Title
A Unified Approach Toward the Total Syntheses of Prenylated Indole Alkaloid Natural Products

Author
Mercado-Marin, Eduardo Valentin

Publication Date
2016

Peer reviewed|Thesis/dissertation

A Unified Approach Toward the Total Syntheses of Prenylated Indole Alkaloid Natural Products

by

Eduardo Valentin Mercado-Marin

A dissertation submitted in partial satisfaction of the

requirements for the degree of

Doctor of Philosophy

in

Chemistry

in the

GRADUATE DIVISION

of the

UNIVERSITY OF CALIFORNIA, BERKELEY

Committee in Charge:

Professor Richmond Sarpong

Professor Thomas J. Maimone

Professor Mary C. Wildermuth

Spring 2016

Abstract

A Unified Approach Toward the Total Syntheses of

Prenylated Indole Alkaloid Natural Products

by

Eduardo Valentin Mercado-Marin

Doctor of Philosophy in Chemistry

University of California, Berkeley

Professor Richmond Sarpong, Chair

This dissertation describes our approach toward a unifying synthesis of prenylated indole alkaloid natural products. Chapter 1 is an introduction and provides background to this class of natural products, focusing primarily on the isolation, biological activity, biosynthetic, and previous synthetic work of these natural products. This section also includes a discussion of synthetic approaches to the common bicyclo[2.2.2]diazaoctane core embodied in many of these natural products, which sets the stage for our entry into these molecules by a unifying route.

Chapter 2 describes our entry into this class of natural products focused primarily on our synthetic and biosynthetic work toward natural products lacking the bicyclo[2.2.2]diazaoctane core. In particular, we discuss the first chemical syntheses of the prenylated indole alkaloids citrinalin B and cyclopiamine B. Along with unambiguously establishing the structures of these natural products, in collaboration with the Berlinck group, we provide evidence for the existence of a common bicyclo[2.2.2]diazaoctane containing precursor as an intermediate to natural products that lack this structural feature.

Lastly, Chapter 3 describes our unified strategy for the synthesis of prenylated indole alkaloid natural products, capitalizing on our results described in Chapter 2. This unifying strategy has resulted in the syntheses of stephacidin A and 17-hydroxy-citrinalin B. Key to the success of this approach in accessing congeners containing and lacking the bicyclo[2.2.2]diazaoctane core was a complexity building isocyanate capture to forge the bicyclo[2.2.2]diazaoctane core from a common all fused precursor.

Dedicated in loving memory of
Ivan Valentin Mercado:
family, friend, and fellow scientist.

Table of Contents

Chapter 3: Toward the Bicyclo[2.2.2]diazaoctane Ring – A Unified Approach to Prenylated Indole Alkaloid Natural Products

Acknowledgements

I am first and foremost grateful to Professor Richmond Sarpong. I certainly could not have asked for a better mentor. Without his positive attitude, encouragement, ideas, and teaching-focused environment, I would not have been successful. I am grateful to him for letting me be a part of his group and for taking the time to develop me as a scientist.

I am also thankful to Dr. Pablo Gacia-Reynaga, for taking me under his wing as a first year graduate student and laying a strong foundation to begin my graduate studies. His training and scientific discussions were both enlightening and imperative to my success as a graduate student.

I also thank, in no particular order, my colleagues from the prenylated indole alkaloid team: Dr. Yingda Ye, Dr. Ken Mukai, Dr. Danilo Pereira de Santana, Jose Roque, Luis Angel Vazquez Maldonado. I have learned so much as a scientist and about myself as a mentor, having worked with each of them. I would also like to thank the rest of the Sarpong group, both past and present, for providing an intellectually stimulating and challenging environment. In particular, I would like to thank my fellow lab-mates in 836 Latimer over the years; Dr. Rebecca Murphy, Dr. James Newton, and Dr. Vincent Lindsay, for providing an uplifting and encouraging environment; especially when chemistry was not working the way we wanted it to. I certainly learned more in discussions with them than I could ever imagine, and have become a better scientist as a result of it, so for that I am also grateful.

I am also appreciative to my past mentors, Professor Thomas R. R. Pettus, Dr. Kun (Phil) Liang-Wu, and McNair Scholars program at UC Santa Barbara, for the encouragement and guidance to pursue graduate school. All their wisdom and knowledge undeniably contributed to my graduate success.

To my parents: *A mis amados padres: Verdaderamente he sido bendecido de tener su amor y apoyo. Las palabras nunca podrán expresar la alegría de contar con ustedes, ni mi gratitud por todo su arduo trabajo y sacrificios. Sus esfuerzos no han pasado desapercibidos, ni han sido en vano. Gracias por todas sus enseñanzas durante toda mi vida porque me hicieron el hombre que ahora soy. Mi mayor motivación a lo largo de los años se refleja en la creencia de que si ustedes hubieran tenido las mismas oportunidades que me procuraron, estarían en mi posición. Estoy eternamente agradecido con Dios por bendecirme con padres tan especiales y maravillosos. Este doctorado es tan suyo como mío. Los quiero mucho.*

To my siblings: Fernando, Jose, Alondra, Alex, James, Uriel, Uziel, Cindy, and Lindsay, thank you for being my role models, friends, and family. We are the products of our love for one another, and I couldn't be happier to have you all as my siblings. I love you all very much.

Most of all, I could not have done this without the love and support of my best friend and fiancée, Margaret Alexandra Sanchez. Ever since the 10th of October 2007, my life changed for the better and each day has been a blessing. Your love and friendship never fails to lift my spirits and provide encouragement to push forward. Thank you for accompanying me on this journey and I look forward to what adventures awaits us in the future. You are my yellow bird. I love you.

CHAPTER 1:

PRENYLATED INDOLE ALKALOID NATURAL PRODUCTS: INTRODUCTION AND BACKGROUND

Presented herein is a discussion regarding the isolation and structural features of several prenylated indole alkaloid natural products. In addition, this discussion will also highlight aspects regarding the biological activities discovered thus far for several families of these secondary metabolites, as well as a summary presenting the current discoveries and hypotheses concerning the biosynthesis of these natural products. Lastly, an overview of synthetic approaches to the common bicyclo[2.2.2]diazaoctane core embodied in many of these metabolites is presented, as well as approaches to related natural products that lack this structural feature.

1.1 – Overview: Isolation and Structure

Secondary metabolites, often referred to as natural products, continue to be the basis for the development of drug candidates for the treatment of various human health problems. For example, of all the drugs on the market in 2010, 50% were either natural products or natural product derivatives.[1] Therefore it is not surprising that novel strategies aimed at streamlining access to these secondary metabolites are extremely important for the treatment of illness and disease. However, initial access to these secondary metabolites requires the laborious isolation and multi-faceted purifications to often obtain minute quantities for a preliminary investigation of the biological activity, which is both inefficient and uneconomical for its development into a drug candidate. Although scientific areas such as synthetic biology have addressed this need by using genetic engineering to override the expression of genes for the production of a subset of secondary metabolites, this is restricted by the structures sanctioned by the biosynthetic machinery and still in its infancy.[2] Over the last seven decades, the field of total synthesis has been the primary means to a) unambiguously validate the structures of natural products, b) access sufficient quantities of otherwise scarce materials, and more importantly, c) access unnatural derivatives for further biological studies.[3,4] Moreover, the field of total synthesis allows the evaluation of modern methodologies in arguably more complex chemical systems, and continues to inspire the development of new organic reactions. As discussed herein, natural products belonging to the prenylated indole alkaloid family has been the backdrop of much scientific inquiry over the last four decades, focused on their diverse biological activities, biosynthetic investigations and the synthetic challenge they impose.

Prenylated indole alkaloids are a growing class of natural products characterized by the presence of an indole ring or derivatives thereof (such as a pseudoindoxyl or spirooxindole, see **1.1** and **1.2**, respectively), which is decorated by one or more prenyl groups (Figure 1.1). Over 70 members of this class of secondary metabolites that contain a unique bicyclo[2.2.2]diazaoctane ring (highlighted in red in **1.1**) have been isolated from various sources of marine and terrestrial fungi including; *Aspergillus, Penicillium,* and *Malbranchea* species.[5] Since 1968 this class of natural products has received continued attention from the scientific community including but

not limited to synthetic, biosynthetic and biological activity studies. Of the natural products containing the unusual bridged bicycle, two distinct stereochemical configurations have been disclosed; the rare *anti*-configuration and the more common *syn*-configuration, which are designated by the position of the bridging C–H proton in relation to the bridging secondary lactam. For example, brevianamides[6] (e.g., brevianamide B (**1.1**), Figure 1.1), chrysogenamide A[7], versicolamide B[8], citrinalin C[9] and 6-*epi*-stephacidin A[10] display the rare *anti*-configuration about the bridged bicycle, whereas the majority of the secondary metabolites, which is the main focus of this Chapter, display the *syn*-configuration as represented by paraherquamide A[11] (**1.2**, Figure 1.1).

Structurally, these secondary metabolites originate from a cyclic amino acid (proline or pipecolic acid, or derivatives thereof, highlighted in pink in **1.4**), tryptophan (highlighted in blue in **1.4**) and one or two isoprene units (highlighted in red in **1.4**, Figure 1.1).

The paraherquamide (**1.2**) and marcfortine[12] (**1.3**) sub-classes are structurally similar in that they contain a spiro-oxindole moiety with a dioxepin ring at the C-6 and C-7 positions of the indole moiety, but differ in possessing a pyrrolidine or piperidine ring, respectively (Figure 1.1). The stephacidin sub-classs[13] (e.g., **1.4–1.6**) closely resemble the paraherquamides (**1.2**) and mangrovamides[14] (e.g., **1.7**) in structure, but lack both the spiro-oxindole and the pyrrolidine ring substituent. Members of this class also possess a chromene moiety at the C-6 and C-7 positions of the indole instead of the dioxepin ring present in **1.2** or the chromanone in **1.7**.

The cyclopiamines[15] (**1.8–1.9**) and citrinalins[16] (**1.10–1.11**) closely resemble the mangrovamides (e.g., **1.7**), in that they contain a pyrrolidine ring, a spiro-oxindole moiety, and substitution at the C-6 and C-7 positions of the indole. However, they lack the bicyclo[2.2.2]diazaoctane ring system and the substitution on the pyrrolidine ring system. The citrinadins[17] (**1.12–1.13**) and the PF1270A–C[18] (**1.14–1.16**) are structurally related to the marcfortine (**1.3**) family of natural products, in that they also contain a substituted pipecolate moiety, C-7 indole substitution, and a spiro-oxindole ring system. However, like the cyclopiamine and citrinalin families, the citrinadins and PF1270A–C families lack the bicyclo[2.2.2]diazaoctane ring system. Since the isolation of the secondary metabolites that lack the characteristic bicyclo[2.2.2]diazaoctane ring system (e.g., cyclopiamines, citrinalins, citrinadins, and PF1270s) from related *Penicillium* species, there has been speculation as to whether these structurally related metabolites share a common biosynthetic pathway or precursor to those which contain the bridged bicycle.

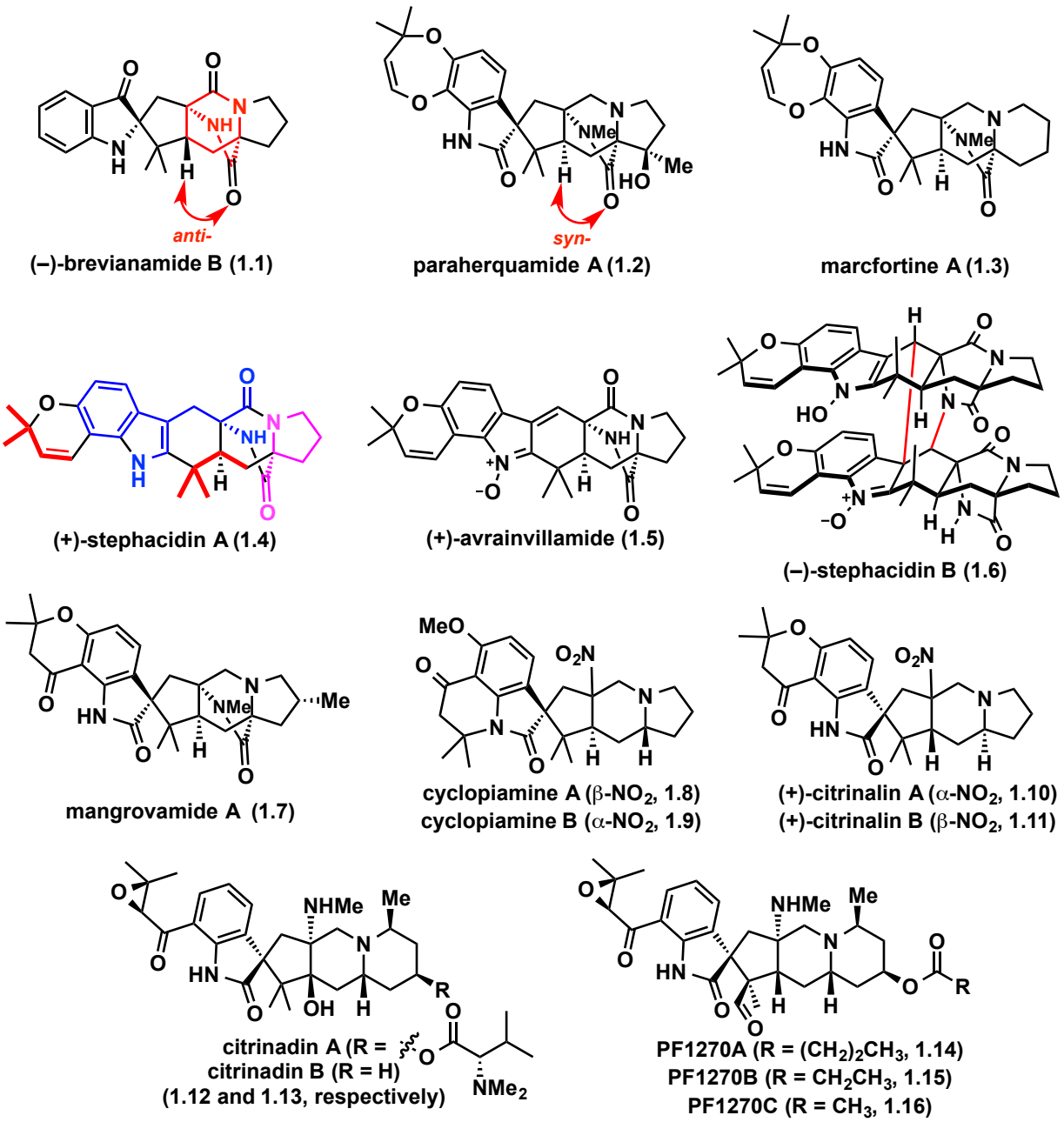

Figure 1.1: Selected Prenylated Indole Alkaloid Natural Products.

1.2 – Biological Activity

Collectively, the prenylated indole alkaloids display a diverse range of biological activities including but not limited to insecticidal, cytotoxic, anthelmintic, calmodulin-inhibition and antibacterial properties.[5] For example, the paraherquamides (**1.2**) and marcfortines (**1.3**) are widely recognized as potent anthelmintics,[19] and in particular, the paraherquamides have been shown to act as antagonists of cholinergic neuromuscular transmission in gastrointestinal nematodes and thus, rapidly inducing paralysis.[20] However, the high toxicity of paraherquamide A needed to be addressed and can be mitigated by removing the carbonyl functional group of the

spirooxindole moiety to afford 2-deoxyparaherquamide A (not shown).[21] This derivative, which is produced semi-synthetically from large-scale fermentation of *P. simplicissimum*, is currently used in a combination therapy as an anthelmintic in sheep and is marketed by Pfizer under the name of Startect®.[22] Other members in this class of natural products, such as the malbrancheamides (not shown) are known to have calmodulin (CaM)-dependent phosphodiesterase (PDE1) inhibitory activity which has important implications in cancer, neurodegenerative and vascular diseases due to its effect on intercellular cAMP and cGMP concentrations.[23]

Arguably, the most intriguing of the secondary metabolites include avrainvillamide and the stephacidins, which have been studied for their biological activity, biosynthetic origins (Section 1.3), and synthetic challenge (Section 1.4). Since its initial isolation in 2001 from *Aspergillus sp.* by a group at Pfizer, avrainvillamide (CJ-17,665) (**1.5**) has been reported to exhibit antibacterial activities against MDR *S. aureus, S. pyogenes,* and *E. faecalis* as well as cytotoxicity against HeLa cells.[24] Most recently, avrainvillamide (**1.5**) has demonstrated global disruption of cellular structure and function by the relocalization of certain cytoplasmic nucleophosmin mutants to the nucleoli of HCT-116 and HeLa S3 cells.[25] The structurally similar stephacidins (**1.4** and **1.6**) showed *in vitro* cytotoxicity against a panel of human tumor cell lines. While stephacidin A (**1.4**) demonstrated IC_{50} values ($IC_{50;}$ half maximal inhibitory concentration) in the single digit micromolar range for ovarian, colon, breast, lung and prostate cancer cell lines, the higher oxidation state and more complex stephacidin B (**1.6**) showed a 5- to 30- fold increase in activity.[13] The strongest activity for **1.5** and **1.6** was observed for testosterone-sensitive prostate LNCaP cancer cells. Of note, the cytotoxicity of these secondary metabolites are not mediated by p53, mdr (multi-drug resistance), bc12, tubulin- or topoisomerase II, which suggests a novel mechanism of action. It was proposed in the original isolation[13, 26] and then later confirmed that stephacidin B (**1.6**) arises from a dimerization of two avrainvillamide (**1.5**) monomers (see bonds highlighted in red in **1.6**, Figure 1.1).[27] The dimerization sequence (**1.5→1.6**) is thought to take place through a double 1,4-addition into the α,β-unsaturated nitrone unit in **1.5** (see Scheme 1.1 for detailed arrow pushing). Thus attack of the secondary amide of one molecule of **1.5** onto the electrophilic β-carbon of the nitrone unit of the second molecule of **1.5** would generate a nucleophilic 1-hydroxyindole species. This 1-hyroxyindole species would react with the proximate α,β-unsaturated nitrone of the second molecule (see bonds highlighted in red in **1.6**) to generate the highly substituted pyrrolidine ring in **1.6**. Myers and co-workers have demonstrated that the nitrone functional group in **1.5** is capable of reversible covalent bond formation with heteroatom-based nucleophiles,[28] such as with intracellular cysteine-containing proteins,[25, 29] and demonstrated the retro-dimerization of stephacidin B (**1.6**) to avrainvillamide (**1.5**) accounted for the higher antiproliferative activity exhibited by stephacidin B.[30]

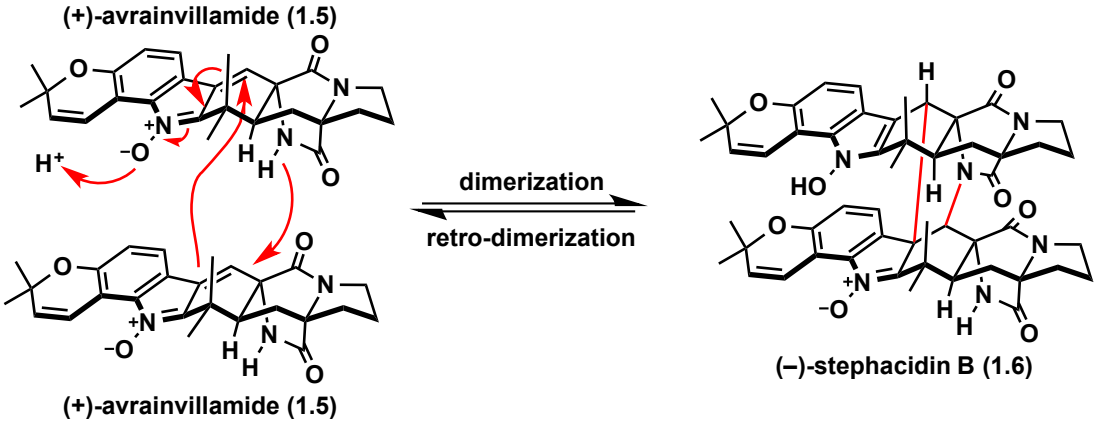

Scheme 1.1: Dimerization sequence of stephacidin B.

The related alkaloids PF1270A-C (**1.14**–**1.16**), show submicromolar affinities for the human H3 histamine receptor with PF1270A being the most active.[18] Citrinadin A (**1.12**) displayed modest cytotoxicity against murine leukemia L1210 cells and human epidermoid carcinoma KB cells with IC_{50} values of 6.2 and 10 μg/mL, respectively.[17a] Citrinadin B (**1.13**) demonstrated nearly identical cytotoxicity against murine leukemia L1210 cells as **1.12** with an IC_{50} of 10 μg/mL.[17b] The citrinalins **1.10** and **1.11** were assayed against the HTB-129 breast cell line but showed no cytotoxic activity, as their IC_{50} values were 174 and 194 micromolar, respectively. No biological activity has been reported for the structurally related cyclopiamines (**1.8**–**1.9**). The development of a unified approach, a goal of this dissertation, to the citrinalins and cyclopiamines may give way to a more comprehensive screening process.

1.3 – Biosynthetic Studies

Since their isolation, the prenylated indole alkaloids have been the subject of intense research aimed at elucidating the biosynthesis of these complex but structurally related metabolites. Birch and co-workers, who isolated the brevianamides in 1969 (e.g. **1.1**, Figure 1.1), demonstrated early on that L-tryptophan, L-proline and isoprene, arising from the mevalonate pathway,[31] were biosynthetically incorporated into these secondary metabolites through the use of ^{13}C-labeled feeding experiments.[32] Since this pioneering work, other groups have shown that amino- acids such as L-isoleucine (in the case of paraherquamide A[33]), L-lysine (in the case of marcfortine A[34]) and *not necessarily L-proline* form cyclic dipeptides with L-tryptophan resulting in the diketopiperazine structural moiety (**1.19**, Scheme 1.2). More importantly, the unique bicyclo[2.2.2]diazaoctane core present in many of these compounds has been proposed to arise through a stereo- and enantio-controlled intramolecular Diels–Alder (IMDA) cycloaddition reaction between an achiral azadiene and an isoprene group (see **1.21**→**1.22**). Since detailed reviews discussing the biosynthesis of the paraherquamides, brevianamides and related metabolites have previously been disclosed,[31, 35] the majority of the discussion to follow will summarize the most current findings regarding the biosynthesis of stephacidin A and structurally related metabolites.[36]

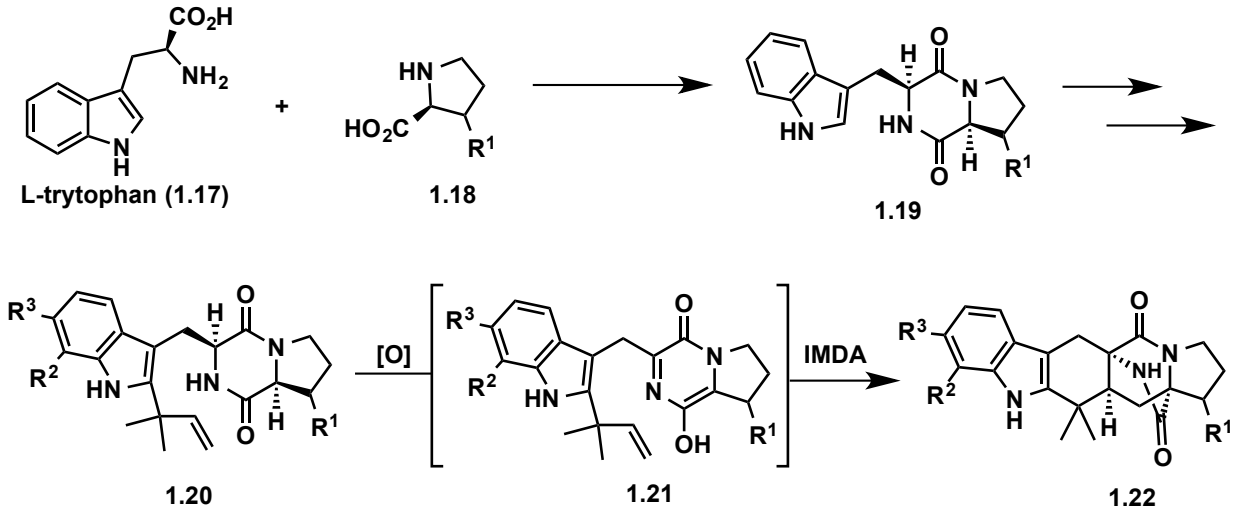

Scheme 1.2: Proposed biosynthesis of prenylated indole alkaloids.

The biosynthesis of the stephacidins attracted much more attention after Gloer and co-workers reported the isolation of the corresponding optically pure enantiomers of stephacidin A and notoamide B from a related terrestrial fungus,[8] which represented the first known occurrence of antipodal prenylated indole alkaloids natural products. The isolation of antipodal forms of stephacidin A and related metabolites implies that the different species of *Aspergillus* have evolved enantiomerically distinct genes responsible for the enantiospecific biosynthesis of these natural products. In order to investigate this further, the Williams and Sherman groups undertook genome sequencing and data mining of *Aspergillus* sp. MF297-2 and *Aspergillus versicolor*, the two fungi responsible for the enantiomeric series of these molecules, which resulted in the identification and characterization of the biosynthetic gene clusters responsible for the production of stephacidin A and notoamide B.[37] Bioinformatics analysis not only revealed a gene cluster, notoamide (*not*), containing 18 genes encompassing ~44 kb (kilo base pairs) of DNA, but also helped predict the function of the majority of the *Not* genes. As shown in Scheme 1.3, two of the genes were identified as aromatic prenyltransferases, *notF* and *notC*, which catalyze the reverse- and normal- prenylation steps, respectively, in the biosynthesis of stephacidin A. Both *notC* and *notF* were independently expressed in *E coli*., the recombinant proteins were isolated, purified and shown to be highly substrate-selective and to catalyze the reverse prenylation on brevianamide F (**1.23→1.24**, Scheme 1.3) and normal prenylation on 6-hydroxy-deoxybrevianamide E (**1.25→1.26**), respectively, with dimethylallylpyrophosphate (DMAPP). On the basis of the genome sequencing, bioinformatics, and double ^{13}C-labeling studies, a biosynthetic sequence for the stephacidins was proposed. Starting from brevianamide F (**1.23**), the *notF* gene product catalyzes the reverse prenylation at the C2 position of the indole to provide deoxybrevianamide E (**1.24**). Then an oxidase, the *notG* gene product, converts **1.24** into 6-hydroxy-deoxybrevianamide E (**1.25**), which is prenylated in the normal sense by the *notC* gene product to give notoamide S (**1.26**).

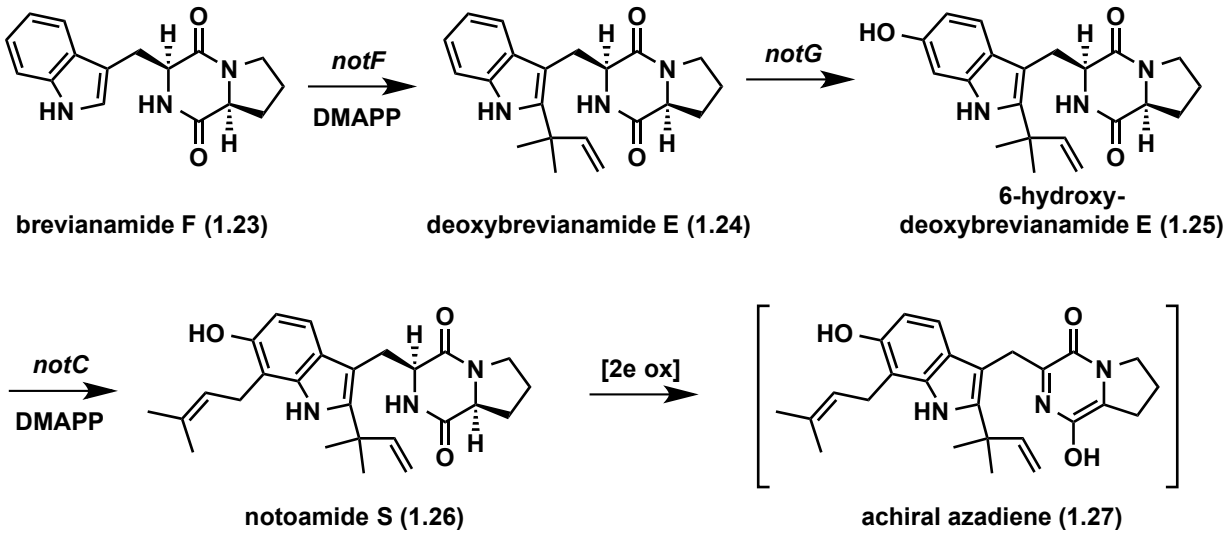

Scheme 1.3: Biosynthesis of achiral azadiene precursor, notoamide S.

Notoamide S (**1.26**, Scheme 1.3) serves as the precursor to the achiral azadiene (**1.27**). Thus, oxidation and tautomerization would yield the key achiral azadiene species (**1.27**), which would undergo an enzymatic enantioselective IMDA reaction, which after oxidative ring closure of the phenol to the chromene,[38] would produce either *syn*-stereoisomer of (+) and (–) enantiomers of stephacidin A (**1.4**) by the respective organism (Scheme 1.4). Each enantiomer of stephacidin A (**1.4**) would then undergo a face-selective oxidative rearrangement of the 2,3-disubstituted indole to provide the corresponding spirooxindoles, (–)- and (+)-notoamide B (**1.28**), respectively. Alternatively, the enantioselective IMDA may also be diastereoselective in regards to the orientation of the olefin (*endo* vs. *exo*) and produce the *anti*-stereoisomers, (+)- and (–)-6-*epi*-stephacidin A (**1.29**), which would undergo the same face-selective oxidative rearrangement of the 2,3-disubstituted indole to yield the corresponding spirooxindoles, (+)- and (–)-versicolamide B (**1.30**), respectively.[10c] Evidence of the putative late stage oxidative rearrangement steps of stephacidin A (**1.4**) to notoamide B (**1.28**) is supported by incorporation studies with ^{13}C-labeled racemic stephacidin A. Whereby doubly ^{13}C-labeled (±)-stephacidin A was fed to cultures of the terrestrial-derived fungus, *Aspergillus versicolor* NRRL 35600, and the marine-derived fungus, *Aspergillus* sp. MF297-2. Analysis of the products revealed complementary, face-selective oxidative enzymes are responsible for the enantiospecific conversion of (+)-stephacidin A to (–)-notoamide B in *Aspergillus* sp. MF297-2, and (–)-stephacidin A to (+)-notoamide B in *Aspergillus versicolor*, with the recovery of the unreacted enantiomer of stephacidin A from each respective organism.[39] Moreover, Williams and co-workers were able to demonstrate the proposed biosynthetic oxidative rearrangement of stephacidin A to notoamide B in a laboratory setting by employing Davis' oxaziridine.[40] The proposed biosynthetic IMDA reaction has been validated by its application to the biomimetic total synthesis of several members of this family of prenylated indole alkaloids including stephacidin A[41] (see Section 1.4.1). However, no evidence for, or against, the presence of a Diels–Alderase that has been proposed in this biosynthetic pathway has been disclosed. Therefore, the possibility exists that these metabolites are produced as *syn*- and/or *anti*-racemates and one enantiomer leads to isolated natural products while the other is catabolized.

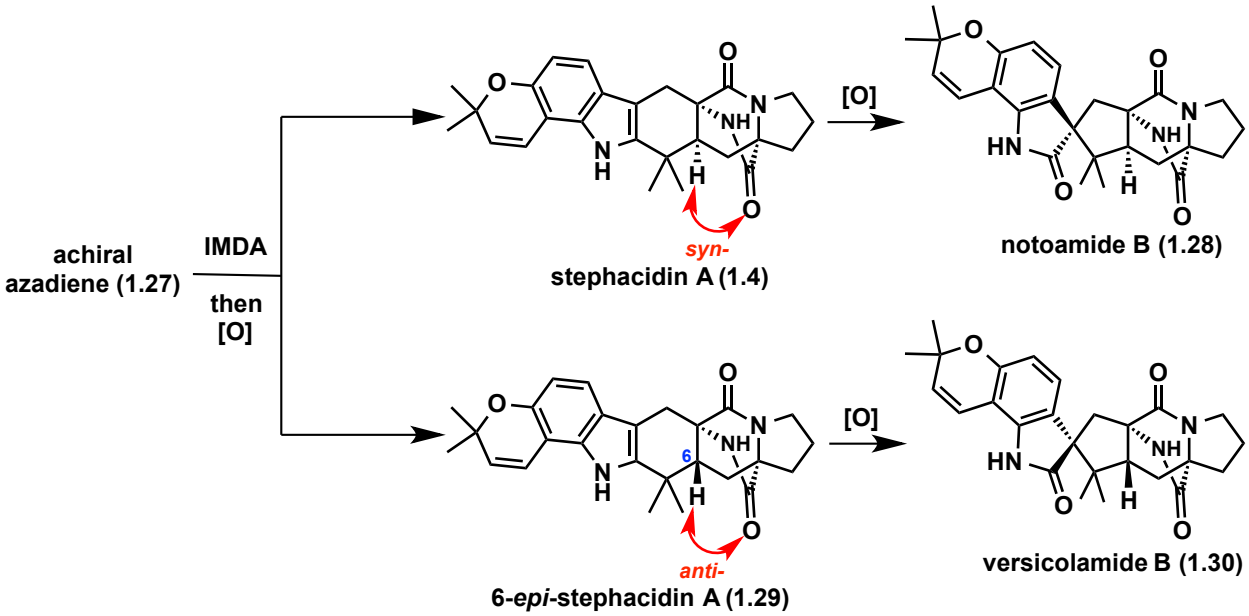

Scheme 1.4: Biosynthesis of stephacidin A and related prenylated indole alkaloids.

From a structural standpoint, the cyclopiamines (**1.8–1.9**, Figure 1.1), citrinalins (**1.10–1.11**), citrinadins (**1.12–1.13**) and PF1270A-C (**1.14–1.16**) appear to be closely related to the previously discussed indole alkaloids, albeit lacking the unique bicyclo[2.2.2]diazaoctane core. Although no biosynthetic studies have been conducted on these related metabolites, with the exception of the research presented in Chapter 2.5,[9] it was proposed by Kobayashi and co-workers[17b] that the citrinadins likely arise from the marcfortine skeleton. As demonstrated in Scheme 1.5, chrysogeanamide A[7] (**1.31**), like the citrinadins and PF1270A-C, contains a substituted pipecolate moiety, C-7 indole substitution, and the spirooxindole ring system. Therefore, loss of an amide carbonyl group occurring by a hydrolysis/decarboxylation event (C13–C18 bond cleavage, see numbering in **1.31**) would take **1.31** to the relatively flat framework found in the citrinadins **1.32** (following additional peripheral oxygenations outlined in red). From a structural point of view, the citrinalins and cyclopiamines are pseudo-enantiomeric (the difference arising from the substitution on the indole moiety) and most likely arise from enantiomeric bicyclo[2.2.2]diazaoctane containing metabolites such as stephacidin A. However, no antipodal natural products lacking the bicyclo[2.2.2]diazaoctane has been reported thus far. Curiously, cyclopiamine B was originally isolated from *Penicillium cyclopium* in 1979[15] and again in 1981[42] from *Aspergillus caespitosus*; both these genera of fungus are closely related and contain species that can produce optical enantiomers of the same or nearly the same molecule.[5] Unfortunately, no optical rotation was reported in either case. Therefore, whether these closely related metabolites share a bicyclo[2.2.2]diazaoctane containing precursor in their biosynthetic pathways remains unclear.

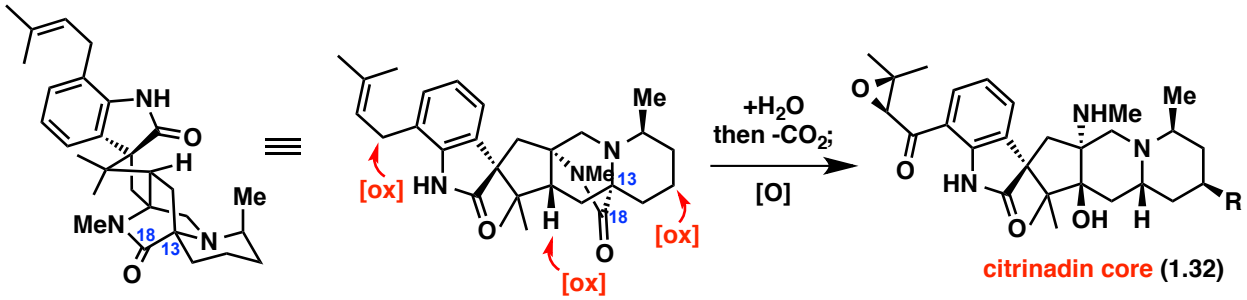

Scheme 1.5: Proposed biosynthesis of the citrinadin family of prenylated indole alkaloids.

1.4 – Previous Synthetic Studies

Over the last three decades, several groups have disclosed synthetic strategies to construct the bicyclo[2.2.2]diazaoctane core found in the majority of prenylated indole alkaloids. Some of the key disconnections include intramolecular S_N2' cyclization, intramolecular Diels–Alder cycloaddition, *N*-acyl radical cyclization, oxidative enolate coupling, radical cyclization, and carbocation cascade cyclization reactions to prepare the bridged bicycle. These approaches are presented in chronological order as they appeared in the literature. Since their isolation in 2001 and 2002 respectively,[13] avrainvillamide (**1.5**, Figure 1.1) and the stephacidins (**1.4** and **1.6**) have garnered much attention from the synthetic community due to their unique biological activities (Section 1.3) and unprecedented molecular scaffolds. They will therefore be the main focus of this section. Reviews covering the synthetic strategies for preparing the bicyclo[2.2.2]diazaoctane ring have previously been reported[43] and only a brief summary of the key steps utilized by various groups will be outlined below.

1.4.1: Synthetic Approaches to the Bicyclo[2.2.2]diazaoctane Ring System

The Williams group developed an intramolecular S_N2' cyclization reaction to build the bicyclo[2.2.2]diazaoctane ring found in the prenylated indole alkaloids, which proved useful in the syntheses of various alkaloids in the family. The first prenylated indole alkaloid synthesized using this approach was (+)-brevianamide B[6b] (Scheme 1.6). The known allylated proline derivative **1.33**, accessed in 3 steps from L-proline following standard chemistry, was converted to diketopiperazine **1.34**. Wittig olefination followed by reduction of the aldehyde provided an allylic alcohol (not shown) which was subsequently protected as the *tert*-butyldimethyl (TBS) -silyl ether. Deprotonation of the diketopiperazine followed by quenching with methyl chloroformate led to methyl ester **1.35**. Treatment of **1.35** with gramine (**1.36**) and tributylphosphine (Bu_3P) furnished the coupled product **1.37** as a single diastereomer. A straightforward sequence was employed to remove the methyl ester, protect the indole nitrogen, and convert the protected primary alcohol group to the corresponding allylic chloride **1.38**, which would serve as the substrate for the key intramolecular S_N2' cyclization (see carbon atoms highlighted in red, **1.38→1.39**). After extensive optimization, it was determined that the addition of 18-crown-6 was essential to obtain the desired *anti*-diastereomer of the bicyclo[2.2.2]diazaoctane core present in **1.41**. The authors propose that the diastereoselectivity is governed by the solvation of the sodium cation of the amide enolate, by either the 18-crown-6 or solvent, resulting in an open transition state leading to the *anti*-product as the major isomer.

With the development of an *anti*-selective route to the bicyclo[2.2.2]diazaoctane core of **1.39**, **1.39** was taken forward to the complete the synthesis of (+)-brevianamide B (**1.41**). Treatment of alkene **1.39** with concentrated HCl led to indole deprotection and olefin-cation cyclization to afford the hexacyclic indole **1.40**. The oxidative rearrangement of the indole to the corresponding pseudoindoxyl was effected by sequential treatment of **1.40** with *m*-CPBA and NaOMe. Removal of the PMB-group proved to be difficult, as standard oxidative conditions for its cleavage proved ineffective. Success was ultimately achieved by deprotonation with *t*-BuLi at the benzylic position followed by quenching with oxygen to give (+)-brevianamide B (**1.41**) in modest yield.

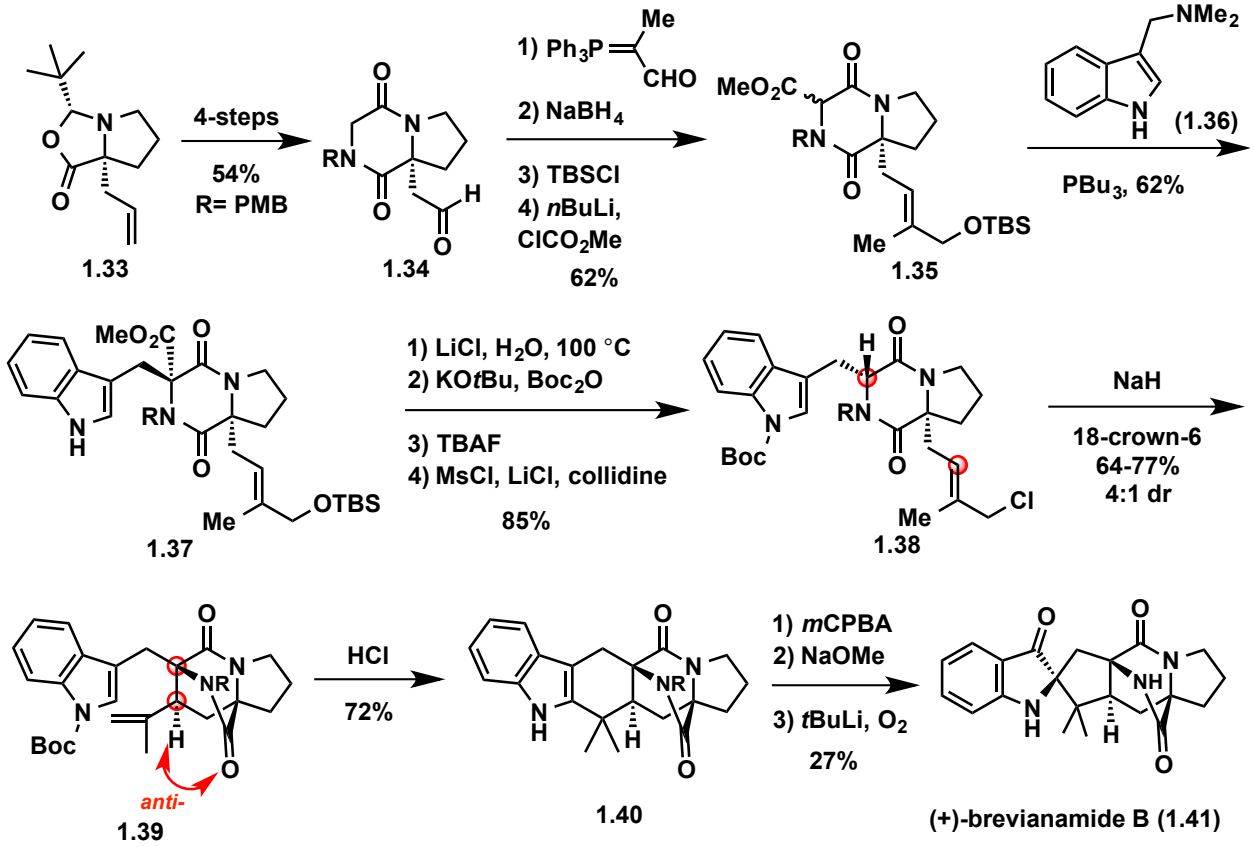

Scheme 1.6: Williams' S_N2' approach to (+)-brevianamide B.

Following the successful application of the S_N2' methodology to (+)-brevianamide B, the Williams research group later applied the same strategy to complete the syntheses of paraherquamide B[44] (not shown) as well as (–)-stephacidin A[40] (**1.45**, Scheme 1.7). Advanced protected tryptophan derivative **1.42** was converted, in 7 steps, to the S_N2' precursor **1.43**. Allylic chloride **1.43** underwent a *syn*-selective intramolecular S_N2' cyclization reaction when treated with NaH in refluxing benzene to give **1.44** as a single diastereomer, which is believed to arise through a tight ion-pair-driven closed transition state. Unfortunately, due to the density of functional groups present in **1.44**, the strongly protic conditions utilized for the cation-olefin cyclization in the synthesis of (+)-brevianamide B (**1.41**, Scheme 1.6) were ineffective. After a screen of various Brønsted and Lewis acids, Pd(II)-mediated cyclization was effective to provide (–)-stephacidin A (**1.45**) upon thermal removal of the indole Boc-group. Following chemistry

discovered by Baran and Myers (*vide infra)*, synthetic (–)-stephacidin A was used to prepare (–)-avrainvillamide and (+)-stephacidin B in two and three steps, respectively.

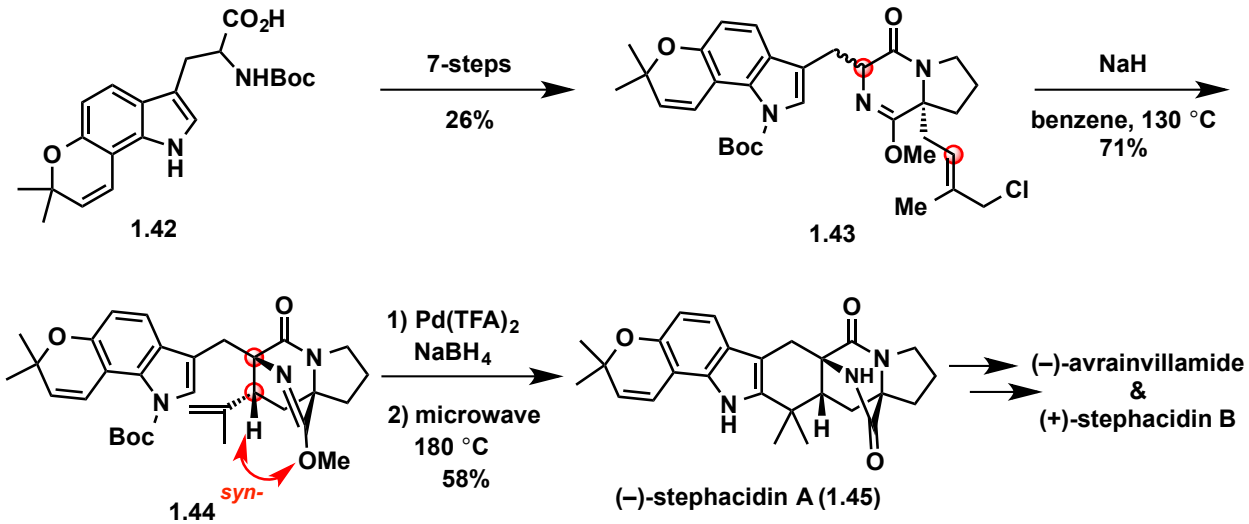

Scheme 1.7: Williams' S_N2' approach to (–)-stephacidin A.

As discussed in Section 1.3, the majority of these compounds share a bicyclo[2.2.2]diazaoctane core, which is postulated to arise biosynthetically through a hetero-Diels–Alder reaction. Williams and co-workers were the first to apply a biomimetic Diels–Alder reaction in the context of accessing the bicyclo[2.2.2]diazaoctane ring present in many of these prenylated indole alkaloids, as demonstrated in the total synthesis of (±)-brevianamide B[45] (**1.1**, Scheme 1.8). Starting with diketopiperazine **1.46**, formation of the amidate ether was followed by oxidation to give the Diels–Alder precursor **1.47**. Treatment of **1.47** under basic conditions resulted in tautomerization to form azadiene **1.48**, which underwent the intramolecular Diels–Alder (IMDA) (see carbon atoms highlighted in red, **1.48→1.49**, **1.50**) to give a 2:1 mixture of the *syn*- to *anti*- diastereomers, **1.49** and **1.50**, respectively. Unfortunately, the diastereofacial bias of the Diels–Alder cyclization (**1.48→1.49**, **1.50**) is not affected by solvent effects as the same ratio of **1.49:1.50** (2:1) was obtained in THF as in aqueous methanol. Nevertheless, the minor *anti*-diastereomer **1.50** was transformed to (±)-brevianamide B (**1.1**) following a four-step sequence involving oxidative rearrangement of the indole to pseudoindoxyl and amidate ether deprotection.

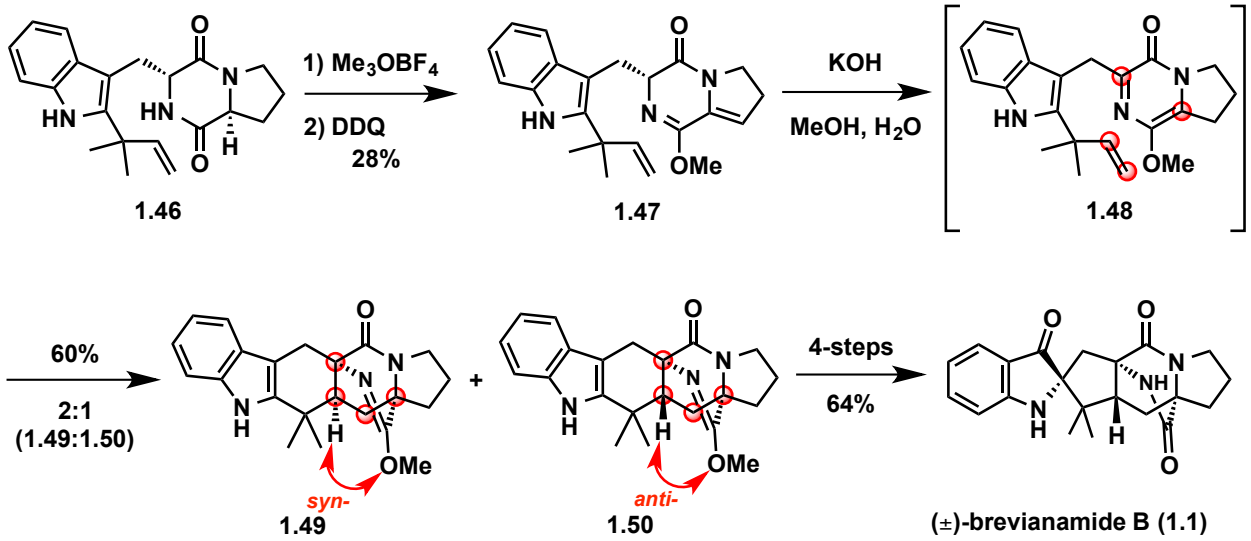

Scheme 1.8: Williams' biomimetic intramolecular Diels–Alder approach to (±)-brevianamide B.

This methodology was also utilized in the synthesis of (±)-stephacidin A[46] (**1.4**, Scheme 1.9) which proved to be more efficient and concise than the S_N2' route previously reported by Williams (see Scheme 1.7). The reverse-prenylated tryptophan derivative **1.51** was prepared in 11-steps from commercially available 6-hydroxyindole and was coupled to form diketopiperazine **1.52**. Treatment of **1.52** with PBu_3 and DEAD resulted in a Mitsunobu dehydration to afford the corresponding enamide **1.53**. Formation of the amidate with Meerwein's salt was followed by IMDA reaction under basic conditions to give a mixture of cycloadducts *syn*-**1.56** and *anti*-**1.55** in a 2.4:1 ratio, respectively. In this case the major product was the desired *syn*-isomer, which was taken forward to (±)-stephacidin A following amidate ether deprotection. It was later determined that **1.52** can be taken directly to cycloadducts **1.55** and **1.56** under the Mitsunobu conditions without the need for amidate formation. This propensity for the formation of the azadiene lends support for the possible construction of this ring system by generation of the putative biosynthetic azadiene species within this family of secondary metabolites.[41]

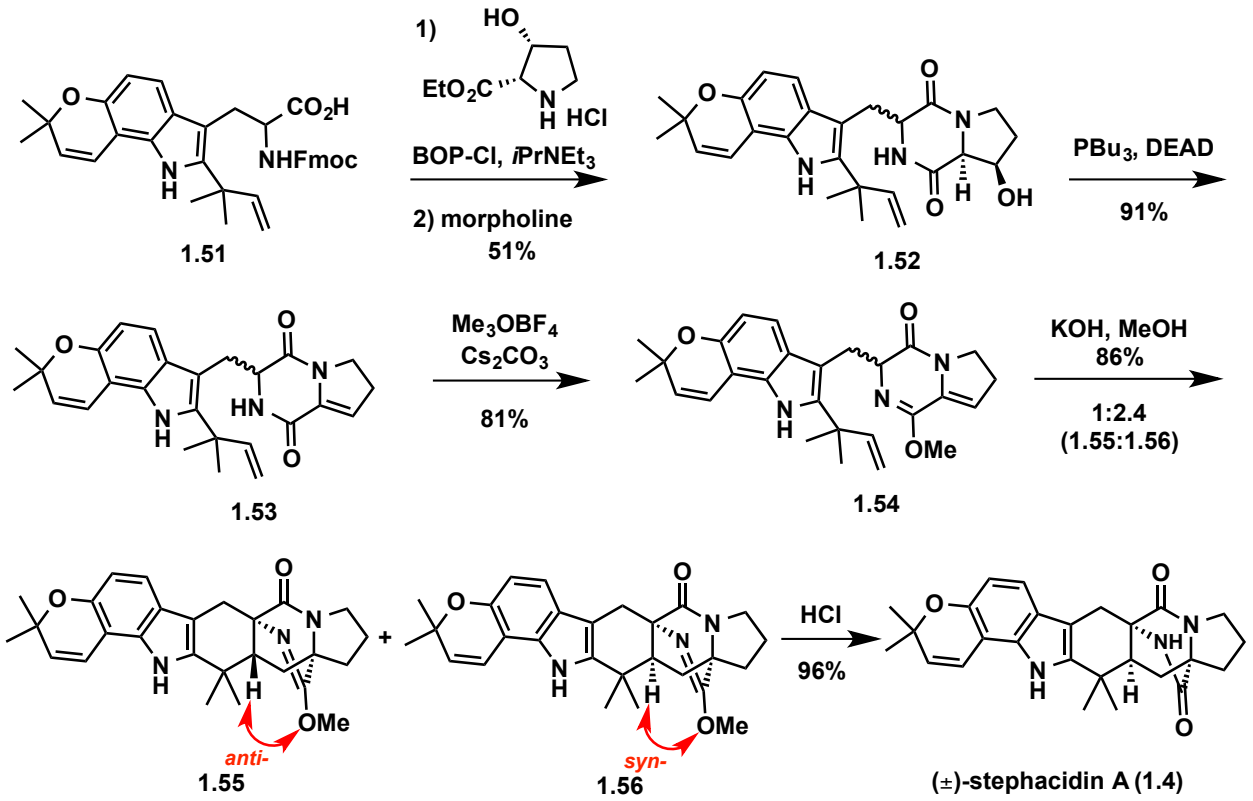

Scheme 1.9: Williams' biomimetic intramolecular Diels–Alder approach to (±)-stephacidin A.

The synthesis of (±)-brevianamide B constitutes the first application of the biomimetic IMDA reaction to the synthesis of the prenylated indole alkaloids. Since the first report in 1998, Williams was able to apply this methodology in the synthesis of several other prenylated indole alkaloids including VM55599,[47] marcfortine C,[48] malbrancheamides,[49] and versicolamide B.[50] However, all the syntheses employing the IMDA reaction rely on the intermediacy of a prochiral azadiene in their sequences, with the exception of versicolamide B, which is diastereoselective, and led to racemic product. Recently, Johnston and co-workers[51] have rendered the IMDA reaction enantioselective using catalytic chiral diamine-derived hydrogen bond donors to access the *syn*-stereoisomer as the major product (*syn:anti*, 2.1:1) in a modest 44% e.e. However, no enantioselective IMDA method for accessing *exclusively* the *syn*-connectivity, which is the most common among the prenylated indole alkaloids, has been reported thus far. Of note, Scheerer and co-workers utilized a similar IMDA reaction in their asymmetric synthesis of (+)-malbrancheamide B,[52] in which the diastereofacial selection of the IMDA was enforced with a chiral aminal auxiliary.

In contrast to William's biomimetic approaches, Myers and co-worker utilized an *N*-acyl radical cyclization to construct the bicyclo[2.2.2]diazaoctane core present in (–)-avrainvillamide (**1.64**, Scheme 1.10) and demonstrated its putative dimerization to form (+)-stephacidin B.[27a] Their synthetic route began with known, achiral cyclohexanone derivative **1.57**, which was transformed to enone **1.58** by a seven-step sequence, one of which was a catalytic enantioselective Corey–Bakshi–Shibata (CBS) reduction.[53] The stereochemistry of the single stereogenic center introduced in the CBS reduction step was subsequently used to control all other stereocenters of avrainvillamide. Next, a four step sequence involving hydration of the

nitrile to the corresponding primary amide, diastereoselective 1,4-addition of thiophenol to the enone moiety accompanied by cyclic hemiaminal formation, acid-mediated cleavage of the *N*-Boc group was accompanied by dehydration of the cyclic aminal, and acylation of the free amine, resulting in radical cyclization precursor **1.59**. When **1.59** is heated with *tert*-amyl peroxybenzoate, the *N*-acyl radical **1.60** is presumably formed, which then attacks the enamide double bond (see carbon atoms highlighted in red in **1.59→1.61**) and expels the phenylthinyl radical to give the bicyclo[2.2.2]diazaoctane core structure **1.61**. Synthesis of avrainvillamide and stephacidin B was straightforward from here, as **1.61** was subjected to a three-step sequence to remove the silyl protecting group, oxidize the allylic alcohol to the corresponding enone, and introduce the vinyl iodide to give coupling partner **1.62**. Ullman coupling with readily accessible aryl iodide **1.63** provided a nitro-aryl enone (not shown) which was reduced in the presence of activated zinc powder to form the heptacyclic unsaturated nitrone **1.64** in modest yields. Simply stirring **1.64** in a triethylamine solution resulted in a spontaneous dimerization to form stephacidin B. This constituted the first asymmetric total synthesis of the stephacidins and avrainvillamide congeners.

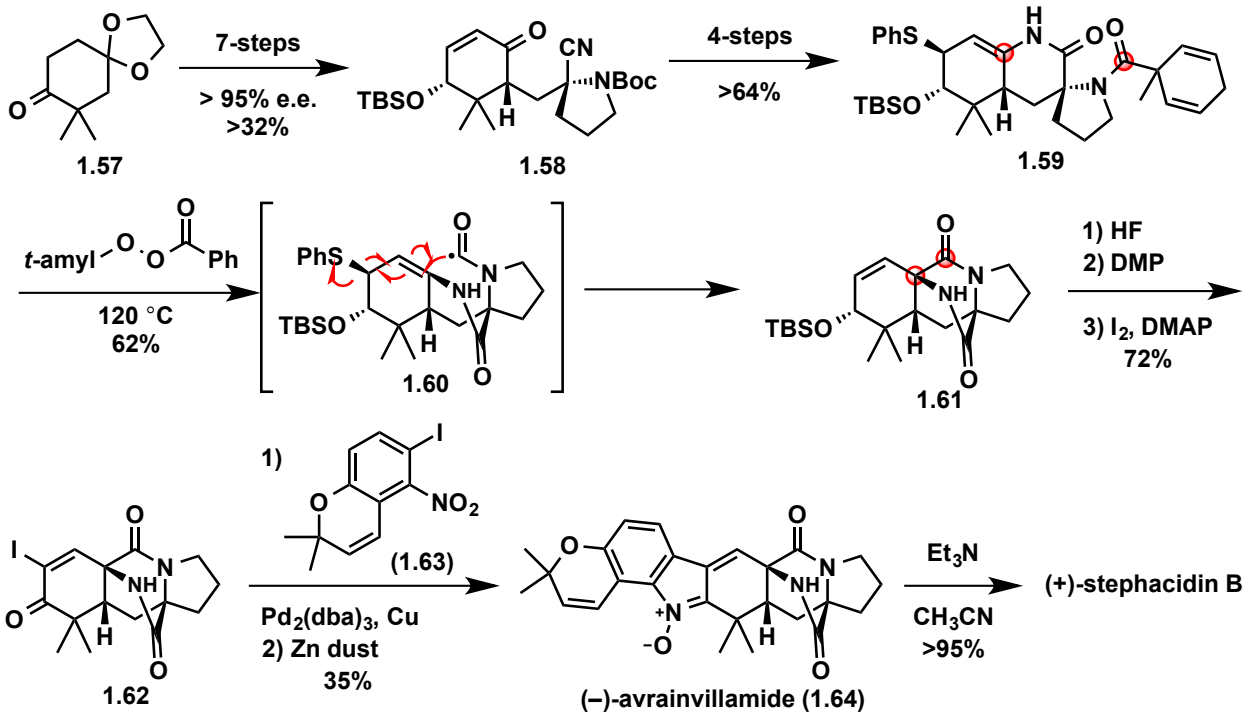

Scheme 1.10: Myers' *N*-acyl radical cyclization approach to (–)-avrainvillamide and (+)-stephacidin B.

The Baran research group utilized an oxidative coupling of enolates to construct the bicyclo[2.2.2]diazaoctane core present in the stephacidins and avrainvillamide (Scheme 1.11).[27b, 54] The protected tryptophan derivative **1.65** was coupled to the proline derivative **1.66** under standard conditions to provide **1.67**, which underwent carbamate cleavage, diketopiperazine formation, and subsequent protection of the secondary amide as the MOM-ether to afford the key oxidative enolate coupling precursor **1.68**. After screening a variety of oxidants, $Fe(acac)_3$ proved to be most effective. Thus, treating **1.68** with LDA and $Fe(acac)_3$ led to effective

coupling (see carbon atoms highlighted in red in **1.68→1.69**) and following cleavage of the MOM-ether gave **1.69** as a single *syn*-diastereomer. The stereochemical outcome of this oxidative enolate coupling is believed to arise from a metal-chelated transition state in which the two enolates are orientated in a head-to-head fashion upon binding a single, multivalent metal counterion.[54a] The resulting free diketopiperazine **1.69** was treated with an excess of MeMgBr to furnish the tertiary alcohol (not shown) that was dehydrated to the corresponding alkene **1.70** upon treatment with Burgess reagent. Attempts at converting **1.70** to (+)-stephacidin A under acidic conditions were ineffective due to the acid-labile nature of the substrate. Surprisingly, simply heating **1.70** at 200 °C results in the formation of (+)-stephacidin A (**1.4**). The authors believe this occurs by the thermal removal of the Boc-group through a retro-ene reaction/formal ene reaction leading to a spirocyclic intermediate (not shown) which undergoes a 1,2-shift to furnish **1.4**. All attempts to facilitate a proposed biomimetic stepwise oxidation sequence of (+)-stephacidin A to access (+)-avrainvillamide via the intermediacy of aspergamides A and/or B (not shown) were unsuccessful. Therefore, the indole was first reduced to the indoline and treatment with SeO_2/H_2O_2 resulted in a synthesis of **1.5**, albeit in modest yield due to the instability of the product under the reaction conditions. In accord with Myers' observations (Scheme 1.10), **1.5** underwent spontaneous dimerization to **1.6** under a variety of conditions, including treatment with base (Et_3N), evaporation from DMSO or even exposure to silica gel.

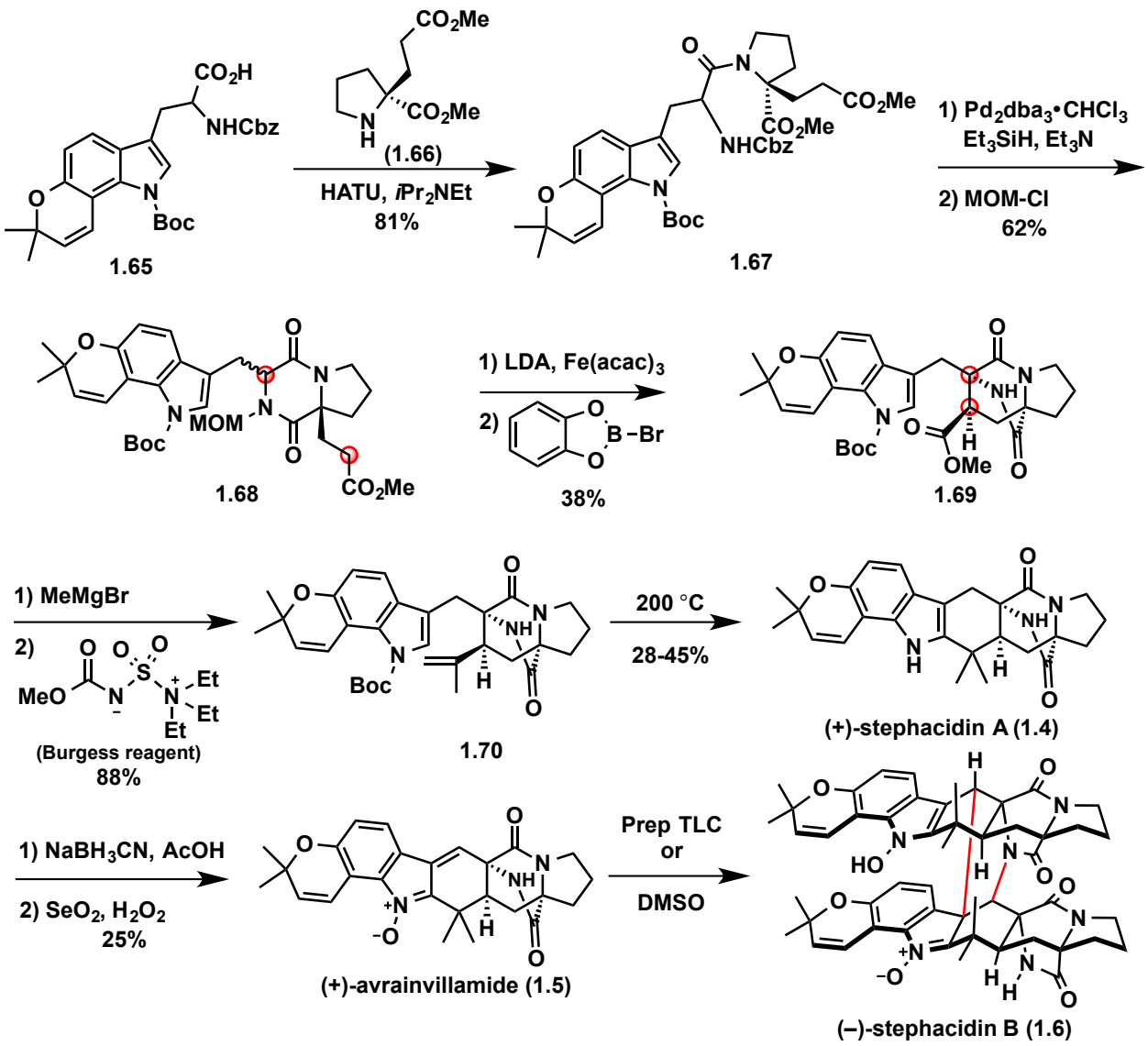

Scheme 1.11: Baran's oxidative coupling of enolates approach to (+)-stephacidin A.

Trost and co-workers devised a radical cyclization route to the bicyclo[2.2.2]diazaoctane core of (±)-marcfortine B[55] (**1.79**, Scheme 1.12). Starting with trimethylenemethane (TMM) acceptor oxindole **1.71**, clean [3+2]-cycloaddition and methylation of the resulting carboxylic acid provided the highly substituted cyclopentane ring in **1.73**. Epoxidation and elimination afforded allylic alcohol **1.74**. Mesylation, displacement with a pipecolic derivative, and an elimination sequence provided enamide **1.75**. Deprotonation of the primary amide resulted in addition to the methyl enoate to give the cyclized product (**1.76**), after protection of the spirooxindole moiety with a PMB group. The diastereoselectivity of this transformation is speculated to arise from addition of the amide to the more accessible α-face of the alkene and internal protonation of the resulting anion by the secondary amide hydrogen. Reduction of the ester in **1.76** with DIBAL-H and installation of the xanthate ester using standard chemistry afforded the radical cyclization precursor **1.77**. Treatment of **1.77** with AIBN and Bu_3SnH generated the primary alkyl radical, which attacked the more-substituted carbon of the enamide double bond to give the bridged bicycle **1.78** (see carbon atoms highlighted in red in **1.77**→**1.78**).

A number of subsequent steps, including reduction of the double bond (which resulted from trapping of the secondary radical with AIBN, C–H abstraction and fragmentation), and installation of the final dioxepin ring were required to complete the synthesis of (±)-marcfortine B (**1.79**).

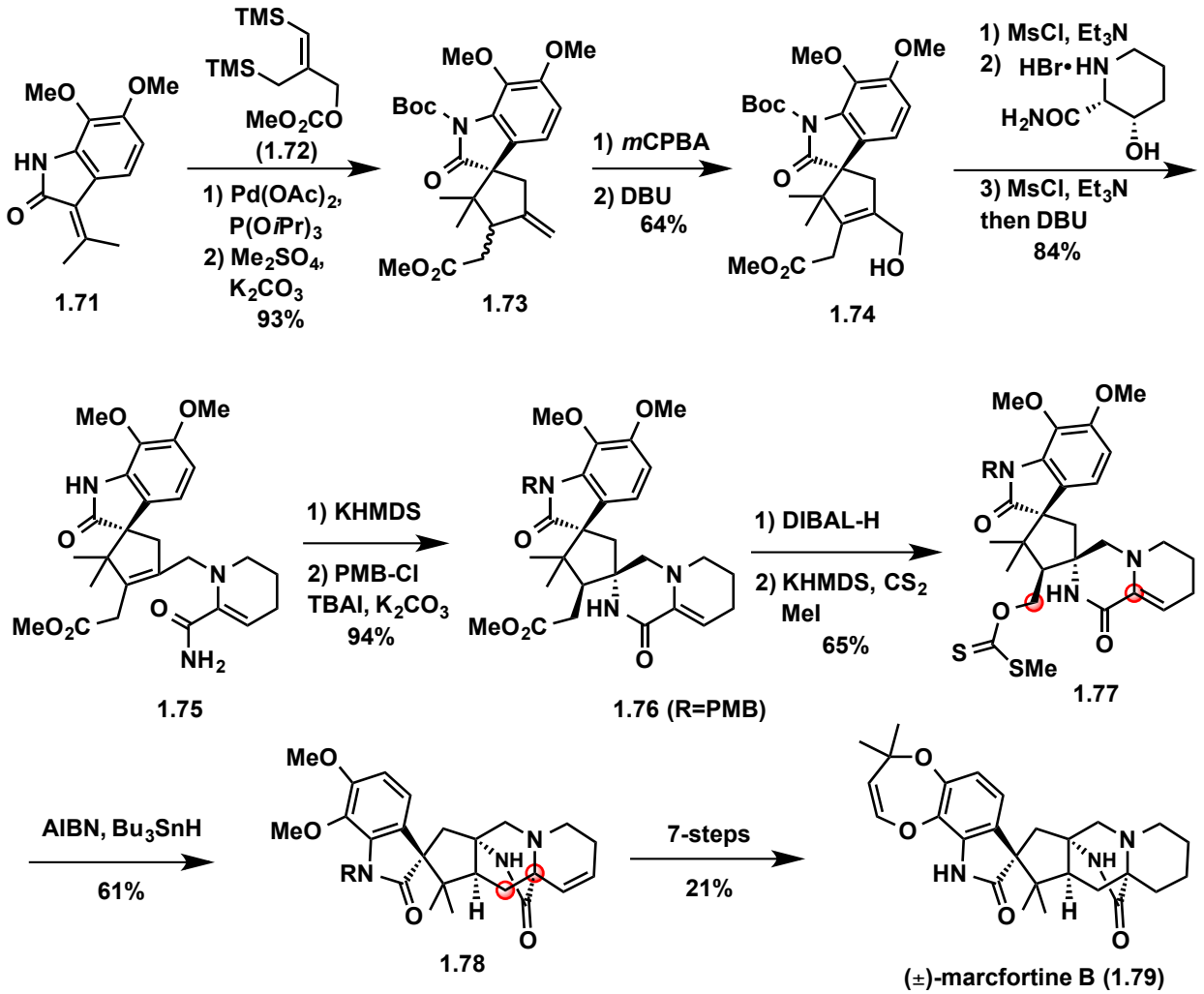

Scheme 1.12: Trost's radical cyclization approach to (±)-marcfortine B.

Simpkins and co-workers developed two separate but analogous approaches to form the bicyclo[2.2.2]diazaoctane ring present in many of these secondary metabolites. The first approach relied on a cationic cascade which was applied to an asymmetric total synthesis of (–)-malbrancheamide B[56] (**1.84**, Scheme 1.13). Readily available aldehyde **1.80** was converted in 5-steps to key diketopiperazine **1.81**, which upon treatment with TMSOTf resulted in simultaneous indole deprotection, ionization and cyclization of the prenyl group onto the diketopiperazine (atoms highlighted in red in **1.81**), followed by ring closure/aromatization of the indole moiety onto the resulting tertiary carbocation (atoms highlighted in blue in **1.81**). This cationic cascade sequence resulted in a separable 1:4 mixture of the *anti*- to *syn*- diastereomers, **1.82** and **1.83**, respectively. From **1.83**, reductive fragmentation of the *N*-(benzyloxy)amide bond was achieved with SmI_2 followed by reduction of the tertiary amide with DIBAL-H, to provide (–)-malbrancheamide B (**1.84**).

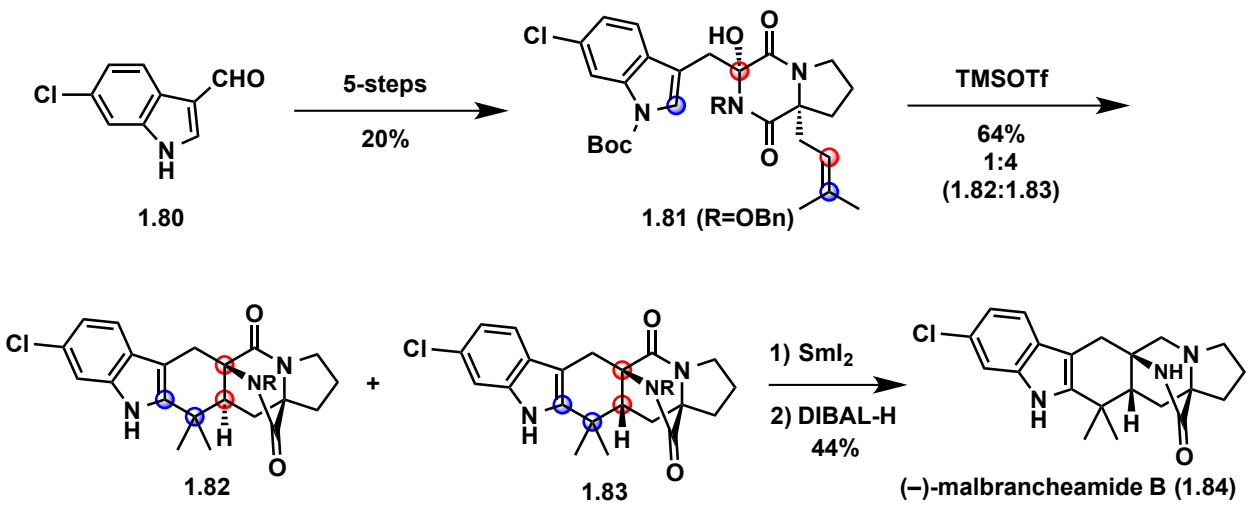

Scheme 1.13: Simpkins' cationic cascade sequence to (–)-malbrancheamide B.

Simpkins' alternative approach to the bicyclo[2.2.2]diazaoctane ring system employed a radical cascade cyclization sequence to access (–)-stephacidin A[57] (**1.45**, Scheme 1.14). Attempts at employing the cationic cyclization sequence, previously demonstrated in the synthesis of (–)-malbrancheamide B (Scheme 1.13), was unsuccessful due to the acid sensitive chromene moiety present in (–)-stephacidin A. Therefore, a process analogous to their previous reports was envisioned to give rise to the bicyclo[2.2.2]diazaoctane core. Coupling advanced protected tryptophan derivative **1.42** with proline derivative **1.85** followed by thermal cleavage of the *N*-Boc group/cyclization to form the diketopiperazine, and double-Boc protection provided **1.86**. The mixture of diastereomers of **1.86** were then treated with LDA at low temperature followed by treatment with phenyl disulfide which resulted in radical cyclization precursor **1.87**. Subjecting **1.87** to thermal reductive Bu_3SnH conditions resulted in the formation of indoline products **1.89**:**1.88**:**1.90** in a 3.3:1.0:0.7 ratio, respectively (see atoms highlighted in red and blue in **1.87**, respectively). Fortunately, the majority of the mixture displayed the *syn*-stereochemistry (**1.89** and **1.90**) found in the natural product. Next, dehydrogenation of the mixture of **1.89**+**1.90** was accomplished by treatment with DDQ, and a final thermal removal of the Boc-group yielded (–)-stephacidin A (**1.45**).

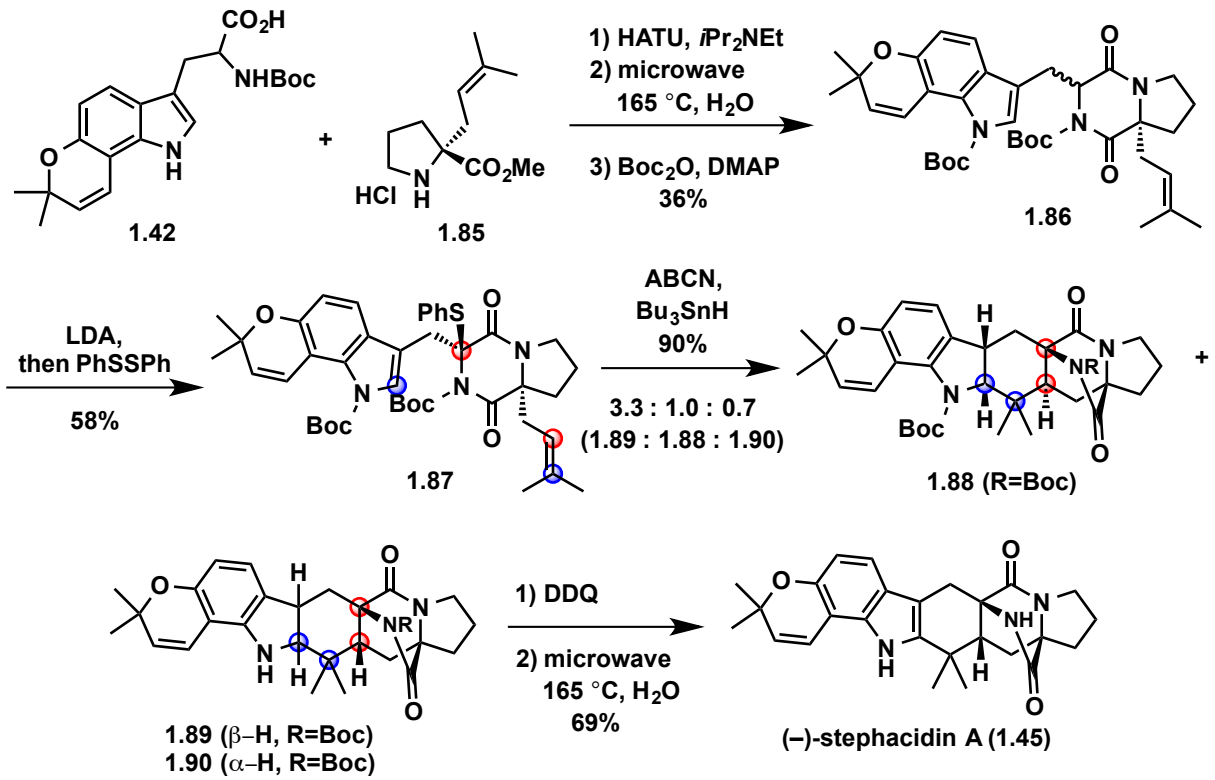

Scheme 1.14: Simpkins' radical cyclization cascade to (–)-stephacidin A.

1.4.2: Synthesis of Congeners Lacking the Bicyclo[2.2.2]diazaoctane Ring

Until recently, the synthetic community has focused on the synthesis of prenylated indole alkaloid congeners possessing the unique bicyclo[2.2.2]diazaoctane core (see Section 1.4.1). However, with the discovery of several prenylated indole alkaloids lacking the bicyclo[2.2.2]diazaoctane ring system that display unique and comparable biological activities (see Section 1.3), there has been an emergence of synthetic work geared toward their syntheses. In particular, the citrinadins (**1.12** and **1.13**, Figure 1.1) has been a focus of the synthetic community over the last decade and recently resulted in the synthesis and structural reassignment of (–)-citrinadin A (**1.12**) and (+)-citrinadin B (**1.13**) by the groups of Martin[58] and Wood[59], respectively. These two natural products will be the focus of this section. Of note, the Sorensen[60] and Sarpong[61] groups have also published routes to the cores of citrinadins. However, that work will not be discussed.

Martin and co-worker's[58a] synthesis of (–)-citrinadin A (**1.12**) was focused on establishing the relative stereochemistry of the α,β-epoxy ketone and the pentacyclic core, which at the time was unknown. Their synthetic route features a diastereoselective vinylogous Mannich addition of a dienolate to a chiral pyridinium salt to set the initial chiral center (Scheme 1.15). The total synthesis of citrinadin A began with the preparation of **1.91** from commercially available 2,2-dimethylcyclohexane-1,3-dione (not shown) through a four-step sequence. Deprotonation of **1.91** with LDA, followed by transmetallation to the zinc-enolate, set the stage for the key diastereoselective vinylogous Mannich reaction with chiral pyridinium salt **1.92** to

provide **1.93** after acid workup. Tricyclic intermediate **1.94** was obtained by base-induced cleavage of the chiral auxiliary/spontaneous cyclization, protodesilylation, copper-mediated 1,4-addition, followed by a highly stereoselective reduction of the resulting ketone group with L-Selectride. Heating this compound (**1.94**) with TBAF resulted in a second protodesilylation reaction, which was followed by epoxidation with peroxytrifluoroacetic acid and opening with methylamine furnished amino-alcohol **1.95**. The diastereoselectivity of the epoxidation is believed to arise by sterics associated with the adjacent quaternary center in which the axial methyl group blocks the α-face of the alkene. Treatment of **1.95** under conditions known to promote the Fischer indole synthesis simultaneously cleaved the ketone protecting group and allowed the installation of the indole moiety, which was followed by an amide reduction resulting in amino-indole **1.96**. Compound **1.96** was first treated with pyridinium *para*-toluenefulfonate (PPTS) to protect the amino groups from oxidation, and an excess of Davis' oxaziridine was added to afford spirooxindole **1.97**, upon acid work up. A subsequent four-step sequence resulted in a synthesis of (–)-citrinadin A (**1.12**) from **1.97**. A final diastereoselective epoxidation of a penultimate enone (not shown) to afford (–)-citrinadin A was necessary to establish the correct stereochemical structure of this prenylated indole alkaloid as **1.12**. Martin and co-workers later published a detailed full account which also described a synthesis of (+)-citrinadin B (**1.13**) employing the synthetic route described above.[58b]

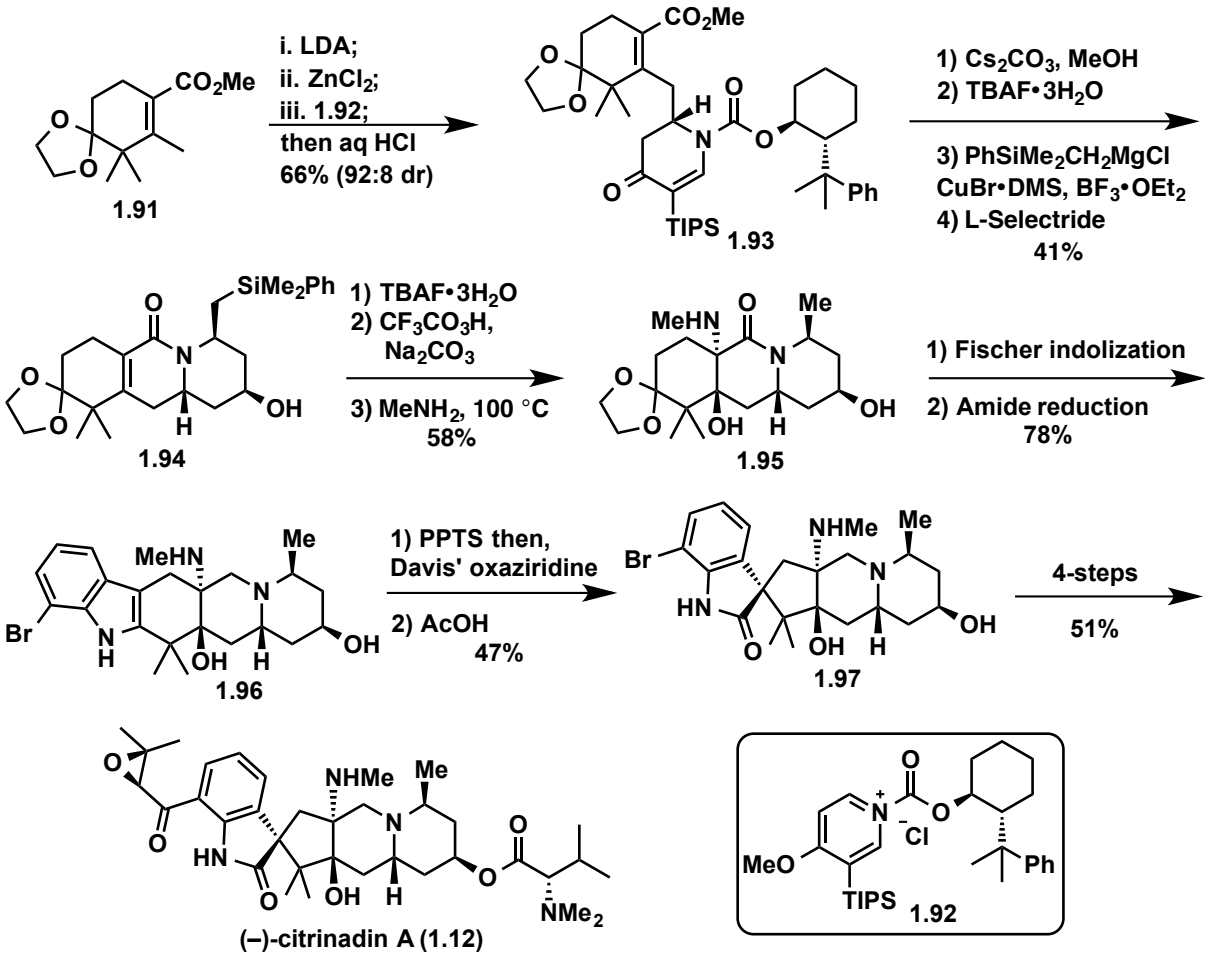

Scheme 1.15: Martin and co-worker's synthesis of (–)-citrinadin A.

Wood and co-workers[59] utilized a stereoselective intermolecular nitrone cycloaddition reaction and an intramolecular opening of an epoxide to construct the carbocyclic core of (+)-citrinadin B (**1.13**, Scheme 1.16). Dibromoaniline **1.98** was subjected to an 11-step sequence to provide the dipolar cycloaddition substrate, **1.99**. After optimization, it was found that L-proline is beneficial to both the rate and diastereoselectivity of the cycloaddition reaction. Thus, a mixture of **1.99** and nitrone **1.100** resulted in the cycloadducts (not shown) in which the desired diastereomer at the C-3 carbon, that shown in **1.101**, resulted from the minor product of the reaction (d.r. 1.4:1). A Corey–Chaykovsky epoxidation on the minor cycloadduct provided epoxide **1.101**, which set the stage for the subsequent ring closure by intramolecular attack of the nucleophilic proximal nitrogen on the epoxide (see carbon atom highlighted in red in **1.101→1.102**). Thus, exposure of epoxide **1.101** to *in situ* generated TMSI furnished the ammonium salt (not shown) which was subsequently treated with Zn to effect N–O bond cleavage reaction to furnish diol **1.102**. The corresponding epoxide (**1.103**) was obtained using standard chemistry. Sonogashira coupling of **1.103** with 3-methyl-1-butyne, benzyl cleavage, and subsequent epoxide opening with $MgCl_2/NaN_3$ furnished azide **1.104**. Amino-azide **1.104** was carried through a 6-step sequence to complete the total synthesis of (+)-citrinadin B (**1.13**) and simultaneously establish the correct stereochemical structure of this prenylated indole alkaloid as **1.13**.

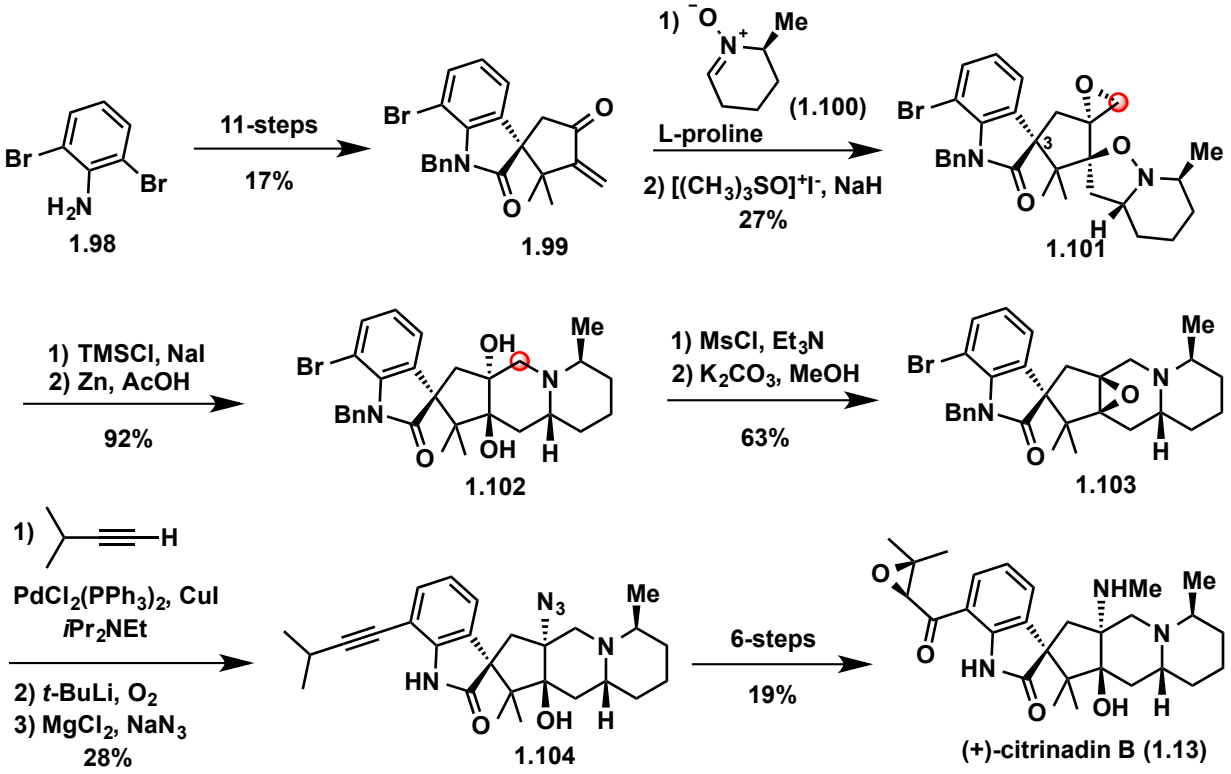

Scheme 1.16: Wood and co-worker's synthesis of (+)-citrinadin B.

1.4.3: Summary of Previous Synthetic Studies

As demonstrated in sections 1.4.1 and 1.4.2, all the existing syntheses toward the prenylated indole alkaloids have targeted either the subset that contains the bicyclo[2.2.2]diazaoctane core (e.g., stephacidin A, section 1.4.1) or those which lack this structural feature (e.g., citrinadins, section 1.4.2). A synthetic approach that would afford both the prenylated indole alkaloids containing as well as lacking the bicyclo[2.2.2]diazaoctane core would be strategically efficient and unifying. However, this was yet to be demonstrated when we began our studies (*vide infra*). As summarized in Scheme 1.17a, all previous syntheses of natural products that contain the [2.2.2] diazaoctane bicycle have centered around constructing the 2,5-diketopiperazine ring (highlighted in red in structures **1.105–1.110**, Scheme 1.17a) early in their synthetic routes, and rely on forming a C–C bond to construct the [2.2.2] bridged bicycle. As demonstrated in **1.105**, the C4 tetrasubstituted center (stephacidin A numbering) at the bicyclo[2.2.2] bridgehead is constructed at an early stage or through C4–C5 bond formation. However, in order to apply these synthetic routes to secondary metabolites lacking the [2.2.2] bicycle, a late-stage cleavage of the C4–C26 bond would be required, which is a complexity minimizing sequence and has not been achieved in the literature. This type of transformation would constitute a biomimetic cleavage of the bicyclo[2.2.2]diazaoctane core as proposed by Kobayashi and co-workers,[17b] see Section 1.3. In this scenario (see Scheme 1.17b), selective amide hydrolysis of the secondary amide of the bicycle in **1.105** would produce **1.111**, which upon decarboxylation (cleavage of C4–C26), and a *diastereoselective* protonation at the resulting C4 ring junction would then convert **1.105** to the sub-family that lacks the [2.2.2]diazaoctane structural moiety, **1.112**. However, this type of transformation has not been reported thus far. From our perspective, a synthetic route which constructs the bicyclo[2.2.2]diazaoctane ring late-stage from an advanced, all-fused precursor such as **1.112**, would provide the most strategically efficient and unifying route to these molecules and would be complementary to the biosynthetic proposal (**1.105→1.112**) as well as all previous syntheses.

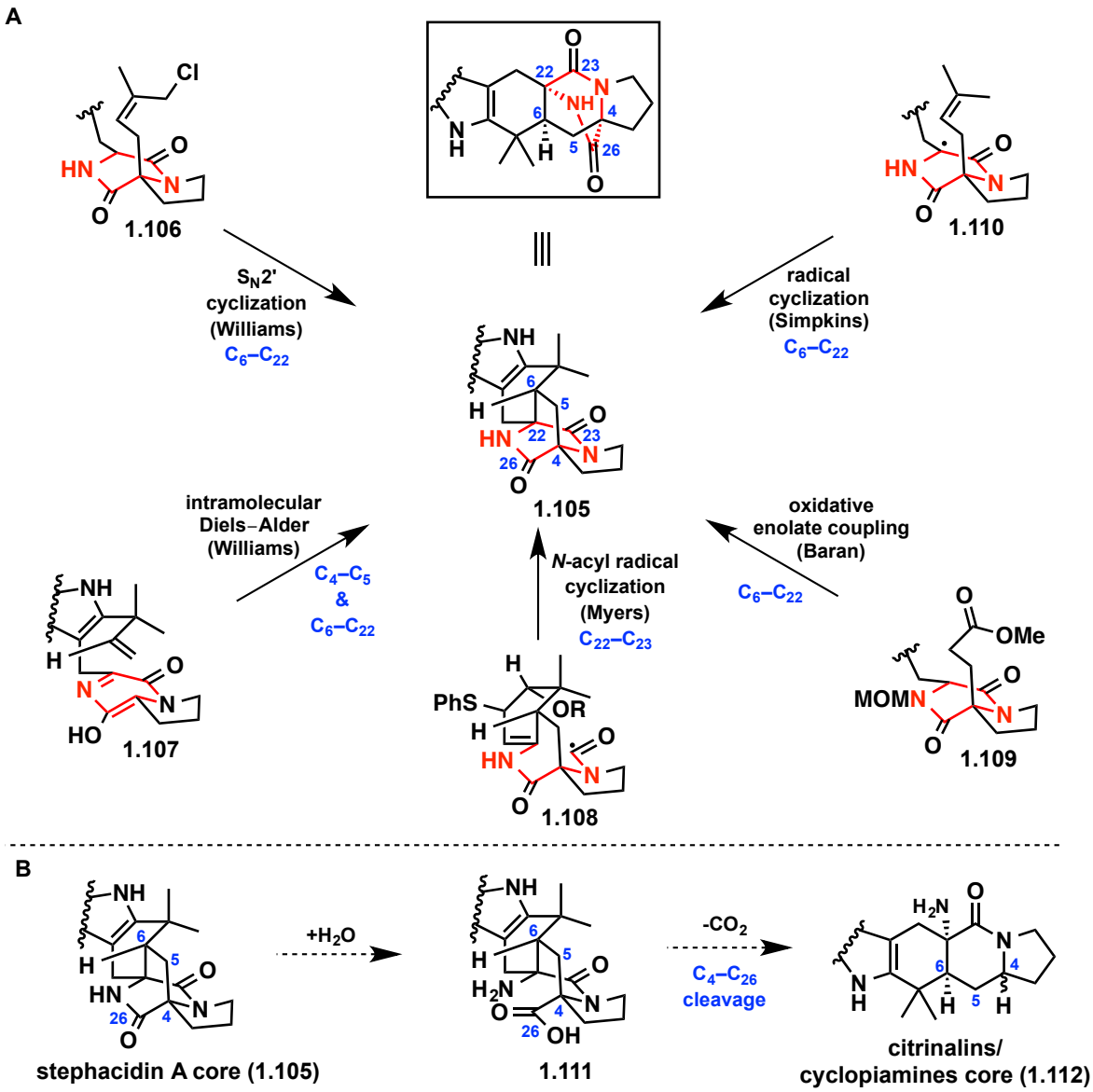

Scheme 1.17: a) Established approaches to the bicyclo[2.2.2]diazaoctane ring system of avrainvillamide and the stephacidins (numbering of **1.105** is based on stephacidin A).[13] **b)** Proposed biomimetic degradation of the bicyclo[2.2.2]diazaoctane ring system.

1.5 – Summary and Outlook

The prenylated indole alkaloids have been the subject of various scientific fields aimed at elucidating their bioactivity, biosynthesis and total syntheses. Although structurally similar, collectively these secondary metabolites have demonstrated insecticidal, antitumor, anthelmintic, calmodulin inhibitory, and antibacterial properties. Pioneering work by the Williams and Sherman groups has culminated in a proposed enzymatic intramolecular Diels–Alder reaction that is both diastereo- and enantioselective for the construction of the key bicyclo[2.2.2]diazaoctane core common to many of these molecules. Although no biosynthetic

studies have been conducted on metabolites which lack the bicyclo[2.2.2]diazaoctane core, it has been proposed that they arise from a bicyclo[2.2.2]diazaoctane containing metabolite which undergoes degradation of the bridged bicycle. However, it remains to be established whether a Diels–Alderase is responsible for construction of the [2.2.2] bicycle and if these two sub-families share common biosynthetic pathways. Moreover, due to their unique bioactivities along with interesting biosynthetic proposals, this family of secondary metabolites has been a fertile area of research for the synthetic community and resulted in powerful synthetic methodologies. However, no unifying synthetic route encompassing both structural sub-types has been disclosed, and our work in this area (described in the preceding Chapters) validates the value of such an approach.

1.6 – References and Notes

1. Newman, D. J.; Cragg, G. M. *J. Nat. Prod.* **2012,** *75*, 311–335.

2. (a) Seyedsayamdost, M. R.; Clardy, J. *ACS Synth. Biol.* **2014,** *3*, 745–747; (b) Kim, E.; Moore, B. S.; Yoon, Y. J. *Nat. Chem. Biol.* **2015,** *11*, 649–659.

3. Hudlicky, T.; Reed, J. W. *The Way of Synthesis*; Wiley-VCH: Weinheim, Germany, **2007**; pp 1-40.

4. Keasling, J. D.; Mendoza, A.; Baran, P. S. *Nature* **2012,** *492*, 188–189.

5. Finefield, J. M.; Frisvad, J. C.; Sherman, D. H.; Williams, R. M. *J. Nat. Prod.* **2012,** *75*, 812–833.

6. (a) Birch, A. J.; Wright, J. J. *J. Chem. Soc., D: Chem. Commun.* **1969**, 644–645; (b) Williams, R. M.; Glinka, T.; Kwast, E.; Coffman, H.; Stille, J. K. *J. Am. Chem. Soc.* **1990,** *112*, 808–821.

7. Lin, Z.; Wen, J.; Zhu, T.; Fang, Y.; Gu, Q.; Zhu, W. *J. Antibiot. (Tokyo)* **2008,** *61*, 81–85.

8. Greshock, T. J.; Grubbs, A. W.; Jiao, P.; Wicklow, D. T.; Gloer, J. B.; Williams, R. M. *Angew. Chem. Int. Ed.* **2008,** *47*, 3573–3577.

9. Mercado-Marin, E. V.; Garcia-Reynaga, P.; Romminger, S.; Pimenta, E. F.; Romney, D. K.; Lodewyk, M. W.; Williams, D. E.; Andersen, R. J.; Miller, S. J.; Tantillo, D. J.; Berlinck, R. G. S.; Sarpong, R. *Nature* **2014,** *509*, 318–324.

10. (a) Cai, S.; Luan, Y.; Kong, X.; Zhu, T.; Gu, Q.; Li, D. *Org. Lett.* **2013,** *15*, 2168–2171; (b) Kato, H.; Nakahara, T.; Sugimoto, K.; Matsuo, K.; Kagiyama, I.; Frisvad, J. C.; Sherman, D. H.; Williams, R. M.; Tsukamoto, S.. *Org. Lett.* **2015**, *17*, 700–703.; (c) Kagiyama, I.; Kato, H.; Nehira, T.; Frisvad, J. C.; Sherman, D. H.; Williams, R. M.; Tsukamoto, S. *Angew. Chem. Int. Ed.* **2016**, *55*, 1128–1132.

11. Yamazaki, M.; Okuyama, E.; Kobayashi, M.; Inoue, H. *Tetrahedron Lett.* **1981,** *22*, 135–136.

12. Polonsky, J.; Merrien, M.-A.; Prange, T.; Pascard, C.; Moreau, S. *J. Chem. Soc., Chem. Commun.* **1980**, 601–602.

13. Qian-Cutrone, J.; Huang, S.; Shu, Y.-Z.; Vyas, D.; Fairchild, C.; Menendez, A.; Krampitz, K.; Dalterio, R.; Klohr, S. E.; Gao, Q. *J. Am. Chem. Soc.* **2002,** *124*, 14556–14557.

14. Yang, B.; Dong, J.; Lin, X.; Zhou, X.; Zhang, Y.; Liu, Y. *Tetrahedron* **2014,** *70*, 3859–3863.

15. Bond, R. F.; Boeyens, J. C. A.; Holzapfel, C. W.; Steyn, P. S. *J. Chem. Soc., Perkin Trans. 1,* **1979**, 1751.

16. Pimenta, E. F.; Vita-Marques, A. M.; Tinimis, A.; Seleghim, M. H. R.; Sette, L. D.; Veloso, K.; Ferreira, A. G.; Williams, D. E.; Patrick, B. O.; Dalisay, D. S.; Andersen, R. J.; Berlinck, R. G. S.. *J. Nat. Prod.* **2010,** *73*, 1821–1832.

17. (a) Tsuda, M.; Kasai, Y.; Komatsu, K.; Sone, T.; Tanaka, M.; Mikami, Y.; Kobayashi, J. I. *Org. Lett.* **2004,** *6*, 3087–3089; (b) Mugishima, T.; Tsuda, M.; Kasai, Y.; Ishiyama, H.; Fukushi, E.; Kawabata, J.; Watanabe, M.; Akao, K.; Kobayashi, J. I. *J. Org. Chem.* **2005,** *70*, 9430–9435.

18. Kushida, N.; Watanabe, N.; Okuda, T.; Yokoyama, F.; Gyobu, Y.; Yaguchi, T. *J. Antibiot.* **2007,** *60*, 667–673.

19. (a) Blanchflower, S. E.; Banks, R. M.; Everett, J. R.; Manger, B. R.; Reading, C. *J. Antibiot. (Tokyo),* **1991,** *44*, 492–497; (b) Ondeyka, J. G.; Goegelman, R. T.; Schaeffer, J. M.; Kelemen, L.; Zitano, L. *J. Antibiot. (Tokyo),* **1990,** *43*, 1375–1379.

20. Zinser, E. W.; Wolf, M. L.; Alexander-Bowman, S. J.; Thomas, E. M.; Davis, J. P.; Groppi, V. E.; Lee, B. H.; Thompson, D. P.; Geary, T. G. *J. Vet. Pharmacol. Ther.* **2002,** *25*, 241–250.

21. (a) Shoop, W. L.; Egerton, J. R.; Eary, C. H.; Suhayda, D. *J. Parasitol.* **1990,** *76*, 349–351; (b) Shoop, W. L.; Haines, H. W.; Eary, C. H.; Michael, B. F. *Am. J. Vet. Res.* **1992,** *53*, 2032–2034.

22. (a) Kaminsky, R.; Bapst, B.; Stein, P.; Strehlau, G.; Allan, B.; Hosking, B.; Rolfe, P.; Sager, H. *Parasitol. Res.* **2011,** *109*, 19–23; (b) Little, P. R.; Hodge, A.; Watson, T. G.; Seed, J. A.; Maeder, S. J. *New Zeal. Vet. J.* **2010,** *58*, 121–129; (c) Robertson, A. P.; Clark, C. L.; Burns, T. A.; Thompson, D. P.; Geary, T. G.; Trailovic, S. M.; Martin, R. J.. *J. Pharm. Exp. Ther.* **2002,** *302*, 853–860.

23. Miller, K. A.; Figueroa, M.; Valente, M. W.; Greshock, T. J.; Mata, R.; Williams, R. M. *Bioorg. Med. Chem. Lett.* **2008,** *18*, 6479–6481.

24. Sugie, Y.; Hirai, H.; Inagaki, T.; Ishiguro, M.; Kim, Y.-J.; Kojima, Y.; Sakakibara, T.; Sakemi, S.; Sugiura, A.; Suzuki, Y.; Brennan, L.; Duignan, J.; Huang, L. H.; Sutcliffe, J.; Kojima, N. *J. Antibiot.* **2001,** *54*, 911–916.

25. Mukherjee, H.; Chan, K.-P.; Andresen, V.; Hanley, M. L.; Gjertsen, B. T.; Myers, A. G. *ACS Chem. Bio.* **2015,** *10*, 855–863.

26. von Nussbaum, F. *Angew. Chem. Int. Ed.* **2003,** *42*, 3068–3071.

27. (a) Herzon, S. B.; Myers, A. G. *J. Am. Chem. Soc.* **2005,** *127*, 5342–5344; (b) Baran, P. S.; Guerrero, C. A.; Hafensteiner, B. D.; Ambhaikar, N. B. *Angew. Chem. Int. Ed.* **2005,** *44*, 3892–3895.

28. Myers, A. G.; Herzon, S. B. *J. Am. Chem. Soc.* **2003,** *125*, 12080–12081.

29. Wulff, J. E.; Siegrist, R.; Myers, A. G. *J. Am. Chem. Soc.* **2007,** *129*, 14444–14451.

30. Wulff, J. E.; Herzon, S. B.; Siegrist, R.; Myers, A. G. *J. Am. Chem. Soc.* **2007,** *129*, 4898–4899.

31. Williams, R. M.; Stocking, E. M.; Sanz-Cervera, J. F. *Top. Curr. Chem.* **2000,** *209*, 97–173.

32. Birch, A. J.; Wright, J. J. *Tetrahedron* **1970,** *26*, 2329–2344.

33. Stocking, E. M.; Sanz-Cervera, J. F.; Williams, R. M. *J. Am. Chem. Soc.* **1996,** *118*, 7008–7009.

34. Kuo, M. S.; Willey, V. H.; Cialdella, J. I.; Yurek, D. A.; Whaley, H. A.; Marshall, V. P. *J. Antibio.* **1996,** *49*, 1006–1013.

35. (a) Williams, R. M.; Cox, R. J. *Acc. Chem. Res.* **2003,** *36*, 127–139; (b) Williams, R. M. *Chem. Pharm. Bull.* **2002,** *50*, 711–740.

36. Sunderhaus, J. D.; Sherman, D. H.; Williams, R. M. *Isr. J. Chem.* **2011,** *51*, 442–452.

37. Ding, Y.; Wet, J. R. d.; Cavalcoli, J.; Li, S.; Greshock, T. J.; Miller, K. A.; Finefield, J. M.; Sunderhaus, J. D.; McAfoos, T. J.; Tsukamoto, S.; Williams, R. M.; Sherman, D. H. *J. Am. Chem. Soc.* **2010,** *132*, 12733–12740.

38. Sunderhaus, J. D.; McAfoos, T. J.; Finefield, J. M.; Kato, H.; Li, S.; Tsukamoto, S.; Sherman, D. H.; Williams, R. M. *Org. Lett.* **2013,** *15*, 22–25.

39. Finefield, J. M.; Kato, H.; Greshock, T. J.; Sherman, D. H.; Tsukamoto, S.; Williams, R. M. *Org. Lett.* **2011,** *13*, 3802–3805.

40. Artman III, G. D.; Grubbs, A. W.; Williams, R. M. *J. Am. Chem. Soc.* **2007,** *129*, 6336–6342.

41. Greshock, T. J.; Williams, R. M. *Org. Lett.* **2007,** *9*, 4255–4258.

42. Steyn, P. S.; Vleggaar, R.; Rabie, C. J. *Phytochemistry* **1981,** *20*, 538–539.

43. (a) Miller, K. A.; Williams, R. M. *Chem. Soc. Rev.* **2009,** *38*, 3160–3174; (b) Escolano, C. *Angew. Chem. Int. Ed.* **2005,** *44*, 7670–7673.

44. Cushing, T. D.; Sanz-Cervera, J. F.; Williams, R. M. *J. Am. Chem. Soc.* **1993,** *115*, 9323–9324.

45. Williams, R. M.; Sanz-Cervera, J. F.; Sancenón, F.; Marco, J. A.; Halligan, K. *J. Am. Chem. Soc.* **1998,** *120*, 1090–1091.

46. Greshock, T. J.; Grubbs, A. W.; Tsukamoto, S.; Williams, R. M. *Angew. Chem. Int. Ed.* **2007,** *46*, 2262–2265.

47. Stocking, E. M.; Sanz-Cervera, J. F.; Williams, R. M. *J. Am. Chem. Soc.* **2000,** *122*, 1675–1683.

48. Greshock, T. J.; Grubbs, A. W.; Williams, R. M. *Tetrahedron* **2007,** *63*, 6124–6130.

49. Miller, K. A.; Welch, T. R.; Greshock, T. J.; Ding, Y.; Sherman, D. H.; Williams, R. M. *J. Org. Chem.* **2008,** *73*, 3116–3119.

50. Miller, K. A.; Tsukamoto, S.; Williams, R. M. *Nat. Chem.* **2009,** *1*, 63–68.

51. Sprague, D. J.; Nugent, B. M.; Yoder, R. A.; Vara, B. A.; Johnston, J. N. *Org. Lett.* **2015**, *17*, 880–883.

52. Laws, S. W.; Scheerer, J. R. *J. Org. Chem.* **2013,** *78*, 2422–2429.

53. Corey, E. J.; Bakshi, R. K.; Shibata, S. *J. Am. Chem. Soc.* **1987,** *109*, 5551–5553.

54. (a) Baran, P. S.; Hafensteiner, B. D.; Ambhaikar, N. B.; Guerrero, C. A.; Gallagher, J. D. *J. Am. Chem. Soc.* **2006,** *128*, 8678–8693; (b) Baran, P. S.; Guerrero, C. A.; Ambhaikar, N. B.; Hafensteiner, B. D. *Angew. Chem. Int. Ed.* **2005,** *44*, 606–609.

55. Trost, B. M.; Cramer, N.; Bernsmann, H. *J. Am. Chem. Soc.* **2007,** *129*, 3086–3087.

56. Frebault, F.; Simpkins, N. S.; Fenwick, A. *J. Am. Chem. Soc.* **2009,** *131*, 4214–4215.

57. Simpkins, N. S.; Pavlakos, I.; Weller, M. D.; Male, L. *Org. Biomol. Chem.* **2013,** *11*, 4957–4970.

58. (a) Bian, Z.; Marvin, C. C.; Martin, S. F. *J. Am. Chem. Soc.* **2013,** *135*, 10886–10889; (b) Bian, Z.; Marvin, C. C.; Pettersson, M.; Martin, S. F. *J. Am. Chem. Soc.* **2014,** *136*, 14184–14192.

59. Kong, K.; Enquist, J. A., Jr.; McCallum, M. E.; Smith, G. M.; Matsumaru, T.; Menhaji-Klotz, E.; Wood, J. L. *J. Am. Chem. Soc.* **2013,** *135*, 10890–10893.

60. Guerrero, C. A.; Sorensen, E. J. *Org. Lett.* **2011,** *13*, 5164–5167.

61. Mundal, D. A.; Sarpong, R. *Org. Lett.* **2013,** *15*, 4952–4955.

CHAPTER 2:

TOTAL SYNTHESES OF CITRINALIN-B AND CYCLOPIAMINE-B AND BIOSYNTHETIC CONSIDERATIONS*

Presented herein are the first chemical syntheses of the prenylated indole alkaloids citrinalin B and cyclopiamine B. Key to the success of this approach was a remarkably diastereoselective spirooxindole formation attended by a chemoselective oxidation of an amino group to a nitro group, and a highly chemoselective reduction of a tertiary amide group to the corresponding amine group resident in these secondary metabolites. The chemical connections that have been realized as a result of these syntheses, in addition to the isolation of both 17-hydroxycitrinalin B and citrinalin C through ^{13}C feeding studies, supports the existence of a common bicyclo[2.2.2]diazaoctane containing biogenetic precursor to these compounds as has been proposed previously.

2.1 – Overview and Retrosynthetic Design

2.1.1: Introduction and Background.

The prenylated indole alkaloids are an emerging class of natural products characterized by the presence of an indole ring, or derivatives thereof (e.g., spirooxindole or pseudoindoxyl), decorated by one or more prenyl groups or the vestige of a prenyl group. Isolates from this family of natural products include citrinalins A and B (**2.1** and **2.2**, see Figure 2.1) and cyclopiamines A and B (**2.4** and **2.6**), which are the focus of this Chapter. The prenylation of the indole core in the prenylated indole alkaloid family, which can occur by a reaction with dimethylallyl pyrophosphate (DMAPP),[1] results in the introduction of a chromene unit as is found in (+) stephacidin A (**2.12**; see blue highlighted portion) or a bicyclo[2.2.2]diazaoctane core that is typical of many congeners including **2.12**–**2.14** (see red highlighted portion).[2]

Although structurally related, the prenylated indole alkaloids display a diverse range of bioactivities including antitumor, insecticidal, anthelmintic, calmodulin-inhibition, and antibacterial properties.[3] The recent discovery of citrinadins A[4] and B[5] (**2.7** and **2.8**) and PF1270A–C[6] (**2.9–2.11**) has added an unprecedented dimension to the structural motifs afforded by the *Penicillium* strains as well as raised several questions as to the biogenesis of these structurally related alkaloids (discussed further in section 2.5). Recently, elegant syntheses of citrinadins A and B have been achieved by the groups of Martin[7] and Wood,[8] see Chapter 1.4.2. Particularly intriguing to us is an emerging subset including citrinalins A and B (**2.1** and **2.2**) and

---

* Portions of this Chapter was taken from our work published in: Eduardo V. Mercado-Marin, Pablo Garcia-Reynaga, Stelamar Romminger, Eli F. Pimenta, David K. Romney, Michael W. Lodewyk, David E. Williams, Raymond J. Andersen, Scott J. Miller, Dean J. Tantillo, Roberto G. S. Berlinck, and Richmond Sarpong, *Nature,* **2014**, *509*, 318–324.

cyclopiamines A and B (**2.4** and **2.6**), which like the citrinadins (**2.7–2.8**), lack the bicyclo[2.2.2]diazaoctane framework and, remarkably, possess an alkyl nitro group. Cyclopiamines A and B (**2.4** and **2.6**) were discovered first (in 1979) by Steyn and coworkers[9] from a toxinogenic strain of *P. cyclopium*, whereas citrinalins A and B (**2.1** and **2.2**), were discovered by Berlinck and coworkers in 2010 from a strain of *P. citrinum*.[10] While natural products that possess aryl nitro groups are known, those that contain aliphatic nitro groups are extremely rare.[11] As such, the citrinalins and cyclopiamines are rather unusual and attractive targets for synthesis as they possess three nitrogen atoms in chemically distinct environments. The synthetic studies described herein have culminated in the total syntheses of *ent*-citrinalin B (*ent*-**2.2**; *ent* = enantiomer) and cyclopiamine B (**2.6**) and, along with the isolation of two new citrinalins, provide support for a proposed biogenesis of the subset of prenylated indole alkaloids that lack the bicyclo[2.2.2]diazaoctane core.

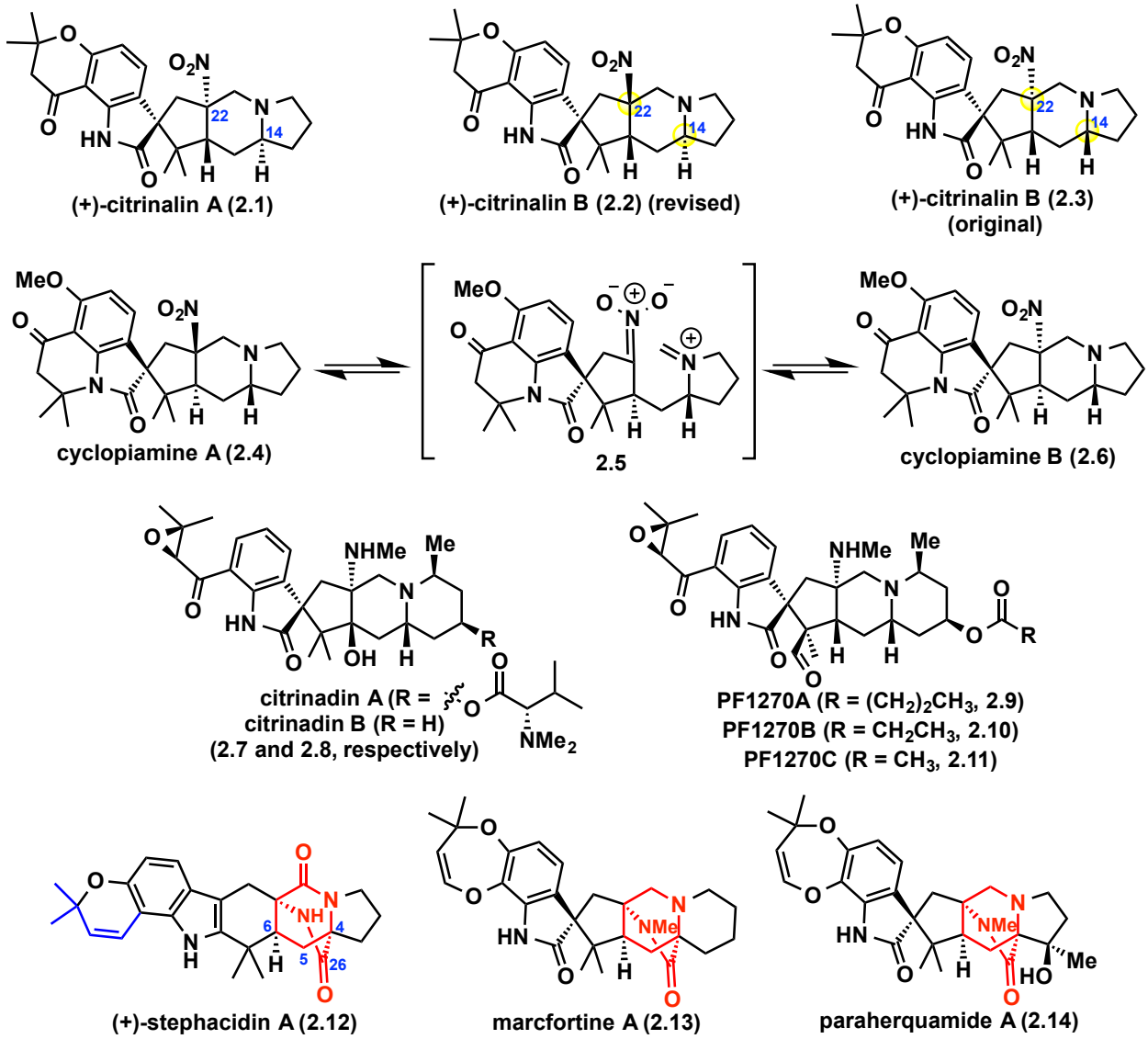

Figure 2.1: Selected prenylated indole alkaloids.

2.1.2: Biosynthetic Connections.

As was proposed by Steyn and coworkers,[9] a stimulating connection may be drawn between cyclopiamine A and B via the intermediacy of zwiterion **2.5** (see Figure 2.1). Steyn and co-workers in fact demonstrated the interconversion of **2.4** and **2.6** by heating either compound in dioxane/water or dimethylformamide (DMF).[9] This led to a proposal that **2.6**, which is the most stable of the two isomers (we have computed **2.6** to be 9.6 kcal/mol lower in energy than **2.4** in a DMF solvent model),[12] may in fact be an isolation artifact. Given the likelihood that the citrinadins, citrinalins and cyclopiamines are all degradation products of a precursor containing a bicyclo[2.2.2]diazaoctane ring, such as marcfortine A (**2.13**; in the case of the citrinadins) or stephacidin A (**2.12**; in the case of the citrinalins and cyclopiamines), we wondered whether the citrinalins could be transformed to the cyclopiamines. As outlined in Scheme 2.1, an amide hydrolysis of the bicyclo[2.2.2]diazaoctane in **2.15**, for example, would produce **2.16**. After which a decarboxylation (cleavage of C4–C26, stephacidin A numbering), and a *diastereoselective* protonation at the ring junction (C4–which may be controlled by an enzyme) would give rise to the sub-family that lacks the diazaoctane structural motif, **2.17**.

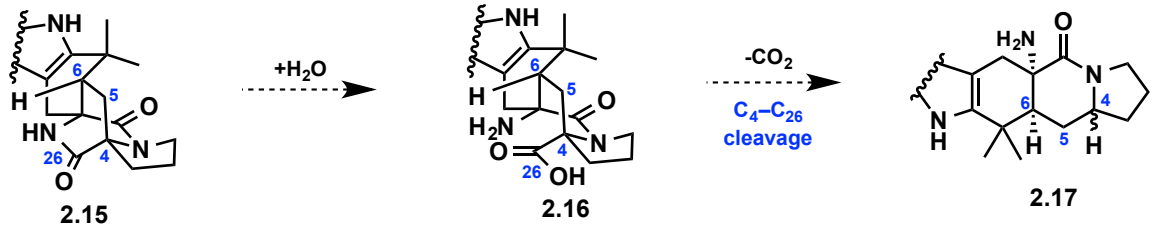

Scheme 2.1: Proposed biomimetic degradation of the bicyclo[2.2.2]diazaoctane ring.

On the basis of this assumption, it is particularly baffling that unlike cyclopiamines A and B, which are related by an aza-Henry (or nitro-Mannich) reaction as shown in Figure 2.1 (**2.4**⇔**2.6**, via **2.5**), citrinalin A (**2.1**) and the originally proposed structure of citrinalin B (**2.3**) would be related not by the formal epimerization of the C22 stereocenter but rather by the nature of the relative configuration of the C14 carbon (highlighted in yellow in **2.2** and **2.3**). Cognizant of the connection between cyclopiamine A (**2.4**) and B (**2.6**) as demonstrated by Steyn, we intuited that the structure of citrinalin B may be better represented by **2.2**, implying their interconversion via a reversible aza-Henry reaction (**2.1**⇔**2.2**).

To support this proposal, we undertook a computational simulation of the ^{1}H and ^{13}C NMR spectra that would be expected for the neutral and salt forms of citrinalins A and B. As has been convincingly demonstrated by Tantillo and coworkers in numerous cases, this method provides an accurate prediction of the structures of complex natural products.[13] During this collaboration,[12] we found that the computed and empirical data for the trifluoroacetic acid (TFA) salt form of citrinalin A is in good agreement with those reported by Berlinck and workers, who isolated these compounds. The corrected mean absolute deviation (CMAD) in the ^{1}H and ^{13}C NMR resonances is 0.21 and 2.0 ppm, respectively (largest outliers are 1.0 and 5.2 ppm, respectively). On the other hand, the computed data for the TFA salt form of **2.3** (the originally proposed structure of citrinalin B) differs significantly from that recorded using the naturally occurring material (CMAD = 0.45 and 2.0 ppm; largest outliers = 2.3 and 9.6 ppm for ^{1}H and ^{13}C, respectively). The best match to the reported spectral data was found to correspond to **2.2** in

its neutral form (CMAD = 0.12 and 1.6 ppm; largest outliers = 0.38 and 4.4 ppm for ^{1}H and ^{13}C, respectively), which corroborates a potentially similar biosynthetic connection as has been established for the cyclopiamines (outlined in Figure 2.1). Moreover, in culture growth experiments reported by Berlinck and co-workers, citrinalin A (**2.1**) production by the fungus begins at day 5, with a maximum concentration at day 13, while citrinalin B production only begins at day 10, with a maximum at day 34.[10] This observation may suggest the conversion of citrinalin A to citrinalin B, via a zwitterionic intermediate similar to **2.5**, in the biological setting. As a result, we chose to proceed with the hypothesis that **2.2** most likely represents the correct structure of citrinalin B. Ultimately, a more thorough analysis of the NMR data of natural citrinalin B, collected in MeOH-d_4, by Berlinck and co-workers with whom we established a collaboration, corroborate the assignment of **2.2** as the true structure of citrinalin B.

2.1.3: Retrosynthetic Design.

As outlined in Scheme 2.2, cyclopiamine B (**2.6**) can be obtained from the enantiomer of citrinalin B (*ent*-**2.2**) by employing a chromanone rearrangement to forge the tetrahydroquinolone structural moiety found in the cyclopiamines. In turn, *ent*-**2.2** could be formed by an 'indole to spirooxindole' conversion on fused hexacycle **2.18**. Introduction of the tertiary amine would take place via a chemoselective reduction of the tertiary amide carbonyl group, which would serve as a nitrogen-protecting group along the synthetic route. Fused indole **2.18** would arise from tricycle **2.19**, via an indolization sequence. A Curtius or Hofmann rearrangement would introduce the primary amine group from the ester group in **2.19**. Tricycle **2.19** would be prepared by a Diels–Alder reaction from diene **2.20**, the *tert*-butyldimethylsilyl (TBS) variant of which was first prepared by Rawal and Jewett,[14] and tetrahydroindolizinone **2.21** (unprecedented prior to this report) that would ultimately arise from D-proline (**2.22**).

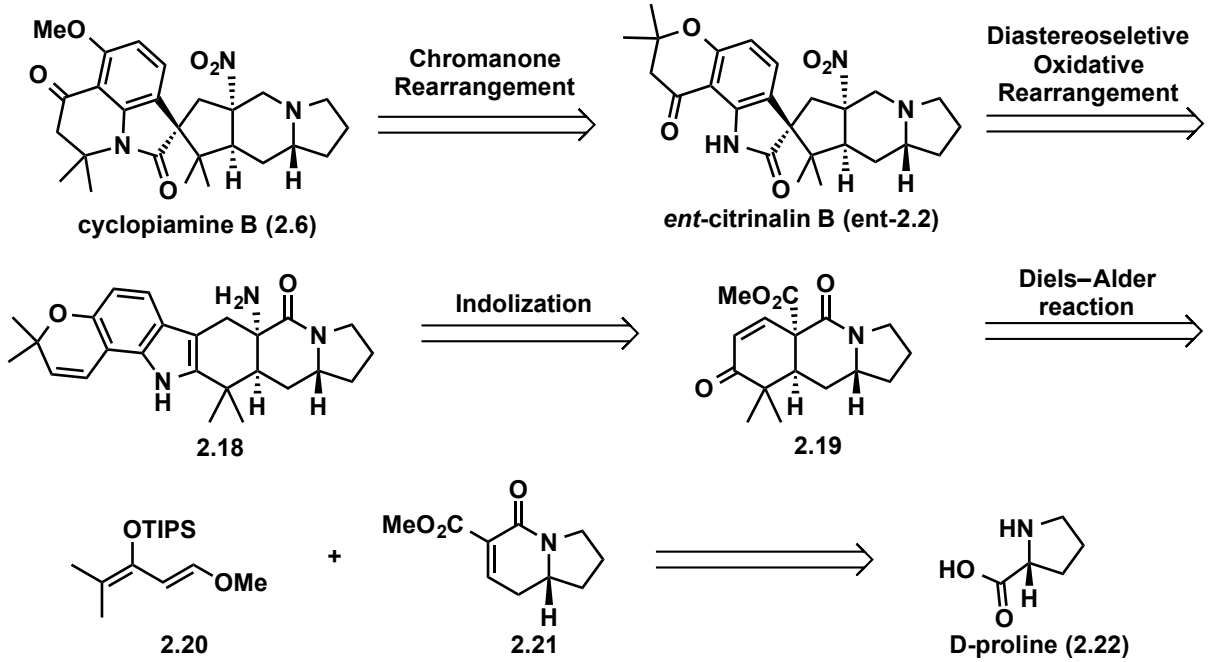

Scheme 2.2: 1st generation retrosynthetic plan for cyclopiamine B and citrinalin B.

2.2 – Initial Synthetic Studies on the Prenylated Indole Alkaloids.

2.2.1: Synthesis of Methyl Ester 6-6-5 Tricycle 2.19.

We initiated our synthetic studies by targeting tricycle **2.19**, which could serve as a divergent intermediate to test different methodologies for the installation of the indole moiety present in the family of prenylated indole alkaloids. We envisioned tricycle **2.19** arising from dienophile **2.21** by a Diels–Alder reaction with an appropriately substituted diene.

In the forward direction, synthesis of the desired chiral, enantiospecific, dienophile **2.21** (Scheme 2.3) commenced with D-proline (**2.22**). First, *tert*-butoxylcarbonyl (Boc) protection of D-proline (**2.22**) was followed by reduction of the carboxylic acid group and a Swern oxidation of the resulting hydroxyl to afford aldehyde **2.23**. One-carbon homologation of the aldehyde group of **2.23** using the Ohira-Bestmann method[15] affords known alkyne **2.24** with no loss of enantiopurity.[16] Removal of the Boc group under acidic (HCl) conditions, followed by acylation with methylmalonyl chloride gave the corresponding acylated pyrrolidine **2.25**. Treating **2.25** with Grotjahn's catalyst (**2.26**) furnished aldehyde **2.27** via an anti-Markovnikov hydration of the alkyne group.[17] On small scales, **2.27** underwent smooth Knoevenagel condensation to the requisite dienophile **2.21** under the Grotjahn conditions. However, intact aldehyde **2.27** was recovered on larger scales, which necessitated an investigation of conditions for the condensation step. It was determined that the product (**2.21**) was sensitive to both the acidic (HCl, $MgBr_2$, $TiCl_4$•Et_3N, $Sc(OTf)_3$) and basic (Et_3N, pyrrolidine) conditions explored. This challenge was ultimately overcome by allowing aldehyde **2.27** to stand in dilute anhydrous HCl which afforded the desired dienophile (**2.21**).

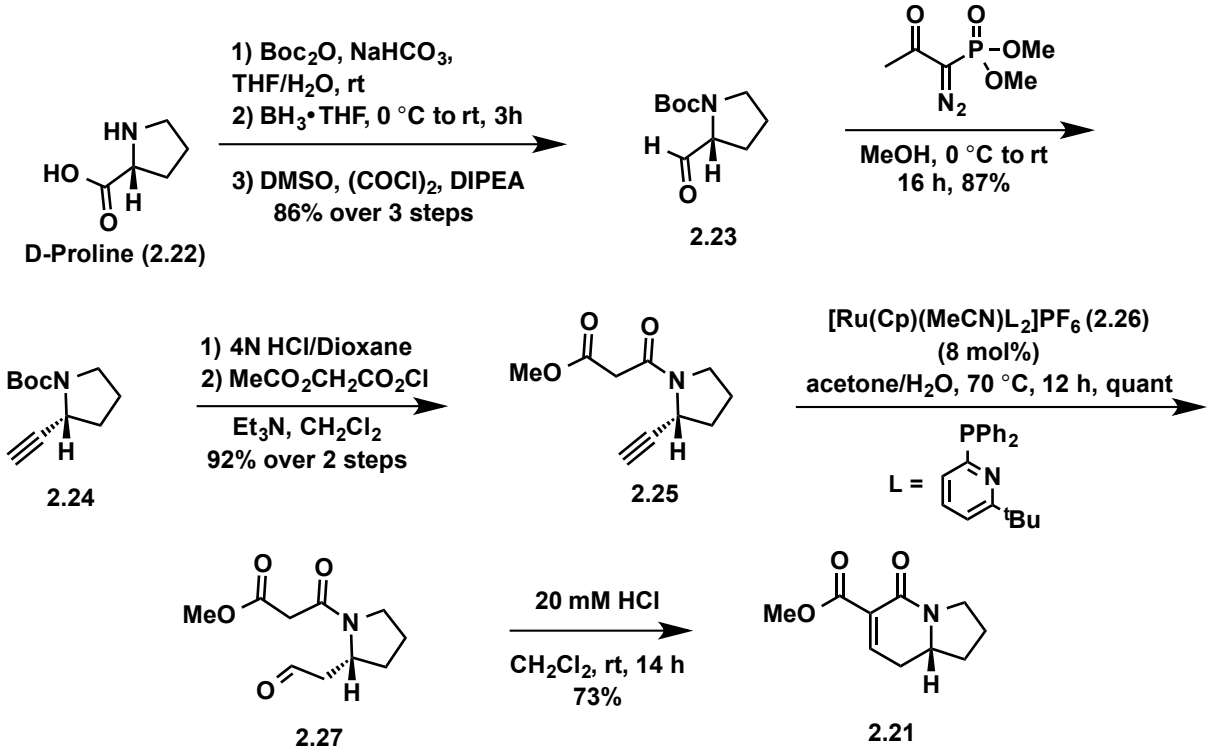

Scheme 2.3: Synthesis of chiral dienophile **2.21**.

With chiral dienophile **2.21** in hand, we proceeded to investigate its reactivity in the Diels–Alder reaction under Lewis acidic conditions, as geminally-substituted dienes such as **2.28** (Table 2.1) are prone to 1,5-hydride shifts under thermal conditions.[18] The use of a mild Lewis acid ($ZnBr_2$) only provided trace amounts of the Diels–Alder adduct as a single diastereomer (Entry 1, Table 2.1). Although, stronger Lewis acids (BF_3•OEt_2, $EtAlCl_2$) provided **2.19** in higher yields, it was accompanied by significant decomposition of both diene **2.28** and dienophile **2.21**, even at low temperatures (Entries 2-3, Table 2.1). Using $EtAlCl_2$ also required a second step to hydrolyze the initially formed silyl-enol ether to the enone with TBAF/THF at room temperature. Ultimately, $SnCl_4$ in combination with the TIPS-protected siloxydiene was required to obtain consistent yields due to the instability of the TBS-diene under the reaction conditions.

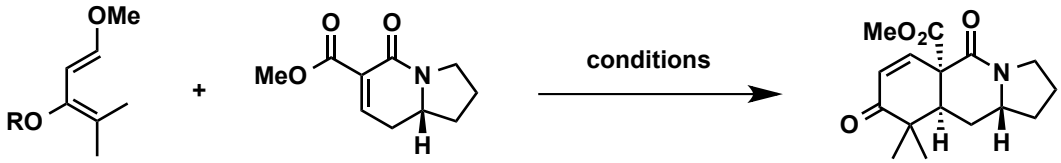

2.28 **2.21** **2.19**

Entry	R	Lewis Acid	Solvent	Temperature (°C)	Time	Yield %
1	TBS	$ZnBr_2$	CH_2Cl_2	–18 to rt	1 h	trace
2	TBS	BF_3•OEt_2	CH_2Cl_2	–78	15 min	50
3	TBS	$EtAlCl_2$	CH_2Cl_2	–78 to rt	30 min	55 (2 steps)
4	TBS	$SnCl_4$	CH_2Cl_2	–42 to rt	30 min	37
5	TIPS	$SnCl_4$	CH_2Cl_2	–78 to –42	1 h	63

Table 2.1: Optimization of the Diels–Alder reaction.

2.2.2: Synthesis of Fused Indoles by Fischer Indole Synthesis.

With access to the Diels–Alder adduct (**2.19**), the installation of the indole moiety was investigated using a Fischer indole synthesis (Scheme 2.4). Initially we found that the reduction of enone **2.19** was effected under standard hydrogenation conditions (Pd/C, H_2) to provide the ketone product (not shown). Treating the hydrogenated product with phenylhydrazine in a mixture of trifluoroacetic acid (TFA) in 1,2-dichloroethane (DCE) at 100 °C provided the desired model compound (indole **2.29**) via a one-pot hydrazone formation-Fischer indolization sequence. The structure of **2.29** is unambiguously supported by single X-ray crystallographic analysis (see CYLview in Scheme 2.4). Unfortunately, 3-methoxyphenylhydrazine, which is more representative of the desired substitution gave an inseparable mixture of C4- and C6-methoxy regioisomers in a 1 : 5 ratio (**2.30** and **2.31**, respectively). In order to circumvent both the regioselectivity and purification issues, we decided to pursue a cross-coupling/condensation approach to forge the indole moiety. This strategy was deemed advantageous as it would allow

the direct installation of the fully functionalized indole, such as the chromanone on the C-6 and C-7 positions, present in the citrinalins and cyclopiamines.

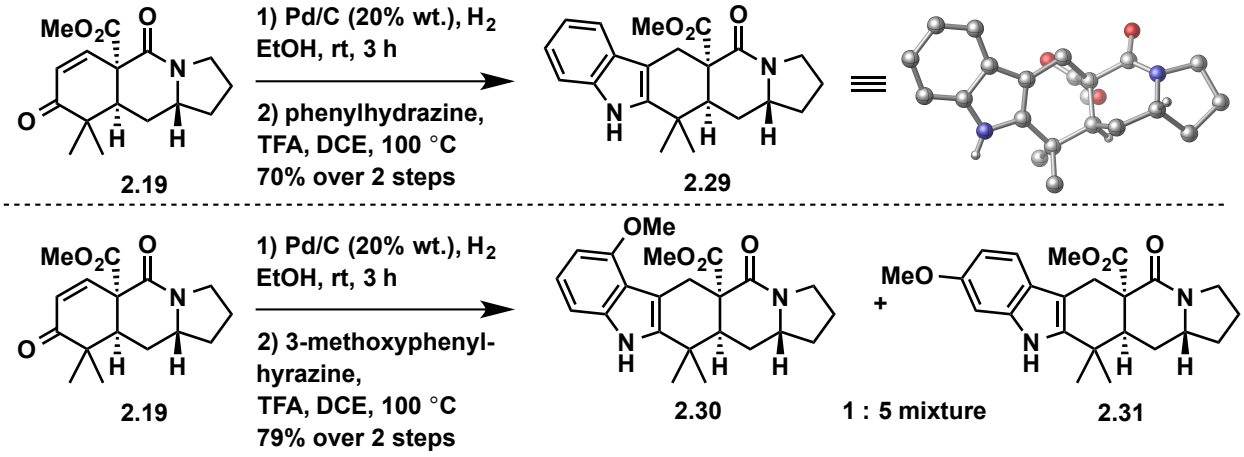

Scheme 2.4: Fischer indolization of tricycle **2.19**.

2.2.3: Synthesis of Hexacyclic Indole 2.35 En Route to Citrinalin B (2.2).

Inspired by the work of Banwell[19] and Myers,[20] we chose to convert tricycle **2.19** to vinyl iodide **2.32** which would serve as a functional handle for a subsequent cross-coupling reaction (Scheme 2.5). Thus, iodination of enone **2.19** utilizing the conditions reported by Johnson and co-workers[21] provided the α-iodoenone, which underwent an Ullmann-like coupling with known aryl iodide **2.33** to give the nitroaryl enone **2.34**.[20a] With access to **2.34**, we investigated conditions for a reductive cyclization to afford the desired indole product. Exploring standard hydrogenation conditions (Pd/C, H_2 or Pt/C, H_2), as demonstrated by Banwell[19] for these reductive cyclization sequences, resulted in competitive reduction of the chromene unit as well. Other reducing agents such as $NiCl_2/NaBH_4$ also gave a complex mixture with competitive reduction of the chromene unit.[22] $SnCl_2$ in MeOH at elevated temperatures returned only the nitroso intermediate (not shown) with no formation of the desired indole product.[23] After much optimization following the conditions reported by Myers,[20a] it was determined that treating **2.34** with activated Zn dust/formic acid/1M HCl, followed by $NaCNBH_3$ reduction of the *in situ* generated indolenine (not shown) affords the desired indole product (**2.35**) in near quantitative yield.

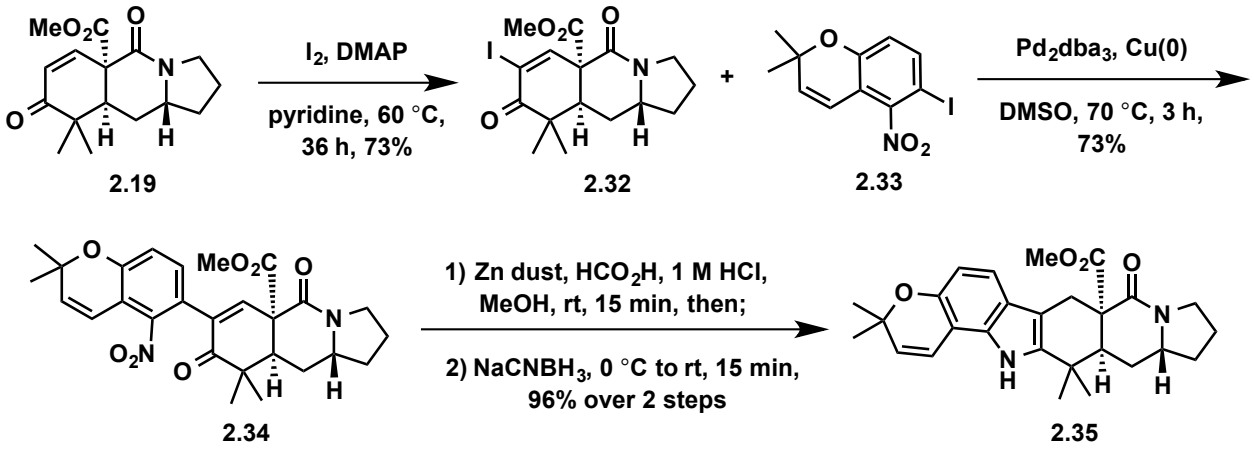

Scheme 2.5: Synthesis of hexacyclic indole **2.35**.

2.2.4: Synthesis of Undesired Spirooxindole 2.37.

Having access to indole **2.35**, we then investigated the substrate's inherent facial bias toward oxidation of the indole moiety *en route* to the desired spirooxindole framework (Scheme 2.6). Utilizing Davis' oxaziridine[24] (**2.36**, which has been shown to give our desired *α*-diastereoselectivity on stephacidin A[25]) on indole **2.35** resulted in undesired *β*-hydroxyl indolenine **2.38** as the major product. The structure of **2.38** is unambiguously supported by single X-ray crystallographic analysis (see CYLview in Scheme 2.6). Of note, **2.38** readily rearranges to the undesired spirooxindole (**2.37**) upon purification by silica gel column chromatography. These results suggest that either the bicyclo[2.2.2]diazaoctane ring system present in stephacidin A (**2.12**) (highlighted in red, Figure 2.1) or the secondary amide N-H of the bridging bicyclic system (possibly via hydrogen bonding) influences the diastereoselectivity for this transformation. Nevertheless, we decided to investigate the forward chemistry on undesired diastereomer **2.37**.

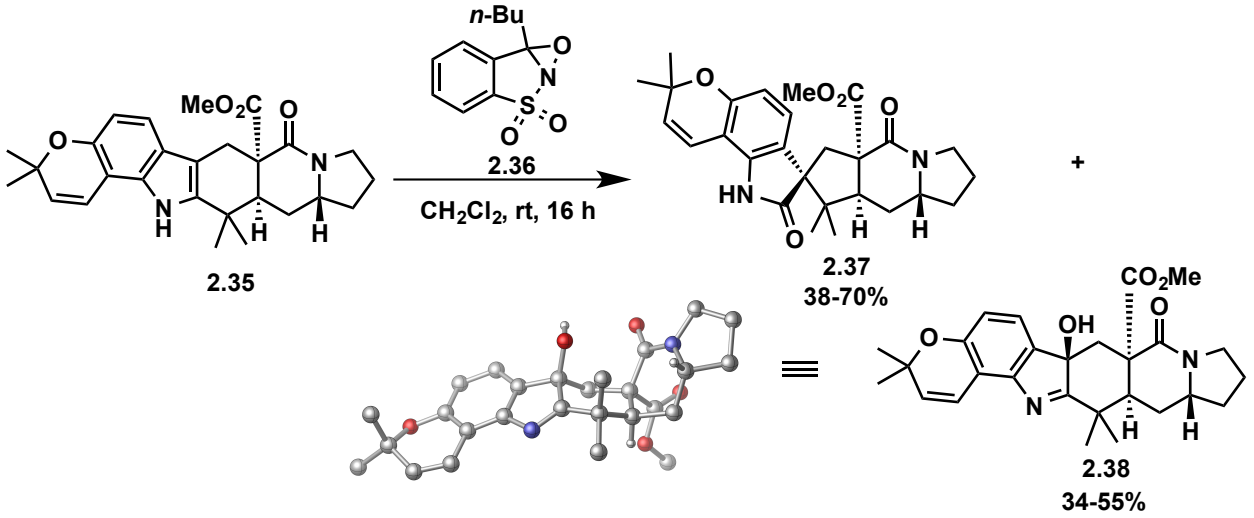

Scheme 2.6: Oxidation of indole **2.35**.

Attempts at converting the ester functionality in **2.37** (Scheme 2.7) to the requisite amino group in **2.40** via the intermediacy of a carboxamide were unsuccessful (not shown). Transformation of the ester group to either an acyl azide for a Curtius rearrangement or a carboxamide for a Hofmann rearrangement were met with difficulty as the carboxylic acid formed from hydrolysis of the methyl ester readily underwent decarboxylation at room temperature. Although we were able to access aldehyde **2.39** by a reduction/oxidation sequence of **2.37** (Scheme 2.7), all attempts to effect a Schmidt reaction or a Beckman rearrangement for the formation of amine **2.40** were met with decomposition of starting material. Consequently, we decided to pursue an alternative approach to install the amine functionality without using an ester as an amino surrogate.

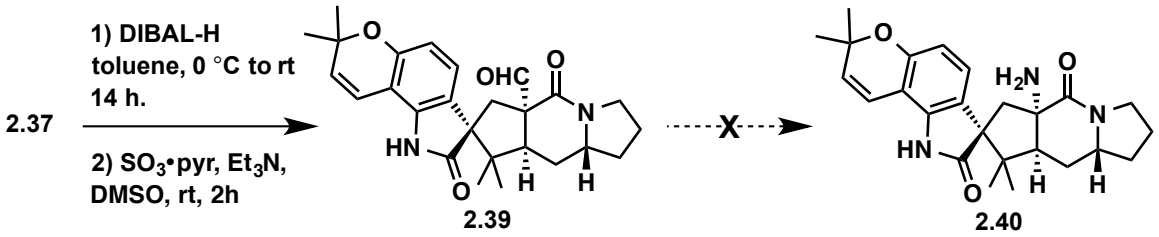

Scheme 2.7: Synthesis of aldehyde **2.39**.

2.2.5: Attempted Synthesis of Nitro-Substituted Dienophile 2.42.

Considering the difficulty in accessing the amino group (which would eventually become the nitro group found in the citrinalins and cyclopiamine) through the use of the methyl ester group in **2.37** (Scheme 2.7), we focused on the synthesis of the nitro-containing dienophile (**2.42**, Scheme 2.8) instead. As outlined in Scheme 2.8, we were unable to successfully access desired α-nitro amide **2.41**, which would have served as the precursor to **2.42** following a formal cycloisomerization with the Grotjahn catalyst (**2.26**).

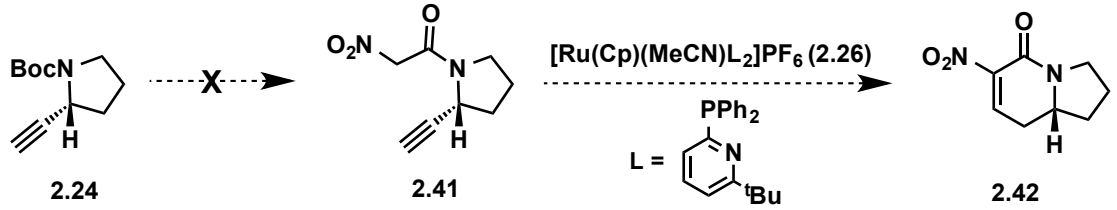

Scheme 2.8: Attempted synthesis of nitro-dienophile **2.42**.

2.3 – Synthesis of Nitrile-Containing 6-6-5 Tricycle and Elaboration to '*Seco*-Stephacidin A'.

2.3.1: Synthesis of Nitrile-Substituted Dienophile 2.45 and Diels–Alder Reaction.

In view of the difficulty of accessing the amino group through the use of the methyl ester group in **2.37** (Scheme 2.7) or accessing the nitro-containing dienophile **2.42** (Scheme 2.8), we chose to employ the nitrile equivalent as a masked carboxamide, which we hoped to transform to the desired amine functionality by a Hofmann rearrangement.

We initiated our synthetic studies (analogous to Scheme 2.3) with the *tert*-butoxycarbonyl (Boc)-protection of D-proline (**2.22**, Scheme 2.9), which was followed by the reduction of the carboxylic acid group and Swern oxidation of the resulting hydroxyl to afford aldehyde **2.23**.[26] Alkynylative homologation of the aldehyde group of **2.23** using the Ohira-Bestmann method[15] was followed by removal of the Boc group and acylation with 2-cyanoacetyl chloride to provide alkyne **2.43**. Applying the method of Grotjahn[17] on substrate **2.43** allows for a formal cycloisomerization, likely proceeding via a metal vinylidene intermediate (not shown), anti-Markovnikov hydration to the incipient aldehyde **2.44**, and Knoevenagel condensation to give tetrahydroindolizinone **2.45** in a single pot transformation.

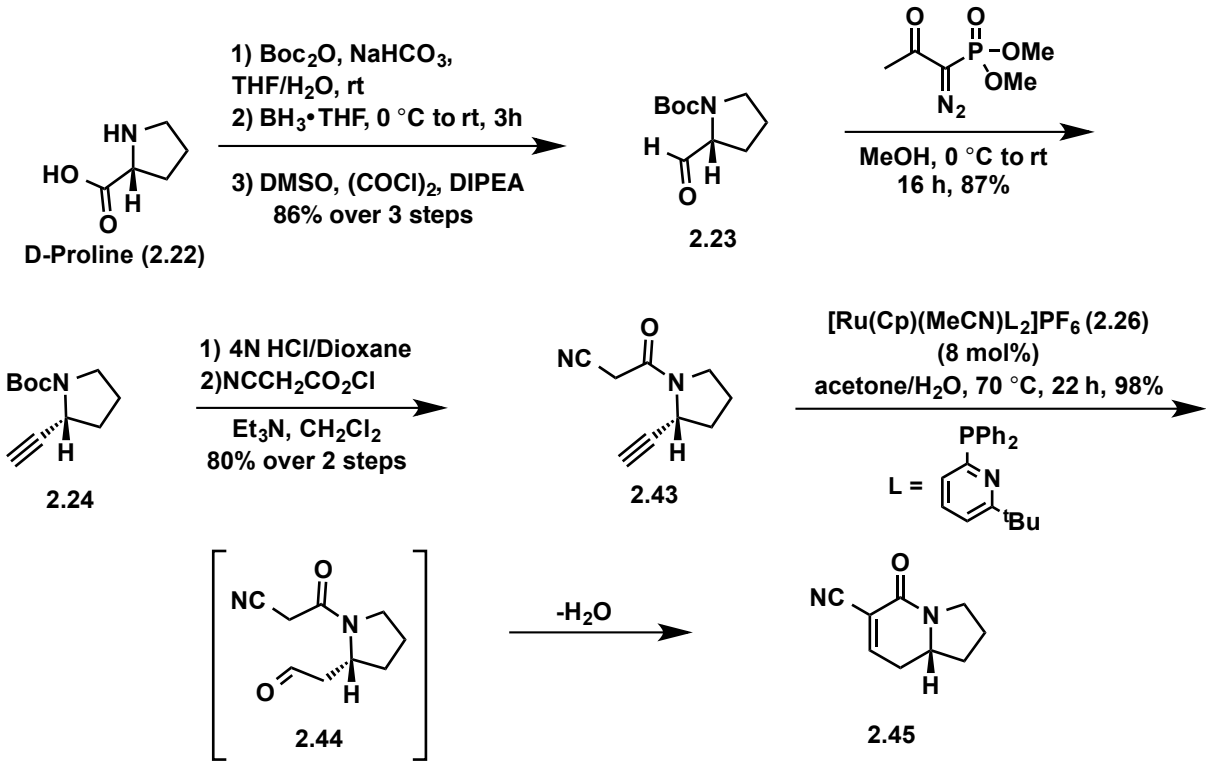

Scheme 2.9: Synthesis of cyano-substituted dienophile **2.45**.

At this stage, a $SnCl_4$-catalyzed Diels–Alder [4+2] reaction[27] between **2.45** and diene **2.20** and a subsequent basic workup affords enone **2.46** (Scheme 2.10) in higher yields than observed for methyl ester dienophile **2.21** (see Entry 5, Table 2.1), possibly due to the increased stability of the cyano-dienophile **2.45** under the reaction conditions. Next, tricycle **2.46** was iodinated using the Johnson protocol[21] to yield α-iodoenone **2.47**, again in higher yields than observed for the analogous ester substrate (**2.19**, Scheme 2.5).

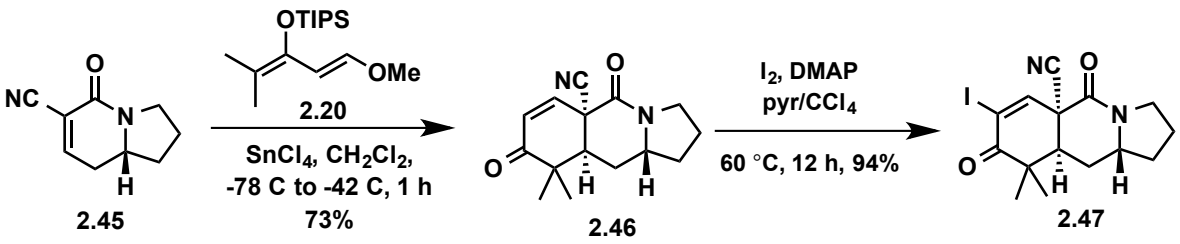

Scheme 2.10: Synthesis of vinyl iodide **2.47**.

2.3.2: Synthesis of 'seco-Stephacidin A' (2.58).

Hydrolysis of the nitrile group of **2.47** using Pt-complex **2.48**, under the conditions introduced by Ghaffar and Parkins (EtOH/H_2O, 70 °C),[28] led to decyanation products **2.49** instead of the corresponding carboxamide (Scheme 2.11). In light of the mechanism proposed by Ghaffar and Parkins, we reasoned that the electron withdrawing effects of both the enone and amide functional groups on the carbon bearing the nitrile group was leading to the decyanation products (**2.49**). As shown in structure **2.50**, collapse of the tetrahedral intermediate (**2.50**) at elevated temperatures results in expulsion of a resonance-stabilized nucleofuge (see red arrows in **2.50**), which is then either protonated under the reaction conditions or leads to various decomposition pathways.

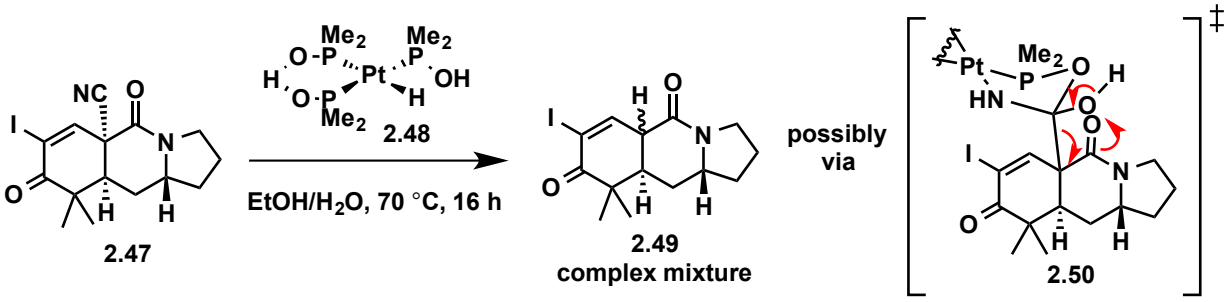

Scheme 2.11: Hydration of nitrile **2.47**.

In light of these observations, we decided to reduce the enone to the corresponding allylic alcohol (**2.51**) using Luche reduction conditions,[29] in hopes of avoiding decomposition. This reaction proceeded in quantitative yield (Scheme 2.12). At this point, subjecting **2.51** to the Ghaffar and Parkins conditions (EtOH/H_2O, 70 °C) resulted in the hydration of the nitrile group to the corresponding carboxamide **2.52** in near quantitative yield. A Hofmann rearrangement was then effected with $Pb(OAc)_4$[30] in the presence of methanol to yield methyl carbamate **2.53**, which was then oxidized to desired enone **2.54** with Dess-Martin periodinane (DMP).

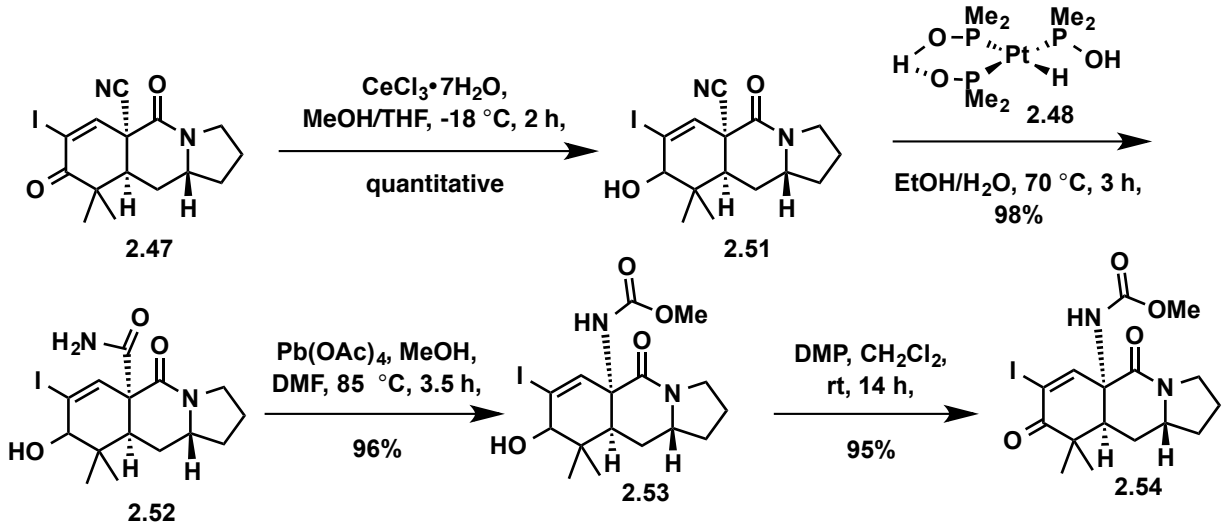

Scheme 2.12: Synthesis of methyl carbamate **2.54**.

Although this sequence of reduction/oxidation allowed access to the desired carbamate **2.54**, it suffered from an increase in step count as well as resources. After optimizing the original conditions reported by Ghaffar and Parkins, treating nitrile **2.47** with Pt-catalyst **2.48** at room temperature effectively accomplishes the desired hydration to carboxamide **2.55** albeit requiring longer reaction times (Scheme 2.13). This alternative hydration protocol was utilized in the forward synthesis. Carboxamide **2.55** serves as a substrate for a Hofmann rearrangement that is effected with phenyliodosylbistrifluoroacetate (PIFA) to yield carbamate **2.54**.[31] Suzuki cross-coupling of **2.54** with known boronic ester **2.56**[20a] gives nitro-aryl enone **2.57**.

Applying the two sequential reduction conditions, effective on the methyl ester analog (**2.34**, Scheme 2.5), resulted in low yields of the desired fused indole (**2.58**, Scheme 2.13) which occurred as a mixture of products, which were later identified by LCMS as the nitroso, the N-OH indole, and dimerization products (not shown). The reaction conditions were ultimately optimized by diluting the reaction mixture (to slow down the dimerization process) and by the addition of ammonium chloride, which proved necessary to ensure reproducibility. Furthermore, the substitution of 1 M HCl with *para*-toluenesulfonic acid (*p*-TsOH) was essential for minimizing the formation of the nitroso compound. Application of these optimized conditions effectively afforded fused-indole **2.58** in a reproducible 82% yield. We chose to label the indole product '*seco*-stephacidin A' given that it is one carbocyclization away from the parent natural product stephacidin A (**2.12**, Figure 2.1). The synthetic strategy outlined thus far would find further application to the synthesis of prenylated indole alkaloids containing the bicyclo[2.2.2]diazaoctane ring system (highlighted in red in **2.12** in Figure 2.1), if we can form a carbon-carbon bond between C4 and C26 (see **2.58**). Successful implementation of this concept will be the topic of Chapter 3.

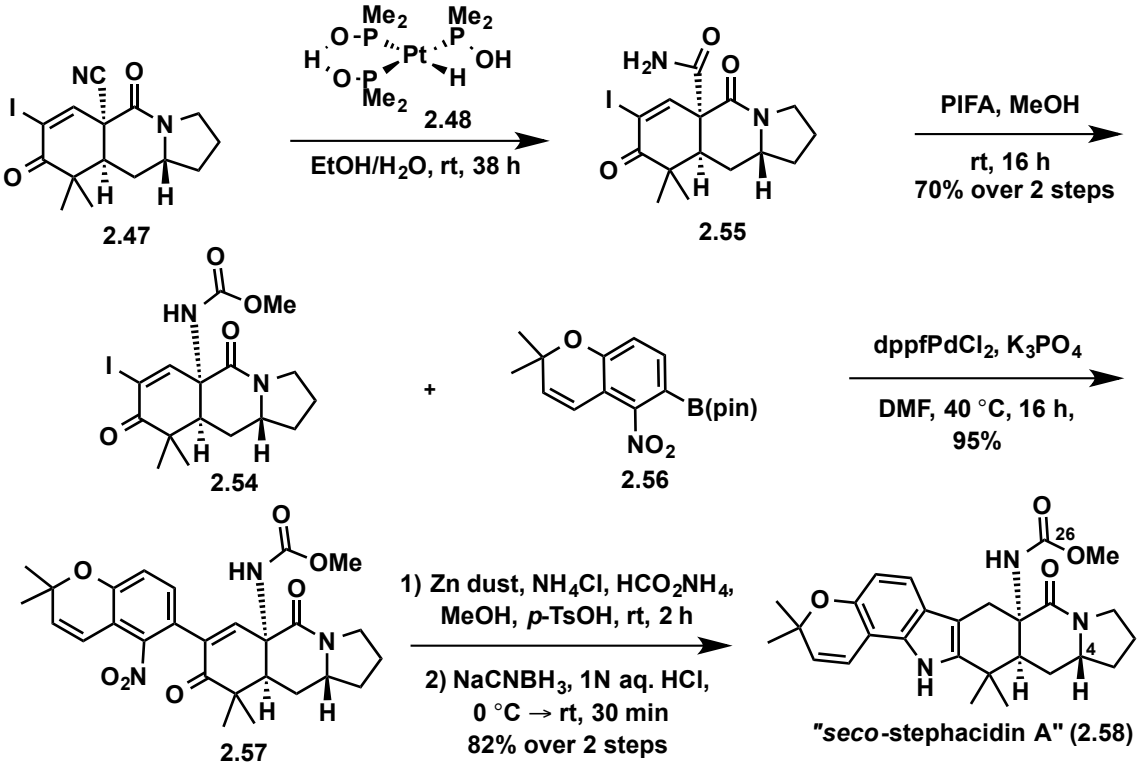

Scheme 2.13: Synthesis of 'seco-stephacidin A' (**2.58**).

2.3.3: Synthesis of 'seco-Stephacidin B' (2.60).

Interestingly, we have been able to show that nitro-aryl enone **2.57** can be converted to the corresponding nitrone **2.59** (Scheme 2.14) in accordance with the effective protocols established by Herzon and Myers.[20a] We have also been able to follow its dimerization to **2.60** by ^{1}H NMR and LCMS as well as after purification by silica gel chromatography.

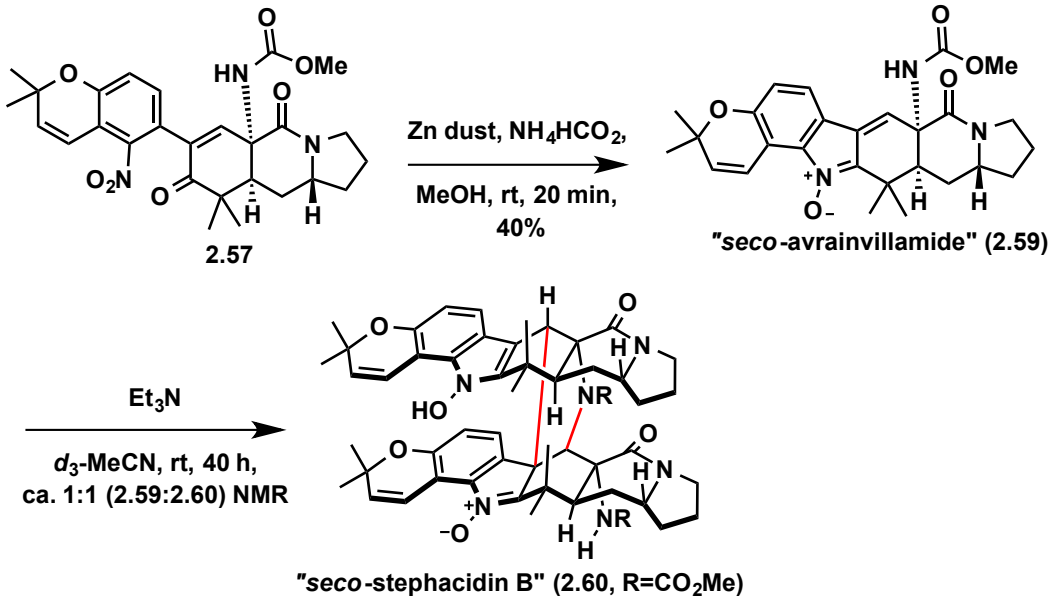

Scheme 2.14: Formation of '*seco*-stephacidin B' (**2.60**).

2.4 – Indole to Spirooxindole Oxidative Rearrangement and Syntheses of Citrinalin B and Cyclopiamine B

2.4.1: Background – Indole to Oxindole Oxidative Rearrangement.

The face-selective oxygenation of C2/C3-fused indoles is a well-established route to hydroxylindolenines, which serve as precursors to the corresponding spirooxindoles (Scheme 2.15).[32] As previously reported by Borschberg[33] and most recently by Movassaghi,[34] among others, initial oxygenation of C2/C3-fused indoles (**2.61**) results in epoxy-intermediate **2.62** (Scheme 2.15). This fleeting intermediate can result in either **2.63** or **2.64**. Intermediates **2.63** (occurring via C2 epoxide opening) and **2.64** (occurring via C3 epoxide opening) may convert in a *stereospecific* manner to either the pseudo-indoxyl (**2.65**) or the oxindole (**2.66**), respectively. In the case of indoles lacking substitution on the benzenoid ring, the oxindole (**2.66**) framework appears to be the thermodynamic product since the pseudoindoxyl converts to the oxindole, via the intermediacy of **2.62**, upon heating with a Lewis acid over time.[33]

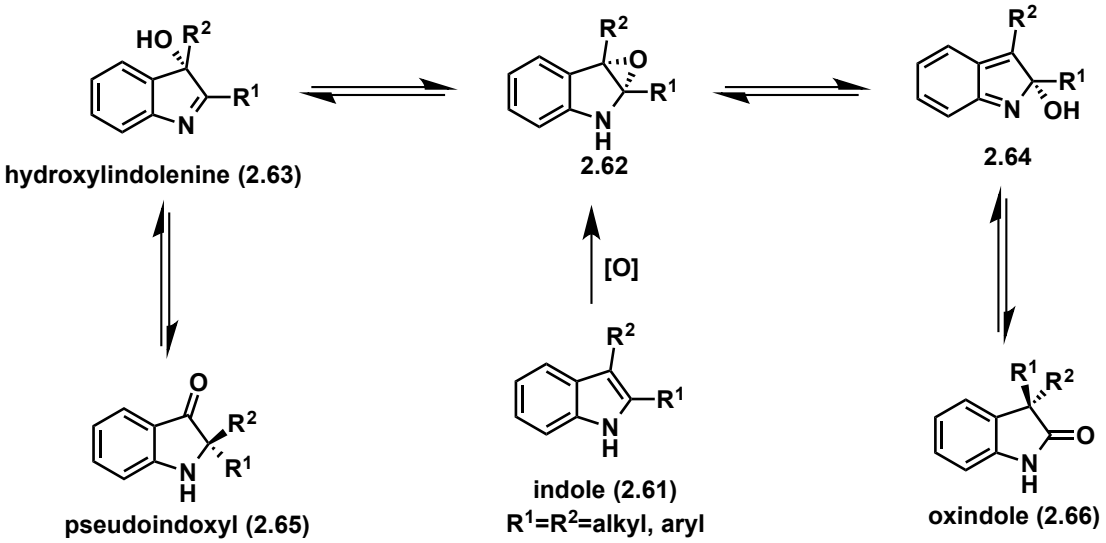

Scheme 2.15: Oxidative rearrangements of C2/C3 fused indoles.

2.4.2: Indole to Spirooxindole Transformation with Oxaziridines.

We envisioned the diastereoselective oxygenation of indole **2.58** (Scheme 2.16) as a path to the spiro-oxindole (i.e. **2.67**) structural moiety found in the citrinalins and cyclopiamines. On the basis of related precedent from Sorensen[35], Williams[36], and Martin[7a] for heteroatom-directed oxygenation, we expected the carbamate group of **2.58** to direct oxygenation to the alpha face and provide **2.67**. We envisioned this carbamate-directed approach would overcome the inherent beta face selectivity previously observed with the analogous methyl ester indole **2.35** (Scheme 2.6).

Scheme 2.16: Envisioned diastereoselective oxidative rearrangement to spiro-oxindole **2.67**.

Surprisingly, the use of the commonly employed Davis' oxaziridine[24] (**2.36**, 3.0 equiv) led to **2.69** and trace amounts of both hydroxyindolenine **2.68** and spirooxindole **2.70** (spirooxindole **2.70** arises via the intermediacy of hydroxylindolenine **2.69**) (Entry 1, Table 2.2). The structure of **2.70** is unambiguously supported by single X-ray crystallographic analysis (see CYLview in Table 2.2). This selectivity was attributed to the angular disposition of one of the methyl groups, adjacent to the C2 position of the indole, which was hindering the delivery of the oxidant to the desired alpha face of the indole. Interstingly, Martin and co-workers observed a similar result in their synthesis of citrinadins A[7a] (see Chapter 1.4.2). A survey of other more sterically demanding oxaziridines including **2.71** and **2.72** leads, at best (using **2.72**), to a 1:1 ratio of the desired hydroxyindolenine **2.68** and both hydroxyindolenine **2.69** and spirooxindole

2.70 (Entries 2 and 3, Table 2.2, respectively). Switching the oxidant to either *meta*-chloroperoxybenzoic acid (*m*CPBA) or dimethyldioxirane (DMDO) gave a complex mixture of products (Entries 4 and 5, Table 2.2, respectively), presumably due to the oxidation of the chromene unit. In light of these results, we suspect the conformation imparted by the bicyclo[2.2.2]diazaoctane ring system in stephacidin A controls the facial selectivity in its oxidation to notoamide B reported as by Williams and co-workers.[37] Thus, the approach of the oxidant is not directed by hydrogen bonding with the secondary amide as we previously proposed (section 2.2.4). Nonetheless, with access to the undersired diastereomer of hydroxylindolenine **2.69** (by oxidation with Davis' oxaziradine **2.36**, Entry 1, Table 2.2) we decided to study the forward chemistry using this material.

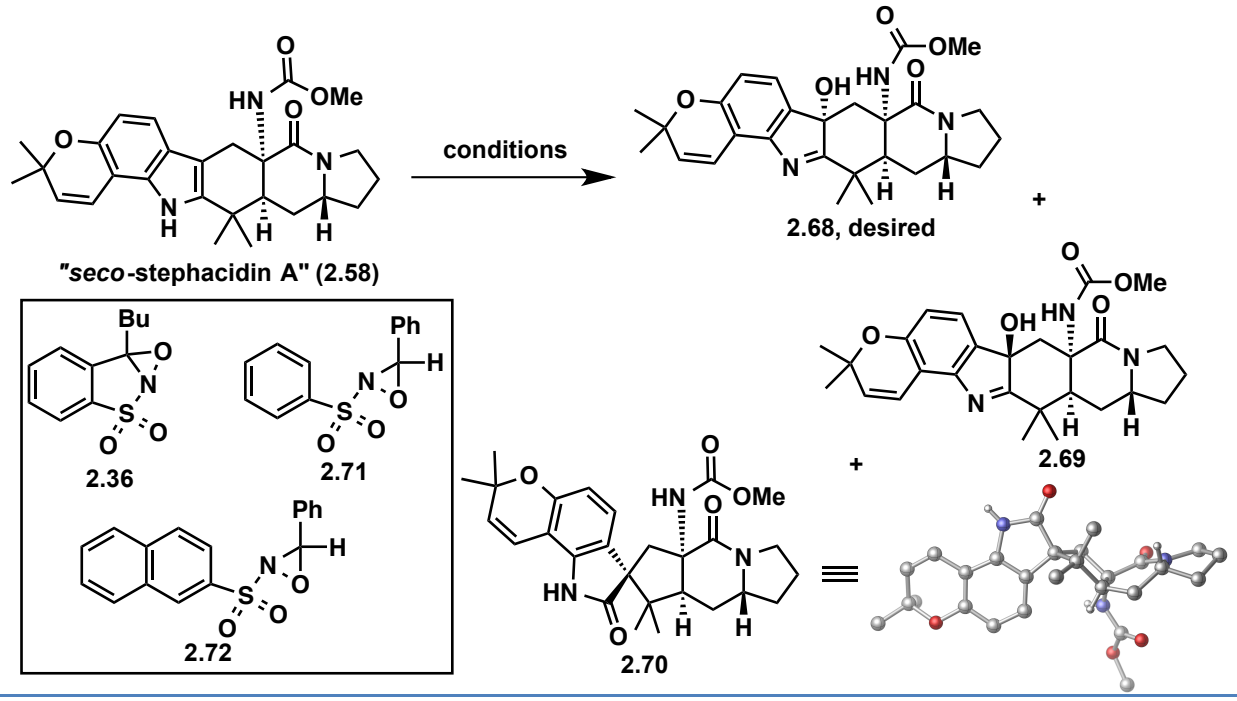

Entry	Oxidant	Solvent	Temperature (°C)	Time	Results
1	**2.36**	THF	23	16 h	>19:1 (**2.69:2.68**)
2	**2.71**	CH_2Cl_2	23	14 h	4:1 (**2.69+2.70:2.68**)
3	**2.72**	CH_2Cl_2	23	14 h	1:1 (**2.69+2.70:2.68**)
4	*m*-CPBA	CH_2Cl_2	–78 to 23	1 h	decomposition
5	DMDO	CH_2Cl_2	–78 to 23	1 h	decomposition

Table 2.2: Oxidation of '*seco*-stephacidin A' (**2.58**).

2.4.3: Forward Chemistry on the Undesired Beta-hydroxylindolenine 2.69.

We decided to first pursue the introduction of the nitro and chromanone groups and the unveiling of the tertiary amine group by amide reduction, on the undesired beta-hydroxylindolenine (**2.69**) as a model substrate (Scheme 2.17). As summarized in Scheme 2.17, hydroxylindolenine **2.69** undergoes conversion to spirooxindole **2.70** when treated with dilute, anhydrous HCl in CH_2Cl_2 at room temperature. Of note, higher concentrations of Brønsted acids lead to decomposition, however, the use of a Lewis acid ($Sc(OTf)_3$/toluene at 110 °C),[38] also effected this rearrangement. Again, the structure of **2.70** is unambiguously supported by single X-ray crystallographic analysis (see CYLview in Table 2.2). Wacker oxidation of the chromene **2.70** to the chromanone **2.73** was achieved with the use of $Pd(OAc)_2$ and $HClO_4$ as a co-catalyst. The methoxycarbonyl group in **2.73** was subsequently cleaved with sodium ethylthiolate (NaSEt) to give the primary amine **2.74**, which was oxidized to a nitro group (**2.75**) with freshly recrystallized *meta*-chloroperoxybenzoic acid[39] (*m*-CPBA) at room temperature. Other oxidants, such as dimethyldioxirane (DMDO),[40] resulted in decomposition of the starting material. At this point, we examined the selective reduction of the tertiary amide in **2.75** to provide the tertiary amine present in the citrinalins and cyclopiamines. Unfortunately, the use of electrophilic reducing agents (DIBAL-H, BH_3•THF, BH_3•SMe_2, AlH_3) resulted in a complex mixture of products with no selectivity as competative reduction of the nitro group was observed by LCMS analysis. On the basis of the more nucleophilic nature of the tertiary amide in comparison to the other functional groups present in **2.75**, we reasoned that activation of the tertiary amide with a strong electrophile followed by reduction with a nucleophilic reducing agent (i.e. $NaBH_4$) would be more effective for this transformation. Before pursuing the optimization of this highly chemoselective reduction of the tertiary amide on this model system, we turned our attention to the use of reagent control to achieve the desired diastereoselective oxygenation of 'seco-stephacidin A' (**2.58**, Table 2.2), given that the inherent facial selectivity observed when using various oxaziridines was very poor.

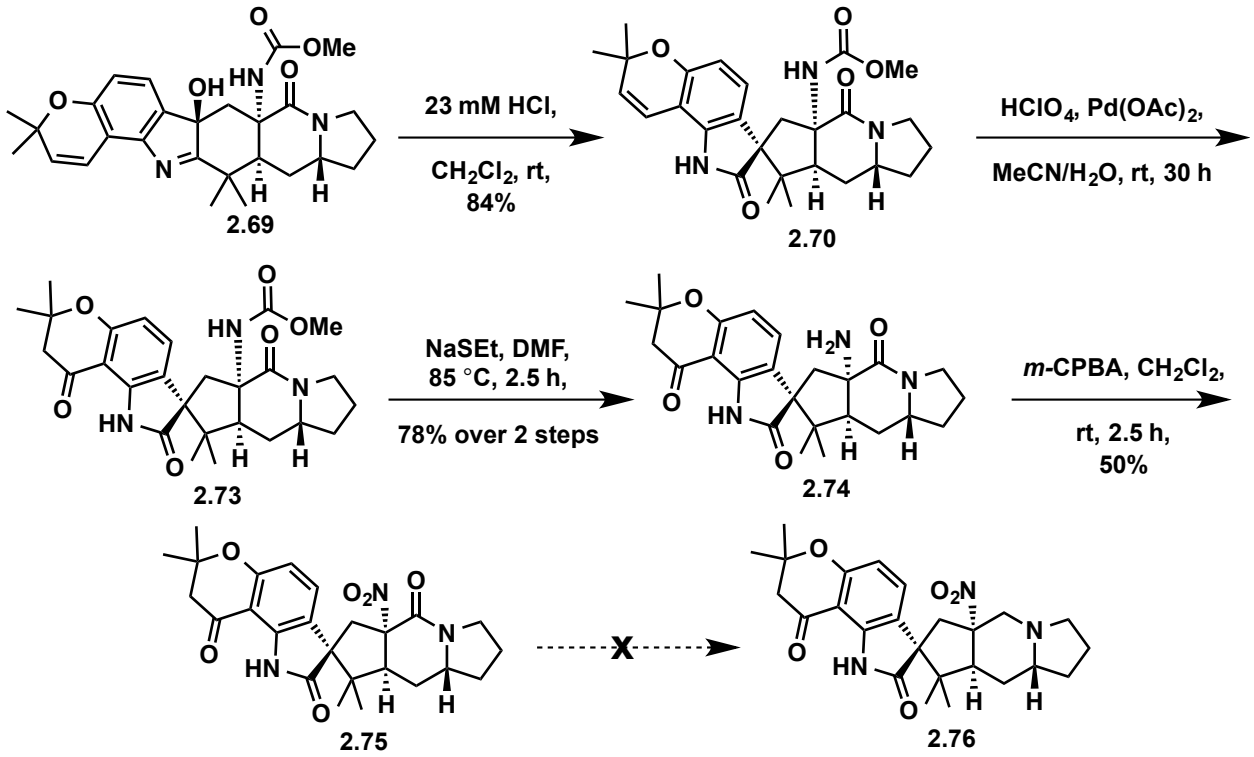

Scheme 2.17: Synthesis of nitro-spirooxindole **2.75**.

2.4.4: Oxidation of 'Seco-Stephacidin A' with Miller's Peptide Catalysts.

After surveying the literature for a reagent to control the face of oxygenation, we were drawn to the peptide-derived catalysts developed by Miller and coworkers.[38, 41] Following an investigation of a focused library of peptide catalysts developed in the Miller laboratory for face-selective oxygenations, **2.77** (Scheme 2.18) emerged as the superior catalyst (20 mol% loading) and provided hydroxylindolenine **2.68** in 83% yield from **2.58**. The oxygenation proceeds by the *in situ* generation of the corresponding peptide-peracid species under the reaction conditions[41b] which acts as the electrophilic oxygen source for the nucleophilic indole moiety. We propose the selectivity is due to hydrogen bonding between the carbamate N-H and one of the the amide carbonyl groups of the peptide backbone to deliver the electrophilic oxygen from the alpha face of the indole moiety (see **2.78** in Scheme 2.18).[41b] It should be noted that it was necessary to run the reaction at low temperature with monitoring to prevent over-oxidation of the chromene unit.

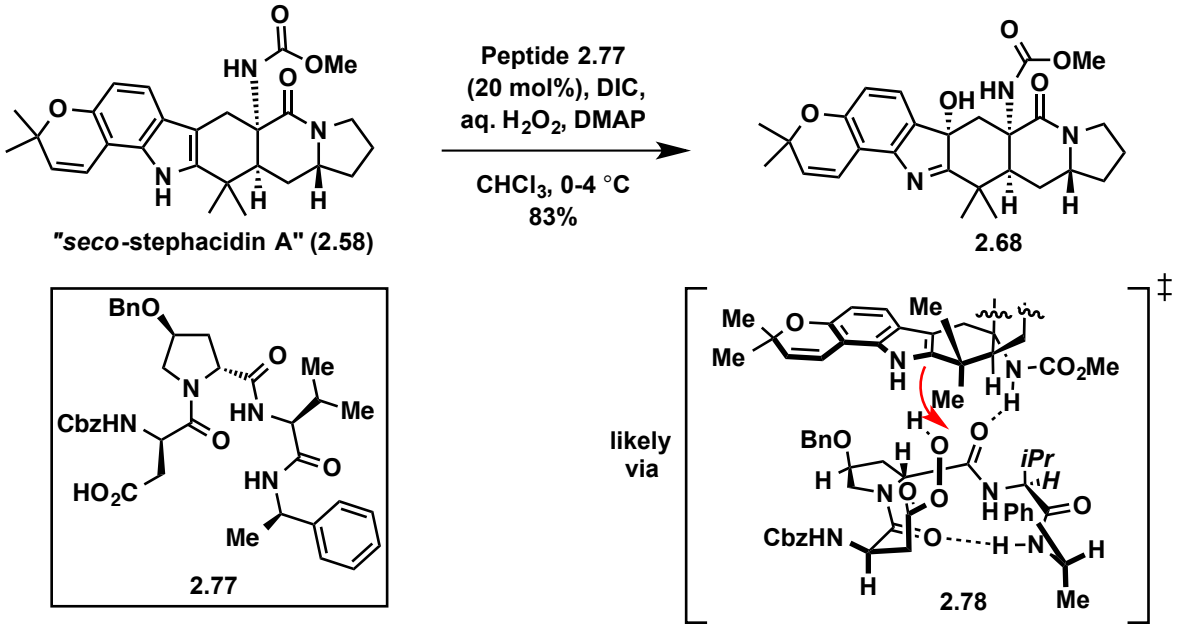

Scheme 2.18: Synthesis of desired hydroxylindolenine **2.68**.

Other peptide catalysts were also examined in hopes of achieving greater selectivities and yields, however none were as effective as **2.77**. Peptide catalyst **2.79** (Figure 2.2) gave comparable selectivities to **2.77** but yielded significantly more decomposition products. The enantiomer of **2.79** (not shown) resulted in a complex mixture. Catalysts **2.80** and **2.81** also favored the desired hydroxylindoline **2.68** (3:1, **2.68:2.69+2.70**) but also provided a complex mixture of decomposition products. The trifluorodioxirane variant of this peptide catalyst, **2.82**, also resulted in a complex reaction mixture.

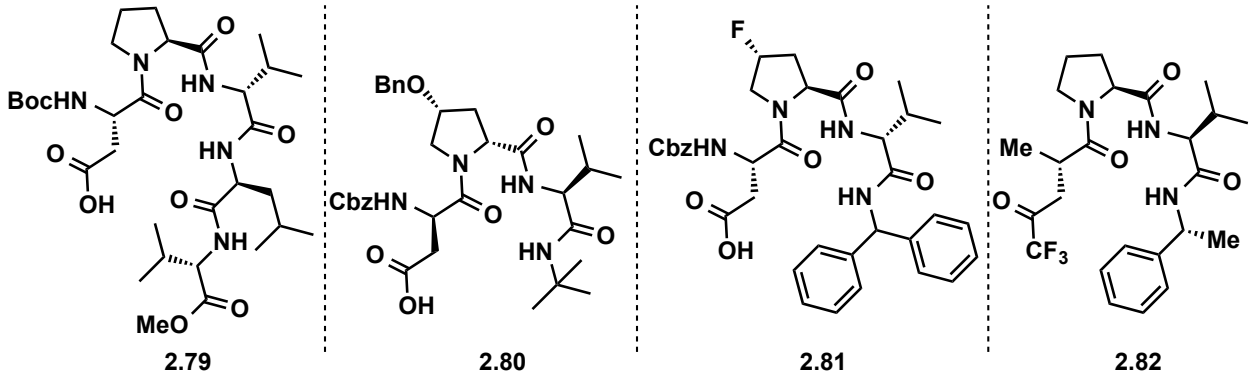

Figure 2.2: Other catalysts provided by Prof. Miller and David Romney (Yale University).

With the desired alpha-hydroxylindolenine **2.68** in hand (accessed using the peptide-catalyzed oxygenations) we were eager to carryout the foward chemistry analogous to the beta-hydroxyindolenine **2.69** in Scheme 2.17. Treating **2.68** with dilute, anhydrous Brønsted acid (23 mM HCl in CH_2Cl_2) or stirring in silica gel at room temperature resulted in decomposition. Suprisingly, however, **2.68** rearranges to afford pseudoindoxyl **2.83** (Scheme 2.19) instead of

desired spirooxindole **2.84** with heating using $Sc(OTf)_3$ over 2 hours. This is consistent with the ^{13}C NMR data ($CDCl_3$) which shows a resonance at δ = 203 ppm for the carbonyl group of the pseudoindoxyl instead of the expected δ = ~180 ppm for the spirooxindole. The equilibrium between pseudoindoxyls and spirooxindoles is well recognized and has been studied for the migration of C2 alkyl substituents by Borschberg[33] (see Scheme 2.15) and recently for C2 aryl substituents by Movassaghi and coworkers.[34] However, despite prolonged heating, further rearrangement of pseudoindoxyl **2.83** to the desired spirooxindole **2.84** was not observed but instead resulted in decomposition. It is possible that an intramolecular hydrogen bond stabilizes pseudoindoxyl **2.83** toward further rearrangement (a bond distance of 2.24Å is computed for the pseudoindoxyl carbonyl group and N-H proton of the carbamate group in **2.83**).[12] A possible stabilizing intramolecular hydrogen bond in **2.83** is supported by the observation that beta-hydroxyindolenine **2.69** (prepared by oxidation of **2.58** with Davis' oxaziridine, Table 2.2) rearranges readily at room temperature in the presence of mild acid (23 mM HCl in CH_2Cl_2) to spirooxindole **2.70** (Scheme 2.17); a pseudoindoxyl generated from **2.70** would lack the analogous stabilizing hydrogen bond.

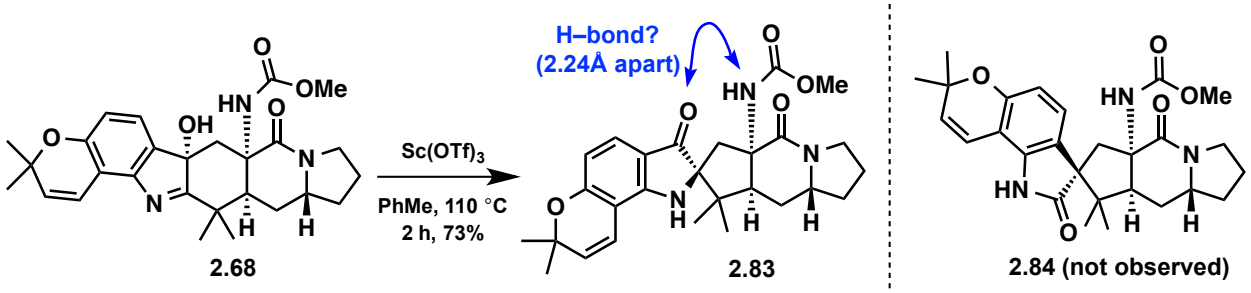

Scheme 2.19: Synthesis of pseudo-indoxyl **2.83**.

At this point we decided to move forward with the installation of the chromanone and attempt the rearrangement at a later stage, following cleavage of the methyl carbamate to remove the presumed pseudoindoxyl-stabilizing hydrogen bonding. Chromene **2.83** readily underwent a Wacker oxidation ($Pd(OAc)_2$, $HClO_4$, *p*-benzoquinone) to provide the requisite chromanone **2.85** (Scheme 2.20). Attempts to cleave the methyl carbamate with sodium ethylthiolate (NaSEt) led to decomposition of starting material but proceeded cleanly with dimethylsulfide (Me_2S) in methylsulfonic acid[42] (MsOH) to afford primary amine **2.86**. With amine **2.86**, lacking the presumed hydrogen bonding, we investigated a series of acids (BF_3•OEt_2, HCl, or $Sc(OTf)_3$), conditions to effect rearrangement to the spirooxindole, but presumably due to the instability of the amine under the reaction conditions, this resulted only in decomposition, with no observable rearranged spirooxindole product. The recalcitrance of pseudoindoxyl **2.86** to undergo further rearrangement caused us to consider alternative tactics that would produce the desired spirooxindole structural moiety of the citrinalins and cyclopiamines.

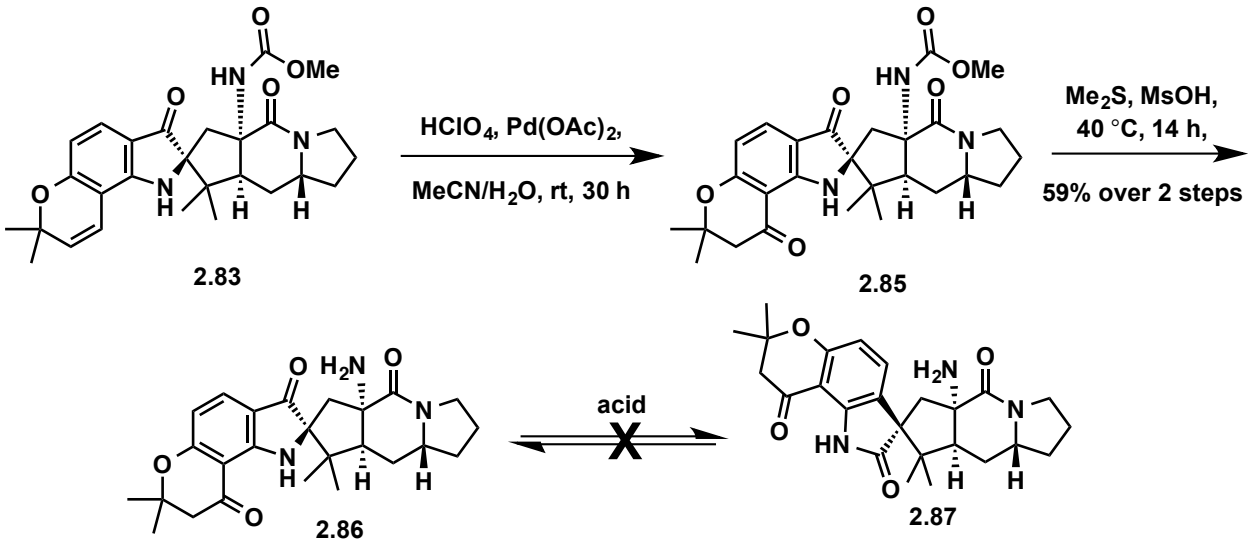

Scheme 2.20: Synthesis of chromanone pseudoindoxyl **2.86**.

2.4.5: Amino-Indole to Nitro-Spirooxindole Transformation with Dimethyldioxirane (DMDO).

Cognizant that the hydrogen bonding is essential for relaying the diastereoselectivity of the oxygenation to the alpha face of the indole (**2.58→2.68**, Scheme 2.18) but is also detrimental to the product formed in the rearrangement step (**2.68→2.83**, Scheme 2.19), we reasoned a transient group that acts as a hydrogen bond donor that is then eliminated under the reaction conditions may effect this transformation. On the basis of this hypothesis we envisioned that an amino group (**2.18**, Scheme 2.21) or some oxidized derivative thereof (e.g., the corresponding hydroxylamine, **2.88**) could serve as a hydrogen bond donor to effect stereoselective oxygenation of the indole C2–C3 bond (**2.88→2.89**) and then, by further oxidation to a nitroso or nitro group (**2.90→2.91**), remove the presumed intramolecular hydrogen bond that may stabilize the pseudoindoxyl form (as in **2.90**), and allow rearrangement to spiro-oxindole **2.92**. It appeared reasonable that this sequence would facilitate the eventual conversion of **2.18** to nitro spirooxindole compound **2.93** (Scheme 2.21).

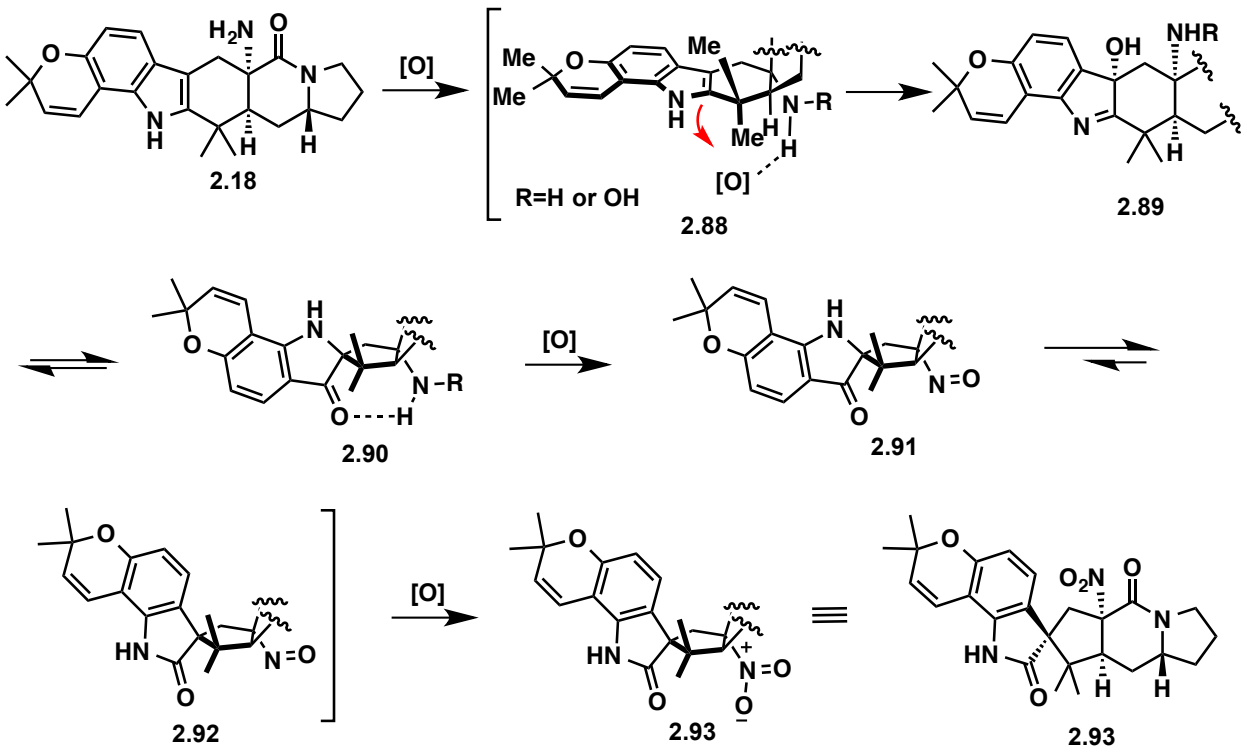

Scheme 2.21: Envisioned global oxidative rearrangement to access nitro-spirooxindole **2.93**.

With this hypothesis in mind, we began investigating conditions for the proposed global oxidative rearrangement to attain the nitro-spirooxindole. We were able to cleave the methoxycarbonyl group present in **2.58** (Scheme 2.22) by treating with sodium ethylthiolate to unveil primary amine **2.18**.

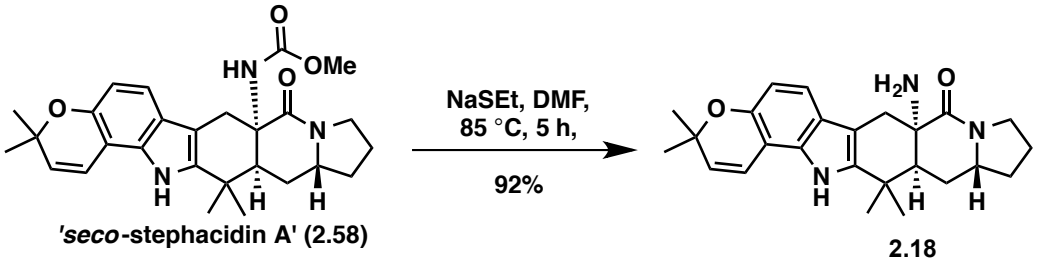

Scheme 2.22: Synthesis of amino-indole **2.18**.

Initial experiments established that oxidation of the chromene ring in **2.18** was a competing reaction that occurred under various oxygenation conditions (*m*CPBA, CH_3CO_3H, Oxone®/acetone). As such, we opted to effect a Wacker oxidation[43] of **2.58** to afford chromanone **2.94** first (Scheme 2.23), which would be advantageous as the chromanone unit is found in the citrinalins and cyclopiamines. Remarkably, treatment of **2.95** (following removal of the methoxycarbonyl group in **2.94** with dimethylsulfide in methylsulfonic acid)[42] with an excess of dimethyldioxirane (DMDO) (formed *in situ* from acetone and Oxone®) affords spirooxindole **2.96** as the major product (4:1 d.r., diastereomeric ratio) where the spiro center is as desired and

the nitro group has been installed. The structure of **2.96** is unambiguously supported by single X-ray crystallographic analysis (see CYLview in Scheme 2.23). Of note, even through optimization we could never achieve greater than 70% recovery of the mass balance after extraction (EtOAc) and we reasoned this was due to decomposition resulting from oxidation of aliphatic C-H groups,[44] which leads to water-soluble products. Support for the amine group acting as a transient directing group comes from the fact that treating methyl carbamate **2.94** under similar *in situ* formed DMDO (four equivalents instead of ten) conditions resulted in the formation of the diastereomeric spirooxindole (**2.73**, Scheme 2.17) as the major product (ca. 4:1 ratio)

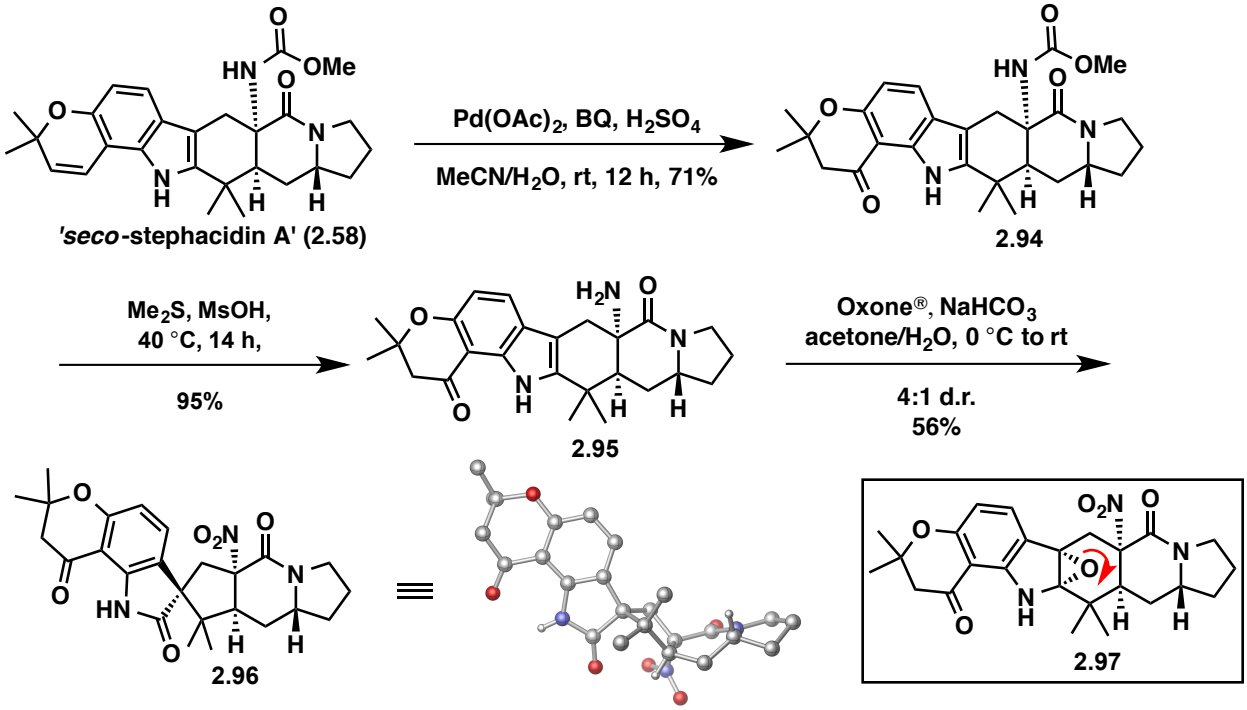

Scheme 2.23: Synthesis of nitro-spirooxindole **2.96**.

It is possible that spirooxindole **2.96** arises from epoxide **2.97** (see inset **2.97** in Scheme 2.23) on the basis of studies by Foote and co-workers for DMDO oxidations of indoles to spirooxindoles.[45] Therefore, it is possible that the introduction of the chromanone diminishes the participatory role of the indole nitrogen lone pair leading, after rearrangement (see direction of red arrow in **2.97**), to **2.96**. This electron-withdrawing nature of the chromanone relative to the chromene is supported by the fact that when chromanone **2.94** is subjected to the peptide-based oxidation conditions described previously (section 2.2.4), only starting material is recovered, even when the reaction is conducted at room temperature over an extended period of time (12 h). With spirooxindole **2.96** in hand, what remained was a selective removal of the tertiary amide carbonyl group by reduction, which had to be accomplished in the presence of the chromanone and secondary amide carbonyl groups as well as the newly introduced nitro group. The meticulous level of chemoselectivity required for this transformation was unprecedented in the literature.

2.4.6: Highly Chemoselective Reduction of the Tertiary Amide Group – Synthesis of ent-Citrinalin B (ent-2.2).

The reduction of amides to the corresponding amine products has been studied for decades using stoichiometric electrophilic (i.e. DIBAL-H) and nucleophilic (i.e. $LiAlH_4$) metal hydride sources, catalytic amounts of transition metal complexes in combination with hydrosilane as reductants,[46] conversion of amides to thioamides prior to reduction,[47] and electrophilic activation of the amide group prior to the reduction step,[48] among other methods.[49]

We began our studies on the chemoselective reduction of the tertiary amide group in **2.96** (Table 2.3) to the tertiary amine group found in the citrinalins and cyclopiamines by looking at both electrophilic and nucleophilic metal hydrides. The use of electrophilic DIBAL-H, which has been previously shown to reduce tertiary amides to the amine products in the presence of secondary amides,[50] resulted in decomposition (Entry 1, Table 2.3). Similarly, $BH_3 \bullet SMe_2$ and alane (AlH_3) did not achieve the selective reduction of the tertiary amide group but instead resulted in the reduction of the ketone group or a global reduction of **2.96** as determined by LCMS analysis (Entries 2 and 3, respectively). Using Schwartz's reagent (Cp_2ZrHCl), known to reduce amides,[51] led to a diastereoselective reduction of the ketone group with no detectable amine product (Entry 4, Table 2.3). Utilizing a nucleophilic metal hydride ($LiAlH_4$) resulted in decomposition (Entry 5, Table 2.3). Lastly, using SmI_2 only returned starting material (Entry 6, Table 2.3).[49d] Having explored both electrophilic and nucleophilic metal hydrides to effect the amide reduction with no success, we decided to explore alternative methods for this transformation.

Next we decided to investigate transition metal catalyzed methods for amide reductions. Employing the conditions of Ito and co-workers,[46a] which demonstrated that tertiary amides are reduced in the presence of both primary or secondary amides with $RhH(CO)(PPh)_3)_3$ as catalyst and diphenylsilane (Ph_2SiH_2) as the reductant, resulted in recovery of starting material (Entry 7, Table 2.3). Similar results were obtained with the use of a platinum-based catalytic system,[46i] which is inert toward the reduction of nitro groups (Entry 8, Table 2.3). Recently, however, Beller and co-workers have demonstrated the use of cost-efficient and environmentally benign methods for the chemoselective reduction of amides. However the use of these catalytic systems resulted in either reduction of the nitro group ($[Fe_3(CO)_{12}]$, Ph_2SiH_2)[46j] or decomposition of starting material ($Zn(OAc)_2$, $(EtO)_3SiH$)[46k] (Entries 9 and 10, respectively). Having explored these catalytic systems, among others, with limited success we chose to focus on electrophilic activation of the amide group prior to reduction.

The idea of amide reductions *via* the intermediacy of electrophilically activated intermediates is well documented in the literature. We reasoned this methodology would be the most effective in terms of chemoselectivity on the basis of the more nucleophilic nature of the tertiary amide in comparison to the other functional groups present in **2.96** (The secondary amide of the spiro-oxindole can be viewed as a vinylogous imide due to the adjacent ketone group). First, we investigated the formation of the thioamide from the corresponding amide group in **2.96** (not shown). Treating **2.96** with either Lawsson's reagent[47a] or phosphorus pentasulfide[52] (P_4S_{10}) resulted in the recovery of starting material; therefore, we looked into electrophilic activators instead. Drawn by the work of André Charette and co-workers,[48e] describing a highly chemoselective metal-free reduction process for the reduction of tertiary amides with

trifluoromethane-sulfonic anhydride (Tf_2O) as the electrophilic activator and Hantzsch ester as the hydride transfer agent, we envisioned this would provide the amine product directly. Unfortunately, employing the Charette conditions on **2.96** only resulted in the recovery of starting material (Entry 11, Table 2.3). Switching the nature of the the reducing agent from Hantzsch ester to either $Me_4NBH(OAc)_3$ or $NaBH_4$ also resulted in starting material (Entries 12 and 13, respectively). Interestingly, the use of Et_3SiH in combination with Tf_2O resulted in decomposition (Entry 14, Table 2.3).

After conducting ^1H NMR studies with **2.96** and Tf_2O (1.1 equiv) in $CDCl_3$, we observed a gradual activation of the amide functional group suggesting either a slow electrophilic activation of the tertiary amide group (possibly due to sterics around the amide group) or a reversible activation process. Modifying the amide activation with Tf_2O at elevated temperatures (>60 °C) and extended reaction times (16 h) led to similar recovery of starting material, **2.96**. Therefore, we decided to look into alternative electrophilic activating agents.

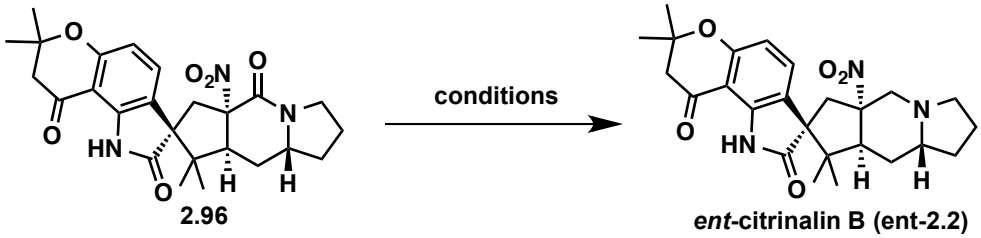

2.96 ***ent*-citrinalin B (ent-2.2)**

Entry	Catalyst/Electrophile	Reducing Agent	Temp (°C)	Solvent	Result
1	–	DIBAL-H	0–23	Toluene	Decomp.
2	–	$BH_3•SMe_2$	23	THF	Ketone Reduction
3	–	AlH_3	0	THF	Global Reduction
4	–	Cp_2ZrHCl	23	THF	Ketone Reduction
5	–	$LiAlH_4$	0	THF	Decomp.
6	–	SmI_2	0	THF	S.M.
7	$RhH(CO)(PPh_3)_3$	Ph_2SiH_2	23	THF	S.M.
8	$H_2PtCl_6•6H_2O$	TMDS	50	THF	S.M.
9	$[Fe_3(CO)_{12}]$	Ph_2SiH_2	100	Toluene	Nitro reduction

10	$Zn(OAc)_2$	$(EtO)_3SiH$	50	THF	Decomp.
11	Tf_2O	Hantzsch ester	23	CH_2Cl_2	S.M.
12	Tf_2O	$Me_4NBH(OAc)_3$	23	CDCl3	S.M.
13	Tf_2O	$NaBH_4$	23	$CDCl_3$/THF	S.M.
14	Tf_2O	Et_3SiH	23	$CDCl_3$	Decomp.
15	MeOTf	$Me_4NBH(OAc)_3$	23	$CDCl_3$	S.M.
16	MeOTf	$NaCNBH_3$	23	CH_2Cl_2	S.M.
17	Et_3OBF_4	$NaBH_4$	23	CH_2Cl_2/MeOH	Ketone Reduction
18	Me_3OBF_4	$NaBH_4$	23	CH_2Cl_2/MeOH	Ketone and 3° Amide Reduction
19	Me_3OBF_4	$NaCNBH_3$	0	CH_2Cl_2/MeOH	**2.2**

Table 2.3: Chemoselective reduction of the tertiary amide group in **2.96**.

Encouraged by the work of Hwu and co-workers,[48c] which showed that either ethyl- or methyl- trifluoromethylsulfonates are effective electrophiles for the activation of amides, we considered these smaller alkylating agents to be more effective at activating the sterically congested tertiary amide group in **2.96** in an irreversible manner (the alpha carbon adjacent to the tertiary amide contains a tetra-substituted carbon). However, MeOTf in combination with either $Me_4NBH(OAc)_3$ or $NaCNBH_3$ (Entries 15 and 16, respectively) resulted in recovered starting material, which suggested that again we may not be achieving the electrophilic activation of the amide group. Next we investigated the use of Meerwein's salt (Et_3OBF_4), as Borch[48a] has convincingly shown its use in the reduction of amides in combination with $NaBH_4$, decades prior to the other methods described above. Unfortunately, application of the Borch procedures (Et_3OBF_4, $NaBH_4$) resulted in the reduction of the ketone group with no observable reduction of the tertiary amide (Entry 17, Table 2.3). However, the methyl variant of Meerwein's salt (Me_3OBF_4) and $NaBH_4$ resulted in the reduction of both the ketone to the alcohol and the tertiary amide to the corresponding amine (Entry 18, Table 2.3). Encouraged by these results, we decided to modify the nature of the reducing agent to $NaCNBH_3$, which is known to be compatible with ketones, finally achieving the highly chemoselective reduction of the tertiary amide group in **2.96** to the tertiary amine group found in the citrinalins and cyclopiamines (Entry 19, Table 2.3). We believe slightly more hindered Meerwein's salt (Et_3OBF_4) is too large to effectively activate the sterically congested tertiary amide in **2.96**. Of note, Evans and co-workers had made analogous findings in reducing amide groups en route to their synthesis of (–)-nakadomarin A.[53]

In summary, after extensive investigation, the chemoselective reduction of the tertiary amide was effectively accomplished using a modification of a procedure developed by Borch[48a] by treating **2.96** (Scheme 2.24) with a variant of Meerwein's salt (Me_3OBF_4), which likely leads to a methylated amidinium intermediate (**2.97**) that is cleanly reduced with sodium cyanoborohydride to give *ent*-citrinalin B (*ent*-**2.2**) in 66% yield (79% brsm; based on recovered starting material). All attempts at pushing the reaction to completion were futile, as we always observed starting material even after changing reaction times, temperature, and equivalents of reagents. We believe this may be due to small amounts of moisture present in $NaCNBH_3$, which hydrolyzes the methylated intermediate **2.97** to **2.96** faster than its reduction. Furthermore, the spectroscopic data for the neutral form of *ent*-**2.2** are fully consistent with the data reported by Berlinck and coworkers for the compound believed to be citrinalin B (corroborating the computational predictions and reanalysis in MeOH-d_4, see Section 2.1.2), except for the sign of optical rotation, which is opposite. The structure of *ent*-**2.2** was unambiguously confirmed by X-ray crystallographic analysis of its HCl salt (see CYLview in Scheme 2.24). Lastly, it provides support for the hypothesis that **2.1** and **2.2** are related by the aza-Henry interversion (see Figure 2.1).

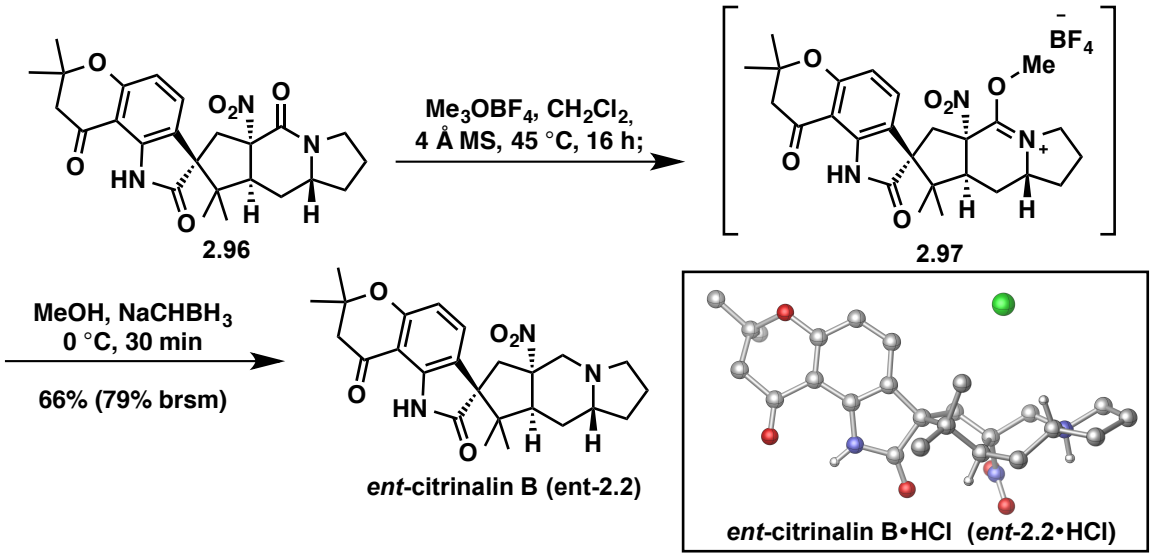

Scheme 2.24: Synthesis of *ent*-citrinalin B **(*ent*-2.2).**

We believe the secondary amide of the spirooxindole in **2.96** is not as nucleophilic as the tertiary amide for the electrophilic activation step due to its resonance stabilization by the electron-poor aromatic ring. Of note, upon addition of $NaCNBH_3$ to the reaction mixure, we observe the generation of bubbles (possibly H_2), which might be attributed to the deprotonation of the spirooxindole N-H on the activated methylated amidinium species. This deprotonation sequence would generate a carboximidate group (not shown) which is no longer susceptiable to reduction under the conditions.

Having effectively accessed *ent*-citrinalin B (***ent*-2.2**) via an unprecedented chemoselective reduction of the tertiary amide group in **2.96** to the corresponding amine present in the natural product, we focused on a chromanone to tetrahydroquinolone rearrangement to access cyclopiamine B (**2.6**, Figure 2.1).

2.4.7: Synthesis of Cyclopiamine B (2.6) by a Chromanone Rearrangement.

ent-Citrinalin B is easily converted to cyclopiamine B (**2.6**, Scheme 2.25) upon treatment of *ent*-**2.2** with sodium hydride and heating (to effect the chromanone to tetrahydroquinolone conversion, presumably via intermediate **2.98**) and subsequent methylation (MeI, K_2CO_3, acetone, 60 °C) of the resulting phenol (**2.99**). The structure of cyclopiamine B (**2.6**) was also unambiguously confirmed by X-ray crystallographic analysis (see CYLview in Scheme 2.25).

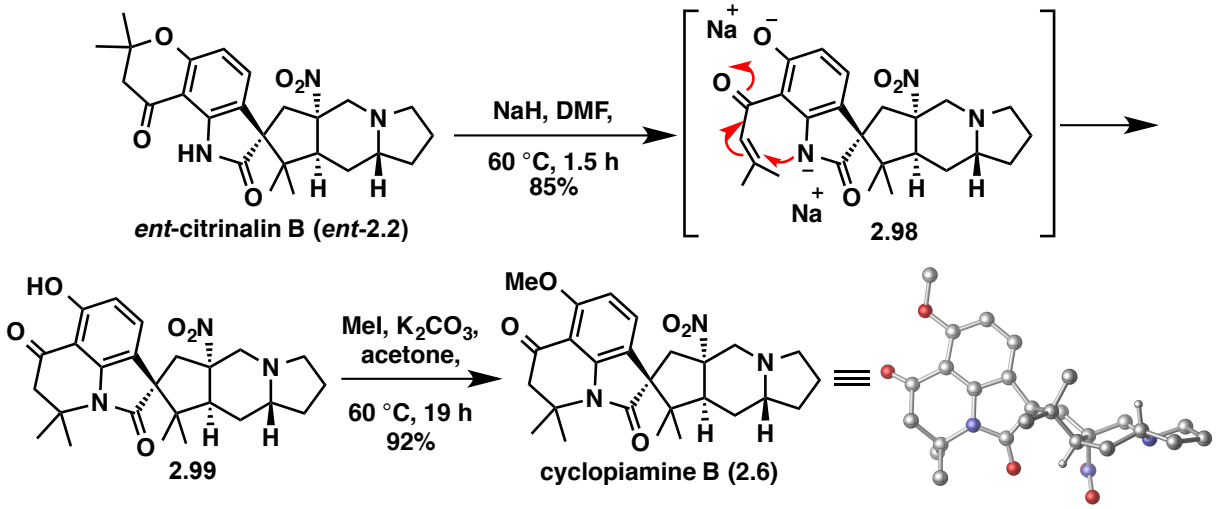

Scheme 2.25: Synthesis of cyclopiamine B **(2.6)** from *ent*-citrinalin B **(*ent*-2.2).**

Alternatively, amide **2.96** (Scheme 2.26) can also be converted to tetrahydroquinolone **2.100** upon treatment under the same conditions described above (NaH, DMF, 60 °C). The resulting phenol (**2.100**) is subsequently methylated (MeI, K_2CO_3, acetone, 60 °C), to provide **2.101**. The structure of **2.101** is unambiguously supported by single X-ray crystallographic analysis (see CYLview in Scheme 2.26). Subjecting **2.101** to the conditions established for the chemoselective reduction of the tertiary amide in **2.96** (Scheme 2.24), resulted in the reduction of the same amide group in 62% yield. As described above, the electronics and sterics of the tertiary amide vs. the vinylogous imide dictates the selectivity for this reduction sequence. Thus, the synthesis of *ent*-**2.2** and its conversion to **2.6** conclusively supports *ent*-**2.2** as the true structure of citrinalin B, albeit the enantiomer of the naturally occurring material.

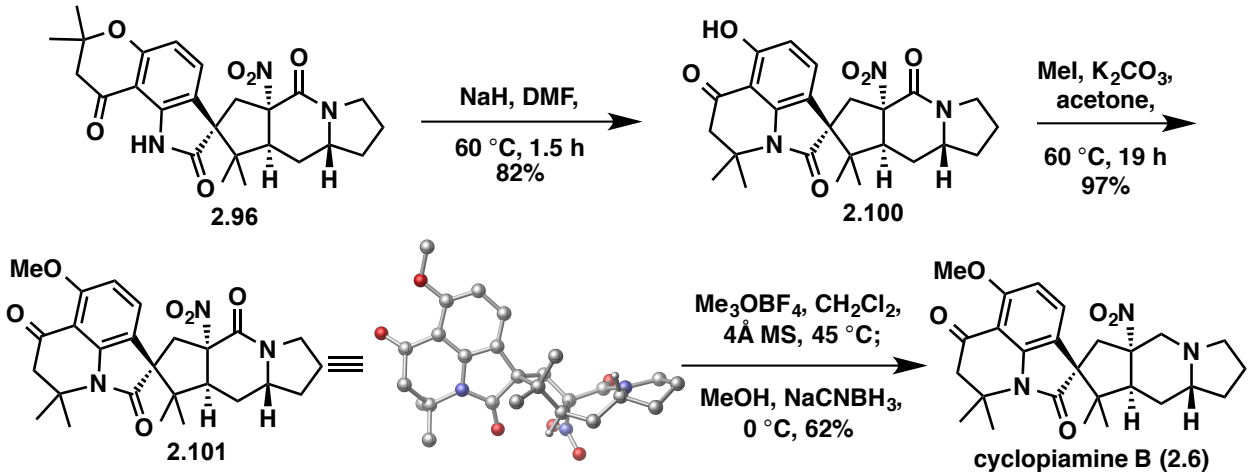

Scheme 2.26: Synthesis of cyclopiamine B (**2.6**) from **2.96**.

2.5 – Biosynthetic Considerations

2.5.1: Proposed Biosynthesis of Congeners Lacking the Bicyclo[2.2.2]diazaoctane Ring.

The total syntheses of *ent*-citrinalin B (*ent*-**2.2**; 19 steps from D-proline, 5.5% overall yield) and cyclopiamine B (**2.6**; 21 steps from D-proline, 4.3% overall yield) not only unambiguously establishes the structures of these metabolites, but also provide possible insight into the biogenesis of these natural products (especially as to the possible formation of the cyclopiamines from the citrinalins).

The citrinalins and cyclopiamines are pseudoenantiomeric natural products, meaning every stereogenic center in citrinalin A (**2.1**, Figure 2.4) is opposite from that found in cyclopiamine A (**2.4**) (the same is true for citrinalin B and cyclopiamine B) and the difference comes from the presence of the chromanone (hightlighted in red in **2.1**) or a rearranged tetrahydroquinolone (highlighted in blue in **2.4**) of the benzenoid ring system. The citrinalins, and in turn the cyclopiamines, likely arise from enantiomeric bicyclo[2.2.2]diazaoctane precursors. However, such a precursor was unknown prior to the findings that are reported herein (*vide infra*). Consistent with numerous biosynthetic studies of the prenylated indole alkaloids, the structural features of the citrinalins (**2.1** and **2.2**) and cyclopiamines (**2.4** and **2.6**) suggest that tryptophan, proline and two isoprene units are biosynthetic precursors to these compounds (see Chapter 1.3 for a more detailed discussion).

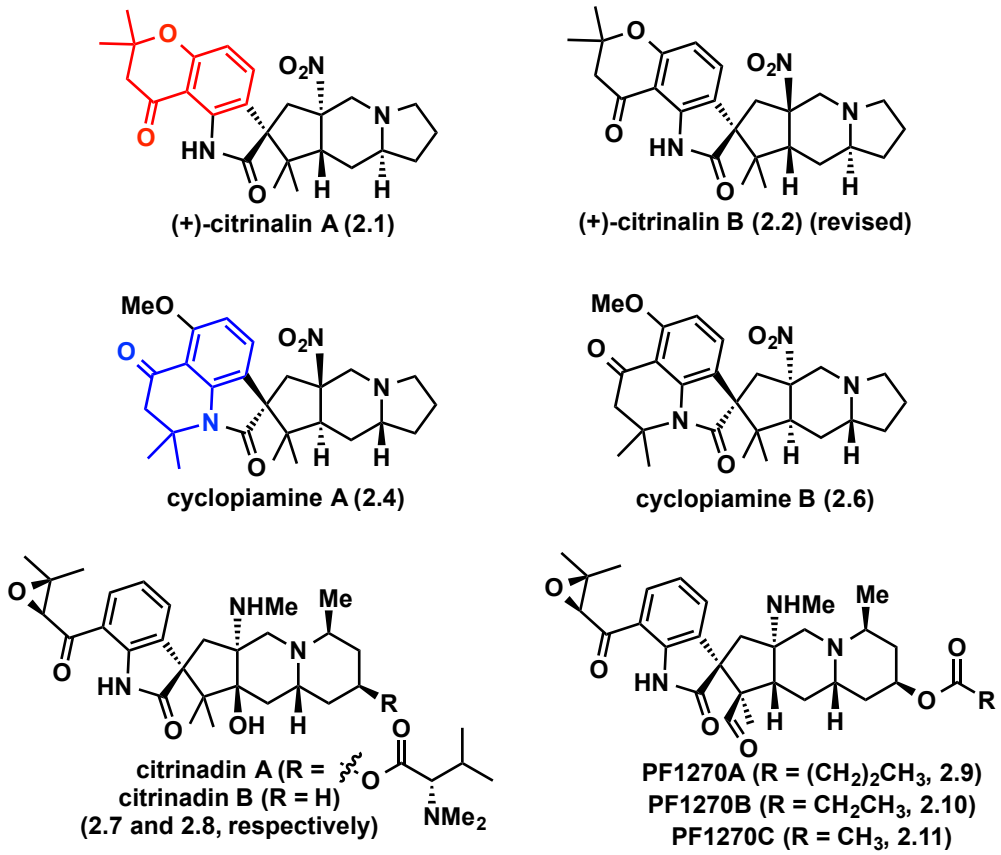

Figure 2.4: Selected prenylated indole alkaloids lacking the bicyclo[2.2.2]diazaoctane.

While no biosynthetic studies on **2.1** and **2.2** or **2.4** and **2.6** or the related citrinadins (**2.7-2.8**) and PF1270 (**2.9-2.11**) alkaloids has appeared, a hypothesis suggesting they are derived from bicyclo[2.2.2]diazaoctane precursors that suffer the "loss" of one diketopiperazine carbonyl group has been advanced by Kobayashi and coworkers.[5] For example, as outlined in Scheme 2.27, a hydrolysis of the amide group of the bicyclo[2.2.2]diazaoctane ring in chrysogenamide A[54] (highlighted in red in **2.102**, Scheme 2.27) followed by a decarboxylation event would take **2.102** to the relatively flat framework found in the citrinadins (see **2.103**) (following additional peripheral oxygenations). However, it was unknown whether organisms producing secondary metabolites containing the bicyclo[2.2.2]diazaoctane ring (i.e. **2.102**) also produce alkaloids which lack this moiety (i.e. **2.103**).

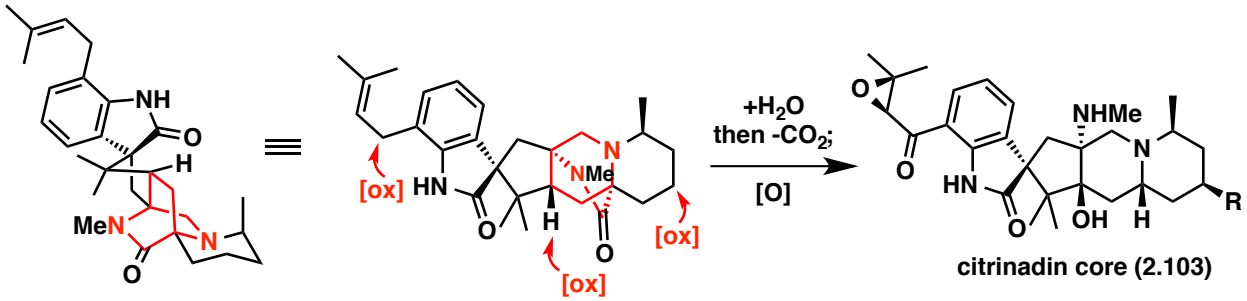

chrysogenamide A (2.102)

citrinadin core (2.103)

Scheme 2.27: Proposed biosynthetic sequence to the citrinalins from chrysogenamide A (**2.102**).

2.5.2: Isolation of Two New Citrinalin Alkaloids and ^{13}C labeling Studies.

In collaboration with Berlinck and co-workers, following the isolation of 17-hydroxy-citrinalin B (**2.104**, Figure 2.5) and more importantly citrinalin C (**2.105**) following a series of stable isotope labeling experiments (summarized in Figure 2.5),[12] we have now obtained support for the possible biogenesis of the citrinalins and cyclopiamines from a precursor bearing the bicyclo[2.2.2]diazaoctane moiety.

The nuclear magnetic resonance (NMR) and mass spectroscopy (MS) characterization data for **2.104** is fully consistent with the assigned structure. Moreover, the assigned relative configuration fully corroborates the revised structure of citrinalin B (**2.2**). By analogy to citrinalin B (**2.2**), the absolute configuration of **2.104** was assigned as 1*S*,14*R*,16*R*,17*R*,22*R*. 17-Hydroxycitrinalin B (**2.104**) was initially isolated from *P. citrinum* F53 grown in a nitrogen depleted culture medium. Stable isotope feeding studies with [U-^{13}C]anthranilic acid (**2.107**) and [1-^{13}C]glucose (**2.106**) gave significant ^{13}C labeling.[12] High levels of [U-^{13}C]ornithine (**2.108**) were also incorporated into **2.104**, while additional feeding studies with [U-^{13}C]proline gave almost undetectable labeling. Ornithine is a well-known biosynthetic precursor to proline, but to our knowledge has never been reported as a efficient substrate for isotopic labeling of the putative proline-derived atoms in the biosynthesis of prenylated indole alkaloids of fungal origin bearing the bicyclo[2.2.2]diazaoctane moiety. The labeling investigations suggest that 17-hydroxy-citrinalin B (**2.104**) might arise from either 3-hydroxyl ornithine, 3-hydroxy proline, or by the late-stage oxygenation of the citrinalin A, B or C skeleton.

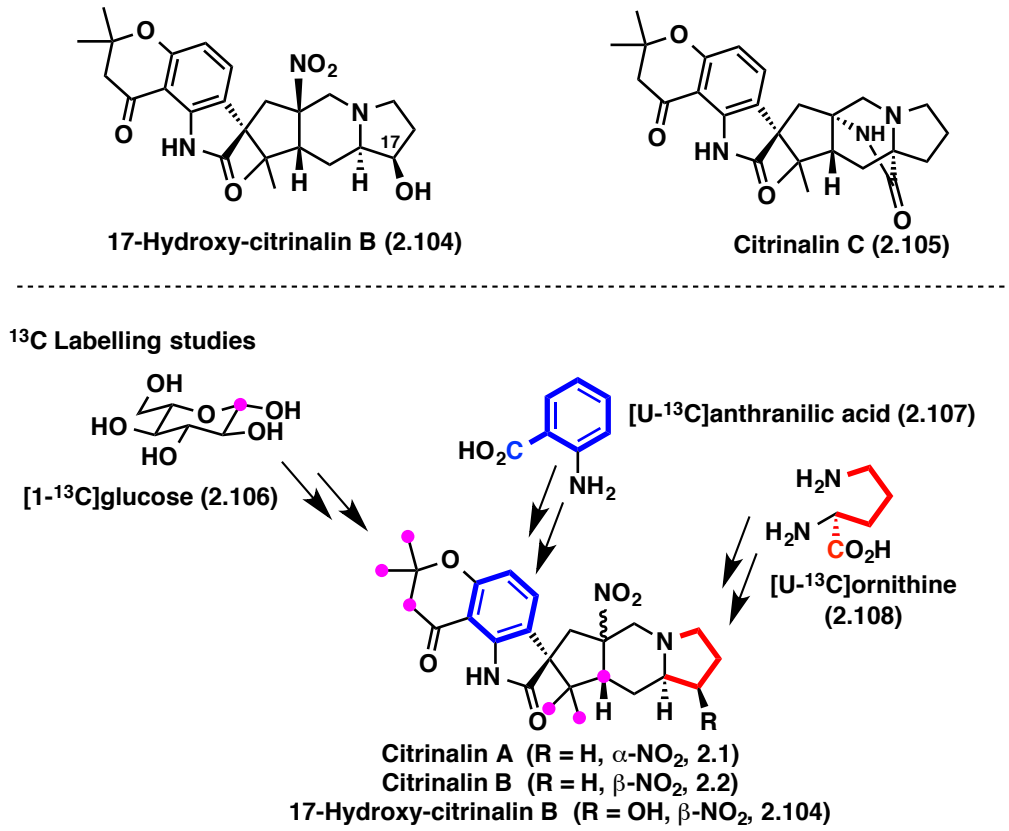

Figure 2.5: Isolation of two new citrinalins and summary of ^{13}C labeling studies.

Citrinalin C (**2.105**), isolated as a minor component from the culture medium of *P. citrinum* F53, gives NMR and MS data that is fully consistent with the relative and absolute configuration illustrated for this natural product. The isolation of **2.105**, along with the congeners lacking the bicyclo[2.2.2]diazaoctane structural moiety from *P. citrinum* F53, lends support to a bicyclo[2.2.2]diazaoctane-containing precursor (i.e. **2.110**, Scheme 2.28), which arises from an intramolecular Diels-Alder (IMDA) cycloaddition step from achiral azadiene **2.109**, as has been studied in detail for other congeners by Williams and Sherman[55] (for a more detailed discussion see Chapter 1.3). Depending on the organism producing either the citrinalins or cyclopiamines, there is an enantioselective IMDA which gives rise to enatiomeric bicyclo[2.2.2]diazaoctane precurors (**2.109** → **2.110**). In accordance with the proposal of Kobayashi, hydrolysis of the amide bridge of citrinalin C (**2.105**, Scheme 2.28), followed by decarboxylation and amino group oxidation to the nitro group, as proposed in the biosynthesis of the structurally related citrinadin B,[5] would then yield citrinalin A (**2.1**). These latter steps are the subject of current biosynthesis studies.

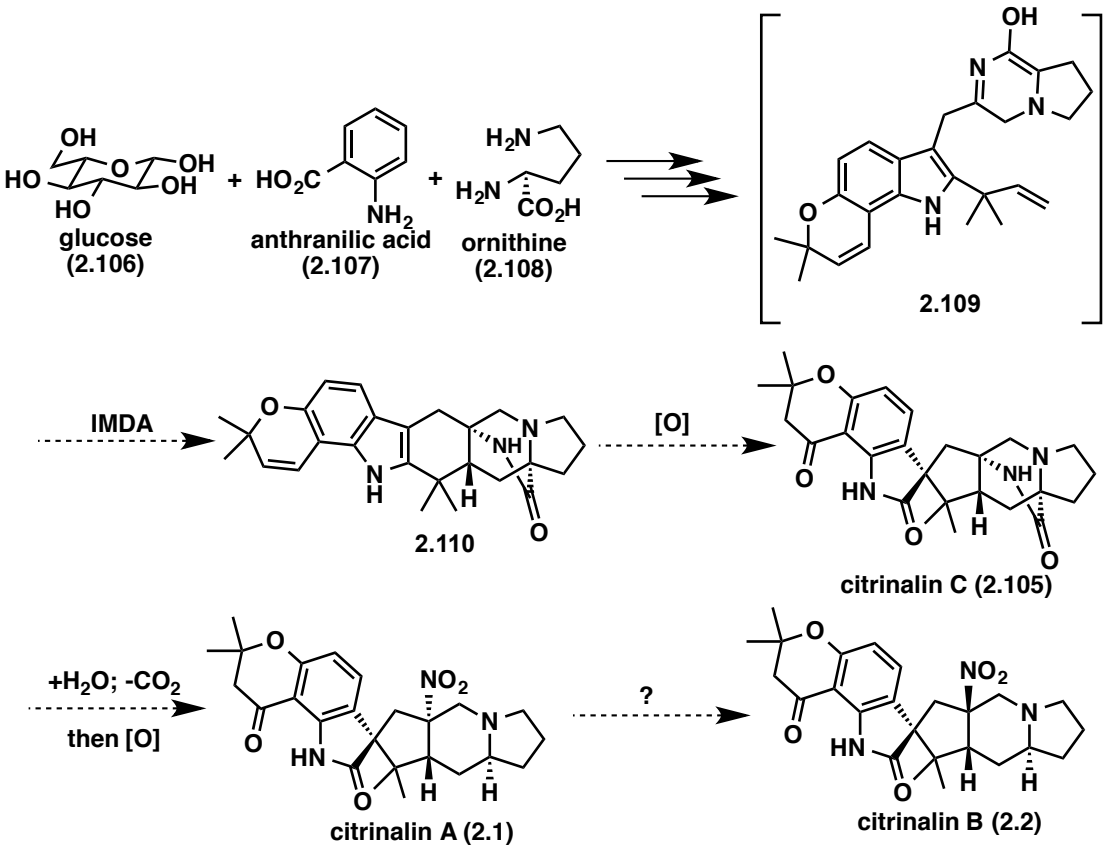

Scheme 2.28: Biosynthetic proposal for the citrinalins.

2.5.3: Conversion of Citrinalin A (2.1) to Citrinalin B (2.2).

A question that remained at this stage concerned the biogenesis of citrinalin B. On the basis of the observations of Steyn in the cyclopiamine series[9] (see **2.4** → **2.6**, Figure 2.1), we anticipated that citrinalin A (**2.1**) might be converted to citrinalin B (**2.2**) via a zwitterionic intermediate analogous to **2.5** (Figure 2.1). In the event, heating a solution of a naturally occurring sample of citrinalin A (**2.1**, Scheme 2.29, obtained from Berlinck and co-workers) in DMF-d_7 at 100 °C for 20 hours leads to a 1:1 ratio of **2.1** and **2.2** (with complete conversion to citrinalin B (**2.2**) after 60 hours, see Appendix 1 for ^{1}H NMR data), confirming the connection of these metabolites, presumably by the same aza-Henry/nitro-Mannich epimerization sequence established for the cyclopiamines by Steyn and coworkers (see proposed intermediate **2.111**).

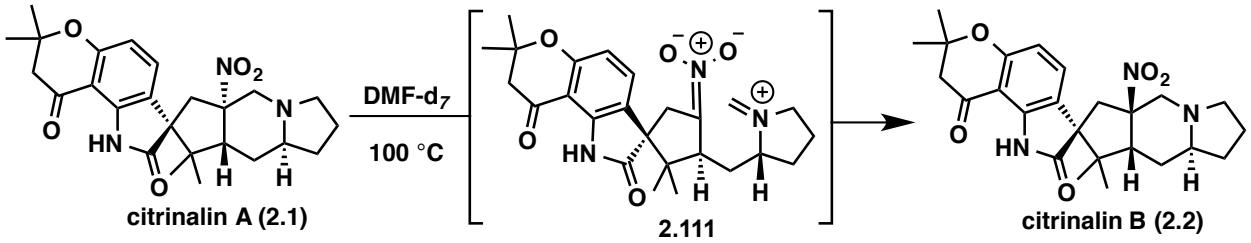

Scheme 2.29: Conversion of citrinalin A (**2.1**) to citrinalin B (**2.2**).

However, we have observed some key differences. First, the epimerization in the citrinalin series occurs at a qualitatively lower rate (likely due to a non-productive proton transfer from the vinylogous imide N–H to the tertiary amine) and higher temperature. In addition, we have not been able to achieve any observable conversion of *ent*-citrinalin B (*ent*-**2.2**) to *ent*-citrinalin A (*ent*-**2.1**) even at elevated temperatures (150 °C) over prolonged periods (24 h) (see Appendix 1 for more details). This observation may suggest that citrinalin B (**2.2**) is the thermodynamically favored diastereomer of this family. Our current efforts are focused on gaining a deeper understanding of these differences and exploring the biosynthetic conversion of citrinalin C to citrinalin A.

2.6 – Conclusion

We have achieved the first total syntheses of the prenylated indole alkaloids *ent*-citrinalin B (*ent*-**2.2**) and cyclopiamine B (**2.6**). Our results secure unambiguously the identity of citrinalin B both through synthesis, a reanalysis of the naturally isolated material, and by an X-ray crystallographic study. Our studies on the isolation of metabolites from *P. citrinum* support a bicyclo[2.2.2]diazaoctane-containing metabolite such as citrinalin C (**2.105**) as an intermediate in the biogenesis of citrinalins A (**2.1**) and B (**2.2**). The extension of the synthetic methods reported herein to the syntheses of other prenylated indole alkaloids such as those containing the bicyclo[2.2.2]diazaoctane is reported in Chapter 3.

2.7 – Experimental Contributors

All the work presented in section 2.2 – Initial Synthetic Studies on the Prenylated Indole Alkaloids is unpublished and was completed solely by Dr. Pablo Garcia-Reynaga (P.G.-R.) and its data is not included in section 2.8 – Experimental Methods with the exception of X-ray crystallographic data. The work presented in sections 2.3 – 2.4.4. was completed by P.G.-R. and Eduardo V. Mercado-Marin (E.V.M.-M.) and the work presented in sections 2.4.5 – 2.4.7. was completed by E.V.M.-M. Luis Angel Vazquez-Maldonado (L.A.V.-M.) (undergraduate, Amgen Scholars Program Summer 2013, Sarpong group) synthesized ~5 g of 6,6,5-tricycle **2.46** (see Scheme 2.10). Oxidation catalysts **2.77, 2.79-2.82** were provided by David K. Romney (D.K.R.) and Prof. Scott J. Miller (S.J.M.), who along with P.G.-R, E.V.M.-M. and Prof. Richmond Sarpong (R.S.) designed the oxidation studies of **2.58**, which were executed by P.G.-R. The computational NMR predictions for **2.1, 2.2** and **2.3** were designed and executed by Dr. Michael W. Lodewyk (M.W.L.) and Prof. Dean J. Tantillo (D.J.T.) with input from P.G.-R., E.V.M.-M. and R.S. Biosynthetic studies, sections 2.5.1 – 2.5.2, were designed and conducted by Stelamar

Romminger (S.R.), Eli F. Pimenta (E.F.P.) and Prof. Roberto G. S. Berlinck (R.G.S.B.) who also isolated and characterized **2.2**, **2.104**, and **2.105**. The conversion of citrinalin A (**2.1**) to citrinalin B (**2.2**), section 2.5.3, was carried out by E.V.M.-M with material supplied by R.G.S.B. David E. Williams (D.E.W.) and Raymond J. Andersen (R.J.A.) provided facilities and contributed to the purification, data analysis and structural analysis of **2.2**, **2.104**, and **2.105**. All data regarding the computational NMR predictions for **2.1**, **2.2** and **2.3** as well as the data on the isolation and characterization of **2.2**, **2.104**, and **2.105** are not included in section 2.8 – Experimental Methods. This data can be found in the Supporting Information for *Nature*, **2014**, *509*, 318–324. doi:10.1038/nature13273.

2.8 – Experimental Method and Procedure

2.8.1. General Experimental for the synthesis of compounds 2.2, 2.6, 2.43-2.101

Unless otherwise noted, all reactions were carried out under an atmosphere of nitrogen, and all reagents were purchased from commercial suppliers and used without further purification. All reactions were carried out in flame-dried glassware under a positive pressure of nitrogen in dry solvents using standard Schlenk techniques. Tetrahydrofuran (THF), diethyl ether (Et_2O), benzene, toluene (PhMe), methanol (MeOH) and triethylamine (Et_3N) were dried over alumina under an argon atmosphere in a GlassContour solvent system. Dichloromethane (CH_2Cl_2) was distilled over calcium hydride under a nitrogen atmosphere. All other solvents and reagents were used as received unless otherwise noted. Reaction temperatures above room temperature (RT), 23 °C, were controlled by an IKA® temperature modulator. Reactions were monitored by thin layer chromatography using SiliCycle silica gel 60 F254 precoated plates (0.25 mm) which were visualized using UV light (254 nm), *p*-anisaldehyde stain, $KMnO_4$ or CAM stain. Sorbtech silica gel (particle size 40-63 μm) was used for flash chromatography. Melting points were recorded on a Mel-Temp II Laboratory Devices, USA. Optical rotation was recorded on a Perkin Elmer Polarimeter 241 at the D line (1.0 dm path length). ^1H and ^{13}C NMR were recorded on Bruker AVB-400, AV-500, DRX-500 or AV-600 MHz spectrometers with ^{13}C operating frequencies of 100, 125, 125, and 150 MHz, respectively, in $CDCl_3$, DMF-d_7, $(CD_3)_2SO$ or C_6D_6 at 23 °C. Chemical shifts (δ) are reported in ppm relative to the residual solvent signal ($CDCl_3$ δ = 7.26 for ^1H NMR and δ = 77.16 for ^{13}C NMR; DMF-d_7 δ = 8.02 for ^1H NMR and δ = 163.15 for ^{13}C NMR; $(CD_3)_2SO$ δ = 2.50 for ^1H NMR and δ = 39.52 for ^{13}C NMR; C_6D_6 δ = 7.16 for ^1H NMR and δ = 128.06 for ^{13}C NMR). Data for ^1H NMR are reported as follows: chemical shift (multiplicity, coupling constant, number of hydrogens). Multiplicity is abbreviated as follows: s (singlet), d (doublet), t (triplet), q (quartet), m (multiplet), br (broad). IR spectra were recorded on a Nicolet MAGNA-IR 850 spectrometer and are reported in frequency of absorption (cm^{-1}). Mass spectral data were obtained from the Mass Spectral Facility at the University of California, Berkeley.

2.8.2. General Experimental for the synthesis of indole oxidation catalyst 2.77

Dichloromethane (CH_2Cl_2) was dried in a Seca Solvent Purification System by Glass Contour. Normal phase flash chromatography was performed using Dynamic Adsorbents silica gel (particle size 32-63 μm). Reversed phase chromatography used C-18 silica and was performed

on a Biotage Isolera One purification system. Products were analyzed by thin-layer chromatography using EMD Millipore silica gel 60 F254 precoated plates (0.25 mm thickness) and were visualized by irradiation with UV light (254 nm) or staining with $KMnO_4$. Optical rotation was recorded on a Perkin Elmer Polarimeter 341 at the D line (1.0 dm path length). ^1H and ^{13}C NMR were recorded on an Agilent DD2 600 MHz spectrometer, equipped with a cold probe, with a ^{13}C operating frequency of 150 MHz. Spectra were recorded in $CDCl_3$ at ambient temperature and chemical shifts (δ) are reported in ppm relative to the residual solvent signal ($CDCl_3$ δ = 7.26 for ^1H NMR and δ = 77.16 for ^{13}C NMR). Data for ^1H NMR are reported as follows: chemical shift (multiplicity, coupling constant, number of hydrogens). Multiplicity is abbreviated as follows: s (singlet), d (doublet), t (triplet), p (pentet), dt (doublet of triplets), td (triplet of doublets), m (multiplet). IR spectrum was recorded on a Nicolet 6700 FT-IR spectrometer and is reported in frequency of absorption (cm^{-1}). High resolution mass spectra were acquired from the Mass Spectrometry Facility at the Keck Center of Yale University.All reactions were performed at ambient temperature (21 °C). Boc-*trans*-4-benzyloxy-D-proline (Boc-DHyp(Bn)-OH) was prepared from Boc-*trans*-4-hydroxy-D-proline by a method reported in the literature.[56]

2.8.3. Experimental Procedures for Compounds 2.43-2.101.

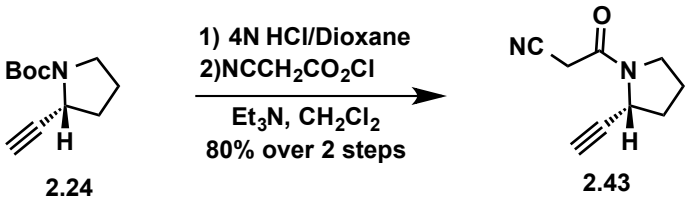

2.24 **2.43**

To a flask charged with known **(*R*)-*tert*-**butyl 2-ethynylpyrrolidine-1-carboxylate[57] (**2.24**) (500 mg, 2.56 mmol, 1.0 equiv) was added 4 N HCl/dioxane (12.8 mL, 51.2 mmol, 20.0 equiv) dropwise at 0 °C. The resulting brown mixture was stirred for 10 min at the same temperature then warmed to room temperature for 1 h. The solvent was removed *in vacuo* and excess HCl/dioxane was azeotroped off with diethyl ether (4 x 10 mL) then ethyl acetate (3 x 10 mL) then placed *in vacuo* overnight. The resulting beige crystals were suspended in dichloromethane (8.5 mL) and triethylamine (1.0 mL, 7.10 mmol, 2.77 equiv) was added drop-wise at 0 °C, followed by the drop-wise addition of cyanoacetylchloride (727 mg, 7.10 mmol, 2.77 equiv) as a solution in dichloromethane (2 mL). The resulting red solution was stirred at the same temperature for 2 h and then warmed to room temperature for 3 h, at which time saturated aqueous $NaHCO_3$ (10 mL) was added and volatiles removed *in vacuo*. The resulting aqueous solution was extracted with ethyl acetate (3 x 10 mL) and the combined organic extracts were dried over $MgSO_4$, filtered, and concentrated *in vacuo*. The resulting red oil was purified by silica gel chromatography (1:2 hexanes:ethyl acetate) to provide **2.43** (330 mg, 2.03 mmol, 80%) as a yellow solid. **m.p.** 88–89 °C; **TLC** (hexanes:EtOAc, 1:2 v/v): R_f=0.34; **^{1}H NMR** (600 MHz, $CDCl_3$, mixture of amide rotomers 1.4:1) δ = 4.75–4.60 (s, 0.4H), 4.52–4.38 (d, *J* = 6.4 Hz, 0.6H), 3.78–3.53 (m, 2H), 3.50–3.36 (m, 2H), 2.56–2.42 (m, 0.4H), 2.30–2.10 (m, 2H), 2.10–1.98 (m, 2H), 1.98–1.85 (m, 0.6H); **^{13}C NMR** (150 MHz, $CDCl_3$) δ = 160.4, 159.9, 114.0, 113.7, 82.1, 81.4, 73.4, 70.7, 48.4, 48.1, 46.7, 46.6, 34.0, 32.0, 25.8, 25.6, 24.6, 22.8; **IR** (NaCl, thin film) ν_{max}: 3276, 2955, 2883, 2262, 1655, 1437 cm^{-1}; **HRMS** (ESI) (*m/z*) $[M]^+$ calcd for $C_9H_{11}N_2O$, 163.0866; found, 163.0866.

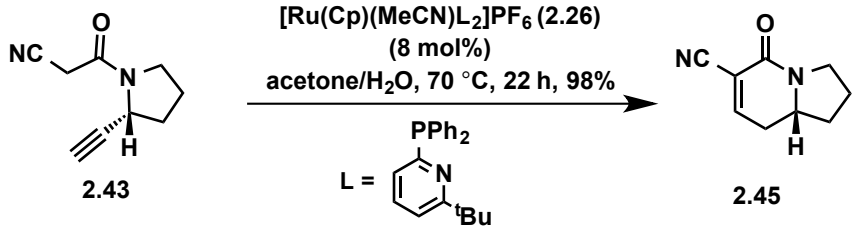

This procedure was adapted from a known procedure.[17] To a Schlenk flask charged with (*R*)-3-(2-ethynylpyrrolidin-1-yl)-3-oxopropanenitrile (**2.43**) (750 mg, 4.62 mmol, 1.0 eqiuv) and a stir bar in an inert atmosphere glovebox was added acetonitrilebis[2-diphenylphosphino-6-*t*-butylpyridine]cyclopentadienylruthenium(II) hexafluorophosphate (**2.26**, 367 mg, 0.370 mmol, 0.08 equiv). A degassed (via three cycles of freeze, pump, thaw) mixture of acetone (9.6 mL) and water (400 µL) was added under a nitrogen atmosphere via syringe. The resulting yellow solution was stirred at 70 °C for 22 h, at which time the reaction was diluted with ethyl acetate (10 mL) and concentrated *in vacuo*. The resulting yellow oil was purified by silica gel chromatography (1:4 hexanes:ethyl acetate) to yield **2.45** (732 mg, 4.53 mmol, 98%) as a yellow solid. **m.p.:** 85–87 °C; **TLC** (hexanes:EtOAc, 1:4 v/v); R_f=0.19; **^{1}H NMR** (600 MHz, $CDCl_3$) δ = 7.35–7.30 (dd, *J* = 6.8, 2.3 Hz, 1H), 3.80–3.72 (m, 1H), 3.68–3.61 (ddd, *J* = 12.0, 9.4, 2.3 Hz, 1H), 3.50–3.42 (m, 1H), 2.78–2.69 (m, 1H), 2.37–2.22 (m, 2H), 2.09–2.01 (m, 1H), 1.87–1.77 (m, 1H), 1.71–1.61 (m, 1H); **^{13}C NMR** (150 MHz, $CDCl_3$) δ = 157.1, 152.2, 114.6, 114.2, 55.8, 44.6, 33.2, 31.0, 22.7; **IR** (NaCl, thin film) ν_{max}: 3046, 2980, 2235, 1661, 1606 cm^{-1}; **HRMS** (ESI) (*m/z*) $[M]^+$ calcd for $C_9H_{11}N_2O$, 163.0866; found, 163.0865.

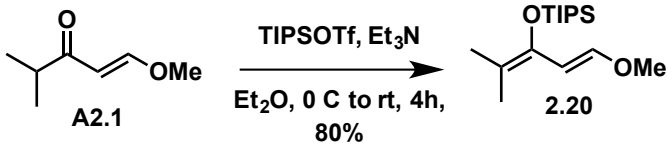

This procedure was adapted from a known procedure.[14] A solution of (*E*)-1-methoxy-4-methylpent-1-en-3-one[14] (**A2.1**) (2.00 g, 15.6 mmol, 1.0 equiv) in diethyl ether (78 mL) was cooled to 0 °C. Triethylamine (13.0 mL, 93.7 mmol, 6.00 equiv) was added quickly, followed by the drop-wise addition of triisopropylsilyl trifluoromethanesulfonate (8.4 mL, 31.2 mmol, 2.00 equiv). After 10 minutes the solution was warmed to room temperature and allowed to stir for an additional 4 h, at which point two distinct layers were formed. The viscous bottom layer was removed and the top layer was diluted with hexanes (50 mL). This solution was washed with saturated aqueous $NaHCO_3$ (1 x 100 mL), and the aqueous layer was extracted with diethyl ether (3 x 100 mL). The combined organic layers were washed with brine (1 x 200 mL), dried over Na_2SO_4, filtered and concentrated *in vacuo.* The crude orange oil was purified by filtration through a plug of silica gel (12 mL SiO_2, 100% pentanes) to yield **2.20** (3.55 g, 12.5 mmol, 80%) as a yellow oil. **TLC** (hexanes:EtOAc, 16:1 v/v); R_f=0.49; **^{1}H NMR** (600 MHz, $CDCl_3$) δ = 6.65 (d, *J* = 12.5 Hz, 1H), 5.54 (d, *J* = 12.5 Hz, 1H), 3.60 (s, 3H), 1.71 (s, 3H), 1.67 (s, 3H), 1.23–1.16 (m, 3H), 1.14–1.09 (m, 18H); **^{13}C NMR** (150 MHz, $CDCl_3$) δ = 149.4, 140.8, 110.4, 101.4, 56.4, 19.4, 18.6, 18.1, 13.7; **IR** (NaCl, thin film) ν_{max}: 2946, 2360, 1717, 1656 cm^{-1}; **HRMS** (ESI) (*m/z*) $[M]^+$ calcd for $C_{16}H_{33}O_2Si$, 285.2244; found, 285.2248

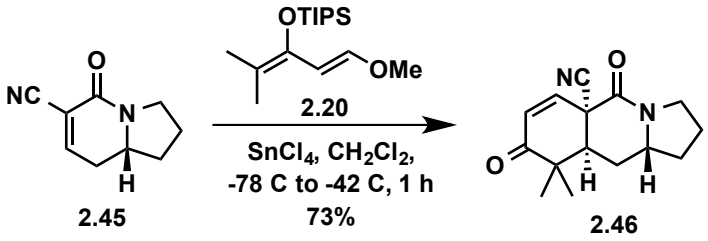

A round-bottom flask charged with (*R*)-5-oxo-1,2,3,5,8,8a-hexahydroindolizine-6-carbonitrile (**2.45**) (2.09 g, 12.9 mmol, 1.00 equiv), (*E*)-triisopropyl((1-methoxy-4-methylpenta-1,3-dien-3-yl)oxy)silane (**2.20**) (7.35 g, 25.8 mmol, 2.00 equiv) and dichloromethane (130 mL) was cooled to –78 °C. Tin tetrachloride (1.0 M in CH_2Cl_2, 15.5 mL, 15.5 mmol, 1.20 equiv) was added dropwise, and the solution was immediately warmed to –42 °C. After 30 minutes the solution was warmed to room temperature and stirred for 15 minutes, after which time saturated aqueous $NaHCO_3$ (130 mL) was slowly added. The resulting mixture was stirred vigorously for 1 h then vacuum filtered through a fritted funnel and the volatiles removed *in vacuo*. The aqueous layer was extracted with ethyl acetate (3 x 150 mL), and the combined organic extracts were dried over Na_2SO_4, filtered and concentrated *in vacuo*. The brown oil was purified by silica gel chromatography (1:2 hexanes:ethyl acetate) to yield **2.46** (2.42 g, 9.37 mmol, 73%) as a yellow solid. **m.p.:** 113–115 °C; **TLC** (hexanes:EtOAc, 1:4 v/v); R_f=0.38; **^{1}H NMR** (400 MHz, $CDCl_3$) δ = 6.78 (d, *J* = 10.0 Hz, 1H), 6.21 (d, *J* = 10.0 Hz, 1H), 3.75–3.61 (m, 1H), 3.55–3.42 (m, 2H), 2.78 (dd, *J* = 7.9, 2.4 Hz, 1H), 2.29 (ddd, *J* = 14.8, 4.3, 2.4 Hz, 1H), 2.24–2.15 (m, 1H), 2.07–1.97 (m, 1H), 1.91 (ddd, *J* = 14.8, 11.6, 7.9 Hz, 1H), 1.86–1.75 (m, 1H), 1.60–1.46 (m, 1H), 1.44 (s, 3H), 1.19 (s, 3H); **^{13}C NMR** (150 MHz, $CDCl_3$) δ = 200.5, 161.4, 138.3, 129.7, 118.2, 55.7, 46.2, 45.9, 45.4, 45.3, 34.1, 30.0, 25.3, 22.4, 22.3; **IR** (NaCl, thin film) ν_{max}: 2976, 2887, 2359, 2341, 1675, 1568, 1443 cm^{-1}; **HRMS** (ESI) (*m/z*) $[M]^+$ calcd for $C_{15}H_{19}O_2N_2$, 259.1441; found, 259.1444.

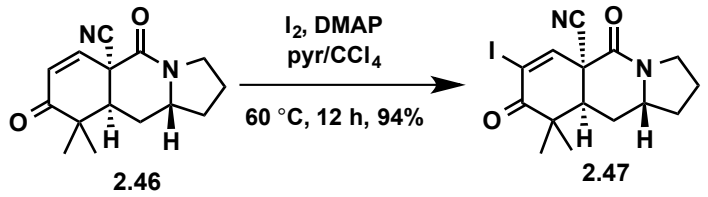

Iodine (383 mg, 1.51 mmol, 3.00 equiv) and 4-dimethylaminopyridine (185 mg, 1.51 mmol, 3.00 equiv) were added sequentially to a solution of (5a*R*,9a*S*,10a*R*)-9,9-dimethyl-5,8-dioxo-1,2,3,5,5a,8,9,9a,10,10a-decahydropyrrolo[1,2-*b*]isoquinoline-5a-carbonitrile (**2.46**) (130 mg, 0.503 mmol, 1.00 equiv) in a mixture of pyridine (0.63 mL) and CCl_4 (0.63 mL). The resulting dark brown mixture was stirred at 60 ºC in the dark for 12 h and then cooled to room temperature. The reaction mixture was poured into saturated aqueous $Na_2S_2O_3$ (60 mL) and the aqueous layer was extracted with 50% EtOAc/Hex (5 x 40 mL). The combined organic extracts were dried with Na_2SO_4, filtered and concentrated *in vacuo*. Purification of the resulting residue by flash chromatography (4:1 to 1:1 hexanes:ethyl acetate), using 10 mL silica gel, afforded **2.47** (179 mg, 0.466 mmol, 93%) as a colorless foam. **TLC** (hexanes:EtOAc, 1:4 v/v); R_f=0.54; **^{1}H NMR** (500 MHz, $CDCl_3$) δ = 7.49 (s, 1H), 3.72–3.61 (m, 1H), 3.56–3.46 (m, 1H), 3.45–3.36 (m, 1H), 2.83 (dd, *J* = 8.0, 2.1 Hz, 1H), 2.33–2.14 (m, 2H), 2.08–1.97 (m, 1H), 1.95–1.76 (m, 2H), 1.58–1.51

(m, 1H), 1.49 (s, 3H), 1.24 (s, 3H); **^{13}C NMR** (150 MHz, $CDCl_3$) δ = 194.8, 160.3, 145.0, 117.2, 105.5, 55.6, 48.7, 46.4, 46.0, 45.6, 34.2, 30.1, 25.8, 23.0, 22.5; **IR** (NaCl, thin film) ν_{max}: 2976, 1692, 1678, 1666, 1659, 1442, 1110, 736; **HRMS**-ESI calcd for $C_{15}H_{18}N_2O_2I$ ($[M+H]^+$): 385.0408, found 385.0407.

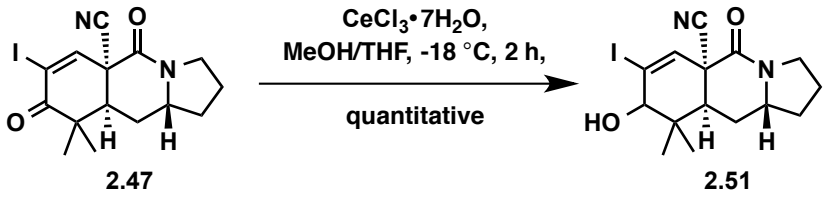

2.47 2.51

Cerium chloride heptaphydrate (645 mg, 1.73 mmol, 1.50 equiv) was added in one portion to a stirring solution of the (5a*S*,9a*S*,10a*R*)-7-iodo-9,9-dimethyl-5,8-dioxo-1,2,3,8,9,9a,10,10a-octahydropyrrolo[1,2-*b*]isoquinoline-5a(5*H*)-carbonitrile (**2.47**) (442 mg, 1.15 mmol, 1.00 equiv) in a mixture of THF (4.8 mL) and MeOH (24 mL). The resulting mixture was cooled to –18 ºC and stirred for 5 min, after which $NaBH_4$ (43.5 mg, 1.15 mmol, 1.00 equiv) was added portion-wise over 1 minute. The reaction mixture was allowed to stir at –18 ºC for 2 h and then poured into saturated aq. NH_4Cl (150 mL). The aqueous layer was extracted with EtOAc (3 x 100 mL). The combined organic extracts were dried with Na_2SO_4, filtered and concentrated in vacuo. Purification of the resulting residue by flash chromatography (20% EtOAc/Hex to 50% EtOAc/Hex), using 5 mL silica gel, afforded **2.51** (445 mg, 1.15 mmol, quantitative) as a colorless foam and a ca. 9:1 mixture of diastereomers. **^{1}H NMR** (500 MHz, CDCl3, major diastereomer**)**) δ = 6.62 (s, 1H), 3.90-3.82 (m, 1H), 3.70-3.59 (m, 2H), 3.50-3.37 (m, 1H), 2.54-2.45 (m, 1H), 2.44 (dd, J = 7.86, 1.64 Hz, 1H), 2.34-2.25 (m, 1H), 2.22-2.11 (m, 1H), 2.04-1.91 (m, 1H), 1.88-1.67 (m, 2H), 1.53-1.41 (m, 1H), 1.28 (s, 3H), 1.08 (s, 3H); **^{13}C NMR** (150 MHz, CDCl3, major diastereomer) δ = 161.6, 130.6, 118.7, 110.3, 78.2, 55.7, 48.1, 46.2, 44.2, 38.9, 34.1, 29.6, 27.2, 22.5; **IR** (film, cm^{-1}) ν_{max}: 3419, 2966, 2925, 2876, 1652, 1446; **HRMS**-ESI calcd for $C_{15}H_{20}N_2O_2I$ ($[M+H]^+$): 387.0564; found 387.0563.

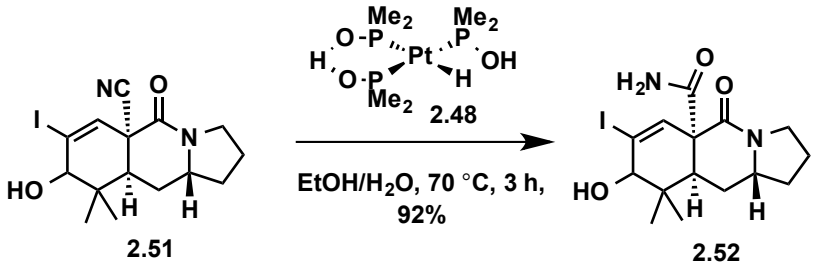

2.51 2.52

$(Me_2POH)_2Pt(H)(Me_2PO)$[28] (**2.48**) (20.0 mg, 0.0466 mmol, 0.10 equiv) was added in one portion to a solution of (5a*S*,9a*S*,10a*R*)-8-hydroxy-7-iodo-9,9-dimethyl-5-oxo-1,2,3,8,9,9a,10,10a-octahydropyrrolo[1,2-*b*]isoquinoline-5a(5*H*)-carbonitrile (**2.51**) (180 mg, 0.466 mmol, 1.00 equiv) in a mixture of H_2O (0.93 mL) and EtOH (3.73 mL). The resulting suspension was stirred at 70 ºC for 3 h and then cooled to room termperature. The reaction mixture was subsequently diluted with CH_2Cl_2, loaded directly on to a short column containing silica (1 mL) and anhydrous Na_2SO_4 (1 mL) and the column eluted with 10% MeOH/CH_2Cl_2. The fractions containing the product were collected and concentrated in vacuo to yield **2.52** (174 mg, 0.43 mmol, 92%) as an off-white crystalline solid. **^{1}H NMR** (500 MHz, 1:1 $CDCl_3$/CD_3OD, major diastereomer) δ =

6.47 (s, 1H), 3.42 (s, 1H), 3.40–3.27 (m, 2H), 3.14 3.02 (m, 1H), 2.49–2.39 (m, 1H), 2.09–2.00 (m, 1H), 1.87–1.77 (m, 1H), 1.75–1.63 (m, 1H), 1.58–1.45 (m, 1H), 1.34–1.24 (m, 1H), 1.09–0.98 (m, 1H), 0.84 (s, 3H), 0.63 (s, 3H); **^{13}C NMR** (150 MHz, 1:1 $CDCl_3/CD_3OD$, major diastereomer) δ = 171.2, 167.7, 135.0, 111.4, 76.6, 58.4, 56.5, 44.8, 41.0, 38.6, 33.7, 29.1, 26.6, 24.4, 21.6; **IR** (film, cm^{-1}) ν_{max}: 3274, 2918, 1658; **HRMS**-ESI calcd for $C_{15}H_{22}N_2O_3I$ ($[M+H]^+$): 405.0670; found 405.0669.

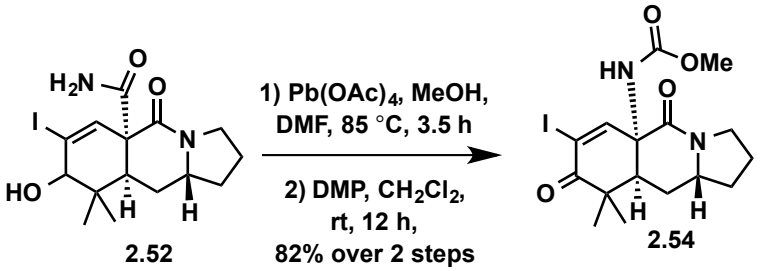

$Pb(OAc)_4$ (2.29 g, 5.17 mmol, 6.63 equiv) was added in one portion to a solution of (5a*S*,9a*S*,10a*R*)-8-hydroxy-7-iodo-9,9-dimethyl-5-oxo-1,2,3,8,9,9a,10,10a-octahydropyrrolo[1,2-*b*]isoquinoline-5a(5*H*)-carboxamide (**2.52**) (348 mg, 0.861 mmol, 1.00 equiv) in MeOH (2.09 mL) and N,N-dimethylformamide (17.2 mL). The resulting orange mixture was stirred at 85 ºC for 3.5 h and then cooled to room temperature. The resulting reaction mixture was poured into saturated aq. $NaHCO_3$ (120 mL) and the aqueous layer extracted with EtOAc (3x 100 mL). The combined organic extracts were dried with Na_2SO_4, filtered and concentrated in vacuo. Purification of the resulting residue by flash chromatography (2% $MeOH/CH_2Cl_2$ to 5% $MeOH/CH_2Cl_2$), using 5 mL silica yielded the methyl carbamate as a yellow oil, which was used directly in the next step. The above alcohol was dissolved in CH_2Cl_2 (17.2 mL) and stirred at room temperature. Dess-Martin periodinane (730 mg, 1.72 mmol, 2.00 equiv) was then added portion-wise over 1 min and the resulting mixture stirred at room temperature overnight. After 12 h, the reaction mixture was poured into saturated aq. $Na_2S_2O_3$ (60 mL) and saturated aq. $NaHCO_3$ (60 mL). The aqueous layer was extracted with EtOAc (3 x 100 mL) and the combined organic extracts dried with Na_2SO_4, filtered and concentrated in vacuo. Purification of the resulting residue by flash chromatography (50% EtOAc/Hex to 80% EtOAc/Hex to 100% EtOAc/Hex), using 5 mL silica yielded **2.54** (305 mg, 0.706 mmol, 82%) as a colorless foam. **^{1}H NMR** (500 MHz, $CDCl_3$) δ = 7.15 (s, 1H), 5.20 (s, 1H), 3.71 (s, 3H), 3.63–3.55 (m, 1H), 3.50–3.41 (m, 1H), 3.23–3.13 (m, 1H), 3.10–3.01 (m, 1H), 2.21–2.14 (m, 1H), 2.14–2.07 (m, 1H), 1.99–1.90 (m, 1H), 1.85–1.70 (m, 2H), 1.51–1.43 (m, 1H), 1.39 (s, 3H), 1.24 (s, 3H); **^{13}C NMR** (150 MHz, $CDCl_3$) δ = 197.4, 166.3, 156.5, 149.6, 108.1, 104.9, 67.8, 62.5, 55.2, 52.6, 46.6, 45.0, 34.1, 30.9, 29.4, 23.8, 23.0; **IR** (NaCl, thin film) ν_{max}: 3294, 2972, 1725, 1692, 1658, 1624, 1109; **HRMS**-ESI calcd for $C_{16}H_{21}N_2O_4I$ ($[M+H]^+$): 433.0619, found 433.0620.

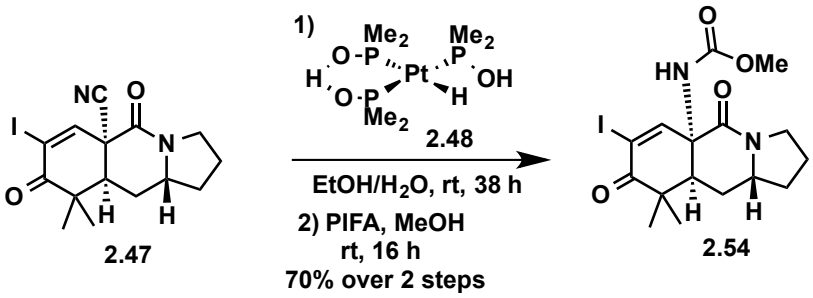

$(Me_2POH)_2Pt(H)(Me_2PO)$[28] (**2.48**) (208 mg, 0.484 mmol, 0.20 equiv) was added in one portion to a solution of (5a*S*,9a*S*,10a*R*)-7-iodo-9,9-dimethyl-5,8-dioxo-1,2,3,5,5a,8,9,9a,10,10a-decahydropyrrolo[1,2-*b*]isoquinoline-5a-carbonitrile (**2.47**) (930 mg, 2.42 mmol, 1.0 equiv) in a mixture of H_2O (2.42 mL) and EtOH (9.68 mL). The resulting suspension was stirred at room temperature for 38 h. The reaction mixture was subsequently diluted with CH_2Cl_2 and passed through a short column containing silica and anhydrous Na_2SO_4. Further purification of the filtrate via silica gel chromatography (2% to 10% MeOH/CH_2Cl_2), using 40 mL silica gave the carboxamide as a creamy orange foam, which was used in the next step without further purification. The carboxamide prepared above was dissolved in MeOH (24 mL) and the flask was placed in a room temperature water bath. [Bis(trifluoroacetoxy)iodo]benzene (PIFA) (1.24 g, 2.88 mmol, 1.20 equiv) was added in one portion and the mixture stirred at room temperature for 16 h. The reaction mixture was subsequently poured into saturated aqueous $NaHCO_3$ (60 mL) and the aqueous layer was extracted with EtOAc (3 x 100 mL). The combined organic extracts were dried with Na_2SO_4, filtered and concentrated *in vacuo*. Purification of the resulting residue by flash chromatography (2% to 5% MeOH/CH_2Cl_2), using 40 mL silica, gave **2.54** (730 mg, 1.69 mmol, 70%, 2 steps) as an orange foam. **TLC** (hexanes:EtOAc, 1:4 v/v); R_f=0.40. The spectral data of this material matched that for the compound prepared via the route reported previously.

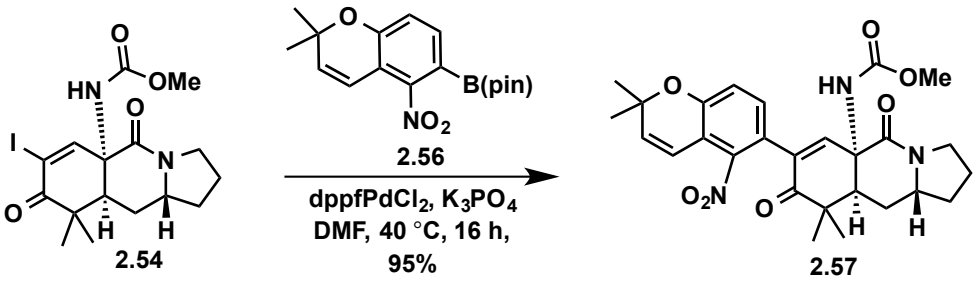

A flask was charged with methyl ((5a*R*,9a*S*,10a*R*)-7-iodo-9,9-dimethyl-5,8-dioxo-1,2,3,5,5a,8,9,9a,10,10a-decahydropyrrolo[1,2-*b*]isoquinolin-5a-yl)carbamate (**2.54**) (659 mg, 1.53 mmol, 1.00 equiv), 2-(2,2-dimethyl-5-nitro-2*H*-chromen-6-yl)-4,4,5,5-tetramethyl-1,3,2-dioxaborolane[20a] (**2.56**) (760 mg, 2.29 mmol, 1.50 equiv), dppfPdCl$_2$ (125 mg, 0.153 mmol, 0.10 equiv) and K_3PO_4 (1.22 g, 5.74 mmol, 3.75 equiv). *N,N*-dimethylformamide (15.3 mL) was added and the mixture degassed by purging with N_2 (3x). The resulting brown mixture was stirred at 40 ºC. After 16 h, the reaction mixture was cooled to room temperature, poured into saturated aqueous NH_4Cl (120 mL) and the aqueous layer extracted with EtOAc (3 x 100 mL). The combined organic extracts were dried with Na_2SO_4, filtered and concentrated *in vacuo*. Purification of the resulting residue by flash chromatography (4:1 to 1:4 hexanes:ethyl acetate),

using 100 mL silica yielded **2.57** (739 mg, 1.45 mmol, 95%) as a brown foam. **TLC** (hexanes:EtOAc, 1:4 v/v); R_f=0.19; **^{1}H NMR** (500 MHz, $CDCl_3$) δ = 6.91 (d, *J* = 8.3 Hz, 1H), 6.87 (d, *J* = 8.3 Hz, 1H), 6.42 (s, 1H), 6.38 (d, *J* = 10.2 Hz, 1H), 5.82 (d, *J* = 10.2 Hz, 1H), 5.48 (s, 1H), 3.70 (s, 3H), 3.63–3.54 (m, 1H), 3.53–3.43 (m, 1H), 3.35–3.21 (m, 1H), 3.02–2.93 (m, 1H), 2.23–2.15 (m, 1H), 2.14–2.05 (m, 1H), 1.98–1.89 (m, 1H), 1.85–1.72 (m, 2H), 1.50–1.44 (m, 1H), 1.45 (s, 6H), 1.43 (s, 3H), 1.19 (s, 3H); **^{13}C NMR** (150 MHz, $CDCl_3$) δ = 201.3, 167.3, 156.9, 154.2, 146.9, 139.9, 136.6, 134.4, 131.0, 121.4, 119.4, 116.6, 114.7, 77.0, 60.0, 55.0, 52.5, 46.6, 46.3, 44.5, 34.1, 31.5, 29.9, 27.9, 23.2, 23.0; **IR** (NaCl, thin film) ν_{max}: 2975, 1725, 1652, 1530, 1361, 1281; **HRMS**-ESI calcd for $C_{27}H_{31}N_3O_7Na$ ($[M+Na]^+$): 532.2054, found 532.2052.

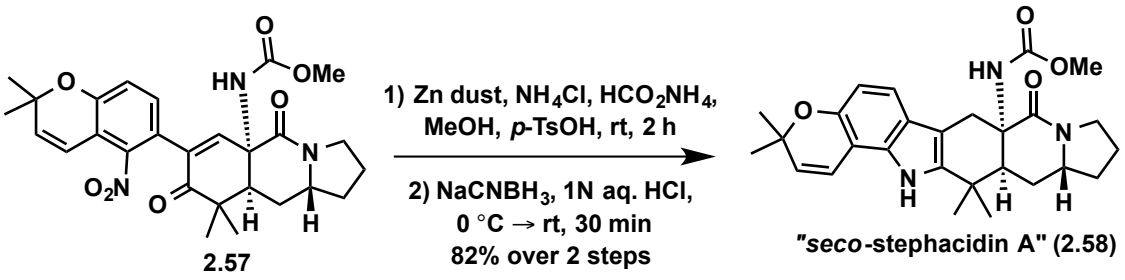

Zinc dust was freshly activated by sequential washing with 0.1 M aq. HCl (3 x 10 mL) and H_2O (10 mL). The solid was collected by filtration and washed with EtOH (2 x 10 mL) and Et_2O (2 x 10 mL), then dried under high vacuum to give a soft blue-gray solid, which was ground to a powder. A separate flask was charged with methyl ((5a*S*,9a*S*,10a*R*)-7-(2,2-dimethyl-5-nitro-2*H*-chromen-6-yl)-9,9-dimethyl-5,8-dioxo-1,2,3,5,5a,8,9,9a,10,10a-decahydropyrrolo[1,2-*b*]isoquinolin-5a-yl)carbamate (**2.57**) (120 mg, 0.236 mmol), NH_4Cl (25.2 mg, 0.472 mmol, 2.00 equiv), HCO_2NH_4 (74.4 mg, 1.18 mmol, 5.00 equiv) and *p*-TsOH·H_2O (449 mg, 2.36 mmol, 10.0 equiv). MeOH (47 mL) was then added and the mixture stirred at room temperature for 5 minutes to ensure complete dissolution of all salts. The above activated zinc dust (77.0 mg, 1.18 mmol, 5.00 equiv) was then added in one portion and the mixture stirred rapidly at room temperature. After 1 h, more NH_4Cl (25.2 mg, 0.472 mmol, 2.00 equiv), HCO_2NH_4 (74.4 mg, 1.18 mmol, 5.00 equiv) and activated zinc dust (77.0 mg, 1.18 mmol, 5.00 equiv) were added sequentially and the reaction mixture stirred at room temperature another 1 h. The reaction mixture above was cooled to 0 ºC and adjusted to pH 2 by the addition of 1 M aq. HCl. $NaCNBH_3$ (29.7 mg, 0.472 mmol, 2.00 equiv) was added in one portion at 0 ºC and allowed to stir at room temperature for 30 min. The resulting reaction mixture was subsequently quenched by the addition of saturated aqueous $NaHCO_3$ (60 mL), at which point the MeOH was removed *in vacuo*. The resulting aqueous mixture was extracted with EtOAc (3 x 30 mL) and the combined organic extracts dried with Na_2SO_4, filtered and concentrated *in vacuo*. Purification of the resulting residue by flash chromatography (1% MeOH/CH_2Cl_2 to 5% MeOH/CH_2Cl_2), using 20 mL silica afforded **2.58** (90.4 mg, 195 μmol, 83%) as an off-white foam. **TLC** (MeOH:CH_2Cl_2, 1:19 v/v); R_f=0.15; **^{1}H NMR** (500 MHz, $CDCl_3$) δ = 7.71 (s, 1H), 7.12 (d, *J* = 8.4 Hz, 1H), 6.66 (d, *J* = 8.4 Hz, 1H), 6.60 (d, *J* = 9.7 Hz, 1H), 5.69 (d, *J* = 9.7 Hz, 1H), 4.93 (s, 1H), 4.02–3.92 (m, 1H), 3.61 (s, 3H), 3.55–3.47 (m, 1H), 3.33–3.24 (m, 1H), 3.14–3.02 (m, 2H), 2.81 (d, *J* = 16.7 Hz, 1H), 2.15–2.04 (m, 1H), 2.04–1.87 (m, 3H), 1.85–1.74 (m, 1H), 1.74–1.63 (m, 1H), 1.48 (s, 3H), 1.46 (s, 6H), 1.34 (s, 3H); **^{13}C NMR** (150 MHz, $CDCl_3$) δ = 170.8, 156.4,

148.7, 138.6, 132.7, 129.9, 121.9, 117.8, 117.3, 110.3, 105.3, 102.7, 75.7, 59.6, 54.7, 52.0, 44.8, 39.4, 34.5, 33.2, 30.1, 28.7, 28.1, 27.5, 27.3, 25.5, 22.0; **IR** (NaCl, thin film) ν_{max}: 3311, 1718, 1639, 1507, 1457, 1267, 1188, 1119, 754; **HRMS**-ESI calcd for $C_{27}H_{34}N_3O_4$ ($[M+H]^+$): 464.2544, found 464.2543.

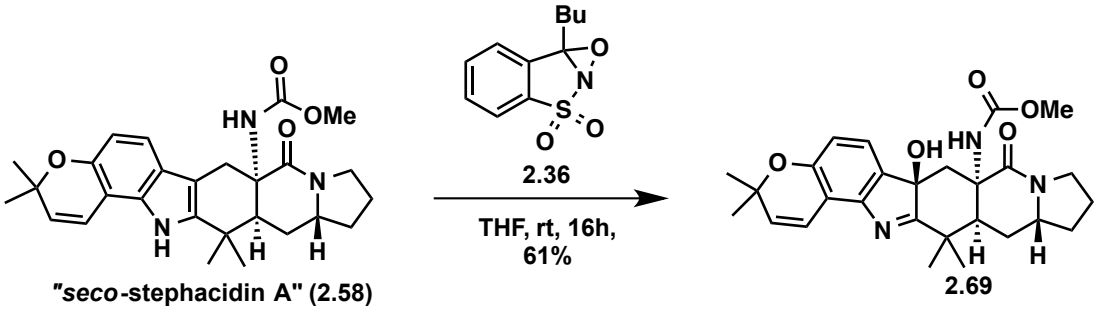

A solution of known saccharin-derived oxaziridine[36] (**2.36**) (177 mg, 0.738 mmol, 3.00 equiv) in THF (6.2 mL) was added drop-wise to a stirring solution of methyl ((7a*S*,12a*R*,13a*S*)-3,3,14,14-tetramethyl-8-oxo-3,7,7a,8,10,11,12,12a,13,13a,14,15-dodecahydroindolizino[6,7-*h*]pyrano[3,2-*a*]carbazol-7a-yl)carbamate (**2.58**) (114 mg, 0.246 mmol, 1.00 equiv) in THF (6.2 mL). The reaction mixture was stirred at room temperature for 16 h. Solvent was removed *in vacuo* at ambient temperature (25 ºC). Purification of the crude mixture by silica gel chromatography (1% MeOH/CH_2Cl_2 to 2% MeOH/CH_2Cl_2 to 5% MeOH/CH_2Cl_2), using 10 mL silica, afforded **2.69** (71.9 mg, 0.150 mmol, 61%) as an orange oil. **TLC** (MeOH:CH_2Cl_2, 1:19 v/v); R_f=0.18; **^{1}H NMR** (600 MHz, $CDCl_3$) δ = 7.06 (d, *J* = 7.9 Hz, 1H), 6.96 (d, *J* = 9.8 Hz, 1H), 6.55 (d, *J* = 7.9 Hz, 1H), 5.69 (d, *J* = 9.8 Hz, 1H), 4.84 (s, 1H), 3.87–3.72 (m, 2H), 3.49 (s, 3H), 3.42–3.30 (m, 1H), 3.30 (d, *J* = 14.5 Hz, 1H), 3.18 (s, 1H), 3.04–2.95 (m, 1H), 2.35–2.24 (m, 1H), 2.20–2.05 (m, 3H), 2.01–1.95 (m, 2H), 1.88–1.74 (m, 1H), 1.50 (s, 3H), 1.49 (s, 3H), 1.43 (s, 3H), 1.41 (s, 3H); **^{13}C NMR** (150 MHz, $CDCl_3$) δ = 188.9, 168.9, 155.1, 154.3, 149.0, 133.7, 131.3, 121.3, 118.2, 114.9, 113.2, 82.1, 76.3, 59.2, 57.5, 52.0, 46.3, 45.3, 42.0, 40.7, 34.5, 28.0, 27.9, 27.9, 25.7, 23.3, 22.4; **IR** (NaCl, thin film) ν_{max}: 3313, 2973, 1725, 1635, 1459, 1246, 1112, 752; **HRMS**-ESI calcd for $C_{27}H_{34}N_3O_5$ ($[M+H]^+$): 480.2493, found 480.2492.

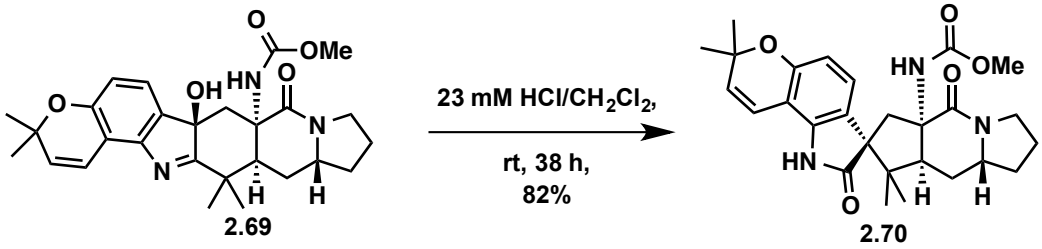

A flask was charged with methyl ((6b*R*,7a*S*,12a*R*,13a*S*)-6b-hydroxy-3,3,14,14-tetramethyl-8-oxo-3,6b,7,7a,8,10,11,12,12a,13,13a,14-dodecahydroindolizino[6,7-*h*]pyrano[3,2-*a*]carbazol-7a-yl)carbamate (**2.69**) (75.0 mg, 0.156 mmol, 1.00 equiv). 23 mM HCl/CH_2Cl_2 (15.6 mL, prepared from AcCl/MeOH) was added and the resulting pale yellow solution was allowed to stir at room temperature for 38 h. Solvent was subsequently removed *in vacuo* and the resulting residue

purified by silica gel chromatography (1% MeOH/CH_2Cl_2 to 2% MeOH/CH_2Cl_2 to 5% MeOH/CH_2Cl_2), using 10 mL silica. The fractions containing the product were concentrated *in vacuo* to yield **2.70** (61.3 mg, 0.128 mmol, 82%) as a pale brown solid. X-ray quality crystals were obtained from slow evaporation of a concentrated solution in 5% MeOH/CH_2Cl_2. **m.p**.: 305–307 ºC (decomp). **TLC** (MeOH:CH_2Cl_2, 1:19 v/v); R_f=0.15; **^{1}H NMR** (500 MHz, $CDCl_3$) δ = 8.25 (s, 1H), 7.34 (d, *J* = 8.3 Hz, 1H), 6.46 (d, *J* = 8.3 Hz, 1H), 6.31 (d, *J* = 9.8 Hz, 1H), 5.69 (d, *J* = 9.8 Hz, 1H), 5.56 (s, 1H), 3.84–3.68 (m, 2H), 3.65 (s, 3H), 3.49–3.39 (m, 1H), 2.99–2.91 (m, 2H), 2.55–2.42 (m, 1H), 2.18–2.08 (m, 1H), 2.07–1.95 (m, 3H), 1.89–1.73 (m, 1H), 1.66–1.51 (m, 1H), 1.47 (s, 3H), 1.42 (s, 3H), 1.22 (s, 3H), 0.74 (s, 3H); **^{13}C NMR** (150 MHz, 20% CD_3OD-$CDCl_3$) δ = 180.2, 171.0, 157.0, 152.5, 137.0, 130.7, 126.5, 123.9, 116.6, 109.4, 105.5, 76.1, 62.6, 61.5, 57.7, 55.4, 52.1, 51.3, 47.0, 45.6, 34.7, 27.9, 27.4, 26.5, 25.6, 23.2, 22.5; **IR** (NaCl, thin film) ν_{max}: 2967, 1729, 1688, 1457, 1250; **HRMS**-ESI calcd for $C_{27}H_{34}N_3O_5$ ($[M+H]^+$): 480.2493, found 480.2493.

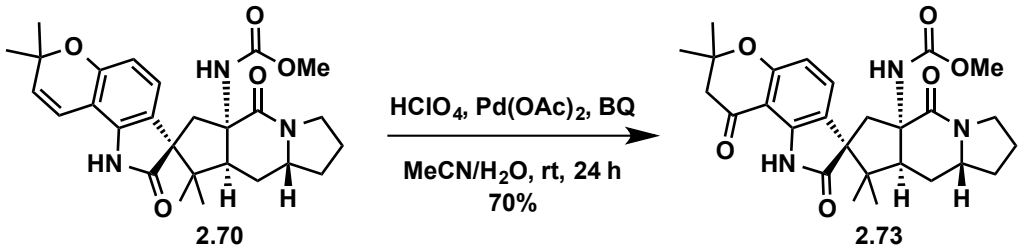

A flask was charged with $Pd(OAc)_2$ (7.49 mg, 0.0334 mmol, 0.40 equiv) and *p*-benzoquinone (BQ) (13.5 mg, 0.125 mmol, 1.50 equiv, recrystallized from CH_2Cl_2/Hex). The flask was fitted with a septum, purged with N_2 (3x) and then MeCN (2.0 mL) and H_2O (0.61 mL) was added via syringe to give an orange solution. $HClO_4$ (86.0 μL, 70% in H_2O) was then added via syringe and the resulting pale yellow solution was stirred at room temperature for 5 min. In a separate flask, methyl ((5a*S*,7*S*,8a*S*,9a*R*)-7',7',8,8-tetramethyl-2',5-dioxo-1',2,3,7',8,8a,9,9a-octahydro-1*H*,2'*H*,5*H*-spiro[cyclopenta[*f*]indolizine-7,3'-pyrano[2,3-*g*]indol]-5a(6*H*)-yl)carbamate (**2.70**) (40 mg, 0.0834 mmol, 1.0 equiv) was dissolved in MeCN (2.0 mL) under an N_2 atmosphere. To this was added, drop-wise, the catalyst-containing solution prepared above and the resulting dark red mixture was stirred at room temperature. After 12 h, TLC analysis indicated remaining starting material, therefore additional $Pd(OAc)_2$ ((7.49 mg, 0.0334 mmol, 0.40 equiv) was added. After another 12 h, TLC analysis indicated complete consumption of starting material. The resulting dark brown reaction mixture was poured into saturated aqueous $NaHCO_3$ (5.0 mL) and the aqueous layer extracted with EtOAc (3 x 5.0 mL). The combined organic extracts were dried with Na_2SO_4, filtered and concentrated *in vacuo*. Purification of the resulting residue by flash chromatography (1% MeOH/CH_2Cl_2 to 2% MeOH/CH_2Cl_2 to 5% MeOH/CH_2Cl_2), using 5.0 mL silica, afforded **2.73** (29 mg, 0.0585 mmol, 70%) as a orange-brown oil. **TLC** (MeOH:CH_2Cl_2, 1:9 v/v); R_f=0.40; **^{1}H NMR** (600 MHz, $CDCl_3$) δ = 9.43 (s, 1H), 7.67 (d, *J* = 8.5 Hz, 1H), 6.52 (d, *J* = 8.5 Hz, 1H), 5.49 (s, 1H), 3.79 (dt, *J* = 11.4, 6.4 Hz, 1H), 3.73 – 3.68 (m, 1H), 3.66 (s, 3H), 3.42 (ddd, *J* = 12.3, 9.7, 2.0 Hz, 1H), 2.95 – 2.87 (m, 2H), 2.74 (d, *J* = 16.7 Hz, 1H), 2.67 (d, *J* = 16.7 Hz, 1H), 2.45 (td, *J* = 13.3, 7.3 Hz, 1H), 2.13 (dt, *J* = 11.7, 5.8 Hz, 1H), 2.05 – 1.96 (m, 3H), 1.84 – 1.76 (m, 1H), 1.59 – 1.53 (m, 1H), 1.49 (s, 3H), 1.44 (s, 3H), 1.23 (s, 4H), 0.75 (s, 3H); **^{13}C NMR** (150 MHz, $CDCl_3$) δ = 193.9, 179.2, 170.0, 159.0, 157.0, 142.2, 133.9, 123.8, 109.7,

105.0, 79.5, 63.2, 60.2, 57.4, 54.9, 52.4, 51.4, 48.9, 47.8, 45.6, 35.0, 27.3, 27.1, 26.5, 26.4, 23.3, 22.7; **IR** (NaCl, thin film) ν_{max}: 3398, 2973, 1729, 1670, 1617, 1463, 1373, 1254, 1171, 1123, 1045; **HRMS**-ESI calcd for $C_{27}H_{34}N_3O_6$ ([M+H]$^+$): 496.2442, found 496.2443.

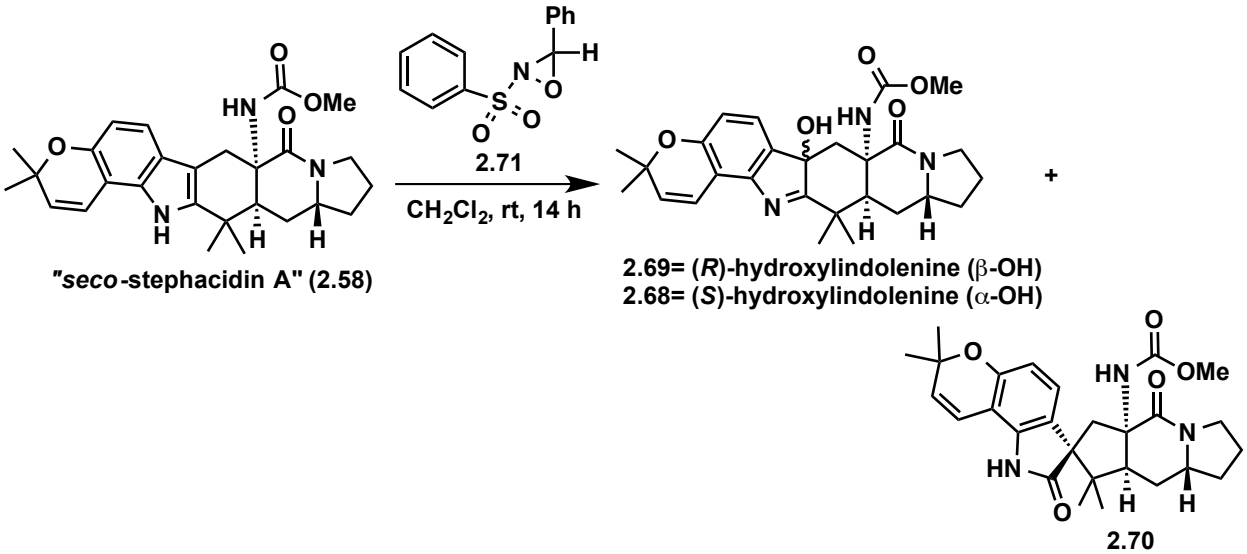

A solution of the oxaziridine[24] (**2.71**) (3.38 mg, 0.0129 mmol, 3.00 equiv) in CH_2Cl_2 (0.10 mL) was added dropwise to a 0 ºC stirring solution of methyl ((7a*S*,12a*R*,13a*S*)-3,3,14,14-tetramethyl-8-oxo-3,7,7a,8,10,11,12,12a,13,13a,14,15-dodecahydroindolizino[6,7-*h*]pyrano[3,2-*a*]carbazol-7a-yl)carbamate (**2.58**) (2.0 mg, 0.00431 mmol, 1.00 equiv) in CH_2Cl_2 (0.12 mL). The reaction mixture was stirred at room temperature for 14 h, at which point TLC indicated complete consumption of starting material. The crude mixture was passed through a quick plug of silica (1 mL) (1% MeOH/CH_2Cl_2 to 5% MeOH/CH_2Cl_2) to remove sulfonamide-based byproducts. Analysis of the combined fractions by ^{1}H NMR indicated a ca. 4:1 mixture of ((*S*)-spiroxindole (**2.70**) + (*R*)-hydroxylindolenine (**2.69**)): (*S*)-hydroxylindolenine (**2.68**).

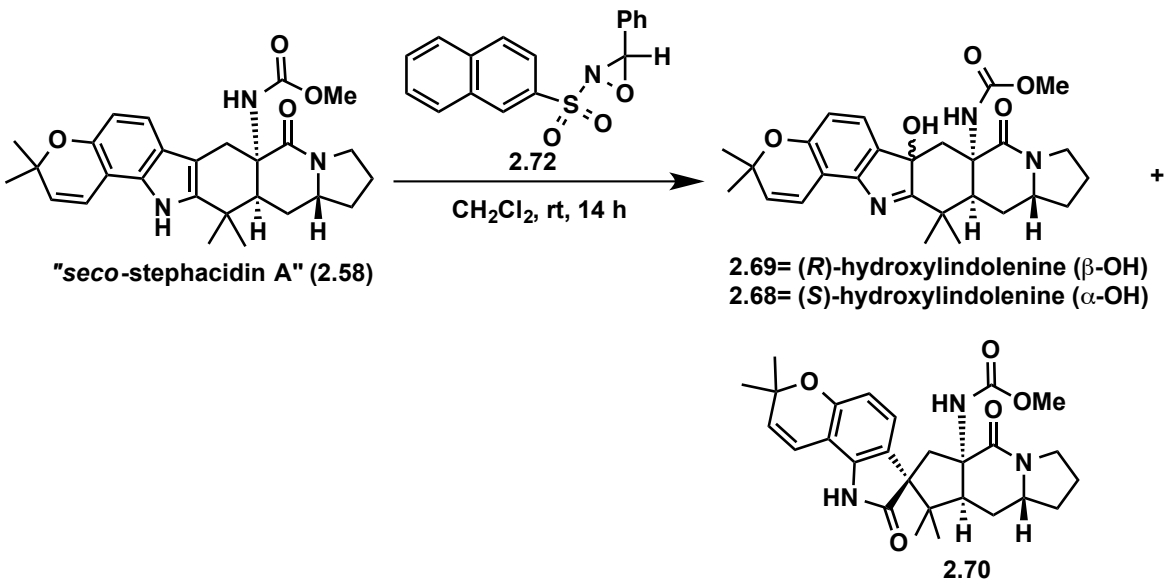

A solution of the napthyl oxaziridine (**2.72**) (10.1 mg, 0.0108 mmol, 3.33 equiv) in CH_2Cl_2 (0.20 mL) was added dropwise to a 0 ºC stirring solution of methyl ((7a*S*,12a*R*,13a*S*)-3,3,14,14-tetramethyl-8-oxo-3,7,7a,8,10,11,12,12a,13,13a,14,15-dodecahydroindolizino[6,7-*h*]pyrano[3,2-*a*]carbazol-7a-yl)carbamate (**2.58**) (5.0 mg, 0.00324 mmol, 1.00 equiv) in CH_2Cl_2 (0.340 mL). The reaction mixture was stirred at room temperature for 14 h, at which point TLC indicated complete consumption of starting material. The crude mixture was passed through a quick plug of silica (1 mL) (1% MeOH/CH_2Cl_2 to 5% MeOH/CH_2Cl_2) to remove sulfonamide-based byproducts. Analysis of the combined fractions by ^{1}H NMR indicated a ca. 1:1 mixture of ((*S*)-spiroxindole (**2.70**) + (*R*)-hydroxylindolenine (**2.69**)): (*S*)-hydroxylindolenine (**2.68**).

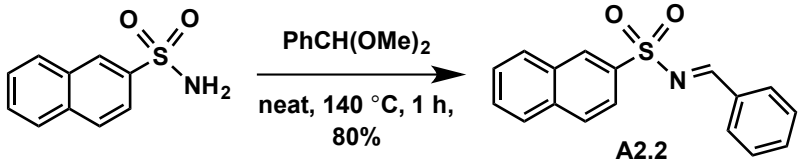

Following the general procedure reported by Davis,[24] a neat mixture of naphthalene-2-sulfonamide (1.04 g, 5.00 mmol, 1.00 equiv) and benzaldehyde dimethylacetal (0.750 mL, 5.00 mmol, 1.00 equiv) was stirred at 140 ºC under a slight flow of N_2 for 1 h. The reaction solution was allowed to cool to room temperature and the resulting pale yellow solid recrystallized from CH_2Cl_2/Hex. Collection of the solid by vacuum filtration afforded **A2.2** (1.22 g, 4.11 mmol, 83%) as a colorless solid. **TLC** (hexanes:EtOAc, 4:1 v/v); R_f=0.19; **^{1}H NMR** (600 MHz, $CDCl_3$) δ = 9.11 (s, 1H), 8.61 (s, 1H), 8.01–7.88 (m, 6H), 7.69–7.57 (m, 3H), 7.50–7.44 (m, 2H); **^{13}C NMR** (150 MHz, $CDCl_3$) δ 170.5, 135.2, 135.0, 135.0, 132.3, 132.3, 132.1, 131.3, 129.6, 129.4, 129.4, 129.2, 129.1, 127.9, 127.6, 122.9; **IR** (NaCl, thin film) ν_{max}: 1597, 1575, 1450, 1348, 1320, 1155, 1130, 1073, 860, 818, 788, 756, 672, 639; **HRMS**-ESI calcd for $C_{17}H_{14}NO_2S_1$ ($[M+H]^+$): 296.0740, found 296.0741.

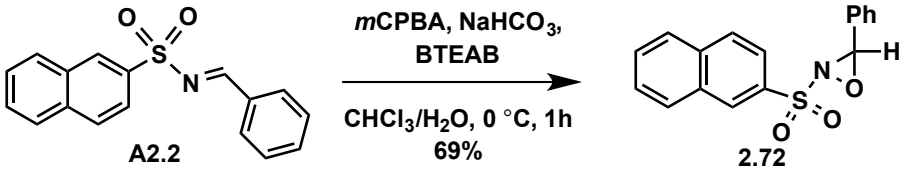

Following the procedure reported by Davis,[24] a mixture of the (*E*)-*N*-benzylidenenaphthalene-2-sulfonamide (**A2.2**) (300 mg, 1.02 mmol, 1.00 equiv), benzyltriethylammonium bromide (BTEAB) (30.5 mg, 1.12 mmol, 1.10 equiv) and saturated aqueous $NaHCO_3$ (3.0 mL) was stirred vigorously at 0 ºC. A solution of *m*CPBA (193 mg, 1.12 mmol, 1.10 equiv) in CH_2Cl_2 (3.0 mL) was then added drop-wise over 30 min, after which the cloudy mixture was stirred another 30 min at 0 ºC. The reaction mixture was subsequently diluted with EtOAc (60 mL) and washed with H_2O, 10% aq. $Na_2S_2O_3$, and brine. The combined organic extracts were concentrated *in vacuo* and the resulting residue purified by silica gel chromatography (10% EtOAc/Hex), using 10 mL silica to yield **2.72** (220 mg, 0.707 mmol, 69%) as a colorless solid. **TLC** (hexanes:EtOAc, 4:1 v/v); R_f=0.31; **^{1}H NMR** (600 MHz, $CDCl_3$) δ = 8.64 (s, 1H), 8.11–7.93 (m, 4H), 7.78–7.60 (m, 2H), 7.51–7.36 (m, 5H), 5.54 (s, 1H); **^{13}C NMR** (150 MHz, $CDCl_3$) δ = 136.1, 132.1, 131.8, 131.6, 131.5, 130.6, 130.0, 129.8, 129.8, 128.8, 128.3, 128.2, 128.0, 76.5; **IR** (NaCl, thin film) ν_{max}: 1348, 1240, 1167, 747; **HRMS**-ESI calcd for $C_{17}H_{13}NO_3NaS$ ($[M+Na]^+$): 334.0508, found 334.0520.

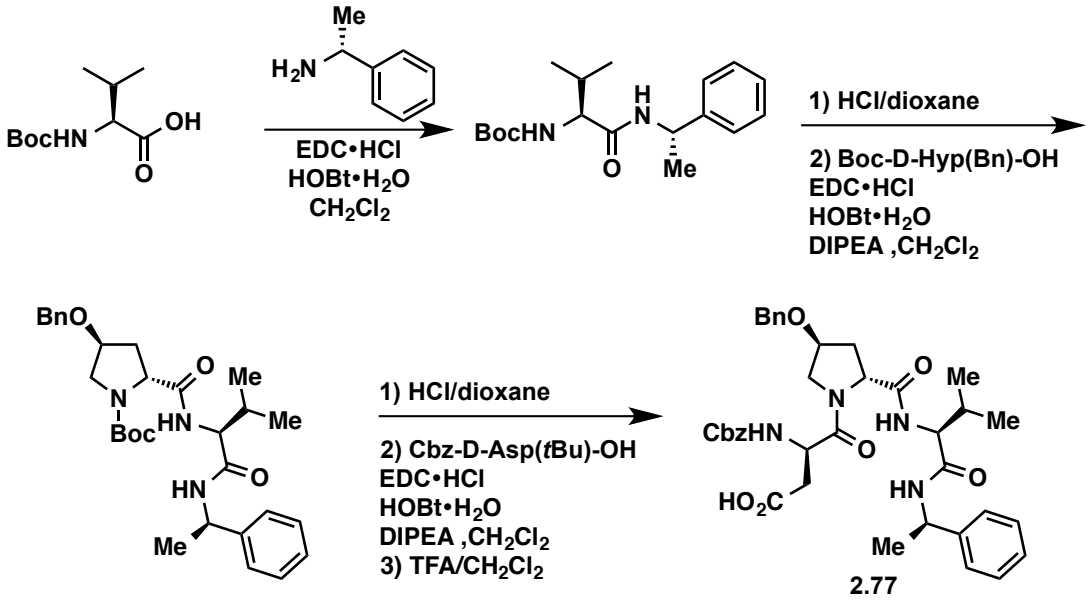

N-Boc-valine (300 mg, 1.38 mmol, 1.00 equiv), EDC•HCl (291 mg, 1.52 mmol, 1.10 equiv), and HOBt•H_2O (232 mg, 1.52 mmol, 1.10 equiv) were suspended in CH_2Cl_2 (7 mL). (*R*)-α-methylbenzylamine (328 μL, 2.60 mmol, 1.88 equiv) was added and the reaction mixture was stirred vigorously. After 4 h, the reaction was diluted with EtOAc (90 mL) and washed with aqueous citric acid (10% w/w, 30 mL), water (30 mL), saturated aqueous $NaHCO_3$ (30 mL), then brine (90 mL). The organic portion was dried over $MgSO_4$ and filtered, then concentrated *in vacuo*. The resulting solid was dissolved in 4.0 M HCl/dioxane (2.8 mL). After 45 min, the mixture was concentrated under a stream of N_2, then *in vacuo*. The residue was dissolved in CH_2Cl_2 with Boc-DHyp(Bn)-OH[56] (488 mg, 1.52 mmol, 1.10 equiv), EDC•HCl (291 mg, 1.52

mmol, 1.10 equiv), and HOBt•H_2O (232 mg, 1.52 mmol, 1.10 equiv). Diisopropylethylamine (0.26 mL, 1.52 mmol, 1.10 equiv) was added, then the resulting suspension was stirred for 12 h. The work-up procedure and Boc removal were conducted as described previously. To the resulting solid were added Cbz-D-Asp(*t*-Bu)-OH (491 mg, 1.52 mmol, 1.10 equiv), EDC•HCl (291 mg, 1.52 mmol, 1.10 equiv), and HOBt•H_2O (232 mg, 1.52 mmol, 1.10 equiv), followed by CH_2Cl_2 (7 mL). Diisopropylethylamine (0.26 mL, 1.52 mmol, 1.10 equiv) was added, then the resulting suspension was stirred vigorously. After 12 h, the reaction was processed as before, then the resulting oil was dissolved in a 1:1 mixture of trifluoroacetic acid and CH_2Cl_2 (9 mL total volume). After 1 h, the solution was concentrated under a stream of N_2, then *in vacuo*. Initial purification was conducted by silica gel chromatography (150 mL of silica, 2 column volumes of 1%, 2%, then 5% MeOH/CH_2Cl_2, all buffered with 1% AcOH). The resulting red oil was purified further by C-18 silica chromatography (120 grams C-18 silica, 5% MeOH/H_2O for 1 CV, 5% to 50% MeOH/H_2O over 2 CV, 50% to 100% MeOH/H_2O over 9 CV, then 100% MeOH for 1 CV) to give **2.77** as a white solid (536 mg, 58% yield). **TLC** (10% MeOH/CH_2Cl_2 with 1% AcOH buffer); R_f =0.54; $[\alpha]_D^{20}$ +23.0° (c = 1.0, MeOH); **^{1}H NMR** (600 MHz, $CDCl_3$) δ = 7.37–7.25 (m, 14H), 7.23–7.19 (m, 1H), 7.13 (d, *J* = 7.8 Hz, 1H), 6.80 (d, *J* = 8.0 Hz, 1H), 5.52 (d, *J* = 9.2 Hz, 1H), 5.10 (p, *J* = 7.2 Hz, 1H), 5.08–4.93 (m, 2H), 4.86 (td, *J* = 8.8, 5.3 Hz, 1H), 4.67 (t, *J* = 7.2 Hz, 1H), 4.52–4.37 (m, 2H), 4.09–4.01 (m, 3H), 3.68–3.62 (m, 1H), 2.75 (**AB**X, J_{AX} = 5.4 Hz, J_{BX} = 8.4 Hz, J_{AB} = 16.2 Hz, ν_{AB} = 93.0 Hz, 2H), 2.30 (dt, *J* = 11.8, 5.6 Hz, 1H), 2.23–2.09 (m, 2H), 1.46 (d, *J* = 6.9 Hz, 3H), 0.94 (d, *J* = 6.7 Hz, 3H), 0.90 (d, *J* = 6.7 Hz, 3H); **^{13}C NMR** (150 MHz, $CDCl_3$) δ = 173.0, 171.8, 171.2, 171.0, 155.6, 143.1, 137.7, 136.1, 128.6, 128.6, 128.5, 128.3, 128.0, 127.9, 127.7, 127.3, 126.1, 76.5, 71.0, 67.2, 59.7, 59.49, 52.3, 49.2, 49.1, 37.5, 35.2, 29.7, 22.1, 19.5, 18.4; **IR** (NaCl, thin film) ν_{max}: 3274, 2931, 1720, 1655, 1616, 1524, 1432, 1313, 1281, 1238, 1201, 1131, 1075, 1053; **HRMS** (ESI) (*m/z*) $[M+H]^+$ calculated for $C_{37}H_{45}N_4O_8$, 673.3232; found, 673.3213; $[M+Na]^+$ calculated for $C_{37}H_{44}N_4NaO_8$, 695.3051; found, 695.2994.

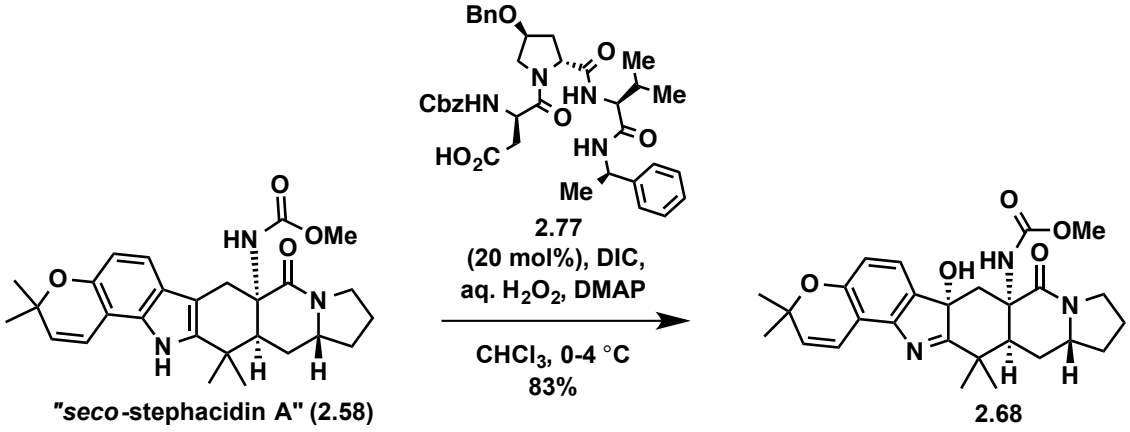

N,N-diisopropyl carbodiimide (25.4 μL, 0.162 mmol, 1.50 equiv) was added drop-wise to a 0 ºC stirring solution of methyl ((7a*S*,12a*R*,13a*S*)-3,3,14,14-tetramethyl-8-oxo-3,7,7a,8,10,11,12,12a,13,13a,14,15-dodecahydroindolizino[6,7-*h*]pyrano[3,2-*a*]carbazol-7a-yl)carbamate (**2.58**) (50.0 mg, 0.108 mmol, 1.00 equiv), the peptide acid (**2.77**) (14.5 mg, 0.0216 mmol, 0.20 equiv) and 4-dimethylaminopyridine (13.2 mg, 0.108 mmol, 1.00 equiv) in $CHCl_3$ (2.2 mL). 30% aq. H_2O_2 (27.6 μL, 0.270 mmol, 2.50 equiv) was then added and the mixture

stirred at 0 ºC for 5 minutes and then allowed to stand in the fridge (4 ºC) overnight. After 24 h, saturated aqueous $Na_2S_2O_3$ (1 mL) and saturated aqueous $NaHCO_3$ was added and the aqueous layer extracted with EtOAc (3 x 2 mL). The combined organic extracts were concentrated *in vacuo*. Purification of resulting residue by silica gel chromatography (1% MeOH/CH_2Cl_2 to 2% MeOH/CH_2Cl_2 to 5% MeOH/CH_2Cl_2), using 20 mL silica, afforded **2.68** (42.8 mg, 0.0892 mmol, 83%) as an orange oil. **TLC** (MeOH:CH_2Cl_2, 1:19 v/v); R_f=0.19; **^{1}H NMR** (600 MHz, $CDCl_3$) δ = 7.05 (d, *J* = 7.9 Hz, 1H), 6.99 (d, *J* = 9.9 Hz, 1H), 6.82 (s, 1H), 6.58 (d, *J* = 7.9 Hz, 1H), 5.74 (d, *J* = 9.9 Hz, 1H), 3.95–3.81 (m, 1H), 3.68 (s, 3H), 3.26–3.11 (m, 3H), 2.79 (s, 1H), 2.66 (d, *J* = 15.2 Hz, 1H), 2.06–1.83 (m, 4H), 1.78 (d, *J* = 15.2 Hz, 1H), 1.73 (s, 3H), 1.56–1.51 (m, 1H) 1.45 (s, 3H), 1.44 (s, 3H), 1.36 (s, 3H); **^{13}C NMR** (150 MHz, $CDCl_3$) δ = 187.8, 169.6, 155.5, 154.7, 148.2, 133.3, 131.7, 121.7, 117.9, 114.7, 113.5, 82.7, 76.6, 59.8, 54.5, 52.0, 45.2, 44.8, 42.3, 41.8, 41.2, 32.9, 28.2, 28.1, 27.0, 26.7, 24.7, 23.6, 22.1; **IR** (NaCl, thin film) ν_{max}: 3392, 2972, 1717, 1637, 1508, 1455, 1270; **HRMS**-ESI calcd for $C_{27}H_{34}N_3O_5$ ($[M+H]^+$): 480.2493, found 480.2492.

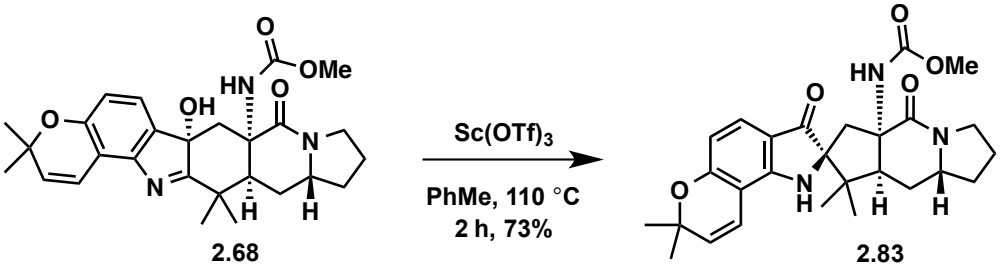

Following Movassaghi's protocol,[34] $Sc(OTf)_3$ (41.0 mg, 0.0834 mmol, 2.00 equiv) was added in one portion to a solution of methyl ((6b*S*,7a*S*,12a*R*,13a*S*)-6b-hydroxy-3,3,14,14-tetramethyl-8-oxo-3,6b,7,7a,8,10,11,12,12a,13,13a,14-dodecahydroindolizino[6,7-*h*]pyrano[3,2-*a*]carbazol-7a-yl)carbamate (**2.68**) (20.0 mg, 0.0417 mmol, 1.00 equiv) in toluene (8.3 mL) under N_2. The resulting solution was heated to 110 ºC for 2 h, then cooled to room temperature. Saturated aqueous $NaHCO_3$ (10 mL) was added and the aqueous layer extracted with EtOAc (3 x 10 mL) and the combined organic extracts dried with Na_2SO_4, filtered and concentrated *in vacuo*. Purification of the resulting residue by flash chromatography (1% MeOH/CH_2Cl_2 to 10% MeOH/CH_2Cl_2), using 5 mL silica afforded **2.83** (14.5 mg, 0.0302 mmol, 73%) as a yellow-orange oil. **TLC** (MeOH:CH_2Cl_2, 1:19 v/v); R_f=0.17; **^{1}H NMR** (600 MHz, $CDCl_3$) δ = 7.29 (d, *J* = 8.5 Hz, 1H), 6.38 (d, *J* = 9.9 Hz, 1H), 6.26–6.19 (m, 2H), 5.53 (d, *J* = 9.9 Hz, 1H), 5.13 (s, 1H), 3.88–3.75 (m, 1H), 3.72–3.63 (m, 1H), 3.59 (s, 3H), 3.42–3.31 (m, 1H), 3.15–3.06 (m, 1H), 2.51 (d, *J* = 15.2 Hz, 1H), 2.31–2.18 (m, 1H), 2.14 (d, *J* = 15.2 Hz, 1H), 2.10–2.05 (m, 1H), 2.03–1.96 (m, 2H), 1.85–1.69 (m, 1H), 1.65–1.50 (m, 1H), 1.45 (s, 3H), 1.41 (s, 3H), 1.14 (s, 3H), 0.86 (s, 3H); **^{13}C NMR** (150 MHz, $CDCl_3$) δ = 203.5, 170.1, 161.1, 157.9, 156.5, 128.0, 125.9, 115.7, 114.1, 109.9, 104.0, 77.7, 77.3, 60.0, 58.1, 53.6, 52.0, 49.5, 45.7, 44.8, 42.2, 34.8, 28.5, 28.3, 25.7, 23.6, 22.7, 22.6, 22.2; **IR** (NaCl, thin film) ν_{max}: 3350, 2971, 1726, 1631, 1602, 1503, 1445, 1317, 1253, 1113; **HRMS**-ESI calcd for $C_{27}H_{34}N_3O_5$ ($[M+H]^+$): 480.2493, found 480.2494.

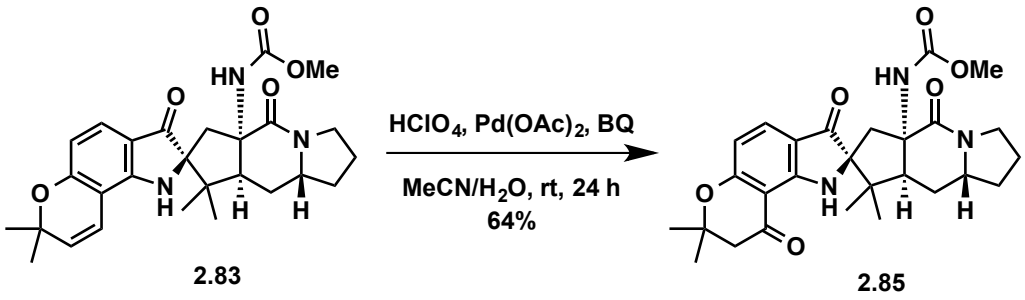

2.83 **2.85**

A flask was charged with $Pd(OAc)_2$ (2.34 mg, 0.0104 mmol, 0.20 equiv) and *p*-benzoquinone (BQ) (8.45 mg, 0.0782 mmol, 1.50 equiv, recrystallized from CH_2Cl_2/Hex). The flask was fitted with a septum, purged with N_2 (3x) and then MeCN (1.25 mL) and H_2O (0.380 mL) added via syringe to give an orange solution. H_2SO_4 (5.50 µL, 95% wt in H_2O) was then added via syringe and the resulting pale yellow solution was stirred at room temperature for 5 min. In a separate flask, methyl ((5a*S*,7*S*,8a*S*,9a*R*)-7',7',8,8-tetramethyl-3',5-dioxo-1',2,3,7',8,8a,9,9a-octahydro-1*H*,3'*H*,5*H*-spiro[cyclopenta[*f*]indolizine-7,2'-pyrano[2,3-*g*]indol]-5a(6*H*)-yl)carbamate (**2.83**) (25.0 mg, 0.0521 mmol, 1.0 equiv) was dissolved in MeCN (1.25 mL) under an N_2 atmosphere. To this was added, drop-wise, the catalyst-containing solution prepared above and the resulting dark red mixture was stirred at room temperature. After 12 h, TLC analysis indicated complete consumption of starting material. The resulting dark brown reaction mixture was poured into saturated aqueous $NaHCO_3$ (5 mL) and the aqueous layer extracted with EtOAc (3 x 5 mL). The combined organic extracts were dried with Na_2SO_4, filtered and concentrated *in vacuo*. Purification of the resulting residue by flash chromatography (1% MeOH/CH_2Cl_2 to 2% MeOH/CH_2Cl_2 to 5% MeOH/CH_2Cl_2), using 1 mL silica, afforded **2.85** (16.6 mg, 0.0335mol, 64%) as a yellow oil. **TLC** (MeOH:CH_2Cl_2, 1:19 v/v); R_f=0.32; **^{1}H NMR** (600 MHz, $CDCl_3$) δ =7.59 (d, *J* = 8.5 Hz, 1H), 7.42 (s, 1H), 6.23 (d, *J* = 8.5 Hz, 1H), 6.12 (s, 1H), 3.86 – 3.79 (m, 1H), 3.75 – 3.69 (m, 1H), 3.62 (s, 3H), 3.50 (dd, *J* = 12.5, 9.3 Hz, 1H), 3.04 (dd, *J* = 7.1, 1.6 Hz, 1H), 2.74 – 2.65 (m, 2H), 2.52 (d, *J* = 15.2 Hz, 1H), 2.31 (d, *J* = 15.1 Hz, 1H), 2.29 – 2.23 (m, 1H), 2.11 (dt, *J* = 11.5, 5.6 Hz, 1H), 2.05 – 1.98 (m, 2H), 1.90 – 1.83 (m, 1H), 1.63 – 1.56 (m, 1H), 1.51 (s, 3H), 1.49 (s, 3H), 1.14 (s, 3H), 0.95 (s, 3H); **^{13}C NMR** (150 MHz, $CDCl_3$) δ = 200.8, 192.9, 170.0, 167.8, 160.6, 156.5, 133.0, 113.4, 108.2, 103.6, 81.0, 78.0, 60.7, 58.0, 53.8, 52.1, 49.7, 48.3, 45.9, 44.8, 35.0, 27.2, 26.7, 26.3, 24.2, 22.7, 21.8; **IR** (NaCl, thin film) ν_{max}: 3373, 2970, 1725, 1658, 1596, 1510, 1452, 1317; **HRMS**-ESI calcd for $C_{27}H_{34}N_3O_6$ ($[M+H]^+$): 496.2442, found 496.2440.

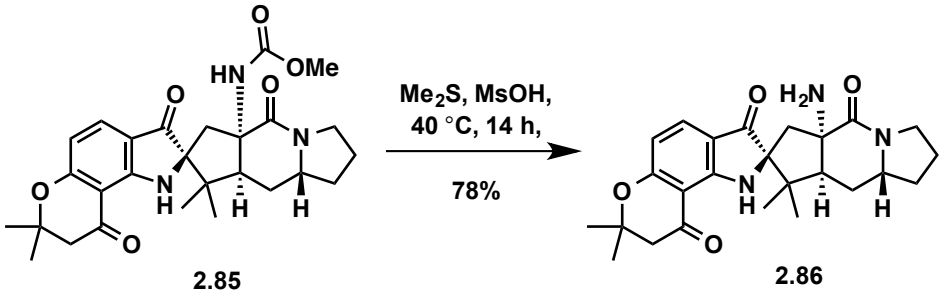

2.85 2.86

Dimethylsulfide (19.1 µL, 0.260 mmol, 10.0 equiv) was added to a solution of methyl ((5a*S*,7*S*,8a*S*,9a*R*)-7',7',8,8-tetramethyl-3',5,9'-trioxo-1',2,3,7',8,8a,8',9,9a,9'-decahydro-1*H*,3'*H*,5*H*-spiro[cyclopenta[*f*]indolizine-7,2'-pyrano[2,3-*g*]indol]-5a(6*H*)-yl)carbamate (**2.85**) (12.9 mg, 0.026 mmol, 1.0 equiv) in MsOH (0.20 mL). The reaction mixture was stirred at 40 ºC for 14 h. After cooling to room temperature, the resulting dark red reaction mixture was slowly added to a 0 ºC stirring mixture of EtOAc (10 mL) and sat'd aq. $NaHCO_3$ (10 mL). The aqueous layer extracted with EtOAc (4 x 10 mL) and the combined organic extracts dried with Na_2SO_4, filtered and concentrated in vacuo. Purification of the resulting residue by flash chromatography (2% MeOH/CH2Cl2 to 10% MeOH/CH2Cl2), using 1 mL silica, afforded **2.86** (9.2 mg, 0.0203 mmol, 78%) as a yellow oil. **^{1}H NMR** (600 MHz, CDCl3) δ = 7.60 (d, J = 8.48 Hz, 1H), 7.30 (s, 1H), 6.22 (d, J = 8.49 Hz, 1H), 3.81-3.55 (m, 2H), 3.51-3.32 (m, 1H), 2.98-2.85 (m, 1H), 2.77-2.66 (m, 2H), 2.58 (d, J = 14.88 Hz, 1H), 2.16 (d, J = 14.94 Hz, 1H), 2.13-2.06 (m, 1H), 2.07-1.92 (m, 3H), 1.87-1.73 (m, 1H), 1.62-1.37 (m, 7H), 1.15 (s, 3H), 0.89 (s, 3H); **^{13}C NMR** (150 MHz, CDCl3) δ = 201.8, 192.9, 172.7, 167.7, 160.7, 133.0, 113.4, 107.9, 103.6, 80.9, 78.2, 59.7, 57.7, 50.7, 48.8, 48.3, 46.4, 45.2, 35.1, 27.1, 26.8, 25.2, 22.5, 22.4, 22.0; **IR** (film, cm^{-1}) ν_{max}: 2970, 1666, 1597, 1453, 1316, 1194; **HRMS**-ESI calcd for $C_{25}H_{32}N_3O_4$ ($[M+H]^+$): 438.2387; found 438.2385.

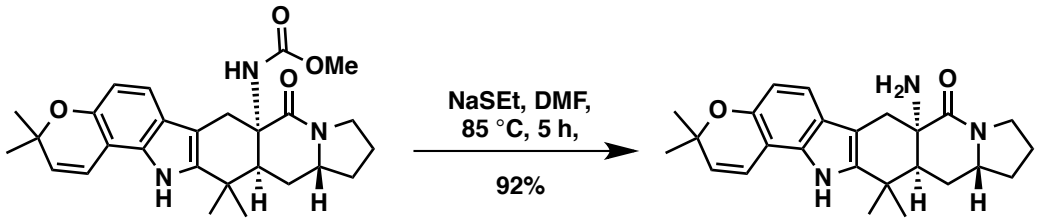

'seco-stephacidin A' (2.58) 2.18

NaH (60 wt% in mineral oil, 34.3 mg, 0.431 mmol, 10.0 equiv) was added portionwise to a solution of methyl ((7a*S*,12a*R*,13a*S*)-3,3,14,14-tetramethyl-8-oxo-3,7,7a,8,10,11,12,12a,13,13a,14,15-dodecahydroindolizino[6,7-*h*]pyrano[3,2-*a*]carbazol-7a-yl)carbamate (**2.58**) (20.0 mg, 0.0431 mmol, 1.0 equiv) and ethanethiol (62.3 µL, 0.862 mmol, 20.0 equiv) in DMF (0.86 mL). The resulting yellow mixture was stirred at 85 ºC for 5 h. After cooling to room temperature, the reaction mixture was poured into sat'd aq. $NaHCO_3$ (15 mL) and the aqueous layer extracted with EtOAc (3x 15 mL). The combined organic extracts dried with Na_2SO_4, filtered and concentrated in vacuo. Purification of the resulting residue by flash chromatography (1% MeOH/CH_2Cl_2 to 10% MeOH/ CH_2Cl_2), using 1 mL silica, afforded **2.18** (16.0 mg, 0.0395 mmol, 92%) as a beige powder. **^{1}H NMR** (500 MHz, $CDCl_3$) δ = 7.65 (s, 1H), 7.14 (d, *J* = 8.4 Hz, 1H), 6.64 (d, *J* = 8.4 Hz, 1H), 6.60 (d, *J* = 9.70 Hz, 1H), 5.68 (d, *J* = 9.7 Hz,

1H), 3.86 3.74 (m, 1H), 3.61–3.50 (m, 1H), 3.41–3.31 (m, 1H), 2.96 (d, J = 15.87 Hz, 1H), 2.68 (d, J = 15.94 Hz, 1H), 2.07–1.68 (m, 6H), 1.66 (s, 3H), 1.60–1.48 (m, 1H), 1.45 (s, 3H), 1.45 (s, 3H), 1.34 (s, 1H)); **^{13}C NMR** (150 MHz, $CDCl_3$) δ = 173.6, 148.6, 137.8, 132.9, 129.7, 122.6, 118.0, 117.4, 110.0, 105.2, 104.7, 75.6, 57.4, 54.3, 44.9, 34.9, 34.4, 30.8, 28.3, 27.4, 27.3, 26.7, 21.9; **IR** (film, cm^{-1}) ν_{max}: 3293, 2969, 1640, 1631, 1552, 1461, 1186; **HRMS**-ESI calcd for $C_{25}H_{32}N_3O_2$ ($[M+H]^+$): 406.2489; found 406.2485.

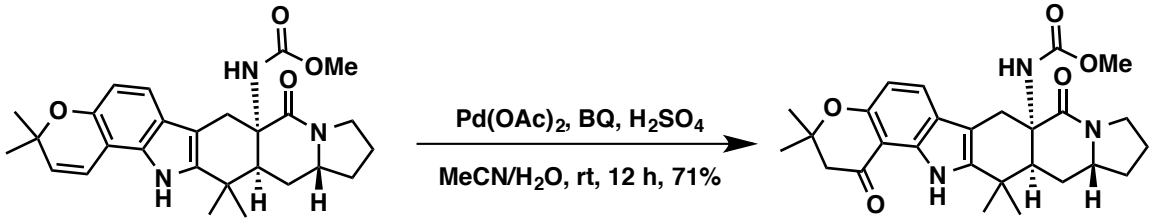

'seco-stephacidin A' (2.58) **2.94**

A flask was charged with $Pd(OAc)_2$ (50.4 mg, 0.224 mmol, 0.40 equiv) and *p*-benzoquinone (BQ) (91.0 mg, 0.842 mmol, 1.50 equiv, recrystallized from CH_2Cl_2/Hex). The flask was fitted with a septum, purged with N_2 (3x) and then MeCN (13.4 mL) and H_2O (4.06 mL) added via syringe to give an orange solution. H_2SO_4 (60.0 µL, 95% wt in H_2O) was then added via syringe and the resulting pale yellow solution was stirred at room temperature for 5 min. In a separate flask, methyl ((7a*S*,12a*R*,13a*S*)-3,3,14,14-tetramethyl-8-oxo-3,7,7a,8,10,11,12,12a,13,13a,14,15-dodecahydroindolizino[6,7-*h*]pyrano[3,2-*a*]carbazol-7a-yl)carbamate (**2.58**) (260 mg, 0.561 mmol, 1.00 equiv) was dissolved in MeCN (13.4 mL) under an N_2 atmosphere. To this was added, drop-wise, the catalyst-containing solution prepared above and the resulting dark red mixture was stirred at room temperature. After 12 h, TLC analysis indicated complete consumption of starting material. The resulting dark brown reaction mixture was poured into saturated aqueous $NaHCO_3$ (120 mL) and the aqueous layer extracted with EtOAc (3 x 100 mL). The combined organic extracts were dried with Na_2SO_4, filtered and concentrated *in vacuo*. Purification of the resulting residue by flash chromatography (1% MeOH/CH_2Cl_2 to 2% MeOH/CH_2Cl_2 to 5% MeOH/CH_2Cl_2), using 50 mL silica, afforded **2.94** (190 mg, 396 µmol, 71%) as a brown foam. **TLC** (MeOH:CH_2Cl_2, 1:19 v/v); R_f=0.14; **^{1}H NMR** (600 MHz, $CDCl_3$) δ = 9.73 (s, 1H), 7.47 (d, J = 8.5 Hz, 1H), 6.63 (d, J = 8.5 Hz, 1H), 4.94 (s, 1H), 4.00–3.89 (m, 1H), 3.59 (s, 3H), 3.53–3.44 (m, 1H), 3.32–3.21 (m, 1H), 3.11–3.01 (m, 2H), 2.82 (d, J = 16.6 Hz, 1H), 2.74 (s, 2H), 2.13–2.03 (m, 1H), 2.02–1.83 (m, 3H), 1.82–1.72 (m, 1H), 1.72–1.63 (m, 1H), 1.52–1.43 (m, 9H), 1.35 (s, 3H); **^{13}C NMR** (150 MHz, $CDCl_3$) δ = 194.2, 170.6, 157.6, 156.4, 139.8, 134.0, 126.9, 121.5, 110.0, 105.3, 102.6, 79.6, 59.6, 54.7, 52.0, 48.8, 44.8, 39.3, 34.5, 33.1, 30.1, 28.5, 28.0, 26.7, 26.6, 25.5, 22.0; **IR** (NaCl, thin film) ν_{max}: 3443, 2970, 1729, 1655, 1619, 1581, 1458, 1370, 1289, 1210; **HRMS**-ESI calcd for $C_{27}H_{34}N_3O_5$ ($[M+H]^+$): 480.2493, found 480.2492.

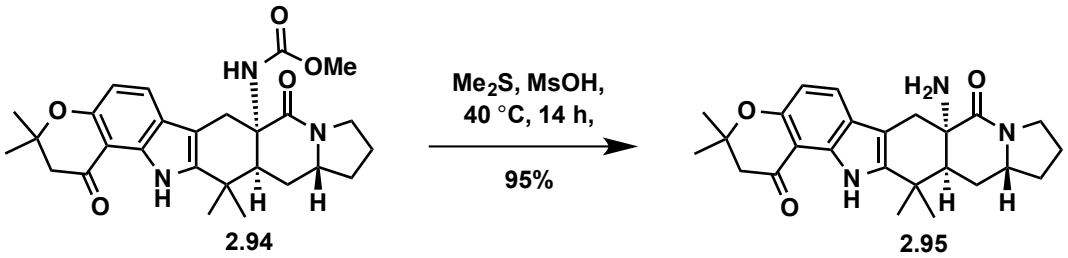

2.94 2.95

Dimethylsulfide (0.40 mL, 5.42 mmol, 20.0 equiv) was added to a solution of methyl ((7a*S*,12a*R*,13a*S*)-3,3,14,14-tetramethyl-1,8-dioxo-1,2,3,7,7a,8,10,11,12,12a,13,13a,14,15-tetradecahydroindolizino[6,7-*h*]pyrano[3,2-*a*]carbazol-7a-yl)carbamate (**2.94**) (130 mg, 0.271 mmol, 1.00 equiv) in MsOH (5.4 mL). The reaction mixture was stirred at 40 ºC for 14 h. After cooling to room temperature, the resulting dark red reaction mixture was slowly added to a 0 ºC stirring mixture of EtOAc (100 mL) and saturated aqueous $NaHCO_3$ (100 mL). The aqueous layer was extracted with EtOAc (4 x 100 mL) and the combined organic extracts were dried with Na_2SO_4, filtered and concentrated *in vacuo*. Purification of the resulting residue by flash chromatography (2% MeOH/CH_2Cl_2 to 5% MeOH/CH_2Cl_2), using 40 mL silica, afforded **2.95** (110 mg, 0.261 mmol, 96%) as a yellow foam. **TLC** (MeOH:CH_2Cl_2, 1:9 v/v); R_f=0.17; **^{1}H NMR** (600 MHz, $CDCl_3$) δ = 9.72 (s, 1H), 7.50 (d, *J* = 8.4 Hz, 1H), 6.63 (d, *J* = 8.4 Hz, 1H), 3.86–3.74 (m, 1H), 3.59–3.49 (m, 1H), 3.40–3.29 (m, 1H), 2.96 (d, *J* = 15.8 Hz, 1H), 2.76 (br s, 2H), 2.69 (d, *J* = 15.8 Hz, 1H), 2.19 (s, 2H), 2.07–1.83 (m, 5H), 1.83–1.73 (m, 1H), 1.66 (s, 3H), 1.59–1.51 (m, 1H), 1.49 (s, 3H), 1.48 (s, 3H), 1.36 (s, 3H); **^{13}C NMR** (150 MHz, $CDCl_3$) δ = 194.2, 173.7, 157.5, 138.8, 134.2, 127.2, 122.2, 109.7, 105.3, 104.7, 79.5, 57.6, 54.3, 48.8, 44.9, 44.8, 34.9, 34.4, 30.8, 30.4, 28.2, 26.8, 26.7, 26.6, 22.0; **IR** (NaCl, thin film) ν_{max}: 3443, 3372, 2971, 1652, 1579, 1459, 1370, 1285, 1209; **HRMS**-ESI calcd for $C_{25}H_{32}N_3O_3$ ($[M+H]^+$): 422.2438, found 422.2442.

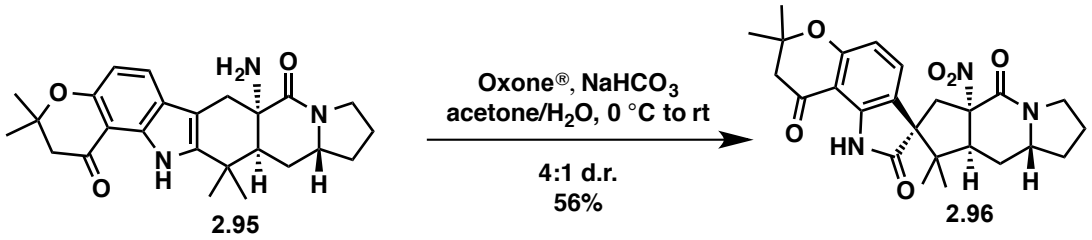

2.95 2.96

A saturated aqueous solution of $NaHCO_3$ (3.0 mL) was added to a solution of (7a*S*,12a*R*,13a*S*)-7a-amino-3,3,14,14-tetramethyl-2,3,7,7a,11,12,12a,13,13a,14-decahydroindolizino[6,7-*h*]pyrano[3,2-*a*]carbazole-1,8(10*H*,15*H*)-dione (**2.95**) (40.0 mg, 0.095 mmol, 1.00 equiv) in acetone (4.0 mL) at 0 ºC, resulting in precipitate formation. A solution of Oxone® (145 mg, 0.95 mmol, 10.0 equiv) in deionized water (2.00 mL) was added drop-wise and the mixture was warmed to room temperature by allowing the ice bath to expire. After 2 h, the resulting mixture was diluted with deionized water (40 mL) and extracted with ethyl acetate (3 x 40 mL). The combined organic extracts were dried with Na_2SO_4, filtered and concentrated *in vacuo*. Purification of the resulting residue by flash chromatography (1% MeOH/CH_2Cl_2), using 10 mL silica, afforded **2.96** (25 mg, 0.054 mmol, 56%) as a yellow foam and ca. 4:1 mixture of

diastereomers. X-ray quality crystals of the major diastereomer were obtained from slow evaporation of a dilute solution in 5% MeOH/Et_2O. **m.p.:** 174–176 ºC; **TLC** (MeOH:CH_2Cl_2, 1:19 v/v); R_f=0.38; ^{1}H NMR (500 MHz, $CDCl_3$, major diastereomer) δ = 9.30 (s, 1H), 7.14 (d, *J* = 8.3 Hz, 1H), 6.52 (d, *J* = 8.3 Hz, 1H), 3.87–3.83 (m, 1H), 3.79–3.66 (m, 2H), 3.61 (d, *J* = 16.6 Hz, 1H), 3.55–3.49 (m, 1H), 2.71 (s, 2H), 2.65 (d, *J* = 16.6 Hz, 1H), 2.44–2.36 (m, 1H), 2.26–2.15 (m, 2H), 2.10–2.03 (m, 1H), 1.90–1.79 (m, 1H), 1.65–1.55 (m, 1H), 1.48 (s, 3H), 1.47 (s, 3H), 1.15 (s, 3H), 0.91 (s, 3H); **^{13}C NMR** (125 MHz, $CDCl_3$, major diastereomer) δ = 193.7, 180.7, 163.3, 159.7, 143.3, 132.6, 118.7, 109.8, 105.2, 93.9, 79.7, 59.3, 57.9, 50.2, 49.7, 48.8, 45.9, 40.0, 35.0, 26.9, 26.8, 25.6, 22.8, 22.5, 22.2; **IR** (NaCl, thin film) ν_{max}: 3402, 2976, 1724, 1652, 1619, 1555, 1463, 1374, 1320, 1257, 1216; **HRMS**-ESI calcd for $C_{25}H_{29}N_3O_6Na$ ($[M+Na]^+$): 490.1949, found 490.1954.

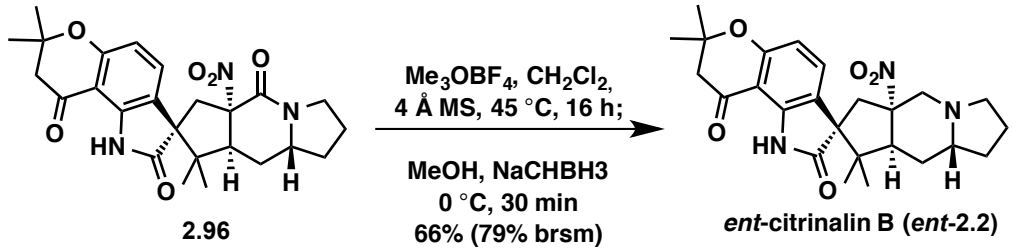

2.96 ***ent*-citrinalin B (*ent*-2.2)**

A Schlenk tube was charged with (3'*R*,5a*S*,8a*S*,9a*R*)-7',7',8,8-tetramethyl-5a-nitro-2,3,5a,6,7',8,8a,8',9,9a-decahydro-1'*H*-spiro[cyclopenta[*f*]indolizine-7,3'-pyrano[2,3-*g*]indole]-2',5,9'(1*H*)-trione (**2.96**) (10.0 mg, 0.0214 mmol, 1.00 equiv), Me_3OBF_4 (38.0 mg, 0.257 mmol, 12.0 equiv) and activated 4 Å MS (100 mg). CH_2Cl_2 (1.5 mL) was added via syringe and the mixture was stirred at 45 ºC for 16 h. After cooling to 0 ºC, anhydrous MeOH (1.5 mL) was added drop-wise followed by $NaCNBH_3$ (20.0 mg, 0.321 mmol, 15.0 equiv) in one portion. After 5 min, more $NaCNBH_3$ (15.0 mg, 0.241 mmol, 10.0 equiv) was added in one portion and the reaction mixture stirred at 0 ºC for 30 min. The resulting reaction mixture was subsequently quenched by the addition of saturated aqueous $NaHCO_3$ (3.0 mL) and extracted with EtOAc (4 x 3.0 mL). The combined organic extracts dried with Na_2SO_4, filtered and concentrated *in vacuo*. The reaction mixture was subsequently diluted with CH_2Cl_2 and passed through a short column containing silica (2 mL) with 1% MeOH/CH_2Cl_2. The fractions containing the product were collected and concentrated *in vacuo*. Further purification of the filtrate via silica gel chromatography (1% to 2% MeOH/toluene), using 5 mL silica, afforded ***ent*-2.2** (6.4 mg, 0.0141 mmol, 66% (79% brsm)) as a yellow oil. X-ray quality crystals of the HCl salt were obtained from a supersaturated solution of a 2:1 mixture of ethyl acetate and methanol. **m.p**.: 238–240 ºC (HCl salt, decomp). **TLC** (MeOH:CH_2Cl_2, 1:19 v/v); R_f=0.38; $[\alpha]_D^{25}$ –125° (c = 2.53, MeOH); **^{1}H NMR** (600 MHz, DMSO-d_6) δ = 10.12 (s, 1H), 7.51 (d, *J* = 8.3 Hz, 1H), 6.53 (d, *J* = 8.3 Hz, 1H), 3.67–3.59 (m, 2H), 2.93–2.85 (m, 1H), 2.84–2.78 (m, 1H), 2.78–2.72 (m, 1H), 2.71–2.60 (m, 3H), 2.00–1.81 (m, 4H), 1.75–1.60 (m, 3H), 1.40 (s, 3H), 1.38 (s, 3H), 1.25–1.15 (m, 1H), 0.98 (s, 3H), 0.70 (s, 3H); **^{13}C NMR** (150 MHz, DMSO-d_6) δ = 192.6, 182.4, 158.7, 142.8, 132.7, 119.5, 108.8, 104.9, 94.6, 79.2, 64.1, 61.2, 58.3, 52.9, 48.7, 48.0, 43.9, 41.4, 30.9, 26.8, 26.3, 26.0, 22.9, 22.7, 20.8; **IR** (NaCl, thin film) ν_{max}: 3402, 2972, 2936, 1725, 1673, 1619, 1594, 1542, 1464, 1372, 1323; **HRMS**-ESI calcd for $C_{25}H_{32}O_5N_3$ ($[M+H^+]$): 454.2336, found 454.2344.

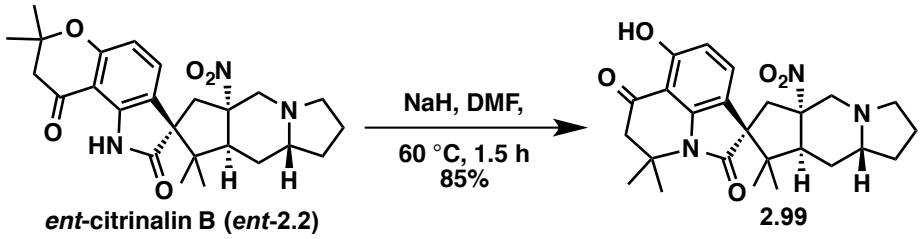

ent-citrinalin B (*ent*-2.2) 2.99

To a solution of *ent*-citrinalin B (*ent*-**2.2**) (5.0 mg, 0.0110 mmol, 1.00 equiv) in anhydrous DMF (1.0 mL) was added NaH (1.32 mg, 0.033 mmol, 3.00 equiv) as a solution in anhydrous DMF (0.10 mL) under an N_2 atmosphere. The resulting yellow solution was stirred at 60 ºC for 1.5 h. The reaction mixture was cooled to room temperature, poured into saturated aqueous NH_4Cl (1.0 mL) and the aqueous layer extracted with CH_2Cl_2 (4 x 1.0 mL). The combined organic extracts were dried with Na_2SO_4, filtered and concentrated *in vacuo*. Purification of the resulting residue by flash chromatography (1% MeOH/CH_2Cl_2 to 2% MeOH/CH_2Cl_2), using 2 mL silica, afforded **2.99** (4.3 mg, 0.00935 mmol, 85%) as a yellow oil. **TLC** (MeOH:CH_2Cl_2, 1:19 v/v); R_f=0.35; **^{1}H NMR** (600 MHz, $CDCl_3$) δ = 10.59 (s, 1H), 7.20 (d, *J* = 8.3 Hz, 1H), 6.48 (d, *J* = 8.3 Hz, 1H), 3.88 (d, *J* = 12.6 Hz, 1H), 3.81–3.77 (m, 1H), 3.00–2.94 (m, 1H), 2.88 (d, *J* = 15.8 Hz, 1H), 2.83 (d, *J* = 16.9 Hz, 1H), 2.56 (d, *J* = 16.9 Hz, 1H), 2.48 (d, *J* = 12.6 Hz, 1H), 2.38 (d, *J* = 15.8 Hz, 1H), 2.06–1.99 (m, 1H), 1.99–1.88 (m, 3H), 1.86–1.76 (m, 2H), 1.73 (s, 3H), 1.71–1.60 (m, 2H), 1.41 (s, 3H), 1.03 (s, 3H), 0.89 (s, 3H); **^{13}C NMR** (125 MHz, $CDCl_3$) δ = 196.9, 181.1, 159.8, 147.6, 133.4, 116.4, 108.4, 104.2, 94.7, 65.5, 62.0, 61.6, 57.2, 53.7, 51.5, 49.6, 44.6, 43.2, 31.6, 27.5, 26.8, 24.1, 23.9, 23.2, 21.3; **IR** (NaCl, thin film) ν_{max}: 2970, 2937, 1717, 1651, 1605, 1542, 1487, 1370, 1242; **HRMS**-ESI calcd for $C_{25}H_{32}O_5N_3$ ([M+H$^+$]): 454.2336, found 454.2333.

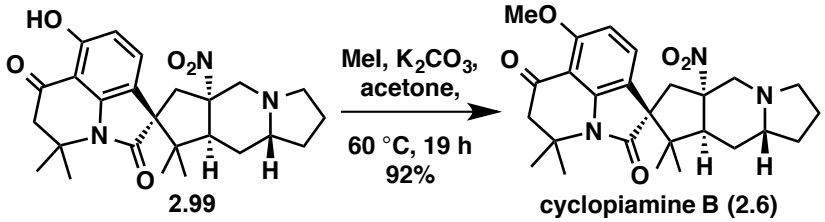

2.99 cyclopiamine B (2.6)

To a flame-dried vial containing (1'*R*,5a*S*,8a*S*,9a*R*)-7'-hydroxy-4',4',8,8-tetramethyl-5a-nitro-1,2,3,4',5,5a,5',6,8,8a,9,9a-dodecahydrospiro[cyclopenta[*f*]indolizine-7,1'-pyrrolo[3,2,1-*ij*]quinoline]-2',6'-dione (**2.99**) (4.2 mg, 0.0093 mmol, 1.00 equiv) and K_2CO_3 (6.4 mg, 0.046 mmol, 5.00 equiv) was added anhydrous acetone (1.0 mL) via syringe under an N_2 atmosphere. Iodomethane (0.7 µL, 0.0011 mmol, 1.18 equiv) was added as a solution in anhydrous acetone (0.10 mL) and the resulting mixture was heated to 60 ºC for 19 h. The reaction mixture was cooled to room temperature, poured into saturated aqueous $NaHCO_3$ (1.0 mL) and the aqueous layer extracted with CH_2Cl_2 (4 x 1.0 mL). The combined organic extracts were dried with Na_2SO_4, filtered and concentrated *in vacuo*. Purification of the resulting residue by flash chromatography (1% MeOH/CH_2Cl_2 to 2% MeOH/CH_2Cl_2), using 2 mL silica, afforded **2.6** (4.0 mg, 0.0086 mmol, 92%) as a yellow oil. X-ray quality crystals were obtained from a supersaturated solution of a 2:1 mixture of ethyl acetate and methanol. **m.p**.: 241–243 ºC (lit.[9] 245–246 ºC); **TLC** (MeOH:CH_2Cl_2, 1:19 v/v): R_f=0.37; $[\alpha]_D^{25}$ –97.9° (c = 1.90, MeOH); **^{1}H**

NMR (600 MHz, $CDCl_3$) δ = 7.22 (d, *J* = 8.3 Hz, 1H), 6.50 (d, *J* = 8.3 Hz, 1H), 3.93 (s, 3H), 3.92–3.88 (m, 1H), 3.85–3.81 (m, 1H), 3.02–2.96 (m, 1H), 2.93 (d, *J* = 15.8 Hz, 1H), 2.80 (d, *J* = 15.3 Hz, 1H), 2.55–2.48 (m, 2H), 2.39 (d, *J* = 15.8 Hz, 1H), 2.07–2.01 (m, 1H), 2.01–1.88 (m, 3H), 1.87–1.79 (m, 2H), 1.71 (s, 3H), 1.70–1.54 (m, 2H), 1.41 (s, 3H), 1.04 (s, 3H), 0.90 (s, 3H); **^{13}C NMR** (125 MHz, $CDCl_3$) δ = 190.5, 180.3, 159.1, 149.1, 131.2, 118.6, 107.6, 103.4, 94.7, 65.5, 62.0, 60.7, 56.9, 56.3, 53.7, 53.6, 49.7, 44.6, 43.2, 31.6, 27.5, 26.6, 23.9, 23.8, 23.2, 21.3; **IR** (NaCl, thin film) ν_{max}: 2968, 2936, 1715, 1688, 1610, 1541, 1488, 1456, 1367, 1248; **HRMS**-ESI calcd for $C_{26}H_{34}O_5N_3$ ([M+H$^+$]): 468.2493, found 468.2497.

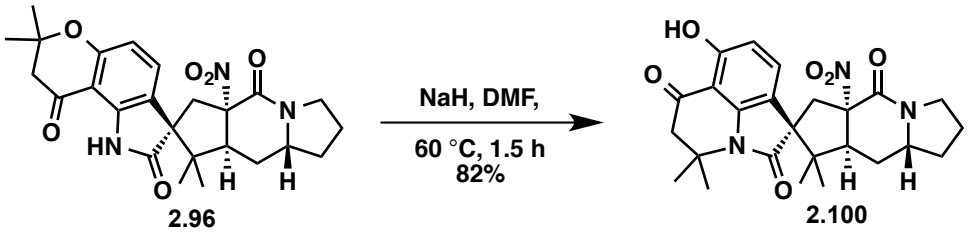

To a solution of (3'*R*,5a*S*,8a*S*,9a*R*)-7',7',8,8-tetramethyl-5a-nitro-2,3,5a,6,7',8,8a,8',9,9a-decahydro-1'*H*-spiro[cyclopenta[*f*]indolizine-7,3'-pyrano[2,3-*g*]indole]-2',5,9'(1*H*)-trione (**2.96**) (5.5 mg, 0.0118 mmol, 1.0 equiv) in anhydrous DMF (1.0 mL) was added NaH (1.41 mg, 0.0353 mmol, 3.0 equiv) as a solution in anhydrous DMF (100 μL) under an N_2 atmosphere. The resulting yellow solution was stirred at 60 ºC for 1.5 h. The reaction mixture was cooled to room temperature, poured into saturated aqueous NH_4Cl (1.0 mL) and the aqueous layer extracted with EtOAc (4 x 1.0 mL). The combined organic extracts were dried with Na_2SO_4, filtered and concentrated *in vacuo*. Purification of the resulting residue by flash chromatography (1% MeOH/CH_2Cl_2 to 2% MeOH/CH_2Cl_2), using 1 mL silica, afforded **2.100** (4.5 mg, 0.0964 mmol, 82%) as a yellow powder. **^{1}H NMR** (600 MHz, $CDCl_3$) δ = 10.62 (s, 1H), 7.15 (d, *J* = 8.4 Hz, 1H), 6.49 (d, *J* = 8.4 Hz, 1H), 3.80 (d, *J* = 7.3 Hz, 1H), 3.78 – 3.66 (m, 2H), 3.57 (d, *J* = 16.9 Hz, 1H), 3.55 – 3.50 (m, 1H), 2.80 (d, *J* = 16.9 Hz, 1H), 2.65 (d, *J* = 17.5 Hz, 1H), 2.62 (d, *J* = 17.5 Hz, 1H), 2.40 (ddd, *J* = 14.7, 11.9, 7.5 Hz, 1H), 2.25 – 2.16 (m, 2H), 2.07 (dt, *J* = 14.7, 8.0 Hz, 1H), 1.85 (ddt, *J* = 12.6, 9.7, 4.8 Hz, 1H), 1.70 (s, 3H), 1.63 – 1.59 (m, 1H), 1.51 (s, 3H), 1.14 (s, 3H), 0.94 (s, 3H); **^{13}C NMR** (150 MHz, CDCl3) δ = 196.8, 179.6, 163.2, 160.0, 147.6, 133.8, 115.4, 108.7, 104.3, 94.0, 61.7, 57.9, 57.3, 51.4, 50.4, 49.6, 46.0, 40.4, 35.1, 26.6, 25.7, 24.7, 22.8, 22.5, 22.2; **IR** (film, cm^{-1}) ν_{max}: 2968, 2927, 1724, 1651, 1548, 1488, 1471, 1455, 1367, 1241, 1209, 1178; **HRMS**-ESI calcd for $C_{25}H_{30}N_3O_6$ ([M+H]+): 468.2129; found 468.2140.

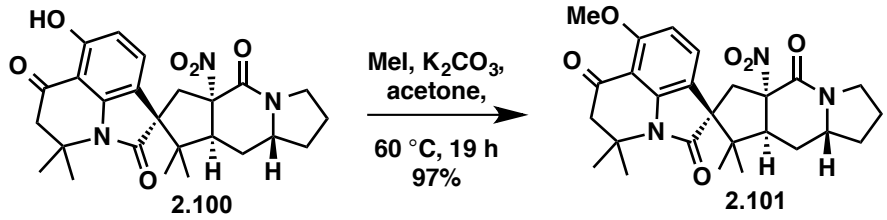

To a flame-dried vial containing (5a*S*,7*R*,8a*S*,9a*R*)-7'-hydroxy-4',4',8,8-tetramethyl-5a-nitro-2,3,4',5a,5',6,8,8a,9,9a-decahydro-1*H*,2'*H*,5*H*,6'*H*-spiro[cyclopenta[*f*]indolizine-7,1'-pyrrolo[3,2,1-*ij*]quinoline]-2',5,6'-trione (**2.100**) (13.0 mg, 0.0278 mmol, 1.0 equiv) and K_2CO_3 (19.2 mg, 0.140 mmol, 5.0 equiv) was added anhydrous acetone (3.7 mL) via syringe under an N_2 atmosphere. Iodomethane (2.1 µL, 0.0334 mmol, 1.2 equiv) was added as a solution in anhydrous acetone (100 µL) and the resulting mixture was heated to 60 ºC for 19 h. The reaction mixture was cooled to room temperature, poured into saturated aqueous $NaHCO_3$ (5.0 mL) and the aqueous layer extracted with CH_2Cl_2 (4 x 5.0 mL). The combined organic extracts were dried with Na_2SO_4, filtered and concentrated *in vacuo*. Purification of the resulting residue by flash chromatography (1% MeOH/CH_2Cl_2 to 2% MeOH/CH_2Cl_2), using 2 mL silica, afforded **2.101** (12.9 mg, 0.0268 mmol, 96%) as a yellow powder. **^{1}H NMR** (600 MHz, $CDCl_3$) δ = 7.16 (d, *J* = 8.4 Hz, 1H), 6.50 (d, *J* = 8.4 Hz, 1H), 3.92 (s, 3H), 3.82 (d, *J* = 7.3 Hz, 1H), 3.78 – 3.72 (m, 1H), 3.71 – 3.66 (m, 1H), 3.60 (d, *J* = 16.5 Hz, 1H), 3.53 (ddd, *J* = 12.6, 9.9, 2.2 Hz, 1H), 2.74 (d, *J* = 15.4 Hz, 1H), 2.66 (d, *J* = 16.5 Hz, 1H), 2.57 (d, *J* = 15.4 Hz, 1H), 2.41 (ddd, *J* = 14.6, 11.8, 7.5 Hz, 1H), 2.25 – 2.16 (m, 2H), 2.07 (dt, *J* = 13.8, 7.7 Hz, 1H), 1.90 – 1.80 (m, 1H), 1.65 (s, 3H), 1.63 – 1.57 (m, 2H), 1.48 (s, 3H), 1.13 (s, 3H), 0.93 (s, 3H); **^{13}C NMR** (150 MHz, CDCl3) δ = 190.4, 179.0, 163.3, 159.2, 149.0, 131.6, 117.6, 107.7, 103.7, 94.0, 60.9, 57.9, 57.0, 56.4, 53.5, 50.5, 49.6, 46.0, 40.4, 35.1, 26.4, 25.7, 24.4, 22.8, 22.4, 22.3; **IR** (film, cm^{-1}) ν_{max}: 2969, 1716, 1686, 1652, 1610, 1552, 1487, 1455, 1367, 1246; **HRMS**-ESI calcd for $C_{26}H_{31}N_3O_6$ ([M+Na]+): 504.2105; found 504.2122.

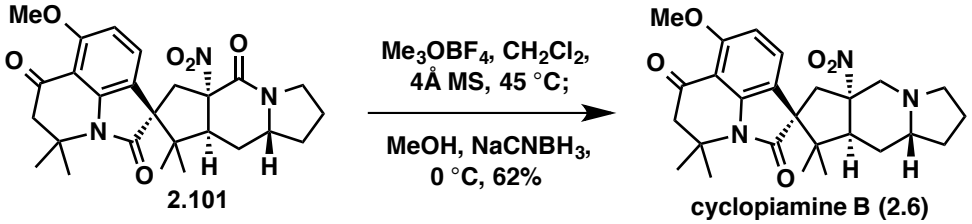

A Schlenk tube was charged with (5a*S*,7*R*,8a*S*,9a*R*)-7'-methoxy-4',4',8,8-tetramethyl-5a-nitro-2,3,4',5a,5',6,8,8a,9,9a-decahydro-1*H*,2'*H*,5*H*,6'*H*-spiro[cyclopenta[*f*]indolizine-7,1'-pyrrolo[3,2,1-*ij*]quinoline]-2',5,6'-trione (**2.101**) (13.4 mg, 0.0278 mmol, 1.00 equiv), Me_3OBF_4 (49.4 mg, 0.334 mmol, 12.0 equiv) and activated 4 Å MS (100 mg). CH_2Cl_2 (1.5 mL) was added via syringe and the mixture was stirred at 45 ºC for 16 h. After cooling to 0 ºC, anhydrous MeOH (1.5 mL) was added drop-wise followed by $NaCNBH_3$ (26.0 mg, 0.417 mmol, 15.0 equiv) in one portion. After 15 min, more $NaCNBH_3$ (10.0 mg, 0.159 mmol, 5.70 equiv) was added in one portion and the reaction mixture stirred at 0 ºC for 15 min. The resulting reaction mixture was subsequently quenched by the addition of saturated aqueous $NaHCO_3$ (3.0 mL) and extracted with EtOAc (4 x 3.0 mL). The combined organic extracts dried with Na_2SO_4, filtered

and concentrated *in vacuo*. The reaction mixture was subsequently diluted with CH_2Cl_2 and passed through a short column containing silica (2 mL) with 1% MeOH/CH_2Cl_2. The fractions containing the product were collected and concentrated *in vacuo*. Further purification of the filtrate via silica gel chromatography (1% to 2% MeOH/toluene), using 5 mL silica, afforded **2.6** (8.0 mg, 0.0171 mmol, 62% (72% brsm)) as a yellow oil. The spectral data of this material matched that for the compound prepared via the route reported previously.

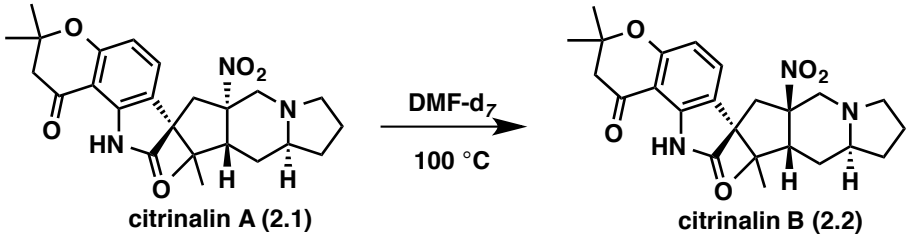

Conversion of citrinalin A (2.1) to citrinalin B (2.2). An NMR tube was charged with a degassed (freeze, pump, thaw) solution of citrinalin A (**2.1**) (0.3 mg, 0.066 μmol) in DMF-d_7 (300 μL). The resulting solution was heated to 100 ºC. After 20 h, ^{1}H NMR shows ca. 1:1 ratio of citrinalin A (**2.1**) : citrinalin B (**2.2**) with complete conversion to citrinalin B (**2**) after 60 h. See Appendix 1, Figure A1.59, for ^{1}H NMR studies.

2.9 – X-Ray Crystallography Data

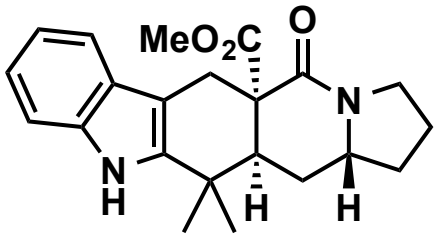

2.29

A colorless block 0.13 x 0.07 x 0.05 mm in size was mounted on a Cryoloop with Paratone oil. Data were collected in a nitrogen gas stream at 100(2) K using phi and omega scans. Crystal-to-detector distance was 60 mm and exposure time was 5 seconds per frame using a scan width of 1.0°. Data collection was 100.0% complete to 25.00° in θ. A total of 48435 reflections were collected covering the indices, -10<=*h*<=10, -19<=*k*<=19, -19<=*l*<=19. 4255 reflections were found to be symmetry independent, with an R_{int} of 0.0642. Indexing and unit cell refinement indicated a primitive, orthorhombic lattice. The space group was found to be P2(1)2(1)2(1) (No. 19). The data were integrated using the Bruker SAINT software program and scaled using the SADABS software program. Solution by direct methods (SIR-2008) produced a complete heavy-atom phasing model consistent with the proposed structure. All non-hydrogen atoms were refined anisotropically by full-matrix least-squares (SHELXL-97). All hydrogen atoms were placed using a riding model. Their positions were constrained relative to their parent atom using the appropriate HFIX command in SHELXL-97. Absolute stereochemistry was unambiguously determined to be *S* at C1, *R* at C3, and *S* at C8, respectively.

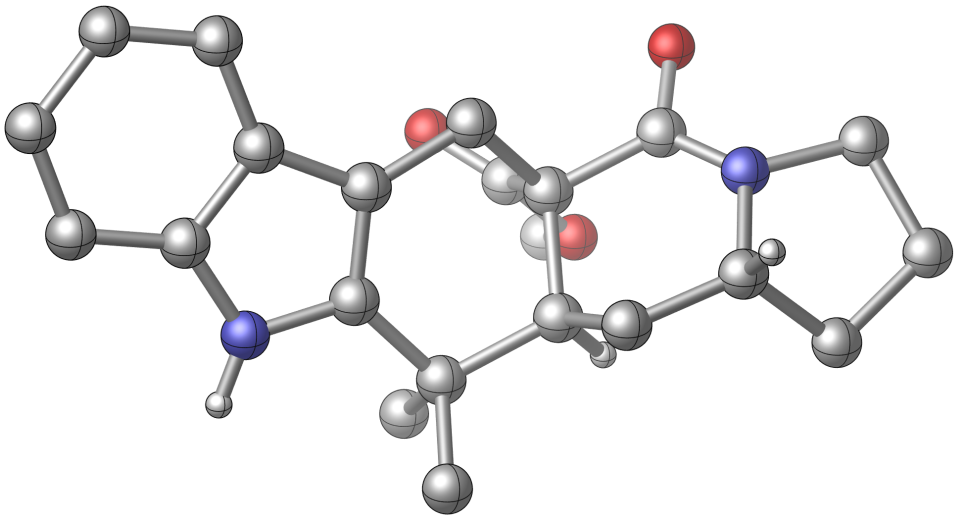

CYLView representation of **2.29**

Table 1. Crystal data and structure refinement for **2.29**.

X-ray ID	sarpong20	
Sample/notebook ID	PG2-165B	
Empirical formula	C23 H27 Cl3 N2 O3	
Formula weight	485.82	
Temperature	100(2) K	
Wavelength	0.71073 Å	
Crystal system	Orthorhombic	
Space group	P2(1)2(1)2(1)	
Unit cell dimensions	a = 9.0740(3) Å	α= 90°.
	b = 15.9454(5) Å	β= 90°.
	c = 16.0432(6) Å	γ = 90°.
Volume	2321.27(14) $Å^3$	
Z	4	
Density (calculated)	1.390 Mg/m^3	
Absorption coefficient	0.423 mm^{-1}	
F(000)	1016	
Crystal size	0.13 x 0.07 x 0.05 mm^3	
Crystal color/habit	colorless block	
Theta range for data collection	1.80 to 25.38°.	
Index ranges	-10<=h<=10, -19<=k<=19, -19<=l<=19	
Reflections collected	48435	
Independent reflections	4255 [R(int) = 0.0642]	
Completeness to theta = 25.00°	100.0 %	
Absorption correction	Semi-empirical from equivalents	
Max. and min. transmission	0.9792 and 0.9471	
Refinement method	Full-matrix least-squares on F^2	
Data / restraints / parameters	4255 / 0 / 283	
Goodness-of-fit on F^2	1.055	
Final R indices [I>2sigma(I)]	R1 = 0.0679, wR2 = 0.1607	
R indices (all data)	R1 = 0.0772, wR2 = 0.1684	
Absolute structure parameter	-0.01(12)	
Largest diff. peak and hole	1.420 and -1.402 e.$Å^{-3}$	

Table 2. Atomic coordinates (x 10^4) and equivalent isotropic displacement parameters ($Å^2$x 10^3) for **2.29**. U(eq) is defined as one third of the trace of the orthogonalized U^{ij} tensor.

	x	y	z	U(eq)
C(1)	1804(5)	6246(2)	2371(3)	15(1)
C(2)	2943(5)	6507(3)	1720(3)	19(1)
C(3)	3911(5)	5787(3)	1455(3)	20(1)
C(4)	5207(5)	5525(3)	2001(3)	24(1)
C(5)	5642(5)	4665(3)	1636(4)	33(1)
C(6)	4225(5)	4310(3)	1250(3)	27(1)
C(7)	1771(5)	4832(3)	1616(2)	15(1)
C(8)	842(4)	5537(3)	1982(2)	14(1)
C(9)	-171(5)	5856(3)	1274(3)	15(1)
C(10)	-877(4)	6665(3)	1505(3)	15(1)
C(11)	-2152(4)	7068(3)	1161(2)	14(1)
C(12)	-3092(5)	6895(3)	480(3)	17(1)
C(13)	-4247(5)	7428(3)	314(3)	19(1)
C(14)	-4498(5)	8150(3)	805(3)	21(1)
C(15)	-3577(5)	8340(3)	1470(3)	21(1)
C(16)	-2409(5)	7796(3)	1640(3)	17(1)
C(17)	-418(4)	7152(3)	2154(3)	16(1)
C(18)	872(5)	7001(3)	2727(3)	18(1)
C(19)	278(5)	6798(3)	3601(3)	24(1)
C(20)	1806(5)	7800(3)	2800(3)	23(1)
C(21)	-89(5)	5106(2)	2656(2)	15(1)
C(22)	105(6)	4412(3)	3949(3)	25(1)
C(23)	-129(6)	3871(4)	-227(3)	37(1)
N(1)	3128(4)	4982(2)	1376(2)	18(1)
N(2)	-1337(4)	7840(2)	2239(2)	20(1)
O(1)	-1389(3)	5027(2)	2671(2)	24(1)
O(2)	823(3)	4814(2)	3262(2)	18(1)
O(3)	1194(3)	4117(2)	1541(2)	17(1)
Cl(1)	1297(2)	4527(1)	-585(1)	45(1)
Cl(2)	-67(3)	2905(1)	-724(1)	66(1)
Cl(3)	-1791(2)	4387(2)	-454(2)	141(2)

Table 3. Bond lengths [Å] and angles [°] for **2.29**.

C(1)-C(2)	1.527(6)	C(6)-H(6A)	0.9900
C(1)-C(8)	1.559(6)	C(6)-H(6B)	0.9900
C(1)-C(18)	1.577(6)	C(7)-O(3)	1.260(5)
C(1)-H(1)	1.0000	C(7)-N(1)	1.313(6)
C(2)-C(3)	1.507(6)	C(7)-C(8)	1.524(6)
C(2)-H(2A)	0.9900	C(8)-C(21)	1.534(6)
C(2)-H(2B)	0.9900	C(8)-C(9)	1.548(5)
C(3)-N(1)	1.472(6)	C(9)-C(10)	1.487(6)
C(3)-C(4)	1.525(6)	C(9)-H(9A)	0.9900
C(3)-H(3)	1.0000	C(9)-H(9B)	0.9900
C(4)-C(5)	1.543(7)	C(10)-C(17)	1.364(6)
C(4)-H(4A)	0.9900	C(10)-C(11)	1.434(6)
C(4)-H(4B)	0.9900	C(11)-C(16)	1.412(6)
C(5)-C(6)	1.535(7)	C(11)-C(12)	1.412(6)
C(5)-H(5A)	0.9900	C(12)-C(13)	1.376(6)
C(5)-H(5B)	0.9900	C(12)-H(12)	0.9500
C(6)-N(1)	1.476(6)	C(13)-C(14)	1.413(7)

C(13)-H(13)	0.9500	C(20)-H(20B)	0.9800
C(14)-C(15)	1.389(6)	C(20)-H(20C)	0.9800
C(14)-H(14)	0.9500	C(21)-O(1)	1.187(5)
C(15)-C(16)	1.396(6)	C(21)-O(2)	1.360(5)
C(15)-H(15)	0.9500	C(22)-O(2)	1.433(5)
C(16)-N(2)	1.370(6)	C(22)-H(22A)	0.9800
C(17)-N(2)	1.385(5)	C(22)-H(22B)	0.9800
C(17)-C(18)	1.508(6)	C(22)-H(22C)	0.9800
C(18)-C(20)	1.535(6)	C(23)-Cl(2)	1.734(6)
C(18)-C(19)	1.537(6)	C(23)-Cl(3)	1.757(6)
C(19)-H(19A)	0.9800	C(23)-Cl(1)	1.760(6)
C(19)-H(19B)	0.9800	C(23)-H(23)	1.0000
C(19)-H(19C)	0.9800	N(2)-H(2)	0.8800
C(20)-H(20A)	0.9800		

C(2)-C(1)-C(8)	107.6(3)	C(21)-C(8)-C(9)	109.7(3)
C(2)-C(1)-C(18)	113.8(3)	C(7)-C(8)-C(1)	112.4(3)
C(8)-C(1)-C(18)	113.5(3)	C(21)-C(8)-C(1)	110.6(3)
C(2)-C(1)-H(1)	107.2	C(9)-C(8)-C(1)	112.8(3)
C(8)-C(1)-H(1)	107.2	C(10)-C(9)-C(8)	111.0(3)
C(18)-C(1)-H(1)	107.2	C(10)-C(9)-H(9A)	109.4
C(3)-C(2)-C(1)	112.4(3)	C(8)-C(9)-H(9A)	109.4
C(3)-C(2)-H(2A)	109.1	C(10)-C(9)-H(9B)	109.4
C(1)-C(2)-H(2A)	109.1	C(8)-C(9)-H(9B)	109.4
C(3)-C(2)-H(2B)	109.1	H(9A)-C(9)-H(9B)	108.0
C(1)-C(2)-H(2B)	109.1	C(17)-C(10)-C(11)	106.5(4)
H(2A)-C(2)-H(2B)	107.9	C(17)-C(10)-C(9)	123.5(4)
N(1)-C(3)-C(2)	114.0(3)	C(11)-C(10)-C(9)	129.9(4)
N(1)-C(3)-C(4)	100.6(3)	C(16)-C(11)-C(12)	118.8(4)
C(2)-C(3)-C(4)	119.7(4)	C(16)-C(11)-C(10)	107.0(4)
N(1)-C(3)-H(3)	107.3	C(12)-C(11)-C(10)	134.1(4)
C(2)-C(3)-H(3)	107.3	C(13)-C(12)-C(11)	119.3(4)
C(4)-C(3)-H(3)	107.3	C(13)-C(12)-H(12)	120.4
C(3)-C(4)-C(5)	102.8(4)	C(11)-C(12)-H(12)	120.4
C(3)-C(4)-H(4A)	111.2	C(12)-C(13)-C(14)	121.1(4)
C(5)-C(4)-H(4A)	111.2	C(12)-C(13)-H(13)	119.4
C(3)-C(4)-H(4B)	111.2	C(14)-C(13)-H(13)	119.4
C(5)-C(4)-H(4B)	111.2	C(15)-C(14)-C(13)	120.6(4)
H(4A)-C(4)-H(4B)	109.1	C(15)-C(14)-H(14)	119.7
C(6)-C(5)-C(4)	105.5(4)	C(13)-C(14)-H(14)	119.7
C(6)-C(5)-H(5A)	110.6	C(14)-C(15)-C(16)	118.1(4)
C(4)-C(5)-H(5A)	110.6	C(14)-C(15)-H(15)	120.9
C(6)-C(5)-H(5B)	110.6	C(16)-C(15)-H(15)	120.9
C(4)-C(5)-H(5B)	110.6	N(2)-C(16)-C(15)	130.1(4)
H(5A)-C(5)-H(5B)	108.8	N(2)-C(16)-C(11)	107.9(4)
N(1)-C(6)-C(5)	104.0(4)	C(15)-C(16)-C(11)	122.0(4)
N(1)-C(6)-H(6A)	111.0	C(10)-C(17)-N(2)	110.1(4)
C(5)-C(6)-H(6A)	111.0	C(10)-C(17)-C(18)	127.7(4)
N(1)-C(6)-H(6B)	111.0	N(2)-C(17)-C(18)	122.2(4)
C(5)-C(6)-H(6B)	111.0	C(17)-C(18)-C(20)	110.1(3)
H(6A)-C(6)-H(6B)	109.0	C(17)-C(18)-C(19)	108.5(4)
O(3)-C(7)-N(1)	121.8(4)	C(20)-C(18)-C(19)	107.4(4)
O(3)-C(7)-C(8)	118.4(4)	C(17)-C(18)-C(1)	108.5(3)
N(1)-C(7)-C(8)	119.8(4)	C(20)-C(18)-C(1)	111.4(3)
C(7)-C(8)-C(21)	104.2(3)	C(19)-C(18)-C(1)	111.0(3)
C(7)-C(8)-C(9)	106.7(3)	C(18)-C(19)-H(19A)	109.5

C(18)-C(19)-H(19B)	109.5
H(19A)-C(19)-H(19B)	109.5
C(18)-C(19)-H(19C)	109.5
H(19A)-C(19)-H(19C)	109.5
H(19B)-C(19)-H(19C)	109.5
C(18)-C(20)-H(20A)	109.5
C(18)-C(20)-H(20B)	109.5
H(20A)-C(20)-H(20B)	109.5
C(18)-C(20)-H(20C)	109.5
H(20A)-C(20)-H(20C)	109.5
H(20B)-C(20)-H(20C)	109.5
O(1)-C(21)-O(2)	123.6(4)
O(1)-C(21)-C(8)	127.6(4)
O(2)-C(21)-C(8)	108.8(3)
O(2)-C(22)-H(22A)	109.5
O(2)-C(22)-H(22B)	109.5
H(22A)-C(22)-H(22B)	109.5
O(2)-C(22)-H(22C)	109.5
H(22A)-C(22)-H(22C)	109.5
H(22B)-C(22)-H(22C)	109.5
Cl(2)-C(23)-Cl(3)	110.4(3)
Cl(2)-C(23)-Cl(1)	110.7(3)
Cl(3)-C(23)-Cl(1)	106.5(4)
Cl(2)-C(23)-H(23)	109.7
Cl(3)-C(23)-H(23)	109.7
Cl(1)-C(23)-H(23)	109.7
C(7)-N(1)-C(3)	125.9(4)
C(7)-N(1)-C(6)	122.7(4)
C(3)-N(1)-C(6)	108.6(4)
C(16)-N(2)-C(17)	108.5(3)
C(16)-N(2)-H(2)	125.7
C(17)-N(2)-H(2)	125.7
C(21)-O(2)-C(22)	115.3(3)

Symmetry transformations used to generate equivalent atoms:

Table 4. Anisotropic displacement parameters ($Å^2 x\ 10^3$)for **2.29**. The anisotropic displacement factor exponent takes the form: $-2\pi^2[\ h^2a^{*2}U^{11} + ... + 2\ h\ k\ a^*\ b^*\ U^{12}\ ]$

	U^{11}	U^{22}	U^{33}	U^{23}	U^{13}	U^{12}
C(1)	14(2)	11(2)	19(2)	0(2)	-3(2)	0(2)
C(2)	19(2)	16(2)	22(2)	7(2)	1(2)	-4(2)
C(3)	19(2)	22(2)	18(2)	1(2)	4(2)	-4(2)
C(4)	17(2)	24(2)	32(2)	2(2)	-6(2)	-1(2)
C(5)	17(2)	30(3)	51(3)	-6(2)	-2(2)	3(2)
C(6)	19(2)	27(3)	36(3)	-2(2)	7(2)	9(2)
C(7)	18(2)	16(2)	11(2)	6(2)	-5(2)	-4(2)
C(8)	15(2)	13(2)	15(2)	3(2)	-2(2)	-1(2)
C(9)	15(2)	14(2)	16(2)	-2(2)	-5(2)	1(2)
C(10)	14(2)	15(2)	16(2)	6(2)	2(2)	0(2)
C(11)	13(2)	15(2)	15(2)	3(2)	-1(2)	-1(2)
C(12)	18(2)	16(2)	16(2)	4(2)	-1(2)	-5(2)
C(13)	17(2)	20(2)	20(2)	6(2)	-2(2)	-2(2)
C(14)	15(2)	21(2)	28(2)	7(2)	-2(2)	1(2)
C(15)	23(2)	13(2)	27(2)	2(2)	0(2)	2(2)
C(16)	16(2)	12(2)	23(2)	3(2)	-2(2)	1(2)
C(17)	15(2)	12(2)	21(2)	-3(2)	-1(2)	-2(2)
C(18)	19(2)	12(2)	24(2)	-2(2)	-7(2)	2(2)
C(19)	30(2)	21(2)	20(2)	-6(2)	0(2)	8(2)
C(20)	22(2)	15(2)	32(3)	-9(2)	-13(2)	2(2)
C(21)	24(2)	7(2)	14(2)	1(2)	-5(2)	-4(2)
C(22)	32(2)	22(2)	20(2)	2(2)	7(2)	1(2)
C(23)	35(3)	50(3)	27(3)	-11(2)	3(2)	1(3)
N(1)	20(2)	14(2)	22(2)	0(2)	1(2)	0(2)
N(2)	21(2)	14(2)	24(2)	-2(2)	-6(2)	1(2)
O(1)	16(2)	28(2)	27(2)	-1(1)	2(1)	-5(1)
O(2)	24(2)	18(2)	13(1)	5(1)	1(1)	-2(1)
O(3)	17(1)	13(1)	20(1)	0(1)	-1(1)	0(1)
Cl(1)	75(1)	34(1)	25(1)	0(1)	11(1)	-8(1)
Cl(2)	102(2)	35(1)	59(1)	-8(1)	20(1)	-16(1)
Cl(3)	38(1)	193(3)	192(3)	-139(3)	-45(2)	44(2)

Table 5. Hydrogen coordinates ($x\ 10^4$) and isotropic displacement parameters ($Å^2 x\ 10^3$) for **2.29**.

	x	y	z	U(eq)
H(1)	2354	5995	2849	18
H(2A)	2427	6734	1225	23
H(2B)	3567	6959	1953	23
H(3)	4316	5928	892	24
H(4A)	4908	5475	2592	29
H(4B)	6029	5931	1957	29
H(5A)	6417	4730	1207	39
H(5B)	6014	4289	2080	39
H(6A)	4363	4191	649	32
H(6B)	3920	3788	1536	32

H(9A)	416	5932	759	18
H(9B)	-943	5432	1159	18
H(12)	-2928	6416	142	20
H(13)	-4888	7310	-140	23
H(14)	-5304	8508	679	25
H(15)	-3737	8826	1800	25
H(19A)	-271	7281	3816	36
H(19B)	1104	6673	3975	36
H(19C)	-377	6310	3570	36
H(20A)	2103	7986	2243	35
H(20B)	2686	7682	3134	35
H(20C)	1226	8241	3070	35
H(22A)	-442	4830	4273	37
H(22B)	844	4143	4306	37
H(22C)	-580	3986	3739	37
H(23)	-37	3790	389	45
H(2)	-1246	8238	2615	23

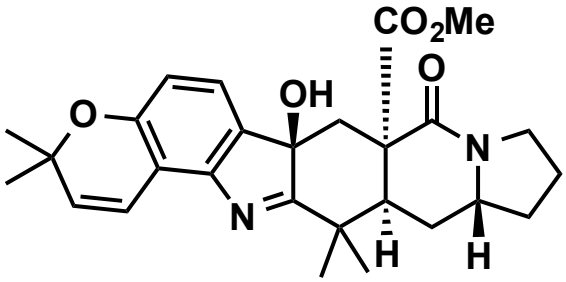

2.38

A colorless plate 0.12 x 0.08 x 0.06 mm in size was mounted on a Cryoloop with Paratone oil. Data were collected in a nitrogen gas stream at 100(2) K using phi and omega scans. Crystal-to-detector distance was 60 mm and exposure time was 10 seconds per frame using a scan width of 0.5°. Data collection was 99.3% complete to 25.00° in θ. A total of 14808 reflections were collected covering the indices, -11<=*h*<=12, -8<=*k*<=12, -29<=*l*<=29. 4812 reflections were found to be symmetry independent, with an R_{int} of 0.0324. Indexing and unit cell refinement indicated a primitive, orthorhombic lattice. The space group was found to be P2(1)2(1)2(1) (No. 19). The data were integrated using the Bruker SAINT software program and scaled using the SADABS software program. Solution by direct methods (SIR-2008) produced a complete heavy-atom phasing model consistent with the proposed structure. All non-hydrogen atoms were refined anisotropically by full-matrix least-squares (SHELXL-97). All hydrogen atoms were placed using a riding model. Their positions were constrained relative to their parent atom using the appropriate HFIX command in SHELXL-97. Absolute stereochemistry was unambiguously determined to be *R* at C1 and C15, and *S* at C13 and C12, respectively.

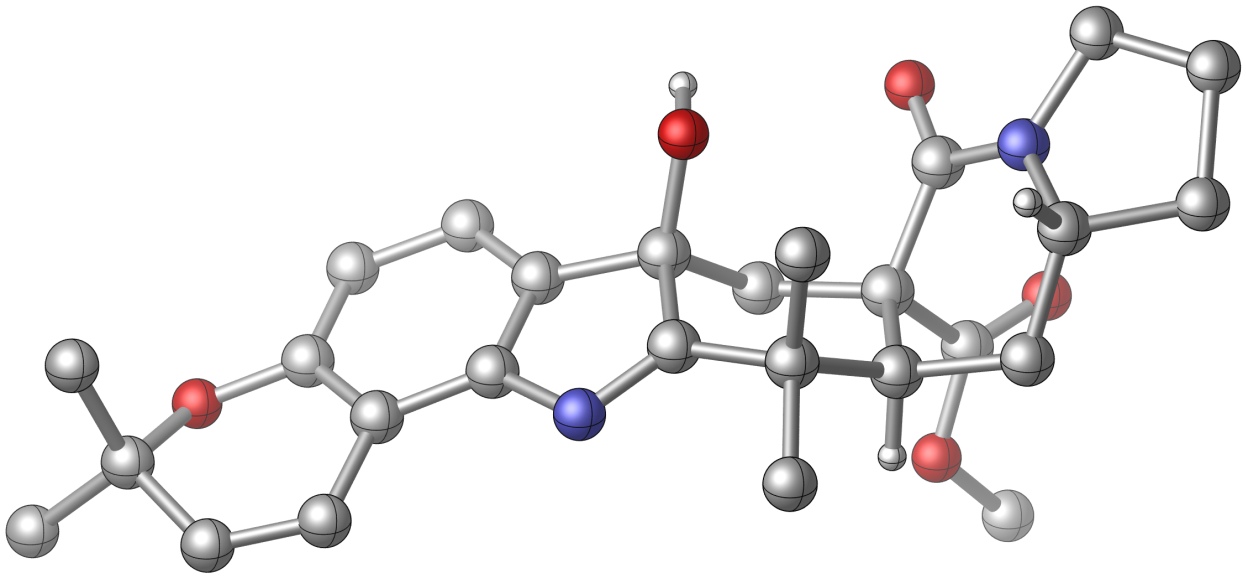

CYLView representation of **2.38**

Table 1. Crystal data and structure refinement for **2.38**.

X-ray ID	sarpong24	
Sample/notebook ID	PG3-192C	
Empirical formula	C29 H36 Cl2 N2 O5	
Formula weight	563.50	
Temperature	100(2) K	
Wavelength	0.71073 Å	
Crystal system	Orthorhombic	
Space group	P2(1)2(1)2(1)	
Unit cell dimensions	a = 10.3813(6) Å	α= 90°.
	b = 10.4519(8) Å	β= 90°.
	c = 24.9335(17) Å	γ = 90°.
Volume	2705.4(3) $Å^3$	
Z	4	
Density (calculated)	1.383 Mg/m^3	
Absorption coefficient	0.283 mm^{-1}	
F(000)	1192	
Crystal size	0.12 x 0.08 x 0.06 mm^3	
Crystal color/habit	colorless plate	
Theta range for data collection	2.11 to 25.35°.	
Index ranges	-11<=h<=12, -8<=k<=12, -29<=l<=29	
Reflections collected	14808	
Independent reflections	4812 [R(int) = 0.0324]	
Completeness to theta = 25.00°	99.3 %	
Absorption correction	Semi-empirical from equivalents	
Max. and min. transmission	0.9832 and 0.9668	
Refinement method	Full-matrix least-squares on F^2	
Data / restraints / parameters	4812 / 0 / 349	
Goodness-of-fit on F^2	1.041	
Final R indices [I>2sigma(I)]	R1 = 0.0351, wR2 = 0.0793	
R indices (all data)	R1 = 0.0400, wR2 = 0.0826	
Absolute structure parameter	-0.01(6)	
Largest diff. peak and hole	0.245 and -0.525 $e.Å^{-3}$	

Table 2. Atomic coordinates (x 10^4) and equivalent isotropic displacement parameters ($Å^2$x 10^3) for **2.38**. U(eq) is defined as one third of the trace of the orthogonalized U^{ij} tensor.

	x	y	z	U(eq)
C(1)	13856(2)	5223(2)	454(1)	14(1)
C(2)	12685(2)	5405(2)	805(1)	14(1)
C(3)	11499(2)	4798(2)	826(1)	16(1)
C(4)	10591(2)	5225(2)	1198(1)	17(1)
C(5)	10868(2)	6245(2)	1537(1)	15(1)
C(6)	9976(2)	7896(2)	2107(1)	18(1)
C(7)	11336(2)	8343(2)	2202(1)	19(1)
C(8)	12305(2)	7890(2)	1913(1)	16(1)
C(9)	12071(2)	6879(2)	1522(1)	14(1)
C(10)	12949(2)	6432(2)	1146(1)	13(1)
C(11)	14703(2)	6305(2)	666(1)	13(1)
C(12)	16050(2)	6504(2)	452(1)	15(1)
C(13)	16751(2)	5169(2)	456(1)	14(1)
C(14)	18021(2)	5124(2)	133(1)	18(1)
C(15)	17829(2)	5030(2)	-467(1)	20(1)
C(16)	18976(2)	4506(2)	-786(1)	27(1)
C(17)	18374(3)	3986(3)	-1301(1)	31(1)
C(18)	16956(3)	3694(3)	-1168(1)	27(1)
C(19)	15852(2)	3676(2)	-302(1)	16(1)
C(20)	15951(2)	3964(2)	306(1)	14(1)
C(21)	14589(2)	3981(2)	568(1)	14(1)
C(22)	9204(2)	7847(3)	2624(1)	26(1)
C(23)	9331(2)	8746(2)	1688(1)	25(1)
C(24)	16805(2)	7401(2)	824(1)	22(1)
C(25)	15927(2)	7155(2)	-101(1)	19(1)
C(26)	16662(2)	2781(2)	529(1)	15(1)
C(27)	17534(2)	1802(3)	1299(1)	27(1)
C(28)	14924(3)	5846(3)	2275(1)	29(1)
C(29)	13796(3)	5037(3)	2403(1)	32(1)
N(1)	14213(2)	6946(2)	1057(1)	14(1)
N(2)	16801(2)	4136(2)	-613(1)	18(1)
O(1)	9970(2)	6573(2)	1916(1)	20(1)
O(2)	13623(2)	5385(1)	-105(1)	15(1)
O(3)	15005(2)	2966(2)	-474(1)	20(1)
O(4)	17017(2)	1883(2)	262(1)	21(1)
O(5)	16835(2)	2859(2)	1057(1)	22(1)
Cl(1)	16232(1)	4929(1)	2038(1)	77(1)
Cl(2)	14109(1)	4009(1)	2962(1)	31(1)

Table 3. Bond lengths [Å] and angles [°] for **2.38**.

C(1)-O(2)	1.423(3)	C(17)-C(18)	1.539(4)
C(1)-C(2)	1.509(3)	C(17)-H(17A)	0.9900
C(1)-C(11)	1.527(3)	C(17)-H(17B)	0.9900
C(1)-C(21)	1.532(3)	C(18)-N(2)	1.469(3)
C(2)-C(3)	1.387(3)	C(18)-H(18A)	0.9900
C(2)-C(10)	1.396(3)	C(18)-H(18B)	0.9900
C(3)-C(4)	1.395(3)	C(19)-O(3)	1.228(3)
C(3)-H(3)	0.9500	C(19)-N(2)	1.342(3)
C(4)-C(5)	1.390(3)	C(19)-C(20)	1.549(3)
C(4)-H(4)	0.9500	C(20)-C(26)	1.544(3)
C(5)-O(1)	1.370(3)	C(20)-C(21)	1.557(3)
C(5)-C(9)	1.414(3)	C(21)-H(21A)	0.9900
C(6)-O(1)	1.463(3)	C(21)-H(21B)	0.9900
C(6)-C(7)	1.506(3)	C(22)-H(22A)	0.9800
C(6)-C(22)	1.518(3)	C(22)-H(22B)	0.9800
C(6)-C(23)	1.527(3)	C(22)-H(22C)	0.9800
C(7)-C(8)	1.326(3)	C(23)-H(23A)	0.9800
C(7)-H(7)	0.9500	C(23)-H(23B)	0.9800
C(8)-C(9)	1.457(3)	C(23)-H(23C)	0.9800
C(8)-H(8)	0.9500	C(24)-H(24A)	0.9800
C(9)-C(10)	1.388(3)	C(24)-H(24B)	0.9800
C(10)-N(1)	1.435(3)	C(24)-H(24C)	0.9800
C(11)-N(1)	1.288(3)	C(25)-H(25A)	0.9800
C(11)-C(12)	1.511(3)	C(25)-H(25B)	0.9800
C(12)-C(24)	1.534(3)	C(25)-H(25C)	0.9800
C(12)-C(25)	1.543(3)	C(26)-O(4)	1.209(3)
C(12)-C(13)	1.574(3)	C(26)-O(5)	1.330(3)
C(13)-C(14)	1.544(3)	C(27)-O(5)	1.454(3)
C(13)-C(20)	1.555(3)	C(27)-H(27A)	0.9800
C(13)-H(13)	1.0000	C(27)-H(27B)	0.9800
C(14)-C(15)	1.513(3)	C(27)-H(27C)	0.9800
C(14)-H(14A)	0.9900	C(28)-C(29)	1.479(4)
C(14)-H(14B)	0.9900	C(28)-Cl(1)	1.764(3)
C(15)-N(2)	1.465(3)	C(28)-H(28A)	0.9900
C(15)-C(16)	1.533(3)	C(28)-H(28B)	0.9900
C(15)-H(15)	1.0000	C(29)-Cl(2)	1.790(3)
C(16)-C(17)	1.528(4)	C(29)-H(29A)	0.9900
C(16)-H(16A)	0.9900	C(29)-H(29B)	0.9900
C(16)-H(16B)	0.9900	O(2)-H(2)	0.8400
O(2)-C(1)-C(2)	114.55(17)	C(3)-C(4)-H(4)	119.7
O(2)-C(1)-C(11)	110.37(17)	O(1)-C(5)-C(4)	118.01(19)
C(2)-C(1)-C(11)	99.79(17)	O(1)-C(5)-C(9)	120.09(19)
O(2)-C(1)-C(21)	111.52(17)	C(4)-C(5)-C(9)	121.8(2)
C(2)-C(1)-C(21)	113.54(17)	O(1)-C(6)-C(7)	110.40(18)
C(11)-C(1)-C(21)	106.07(17)	O(1)-C(6)-C(22)	104.11(18)
C(3)-C(2)-C(10)	120.1(2)	C(7)-C(6)-C(22)	111.79(19)
C(3)-C(2)-C(1)	132.8(2)	O(1)-C(6)-C(23)	108.96(18)
C(10)-C(2)-C(1)	106.99(18)	C(7)-C(6)-C(23)	109.77(19)
C(2)-C(3)-C(4)	118.6(2)	C(22)-C(6)-C(23)	111.7(2)
C(2)-C(3)-H(3)	120.7	C(8)-C(7)-C(6)	121.0(2)
C(4)-C(3)-H(3)	120.7	C(8)-C(7)-H(7)	119.5
C(5)-C(4)-C(3)	120.6(2)	C(6)-C(7)-H(7)	119.5
C(5)-C(4)-H(4)	119.7	C(7)-C(8)-C(9)	119.7(2)

C(7)-C(8)-H(8)	120.1	C(26)-C(20)-C(19)	103.26(17)
C(9)-C(8)-H(8)	120.1	C(26)-C(20)-C(13)	107.85(17)
C(10)-C(9)-C(5)	116.0(2)	C(19)-C(20)-C(13)	115.32(17)
C(10)-C(9)-C(8)	125.9(2)	C(26)-C(20)-C(21)	106.97(17)
C(5)-C(9)-C(8)	118.0(2)	C(19)-C(20)-C(21)	110.67(17)
C(9)-C(10)-C(2)	122.8(2)	C(13)-C(20)-C(21)	112.01(17)
C(9)-C(10)-N(1)	125.3(2)	C(1)-C(21)-C(20)	112.52(17)
C(2)-C(10)-N(1)	111.89(19)	C(1)-C(21)-H(21A)	109.1
N(1)-C(11)-C(12)	124.18(19)	C(20)-C(21)-H(21A)	109.1
N(1)-C(11)-C(1)	114.77(19)	C(1)-C(21)-H(21B)	109.1
C(12)-C(11)-C(1)	120.86(18)	C(20)-C(21)-H(21B)	109.1
C(11)-C(12)-C(24)	110.08(18)	H(21A)-C(21)-H(21B)	107.8
C(11)-C(12)-C(25)	107.43(18)	C(6)-C(22)-H(22A)	109.5
C(24)-C(12)-C(25)	108.25(18)	C(6)-C(22)-H(22B)	109.5
C(11)-C(12)-C(13)	107.68(17)	H(22A)-C(22)-H(22B)	109.5
C(24)-C(12)-C(13)	107.57(18)	C(6)-C(22)-H(22C)	109.5
C(25)-C(12)-C(13)	115.77(17)	H(22A)-C(22)-H(22C)	109.5
C(14)-C(13)-C(20)	107.85(17)	H(22B)-C(22)-H(22C)	109.5
C(14)-C(13)-C(12)	114.74(18)	C(6)-C(23)-H(23A)	109.5
C(20)-C(13)-C(12)	118.03(17)	C(6)-C(23)-H(23B)	109.5
C(14)-C(13)-H(13)	105.0	H(23A)-C(23)-H(23B)	109.5
C(20)-C(13)-H(13)	105.0	C(6)-C(23)-H(23C)	109.5
C(12)-C(13)-H(13)	105.0	H(23A)-C(23)-H(23C)	109.5
C(15)-C(14)-C(13)	113.86(18)	H(23B)-C(23)-H(23C)	109.5
C(15)-C(14)-H(14A)	108.8	C(12)-C(24)-H(24A)	109.5
C(13)-C(14)-H(14A)	108.8	C(12)-C(24)-H(24B)	109.5
C(15)-C(14)-H(14B)	108.8	H(24A)-C(24)-H(24B)	109.5
C(13)-C(14)-H(14B)	108.8	C(12)-C(24)-H(24C)	109.5
H(14A)-C(14)-H(14B)	107.7	H(24A)-C(24)-H(24C)	109.5
N(2)-C(15)-C(14)	112.48(18)	H(24B)-C(24)-H(24C)	109.5
N(2)-C(15)-C(16)	102.05(18)	C(12)-C(25)-H(25A)	109.5
C(14)-C(15)-C(16)	115.8(2)	C(12)-C(25)-H(25B)	109.5
N(2)-C(15)-H(15)	108.7	H(25A)-C(25)-H(25B)	109.5
C(14)-C(15)-H(15)	108.7	C(12)-C(25)-H(25C)	109.5
C(16)-C(15)-H(15)	108.7	H(25A)-C(25)-H(25C)	109.5
C(17)-C(16)-C(15)	104.2(2)	H(25B)-C(25)-H(25C)	109.5
C(17)-C(16)-H(16A)	110.9	O(4)-C(26)-O(5)	123.4(2)
C(15)-C(16)-H(16A)	110.9	O(4)-C(26)-C(20)	124.7(2)
C(17)-C(16)-H(16B)	110.9	O(5)-C(26)-C(20)	111.87(19)
C(15)-C(16)-H(16B)	110.9	O(5)-C(27)-H(27A)	109.5
H(16A)-C(16)-H(16B)	108.9	O(5)-C(27)-H(27B)	109.5
C(16)-C(17)-C(18)	106.33(19)	H(27A)-C(27)-H(27B)	109.5
C(16)-C(17)-H(17A)	110.5	O(5)-C(27)-H(27C)	109.5
C(18)-C(17)-H(17A)	110.5	H(27A)-C(27)-H(27C)	109.5
C(16)-C(17)-H(17B)	110.5	H(27B)-C(27)-H(27C)	109.5
C(18)-C(17)-H(17B)	110.5	C(29)-C(28)-Cl(1)	111.79(19)
H(17A)-C(17)-H(17B)	108.7	C(29)-C(28)-H(28A)	109.3
N(2)-C(18)-C(17)	104.2(2)	Cl(1)-C(28)-H(28A)	109.3
N(2)-C(18)-H(18A)	110.9	C(29)-C(28)-H(28B)	109.3
C(17)-C(18)-H(18A)	110.9	Cl(1)-C(28)-H(28B)	109.3
N(2)-C(18)-H(18B)	110.9	H(28A)-C(28)-H(28B)	107.9
C(17)-C(18)-H(18B)	110.9	C(28)-C(29)-Cl(2)	111.59(18)
H(18A)-C(18)-H(18B)	108.9	C(28)-C(29)-H(29A)	109.3
O(3)-C(19)-N(2)	122.7(2)	Cl(2)-C(29)-H(29A)	109.3
O(3)-C(19)-C(20)	120.43(19)	C(28)-C(29)-H(29B)	109.3
N(2)-C(19)-C(20)	116.54(19)	Cl(2)-C(29)-H(29B)	109.3

H(29A)-C(29)-H(29B)	108.0
C(11)-N(1)-C(10)	106.48(18)
C(19)-N(2)-C(15)	128.32(19)
C(19)-N(2)-C(18)	120.8(2)
C(15)-N(2)-C(18)	110.79(18)
C(5)-O(1)-C(6)	117.31(16)
C(1)-O(2)-H(2)	109.5
C(26)-O(5)-C(27)	115.62(19)

Symmetry transformations used to generate equivalent atoms:

Table 4. Anisotropic displacement parameters ($Å^2 x\ 10^3$)for **2.38**. The anisotropic displacement factor exponent takes the form: $-2\pi^2[\ h^2a^{*2}U^{11} + ... + 2\ h\ k\ a^*\ b^*\ U^{12}\ ]$

	U^{11}	U^{22}	U^{33}	U^{23}	U^{13}	U^{12}
C(1)	16(1)	12(1)	14(1)	1(1)	0(1)	-1(1)
C(2)	16(1)	11(1)	15(1)	4(1)	-2(1)	2(1)
C(3)	18(1)	10(1)	19(1)	0(1)	-3(1)	0(1)
C(4)	16(1)	15(1)	21(1)	2(1)	1(1)	-4(1)
C(5)	15(1)	16(1)	15(1)	3(1)	1(1)	2(1)
C(6)	19(1)	19(1)	17(1)	-4(1)	4(1)	0(1)
C(7)	21(1)	20(1)	15(1)	-3(1)	-2(1)	1(1)
C(8)	18(1)	18(1)	14(1)	1(1)	0(1)	-2(1)
C(9)	16(1)	13(1)	15(1)	3(1)	-2(1)	1(1)
C(10)	14(1)	11(1)	15(1)	5(1)	-2(1)	1(1)
C(11)	15(1)	11(1)	13(1)	2(1)	-2(1)	-1(1)
C(12)	16(1)	13(1)	16(1)	0(1)	2(1)	-3(1)
C(13)	14(1)	14(1)	14(1)	2(1)	-1(1)	-1(1)
C(14)	13(1)	15(1)	28(1)	0(1)	1(1)	-1(1)
C(15)	20(1)	15(1)	26(1)	5(1)	6(1)	3(1)
C(16)	26(1)	16(1)	39(2)	1(1)	17(1)	4(1)
C(17)	43(2)	26(1)	24(1)	8(1)	16(1)	16(1)
C(18)	43(2)	23(1)	15(1)	0(1)	4(1)	7(1)
C(19)	16(1)	13(1)	19(1)	-2(1)	-3(1)	7(1)
C(20)	12(1)	12(1)	17(1)	1(1)	0(1)	0(1)
C(21)	14(1)	11(1)	17(1)	1(1)	2(1)	-1(1)
C(22)	21(1)	33(1)	22(1)	-4(1)	7(1)	-2(1)
C(23)	20(1)	28(1)	29(1)	-6(1)	-2(1)	1(1)
C(24)	18(1)	20(1)	27(1)	-8(1)	7(1)	-6(1)
C(25)	20(1)	14(1)	22(1)	4(1)	6(1)	3(1)
C(26)	9(1)	15(1)	21(1)	3(1)	1(1)	-4(1)
C(27)	27(1)	29(1)	24(1)	10(1)	-2(1)	9(1)
C(28)	31(1)	33(1)	22(1)	5(1)	-6(1)	-2(1)
C(29)	31(2)	34(2)	33(2)	11(1)	-2(1)	6(1)
N(1)	15(1)	13(1)	14(1)	2(1)	1(1)	-1(1)
N(2)	22(1)	17(1)	14(1)	0(1)	2(1)	0(1)
O(1)	18(1)	21(1)	21(1)	-4(1)	7(1)	-2(1)
O(2)	19(1)	14(1)	13(1)	0(1)	-2(1)	-2(1)
O(3)	15(1)	21(1)	24(1)	-7(1)	-6(1)	3(1)
O(4)	19(1)	19(1)	24(1)	-1(1)	-2(1)	5(1)
O(5)	28(1)	22(1)	16(1)	4(1)	-2(1)	10(1)
Cl(1)	48(1)	123(1)	60(1)	59(1)	31(1)	52(1)
Cl(2)	26(1)	32(1)	35(1)	13(1)	2(1)	3(1)

Table 5. Hydrogen coordinates (x 10^4) and isotropic displacement parameters ($Å^2$x 10^3) for **2.38**.

	x	y	z	U(eq)
H(3)	11308	4105	593	19
H(4)	9776	4816	1219	21
H(7)	11501	8959	2474	22
H(8)	13149	8222	1960	20
H(13)	17013	5033	837	17
H(14A)	18526	5904	213	22
H(14B)	18531	4378	255	22
H(15)	17605	5897	-609	24
H(16A)	19603	5193	-866	32
H(16B)	19418	3817	-585	32
H(17A)	18824	3199	-1418	37
H(17B)	18431	4628	-1592	37
H(18A)	16370	4162	-1413	33
H(18B)	16778	2766	-1198	33
H(21A)	14083	3249	431	17
H(21B)	14681	3874	961	17
H(22A)	8341	7512	2549	38
H(22B)	9133	8711	2774	38
H(22C)	9640	7288	2882	38
H(23A)	9803	8684	1349	38
H(23B)	9336	9636	1812	38
H(23C)	8440	8465	1634	38
H(24A)	16379	8237	836	32
H(24B)	17684	7504	687	32
H(24C)	16834	7035	1185	32
H(25A)	15542	6555	-357	28
H(25B)	16783	7409	-228	28
H(25C)	15379	7914	-69	28
H(27A)	17045	1008	1250	40
H(27B)	17649	1967	1683	40
H(27C)	18379	1718	1128	40
H(28A)	15191	6318	2600	34
H(28B)	14678	6481	1999	34
H(29A)	13573	4510	2086	39
H(29B)	13049	5591	2486	39
H(2)	13205	4756	-221	23

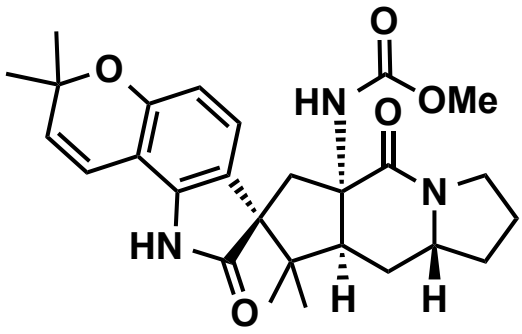

2.70

A colorless rod 0.070 x 0.050 x 0.040 mm in size was mounted on a Cryoloop with Paratone oil. Data were collected in a nitrogen gas stream at 100(2) K using phi and omgea scans. Crystal-to-detector distance was 60 mm and exposure time was 10 seconds per frame using a scan width of 1.0°. Data collection was 100.0% complete to 67.000° in θ. A total of 43987 reflections were collected covering the indices, -14<=*h*<=14, -15<=*k*<=15, -22<=*l*<=22. 5221 reflections were found to be symmetry independent, with an R_{int} of 0.0234. Indexing and unit cell refinement indicated a primitive, orthorhombic lattice. The space group was found to be P 21 21 21 (No. 19). The data were integrated using the Bruker SAINT software program and scaled using the SADABS software program. Solution by direct methods (SIR-2011) produced a complete heavy-atom phasing model consistent with the proposed structure. All non-hydrogen atoms were refined anisotropically by full-matrix least-squares (SHELXL-2012). All hydrogen atoms were placed using a riding model. Their positions were constrained relative to their parent atom using the appropriate HFIX command in SHELXL-2012. Absolute stereochemistry was unambiguously determined to be *R* at C5 and *S* at C1, C3 and C10, respectively. CCDC 984480 (**2.70**) contains the supplementary crystallographic data for this paper. This data can be obtained free of charge from The Cambridge Crystallographic Data Centre via www.ccdc.cam.ac.uk/data_request/cif.

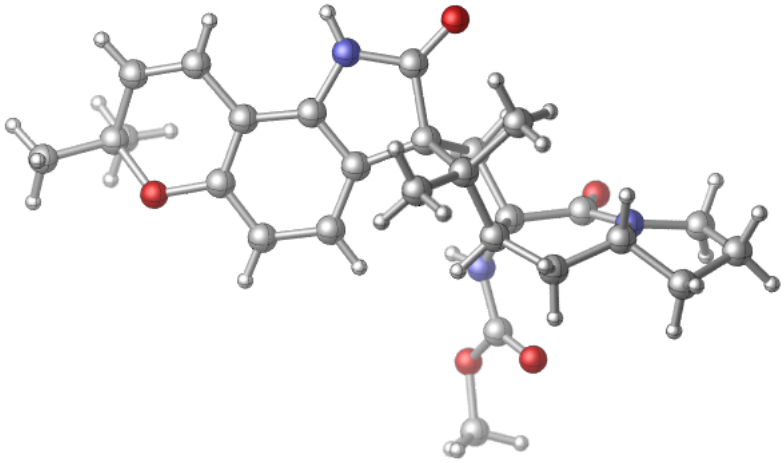

CYLView representation of **2.70**

Table 1. Crystal data and structure refinement for **2.70**.

X-ray ID	sarpong41	
Sample/notebook ID	PG7-196B	
Empirical formula	C28 H34 Cl3 N3 O5	
Formula weight	598.93	
Temperature	100(2) K	
Wavelength	1.54178 Å	
Crystal system	Orthorhombic	
Space group	P 21 21 21	
Unit cell dimensions	a = 12.3041(9) Å	α= 90°.
	b = 12.6161(9) Å	β= 90°.
	c = 18.4443(14) Å	γ = 90°.
Volume	2863.1(4) $Å^3$	
Z	4	
Density (calculated)	1.389 Mg/m^3	
Absorption coefficient	3.255 mm^{-1}	
F(000)	1256	
Crystal size	0.070 x 0.050 x 0.040 mm^3	
Crystal color/habit	colorless rod	
Theta range for data collection	4.246 to 68.125°.	
Index ranges	-14<=h<=14, -15<=k<=15, -22<=l<=22	
Reflections collected	43987	
Independent reflections	5221 [R(int) = 0.0234]	
Completeness to theta = 67.000°	100.0 %	
Absorption correction	Semi-empirical from equivalents	
Max. and min. transmission	0.929 and 0.817	
Refinement method	Full-matrix least-squares on F^2	
Data / restraints / parameters	5221 / 0 / 357	
Goodness-of-fit on F^2	1.071	
Final R indices [I>2sigma(I)]	R1 = 0.0604, wR2 = 0.1713	
R indices (all data)	R1 = 0.0610, wR2 = 0.1720	
Absolute structure parameter	0.010(9)	
Extinction coefficient	n/a	
Largest diff. peak and hole	0.962 and -0.724 e.$Å^{-3}$	

Table 2. Atomic coordinates (x 10^4) and equivalent isotropic displacement parameters ($Å^2$x 10^3) for **2.70**. U(eq) is defined as one third of the trace of the orthogonalized U^{ij} tensor.

	x	y	z	U(eq)
C(1)	5700(4)	12046(4)	1337(3)	18(1)
C(2)	5237(4)	11847(4)	553(2)	19(1)
C(3)	4962(4)	10637(4)	579(3)	19(1)
C(4)	4171(4)	10241(4)	-2(3)	23(1)
C(5)	2985(4)	10380(4)	186(3)	25(1)
C(6)	2191(5)	9645(5)	-210(3)	34(1)
C(7)	1175(5)	9688(4)	261(4)	37(1)
C(8)	1606(4)	9761(4)	1033(3)	30(1)
C(9)	3411(4)	10158(3)	1506(3)	19(1)
C(10)	4626(4)	10381(4)	1371(2)	18(1)
C(11)	4941(4)	11374(4)	1815(3)	19(1)
C(12)	6910(4)	11817(4)	1425(3)	20(1)
C(13)	7541(4)	10914(4)	1308(3)	23(1)
C(14)	8661(4)	10952(4)	1445(3)	26(1)
C(15)	9140(4)	11881(4)	1693(3)	24(1)
C(16)	10715(4)	12655(5)	2297(3)	31(1)
C(17)	10142(4)	13717(5)	2234(3)	31(1)
C(18)	9099(4)	13769(4)	2031(3)	26(1)
C(19)	8538(4)	12802(4)	1810(3)	22(1)
C(20)	7426(4)	12732(4)	1672(3)	21(1)
C(21)	5635(4)	13207(4)	1612(2)	20(1)
C(22)	6051(4)	12080(4)	-52(3)	25(1)
C(23)	4230(4)	12549(4)	408(3)	21(1)
C(24)	5199(4)	8492(4)	1375(3)	21(1)
C(25)	5921(5)	6771(5)	1469(3)	34(1)
C(26)	11902(5)	12731(6)	2077(4)	39(1)
C(27)	10594(6)	12211(6)	3052(3)	42(2)
C(28)	7858(5)	8463(5)	-773(3)	34(1)
N(1)	2741(3)	10119(3)	941(2)	23(1)
N(2)	6660(3)	13551(3)	1764(2)	22(1)
N(3)	5239(3)	9471(3)	1670(2)	19(1)
O(1)	3092(3)	9995(3)	2131(2)	24(1)
O(2)	10245(3)	11886(3)	1780(2)	28(1)
O(3)	4815(3)	13725(3)	1716(2)	22(1)
O(4)	4749(3)	8252(3)	817(2)	29(1)
O(5)	5772(3)	7808(3)	1787(2)	26(1)
Cl(1)	6634(1)	8280(1)	-285(1)	43(1)
Cl(2)	8362(2)	9729(2)	-626(2)	78(1)
Cl(3)	7648(2)	8215(3)	-1692(1)	74(1)

Table 3. Bond lengths [Å] and angles [°] for **2.70**.

C(1)-C(12)	1.525(6)	C(15)-C(19)	1.395(8)
C(1)-C(11)	1.539(6)	C(16)-O(2)	1.477(6)
C(1)-C(21)	1.553(7)	C(16)-C(27)	1.509(8)
C(1)-C(2)	1.574(6)	C(16)-C(26)	1.519(8)
C(2)-C(22)	1.528(6)	C(16)-C(17)	1.519(8)
C(2)-C(23)	1.547(6)	C(17)-C(18)	1.338(8)
C(2)-C(3)	1.564(6)	C(17)-H(17)	0.9500
C(3)-C(4)	1.530(6)	C(18)-C(19)	1.460(7)
C(3)-C(10)	1.553(6)	C(18)-H(18)	0.9500
C(3)-H(3)	1.0000	C(19)-C(20)	1.394(7)
C(4)-C(5)	1.510(7)	C(20)-N(2)	1.409(6)
C(4)-H(4A)	0.9900	C(21)-O(3)	1.217(6)
C(4)-H(4B)	0.9900	C(21)-N(2)	1.363(6)
C(5)-N(1)	1.463(7)	C(22)-H(22A)	0.9800
C(5)-C(6)	1.532(7)	C(22)-H(22B)	0.9800
C(5)-H(5)	1.0000	C(22)-H(22C)	0.9800
C(6)-C(7)	1.524(9)	C(23)-H(23A)	0.9800
C(6)-H(6A)	0.9900	C(23)-H(23B)	0.9800
C(6)-H(6B)	0.9900	C(23)-H(23C)	0.9800
C(7)-C(8)	1.521(9)	C(24)-O(4)	1.207(6)
C(7)-H(7A)	0.9900	C(24)-O(5)	1.348(6)
C(7)-H(7B)	0.9900	C(24)-N(3)	1.351(6)
C(8)-N(1)	1.477(7)	C(25)-O(5)	1.446(6)
C(8)-H(8A)	0.9900	C(25)-H(25A)	0.9800
C(8)-H(8B)	0.9900	C(25)-H(25B)	0.9800
C(9)-O(1)	1.235(6)	C(25)-H(25C)	0.9800
C(9)-N(1)	1.329(6)	C(26)-H(26A)	0.9800
C(9)-C(10)	1.541(6)	C(26)-H(26B)	0.9800
C(10)-N(3)	1.480(6)	C(26)-H(26C)	0.9800
C(10)-C(11)	1.545(6)	C(27)-H(27A)	0.9800
C(11)-H(11A)	0.9900	C(27)-H(27B)	0.9800
C(11)-H(11B)	0.9900	C(27)-H(27C)	0.9800
C(12)-C(13)	1.395(7)	C(28)-Cl(2)	1.735(7)
C(12)-C(20)	1.394(7)	C(28)-Cl(3)	1.744(6)
C(13)-C(14)	1.402(7)	C(28)-Cl(1)	1.770(6)
C(13)-H(13)	0.9500	C(28)-H(28)	1.0000
C(14)-C(15)	1.389(8)	N(2)-H(2)	0.8800
C(14)-H(14)	0.9500	N(3)-H(3A)	0.8800
C(15)-O(2)	1.369(6)		

C(12)-C(1)-C(11)	115.3(4)	C(10)-C(3)-C(2)	106.8(4)
C(12)-C(1)-C(21)	101.2(4)	C(4)-C(3)-H(3)	106.2
C(11)-C(1)-C(21)	107.5(4)	C(10)-C(3)-H(3)	106.2
C(12)-C(1)-C(2)	114.9(4)	C(2)-C(3)-H(3)	106.2
C(11)-C(1)-C(2)	102.6(4)	C(5)-C(4)-C(3)	114.6(4)
C(21)-C(1)-C(2)	115.6(4)	C(5)-C(4)-H(4A)	108.6
C(22)-C(2)-C(23)	106.8(4)	C(3)-C(4)-H(4A)	108.6
C(22)-C(2)-C(3)	110.6(4)	C(5)-C(4)-H(4B)	108.6
C(23)-C(2)-C(3)	113.0(4)	C(3)-C(4)-H(4B)	108.6
C(22)-C(2)-C(1)	113.7(4)	H(4A)-C(4)-H(4B)	107.6
C(23)-C(2)-C(1)	111.0(4)	N(1)-C(5)-C(4)	113.0(4)
C(3)-C(2)-C(1)	101.9(4)	N(1)-C(5)-C(6)	100.7(4)
C(4)-C(3)-C(10)	114.9(4)	C(4)-C(5)-C(6)	115.9(5)
C(4)-C(3)-C(2)	115.8(4)	N(1)-C(5)-H(5)	109.0

C(4)-C(5)-H(5)	109.0	C(17)-C(18)-C(19)	119.4(5)
C(6)-C(5)-H(5)	109.0	C(17)-C(18)-H(18)	120.3
C(7)-C(6)-C(5)	103.3(5)	C(19)-C(18)-H(18)	120.3
C(7)-C(6)-H(6A)	111.1	C(20)-C(19)-C(15)	116.1(5)
C(5)-C(6)-H(6A)	111.1	C(20)-C(19)-C(18)	124.6(5)
C(7)-C(6)-H(6B)	111.1	C(15)-C(19)-C(18)	119.3(5)
C(5)-C(6)-H(6B)	111.1	C(19)-C(20)-C(12)	124.0(5)
H(6A)-C(6)-H(6B)	109.1	C(19)-C(20)-N(2)	126.0(5)
C(8)-C(7)-C(6)	104.4(4)	C(12)-C(20)-N(2)	110.0(4)
C(8)-C(7)-H(7A)	110.9	O(3)-C(21)-N(2)	124.3(4)
C(6)-C(7)-H(7A)	110.9	O(3)-C(21)-C(1)	126.9(4)
C(8)-C(7)-H(7B)	110.9	N(2)-C(21)-C(1)	108.7(4)
C(6)-C(7)-H(7B)	110.9	C(2)-C(22)-H(22A)	109.5
H(7A)-C(7)-H(7B)	108.9	C(2)-C(22)-H(22B)	109.5
N(1)-C(8)-C(7)	104.0(5)	H(22A)-C(22)-H(22B)	109.5
N(1)-C(8)-H(8A)	111.0	C(2)-C(22)-H(22C)	109.5
C(7)-C(8)-H(8A)	111.0	H(22A)-C(22)-H(22C)	109.5
N(1)-C(8)-H(8B)	111.0	H(22B)-C(22)-H(22C)	109.5
C(7)-C(8)-H(8B)	111.0	C(2)-C(23)-H(23A)	109.5
H(8A)-C(8)-H(8B)	109.0	C(2)-C(23)-H(23B)	109.5
O(1)-C(9)-N(1)	121.9(5)	H(23A)-C(23)-H(23B)	109.5
O(1)-C(9)-C(10)	119.3(4)	C(2)-C(23)-H(23C)	109.5
N(1)-C(9)-C(10)	118.8(4)	H(23A)-C(23)-H(23C)	109.5
N(3)-C(10)-C(9)	107.0(4)	H(23B)-C(23)-H(23C)	109.5
N(3)-C(10)-C(11)	107.7(4)	O(4)-C(24)-O(5)	124.1(4)
C(9)-C(10)-C(11)	107.9(4)	O(4)-C(24)-N(3)	126.1(4)
N(3)-C(10)-C(3)	112.0(4)	O(5)-C(24)-N(3)	109.8(4)
C(9)-C(10)-C(3)	116.6(4)	O(5)-C(25)-H(25A)	109.5
C(11)-C(10)-C(3)	105.2(4)	O(5)-C(25)-H(25B)	109.5
C(1)-C(11)-C(10)	107.2(4)	H(25A)-C(25)-H(25B)	109.5
C(1)-C(11)-H(11A)	110.3	O(5)-C(25)-H(25C)	109.5
C(10)-C(11)-H(11A)	110.3	H(25A)-C(25)-H(25C)	109.5
C(1)-C(11)-H(11B)	110.3	H(25B)-C(25)-H(25C)	109.5
C(10)-C(11)-H(11B)	110.3	C(16)-C(26)-H(26A)	109.5
H(11A)-C(11)-H(11B)	108.5	C(16)-C(26)-H(26B)	109.5
C(13)-C(12)-C(20)	118.3(4)	H(26A)-C(26)-H(26B)	109.5
C(13)-C(12)-C(1)	132.9(5)	C(16)-C(26)-H(26C)	109.5
C(20)-C(12)-C(1)	108.8(4)	H(26A)-C(26)-H(26C)	109.5
C(12)-C(13)-C(14)	119.4(5)	H(26B)-C(26)-H(26C)	109.5
C(12)-C(13)-H(13)	120.3	C(16)-C(27)-H(27A)	109.5
C(14)-C(13)-H(13)	120.3	C(16)-C(27)-H(27B)	109.5
C(15)-C(14)-C(13)	120.4(5)	H(27A)-C(27)-H(27B)	109.5
C(15)-C(14)-H(14)	119.8	C(16)-C(27)-H(27C)	109.5
C(13)-C(14)-H(14)	119.8	H(27A)-C(27)-H(27C)	109.5
O(2)-C(15)-C(14)	117.6(5)	H(27B)-C(27)-H(27C)	109.5
O(2)-C(15)-C(19)	120.3(5)	Cl(2)-C(28)-Cl(3)	111.7(4)
C(14)-C(15)-C(19)	121.9(4)	Cl(2)-C(28)-Cl(1)	110.1(3)
O(2)-C(16)-C(27)	108.3(5)	Cl(3)-C(28)-Cl(1)	110.2(3)
O(2)-C(16)-C(26)	104.2(4)	Cl(2)-C(28)-H(28)	108.2
C(27)-C(16)-C(26)	111.4(5)	Cl(3)-C(28)-H(28)	108.2
O(2)-C(16)-C(17)	110.4(4)	Cl(1)-C(28)-H(28)	108.2
C(27)-C(16)-C(17)	110.6(5)	C(9)-N(1)-C(5)	127.7(4)
C(26)-C(16)-C(17)	111.8(5)	C(9)-N(1)-C(8)	120.5(4)
C(18)-C(17)-C(16)	120.7(5)	C(5)-N(1)-C(8)	111.8(4)
C(18)-C(17)-H(17)	119.7	C(21)-N(2)-C(20)	111.1(4)
C(16)-C(17)-H(17)	119.7	C(21)-N(2)-H(2)	124.4

C(20)-N(2)-H(2)	124.4
C(24)-N(3)-C(10)	122.8(4)
C(24)-N(3)-H(3A)	118.6
C(10)-N(3)-H(3A)	118.6
C(15)-O(2)-C(16)	117.9(4)
C(24)-O(5)-C(25)	114.6(4)

Symmetry transformations used to generate equivalent atoms:

Table 4. Anisotropic displacement parameters ($Å^2 x\ 10^3$) for **2.70**. The anisotropic displacement factor exponent takes the form: $-2\pi^2[\ h^2\ a^{*2}U^{11} + ...\ + 2\ h\ k\ a^*\ b^*\ U^{12}\ ]$

	U^{11}	U^{22}	U^{33}	U^{23}	U^{13}	U^{12}
C(1)	13(2)	22(2)	20(2)	0(2)	1(2)	1(2)
C(2)	16(2)	20(2)	21(2)	1(2)	0(2)	1(2)
C(3)	17(2)	18(2)	23(2)	-1(2)	0(2)	2(2)
C(4)	29(3)	21(2)	18(2)	-1(2)	-3(2)	1(2)
C(5)	29(3)	16(2)	30(3)	2(2)	-14(2)	0(2)
C(6)	38(3)	31(3)	33(3)	9(2)	-21(2)	-11(2)
C(7)	30(3)	25(3)	56(4)	9(3)	-17(3)	-5(2)
C(8)	16(2)	27(3)	48(3)	-8(2)	-4(2)	-1(2)
C(9)	20(2)	12(2)	25(2)	0(2)	0(2)	2(2)
C(10)	15(2)	21(2)	19(2)	-2(2)	-4(2)	1(2)
C(11)	14(2)	20(2)	22(2)	-2(2)	-1(2)	0(2)
C(12)	15(2)	23(2)	22(2)	1(2)	0(2)	3(2)
C(13)	19(2)	27(2)	24(2)	-4(2)	1(2)	1(2)
C(14)	22(2)	29(3)	27(2)	-1(2)	0(2)	9(2)
C(15)	15(2)	35(3)	21(2)	1(2)	0(2)	-1(2)
C(16)	21(3)	40(3)	32(3)	-7(2)	-4(2)	-2(2)
C(17)	23(3)	38(3)	31(3)	-5(2)	-4(2)	-10(2)
C(18)	22(2)	26(2)	28(2)	-4(2)	3(2)	-1(2)
C(19)	19(2)	29(2)	19(2)	2(2)	-2(2)	-3(2)
C(20)	20(2)	22(2)	19(2)	0(2)	3(2)	1(2)
C(21)	21(2)	21(2)	18(2)	3(2)	-2(2)	-1(2)
C(22)	21(2)	27(3)	26(2)	3(2)	4(2)	-2(2)
C(23)	18(2)	17(2)	28(2)	1(2)	-2(2)	1(2)
C(24)	20(2)	20(2)	22(2)	4(2)	6(2)	1(2)
C(25)	48(3)	24(3)	28(3)	1(2)	6(2)	17(2)
C(26)	19(3)	53(4)	46(3)	-10(3)	-4(2)	-2(2)
C(27)	40(3)	55(4)	31(3)	1(3)	-6(3)	5(3)
C(28)	32(3)	44(3)	28(3)	1(2)	2(2)	1(2)
N(1)	15(2)	20(2)	35(2)	-3(2)	-2(2)	2(2)
N(2)	19(2)	19(2)	26(2)	-1(2)	-4(2)	0(2)
N(3)	17(2)	21(2)	20(2)	2(2)	-5(2)	2(2)
O(1)	19(2)	23(2)	29(2)	4(1)	1(1)	1(1)
O(2)	15(2)	39(2)	31(2)	-6(2)	-1(1)	2(2)
O(3)	18(2)	22(2)	27(2)	-3(1)	-1(1)	4(1)
O(4)	38(2)	20(2)	28(2)	1(1)	-6(2)	0(2)
O(5)	29(2)	21(2)	27(2)	1(1)	-1(2)	11(1)
Cl(1)	47(1)	38(1)	44(1)	5(1)	16(1)	6(1)
Cl(2)	46(1)	41(1)	146(2)	-21(1)	1(1)	-13(1)
Cl(3)	47(1)	146(2)	31(1)	-18(1)	2(1)	-11(1)

Table 5. Hydrogen coordinates (x 10^4) and isotropic displacement parameters ($Å^2$x 10^3) for **2.70**.

	x	y	z	U(eq)
H(3)	5662	10255	492	23
H(4A)	4321	10623	-460	27
H(4B)	4312	9479	-88	27
H(5)	2772	11133	92	30
H(6A)	2039	9905	-706	41
H(6B)	2481	8914	-239	41
H(7A)	727	10316	140	44
H(7B)	729	9042	196	44
H(8A)	1182	10278	1320	36
H(8B)	1577	9062	1276	36
H(11A)	4284	11785	1944	23
H(11B)	5317	11164	2267	23
H(13)	7214	10280	1137	28
H(14)	9094	10340	1369	31
H(17)	10527	14351	2341	37
H(18)	8728	14430	2030	31
H(22A)	5727	11899	-521	37
H(22B)	6709	11655	23	37
H(22C)	6240	12834	-45	37
H(23A)	4438	13298	437	31
H(23B)	3670	12398	771	31
H(23C)	3945	12397	-77	31
H(25A)	5211	6432	1402	50
H(25B)	6369	6335	1791	50
H(25C)	6283	6843	998	50
H(26A)	12235	12026	2099	59
H(26B)	12284	13210	2409	59
H(26C)	11953	13006	1581	59
H(27A)	9821	12099	3158	63
H(27B)	10899	12712	3404	63
H(27C)	10981	11534	3086	63
H(28)	8404	7941	-588	41
H(2)	6822	14200	1902	26
H(3A)	5647	9572	2056	23

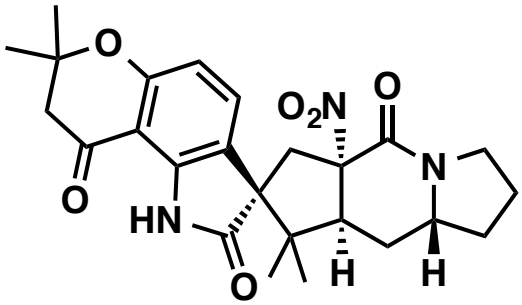

2.96

A colorless plate 0.060 x 0.040 x 0.010 mm in size was mounted on a Cryoloop with Paratone oil. Data were collected in a nitrogen gas stream at 100(2) K using phi and omega scans. Crystal-to-detector distance was 60 mm and exposure time was 20 seconds per frame using a scan width of 2.0°. Data collection was 99.9% complete to 67.000° in θ. A total of 31636 reflections were collected covering the indices, -8<=*h*<=5, -13<=*k*<=13, -35<=*l*<=35. 4203 reflections were found to be symmetry independent, with an R_{int} of 0.0441. Indexing and unit cell refinement indicated a primitive, orthorhombic lattice. The space group was found to be P 21 21 21 (No. 19). The data were integrated using the Bruker SAINT software program and scaled using the SADABS software program. Solution by iterative methods (SHELXT) produced a complete heavy-atom phasing model consistent with the proposed structure. All non-hydrogen atoms were refined anisotropically by full-matrix least-squares (SHELXL-2013). All hydrogen atoms were placed using a riding model. Their positions were constrained relative to their parent atom using the appropriate HFIX command in SHELXL-2013. Absolute stereochemistry was unambiguously determined to be *R* at C1 and C15, and *S* at C13 and C20, respectively. CCDC 984479 (**2.96**) contains the supplementary crystallographic data for this paper. This data can be obtained free of charge from The Cambridge Crystallographic Data Centre via www.ccdc.cam.ac.uk/data_request/cif.

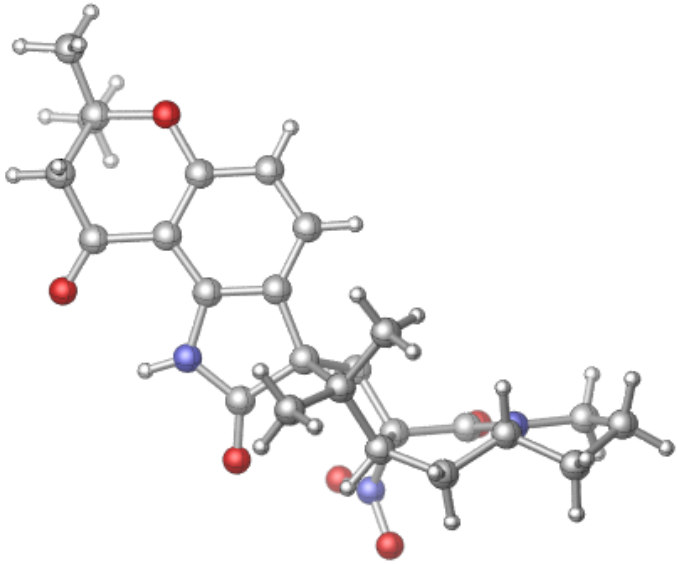

CYLView representation of **2.96**

Table 1. Crystal data and structure refinement for **2.96**.

X-ray ID	sarpong52	
Sample/notebook ID	EM04-013C	
Empirical formula	C25 H29 N3 O6	
Formula weight	467.51	
Temperature	100(2) K	
Wavelength	1.54178 Å	
Crystal system	Orthorhombic	
Space group	P 21 21 21	
Unit cell dimensions	a = 6.8459(5) Å	a= 90°.
	b = 11.5478(9) Å	b= 90°.
	c = 29.618(2) Å	g = 90°.
Volume	2341.5(3) $Å^3$	
Z	4	
Density (calculated)	1.326 Mg/m^3	
Absorption coefficient	0.787 mm^{-1}	
F(000)	992	
Crystal size	0.060 x 0.040 x 0.010 mm^3	
Crystal color/habit	colorless plate	
Theta range for data collection	2.984 to 68.243°.	
Index ranges	-8<=h<=5, -13<=k<=13, -35<=l<=35	
Reflections collected	31636	
Independent reflections	4203 [R(int) = 0.0441]	
Completeness to theta = 67.000°	99.9 %	
Absorption correction	Semi-empirical from equivalents	
Max. and min. transmission	0.929 and 0.781	
Refinement method	Full-matrix least-squares on F^2	
Data / restraints / parameters	4203 / 0 / 311	
Goodness-of-fit on F^2	1.053	
Final R indices [I>2sigma(I)]	R1 = 0.0359, wR2 = 0.0750	
R indices (all data)	R1 = 0.0422, wR2 = 0.0773	
Absolute structure parameter	-0.06(8)	
Extinction coefficient	n/a	
Largest diff. peak and hole	0.154 and -0.171 $e.Å^{-3}$	

Table 2. Atomic coordinates (x 10^4) and equivalent isotropic displacement parameters ($Å^2$x 10^3) for **2.96**. U(eq) is defined as one third of the trace of the orthogonalized U^{ij} tensor.

	x	y	z	U(eq)
C(1)	8956(4)	1404(2)	8450(1)	21(1)
C(2)	9980(4)	554(2)	8755(1)	21(1)
C(3)	10758(4)	-540(2)	8678(1)	24(1)
C(4)	11738(4)	-1111(2)	9021(1)	27(1)
C(5)	11898(4)	-618(2)	9446(1)	27(1)
C(6)	13375(5)	-716(3)	10190(1)	43(1)
C(7)	11796(5)	113(3)	10345(1)	41(1)
C(8)	11233(4)	981(3)	9991(1)	34(1)
C(9)	11152(4)	492(2)	9536(1)	26(1)
C(10)	10249(4)	1060(2)	9176(1)	24(1)
C(11)	8869(4)	2494(2)	8754(1)	24(1)
C(12)	6836(4)	1084(2)	8283(1)	23(1)
C(13)	6540(4)	1934(2)	7877(1)	22(1)
C(14)	5061(4)	1597(2)	7508(1)	25(1)
C(15)	5859(4)	758(2)	7163(1)	26(1)
C(16)	4706(4)	621(3)	6725(1)	38(1)
C(17)	6251(5)	76(3)	6415(1)	44(1)
C(18)	8123(4)	730(2)	6528(1)	28(1)
C(19)	9054(4)	1822(2)	7193(1)	21(1)
C(20)	8601(3)	2192(2)	7684(1)	20(1)
C(21)	10065(4)	1644(2)	8009(1)	21(1)
C(22)	13596(7)	-1723(3)	10516(1)	69(1)
C(23)	15290(5)	-90(3)	10107(1)	61(1)
C(24)	6741(4)	-195(2)	8153(1)	27(1)
C(25)	5282(4)	1292(3)	8646(1)	32(1)
N(1)	9535(3)	2184(2)	9171(1)	28(1)
N(2)	7771(3)	1145(2)	6990(1)	22(1)
N(3)	8890(3)	3502(2)	7650(1)	25(1)
O(1)	12779(3)	-1277(2)	9768(1)	38(1)
O(2)	10782(3)	1977(2)	10078(1)	46(1)
O(3)	8275(3)	3451(2)	8651(1)	30(1)
O(4)	10400(3)	3942(2)	7781(1)	35(1)
O(5)	7576(3)	4040(2)	7460(1)	33(1)
O(6)	10580(3)	2167(2)	7018(1)	28(1)

Table 3. Bond lengths [Å] and angles [°] for **2.96**.

C(1)-C(2)	1.508(3)	C(15)-N(2)	1.475(3)
C(1)-C(21)	1.535(3)	C(15)-C(16)	1.526(4)
C(1)-C(11)	1.549(3)	C(15)-H(15)	1.0000
C(1)-C(12)	1.578(4)	C(16)-C(17)	1.536(4)
C(2)-C(10)	1.387(3)	C(16)-H(16A)	0.9900
C(2)-C(3)	1.390(3)	C(16)-H(16B)	0.9900
C(3)-C(4)	1.384(4)	C(17)-C(18)	1.525(4)
C(3)-H(3)	0.9500	C(17)-H(17A)	0.9900
C(4)-C(5)	1.387(4)	C(17)-H(17B)	0.9900
C(4)-H(4)	0.9500	C(18)-N(2)	1.469(3)
C(5)-O(1)	1.362(3)	C(18)-H(18A)	0.9900
C(5)-C(9)	1.405(4)	C(18)-H(18B)	0.9900
C(6)-O(1)	1.463(3)	C(19)-O(6)	1.232(3)
C(6)-C(7)	1.515(5)	C(19)-N(2)	1.321(3)
C(6)-C(23)	1.516(5)	C(19)-C(20)	1.549(3)
C(6)-C(22)	1.521(5)	C(20)-C(21)	1.526(3)
C(7)-C(8)	1.500(4)	C(20)-N(3)	1.530(3)
C(7)-H(7A)	0.9900	C(21)-H(21A)	0.9900
C(7)-H(7B)	0.9900	C(21)-H(21B)	0.9900
C(8)-O(2)	1.219(3)	C(22)-H(22A)	0.9800
C(8)-C(9)	1.462(4)	C(22)-H(22B)	0.9800
C(9)-C(10)	1.397(4)	C(22)-H(22C)	0.9800
C(10)-N(1)	1.387(3)	C(23)-H(23A)	0.9800
C(11)-O(3)	1.217(3)	C(23)-H(23B)	0.9800
C(11)-N(1)	1.364(3)	C(23)-H(23C)	0.9800
C(12)-C(24)	1.528(4)	C(24)-H(24A)	0.9800
C(12)-C(25)	1.531(3)	C(24)-H(24B)	0.9800
C(12)-C(13)	1.565(3)	C(24)-H(24C)	0.9800
C(13)-C(14)	1.539(4)	C(25)-H(25A)	0.9800
C(13)-C(20)	1.551(3)	C(25)-H(25B)	0.9800
C(13)-H(13)	1.0000	C(25)-H(25C)	0.9800
C(14)-C(15)	1.511(4)	N(1)-H(1)	0.8800
C(14)-H(14A)	0.9900	N(3)-O(4)	1.216(3)
C(14)-H(14B)	0.9900	N(3)-O(5)	1.229(3)

C(2)-C(1)-C(21)	113.4(2)	O(1)-C(6)-C(23)	108.3(3)
C(2)-C(1)-C(11)	101.40(19)	C(7)-C(6)-C(23)	111.4(3)
C(21)-C(1)-C(11)	111.6(2)	O(1)-C(6)-C(22)	103.4(2)
C(2)-C(1)-C(12)	117.6(2)	C(7)-C(6)-C(22)	111.1(3)
C(21)-C(1)-C(12)	103.31(18)	C(23)-C(6)-C(22)	112.4(3)
C(11)-C(1)-C(12)	109.7(2)	C(8)-C(7)-C(6)	113.2(2)
C(10)-C(2)-C(3)	118.7(2)	C(8)-C(7)-H(7A)	108.9
C(10)-C(2)-C(1)	109.0(2)	C(6)-C(7)-H(7A)	108.9
C(3)-C(2)-C(1)	132.1(2)	C(8)-C(7)-H(7B)	108.9
C(4)-C(3)-C(2)	119.8(2)	C(6)-C(7)-H(7B)	108.9
C(4)-C(3)-H(3)	120.1	H(7A)-C(7)-H(7B)	107.8
C(2)-C(3)-H(3)	120.1	O(2)-C(8)-C(9)	123.3(3)
C(3)-C(4)-C(5)	120.6(2)	O(2)-C(8)-C(7)	123.2(2)
C(3)-C(4)-H(4)	119.7	C(9)-C(8)-C(7)	113.3(2)
C(5)-C(4)-H(4)	119.7	C(10)-C(9)-C(5)	116.4(2)
O(1)-C(5)-C(4)	116.3(2)	C(10)-C(9)-C(8)	122.7(2)
O(1)-C(5)-C(9)	122.5(2)	C(5)-C(9)-C(8)	120.9(2)
C(4)-C(5)-C(9)	121.2(2)	C(2)-C(10)-N(1)	109.8(2)
O(1)-C(6)-C(7)	109.8(2)	C(2)-C(10)-C(9)	123.2(2)

N(1)-C(10)-C(9)	127.1(2)
O(3)-C(11)-N(1)	125.2(2)
O(3)-C(11)-C(1)	127.2(2)
N(1)-C(11)-C(1)	107.5(2)
C(24)-C(12)-C(25)	107.4(2)
C(24)-C(12)-C(13)	114.0(2)
C(25)-C(12)-C(13)	110.5(2)
C(24)-C(12)-C(1)	110.2(2)
C(25)-C(12)-C(1)	112.5(2)
C(13)-C(12)-C(1)	102.30(19)
C(14)-C(13)-C(20)	112.7(2)
C(14)-C(13)-C(12)	118.1(2)
C(20)-C(13)-C(12)	106.57(19)
C(14)-C(13)-H(13)	106.2
C(20)-C(13)-H(13)	106.2
C(12)-C(13)-H(13)	106.2
C(15)-C(14)-C(13)	113.9(2)
C(15)-C(14)-H(14A)	108.8
C(13)-C(14)-H(14A)	108.8
C(15)-C(14)-H(14B)	108.8
C(13)-C(14)-H(14B)	108.8
H(14A)-C(14)-H(14B)	107.7
N(2)-C(15)-C(14)	111.2(2)
N(2)-C(15)-C(16)	101.3(2)
C(14)-C(15)-C(16)	117.1(2)
N(2)-C(15)-H(15)	109.0
C(14)-C(15)-H(15)	109.0
C(16)-C(15)-H(15)	109.0
C(15)-C(16)-C(17)	101.2(2)
C(15)-C(16)-H(16A)	111.5
C(17)-C(16)-H(16A)	111.5
C(15)-C(16)-H(16B)	111.5
C(17)-C(16)-H(16B)	111.5
H(16A)-C(16)-H(16B)	109.3
C(18)-C(17)-C(16)	104.2(2)
C(18)-C(17)-H(17A)	110.9
C(16)-C(17)-H(17A)	110.9
C(18)-C(17)-H(17B)	110.9
C(16)-C(17)-H(17B)	110.9
H(17A)-C(17)-H(17B)	108.9
N(2)-C(18)-C(17)	103.2(2)
N(2)-C(18)-H(18A)	111.1
C(17)-C(18)-H(18A)	111.1
N(2)-C(18)-H(18B)	111.1
C(17)-C(18)-H(18B)	111.1
H(18A)-C(18)-H(18B)	109.1
O(6)-C(19)-N(2)	124.3(2)
O(6)-C(19)-C(20)	118.4(2)
N(2)-C(19)-C(20)	117.2(2)
C(21)-C(20)-N(3)	111.6(2)
C(21)-C(20)-C(19)	110.31(19)
N(3)-C(20)-C(19)	100.58(18)
C(21)-C(20)-C(13)	106.62(19)
N(3)-C(20)-C(13)	109.39(19)
C(19)-C(20)-C(13)	118.4(2)
C(20)-C(21)-C(1)	106.6(2)
C(20)-C(21)-H(21A)	110.4
C(1)-C(21)-H(21A)	110.4
C(20)-C(21)-H(21B)	110.4
C(1)-C(21)-H(21B)	110.4
H(21A)-C(21)-H(21B)	108.6
C(6)-C(22)-H(22A)	109.5
C(6)-C(22)-H(22B)	109.5
H(22A)-C(22)-H(22B)	109.5
C(6)-C(22)-H(22C)	109.5
H(22A)-C(22)-H(22C)	109.5
H(22B)-C(22)-H(22C)	109.5
C(6)-C(23)-H(23A)	109.5
C(6)-C(23)-H(23B)	109.5
H(23A)-C(23)-H(23B)	109.5
C(6)-C(23)-H(23C)	109.5
H(23A)-C(23)-H(23C)	109.5
H(23B)-C(23)-H(23C)	109.5
C(12)-C(24)-H(24A)	109.5
C(12)-C(24)-H(24B)	109.5
H(24A)-C(24)-H(24B)	109.5
C(12)-C(24)-H(24C)	109.5
H(24A)-C(24)-H(24C)	109.5
H(24B)-C(24)-H(24C)	109.5
C(12)-C(25)-H(25A)	109.5
C(12)-C(25)-H(25B)	109.5
H(25A)-C(25)-H(25B)	109.5
C(12)-C(25)-H(25C)	109.5
H(25A)-C(25)-H(25C)	109.5
H(25B)-C(25)-H(25C)	109.5
C(11)-N(1)-C(10)	111.9(2)
C(11)-N(1)-H(1)	124.1
C(10)-N(1)-H(1)	124.1
C(19)-N(2)-C(18)	120.5(2)
C(19)-N(2)-C(15)	127.7(2)
C(18)-N(2)-C(15)	111.7(2)
O(4)-N(3)-O(5)	123.9(2)
O(4)-N(3)-C(20)	120.1(2)
O(5)-N(3)-C(20)	115.9(2)
C(5)-O(1)-C(6)	118.3(2)

Symmetry transformations used to generate equivalent atoms:

Table 4. Anisotropic displacement parameters ($Å^2 x\ 10^3$) for **2.96**. The anisotropic displacement factor exponent takes the form: $-2p^2[\ h^2\ a^{*2}U^{11} + ...\ + 2\ h\ k\ a^*\ b^*\ U^{12}\ ]$

	U^{11}	U^{22}	U^{33}	U^{23}	U^{13}	U^{12}
C(1)	19(1)	18(1)	24(1)	-1(1)	2(1)	0(1)
C(2)	18(1)	21(1)	23(1)	0(1)	2(1)	-3(1)
C(3)	26(1)	22(1)	24(1)	-1(1)	0(1)	-2(1)
C(4)	32(1)	18(1)	30(1)	-2(1)	-2(1)	2(1)
C(5)	28(1)	26(2)	28(1)	4(1)	-7(1)	-2(1)
C(6)	59(2)	36(2)	35(2)	-5(1)	-24(2)	8(2)
C(7)	56(2)	40(2)	27(1)	-4(1)	-10(1)	-3(2)
C(8)	36(2)	35(2)	30(1)	-4(1)	-5(1)	2(1)
C(9)	27(1)	26(2)	26(1)	-1(1)	-2(1)	0(1)
C(10)	21(1)	23(1)	26(1)	-2(1)	2(1)	0(1)
C(11)	22(1)	22(2)	29(1)	-3(1)	1(1)	0(1)
C(12)	19(1)	25(1)	25(1)	1(1)	1(1)	-1(1)
C(13)	19(1)	21(1)	27(1)	1(1)	3(1)	2(1)
C(14)	17(1)	28(2)	30(1)	3(1)	0(1)	1(1)
C(15)	20(1)	30(2)	27(1)	2(1)	-2(1)	-2(1)
C(16)	29(2)	52(2)	31(1)	1(1)	-6(1)	-5(2)
C(17)	44(2)	61(2)	28(1)	-9(1)	-4(1)	-6(2)
C(18)	32(2)	30(2)	23(1)	2(1)	0(1)	3(1)
C(19)	18(1)	19(1)	25(1)	5(1)	1(1)	4(1)
C(20)	19(1)	14(1)	27(1)	0(1)	0(1)	1(1)
C(21)	16(1)	22(1)	26(1)	1(1)	1(1)	-1(1)
C(22)	116(4)	49(2)	42(2)	-3(2)	-40(2)	17(2)
C(23)	48(2)	59(2)	75(3)	-23(2)	-28(2)	13(2)
C(24)	26(1)	28(2)	28(1)	4(1)	-5(1)	-7(1)
C(25)	22(1)	45(2)	30(1)	5(1)	4(1)	-2(1)
N(1)	36(1)	23(1)	26(1)	-8(1)	-2(1)	6(1)
N(2)	22(1)	23(1)	23(1)	2(1)	1(1)	1(1)
N(3)	26(1)	23(1)	26(1)	1(1)	4(1)	-1(1)
O(1)	55(1)	29(1)	30(1)	-1(1)	-17(1)	5(1)
O(2)	66(2)	38(1)	34(1)	-13(1)	-11(1)	14(1)
O(3)	35(1)	22(1)	34(1)	-3(1)	0(1)	5(1)
O(4)	37(1)	28(1)	38(1)	1(1)	-3(1)	-14(1)
O(5)	36(1)	23(1)	40(1)	7(1)	1(1)	8(1)
O(6)	22(1)	33(1)	30(1)	3(1)	6(1)	-1(1)

Table 5. Hydrogen coordinates (x 10^4) and isotropic displacement parameters ($Å^2$x 10^3) for **2.96**.

	x	y	z	U(eq)
H(3)	10617	-895	8390	29
H(4)	12306	-1847	8964	32
H(7A)	10625	-338	10432	50
H(7B)	12260	531	10616	50
H(13)	6059	2678	8010	27
H(14A)	3902	1246	7654	30
H(14B)	4626	2308	7351	30
H(15)	6016	-19	7307	31
H(16A)	4255	1378	6608	45
H(16B)	3567	102	6766	45
H(17A)	6398	-762	6478	53
H(17B)	5897	179	6093	53
H(18A)	9273	211	6517	34
H(18B)	8330	1384	6318	34
H(21A)	11171	2177	8065	26
H(21B)	10584	913	7882	26
H(22A)	12380	-2171	10524	104
H(22B)	13878	-1425	10819	104
H(22C)	14671	-2222	10417	104
H(23A)	16260	-640	9992	91
H(23B)	15758	247	10391	91
H(23C)	15088	527	9885	91
H(24A)	6933	-673	8423	41
H(24B)	7767	-367	7932	41
H(24C)	5461	-366	8020	41
H(25A)	3998	1065	8529	48
H(25B)	5262	2115	8727	48
H(25C)	5590	829	8914	48
H(1)	9515	2642	9408	34

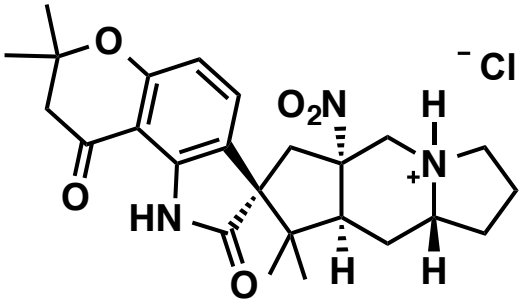

***ent*-citrinalin B•HCl (*ent*-2.2•HCl)**

A colorless plate 0.040 x 0.030 x 0.010 mm in size was mounted on a Cryoloop with Paratone oil. Data were collected in a nitrogen gas stream at 100(2) K using phi and omega scans. Crystal-to-detector distance was 60 mm and exposure time was 20 seconds per frame using a scan width of 2.0°. Data collection was 98.4% complete to 67.000° in θ. A total of 17934 reflections were collected covering the indices, -30<=*h*<=25, -8<=*k*<=8, -19<=*l*<=19. 4686 reflections were found to be symmetry independent, with an R_{int} of 0.0572. Indexing and unit cell refinement indicated a C-centered, monoclinic lattice. The space group was found to be C 2 (No. 5). The data were integrated using the Bruker SAINT software program and scaled using the SADABS software program. Solution by iterative methods (SHELXT) produced a complete heavy-atom phasing model consistent with the proposed structure. All non-hydrogen atoms were refined anisotropically by full-matrix least-squares (SHELXL-2013). All hydrogen atoms were placed using a riding model. Their positions were constrained relative to their parent atom using the appropriate HFIX command in SHELXL-2013. Absolute stereochemistry was unambiguously determined to be *R* at N2, C1, C18, and *S* at C13 and C20, respectively. CCDC 984477 (*ent*-**2.2**•HCl) contains the supplementary crystallographic data for this paper. This data can be obtained free of charge from The Cambridge Crystallographic Data Centre via www.ccdc.cam.ac.uk/data_request/cif.

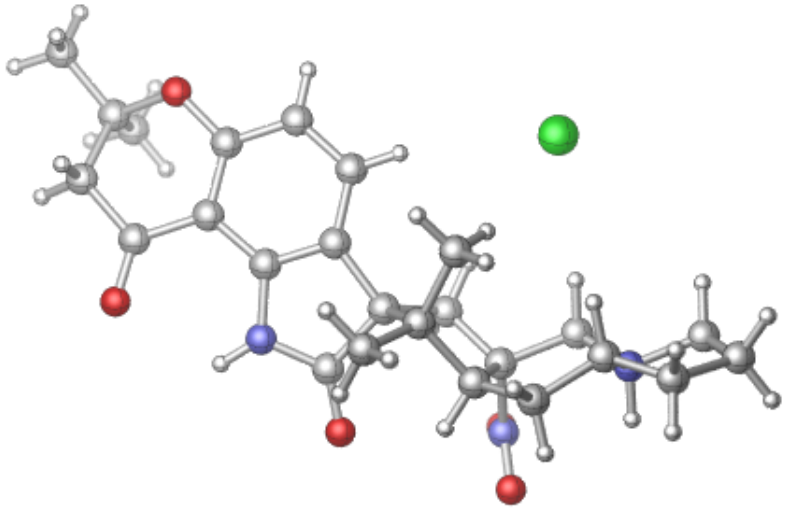

CYLView representation of *ent*-citrinalin B•HCl (*ent*-**2.2**•HCl)

Table 1. Crystal data and structure refinement for *ent*-**2.2**•HCl.

X-ray ID	sarpong75	
Sample/notebook ID	EM05-080D-F3	
Empirical formula	C50 H63 Cl N6 O10	
Formula weight	943.51	
Temperature	100(2) K	
Wavelength	1.54178 Å	
Crystal system	Monoclinic	
Space group	C 2	
Unit cell dimensions	a = 25.8379(8) Å	α= 90°.
	b = 6.7742(2) Å	β= 112.251(2)°.
	c = 16.2191(5) Å	γ = 90°.
Volume	2627.45(14) $Å^3$	
Z	2	
Density (calculated)	1.193 Mg/m^3	
Absorption coefficient	1.131 mm^{-1}	
F(000)	1004	
Crystal size	0.040 x 0.030 x 0.010 mm^3	
Crystal color/habit	colorless plate	
Theta range for data collection	2.944 to 68.356°.	
Index ranges	-30<=h<=25, -8<=k<=8, -19<=l<=19	
Reflections collected	17934	
Independent reflections	4686 [R(int) = 0.0572]	
Completeness to theta = 67.000°	98.4 %	
Absorption correction	Semi-empirical from equivalents	
Max. and min. transmission	0.929 and 0.822	
Refinement method	Full-matrix least-squares on F^2	
Data / restraints / parameters	4686 / 1 / 307	
Goodness-of-fit on F^2	1.092	
Final R indices [I>2sigma(I)]	R1 = 0.0931, wR2 = 0.2547	
R indices (all data)	R1 = 0.1077, wR2 = 0.2701	
Absolute structure parameter	-0.014(18)	
Extinction coefficient	n/a	
Largest diff. peak and hole	2.355 and -0.276 e.$Å^{-3}$	

Table 2. Atomic coordinates (x 10^4) and equivalent isotropic displacement parameters ($Å^2$x 10^3) for *ent*-**2.2**•HCl. U(eq) is defined as one third of the trace of the orthogonalized U^{ij} tensor.

	x	y	z	U(eq)
C(1)	8290(3)	7996(11)	4427(6)	40(2)
C(2)	8170(3)	7126(11)	3505(5)	37(2)
C(3)	8527(3)	6179(10)	3152(5)	37(2)
C(4)	8302(4)	5364(12)	2307(6)	45(2)
C(5)	7734(4)	5512(12)	1804(5)	45(2)
C(6)	6961(5)	4100(20)	621(6)	63(3)
C(7)	6608(5)	5830(20)	668(7)	67(3)
C(8)	6779(4)	6715(15)	1585(6)	54(2)
C(9)	7369(3)	6444(13)	2127(6)	44(2)
C(10)	7609(3)	7212(11)	3005(5)	40(2)
C(11)	7682(3)	8414(11)	4350(5)	36(2)
C(12)	8609(3)	6705(11)	5224(5)	38(2)
C(13)	8863(3)	8120(12)	6004(6)	42(2)
C(14)	9472(4)	7543(11)	6555(6)	43(2)
C(15)	10405(4)	8769(18)	7613(7)	62(3)
C(16)	10682(4)	10800(17)	7816(7)	59(2)
C(17)	10257(4)	12266(16)	7152(7)	57(2)
C(18)	9798(3)	10946(12)	6517(5)	40(2)
C(19)	9208(3)	11802(12)	6106(5)	40(2)
C(20)	8765(3)	10248(11)	5619(5)	38(2)
C(21)	8626(3)	10002(12)	4620(5)	36(2)
C(22)	6839(6)	3620(30)	-360(7)	95(5)
C(23)	6875(5)	2308(16)	1110(8)	70(3)
C(24)	8286(3)	11755(11)	4092(5)	40(2)
C(25)	9155(3)	9794(11)	4387(5)	36(2)
N(1)	7327(2)	8092(9)	3493(5)	37(1)
N(2)	9804(3)	9193(11)	7106(5)	47(2)
N(3)	8572(3)	7928(11)	6668(5)	46(2)
O(1)	7542(3)	4663(10)	978(4)	57(2)
O(2)	6454(3)	7636(11)	1822(5)	57(2)
O(3)	7542(2)	9026(8)	4933(4)	44(1)
O(4)	8455(5)	6300(13)	6834(6)	93(3)
O(5)	8488(4)	9380(12)	7033(5)	80(3)
Cl(1)	10000	5013(4)	5000	43(1)

Table 3. Bond lengths [Å] and angles [°] for *ent*-**2.2**•HCl.

C(1)-C(12)	1.520(11)	C(15)-C(16)	1.527(17)
C(1)-C(2)	1.526(11)	C(15)-H(15A)	0.9900
C(1)-C(11)	1.553(11)	C(15)-H(15B)	0.9900
C(1)-C(21)	1.579(11)	C(16)-C(17)	1.567(14)
C(2)-C(10)	1.369(11)	C(16)-H(16A)	0.9900
C(2)-C(3)	1.411(11)	C(16)-H(16B)	0.9900
C(3)-C(4)	1.385(12)	C(17)-C(18)	1.529(12)
C(3)-H(3)	0.9500	C(17)-H(17A)	0.9900
C(4)-C(5)	1.386(13)	C(17)-H(17B)	0.9900
C(4)-H(4)	0.9500	C(18)-N(2)	1.521(11)
C(5)-O(1)	1.367(10)	C(18)-C(19)	1.529(11)
C(5)-C(9)	1.392(12)	C(18)-H(18)	1.0000
C(6)-O(1)	1.441(13)	C(19)-C(20)	1.535(11)
C(6)-C(7)	1.506(17)	C(19)-H(19A)	0.9900
C(6)-C(23)	1.511(17)	C(19)-H(19B)	0.9900
C(6)-C(22)	1.535(14)	C(20)-C(21)	1.531(10)
C(7)-C(8)	1.507(15)	C(20)-H(20)	1.0000
C(7)-H(7A)	0.9900	C(21)-C(24)	1.531(11)
C(7)-H(7B)	0.9900	C(21)-C(25)	1.556(10)
C(8)-O(2)	1.219(11)	C(22)-H(22A)	0.9800
C(8)-C(9)	1.455(13)	C(22)-H(22B)	0.9800
C(9)-C(10)	1.419(12)	C(22)-H(22C)	0.9800
C(10)-N(1)	1.396(10)	C(23)-H(23A)	0.9800
C(11)-O(3)	1.206(9)	C(23)-H(23B)	0.9800
C(11)-N(1)	1.363(11)	C(23)-H(23C)	0.9800
C(12)-C(13)	1.524(11)	C(24)-H(24A)	0.9800
C(12)-H(12A)	0.9900	C(24)-H(24B)	0.9800
C(12)-H(12B)	0.9900	C(24)-H(24C)	0.9800
C(13)-N(3)	1.535(10)	C(25)-H(25A)	0.9800
C(13)-C(14)	1.536(11)	C(25)-H(25B)	0.9800
C(13)-C(20)	1.553(10)	C(25)-H(25C)	0.9800
C(14)-N(2)	1.485(12)	N(1)-H(1)	0.8800
C(14)-H(14A)	0.9900	N(2)-H(2)	1.0000
C(14)-H(14B)	0.9900	N(3)-O(4)	1.200(11)
C(15)-N(2)	1.484(13)	N(3)-O(5)	1.208(10)

C(12)-C(1)-C(2)	117.0(6)	O(1)-C(6)-C(7)	109.4(9)
C(12)-C(1)-C(11)	112.3(6)	O(1)-C(6)-C(23)	109.9(9)
C(2)-C(1)-C(11)	99.7(6)	C(7)-C(6)-C(23)	112.7(9)
C(12)-C(1)-C(21)	104.2(6)	O(1)-C(6)-C(22)	104.3(9)
C(2)-C(1)-C(21)	114.8(6)	C(7)-C(6)-C(22)	109.1(10)
C(11)-C(1)-C(21)	108.8(6)	C(23)-C(6)-C(22)	111.1(12)
C(10)-C(2)-C(3)	119.2(7)	C(6)-C(7)-C(8)	113.8(8)
C(10)-C(2)-C(1)	109.9(6)	C(6)-C(7)-H(7A)	108.8
C(3)-C(2)-C(1)	130.7(7)	C(8)-C(7)-H(7A)	108.8
C(4)-C(3)-C(2)	119.2(7)	C(6)-C(7)-H(7B)	108.8
C(4)-C(3)-H(3)	120.4	C(8)-C(7)-H(7B)	108.8
C(2)-C(3)-H(3)	120.4	H(7A)-C(7)-H(7B)	107.7
C(3)-C(4)-C(5)	120.5(8)	O(2)-C(8)-C(9)	124.3(9)
C(3)-C(4)-H(4)	119.8	O(2)-C(8)-C(7)	122.3(9)
C(5)-C(4)-H(4)	119.8	C(9)-C(8)-C(7)	113.3(8)
O(1)-C(5)-C(4)	117.1(8)	C(5)-C(9)-C(10)	116.3(7)
O(1)-C(5)-C(9)	120.9(8)	C(5)-C(9)-C(8)	122.3(8)
C(4)-C(5)-C(9)	122.0(7)	C(10)-C(9)-C(8)	121.3(8)

C(2)-C(10)-N(1)	110.3(7)
C(2)-C(10)-C(9)	122.7(7)
N(1)-C(10)-C(9)	127.0(7)
O(3)-C(11)-N(1)	124.6(7)
O(3)-C(11)-C(1)	126.5(7)
N(1)-C(11)-C(1)	108.8(6)
C(1)-C(12)-C(13)	105.6(6)
C(1)-C(12)-H(12A)	110.6
C(13)-C(12)-H(12A)	110.6
C(1)-C(12)-H(12B)	110.6
C(13)-C(12)-H(12B)	110.6
H(12A)-C(12)-H(12B)	108.8
C(12)-C(13)-N(3)	111.0(6)
C(12)-C(13)-C(14)	110.2(7)
N(3)-C(13)-C(14)	103.7(7)
C(12)-C(13)-C(20)	107.3(6)
N(3)-C(13)-C(20)	108.2(6)
C(14)-C(13)-C(20)	116.4(6)
N(2)-C(14)-C(13)	113.0(6)
N(2)-C(14)-H(14A)	109.0
C(13)-C(14)-H(14A)	109.0
N(2)-C(14)-H(14B)	109.0
C(13)-C(14)-H(14B)	109.0
H(14A)-C(14)-H(14B)	107.8
N(2)-C(15)-C(16)	104.5(8)
N(2)-C(15)-H(15A)	110.8
C(16)-C(15)-H(15A)	110.8
N(2)-C(15)-H(15B)	110.8
C(16)-C(15)-H(15B)	110.8
H(15A)-C(15)-H(15B)	108.9
C(15)-C(16)-C(17)	105.9(8)
C(15)-C(16)-H(16A)	110.6
C(17)-C(16)-H(16A)	110.6
C(15)-C(16)-H(16B)	110.6
C(17)-C(16)-H(16B)	110.6
H(16A)-C(16)-H(16B)	108.7
C(18)-C(17)-C(16)	104.8(8)
C(18)-C(17)-H(17A)	110.8
C(16)-C(17)-H(17A)	110.8
C(18)-C(17)-H(17B)	110.8
C(16)-C(17)-H(17B)	110.8
H(17A)-C(17)-H(17B)	108.9
N(2)-C(18)-C(19)	109.9(6)
N(2)-C(18)-C(17)	102.3(7)
C(19)-C(18)-C(17)	117.6(7)
N(2)-C(18)-H(18)	108.9
C(19)-C(18)-H(18)	108.9
C(17)-C(18)-H(18)	108.9
C(18)-C(19)-C(20)	113.0(6)
C(18)-C(19)-H(19A)	109.0
C(20)-C(19)-H(19A)	109.0
C(18)-C(19)-H(19B)	109.0
C(20)-C(19)-H(19B)	109.0
H(19A)-C(19)-H(19B)	107.8
C(21)-C(20)-C(19)	116.7(6)
C(21)-C(20)-C(13)	105.2(6)
C(19)-C(20)-C(13)	117.0(6)
C(21)-C(20)-H(20)	105.6
C(19)-C(20)-H(20)	105.6
C(13)-C(20)-H(20)	105.6
C(20)-C(21)-C(24)	111.2(6)
C(20)-C(21)-C(25)	113.1(6)
C(24)-C(21)-C(25)	107.7(6)
C(20)-C(21)-C(1)	101.2(6)
C(24)-C(21)-C(1)	113.6(6)
C(25)-C(21)-C(1)	110.0(6)
C(6)-C(22)-H(22A)	109.5
C(6)-C(22)-H(22B)	109.5
H(22A)-C(22)-H(22B)	109.5
C(6)-C(22)-H(22C)	109.5
H(22A)-C(22)-H(22C)	109.5
H(22B)-C(22)-H(22C)	109.5
C(6)-C(23)-H(23A)	109.5
C(6)-C(23)-H(23B)	109.5
H(23A)-C(23)-H(23B)	109.5
C(6)-C(23)-H(23C)	109.5
H(23A)-C(23)-H(23C)	109.5
H(23B)-C(23)-H(23C)	109.5
C(21)-C(24)-H(24A)	109.5
C(21)-C(24)-H(24B)	109.5
H(24A)-C(24)-H(24B)	109.5
C(21)-C(24)-H(24C)	109.5
H(24A)-C(24)-H(24C)	109.5
H(24B)-C(24)-H(24C)	109.5
C(21)-C(25)-H(25A)	109.5
C(21)-C(25)-H(25B)	109.5
H(25A)-C(25)-H(25B)	109.5
C(21)-C(25)-H(25C)	109.5
H(25A)-C(25)-H(25C)	109.5
H(25B)-C(25)-H(25C)	109.5
C(11)-N(1)-C(10)	110.6(6)
C(11)-N(1)-H(1)	124.7
C(10)-N(1)-H(1)	124.7
C(15)-N(2)-C(14)	115.7(7)
C(15)-N(2)-C(18)	105.0(7)
C(14)-N(2)-C(18)	110.1(6)
C(15)-N(2)-H(2)	108.6
C(14)-N(2)-H(2)	108.6
C(18)-N(2)-H(2)	108.6
O(4)-N(3)-O(5)	122.1(7)
O(4)-N(3)-C(13)	117.8(7)
O(5)-N(3)-C(13)	120.0(7)
C(5)-O(1)-C(6)	116.2(7)

Table 4. Anisotropic displacement parameters ($Å^2 x\ 10^3$) for *ent*-**2.2**•HCl. The anisotropic displacement factor exponent takes the form: $-2\pi^2[\ h^2\ a^{*2}U^{11} + ...\ + 2\ h\ k\ a^*\ b^*\ U^{12}\ ]$

	U^{11}	U^{22}	U^{33}	U^{23}	U^{13}	U^{12}
C(1)	53(4)	24(3)	48(4)	-2(3)	24(4)	3(3)
C(2)	45(4)	30(3)	41(4)	-1(3)	21(3)	-5(3)
C(3)	45(4)	26(3)	44(4)	-2(3)	23(3)	2(3)
C(4)	59(5)	35(4)	50(5)	1(3)	31(4)	6(4)
C(5)	65(5)	39(4)	39(4)	0(3)	27(4)	0(4)
C(6)	63(6)	83(7)	37(5)	-19(5)	11(4)	-2(5)
C(7)	64(6)	86(8)	46(5)	6(5)	14(4)	9(5)
C(8)	56(5)	62(6)	45(4)	8(4)	22(4)	8(4)
C(9)	46(4)	48(4)	43(4)	3(4)	23(4)	-1(3)
C(10)	52(4)	28(3)	44(4)	5(3)	24(4)	2(3)
C(11)	45(4)	29(3)	39(4)	1(3)	20(3)	-2(3)
C(12)	44(4)	31(4)	48(4)	1(3)	28(3)	0(3)
C(13)	42(4)	38(4)	51(5)	3(4)	24(4)	1(3)
C(14)	53(4)	30(4)	53(5)	10(3)	28(4)	12(3)
C(15)	60(6)	73(7)	55(6)	12(5)	24(5)	16(5)
C(16)	51(5)	71(6)	50(5)	6(5)	11(4)	18(5)
C(17)	53(5)	58(6)	54(5)	-11(4)	15(4)	-3(4)
C(18)	39(4)	44(4)	35(4)	4(3)	14(3)	0(3)
C(19)	45(4)	40(4)	36(4)	3(3)	16(3)	10(3)
C(20)	45(4)	29(4)	44(4)	2(3)	21(3)	1(3)
C(21)	45(4)	31(3)	39(4)	0(3)	22(3)	-2(3)
C(22)	91(8)	137(14)	43(6)	-29(7)	11(6)	1(9)
C(23)	62(6)	49(5)	81(7)	-15(5)	7(5)	-13(4)
C(24)	48(4)	32(4)	41(4)	5(3)	19(3)	1(3)
C(25)	38(3)	32(3)	42(4)	4(3)	18(3)	-7(3)
N(1)	29(3)	32(3)	54(4)	4(3)	19(3)	0(2)
N(2)	52(4)	39(3)	53(4)	0(3)	24(3)	3(3)
N(3)	62(4)	40(4)	47(4)	4(3)	34(3)	4(3)
O(1)	80(4)	59(4)	36(3)	-9(3)	25(3)	-4(3)
O(2)	55(3)	63(4)	56(4)	0(3)	23(3)	7(3)
O(3)	53(3)	34(3)	57(3)	-2(3)	34(3)	-3(2)
O(4)	164(9)	68(5)	85(6)	-29(4)	90(6)	-57(6)
O(5)	139(7)	61(5)	77(5)	6(4)	83(6)	15(5)
Cl(1)	43(1)	34(1)	57(2)	0	25(1)	0

Table 5. Hydrogen coordinates (x 10^4) and isotropic displacement parameters ($Å^2$x 10^3) for *ent*-**2.2**•HCl.

	x	y	z	U(eq)
H(3)	8918	6102	3490	44
H(4)	8539	4699	2070	54
H(7A)	6213	5397	468	81
H(7B)	6630	6861	251	81
H(12A)	8906	5955	5115	45
H(12B)	8354	5760	5344	45
H(14A)	9474	6425	6949	52
H(14B)	9651	7091	6146	52
H(15A)	10562	7971	7252	75
H(15B)	10458	8048	8170	75
H(16A)	11040	10793	7726	71
H(16B)	10756	11184	8440	71
H(17A)	10101	13184	7473	68
H(17B)	10441	13044	6822	68
H(18)	9916	10491	6027	47
H(19A)	9203	12857	5681	48
H(19B)	9110	12408	6584	48
H(20)	8411	10708	5672	46
H(22A)	6970	4703	-630	142
H(22B)	6435	3444	-679	142
H(22C)	7033	2398	-397	142
H(23A)	6956	2653	1733	104
H(23B)	7127	1249	1084	104
H(23C)	6487	1860	830	104
H(24A)	7948	11910	4221	60
H(24B)	8182	11517	3454	60
H(24C)	8512	12960	4264	60
H(25A)	9396	10951	4608	54
H(25B)	9042	9701	3740	54
H(25C)	9360	8600	4668	54
H(1)	6969	8396	3277	45
H(2)	9630	9605	7535	56

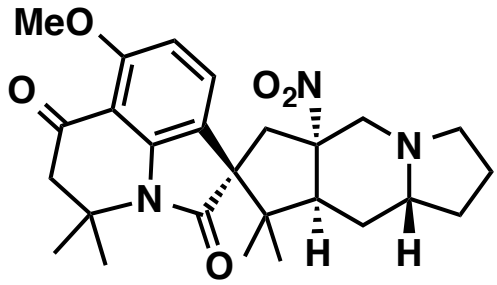

cyclopiamine B (2.6)

A colorless blade 0.050 x 0.040 x 0.020 mm in size was mounted on a Cryoloop with Paratone oil. Data were collected in a nitrogen gas stream at 100(2) K using phi and omega scans. Crystal-to-detector distance was 60 mm and exposure time was 5 seconds per frame using a scan width of 1.0°. Data collection was 100.0% complete to 67.000° in θ. A total of 43571 reflections were collected covering the indices, -12<=*h*<=12, -16<=*k*<=16, -19<=*l*<=19. 4544 reflections were found to be symmetry independent, with an R_{int} of 0.0179. Indexing and unit cell refinement indicated a primitive, orthorhombic lattice. The space group was found to be P 21 21 21 (No. 19). The data were integrated using the Bruker SAINT software program and scaled using the SADABS software program. Solution by iterative methods (SHELXT) produced a complete heavy-atom phasing model consistent with the proposed structure. All non-hydrogen atoms were refined anisotropically by full-matrix least-squares (SHELXL-2013). All hydrogen atoms were placed using a riding model. Their positions were constrained relative to their parent atom using the appropriate HFIX command in SHELXL-2013. Absolute stereochemistry was unambiguously determined to be *R* at C1 and C8, and *S* at C3 and C10, respectively. CCDC 984478 (**2.6**) contains the supplementary crystallographic data for this paper. This data can be obtained free of charge from The Cambridge Crystallographic Data Centre via www.ccdc.cam.ac.uk/data_request/cif.

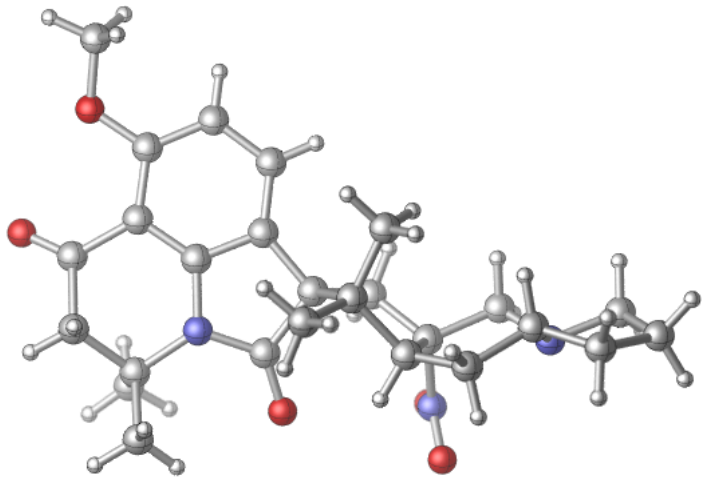

CYLView representation of **cyclopiamine B (2.6)**

Table 1. Crystal data and structure refinement for **2.6**.

X-ray ID	sarpong70	
Sample/notebook ID	EM05-028B	
Empirical formula	C27 H37 N3 O6	
Formula weight	499.59	
Temperature	100(2) K	
Wavelength	1.54178 Å	
Crystal system	Orthorhombic	
Space group	P 21 21 21	
Unit cell dimensions	a = 10.7754(6) Å	α= 90°.
	b = 14.1165(8) Å	β= 90°.
	c = 16.3912(9) Å	γ = 90°.
Volume	2493.3(2) $Å^3$	
Z	4	
Density (calculated)	1.331 Mg/m^3	
Absorption coefficient	0.769 mm^{-1}	
F(000)	1072	
Crystal size	0.050 x 0.040 x 0.020 mm^3	
Crystal color/habit	colorless blade	
Theta range for data collection	4.133 to 68.289°.	
Index ranges	-12<=h<=12, -16<=k<=16, -19<=l<=19	
Reflections collected	43571	
Independent reflections	4544 [R(int) = 0.0179]	
Completeness to theta = 67.000°	100.0 %	
Absorption correction	Semi-empirical from equivalents	
Max. and min. transmission	0.929 and 0.881	
Refinement method	Full-matrix least-squares on F^2	
Data / restraints / parameters	4544 / 0 / 332	
Goodness-of-fit on F^2	1.074	
Final R indices [I>2sigma(I)]	R1 = 0.0304, wR2 = 0.0886	
R indices (all data)	R1 = 0.0306, wR2 = 0.0887	
Absolute structure parameter	-0.02(2)	
Extinction coefficient	n/a	
Largest diff. peak and hole	0.235 and -0.332 e.$Å^{-3}$	

Table 2. Atomic coordinates (x 10^4) and equivalent isotropic displacement parameters ($Å^2$x 10^3) for **2.6**. U(eq) is defined as one third of the trace of the orthogonalized U^{ij} tensor.

	x	y	z	U(eq)
C(1)	9601(2)	6235(2)	3390(1)	16(1)
C(2)	10240(2)	5593(1)	2751(1)	16(1)
C(3)	11251(2)	6206(2)	2348(1)	16(1)
C(4)	11254(2)	6108(2)	1411(1)	18(1)
C(5)	11985(2)	6819(2)	134(1)	24(1)
C(6)	12356(2)	7825(2)	-123(2)	30(1)
C(7)	11953(3)	8457(2)	596(2)	29(1)
C(8)	11333(2)	7780(2)	1194(1)	21(1)
C(9)	11465(2)	8024(2)	2091(1)	21(1)
C(10)	11068(2)	7229(2)	2675(1)	17(1)
C(11)	9720(2)	7255(2)	3009(1)	18(1)
C(12)	8740(2)	7404(2)	2344(1)	22(1)
C(13)	9572(2)	8039(2)	3646(1)	24(1)
C(14)	8314(2)	5973(2)	3662(1)	16(1)
C(15)	7227(2)	5771(2)	3251(1)	18(1)
C(16)	6142(2)	5571(2)	3685(1)	18(1)
C(17)	6149(2)	5537(1)	4538(1)	16(1)
C(18)	7259(2)	5705(1)	4974(1)	16(1)
C(19)	7439(2)	5631(2)	5866(1)	18(1)
C(20)	8550(2)	6189(2)	6176(1)	22(1)
C(21)	9768(2)	6004(2)	5713(1)	18(1)
C(22)	10322(2)	6189(2)	4199(1)	17(1)
C(23)	8294(2)	5942(1)	4515(1)	16(1)
C(24)	3948(2)	5496(2)	4599(1)	22(1)
C(25)	10741(2)	6734(2)	5977(2)	28(1)
C(26)	10225(2)	4995(2)	5868(1)	27(1)
C(27)	15124(3)	7835(2)	1748(2)	44(1)
N(1)	11951(2)	6868(1)	1031(1)	19(1)
N(2)	12545(2)	5849(1)	2601(1)	21(1)
N(3)	9480(2)	6118(1)	4830(1)	16(1)
O(1)	13359(2)	6430(1)	2744(1)	27(1)
O(2)	12720(2)	4990(1)	2605(1)	29(1)
O(3)	5127(1)	5358(1)	4989(1)	19(1)
O(4)	6783(1)	5175(1)	6320(1)	26(1)
O(5)	11446(1)	6198(1)	4276(1)	24(1)
O(6)	14649(2)	7307(2)	1098(1)	45(1)

Table 3. Bond lengths [Å] and angles [°] for **2.6**.

C(1)-C(14)	1.503(3)	C(14)-C(15)	1.381(3)
C(1)-C(22)	1.539(3)	C(14)-C(23)	1.399(3)
C(1)-C(2)	1.547(3)	C(15)-C(16)	1.397(3)
C(1)-C(11)	1.575(3)	C(15)-H(15)	0.9500
C(2)-C(3)	1.541(3)	C(16)-C(17)	1.398(3)
C(2)-H(2A)	0.9900	C(16)-H(16)	0.9500
C(2)-H(2B)	0.9900	C(17)-O(3)	1.351(3)
C(3)-N(2)	1.540(3)	C(17)-C(18)	1.413(3)
C(3)-C(4)	1.541(3)	C(18)-C(23)	1.386(3)
C(3)-C(10)	1.554(3)	C(18)-C(19)	1.480(3)
C(4)-N(1)	1.451(3)	C(19)-O(4)	1.212(3)
C(4)-H(4A)	0.9900	C(19)-C(20)	1.520(3)
C(4)-H(4B)	0.9900	C(20)-C(21)	1.539(3)
C(5)-N(1)	1.473(3)	C(20)-H(20A)	0.9900
C(5)-C(6)	1.534(3)	C(20)-H(20B)	0.9900
C(5)-H(5A)	0.9900	C(21)-N(3)	1.488(3)
C(5)-H(5B)	0.9900	C(21)-C(26)	1.528(3)
C(6)-C(7)	1.541(4)	C(21)-C(25)	1.533(3)
C(6)-H(6A)	0.9900	C(22)-O(5)	1.217(3)
C(6)-H(6B)	0.9900	C(22)-N(3)	1.380(3)
C(7)-C(8)	1.523(3)	C(23)-N(3)	1.400(3)
C(7)-H(7A)	0.9900	C(24)-O(3)	1.435(3)
C(7)-H(7B)	0.9900	C(24)-H(24A)	0.9800
C(8)-N(1)	1.474(3)	C(24)-H(24B)	0.9800
C(8)-C(9)	1.516(3)	C(24)-H(24C)	0.9800
C(8)-H(8)	1.0000	C(25)-H(25A)	0.9800
C(9)-C(10)	1.536(3)	C(25)-H(25B)	0.9800
C(9)-H(9A)	0.9900	C(25)-H(25C)	0.9800
C(9)-H(9B)	0.9900	C(26)-H(26A)	0.9800
C(10)-C(11)	1.553(3)	C(26)-H(26B)	0.9800
C(10)-H(10)	1.0000	C(26)-H(26C)	0.9800
C(11)-C(13)	1.530(3)	C(27)-O(6)	1.397(4)
C(11)-C(12)	1.533(3)	C(27)-H(27A)	0.9800
C(12)-H(12A)	0.9800	C(27)-H(27B)	0.9800
C(12)-H(12B)	0.9800	C(27)-H(27C)	0.9800
C(12)-H(12C)	0.9800	N(2)-O(1)	1.223(3)
C(13)-H(13A)	0.9800	N(2)-O(2)	1.227(3)
C(13)-H(13B)	0.9800	O(6)-H(6)	0.8400
C(13)-H(13C)	0.9800		

C(14)-C(1)-C(22)	101.52(16)	C(2)-C(3)-C(4)	112.26(17)
C(14)-C(1)-C(2)	117.90(18)	N(2)-C(3)-C(10)	108.99(17)
C(22)-C(1)-C(2)	109.52(17)	C(2)-C(3)-C(10)	106.52(16)
C(14)-C(1)-C(11)	114.68(17)	C(4)-C(3)-C(10)	115.30(17)
C(22)-C(1)-C(11)	109.79(17)	N(1)-C(4)-C(3)	111.26(17)
C(2)-C(1)-C(11)	103.39(16)	N(1)-C(4)-H(4A)	109.4
C(3)-C(2)-C(1)	106.04(16)	C(3)-C(4)-H(4A)	109.4
C(3)-C(2)-H(2A)	110.5	N(1)-C(4)-H(4B)	109.4
C(1)-C(2)-H(2A)	110.5	C(3)-C(4)-H(4B)	109.4
C(3)-C(2)-H(2B)	110.5	H(4A)-C(4)-H(4B)	108.0
C(1)-C(2)-H(2B)	110.5	N(1)-C(5)-C(6)	103.73(19)
H(2A)-C(2)-H(2B)	108.7	N(1)-C(5)-H(5A)	111.0
N(2)-C(3)-C(2)	109.96(16)	C(6)-C(5)-H(5A)	111.0
N(2)-C(3)-C(4)	103.74(16)	N(1)-C(5)-H(5B)	111.0

C(6)-C(5)-H(5B)	111.0	C(15)-C(16)-C(17)	120.8(2)
H(5A)-C(5)-H(5B)	109.0	C(15)-C(16)-H(16)	119.6
C(5)-C(6)-C(7)	104.59(18)	C(17)-C(16)-H(16)	119.6
C(5)-C(6)-H(6A)	110.8	O(3)-C(17)-C(16)	123.36(19)
C(7)-C(6)-H(6A)	110.8	O(3)-C(17)-C(18)	116.38(18)
C(5)-C(6)-H(6B)	110.8	C(16)-C(17)-C(18)	120.25(19)
C(7)-C(6)-H(6B)	110.8	C(23)-C(18)-C(17)	116.60(19)
H(6A)-C(6)-H(6B)	108.9	C(23)-C(18)-C(19)	116.57(19)
C(8)-C(7)-C(6)	104.68(19)	C(17)-C(18)-C(19)	126.81(19)
C(8)-C(7)-H(7A)	110.8	O(4)-C(19)-C(18)	124.7(2)
C(6)-C(7)-H(7A)	110.8	O(4)-C(19)-C(20)	121.98(19)
C(8)-C(7)-H(7B)	110.8	C(18)-C(19)-C(20)	113.37(18)
C(6)-C(7)-H(7B)	110.8	C(19)-C(20)-C(21)	114.77(17)
H(7A)-C(7)-H(7B)	108.9	C(19)-C(20)-H(20A)	108.6
N(1)-C(8)-C(9)	109.43(18)	C(21)-C(20)-H(20A)	108.6
N(1)-C(8)-C(7)	103.43(19)	C(19)-C(20)-H(20B)	108.6
C(9)-C(8)-C(7)	116.09(19)	C(21)-C(20)-H(20B)	108.6
N(1)-C(8)-H(8)	109.2	H(20A)-C(20)-H(20B)	107.6
C(9)-C(8)-H(8)	109.2	N(3)-C(21)-C(26)	109.24(17)
C(7)-C(8)-H(8)	109.2	N(3)-C(21)-C(25)	110.19(18)
C(8)-C(9)-C(10)	114.31(18)	C(26)-C(21)-C(25)	111.05(19)
C(8)-C(9)-H(9A)	108.7	N(3)-C(21)-C(20)	106.45(17)
C(10)-C(9)-H(9A)	108.7	C(26)-C(21)-C(20)	110.54(19)
C(8)-C(9)-H(9B)	108.7	C(25)-C(21)-C(20)	109.27(18)
C(10)-C(9)-H(9B)	108.7	O(5)-C(22)-N(3)	125.3(2)
H(9A)-C(9)-H(9B)	107.6	O(5)-C(22)-C(1)	126.21(19)
C(9)-C(10)-C(11)	117.61(18)	N(3)-C(22)-C(1)	108.48(17)
C(9)-C(10)-C(3)	115.40(17)	C(18)-C(23)-C(14)	124.16(19)
C(11)-C(10)-C(3)	105.20(16)	C(18)-C(23)-N(3)	125.28(19)
C(9)-C(10)-H(10)	105.9	C(14)-C(23)-N(3)	110.42(18)
C(11)-C(10)-H(10)	105.9	O(3)-C(24)-H(24A)	109.5
C(3)-C(10)-H(10)	105.9	O(3)-C(24)-H(24B)	109.5
C(13)-C(11)-C(12)	108.34(18)	H(24A)-C(24)-H(24B)	109.5
C(13)-C(11)-C(10)	110.81(17)	O(3)-C(24)-H(24C)	109.5
C(12)-C(11)-C(10)	113.38(17)	H(24A)-C(24)-H(24C)	109.5
C(13)-C(11)-C(1)	112.47(17)	H(24B)-C(24)-H(24C)	109.5
C(12)-C(11)-C(1)	110.57(17)	C(21)-C(25)-H(25A)	109.5
C(10)-C(11)-C(1)	101.22(16)	C(21)-C(25)-H(25B)	109.5
C(11)-C(12)-H(12A)	109.5	H(25A)-C(25)-H(25B)	109.5
C(11)-C(12)-H(12B)	109.5	C(21)-C(25)-H(25C)	109.5
H(12A)-C(12)-H(12B)	109.5	H(25A)-C(25)-H(25C)	109.5
C(11)-C(12)-H(12C)	109.5	H(25B)-C(25)-H(25C)	109.5
H(12A)-C(12)-H(12C)	109.5	C(21)-C(26)-H(26A)	109.5
H(12B)-C(12)-H(12C)	109.5	C(21)-C(26)-H(26B)	109.5
C(11)-C(13)-H(13A)	109.5	H(26A)-C(26)-H(26B)	109.5
C(11)-C(13)-H(13B)	109.5	C(21)-C(26)-H(26C)	109.5
H(13A)-C(13)-H(13B)	109.5	H(26A)-C(26)-H(26C)	109.5
C(11)-C(13)-H(13C)	109.5	H(26B)-C(26)-H(26C)	109.5
H(13A)-C(13)-H(13C)	109.5	O(6)-C(27)-H(27A)	109.5
H(13B)-C(13)-H(13C)	109.5	O(6)-C(27)-H(27B)	109.5
C(15)-C(14)-C(23)	117.93(19)	H(27A)-C(27)-H(27B)	109.5
C(15)-C(14)-C(1)	133.48(19)	O(6)-C(27)-H(27C)	109.5
C(23)-C(14)-C(1)	108.59(18)	H(27A)-C(27)-H(27C)	109.5
C(14)-C(15)-C(16)	120.2(2)	H(27B)-C(27)-H(27C)	109.5
C(14)-C(15)-H(15)	119.9	C(4)-N(1)-C(5)	114.03(17)
C(16)-C(15)-H(15)	119.9	C(4)-N(1)-C(8)	109.50(16)

C(5)-N(1)-C(8)	103.52(17)
O(1)-N(2)-O(2)	123.5(2)
O(1)-N(2)-C(3)	118.84(18)
O(2)-N(2)-C(3)	117.59(18)
C(22)-N(3)-C(23)	109.69(17)
C(22)-N(3)-C(21)	126.81(17)
C(23)-N(3)-C(21)	121.99(17)
C(17)-O(3)-C(24)	116.84(16)
C(27)-O(6)-H(6)	109.5

Symmetry transformations used to generate equivalent atoms:

Table 4. Anisotropic displacement parameters ($Å^2 x\ 10^3$) for **2.6**. The anisotropic displacement factor exponent takes the form: $-2\pi^2[\ h^2\ a^{*2}U^{11} + ...\ + 2\ h\ k\ a^*\ b^*\ U^{12}\ ]$

	U^{11}	U^{22}	U^{33}	U^{23}	U^{13}	U^{12}
C(1)	14(1)	20(1)	14(1)	0(1)	-2(1)	-1(1)
C(2)	16(1)	17(1)	15(1)	-1(1)	1(1)	1(1)
C(3)	15(1)	18(1)	16(1)	1(1)	0(1)	1(1)
C(4)	21(1)	19(1)	14(1)	-1(1)	1(1)	1(1)
C(5)	28(1)	29(1)	16(1)	3(1)	1(1)	0(1)
C(6)	34(1)	34(1)	22(1)	5(1)	3(1)	-7(1)
C(7)	37(1)	24(1)	25(1)	4(1)	2(1)	-7(1)
C(8)	22(1)	20(1)	22(1)	4(1)	-1(1)	-2(1)
C(9)	22(1)	20(1)	22(1)	-2(1)	1(1)	-5(1)
C(10)	17(1)	18(1)	15(1)	-2(1)	0(1)	-3(1)
C(11)	16(1)	18(1)	18(1)	-1(1)	0(1)	0(1)
C(12)	19(1)	23(1)	23(1)	4(1)	0(1)	1(1)
C(13)	26(1)	22(1)	24(1)	-4(1)	5(1)	-1(1)
C(14)	15(1)	17(1)	17(1)	2(1)	1(1)	0(1)
C(15)	18(1)	21(1)	16(1)	0(1)	0(1)	-1(1)
C(16)	14(1)	20(1)	19(1)	0(1)	-2(1)	-1(1)
C(17)	15(1)	15(1)	18(1)	0(1)	1(1)	1(1)
C(18)	14(1)	15(1)	18(1)	-1(1)	0(1)	2(1)
C(19)	14(1)	23(1)	17(1)	0(1)	1(1)	4(1)
C(20)	20(1)	30(1)	16(1)	-4(1)	1(1)	1(1)
C(21)	15(1)	26(1)	13(1)	-1(1)	-2(1)	-1(1)
C(22)	16(1)	20(1)	16(1)	-2(1)	0(1)	-1(1)
C(23)	14(1)	16(1)	18(1)	-2(1)	-2(1)	2(1)
C(24)	13(1)	32(1)	22(1)	5(1)	0(1)	-1(1)
C(25)	23(1)	39(1)	22(1)	-7(1)	-1(1)	-8(1)
C(26)	23(1)	34(1)	23(1)	3(1)	-2(1)	6(1)
C(27)	39(2)	56(2)	37(2)	-6(1)	2(1)	-9(1)
N(1)	19(1)	21(1)	16(1)	0(1)	1(1)	-1(1)
N(2)	18(1)	29(1)	15(1)	3(1)	2(1)	3(1)
N(3)	13(1)	21(1)	15(1)	-2(1)	-1(1)	0(1)
O(1)	16(1)	39(1)	27(1)	4(1)	-1(1)	-3(1)
O(2)	27(1)	27(1)	33(1)	4(1)	3(1)	10(1)
O(3)	12(1)	27(1)	17(1)	2(1)	0(1)	0(1)
O(4)	19(1)	40(1)	19(1)	7(1)	2(1)	-2(1)
O(5)	13(1)	38(1)	20(1)	1(1)	0(1)	0(1)
O(6)	34(1)	58(1)	42(1)	-11(1)	3(1)	-7(1)

Table 5. Hydrogen coordinates (x 10^4) and isotropic displacement parameters ($Å^2$x 10^3) for **2.6**.

	x	y	z	U(eq)
H(2A)	10614	5032	3018	19
H(2B)	9632	5373	2339	19
H(4A)	11625	5491	1258	21
H(4B)	10389	6118	1208	21
H(5A)	11162	6648	-90	29
H(5B)	12605	6350	-54	29
H(6A)	11924	8013	-631	36
H(6B)	13263	7868	-213	36
H(7A)	12680	8768	850	34
H(7B)	11363	8950	413	34
H(8)	10432	7725	1056	25
H(9A)	10960	8594	2207	25
H(9B)	12343	8186	2202	25
H(10)	11621	7286	3162	20
H(12A)	7914	7426	2593	32
H(12B)	8777	6880	1953	32
H(12C)	8902	8003	2060	32
H(13A)	9629	8658	3379	36
H(13B)	10231	7982	4056	36
H(13C)	8762	7978	3913	36
H(15)	7217	5768	2671	22
H(16)	5392	5457	3397	21
H(20A)	8679	6034	6759	26
H(20B)	8354	6873	6141	26
H(24A)	3925	6126	4348	33
H(24B)	3284	5446	5005	33
H(24C)	3830	5012	4178	33
H(25A)	11520	6615	5686	42
H(25B)	10883	6681	6566	42
H(25C)	10443	7373	5848	42
H(26A)	9566	4544	5730	40
H(26B)	10446	4925	6445	40
H(26C)	10955	4869	5529	40
H(27A)	15954	8067	1607	66
H(27B)	15175	7435	2235	66
H(27C)	14577	8375	1857	66
H(6)	13924	7131	1209	67

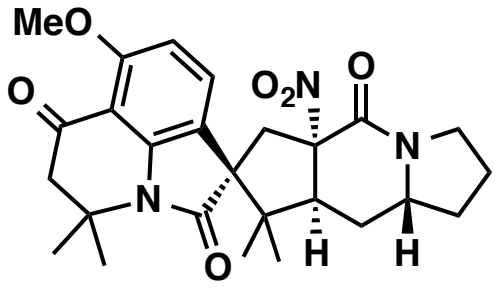

2.101

A colorless prism 0.040 x 0.040 x 0.020 mm in size was mounted on a Cryoloop with Paratone oil. Data were collected in a nitrogen gas stream at 100(2) K using phi and omega scans. Crystal-to-detector distance was 60 mm and exposure time was 10 seconds per frame using a scan width of 1.0°. Data collection was 99.8% complete to 67.000° in θ. A total of 18675 reflections were collected covering the indices, -9<=*h*<=9, -10<=*k*<=11, -21<=*l*<=21. 4856 reflections were found to be symmetry independent, with an R_{int} of 0.0357. Indexing and unit cell refinement indicated a primitive, monoclinic lattice. The space group was found to be P 21 (No. 4). The data were integrated using the Bruker SAINT software program and scaled using the SADABS software program. Solution by iterative methods (SHELXT) produced a complete heavy-atom phasing model consistent with the proposed structure. All non-hydrogen atoms were refined anisotropically by full-matrix least-squares (SHELXL-2013). All hydrogen atoms were placed using a riding model. Their positions were constrained relative to their parent atom using the appropriate HFIX command in SHELXL-2013. Absolute stereochemistry was unambiguously determined to be *R* at C1 and C8, and *S* at C3 and C10, respectively.

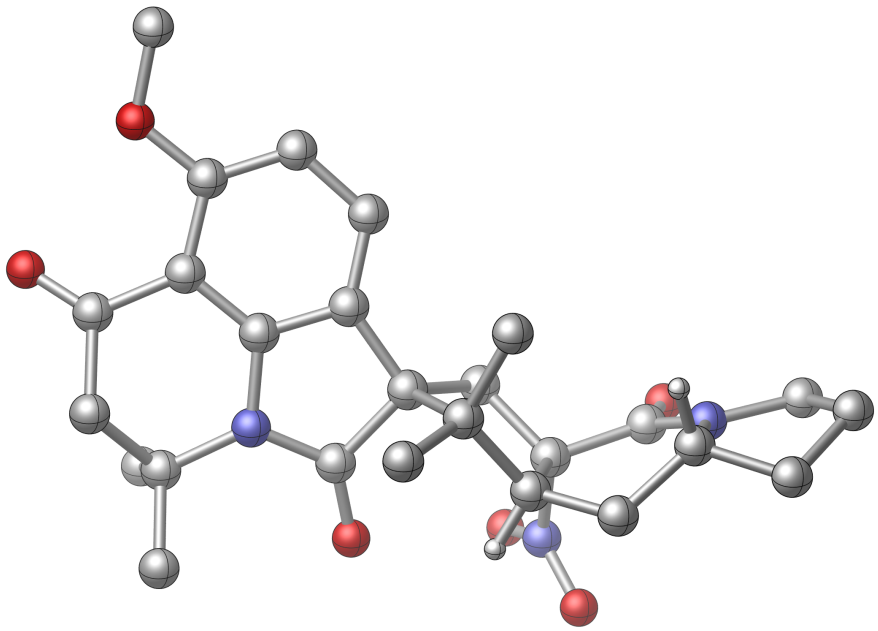

CYLView representation of **2.101**

Table 1. Crystal data and structure refinement for **2.101**.

X-ray ID	sarpong65	
Sample/notebook ID	EM04-184A	
Empirical formula	C26.73 H31.73 Cl2.19 N3 O6	
Formula weight	568.56	
Temperature	100(2) K	
Wavelength	1.54178 Å	
Crystal system	Monoclinic	
Space group	P 21	
Unit cell dimensions	a = 7.9739(4) Å	α= 90°.
	b = 9.6194(5) Å	β= 97.348(3)°.
	c = 18.2544(9) Å	γ = 90°.
Volume	1388.69(12) $Å^3$	
Z	2	
Density (calculated)	1.360 Mg/m^3	
Absorption coefficient	2.652 mm^{-1}	
F(000)	596.6	
Crystal size	0.040 x 0.040 x 0.020 mm^3	
Crystal color/habit	colorless prism	
Theta range for data collection	2.440 to 68.257°.	
Index ranges	-9<=h<=9, -10<=k<=11, -21<=l<=21	
Reflections collected	18675	
Independent reflections	4856 [R(int) = 0.0357]	
Completeness to theta = 67.000°	99.8 %	
Absorption correction	Semi-empirical from equivalents	
Max. and min. transmission	0.929 and 0.778	
Refinement method	Full-matrix least-squares on F^2	
Data / restraints / parameters	4856 / 1 / 358	
Goodness-of-fit on F^2	1.077	
Final R indices [I>2sigma(I)]	R1 = 0.0763, wR2 = 0.2026	
R indices (all data)	R1 = 0.0788, wR2 = 0.2064	
Absolute structure parameter	0.012(15)	
Extinction coefficient	n/a	
Largest diff. peak and hole	0.939 and -0.289 e.$Å^{-3}$	

Table 2. Atomic coordinates (x 10^4) and equivalent isotropic displacement parameters ($Å^2$x 10^3) for **2.101**. U(eq) is defined as one third of the trace of the orthogonalized U^{ij} tensor.

	x	y	z	U(eq)
C(1)	14499(6)	3754(6)	7699(3)	33(1)
C(2)	14167(7)	2182(6)	7692(3)	34(1)
C(3)	14407(7)	1720(6)	8503(3)	36(1)
C(4)	15297(7)	298(6)	8601(3)	38(1)
C(5)	17574(8)	-1137(6)	9206(4)	44(1)
C(6)	19080(8)	-799(7)	9774(4)	47(1)
C(7)	18605(8)	577(7)	10116(3)	44(1)
C(8)	17677(7)	1356(6)	9458(3)	37(1)
C(9)	16486(7)	2502(6)	9630(3)	36(1)
C(10)	15222(6)	2952(6)	8962(3)	33(1)
C(11)	15886(7)	3969(6)	8393(3)	34(1)
C(12)	14947(7)	4376(6)	6992(3)	36(1)
C(13)	16064(7)	3981(6)	6507(3)	37(1)
C(14)	16191(7)	4782(8)	5869(3)	43(1)
C(15)	15198(7)	5941(7)	5715(3)	42(1)
C(16)	13992(7)	6342(7)	6191(3)	39(1)
C(17)	12814(8)	7527(7)	6080(3)	44(1)
C(18)	12131(8)	7984(7)	6780(4)	47(1)
C(19)	11426(7)	6773(6)	7207(3)	39(1)
C(20)	12900(7)	4595(6)	7811(3)	34(1)
C(21)	13944(7)	5520(7)	6820(3)	37(1)
C(22)	15970(8)	5448(6)	8679(3)	41(1)
C(23)	17639(7)	3572(7)	8192(3)	40(1)
C(24)	16644(9)	6559(8)	4702(4)	52(2)
C(25)	10973(8)	7330(7)	7941(3)	45(1)
C(26)	9889(8)	6125(8)	6750(3)	47(1)
C(27)	8193(10)	10927(9)	5858(4)	41(2)
N(1)	16752(6)	220(5)	9040(3)	37(1)
N(2)	12785(6)	5708(5)	7332(2)	36(1)
N(3)	12670(6)	1393(5)	8769(3)	40(1)
O(1)	12673(6)	1347(6)	9439(2)	52(1)
O(2)	11456(6)	1130(6)	8319(3)	52(1)
O(3)	14621(6)	-719(5)	8268(3)	52(1)
O(4)	15261(5)	6759(5)	5117(2)	48(1)
O(5)	12403(6)	8082(6)	5484(3)	57(1)
O(6)	11923(5)	4323(4)	8249(2)	40(1)
Cl(1)	7122(4)	10002(3)	6510(2)	67(1)
Cl(2)	9875(3)	11900(3)	6325(1)	66(1)
Cl(3)	8946(3)	9746(2)	5252(1)	50(1)

Table 3. Bond lengths [Å] and angles [°] for **2.101**.

C(1)-C(12)	1.506(7)	C(15)-O(4)	1.352(7)
C(1)-C(2)	1.535(8)	C(15)-C(16)	1.429(8)
C(1)-C(20)	1.545(7)	C(16)-C(21)	1.397(8)
C(1)-C(11)	1.585(7)	C(16)-C(17)	1.475(9)
C(2)-C(3)	1.535(7)	C(17)-O(5)	1.219(8)
C(2)-H(2A)	0.9900	C(17)-C(18)	1.516(9)
C(2)-H(2B)	0.9900	C(18)-C(19)	1.547(8)
C(3)-C(4)	1.541(8)	C(18)-H(18A)	0.9900
C(3)-C(10)	1.546(7)	C(18)-H(18B)	0.9900
C(3)-N(3)	1.558(7)	C(19)-N(2)	1.488(7)
C(4)-O(3)	1.238(7)	C(19)-C(26)	1.525(8)
C(4)-N(1)	1.325(8)	C(19)-C(25)	1.529(8)
C(5)-N(1)	1.475(7)	C(20)-O(6)	1.215(7)
C(5)-C(6)	1.518(9)	C(20)-N(2)	1.378(7)
C(5)-H(5A)	0.9900	C(21)-N(2)	1.408(7)
C(5)-H(5B)	0.9900	C(22)-H(22A)	0.9800
C(6)-C(7)	1.532(10)	C(22)-H(22B)	0.9800
C(6)-H(6A)	0.9900	C(22)-H(22C)	0.9800
C(6)-H(6B)	0.9900	C(23)-H(23A)	0.9800
C(7)-C(8)	1.524(8)	C(23)-H(23B)	0.9800
C(7)-H(7A)	0.9900	C(23)-H(23C)	0.9800
C(7)-H(7B)	0.9900	C(24)-O(4)	1.429(8)
C(8)-N(1)	1.476(7)	C(24)-H(24A)	0.9800
C(8)-C(9)	1.514(8)	C(24)-H(24B)	0.9800
C(8)-H(8)	1.0000	C(24)-H(24C)	0.9800
C(9)-C(10)	1.542(7)	C(25)-H(25A)	0.9800
C(9)-H(9A)	0.9900	C(25)-H(25B)	0.9800
C(9)-H(9B)	0.9900	C(25)-H(25C)	0.9800
C(10)-C(11)	1.567(7)	C(26)-H(26A)	0.9800
C(10)-H(10)	1.0000	C(26)-H(26B)	0.9800
C(11)-C(22)	1.514(8)	C(26)-H(26C)	0.9800
C(11)-C(23)	1.538(8)	C(27)-Cl(3)	1.746(8)
C(12)-C(21)	1.374(9)	C(27)-Cl(2)	1.762(9)
C(12)-C(13)	1.386(8)	C(27)-Cl(1)	1.788(9)
C(13)-C(14)	1.411(8)	C(27)-H(27)	1.0000
C(13)-H(13)	0.9500	N(3)-O(2)	1.214(7)
C(14)-C(15)	1.376(10)	N(3)-O(1)	1.224(7)
C(14)-H(14)	0.9500		

C(12)-C(1)-C(2)	116.3(5)	C(2)-C(3)-N(3)	110.7(4)
C(12)-C(1)-C(20)	101.3(4)	C(4)-C(3)-N(3)	101.5(4)
C(2)-C(1)-C(20)	111.9(4)	C(10)-C(3)-N(3)	108.4(4)
C(12)-C(1)-C(11)	114.5(4)	O(3)-C(4)-N(1)	123.0(5)
C(2)-C(1)-C(11)	103.7(4)	O(3)-C(4)-C(3)	118.6(5)
C(20)-C(1)-C(11)	109.2(4)	N(1)-C(4)-C(3)	118.4(5)
C(3)-C(2)-C(1)	106.1(4)	N(1)-C(5)-C(6)	104.1(5)
C(3)-C(2)-H(2A)	110.5	N(1)-C(5)-H(5A)	110.9
C(1)-C(2)-H(2A)	110.5	C(6)-C(5)-H(5A)	110.9
C(3)-C(2)-H(2B)	110.5	N(1)-C(5)-H(5B)	110.9
C(1)-C(2)-H(2B)	110.5	C(6)-C(5)-H(5B)	110.9
H(2A)-C(2)-H(2B)	108.7	H(5A)-C(5)-H(5B)	109.0
C(2)-C(3)-C(4)	111.6(5)	C(5)-C(6)-C(7)	104.4(5)
C(2)-C(3)-C(10)	107.0(4)	C(5)-C(6)-H(6A)	110.9
C(4)-C(3)-C(10)	117.6(4)	C(7)-C(6)-H(6A)	110.9

C(5)-C(6)-H(6B)	110.9
C(7)-C(6)-H(6B)	110.9
H(6A)-C(6)-H(6B)	108.9
C(8)-C(7)-C(6)	102.9(5)
C(8)-C(7)-H(7A)	111.2
C(6)-C(7)-H(7A)	111.2
C(8)-C(7)-H(7B)	111.2
C(6)-C(7)-H(7B)	111.2
H(7A)-C(7)-H(7B)	109.1
N(1)-C(8)-C(9)	111.2(4)
N(1)-C(8)-C(7)	101.8(5)
C(9)-C(8)-C(7)	116.7(5)
N(1)-C(8)-H(8)	109.0
C(9)-C(8)-H(8)	109.0
C(7)-C(8)-H(8)	109.0
C(8)-C(9)-C(10)	113.8(4)
C(8)-C(9)-H(9A)	108.8
C(10)-C(9)-H(9A)	108.8
C(8)-C(9)-H(9B)	108.8
C(10)-C(9)-H(9B)	108.8
H(9A)-C(9)-H(9B)	107.7
C(9)-C(10)-C(3)	113.6(5)
C(9)-C(10)-C(11)	117.2(4)
C(3)-C(10)-C(11)	105.9(4)
C(9)-C(10)-H(10)	106.5
C(3)-C(10)-H(10)	106.5
C(11)-C(10)-H(10)	106.5
C(22)-C(11)-C(23)	108.4(5)
C(22)-C(11)-C(10)	111.2(4)
C(23)-C(11)-C(10)	113.4(4)
C(22)-C(11)-C(1)	113.2(5)
C(23)-C(11)-C(1)	109.8(4)
C(10)-C(11)-C(1)	100.8(4)
C(21)-C(12)-C(13)	118.4(5)
C(21)-C(12)-C(1)	108.6(5)
C(13)-C(12)-C(1)	132.9(5)
C(12)-C(13)-C(14)	119.8(5)
C(12)-C(13)-H(13)	120.1
C(14)-C(13)-H(13)	120.1
C(15)-C(14)-C(13)	120.7(5)
C(15)-C(14)-H(14)	119.6
C(13)-C(14)-H(14)	119.6
O(4)-C(15)-C(14)	123.8(5)
O(4)-C(15)-C(16)	115.6(6)
C(14)-C(15)-C(16)	120.6(5)
C(21)-C(16)-C(15)	116.0(6)
C(21)-C(16)-C(17)	117.8(5)
C(15)-C(16)-C(17)	126.2(5)
O(5)-C(17)-C(16)	123.7(6)
O(5)-C(17)-C(18)	122.7(6)
C(16)-C(17)-C(18)	113.6(5)
C(17)-C(18)-C(19)	113.5(5)
C(17)-C(18)-H(18A)	108.9
C(19)-C(18)-H(18A)	108.9
C(17)-C(18)-H(18B)	108.9
C(19)-C(18)-H(18B)	108.9
H(18A)-C(18)-H(18B)	107.7
N(2)-C(19)-C(26)	108.8(5)
N(2)-C(19)-C(25)	110.8(5)
C(26)-C(19)-C(25)	111.1(5)
N(2)-C(19)-C(18)	106.9(5)
C(26)-C(19)-C(18)	110.5(5)
C(25)-C(19)-C(18)	108.6(5)
O(6)-C(20)-N(2)	126.1(5)
O(6)-C(20)-C(1)	125.7(5)
N(2)-C(20)-C(1)	108.2(4)
C(12)-C(21)-C(16)	124.4(5)
C(12)-C(21)-N(2)	111.3(5)
C(16)-C(21)-N(2)	124.2(6)
C(11)-C(22)-H(22A)	109.5
C(11)-C(22)-H(22B)	109.5
H(22A)-C(22)-H(22B)	109.5
C(11)-C(22)-H(22C)	109.5
H(22A)-C(22)-H(22C)	109.5
H(22B)-C(22)-H(22C)	109.5
C(11)-C(23)-H(23A)	109.5
C(11)-C(23)-H(23B)	109.5
H(23A)-C(23)-H(23B)	109.5
C(11)-C(23)-H(23C)	109.5
H(23A)-C(23)-H(23C)	109.5
H(23B)-C(23)-H(23C)	109.5
O(4)-C(24)-H(24A)	109.5
O(4)-C(24)-H(24B)	109.5
H(24A)-C(24)-H(24B)	109.5
O(4)-C(24)-H(24C)	109.5
H(24A)-C(24)-H(24C)	109.5
H(24B)-C(24)-H(24C)	109.5
C(19)-C(25)-H(25A)	109.5
C(19)-C(25)-H(25B)	109.5
H(25A)-C(25)-H(25B)	109.5
C(19)-C(25)-H(25C)	109.5
H(25A)-C(25)-H(25C)	109.5
H(25B)-C(25)-H(25C)	109.5
C(19)-C(26)-H(26A)	109.5
C(19)-C(26)-H(26B)	109.5
H(26A)-C(26)-H(26B)	109.5
C(19)-C(26)-H(26C)	109.5
H(26A)-C(26)-H(26C)	109.5
H(26B)-C(26)-H(26C)	109.5
Cl(3)-C(27)-Cl(2)	110.5(4)
Cl(3)-C(27)-Cl(1)	109.3(5)
Cl(2)-C(27)-Cl(1)	110.0(4)
Cl(3)-C(27)-H(27)	109.0
Cl(2)-C(27)-H(27)	109.0
Cl(1)-C(27)-H(27)	109.0
C(4)-N(1)-C(5)	120.4(5)
C(4)-N(1)-C(8)	127.7(5)
C(5)-N(1)-C(8)	111.7(4)
C(20)-N(2)-C(21)	109.0(5)
C(20)-N(2)-C(19)	128.4(5)
C(21)-N(2)-C(19)	120.9(5)
O(2)-N(3)-O(1)	124.6(5)

O(2)-N(3)-C(3)	119.7(5)
O(1)-N(3)-C(3)	115.5(5)
C(15)-O(4)-C(24)	117.5(5)

Symmetry transformations used to generate equivalent atoms:

Table 4. Anisotropic displacement parameters ($Å^2 x\ 10^3$) for **2.101**. The anisotropic displacement factor exponent takes the form: $-2\pi^2[\ h^2\ a^{*2}U^{11} + ...\ + 2\ h\ k\ a^*\ b^*\ U^{12}\ ]$

	U^{11}	U^{22}	U^{33}	U^{23}	U^{13}	U^{12}
C(1)	30(2)	37(3)	31(2)	-2(2)	2(2)	-4(2)
C(2)	36(2)	31(3)	34(2)	0(2)	2(2)	-3(2)
C(3)	34(2)	36(3)	39(3)	-3(2)	4(2)	-2(2)
C(4)	44(3)	31(3)	38(3)	-1(2)	2(2)	-2(2)
C(5)	43(3)	31(3)	58(3)	4(2)	6(3)	2(2)
C(6)	37(3)	40(3)	62(4)	10(3)	2(3)	4(2)
C(7)	38(3)	42(3)	48(3)	6(3)	-2(2)	-1(2)
C(8)	36(3)	38(3)	36(2)	-1(2)	1(2)	-8(2)
C(9)	38(3)	35(3)	33(2)	-1(2)	-1(2)	-3(2)
C(10)	32(2)	32(3)	35(2)	0(2)	3(2)	-2(2)
C(11)	35(2)	34(3)	31(2)	0(2)	2(2)	-3(2)
C(12)	37(3)	38(3)	32(2)	2(2)	1(2)	-4(2)
C(13)	36(2)	36(3)	40(3)	-2(2)	2(2)	0(2)
C(14)	40(3)	53(3)	35(3)	-1(2)	6(2)	-2(3)
C(15)	36(3)	54(4)	36(3)	3(2)	-2(2)	-6(3)
C(16)	34(2)	44(3)	37(2)	1(2)	0(2)	-3(2)
C(17)	38(3)	44(3)	48(3)	9(3)	2(2)	-3(2)
C(18)	43(3)	37(3)	59(3)	9(3)	6(3)	1(2)
C(19)	36(2)	36(3)	44(3)	3(2)	3(2)	4(2)
C(20)	33(2)	35(3)	33(2)	1(2)	0(2)	-1(2)
C(21)	33(2)	43(3)	35(3)	-4(2)	1(2)	-4(2)
C(22)	47(3)	31(3)	43(3)	0(2)	-2(2)	-7(2)
C(23)	34(2)	46(3)	39(3)	5(2)	2(2)	-4(2)
C(24)	49(3)	60(4)	50(3)	13(3)	16(3)	7(3)
C(25)	42(3)	47(3)	47(3)	1(3)	5(2)	10(3)
C(26)	36(3)	58(4)	47(3)	9(3)	2(2)	0(3)
C(27)	35(4)	49(5)	39(4)	-5(3)	0(3)	17(3)
N(1)	40(2)	27(2)	43(2)	0(2)	2(2)	-2(2)
N(2)	32(2)	40(2)	36(2)	2(2)	4(2)	-2(2)
N(3)	37(2)	42(3)	40(2)	3(2)	4(2)	-6(2)
O(1)	50(2)	62(3)	45(2)	2(2)	10(2)	-13(2)
O(2)	39(2)	58(3)	57(2)	6(2)	-4(2)	-12(2)
O(3)	54(2)	33(2)	65(3)	-7(2)	-12(2)	-3(2)
O(4)	42(2)	61(3)	43(2)	11(2)	11(2)	6(2)
O(5)	54(3)	63(3)	56(3)	19(2)	10(2)	12(2)
O(6)	37(2)	43(2)	40(2)	3(2)	7(2)	-1(2)
Cl(1)	74(2)	62(2)	69(2)	15(1)	30(1)	26(1)
Cl(2)	34(1)	96(2)	64(1)	-34(1)	-9(1)	14(1)
Cl(3)	52(1)	53(1)	45(1)	-6(1)	4(1)	22(1)

Table 5. Hydrogen coordinates (x 10^4) and isotropic displacement parameters ($Å^2$x 10^3) for **2.101**.

	x	y	z	U(eq)
H(2A)	13002	1978	7459	41
H(2B)	14973	1692	7412	41
H(5A)	17946	-1551	8757	53
H(5B)	16797	-1792	9411	53
H(6A)	20121	-694	9536	56
H(6B)	19262	-1537	10154	56
H(7A)	17860	420	10503	52
H(7B)	19625	1091	10334	52
H(8)	18527	1750	9157	44
H(9A)	17162	3321	9818	43
H(9B)	15845	2182	10029	43
H(10)	14282	3447	9166	40
H(13)	16742	3174	6605	45
H(14)	16971	4518	5542	51
H(18A)	11220	8674	6649	56
H(18B)	13047	8450	7107	56
H(22A)	16817	5510	9117	61
H(22B)	14862	5719	8811	61
H(22C)	16284	6073	8295	61
H(23A)	17936	4192	7802	60
H(23B)	17615	2609	8016	60
H(23C)	18482	3662	8629	60
H(24A)	17711	6602	5034	78
H(24B)	16630	7289	4327	78
H(24C)	16540	5648	4460	78
H(25A)	10429	6593	8197	68
H(25B)	10197	8118	7848	68
H(25C)	12005	7635	8249	68
H(26A)	10163	5910	6254	71
H(26B)	8941	6781	6713	71
H(26C)	9575	5268	6989	71
H(27)	7377	11576	5571	50

2.10 – References and Notes

1. Stocking, E. M.; Sanz-Cervera, J. F.; Williams, R. M. *Angew, Chem. Int. Ed.* **1999,** *38*, 786–789.

2. Finefield, J. M.; Frisvad, J. C.; Sherman, D. H.; Williams, R. M. *J. Nat. Prod.* **2012,** *75*, 812–833.

3. Miller, K. A.; Williams, R. M. *Chem. Soc. Rev.* **2009,** *38*, 3160–3174.

4. Tsuda, M.; Kasai, Y.; Komatsu, K.; Sone, T.; Tanaka, M.; Mikami, Y.; Kobayashi, J. *Org. Lett.* **2004,** *6*, 3087–3089.

5. Mugishima, T.; Tsuda, M.; Kasai, Y.; Ishiyama, H.; Fukushi, E.; Kawabata, J.; Watanabe, M.; Akao, K.; Kobayashi, J. *J. Org. Chem.* **2005,** *70*, 9430–9435.

6. Kushida, N.; Watanabe, N.; Okuda, T.; Yokoyama, F.; Gyobu, Y.; Yaguchi, T. *J. Antibiot.* **2007,** *60*, 667–673.

7. (a) Bian, Z.; Marvin, C. C.; Martin, S. F. *J. Am. Chem. Soc.* **2013,** *135*, 10886–10889; (b) Bian, Z.; Marvin, C. C.; Pettersson, M.; Martin, S. F. *J. Am. Chem. Soc.* **2014,** *136*, 14184–14192.

8. Kong, K.; Enquist, J. A., Jr.; McCallum, M. E.; Smith, G. M.; Matsumaru, T.; Menhaji-Klotz, E.; Wood, J. L. *J. Am. Chem. Soc.* **2013,** *135*, 10890–10893.

9. Bond, R. F.; Boeyens, J. C. A.; Holzapfel, C. W.; Steyn, P. S. *J. Chem. Soc., Perkin Trans. 1,* **1979**, 1751.

10. Pimenta, E. F.; Vita-Marques, A. M.; Tinimis, A.; Seleghim, M. H. R.; Sette, L. D.; Veloso, K.; Ferreira, A. G.; Williams, D. E.; Patrick, B. O.; Dalisay, D. S.; Andersen, R. J.; Berlinck, R. G. S. *J. Nat. Prod.* **2010,** *73*, 1821–1832.

11. Parry, R.; Nishino, S.; Spain, J. *Nat. Prod. Rep.* **2011,** *28*, 152–167.

12. Mercado-Marin, E. V.; Garcia-Reynaga, P.; Romminger, S.; Pimenta, E. F.; Romney, D. K.; Lodewyk, M. W.; Williams, D. E.; Andersen, R. J.; Miller, S. J.; Tantillo, D. J.; Berlinck, R. G. S.; Sarpong, R. *Nature* **2014,** *509*, 318–324.

13. Lodewyk, M. W.; Siebert, M. R.; Tantillo, D. J. *Chem. Rev.* **2012,** *112*, 1839–1862.

14. Jewett, J. C.; Rawal, V. H. *Angew. Chem. Int. Ed.* **2007,** *46*, 6502–6504.

15. Ohira, S. *Synth. Commun.* **1989,** *19*, 561–564.

16. Garvey, D. S.; Wasicak, J. T.; Elliott, R. L.; Lebold, S.; Hettinger, A.-M.; Carrera, G. M.; Lin, N.-H.; He, Y.; Holladay, M. W. *J. Med. Chem.* **1994,** *37*, 4455–4463.

17. Grotjahn, D. B.; Lev, D. A. *J. Am. Chem. Soc.* **2004,** *126*, 12232–12233.

18. Kienzle, F.; Mergelsberg, I.; Stadlwieser, J.; Arnold, W. *Helv. Chim. Acta* **1985,** *68*, 1133–1139.

19. Banwell, M. G.; Kelly, B. D.; Kokas, O. J.; Lupton, D. W. *Org. Lett.* **2003,** *5*, 2497–2500.

20. (a) Herzon, S. B.; Myers, A. G. *J. Am. Chem. Soc.* **2005,** *127*, 5342–5344; (b) Myers, A. G.; Herzon, S. B. *J. Am. Chem. Soc.* **2003,** *125*, 12080–12081.

21. Johnson, C. R.; Adams, J. P.; Braun, M. P.; Senanayake, C. B. W.; Wovkulich, P. M.; Uskoković, M. R. *Tetrahedron Lett.* **1992,** *33*, 917–918.

22. Lloyd, D. H.; Nichols, D. E. *J. Org. Chem.* **1986,** *51*, 4294–4295.

23. Bellamy, F. D.; Ou, K. *Tetrahedron Lett.* **1984,** *25*, 839–842.

24. Davis, F. A.; Stringer, O. D. *J. Org. Chem.* **1982,** *47*, 1774–1775.

25. Greshock, T. J.; Grubbs, A. W.; Tsukamoto, S.; Williams, R. M. *Angew. Chem. Int. Ed.* **2007,** *46*, 2262–2265.

26. Omura, K.; Swern, D. *Tetrahedron* **1978,** *34*, 1651–1660.

27. Kishi, Y.; Nakatsubo, F.; Aratani, M.; Goto, T.; Inoue, S.; Kakoi, H.; Sugiura, S. *Tetrahedron Lett.* **1970,** *11*, 5127–5128.

28. Ghaffar, T.; Parkins, A. W. *Tetrahedron Lett.* **1995,** *36*, 8657–8660.

29. Luche, J. L. *J. Am. Chem. Soc.* **1978,** *100*, 2226–2227.

30. Baumgarten, H. E.; Smith, H. L.; Staklis, A. *J. Org. Chem.* **1975,** *40*, 3554–3561.

31. Moriarty, R. M.; Chany, C. J.; Vaid, R. K.; Prakash, O.; Tuladhar, S. M. *J. Org. Chem.* **1993,** *58*, 2478–2482.

32. Marti, C.; Carreira, Erick M. *Eur. J. Org. Chem.* **2003,** *2003*, 2209–2219.

33. Güller, R.; Borschberg, H.-J. *Tetrahedron Lett.* **1994,** *35*, 865–868.

34. Movassaghi, M.; Schmidt, M. A.; Ashenhurst, J. A. *Org. Lett.* **2008,** *10*, 4009–4012.

35. Guerrero, C. A.; Sorensen, E. J. *Org. Lett.* **2011,** *13*, 5164–5167.

36. Artman III, G. D.; Grubbs, A. W.; Williams, R. M. *J. Am. Chem. Soc.* **2007,** *129*, 6336–6342.

37. Greshock, T. J.; Williams, R. M. *Org. Lett,* **2007,** *9*, 4255–4258.

38. Kolundzic, F.; Noshi, M. N.; Tjandra, M.; Movassaghi, M.; Miller, S. J. *J. Am. Chem. Soc.* **2011,** *133*, 9104–9111.

39. Gilbert, K. E.; Borden, W. T. *J. Org. Chem.* **1979,** *44*, 659–661.

40. Murray, R. W.; Jeyaraman, R.; Mohan, L. *Tetrahedron Lett.* **1986,** *27*, 2335–2336.

41. (a) Romney, D. K.; Miller, S. J. *Org. Lett.* **2012,** *14*, 1138–1141; (b) Peris, G.; Jakobsche, C. E.; Miller, S. J. *J. Am. Chem. Soc.* **2007,** *129*, 8710–8711.

42. Irie, H.; Nakanishi, H.; Fujii, N.; Mizuno, Y.; Fushimi, T.; Funakoshi, S.; Yajima, H. *Chem. Lett.* **1980,** *9*, 705–708.

43. Miller, D. G.; Wayner, D. D. M. *J. Org. Chem.* **1990,** *55*, 2924–2927.

44. Curci, R.; D'Accolti, L.; Fusco, C. *Acc. Chem. Res.* **2006,** *39*, 1–9.

45. Zhang, X.; Foote, C. S. *J. Am. Chem. Soc.* **1993,** *115*, 8867–8868.

46. (a) Kuwano, R.; Takahashi, M.; Ito, Y. *Tetrahedron Lett.* **1998,** *39*, 1017–1020; (b) Igarashi, M.; Fuchikami, T. *Tetrahedron Lett.* **2001,** *42*, 1945–1947; (c) Matsubara, K.; Iura, T.; Maki, T.; Nagashima, H. *J. Org. Chem.* **2002,** *67*, 4985–4988; (d) Motoyama,

Y.; Mitsui, K.; Ishida, T.; Nagashima, H. *J. Am. Chem. Soc.* **2005,** *127*, 13150–13151; (e) Ohta, T.; Kamiya, M.; Nobutomo, M.; Kusui, K.; Furukawa, I. *Bull. Chem. Soc. Jpn.* **2005,** *78*, 1856–1861; (f) Fernandes, A. C.; Romão, C. C. *J. Mol. Catal. A: Chem.* **2007,** *272*, 60–63; (g) Hanada, S.; Ishida, T.; Motoyama, Y.; Nagashima, H. *J. Org. Chem.* **2007,** *72*, 7551–7559; (h) Sakai, N.; Fujii, K.; Konakahara, T. *Tetrahedron Lett.* **2008,** *49*, 6873–6875; (i) Hanada, S.; Tsutsumi, E.; Motoyama, Y.; Nagashima, H. *J. Am. Chem. Soc.* **2009,** *131*, 15032–15040; (j) Zhou, S.; Junge, K.; Addis, D.; Das, S.; Beller, M. *Angew. Chem. Int. Ed.* **2009,** *48*, 9507–9510; (k) Das, S.; Addis, D.; Zhou, S.; Junge, K.; Beller, M. *J. Am. Chem. Soc.* **2010,** *132*, 1770–1771; (l) Cheng, C.; Brookhart, M. *J. Am. Chem. Soc.* **2012,** *134*, 11304–11307; (m) Bornschein, C.; Lennox, A. J. J.; Werkmeister, S.; Junge, K.; Beller, M. *Eur. J. Org. Chem.* **2015**, *9*, 1915–1919.

47. (a) Raucher, S.; Klein, P. *Tetrahedron* **1980,** *21*, 4061–4064; (b) Sundberg, R. J.; Walters, C. P.; Bloom, J. D. *J. Org. Chem.* **1981,** *46*, 3730–3732; (c) Mandal, S. B.; Giri, V. S.; Sabeena, M. S.; Pakrashi, S. C. *J. Org. Chem.* **1988,** *53*, 4236–4241.

48. (a) Borch, R. F. *Tetrahedron Lett.* **1968,** *9*, 61–65; (b) Kuehne, M. E.; Shannon, P. J. *J. Org. Chem.* **1977,** *42*, 2082–2087; (c) Tsay, S.-C.; Robl, J. A.; Hwu, J. R. *J. Chem. Soc., Perkin Trans. 1,* **1990**, 757–759; (d) Ito, M.; Clark, C. W.; Mortimore, M.; Goh, J. B.; Martin, S. F. *J. Am. Chem. Soc.* **2001,** *123*, 8003–8010; (e) Barbe, G.; Charette, A. B. *J. Am. Chem. Soc.* **2008,** *130*, 18–19; (f) Pelletier, G.; Bechara, W. S.; Charette, A. B. *J. Am. Chem. Soc.* **2010,** *132*, 12817–12819; (g) Huang, P.-Q.; Xiang, S.-H.; Xu, J.; Yuan, H.-Q. *Synlett* **2010,** *12*, 1829–1832.

49. (a) Collins, C. J.; Lanz, M.; Singaram, B. *Tetrahedron Lett.* **1999,** *40*, 3673–3676; (b) Chadwick, R. C.; Kardelis, V.; Lim, P.; Adronov, A. *J. Org. Chem.* **2014,** *79*, 7728–7733; (c) Smith, A. M.; Whyman, R. *Chem. Rev.* **2014,** *114*, 5477–5510; (d) Szostak, M.; Spain, M.; Eberhart, A. J.; Procter, D. J. *J. Org. Chem.* **2014,** *79* (24), 11988-12003.

50. Ding, Y.; Greshock, T. J.; Miller, K. A.; Sherman, D. H.; Williams, R. M. *Org. Lett.* **2008,** *10*, 4863–4866.

51. White, J. M.; Tunoori, A. R.; Georg, G. I. *J. Am. Chem. Soc.* **2000,** *122*, 11995–11996.

52. Curphey, T. J. *J. Org. Chem.* **2002,** *67*, 6461–6473.

53. Bonazzi, S.; Cheng, B.; Wzorek, J. S.; Evans, D. A. *J. Am. Chem. Soc.* **2013,** *135*, 9338–9341.

54. Lin, Z.; Wen, J.; Zhu, T.; Fang, Y.; Gu, Q.; Zhu, W. *J. Antibiot. (Tokyo)* **2008,** *61*, 81–85.

55. Ding, Y.; Wet, J. R. d.; Cavalcoli, J.; Li, S.; Greshock, T. J.; Miller, K. A.; Finefield, J. M.; Sunderhaus, J. D.; McAfoos, T. J.; Tsukamoto, S.; Williams, R. M.; Sherman, D. H. *J. Am. Chem. Soc.* **2010,** *132*, 12733-12740.

56. Boldi, A. M.; Dener, J. M.; Hopkins, T. P. *J. Comb. Chem.* **2001,** *3*, 367–373.

57. Dickson, H. D.; Smith, S. C.; Hinkle, K. W. *Tetrahedron Lett.* **2004,** *45*, 5597–5599.

Appendix 1:

Attempted Epimerization Data on

ent-Citrinalin B (ent-2.2) and Cyclopiamine B (2.6)

&

Spectra Relevant to Chapter 2

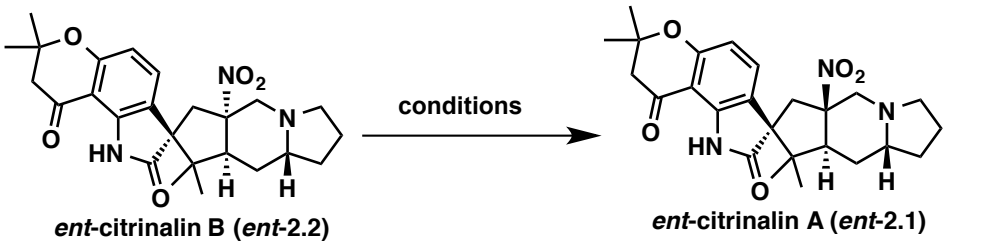

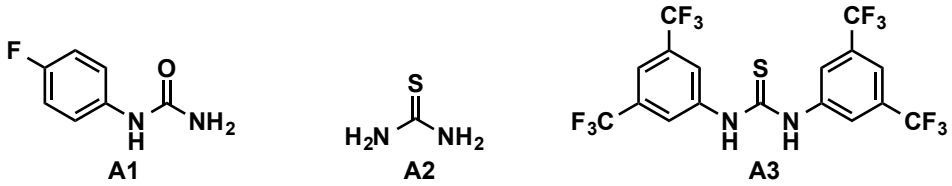

Entry	Solvent	Temperature (°C)	Additive	Result
1	DMF-d_7	80 to 150	–	S.M.
2	MeOH-d_4	65 to 85	–	S.M.
3	Dioxane/H_2O	100 to 120	–	S.M.
4	EtOH/H_2O	100 to 120	–	S.M.
5	$CHCl_3$/MeOH	65 to 85	–	S.M.
6	DMSO-d_6	80 to 150	–	S.M.
7	Dioxane/H_2O	70 to 140	**A1***	S.M.
8	Dioxane/H_2O	70 to 140	**A2***	Decomp.
9	Dioxane/H_2O	70 to 140	**A3***	S.M.
10	Dioxane/H_2O	200 (microwave)	–	Decomp.

Table A1.1: Conditions for the attempted conversion of *ent*-citrinalin B (***ent*-2.2**) to *ent*-citrinalin A (***ent*-2.1**). Note: Analysis of each reaction was conducted using TLC, LCMS, and ^{1}H NMR. (*Urea (**A1**) and thioureas (**A2** and **A3**) were added as additives in hopes of facilitating this epimerization sequence since they are known to activate nitro groups for related nitro-mannich reactions; see: Anderson. *et al. Chem. Rev.* **2013**, *113*, 2887–2939).

We reasoned that the vinylogous imide might be acting as an acid and leading to the protonation of the tertiary amine group, thus shutting down the epimerization event. However, benzylation (benzyl bromide, K_2CO_3, acetone, 60 °C) of the secondary amide (thus, removing the acidic proton) we again did not observe the epimerized product. Therefore, we concluded that *ent*-citrinalin B (***ent*-2.2**) is the thermodynamic product for this transformation. We were able to show that citrinalin A (**2.1**) converts completely to citrinalin B (**2.2**) upon heating in DMF-d_7 (Section 2.5.3).

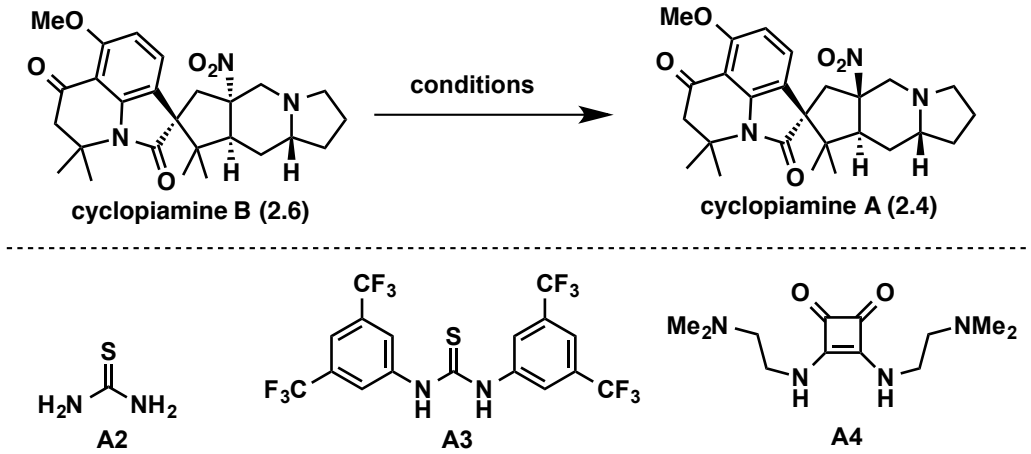

Entry	Solvent	Temperature (°C)	Additive	Result
1	DMF-d_7	80 to 165	–	S.M.
2	Dioxane/H_2O	100 to 140	–	S.M.
3	EtOH/H_2O	100 to 140	–	S.M.
4	$CHCl_3$/MeOH	100 to 140	–	S.M.
5	Dioxane/H_2O	100	1% AcOH	S.M.
6	Dioxane/H_2O	100	1% pyridine	S.M.
7	DMF	100	1% AcOH	S.M.
8	DMF	100	1% pyridine	S.M.
9	Formamide	140 (microwave)	–	Decomp.
10	Dioxane/H_2O	110	Tap water	S.M.
11	Dioxane/H_2O	110	LiCl	S.M.
12	Dioxane/H_2O	110	$CuCl_2$	S.M.
13	Dioxane/H_2O	110	$CuSO_4$•XH_2O	S.M.
14	MeCN	100	**A2***	S.M.
15	MeCN	100	**A3***	S.M.
16	MeCN	100	**A4**	S.M.
17	CF_3CH_2OH/H_2O	100	–	S.M.
18	DMF-d_7	140 to 190	–	S.M.
19	DMF-d_7	140 to 190	1% TFA	S.M.

Table A1.2: Conditions for the attempted conversion of cyclopiamine B (**2.6**) to cyclopiamine A (**2.4**). Note: Analysis of each reaction was conducted using TLC, LCMS, and ^{1}H NMR. (*Thioureas (**A2** and **A3**) were added as additives in hopes of facilitating this epimerization sequence since they are known to activate nitro groups for related nitro-mannich reactions; see: Anderson. *et al. Chem. Rev.* **2013**, *113*, 2887–2939).

Similar to above, we speculated that cyclopiamine B (**2.6**) is the thermodymanic product for this epimerization sequence. The work described in Table A1.2 was conducted prior to our computational work which showed that cyclopiamine B (**2.6**) is lower in energy than cyclopiamine A (**2.4**) by 9.6 kcal/mol in a DMF solvent model, section 2.1.2.

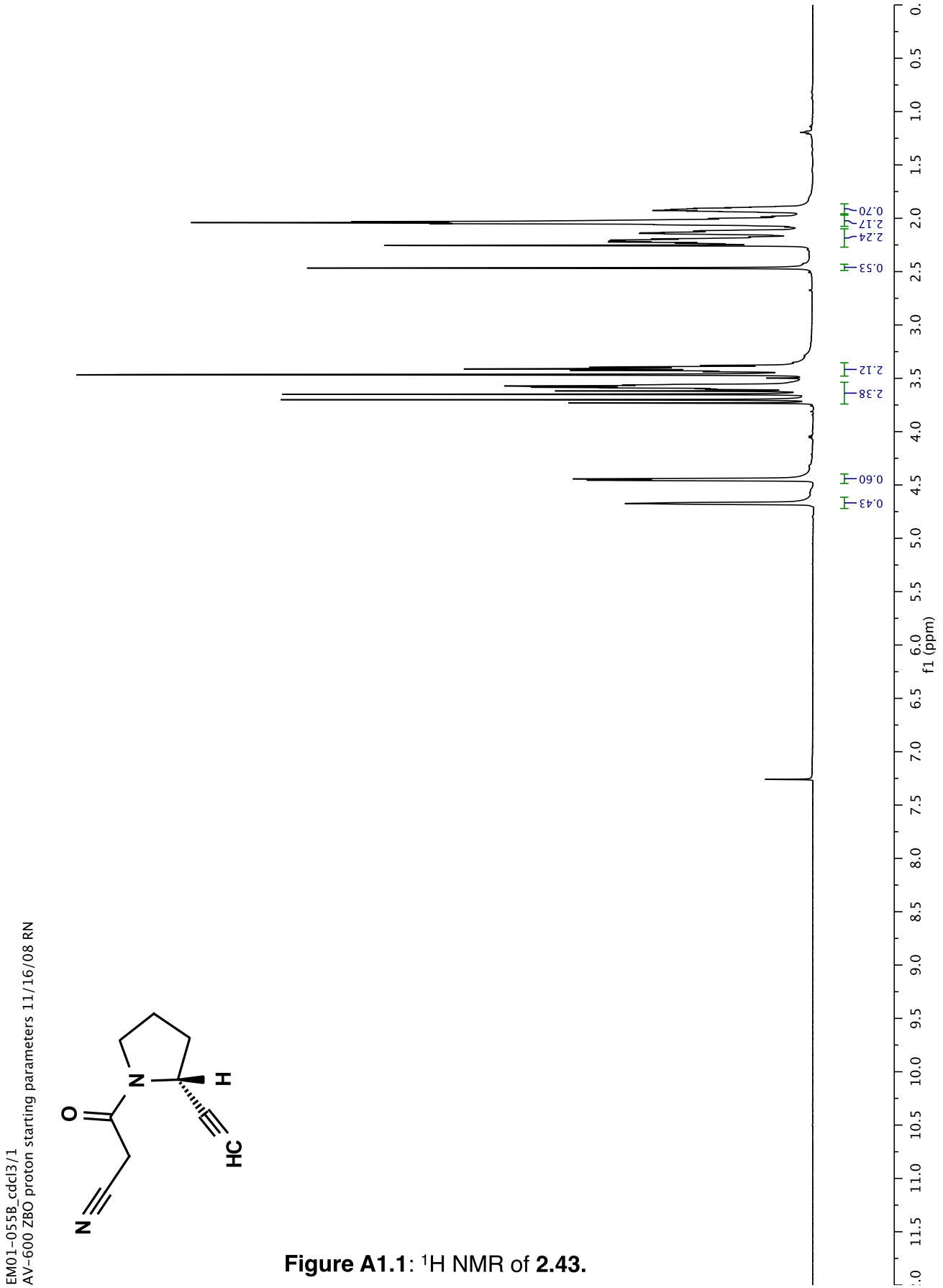

Figure A1.1: ^{1}H NMR of **2.43.**

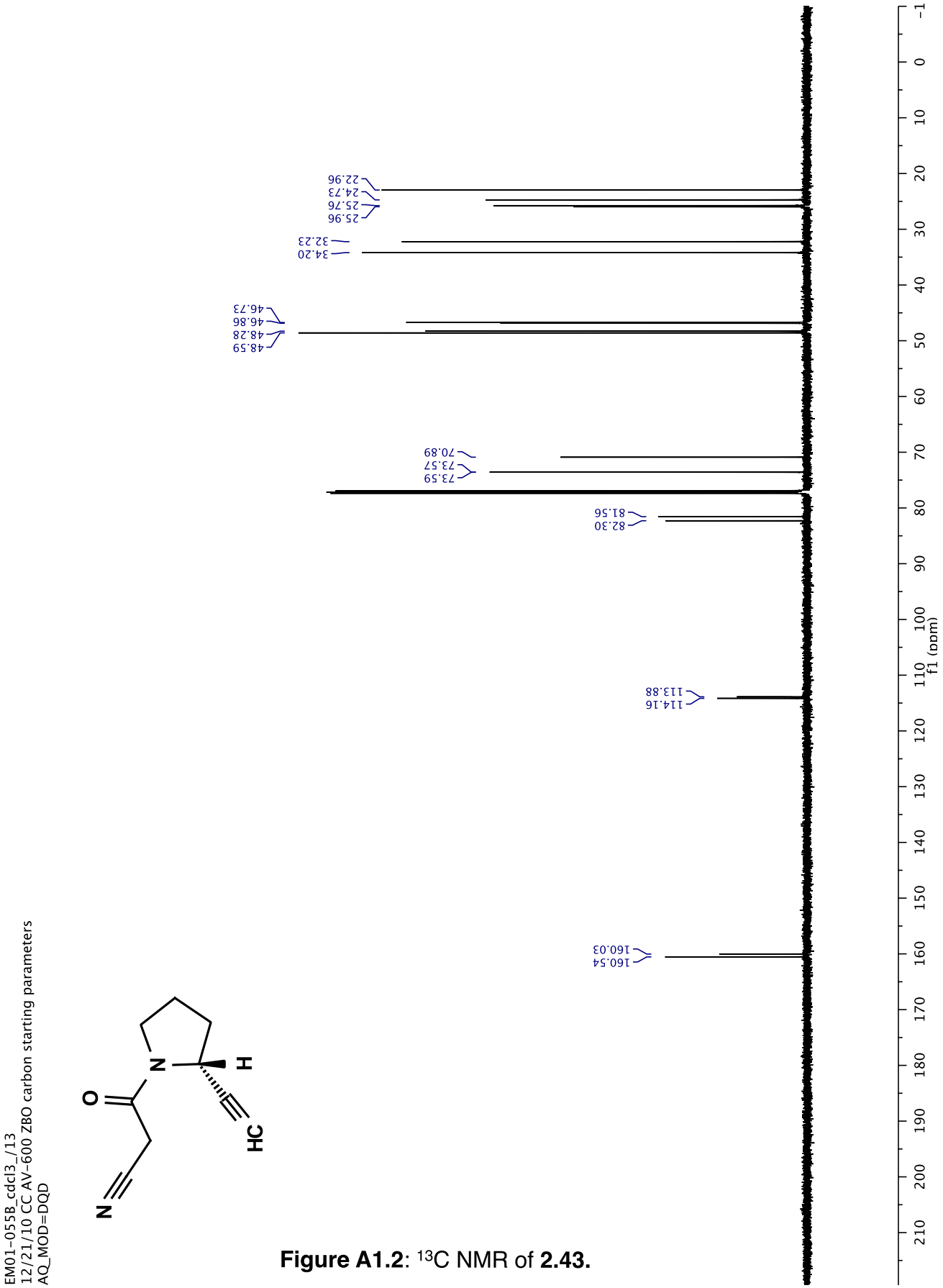

Figure A1.2: ^{13}C NMR of **2.43.**

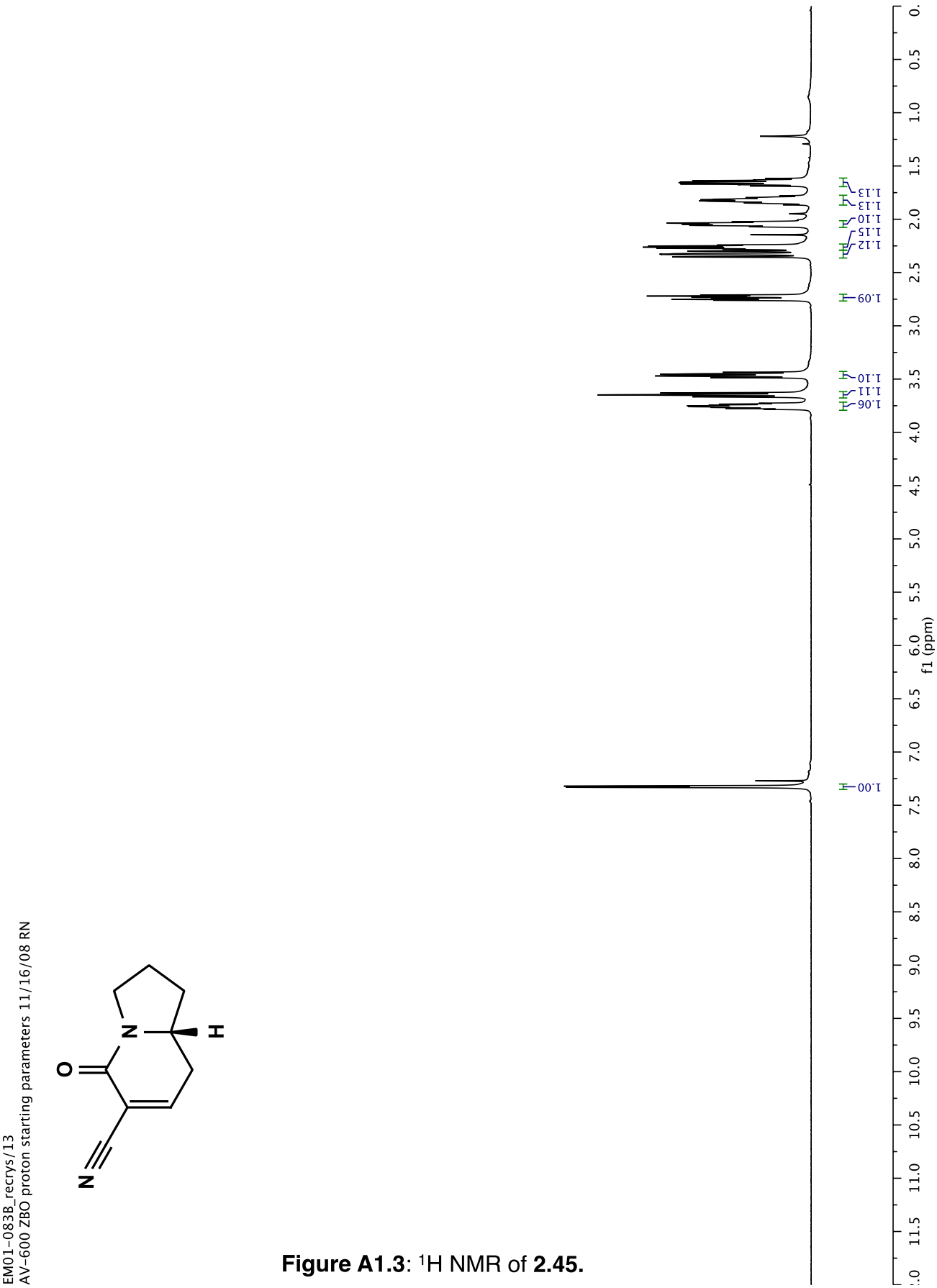

Figure A1.3: ^{1}H NMR of **2.45.**

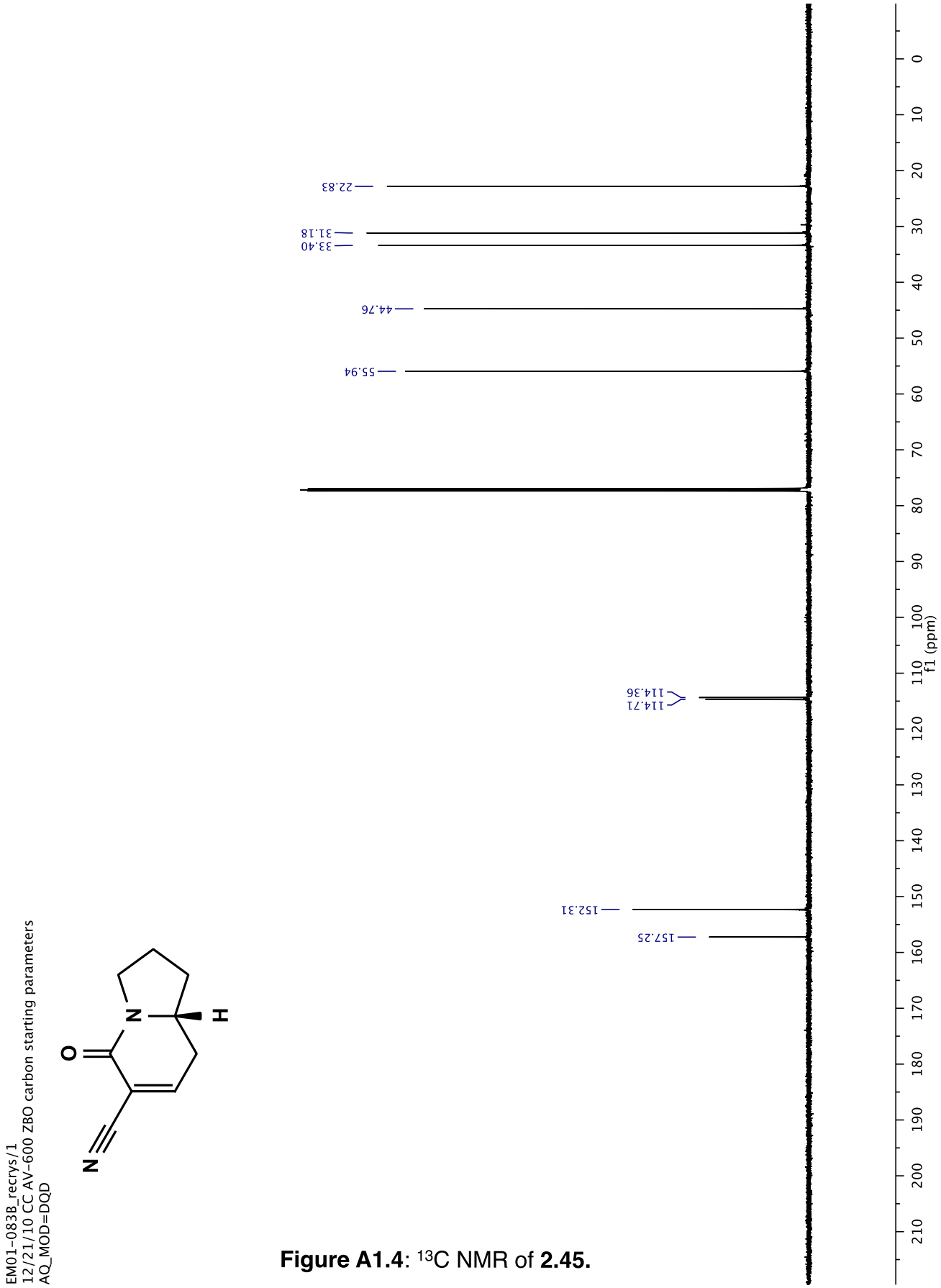

Figure A1.4: ^{13}C NMR of **2.45.**

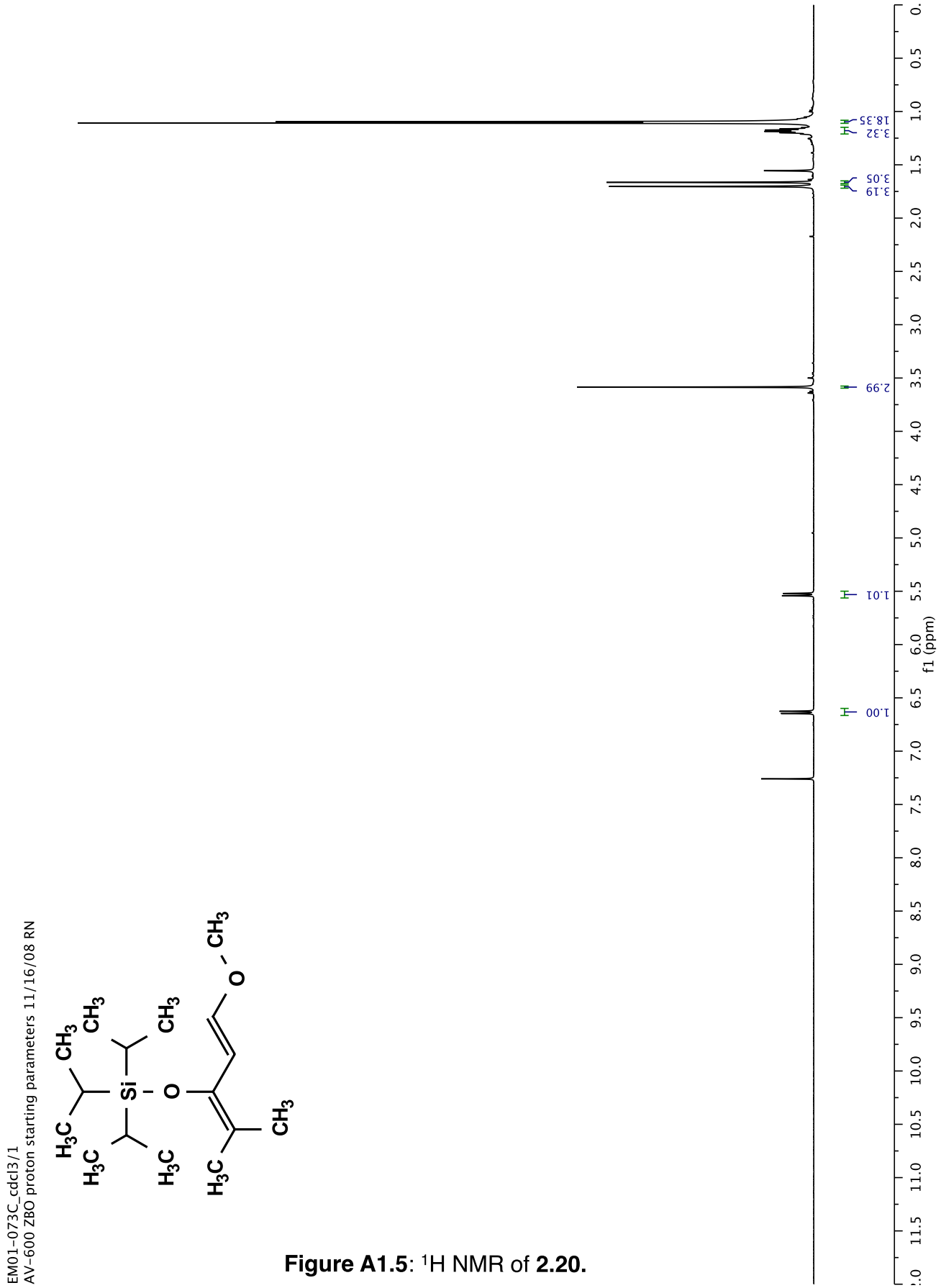

Figure A1.5: ^{1}H NMR of **2.20.**

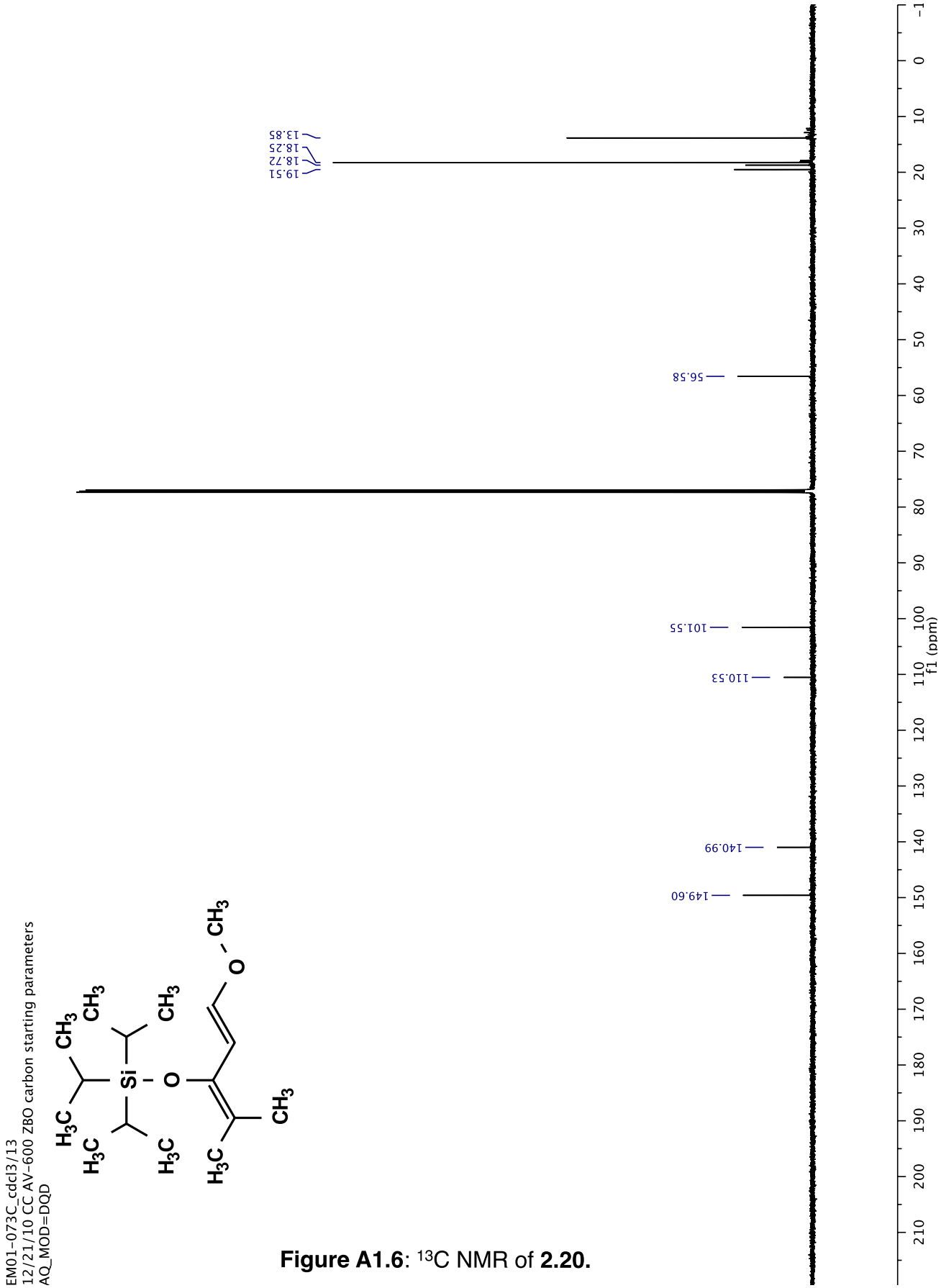

Figure A1.6: ^{13}C NMR of **2.20.**

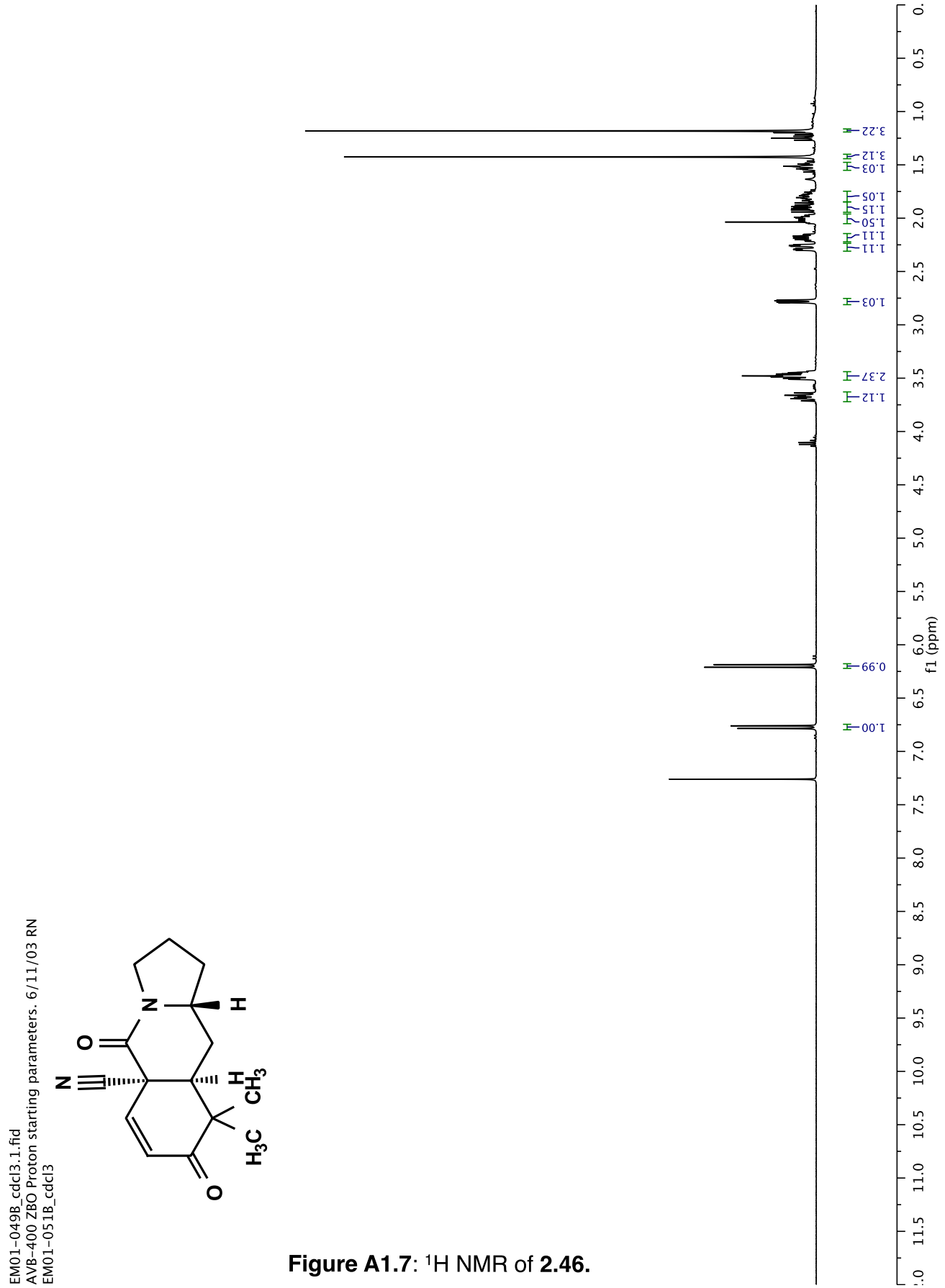

Figure A1.7: ^{1}H NMR of **2.46.**

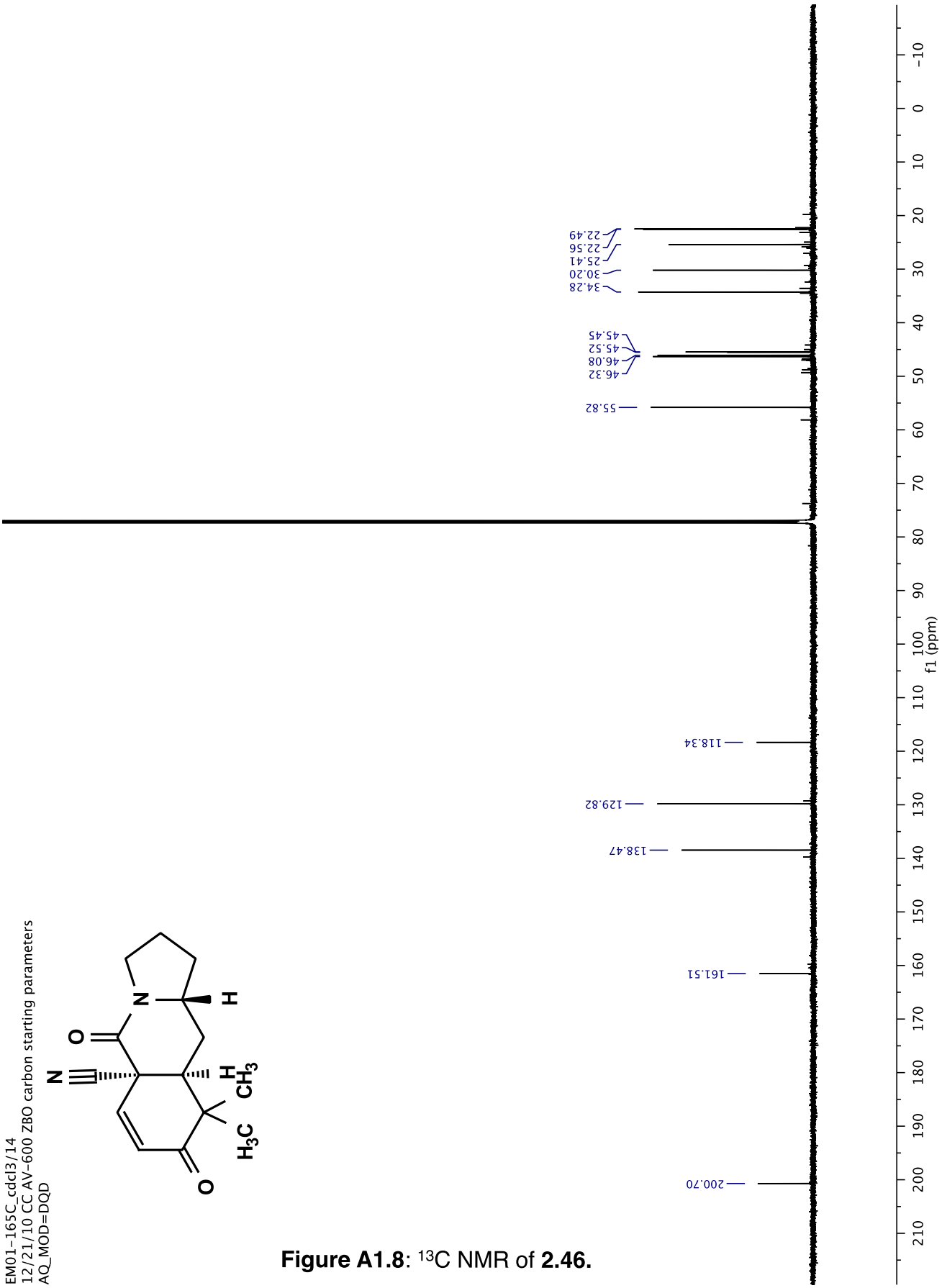

Figure A1.8: ^{13}C NMR of **2.46.**

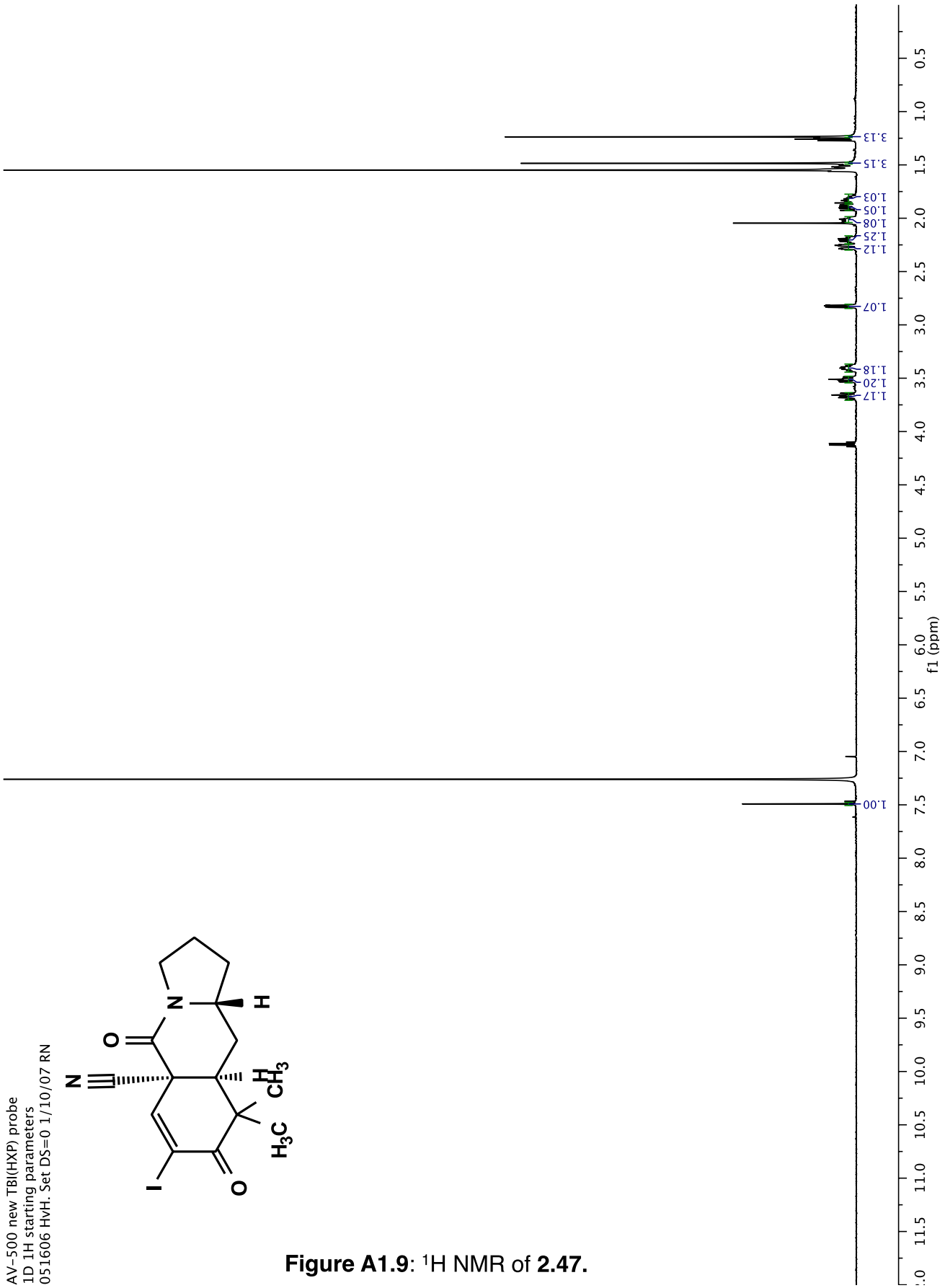

Figure A1.9: ^{1}H NMR of **2.47.**

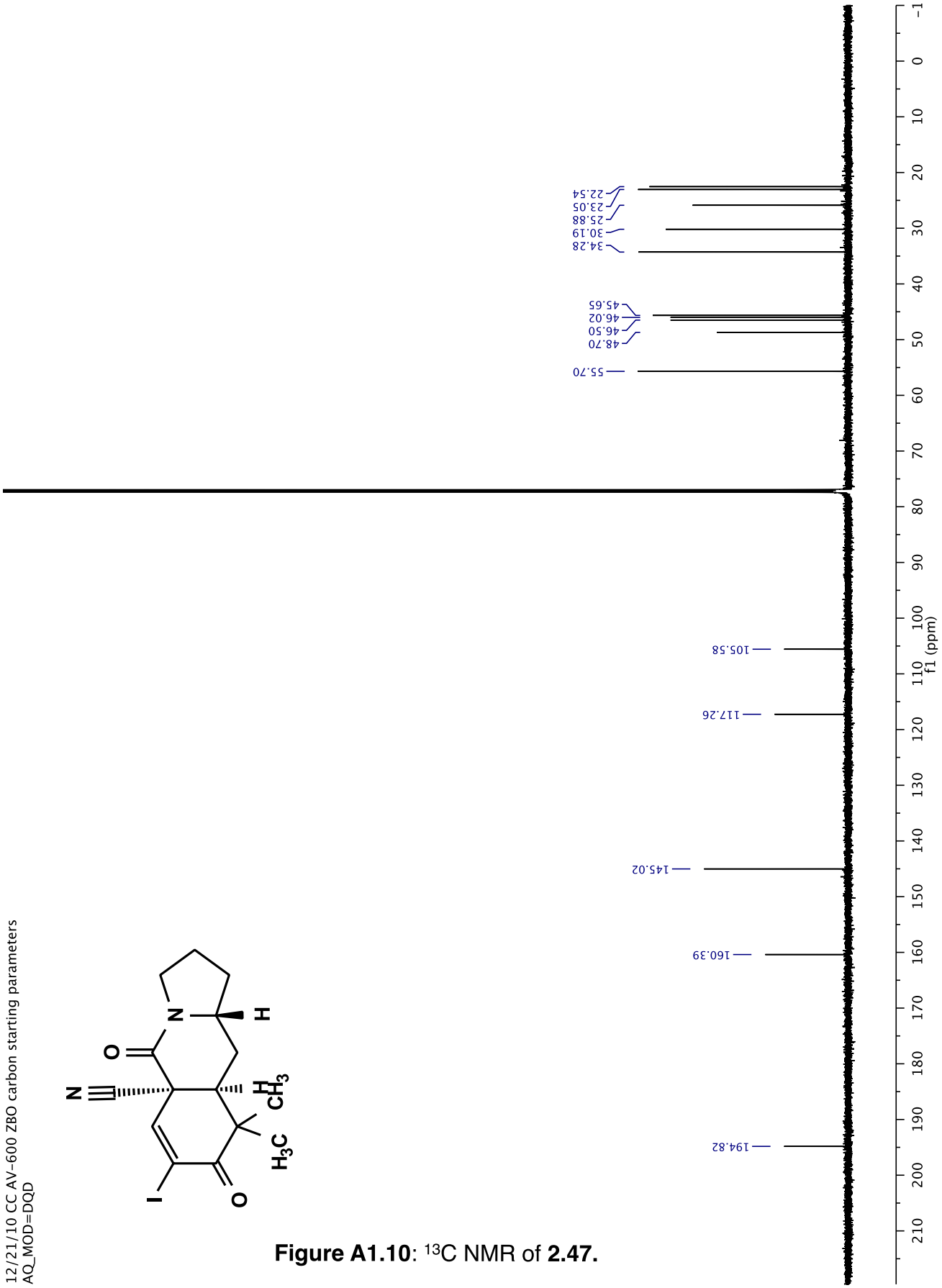

Figure A1.10: ^{13}C NMR of **2.47.**

AV-500 new TBI(HXP) probe
1D 1H starting parameters
051606 HvH. Set DS=0 1/10/07 RN

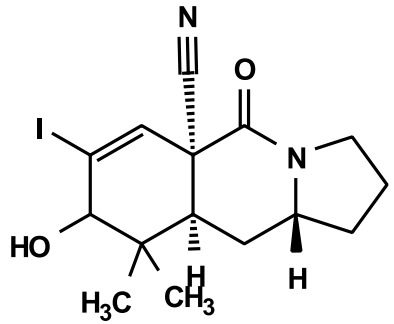

Figure A1.11: ^{1}H NMR of **2.51.**

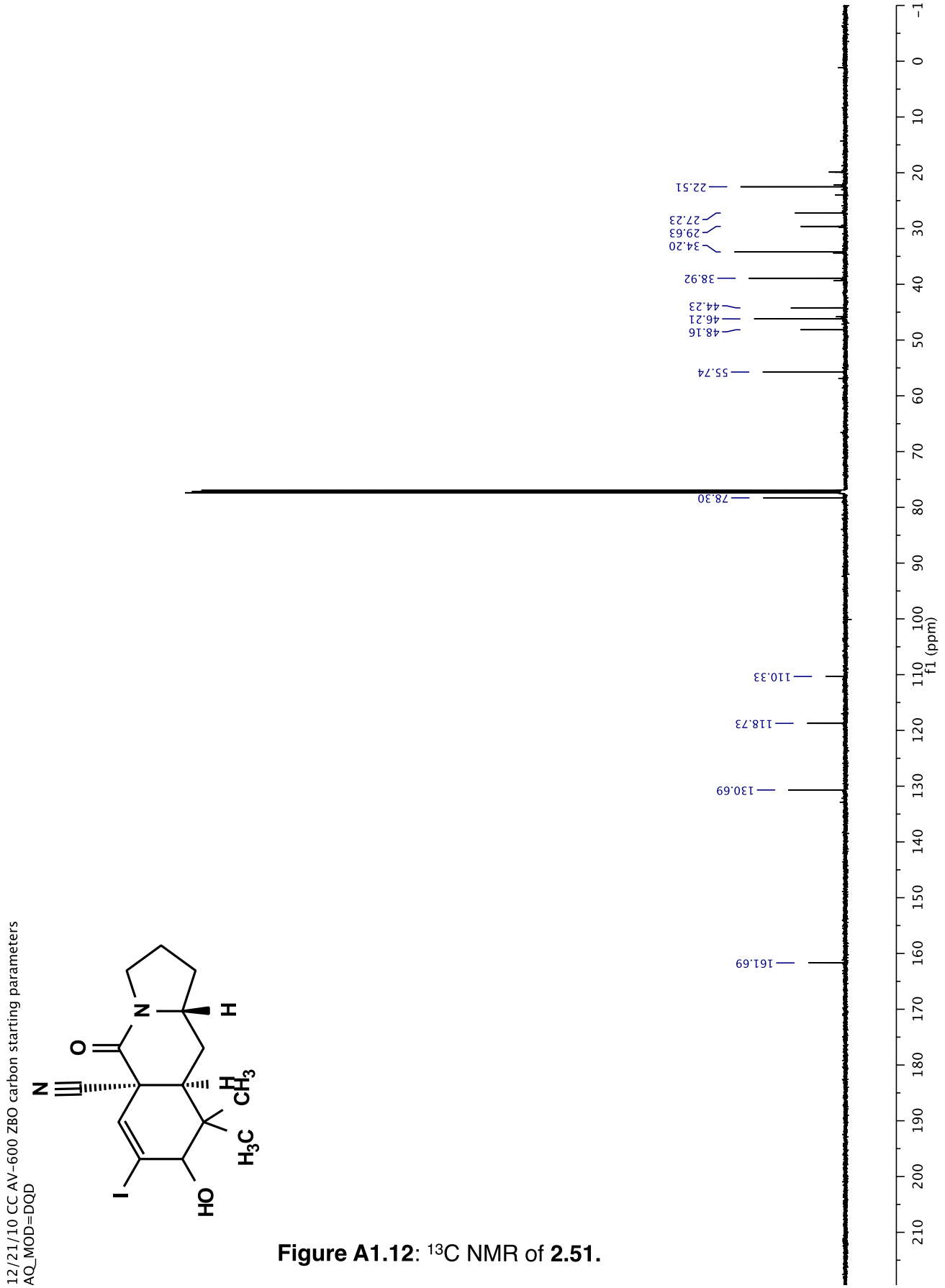

Figure A1.12: ^{13}C NMR of **2.51.**

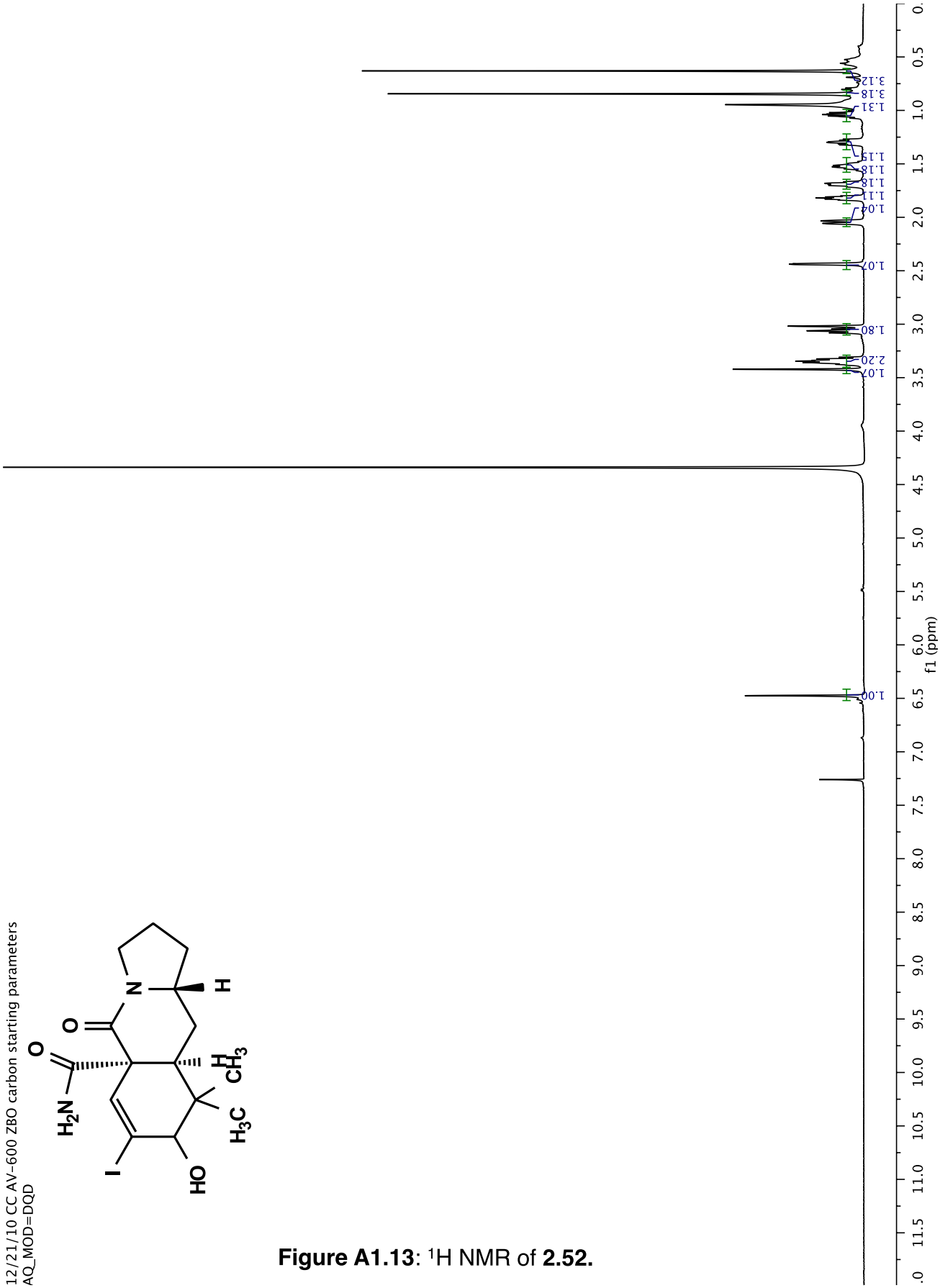

Figure A1.13: ^{1}H NMR of **2.52.**

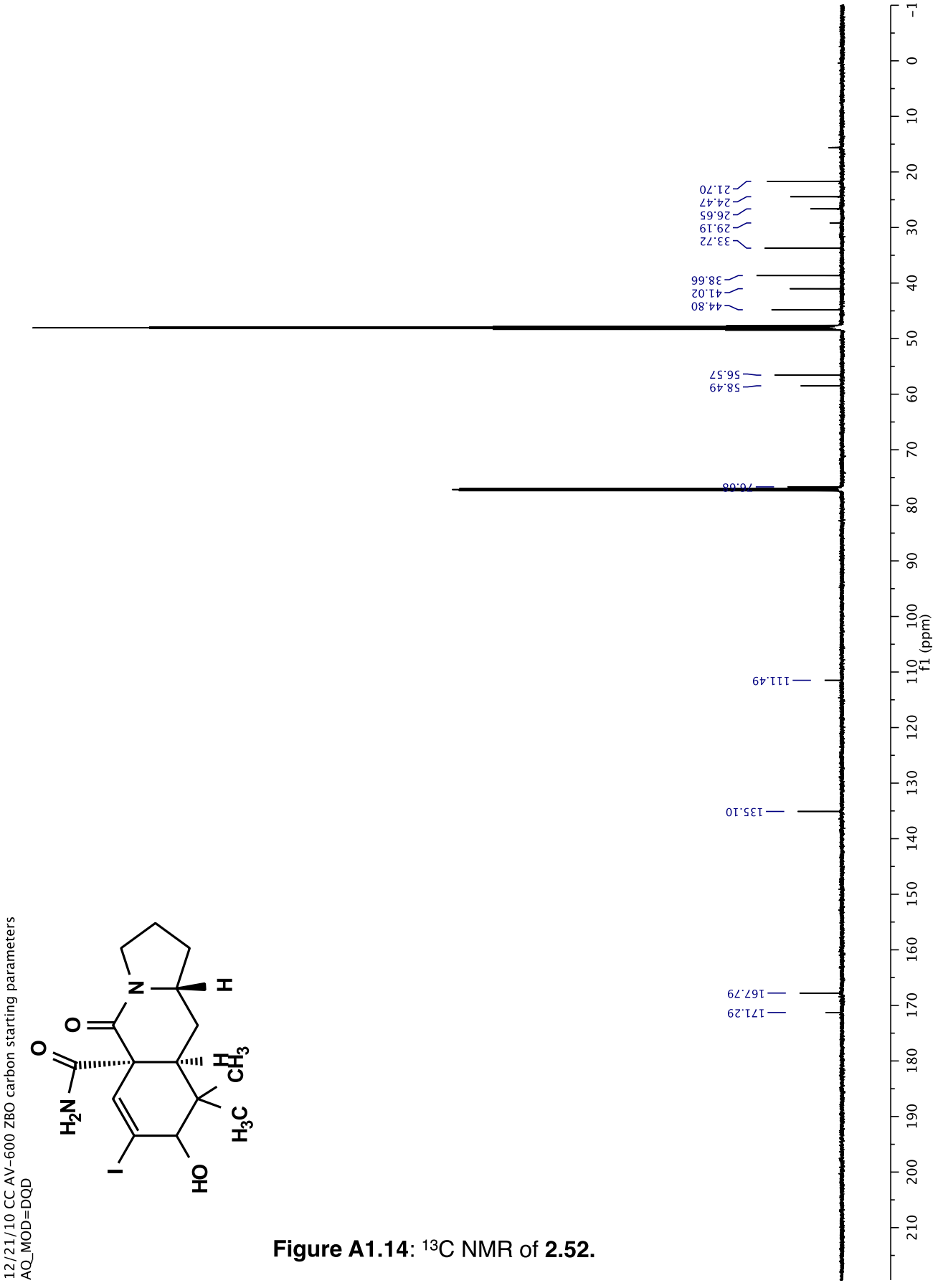

Figure A1.14: ^{13}C NMR of **2.52.**

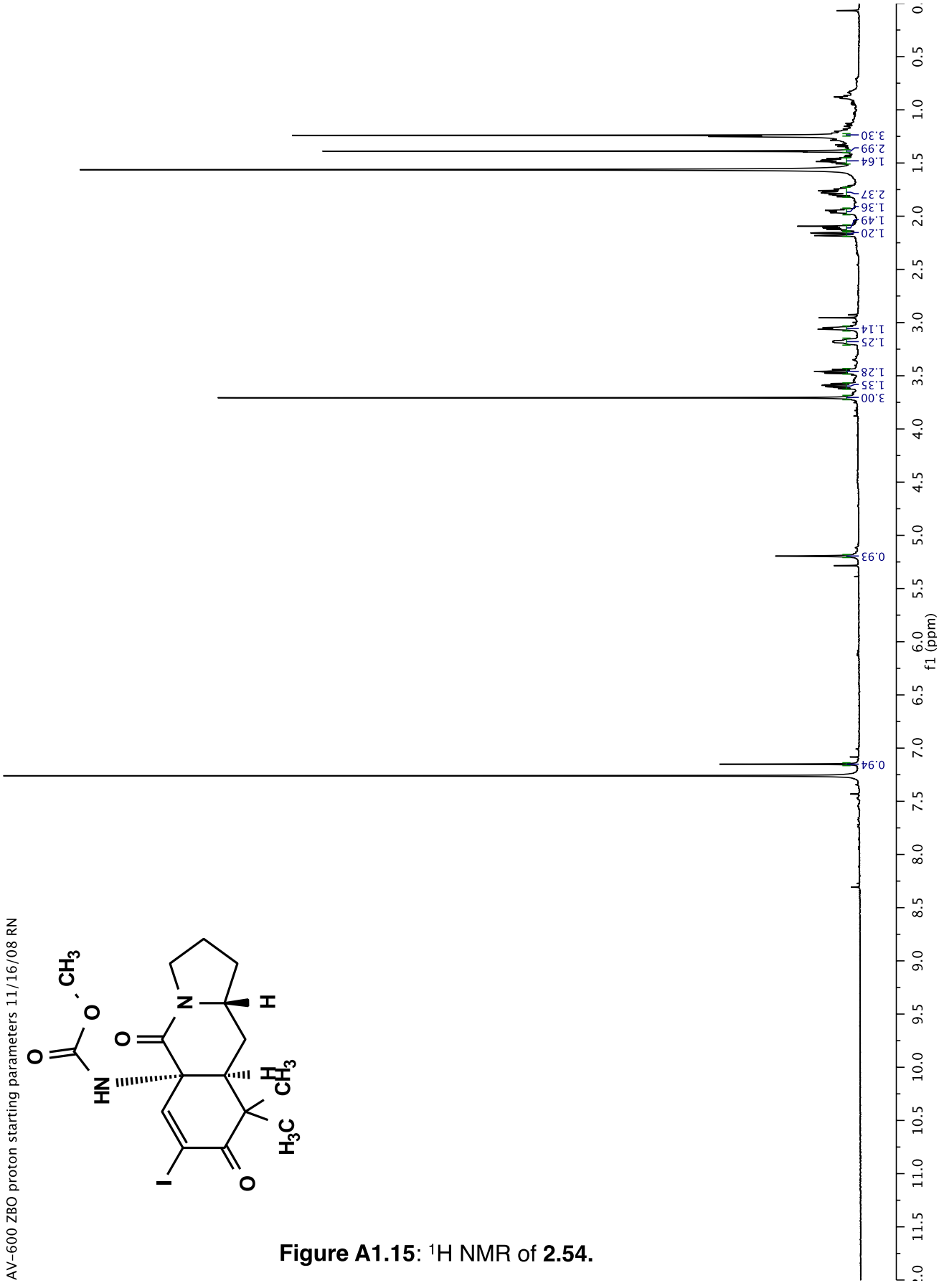

Figure A1.15: ^{1}H NMR of **2.54.**

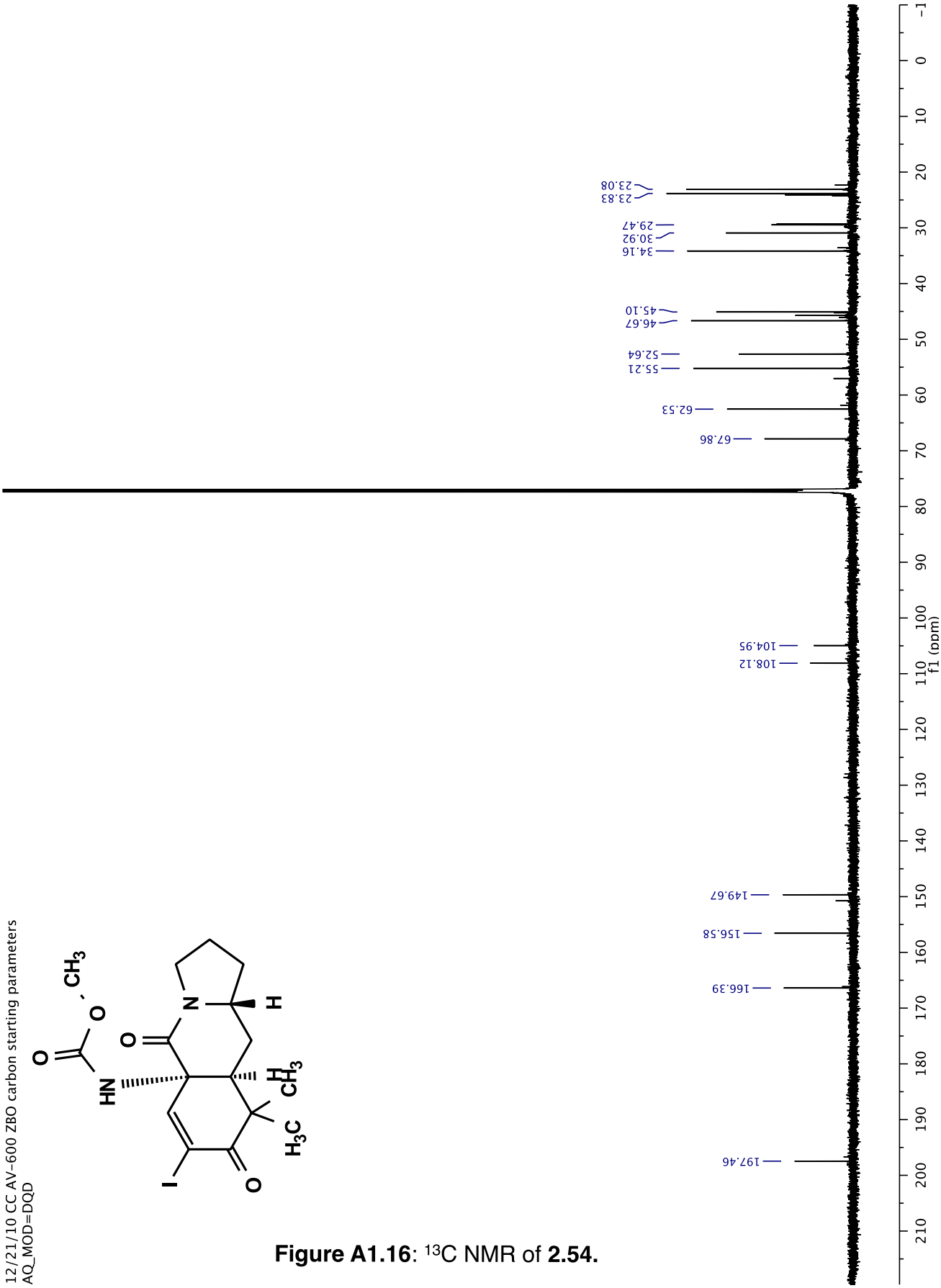

Figure A1.16: ^{13}C NMR of **2.54.**

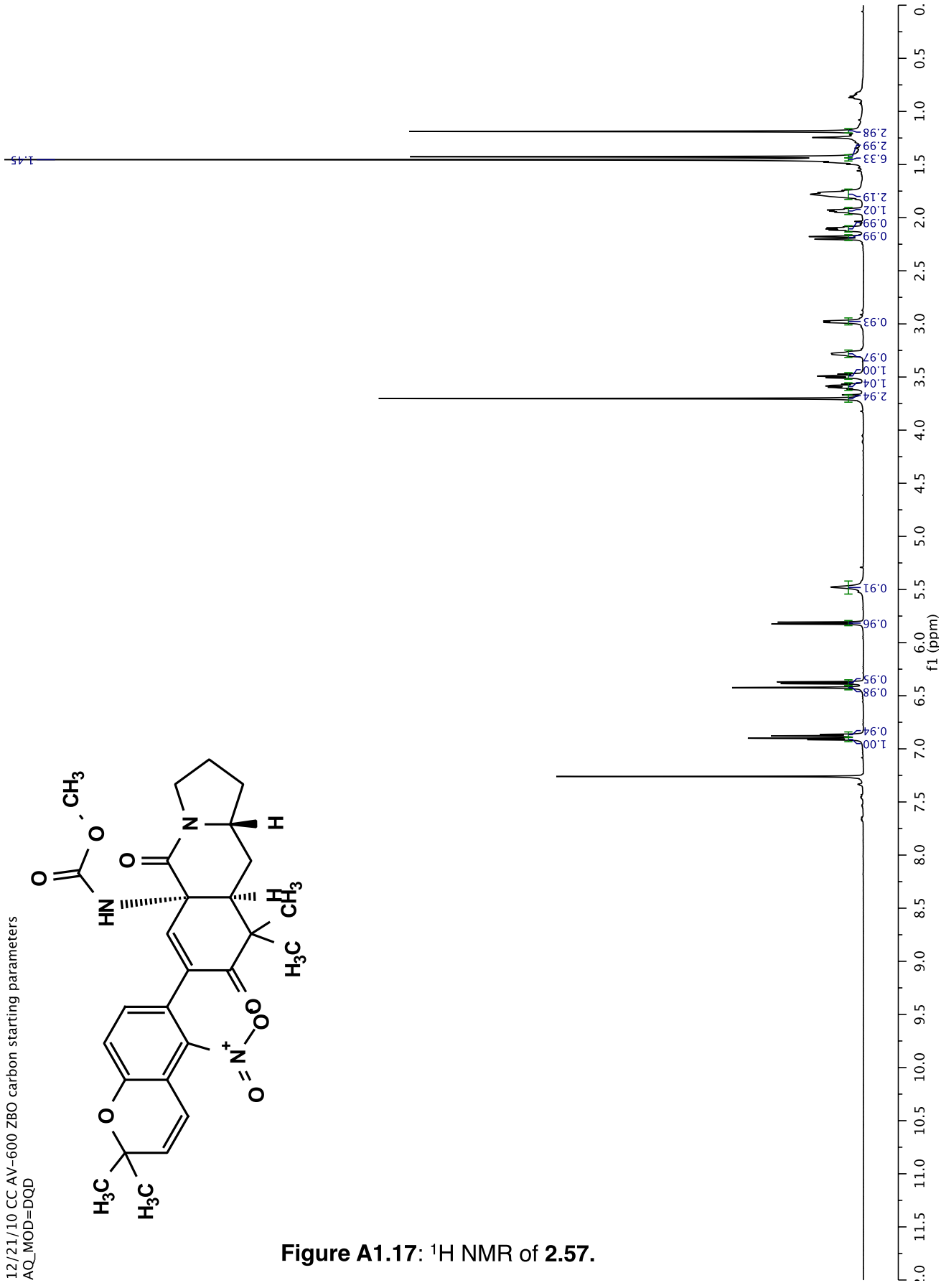

Figure A1.17: ^{1}H NMR of **2.57.**

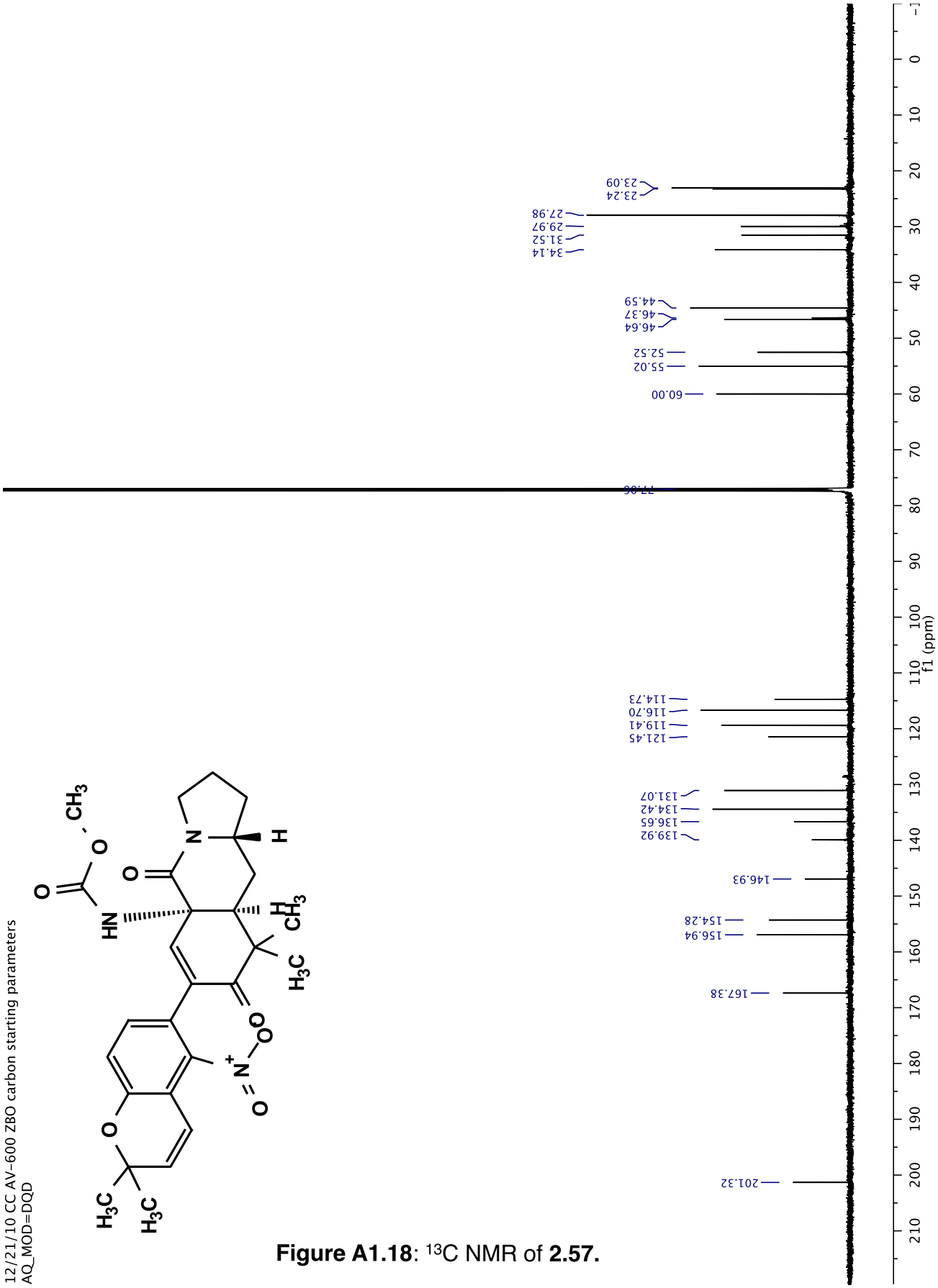

Figure A1.18: ^{13}C NMR of **2.57.**

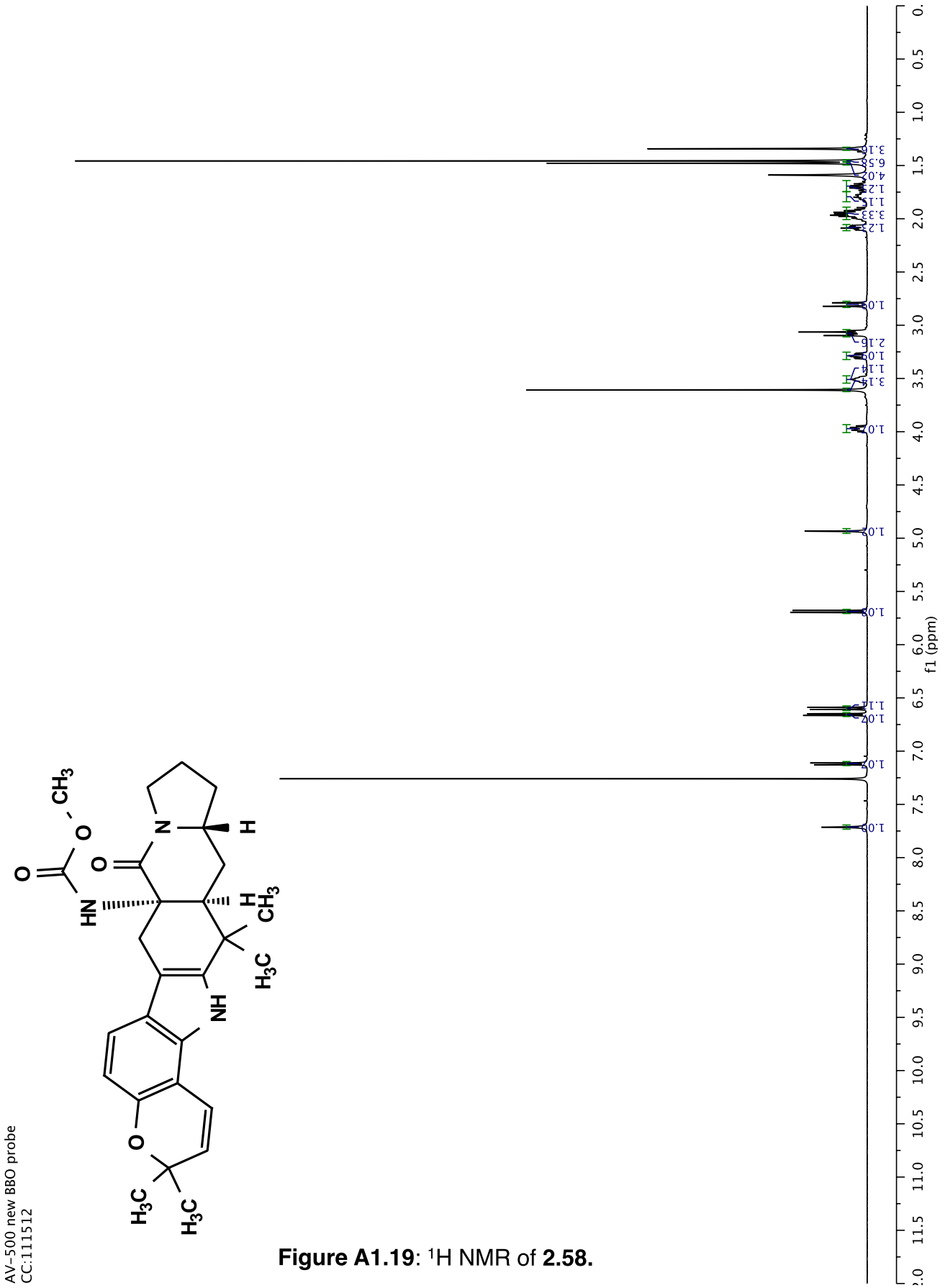

Figure A1.19: ^{1}H NMR of **2.58.**

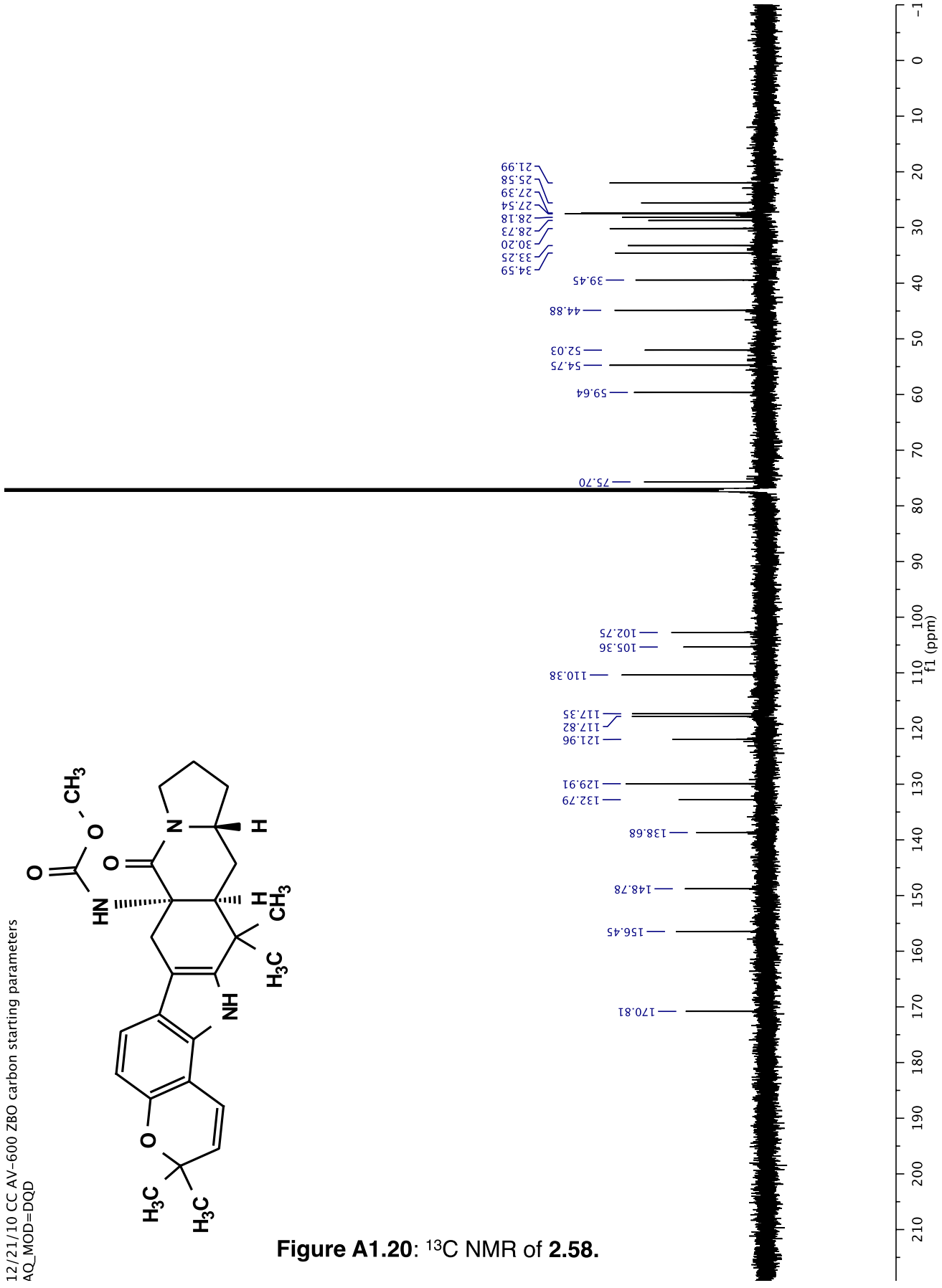

Figure A1.20: ^{13}C NMR of **2.58.**

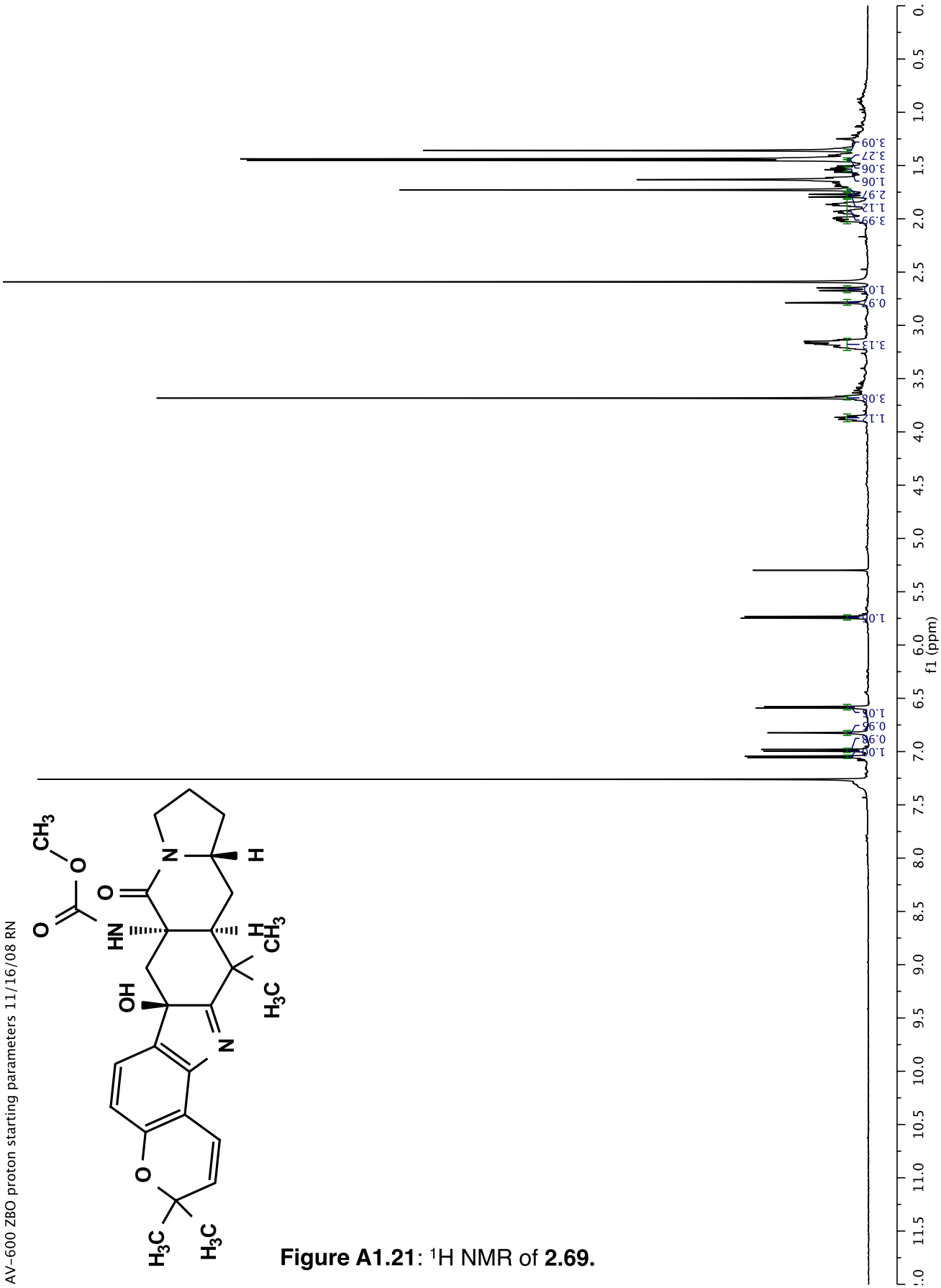

Figure A1.21: ^{1}H NMR of **2.69.**

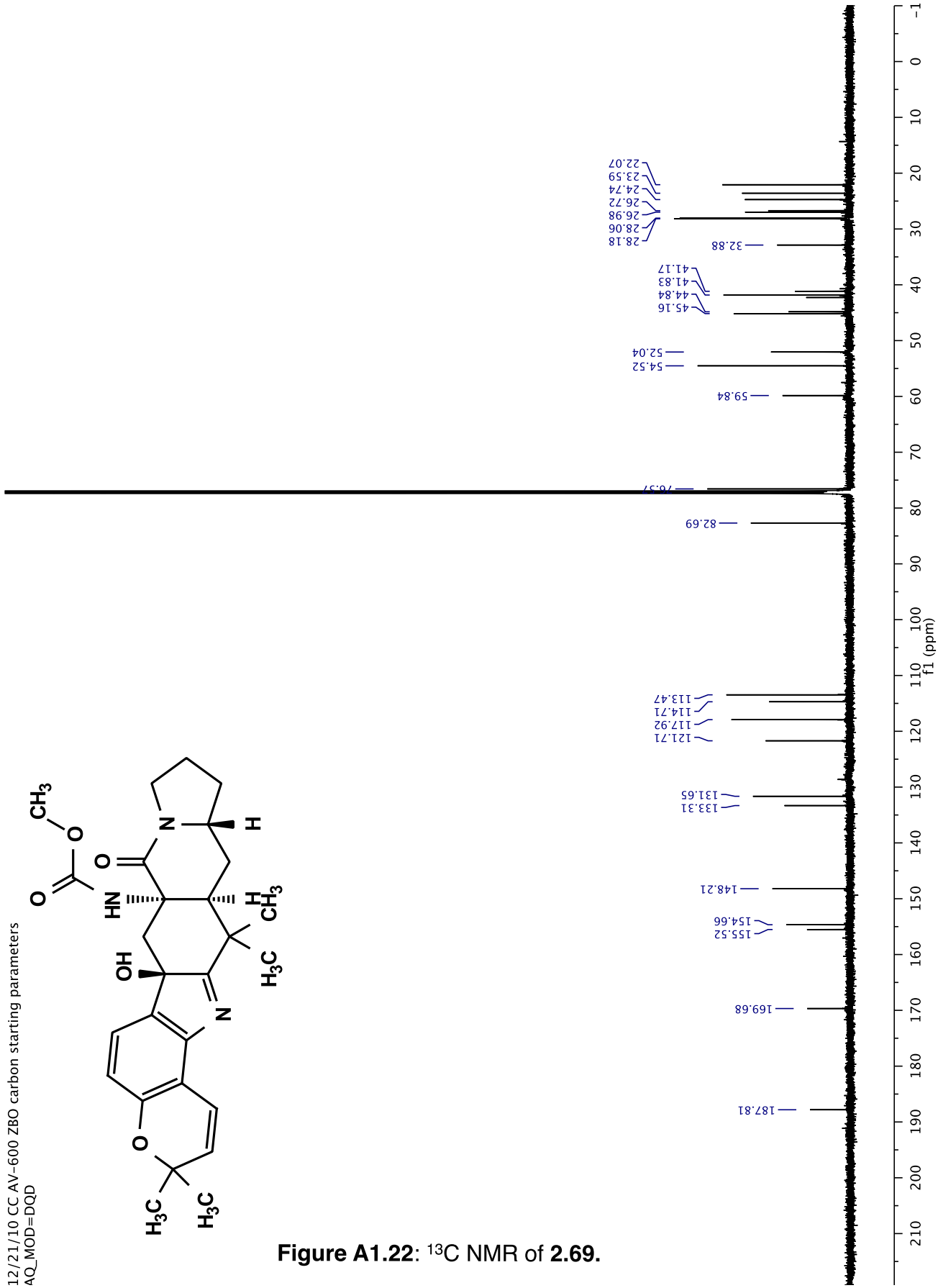

Figure A1.22: ^{13}C NMR of **2.69.**

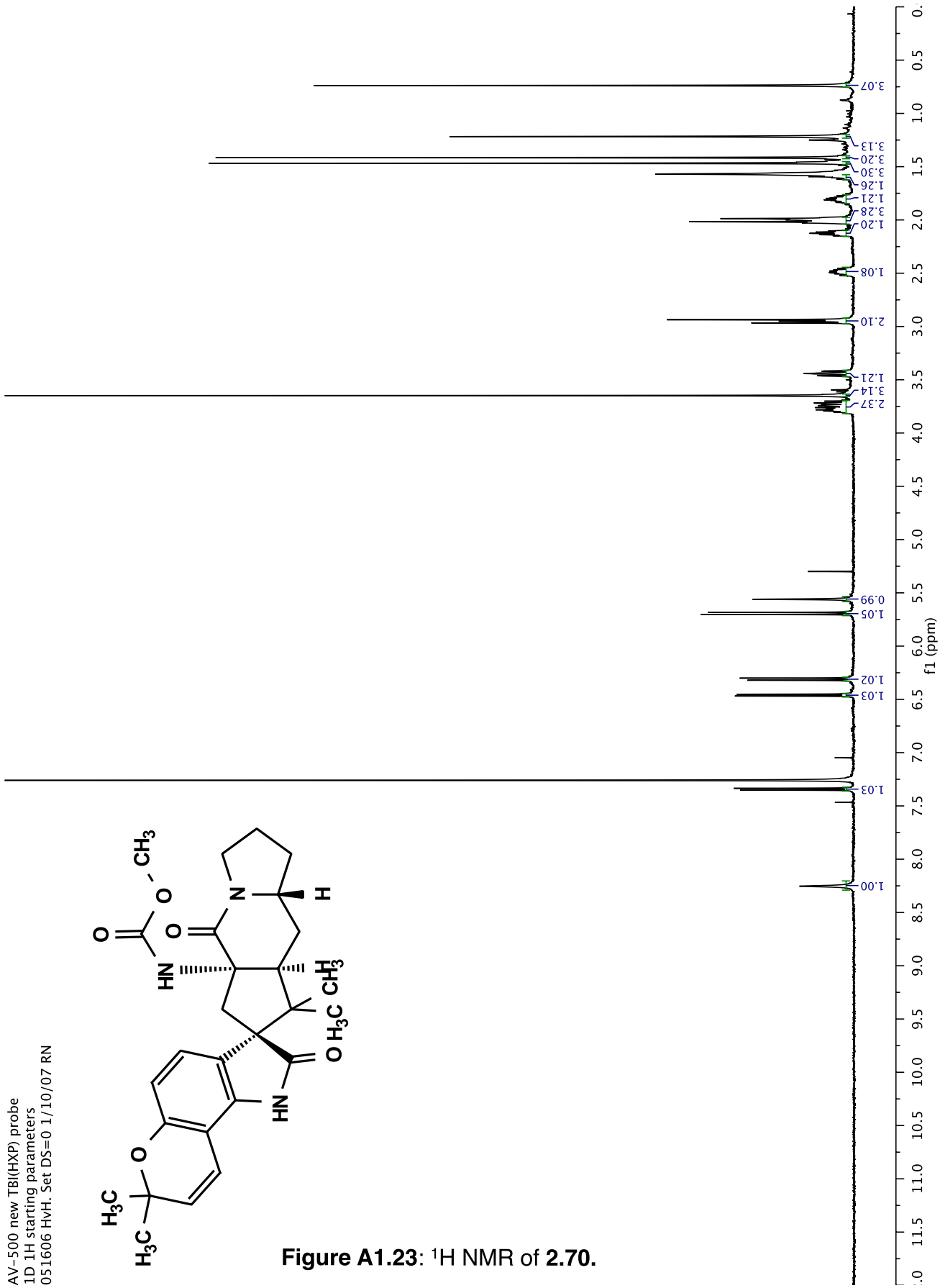

Figure A1.23: ^{1}H NMR of **2.70.**

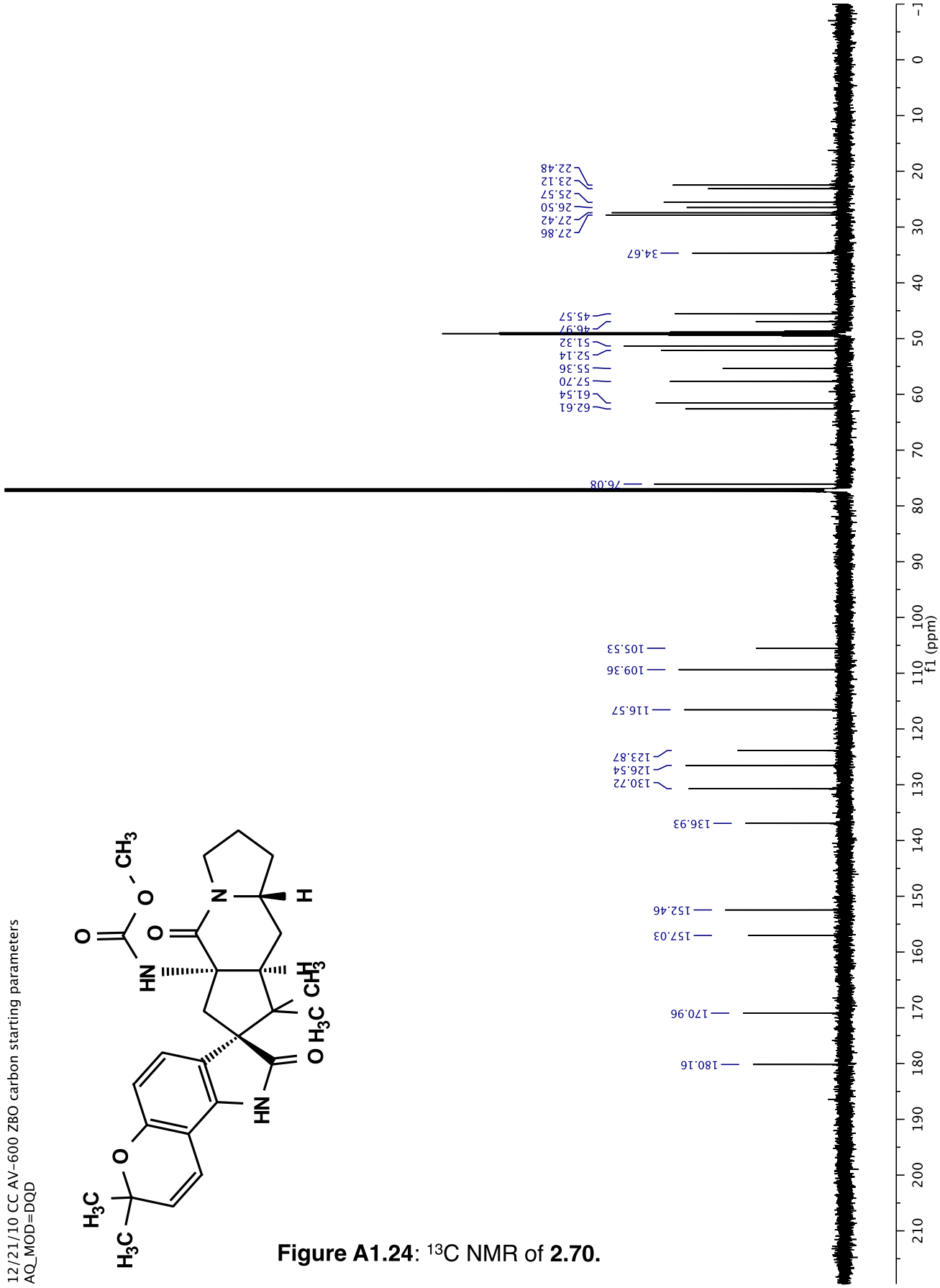

Figure A1.24: ^{13}C NMR of **2.70.**

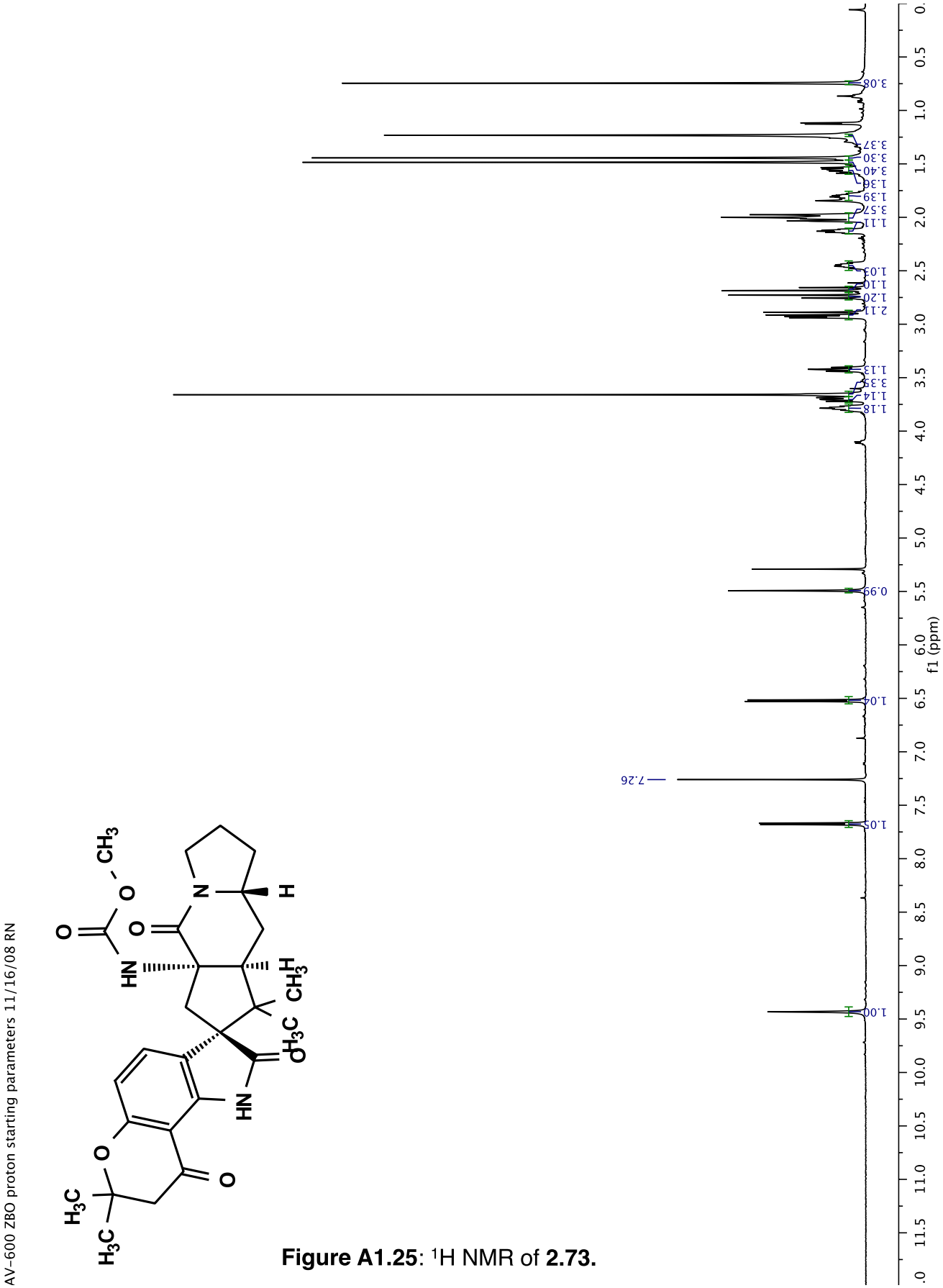

Figure A1.25: ^{1}H NMR of **2.73.**

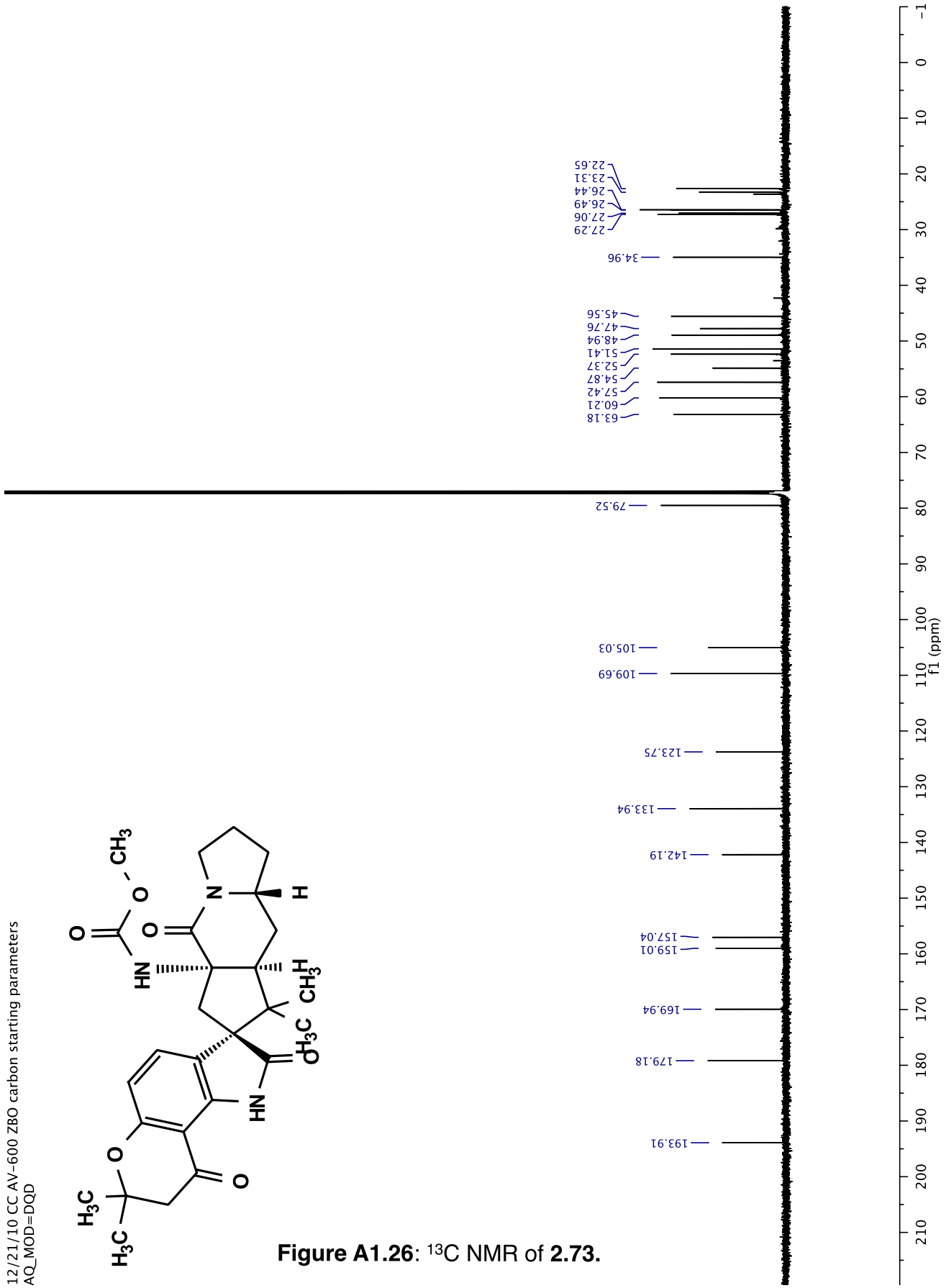

Figure A1.26: ^{13}C NMR of **2.73.**

12/21/10 CC AV-600 ZBO carbon starting parameters
AQ_MOD=DQD

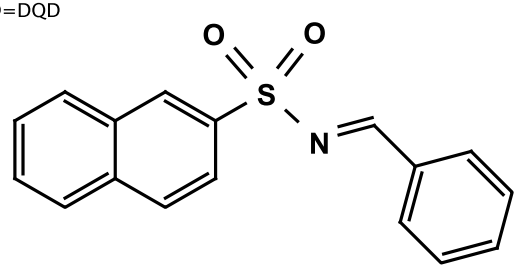

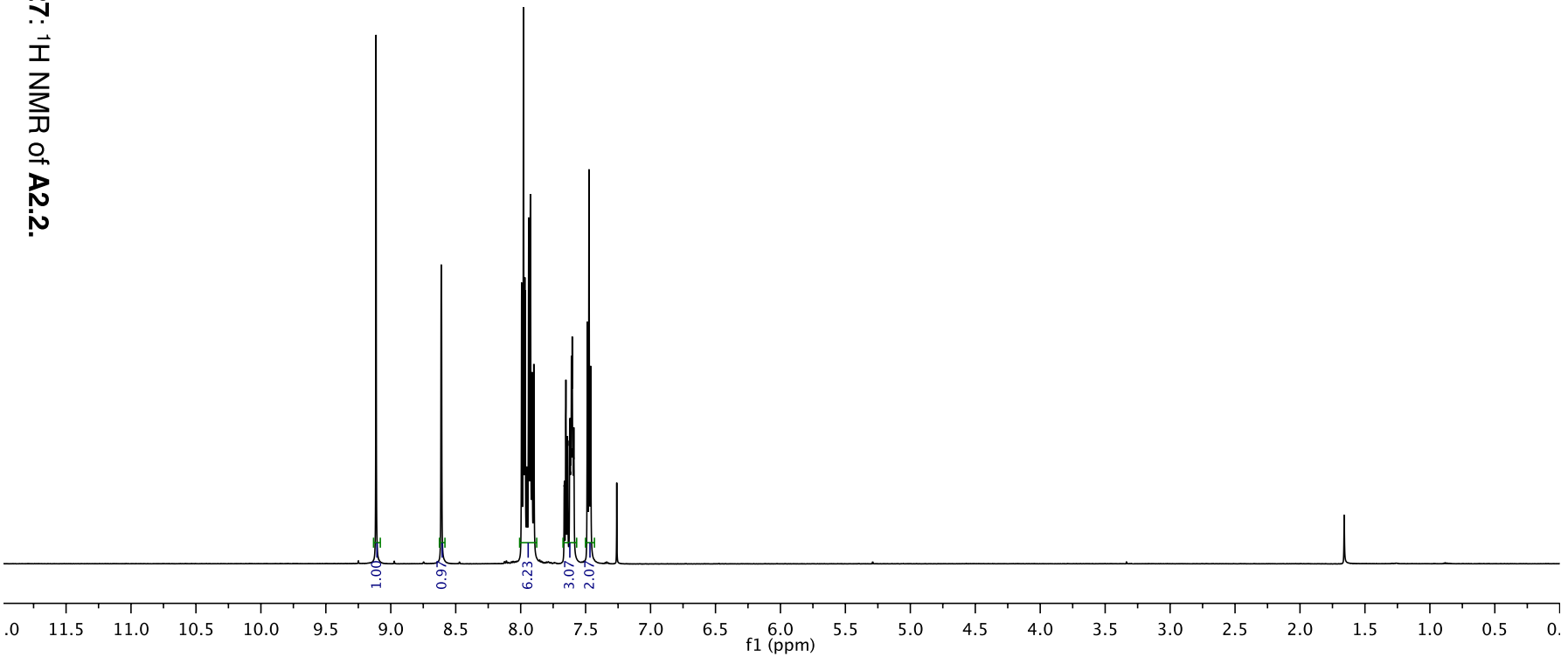

Figure A1.27: ^{1}H NMR of **A2.2.**

12/21/10 CC AV-600 ZBO carbon starting parameters
AQ_MOD=DQD

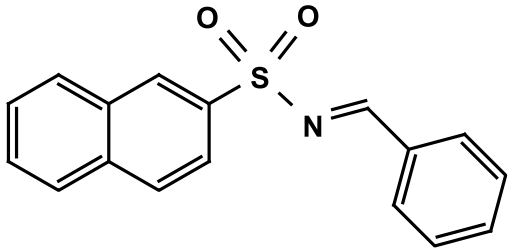

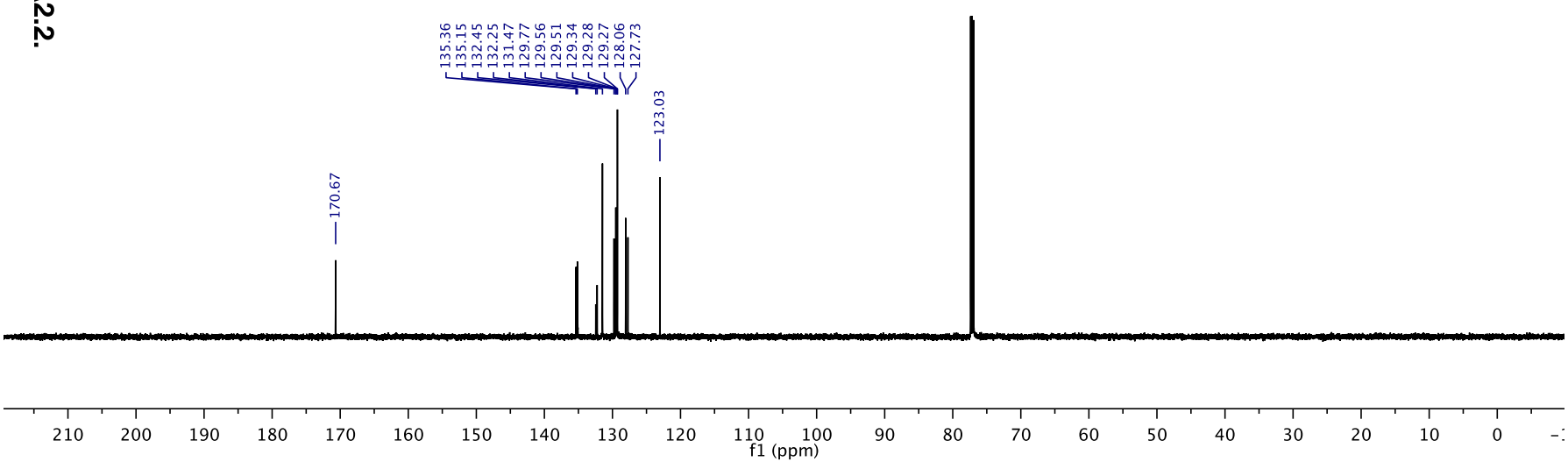

Figure A1.28: ^{13}C NMR of **A2.2.**

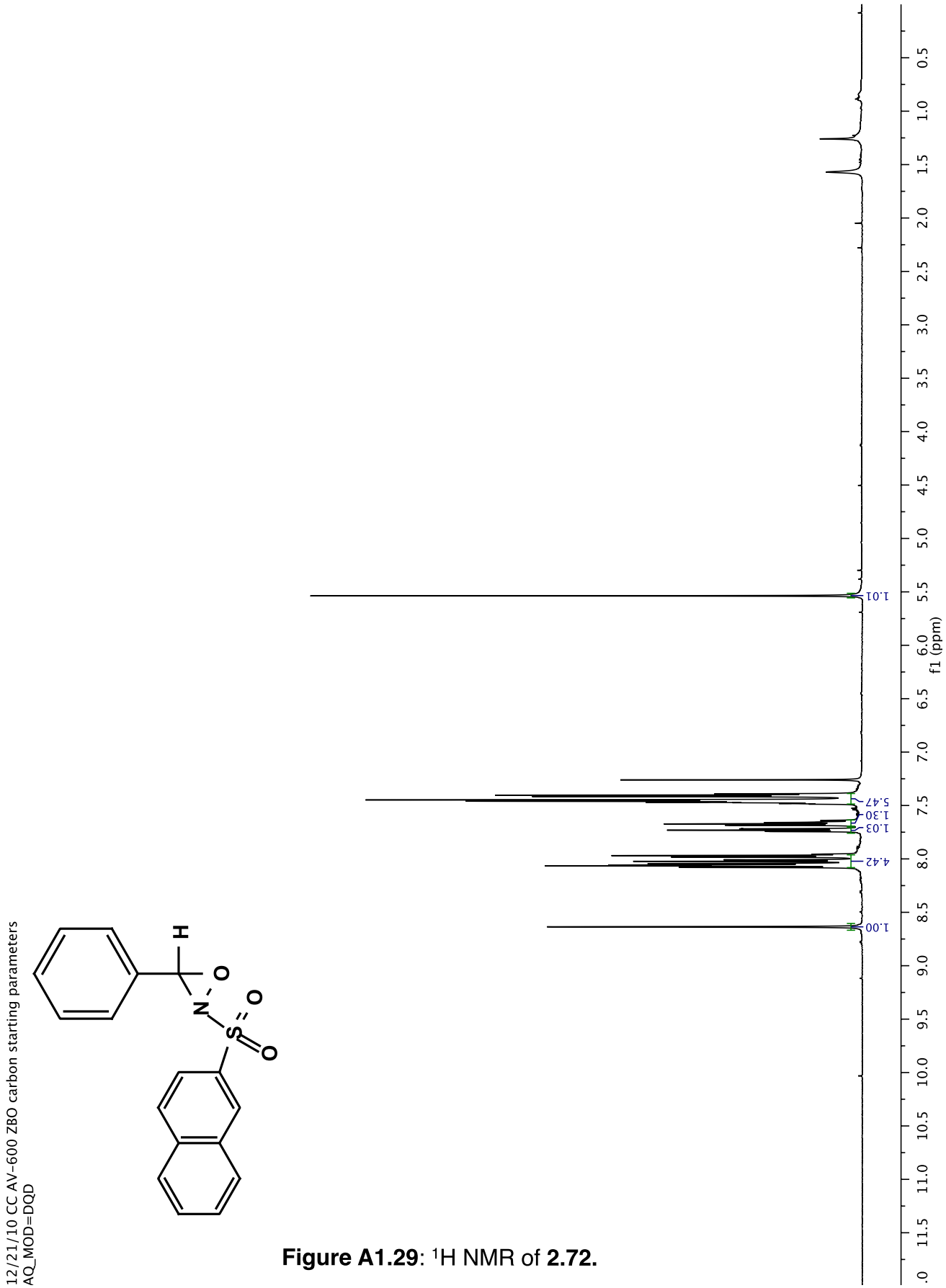

Figure A1.29: ^{1}H NMR of **2.72.**

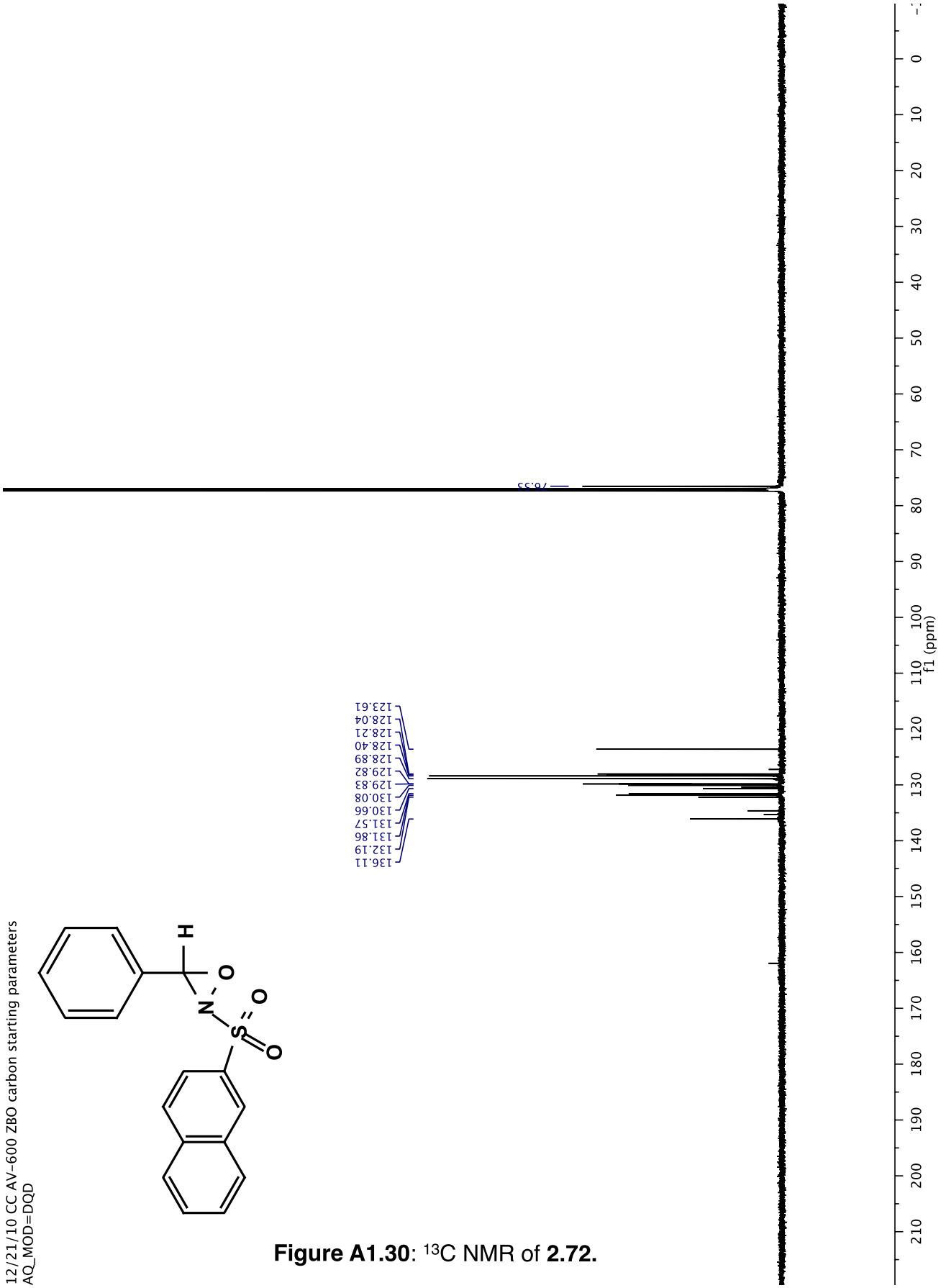

Figure A1.30: ^{13}C NMR of **2.72.**

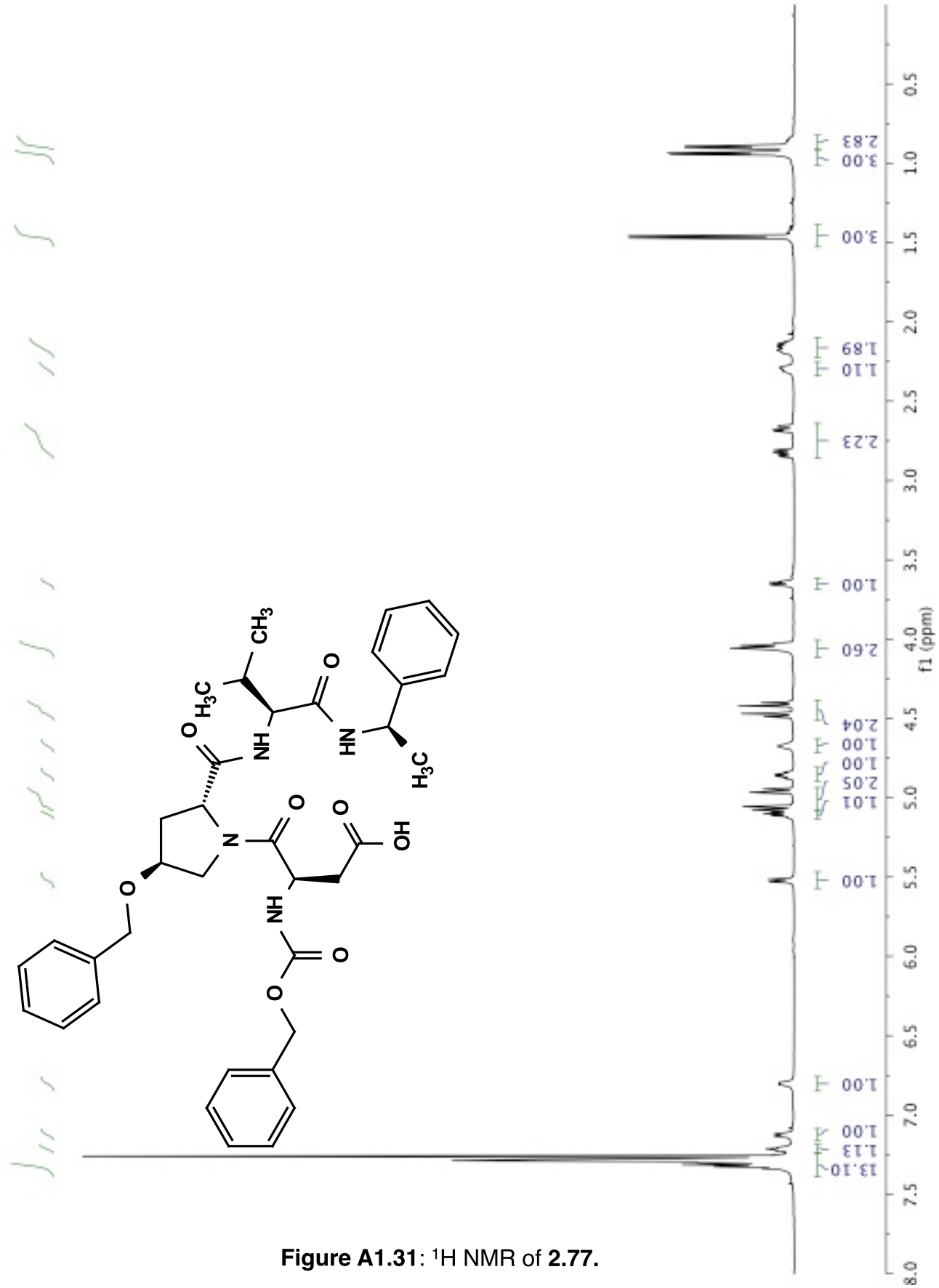

Figure A1.31: ^{1}H NMR of **2.77.**

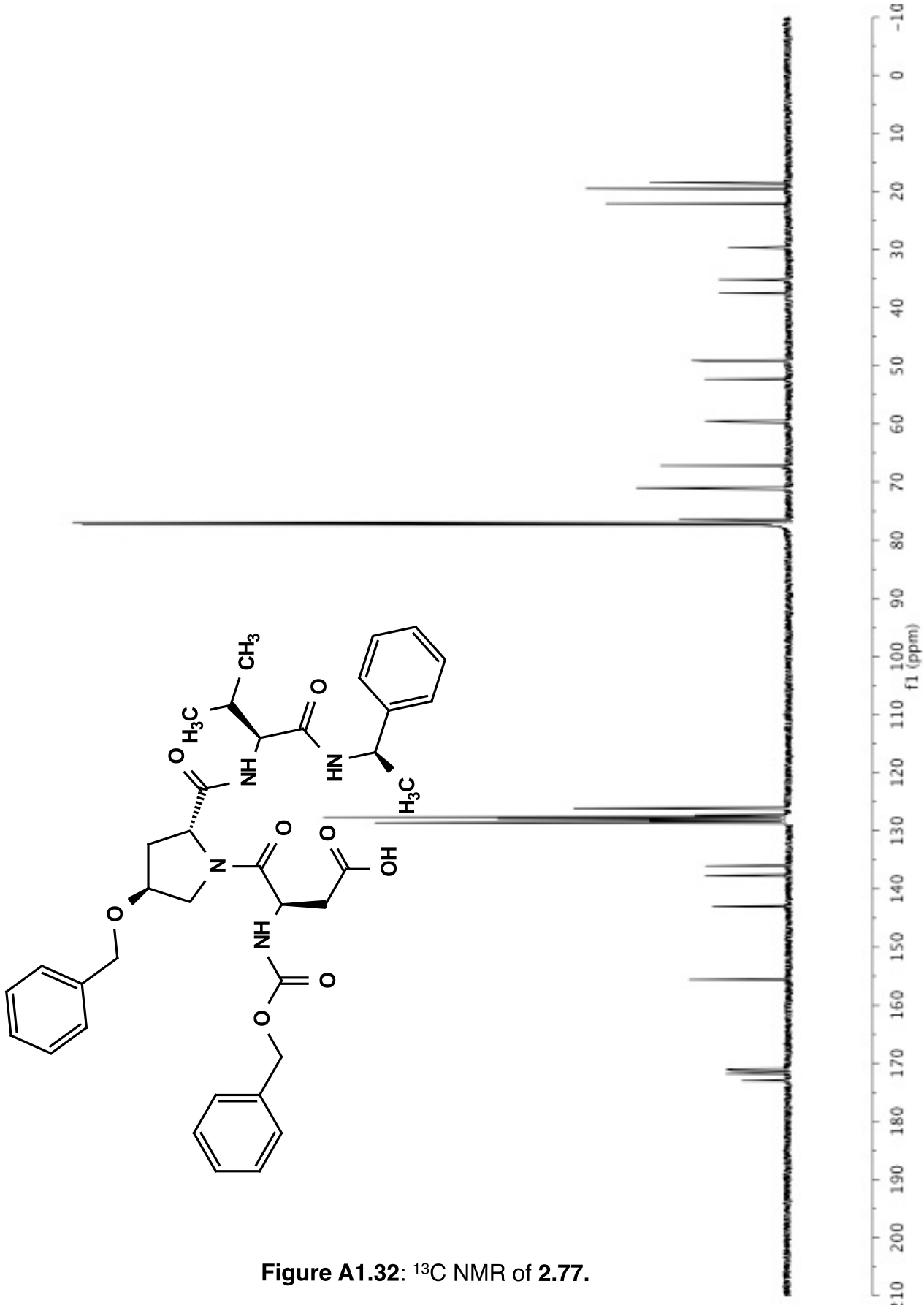

Figure A1.32: ^{13}C NMR of **2.77.**

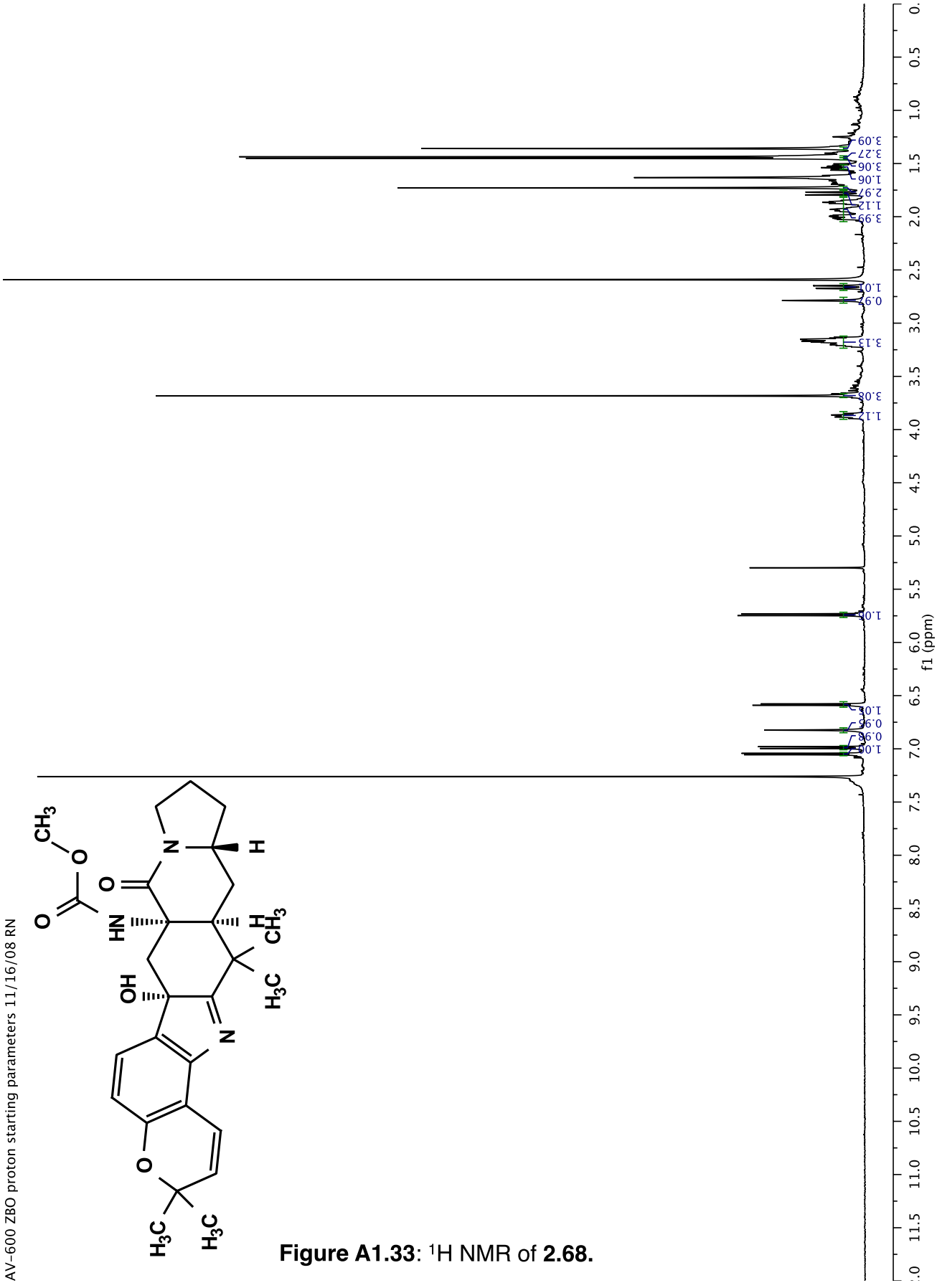

Figure A1.33: ^{1}H NMR of **2.68.**

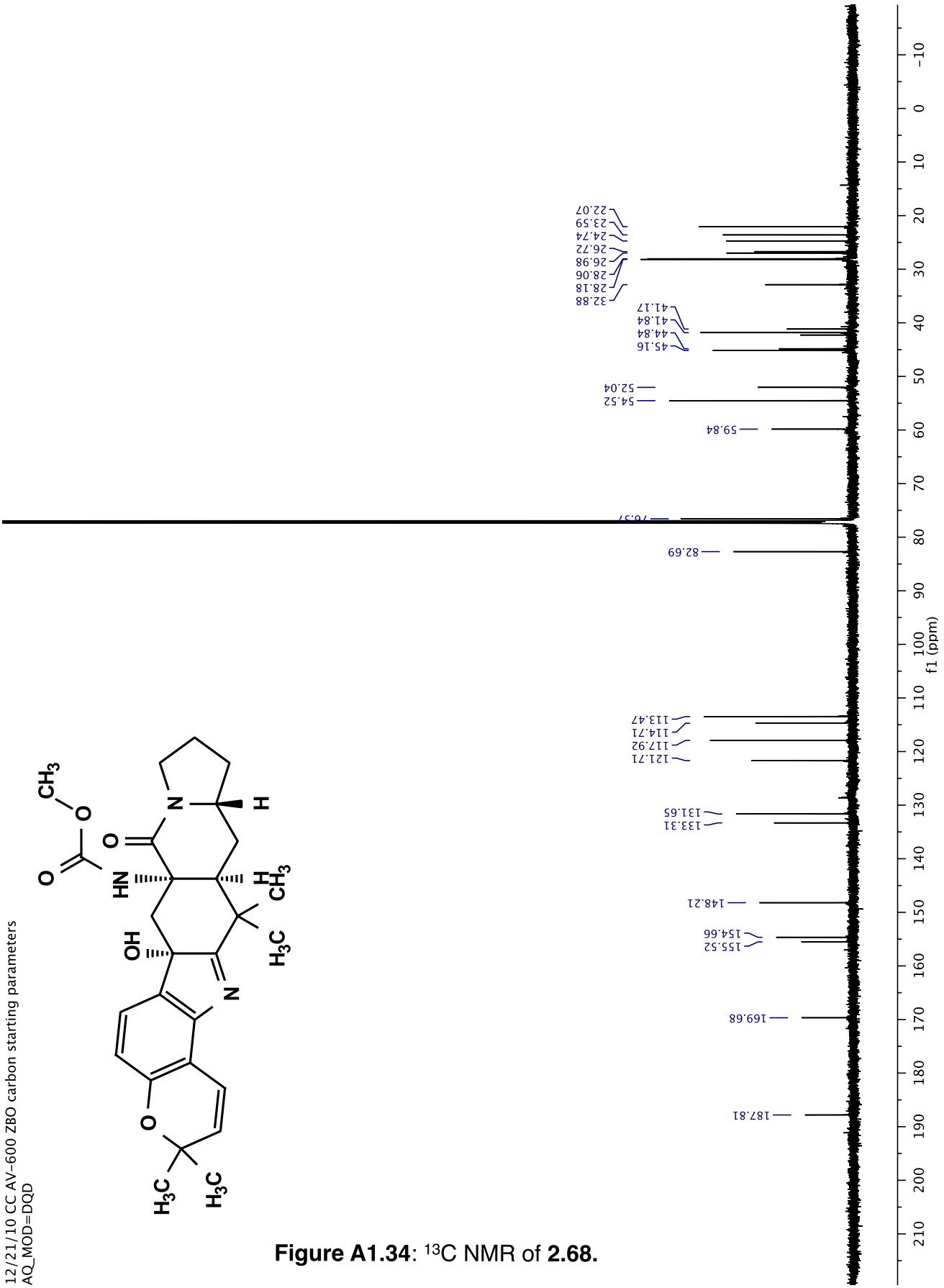

Figure A1.34: ^{13}C NMR of **2.68.**

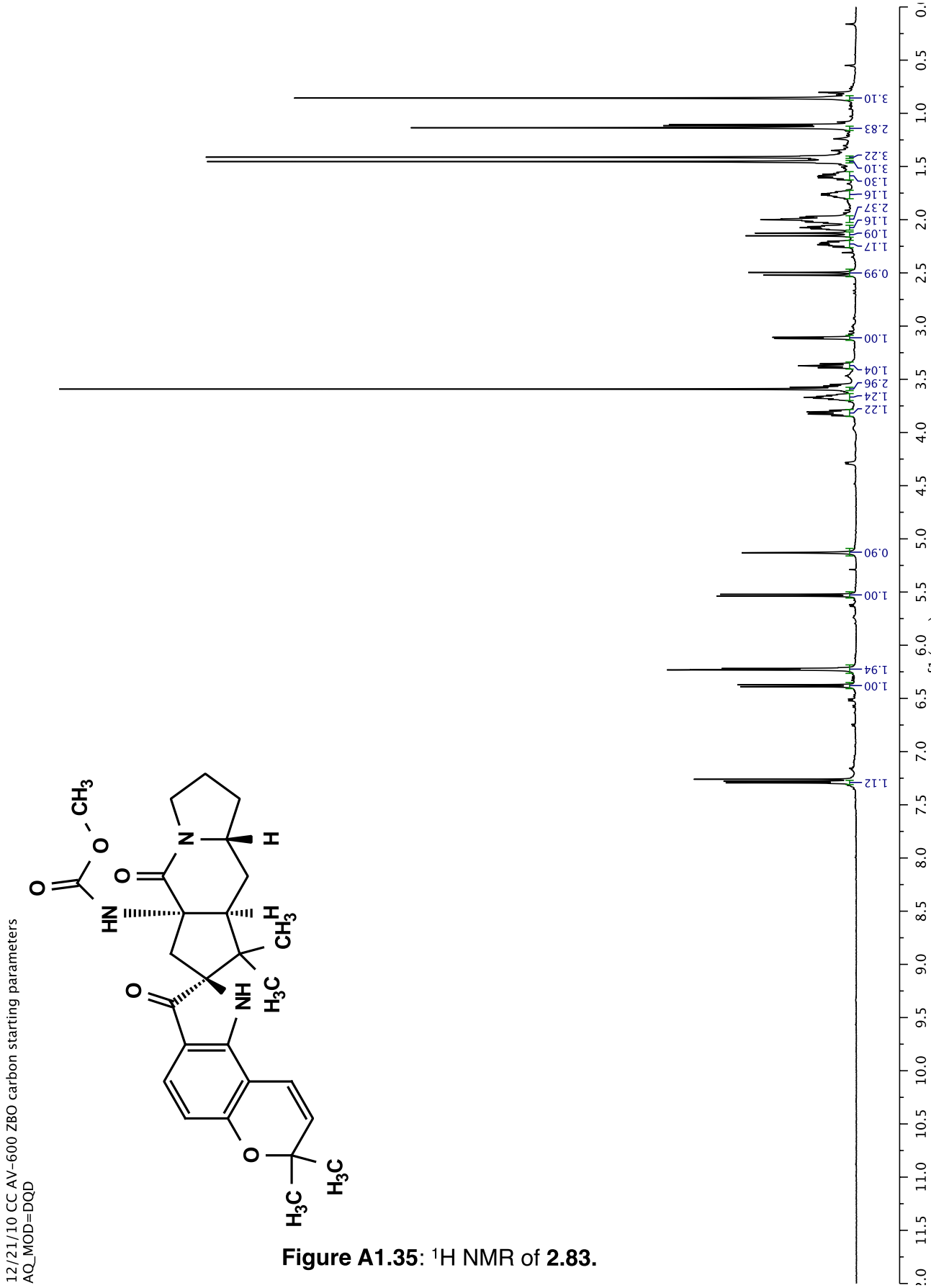

Figure A1.35: ^{1}H NMR of **2.83.**

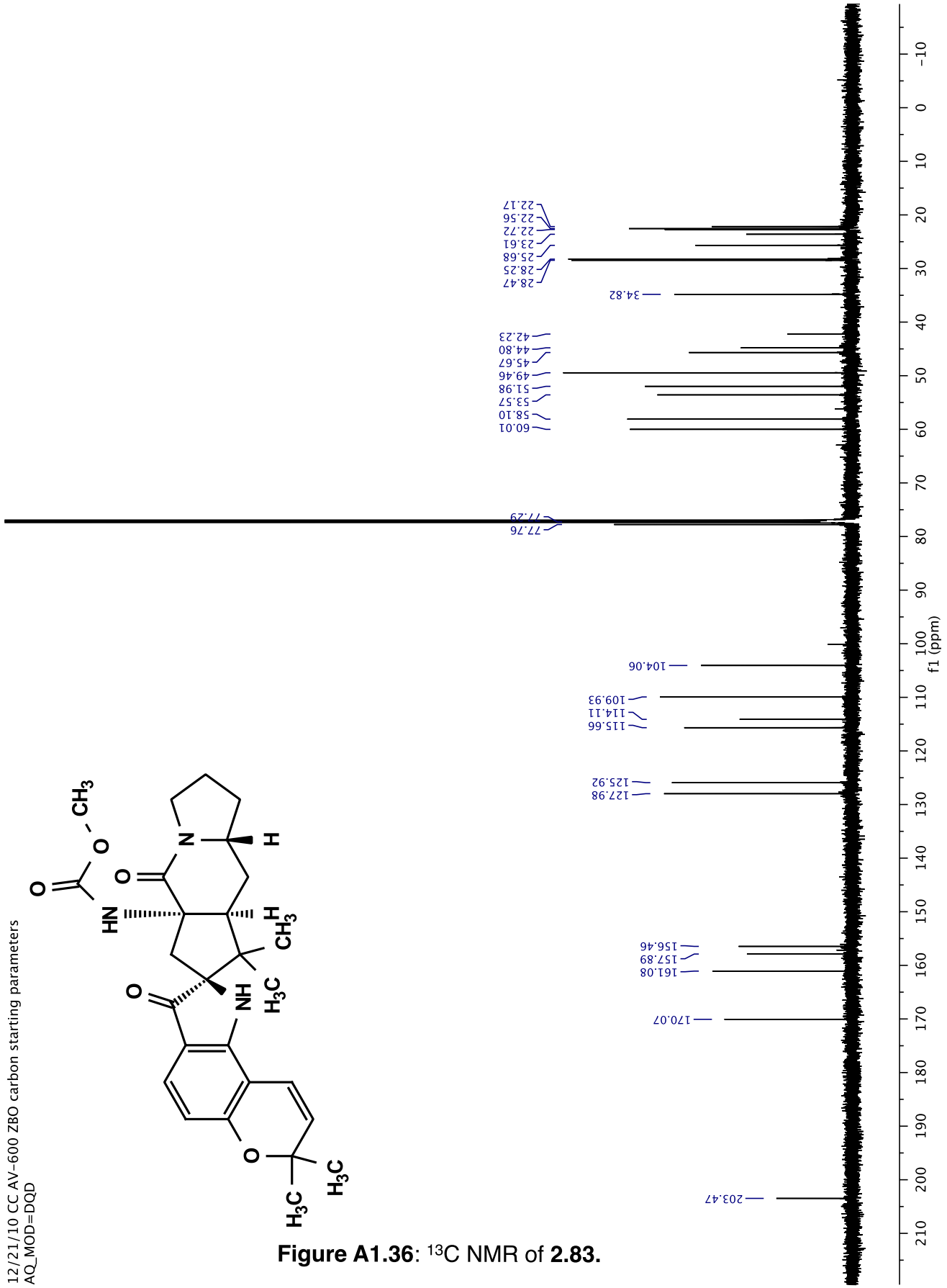

Figure A1.36: ^{13}C NMR of **2.83.**

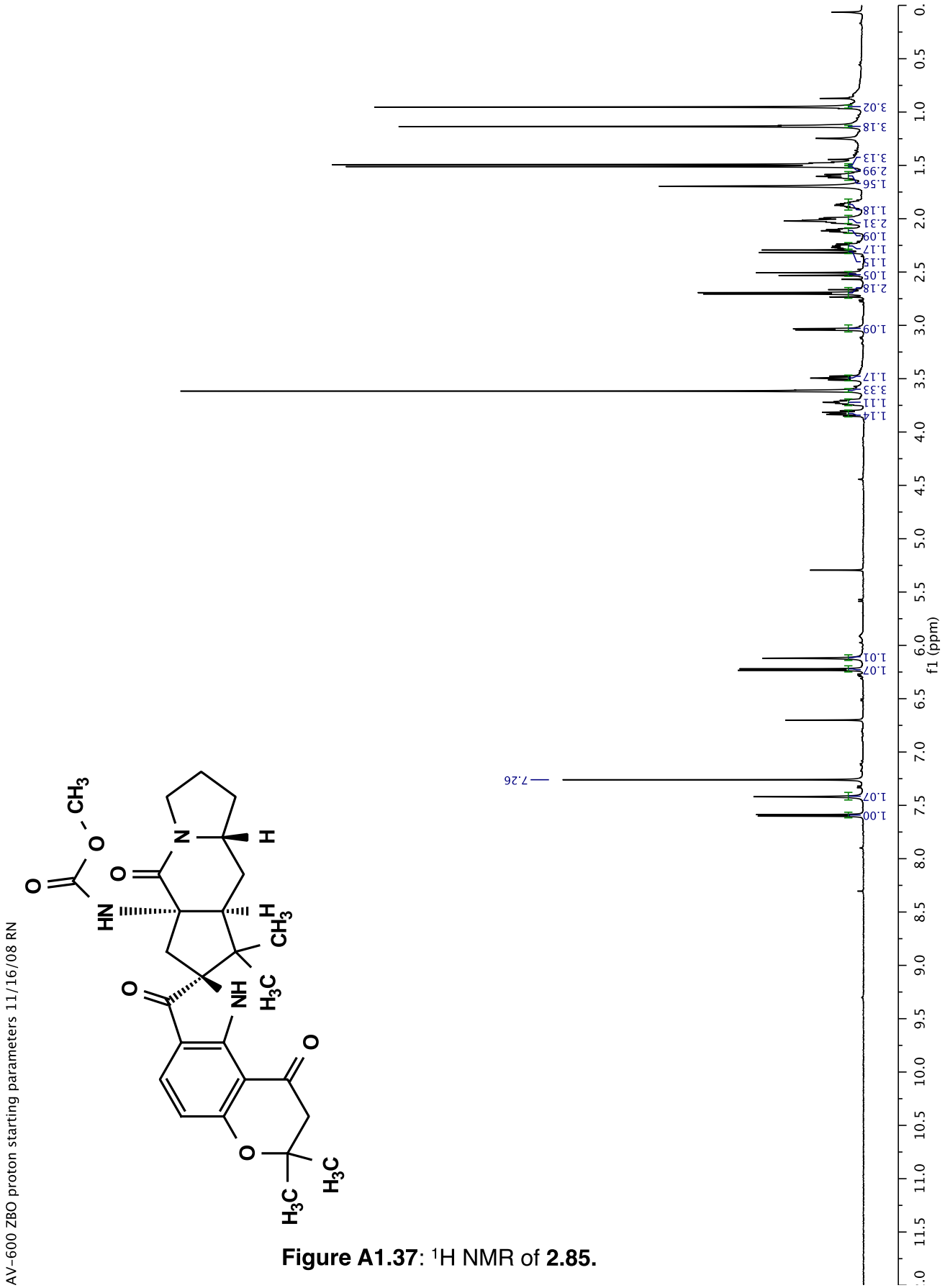

Figure A1.37: ^{1}H NMR of **2.85.**

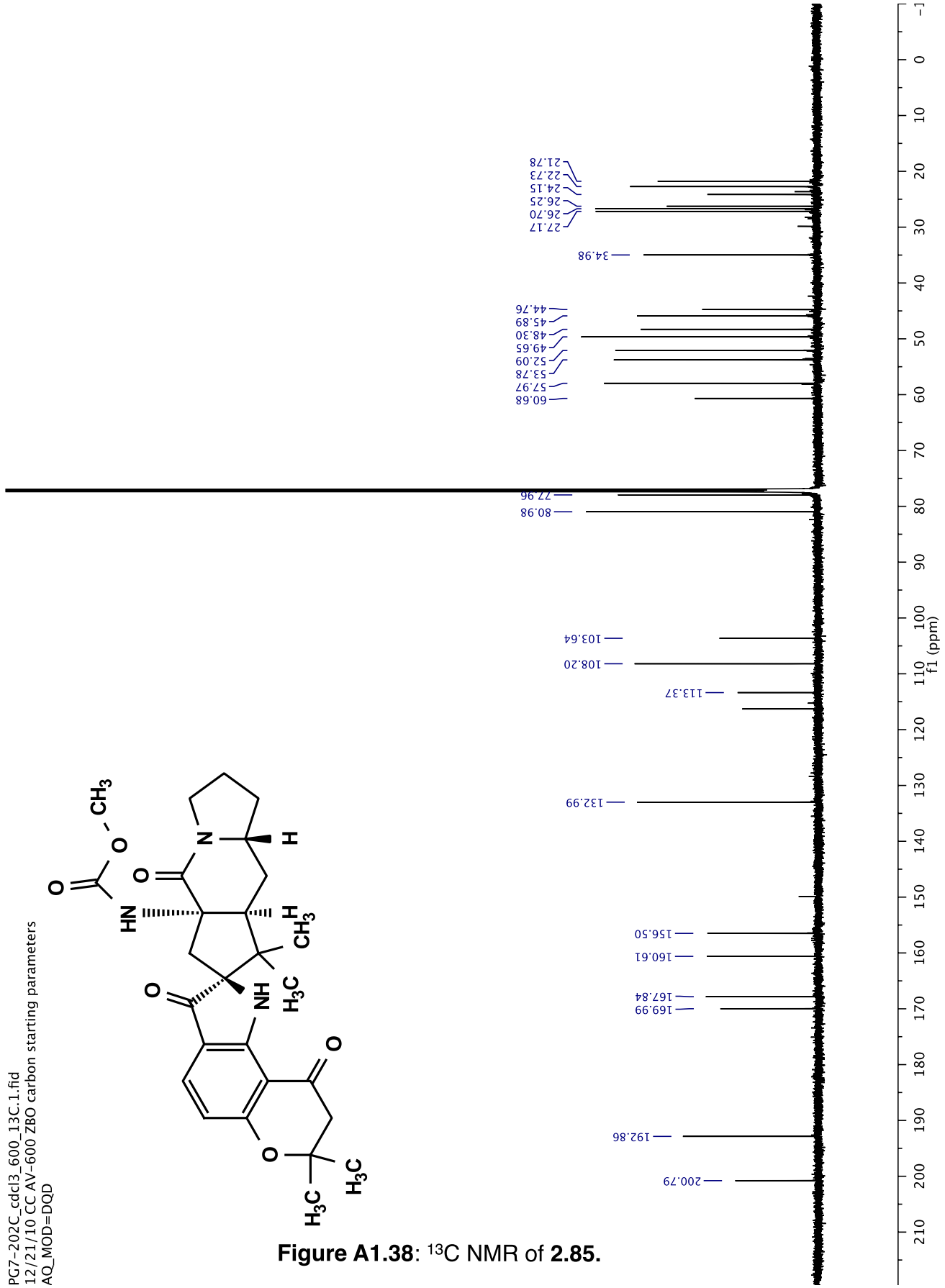

Figure A1.38: ^{13}C NMR of **2.85.**

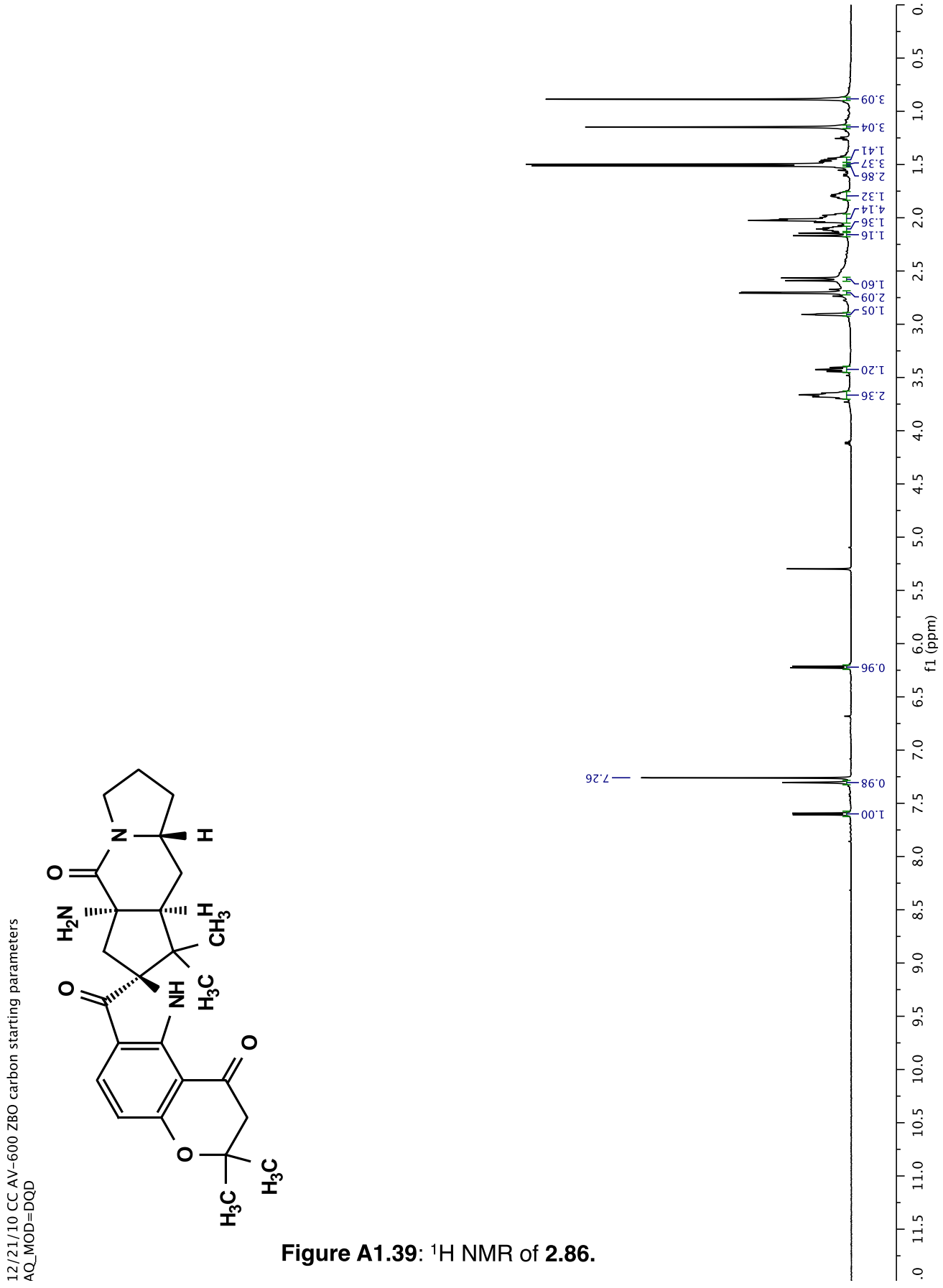

Figure A1.39: ^{1}H NMR of **2.86.**

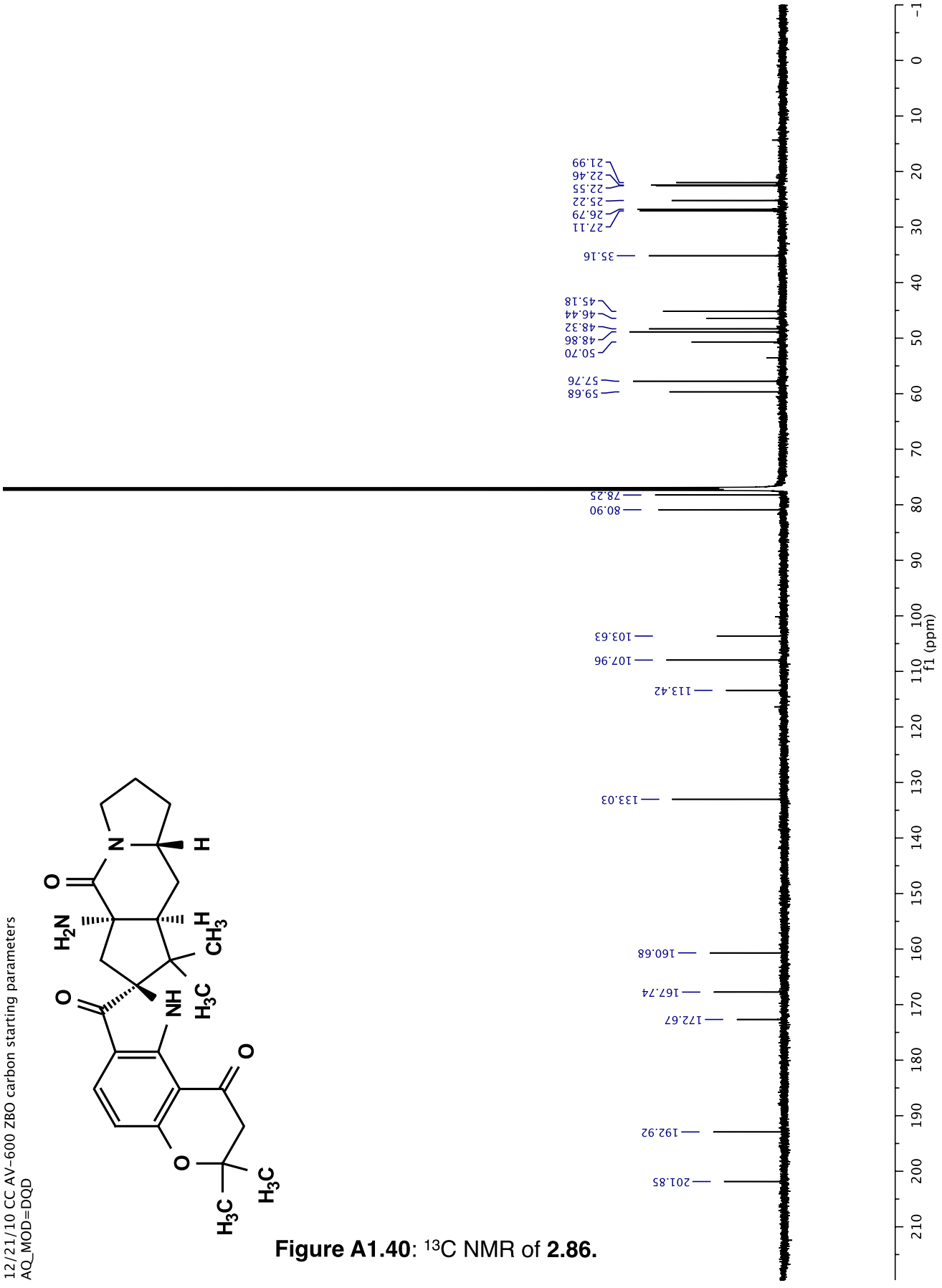

Figure A1.40: ^{13}C NMR of **2.86.**

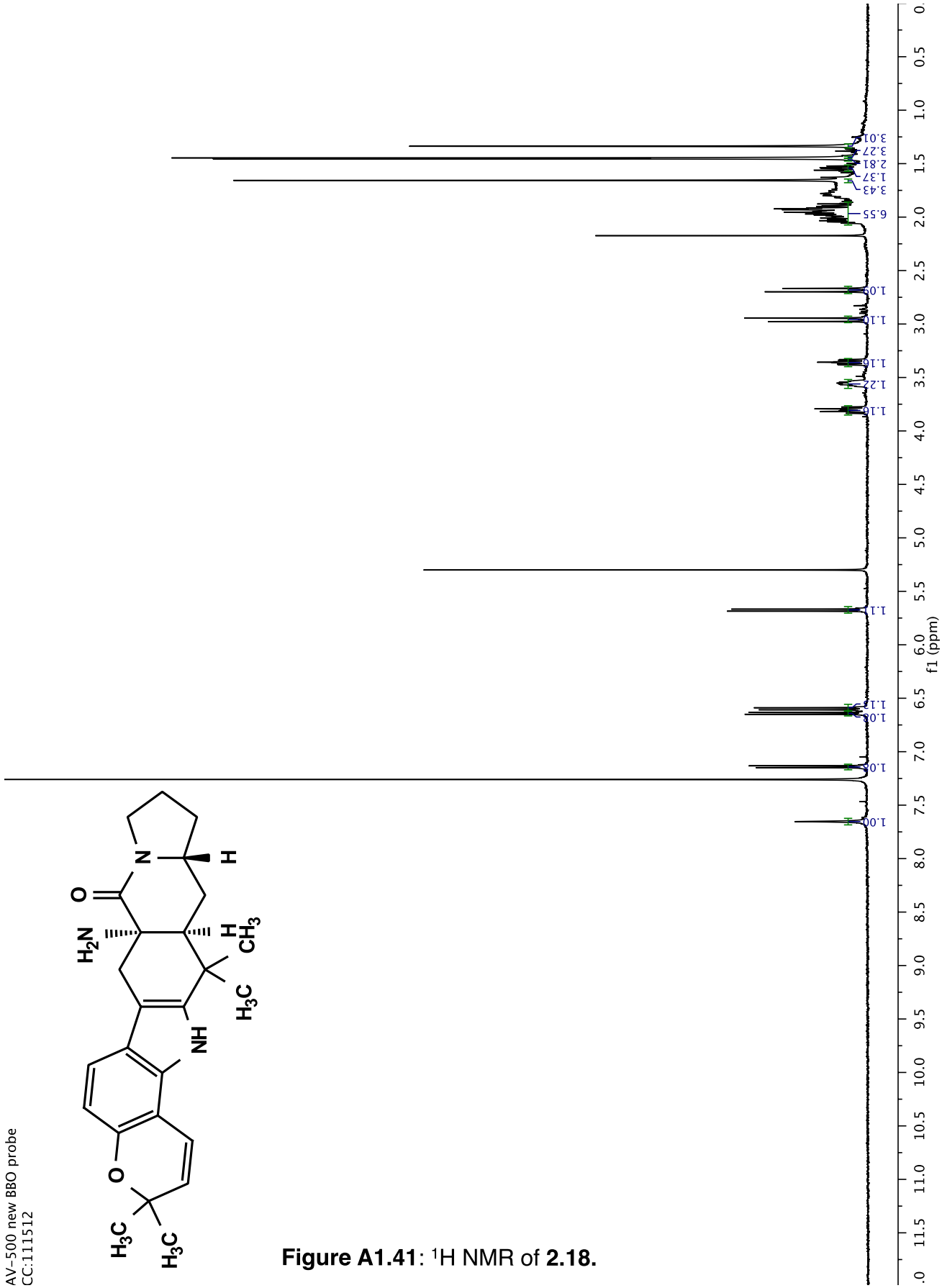

Figure A1.41: ^{1}H NMR of **2.18.**

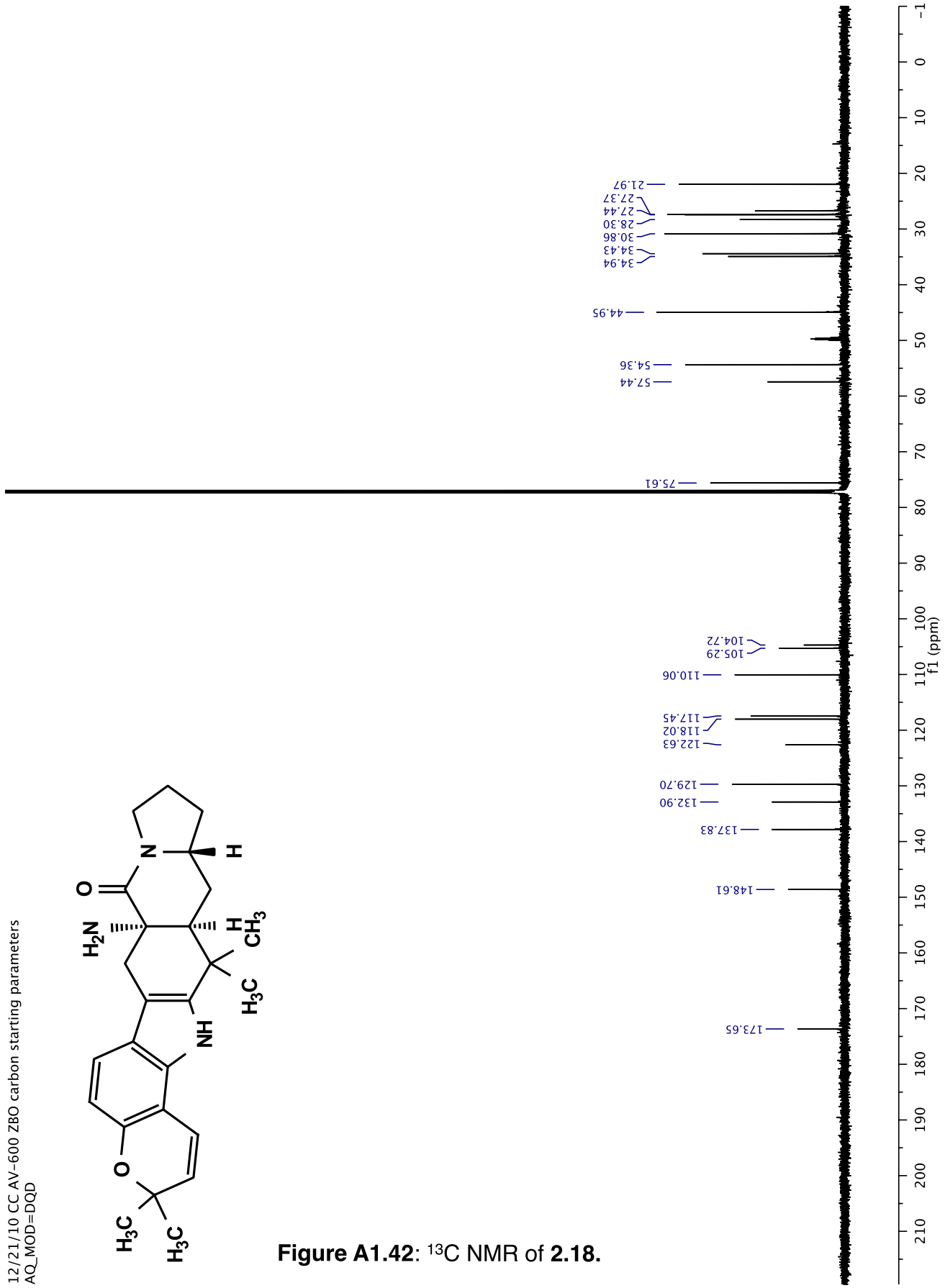

Figure A1.42: ^{13}C NMR of **2.18.**

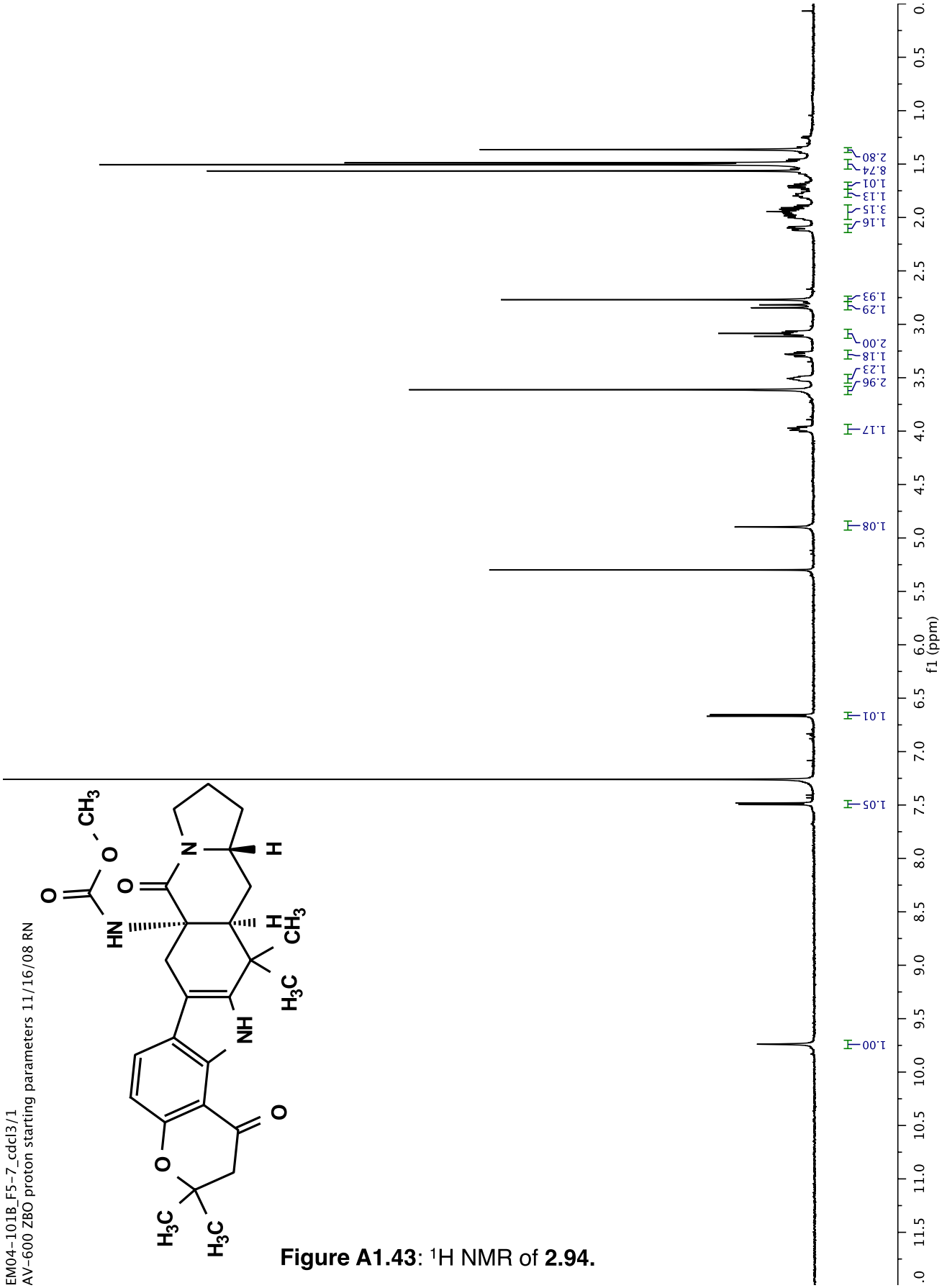

Figure A1.43: ^{1}H NMR of **2.94.**

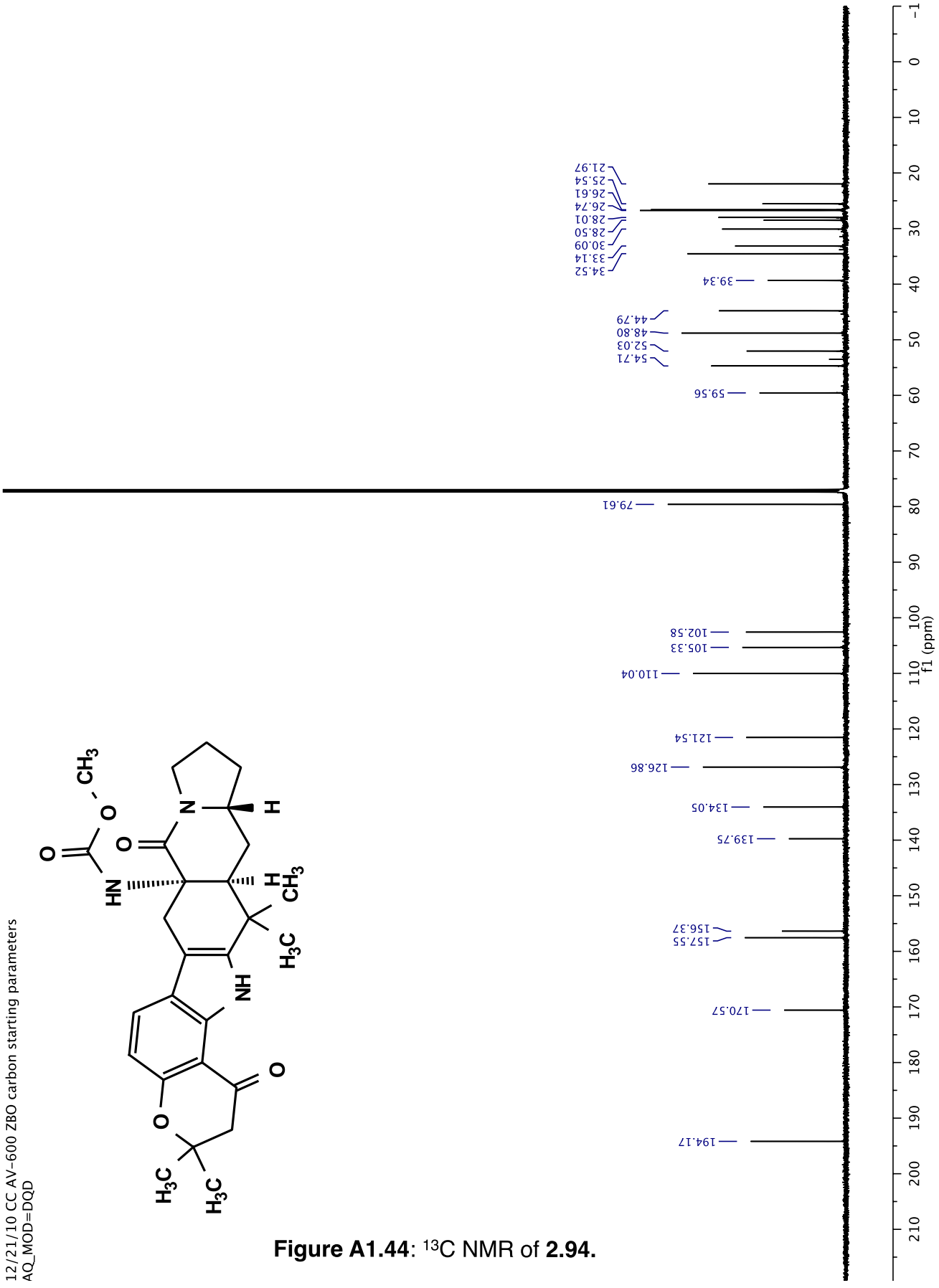

Figure A1.44: ^{13}C NMR of **2.94.**

EM03-151B_dry_cdcl3/1
AV-600 ZBO proton starting parameters 11/16/08 RN

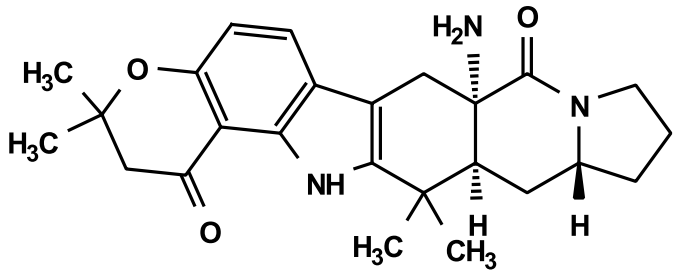

Figure A1.45: ^{1}H NMR of **2.95.**

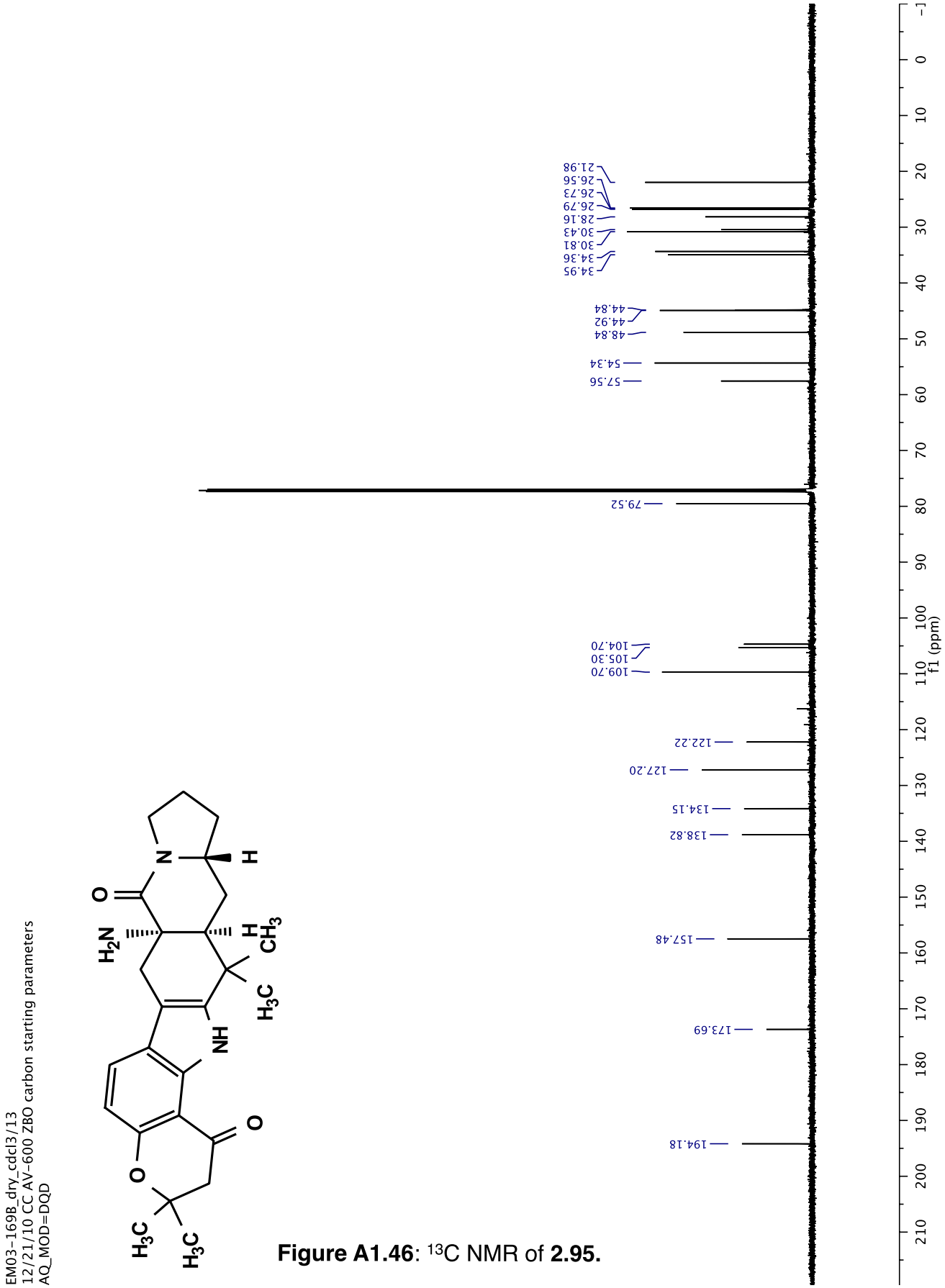

Figure A1.46: ^{13}C NMR of **2.95.**

EM03-187B_dry_cdcl3/1
CC: 12182012 AV-500 TBIP probe
1H 1D NMR

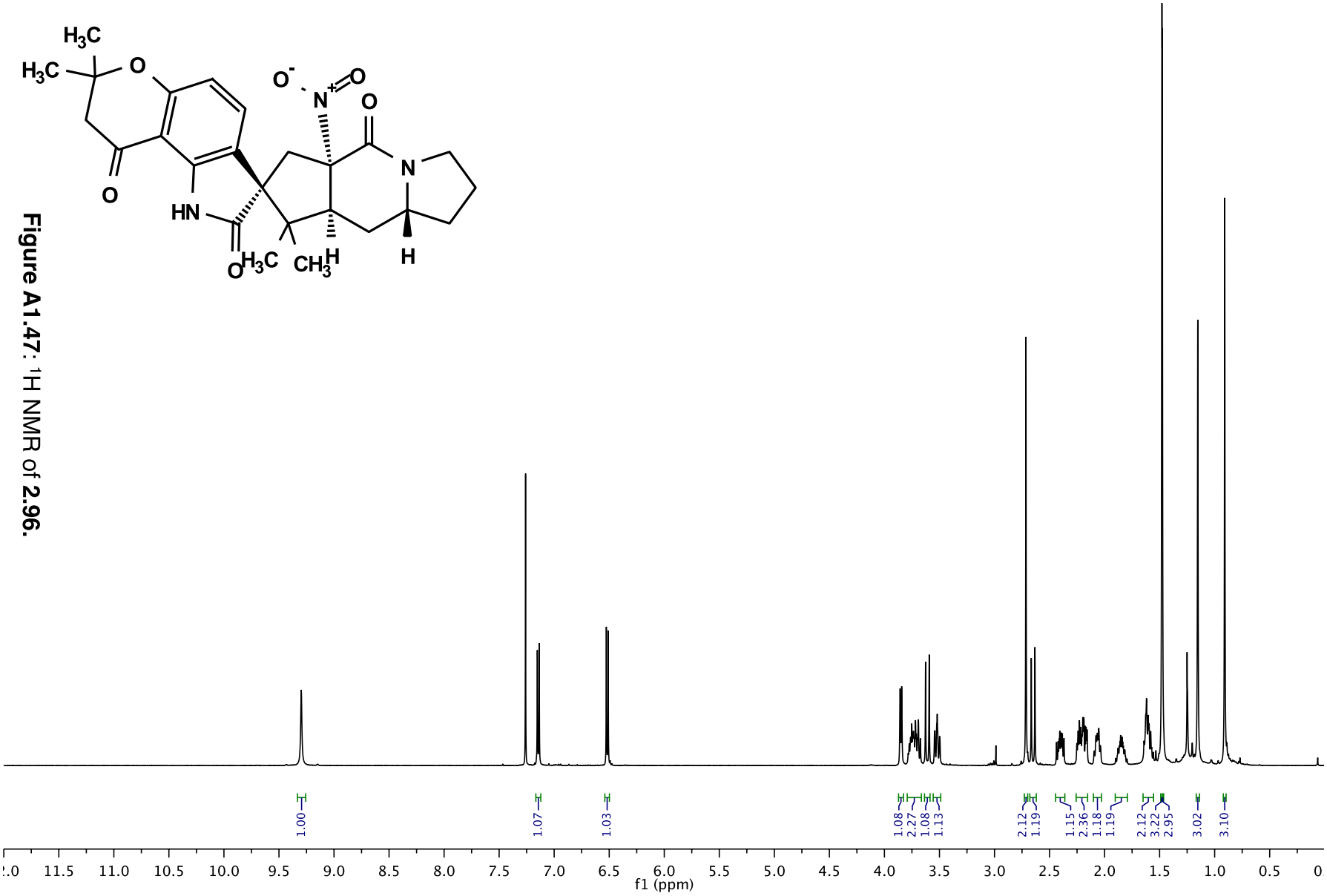

Figure A1.47: ^{1}H NMR of **2.96.**

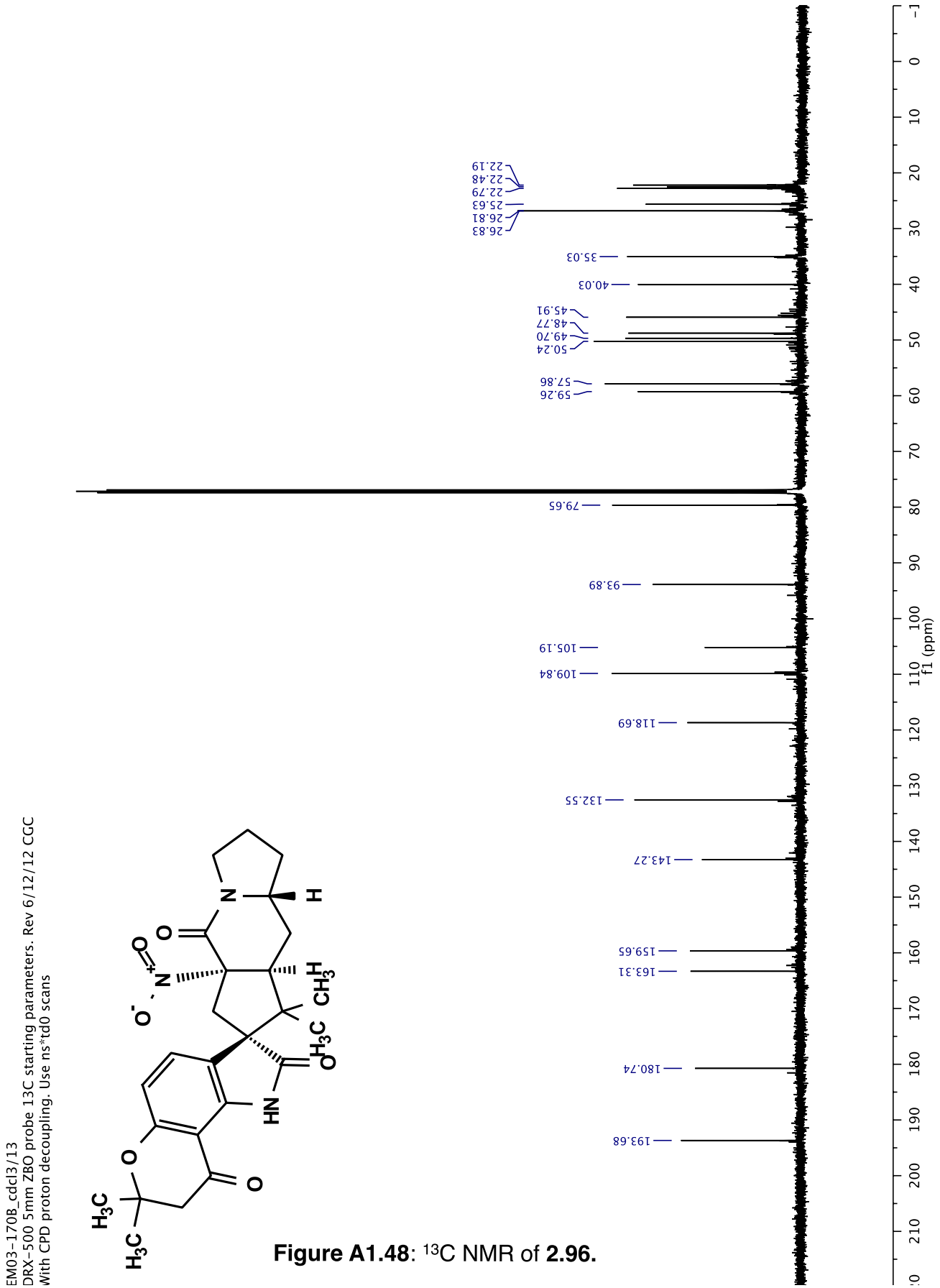

Figure A1.48: ^{13}C NMR of **2.96.**

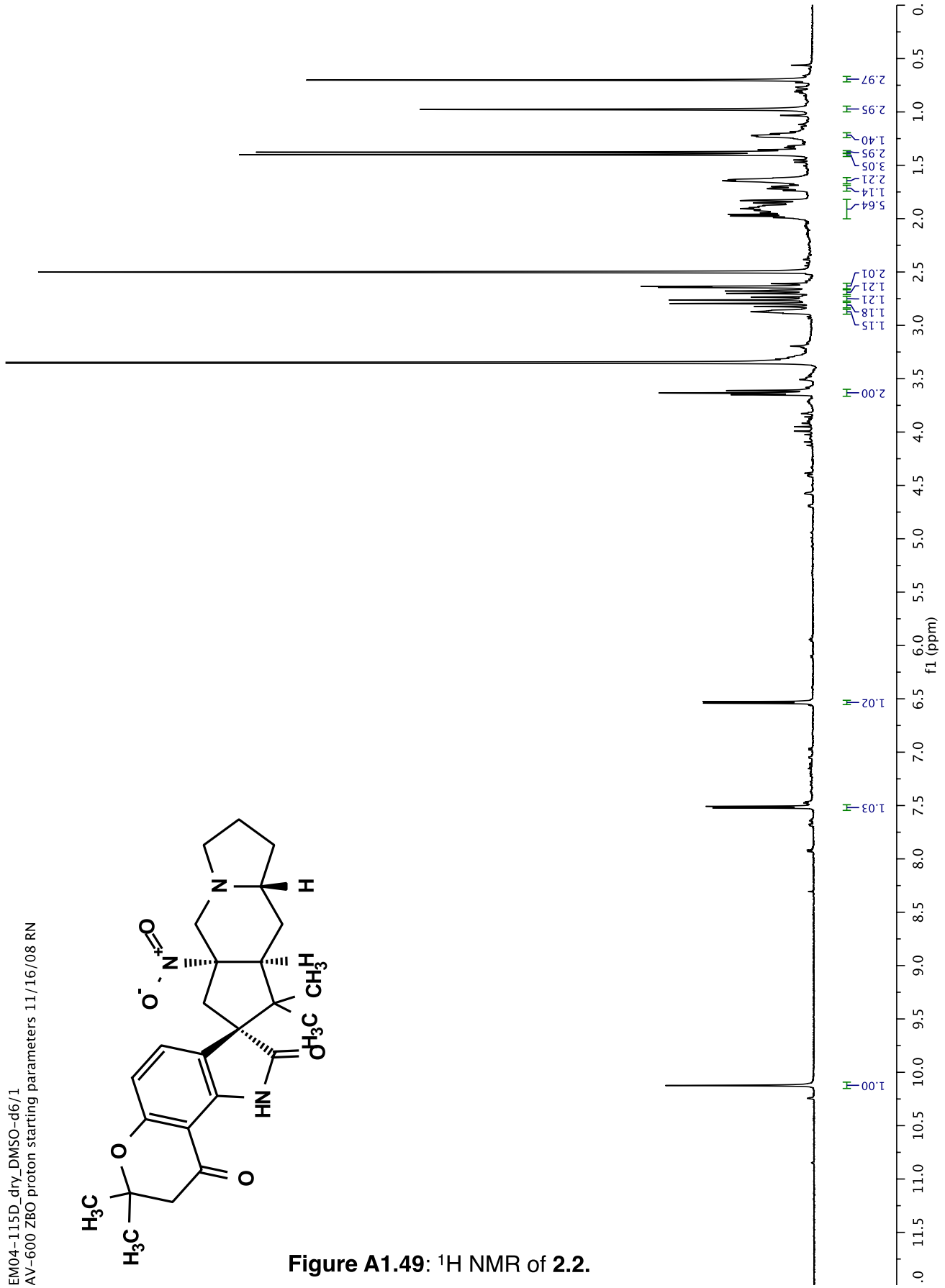

Figure A1.49: ^{1}H NMR of **2.2.**

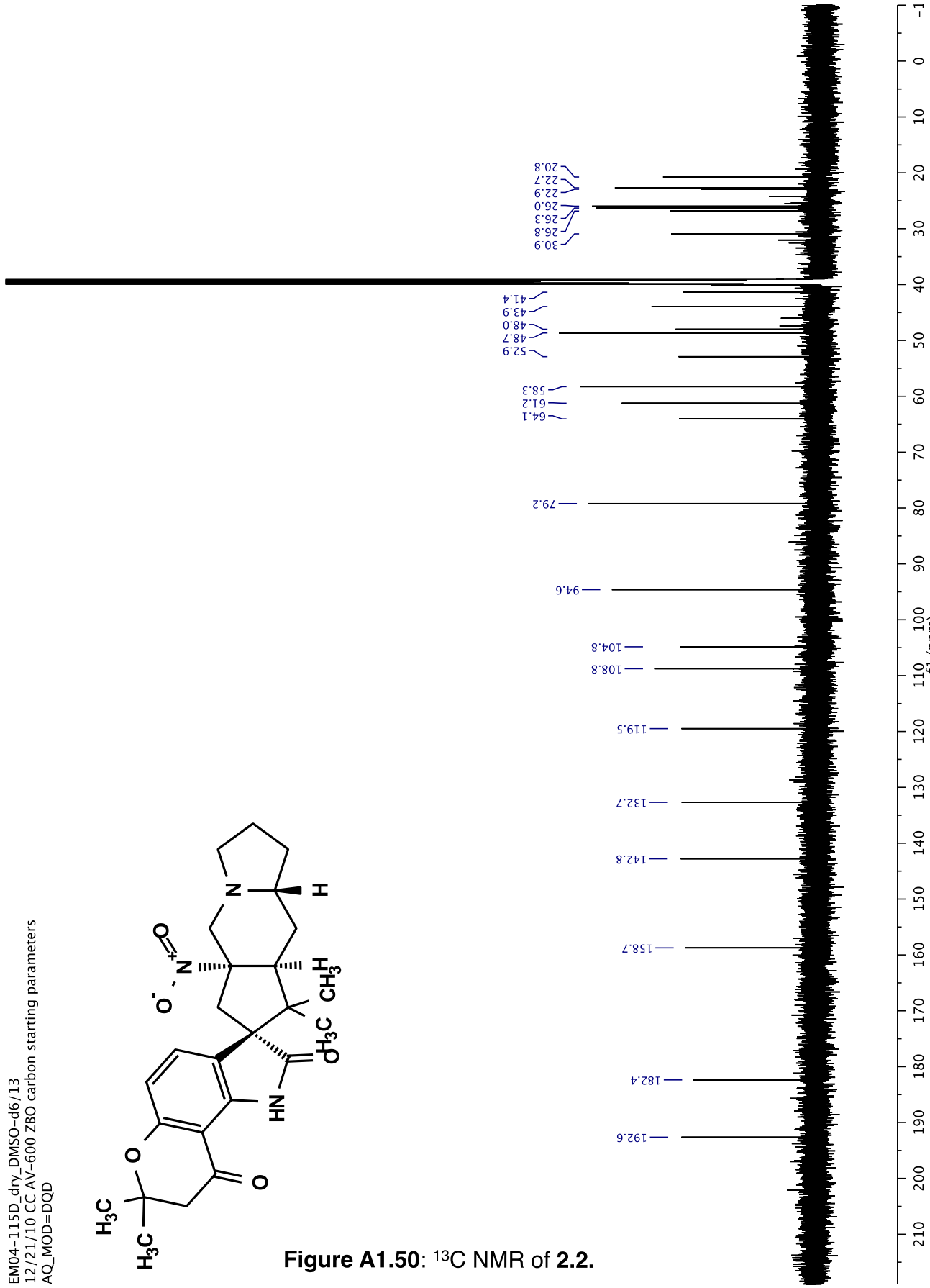

Figure A1.50: ^{13}C NMR of **2.2.**

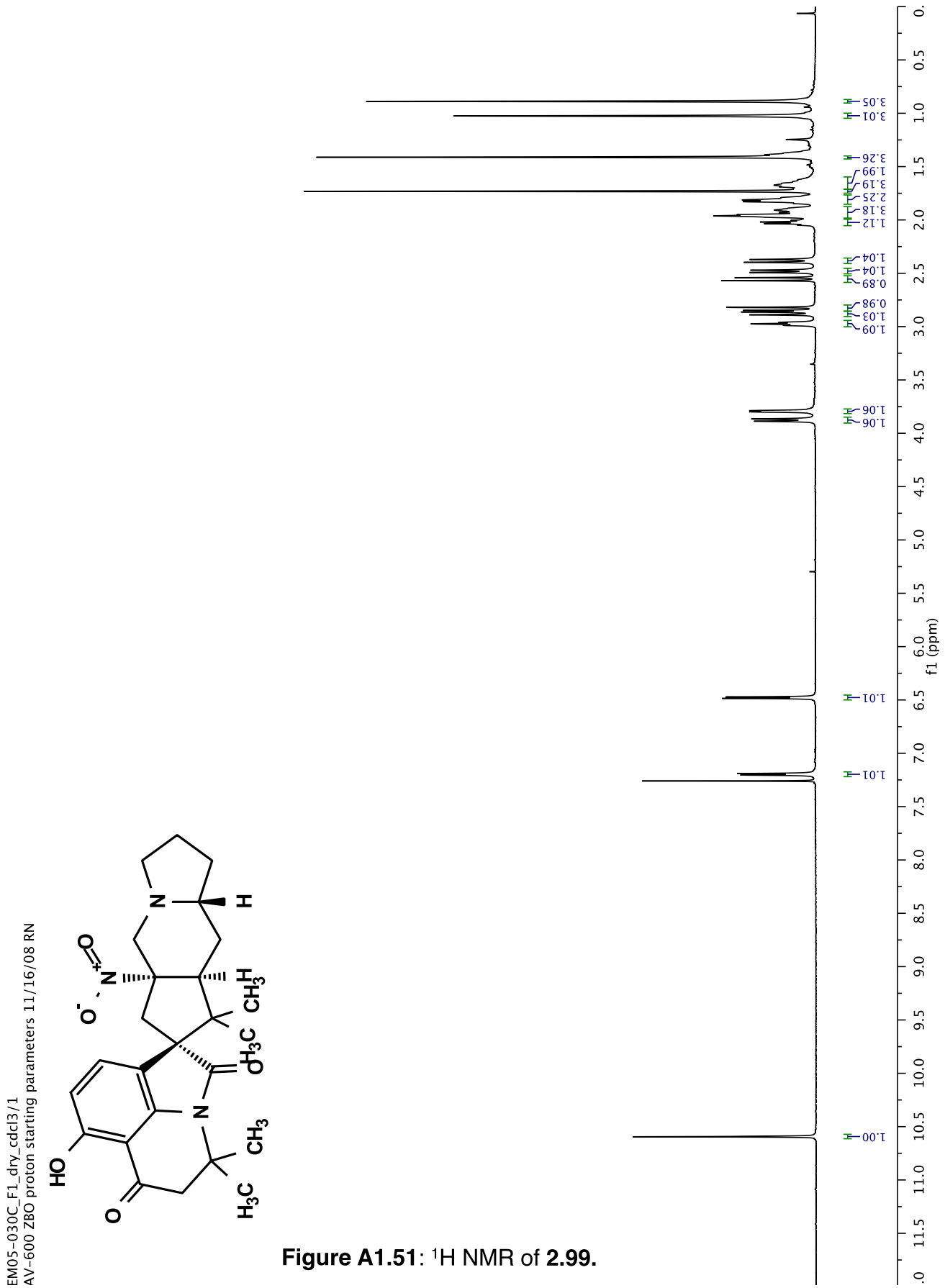

Figure A1.51: ^{1}H NMR of **2.99.**

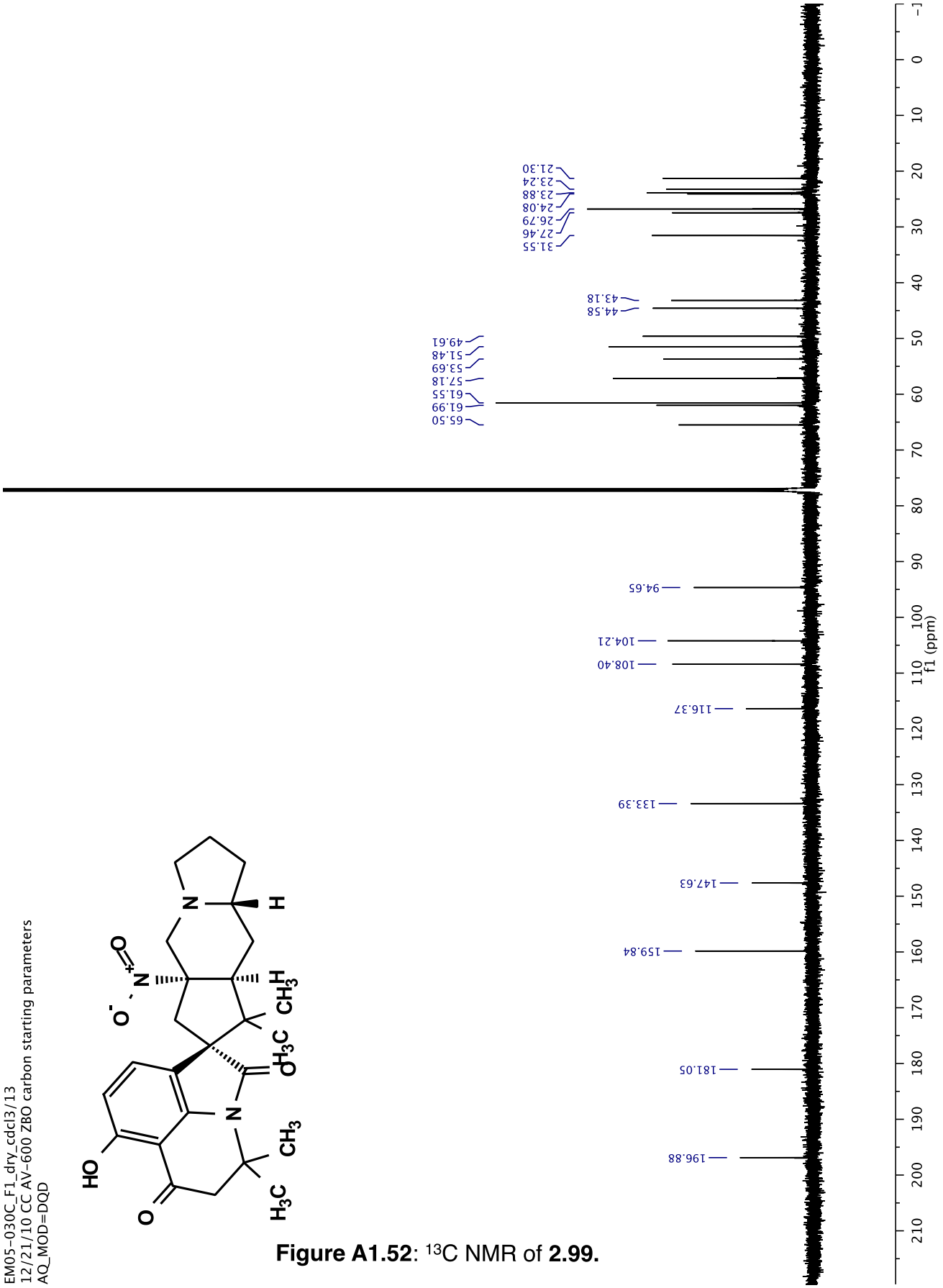

Figure A1.52: ^{13}C NMR of **2.99.**

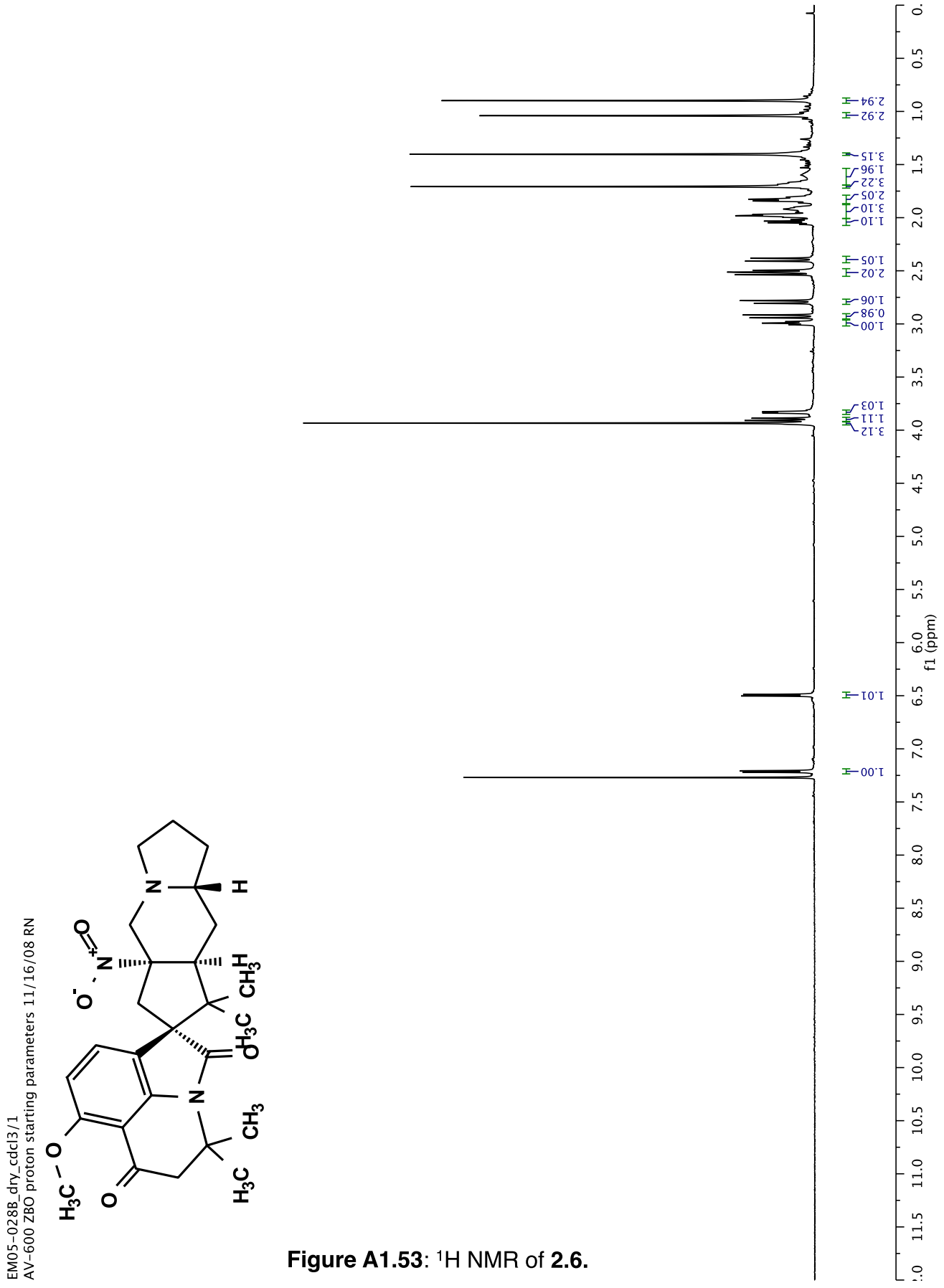

Figure A1.53: ^{1}H NMR of **2.6.**

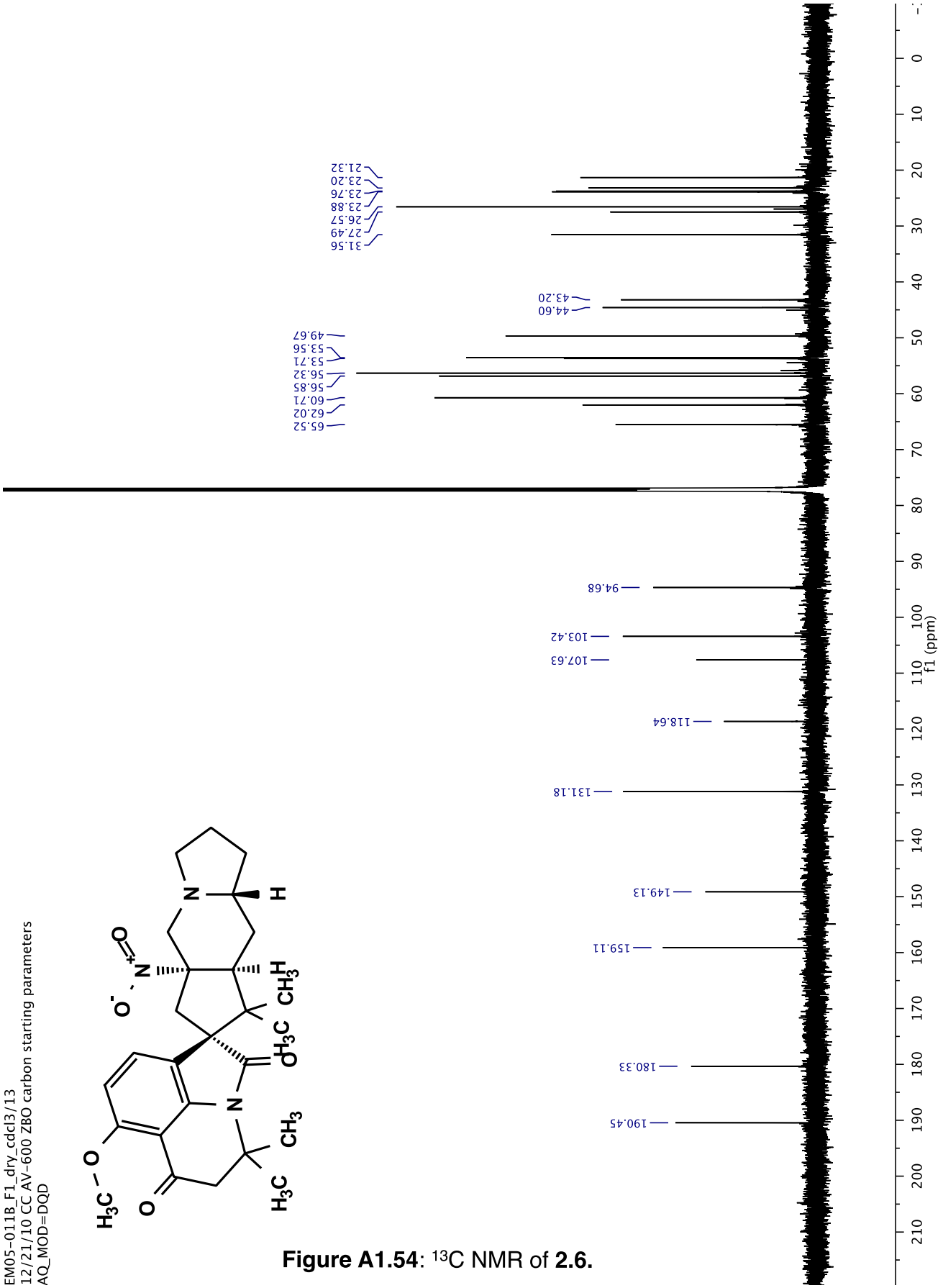

Figure A1.54: ^{13}C NMR of **2.6.**

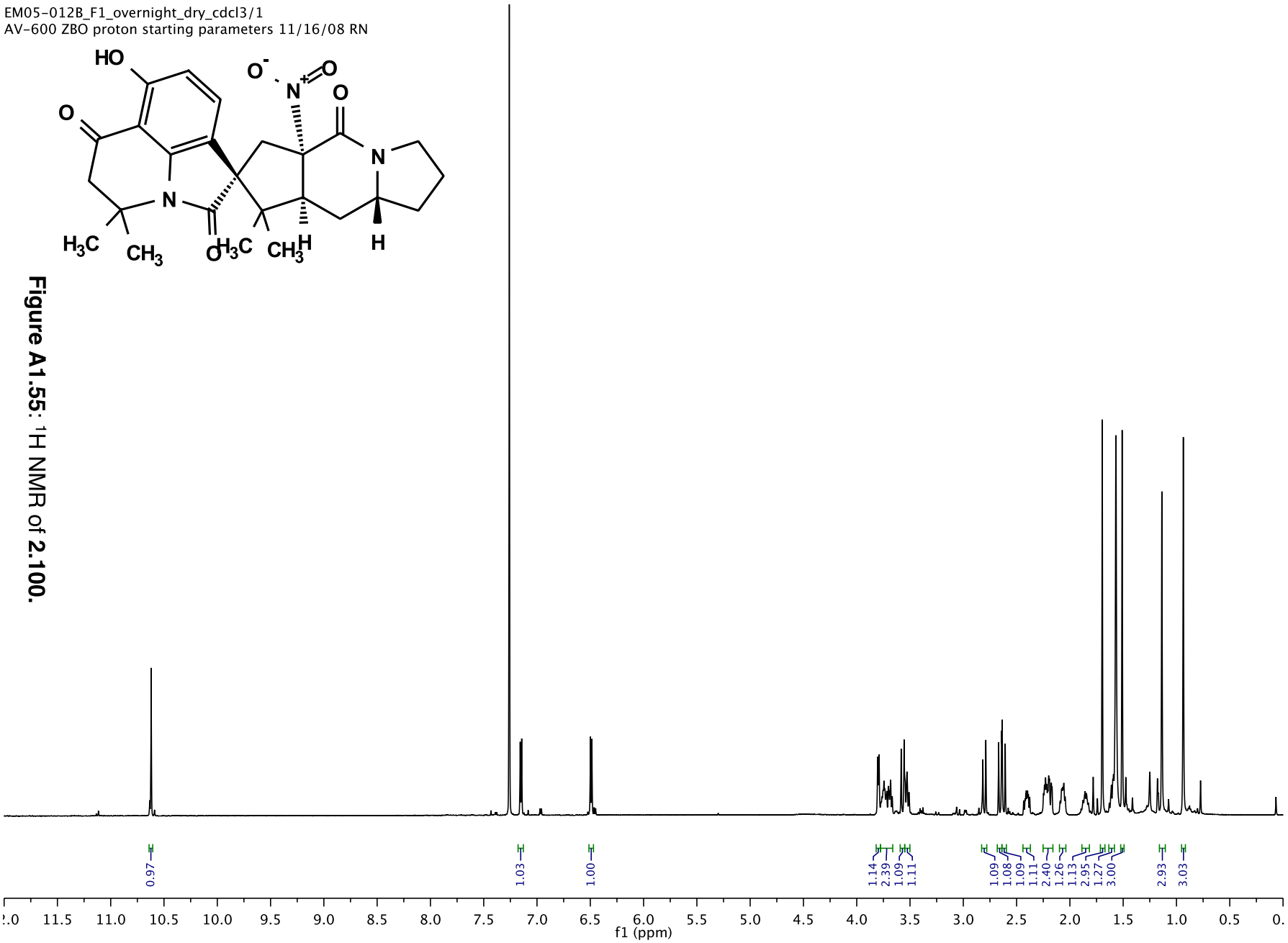

Figure A1.55: ^{1}H NMR of **2.100.**

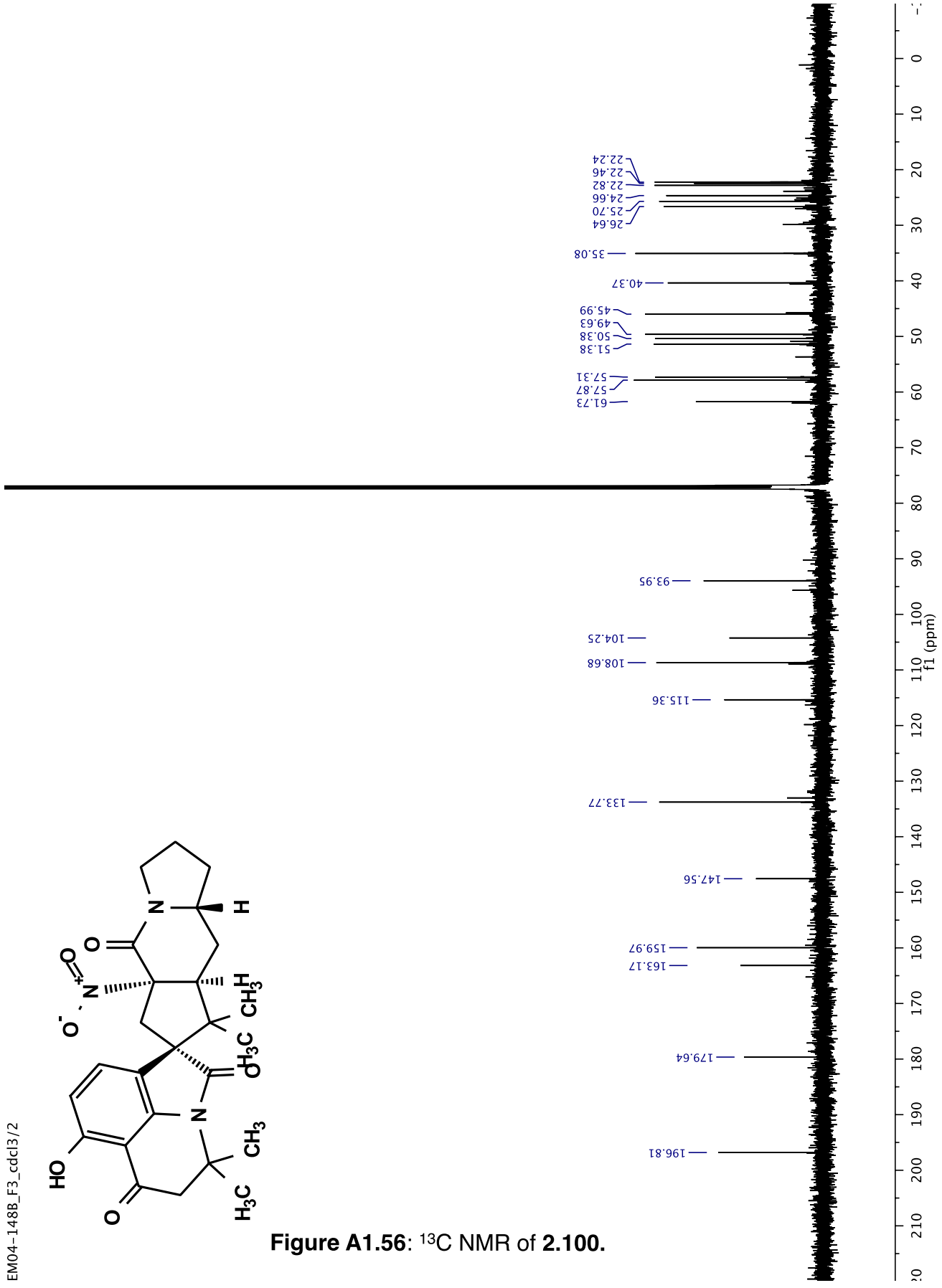

Figure A1.56: ^{13}C NMR of **2.100.**

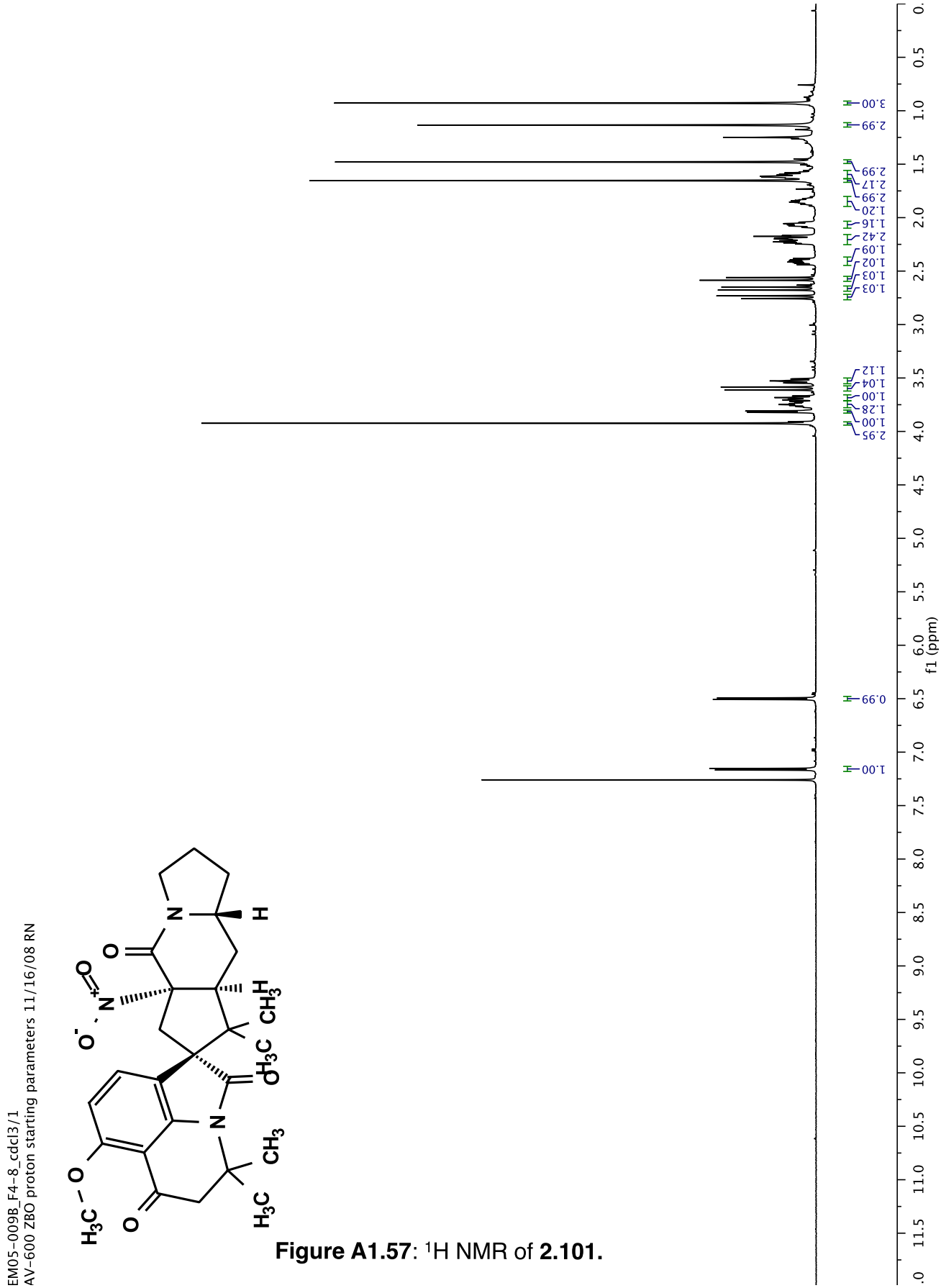

Figure A1.57: ^{1}H NMR of **2.101.**

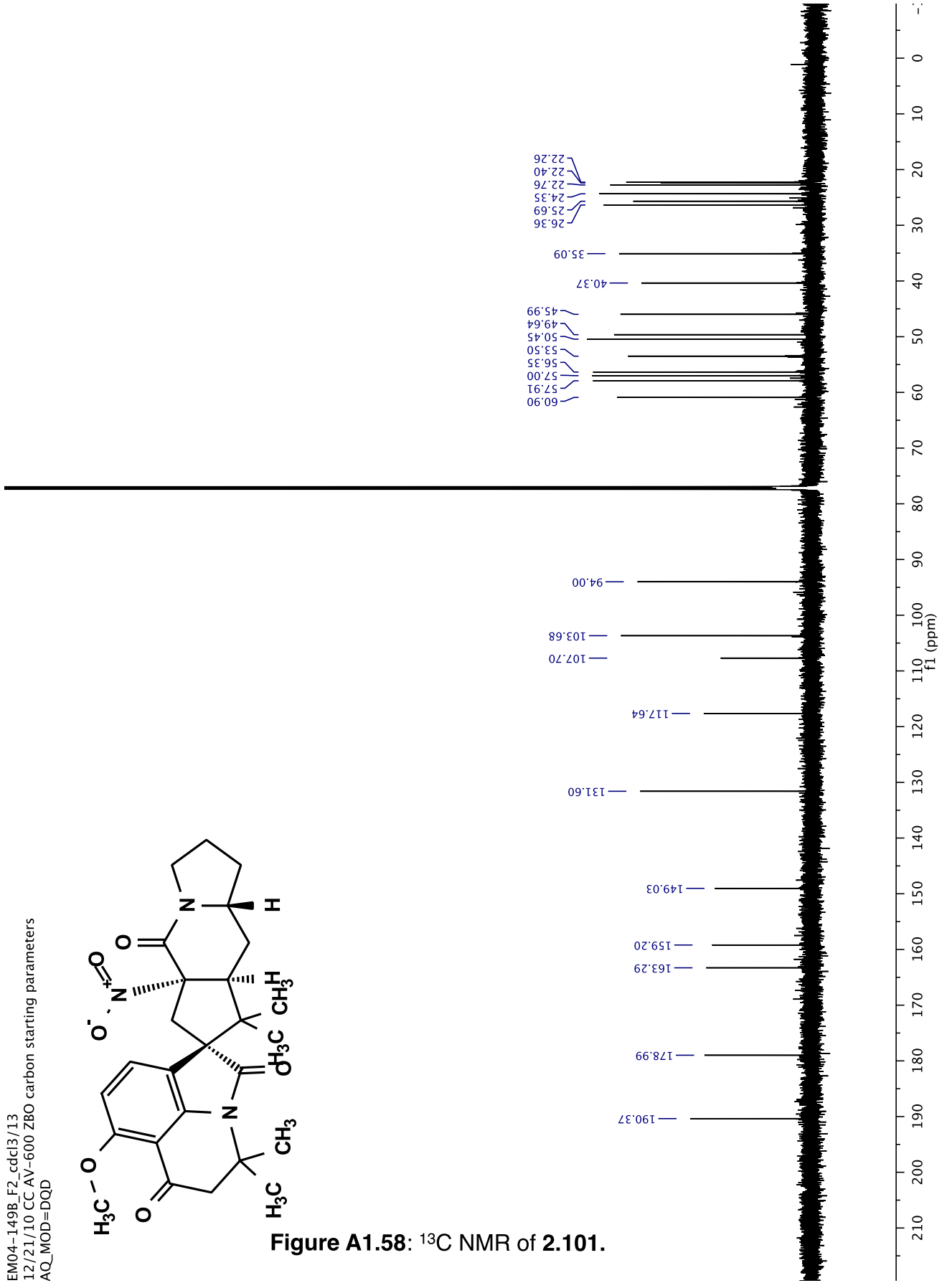

Figure A1.58: ^{13}C NMR of **2.101.**

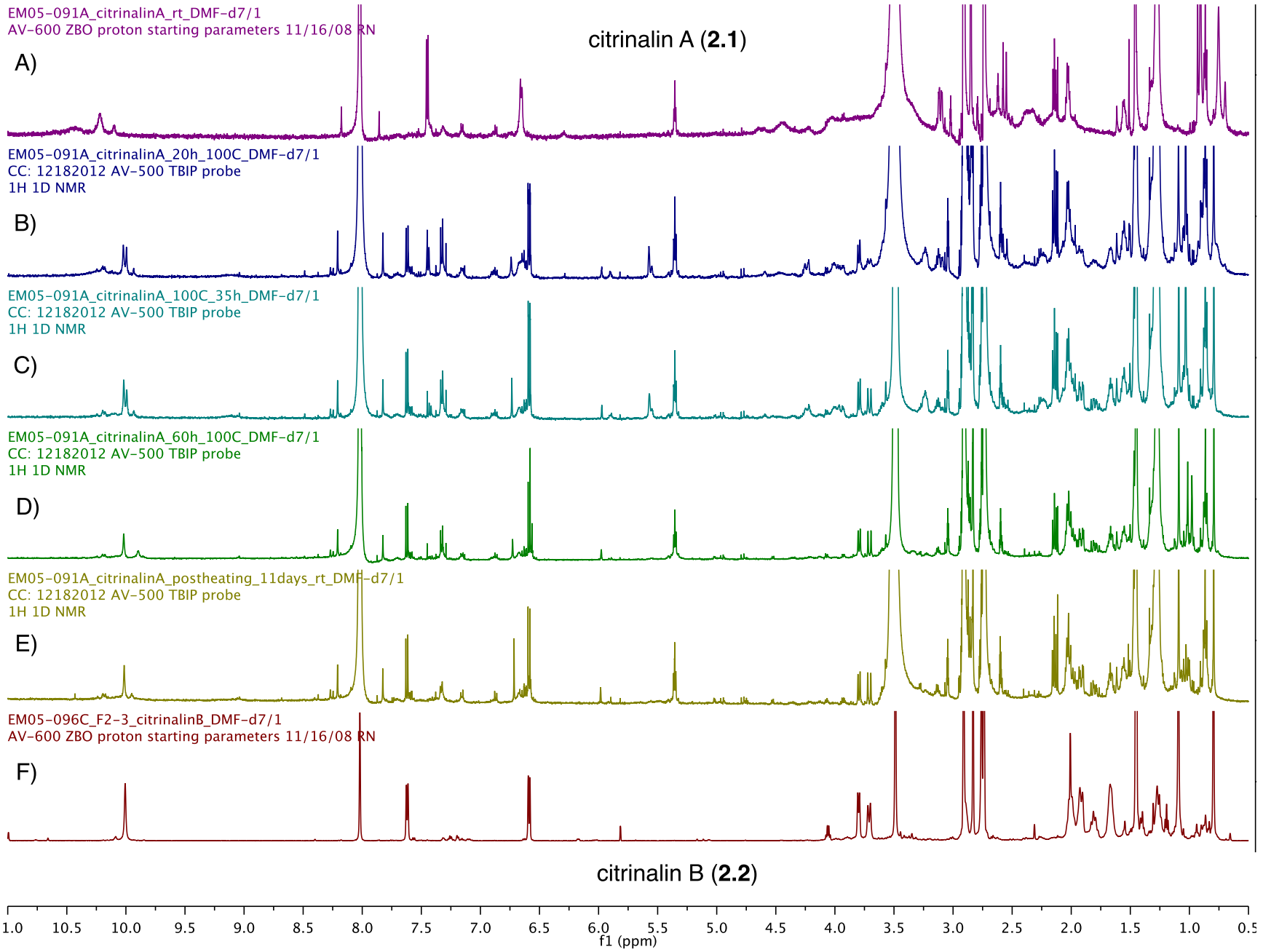

Figure A1.59: ^{1}H NMR conversion of **2.1** to **2.2**.

Figure A1.59. Conversion of citrinalin A (2.1) to citrinalin B (2.2). Solution (**a**) was prepared as follows: To a NMR tube was charged with a degassed (freeze, pump, thaw) solution of citrinalin A (**2.1**) (0.3 mg, 0.066 μmol) in DMF-d_7 (300 μL).

A) ^{1}H (600 MHz) spectra of citrinalin A (**2.1**) in DMF-d_7.

B) ^{1}H (500 MHz) spectra of solution (**a**) after heating at 100 °C for 20 h in DMF-d_7.

C) ^{1}H (500 MHz) spectra of solution (**a**) after heating at 100 °C for 35 h inDMF-d_7.

D) ^{1}H (500 MHz) spectra of solution (**a**) after heating at 100°C for 60h in DMF-d_7.

E) ^{1}H (500MHz) spectra of solution (**a**) post-heating, 11 days at room temperature in DMF-d_7.

F) ^{1}H (600 MHz) spectra of *ent*-citrinalin B (*ent*-**2.2**) in DMF-d_7.

CHAPTER 3:

TOWARD THE BICYCLO[2.2.2]DIAZAOCTANE RING – A UNIFIED APPROACH TO PRENYLATED INDOLE ALKALOID NATURAL PRODUCTS*

A unified strategy for the synthesis of congeners of the prenylated indole alkaloids is presented. This strategy has yielded the first synthesis of the natural product (–)-17-hydroxy-citrinalin B as well as syntheses of (+)-stephacidin A and (+)-notoamide I. An enolate addition to an *in situ* generated isocyanate was utilized in forging a key bicyclo[2.2.2]diazaoctane moiety, connecting the two major structural classes of the prenylated indole alkaloids through synthesis.

3.1 – Overview of Previous Synthetic Approaches and Retrosynthetic Design

3.1.1: Introduction and Background.

Historically, the undertaking of total syntheses of natural products has focused on 'target-oriented' syntheses whereby a single compound is targeted for chemical synthesis to investigate its biological relevance or aspects of its structure.[1] This practice has inspired many new synthesis developments and methodologies. Recently, however, exercises in complex molecule total synthesis are placing a growing emphasis on the preparation of diverse molecular skeletons from a common intermediate.[2] This pursuit, which mirrors the biological production of many secondary metabolites *but does not necessarily follow along biosynthetic lines*, maximizes the opportunities for, and efficiency of, accessing molecular diversity to facilitate structure-activity relationship studies. Over the last 30 years, this concept has led to remarkable unified strategies for the syntheses of various families of natural products.[3] Here, we present the extension of this idea to the syntheses of congeners in the prenylated indole alkaloid family featuring a powerful Dieckmann-type cyclization to forge a key [2.2.2]bicycle.

The prenylated indole alkaloids include some of the most structurally diverse secondary metabolites isolated to date (see Figure 3.1 for selected examples). Many congeners such as stephacidin A (**3.1**), notoamide I (**3.2**), stephacidin B (**3.4**), mangrovamide A (**3.5**), paraherquamide A (**3.6**) and marcfortine A (**3.7**) contain a bicyclo[2.2.2]diazaoctane structural moiety.[4] Over the last decade, additional members of the family that lack the bicyclo[2.2.2]diazaoctane core have begun to emerge. This includes the citrinalins (e.g., **3.11**), citrinadins (e.g., **3.13**), PF1270s (e.g., **3.15**) and the cyclopiamines (e.g., **3.9** – albeit isolated in 1979).[5] While myriad bioactivity has been discovered for various prenylated indole alkaloids (especially anthelmintic activity, see

---

* Portions of this Chapter was taken from our work published in: Eduardo V. Mercado-Marin and Richmond Sarpong, *Chemical Science* **2015**, *6*, 5048–5052.

Chapter 1.2 for more details),[4] the recent emergence of the citrinadins and the related PF1270A-C[6] (**3.15-3.17**) compounds which lack the bicyclo[2.2.2]diazaoctane structural motif, as potent anti-tumor compounds has heightened interest in this whole family of secondary metabolites.

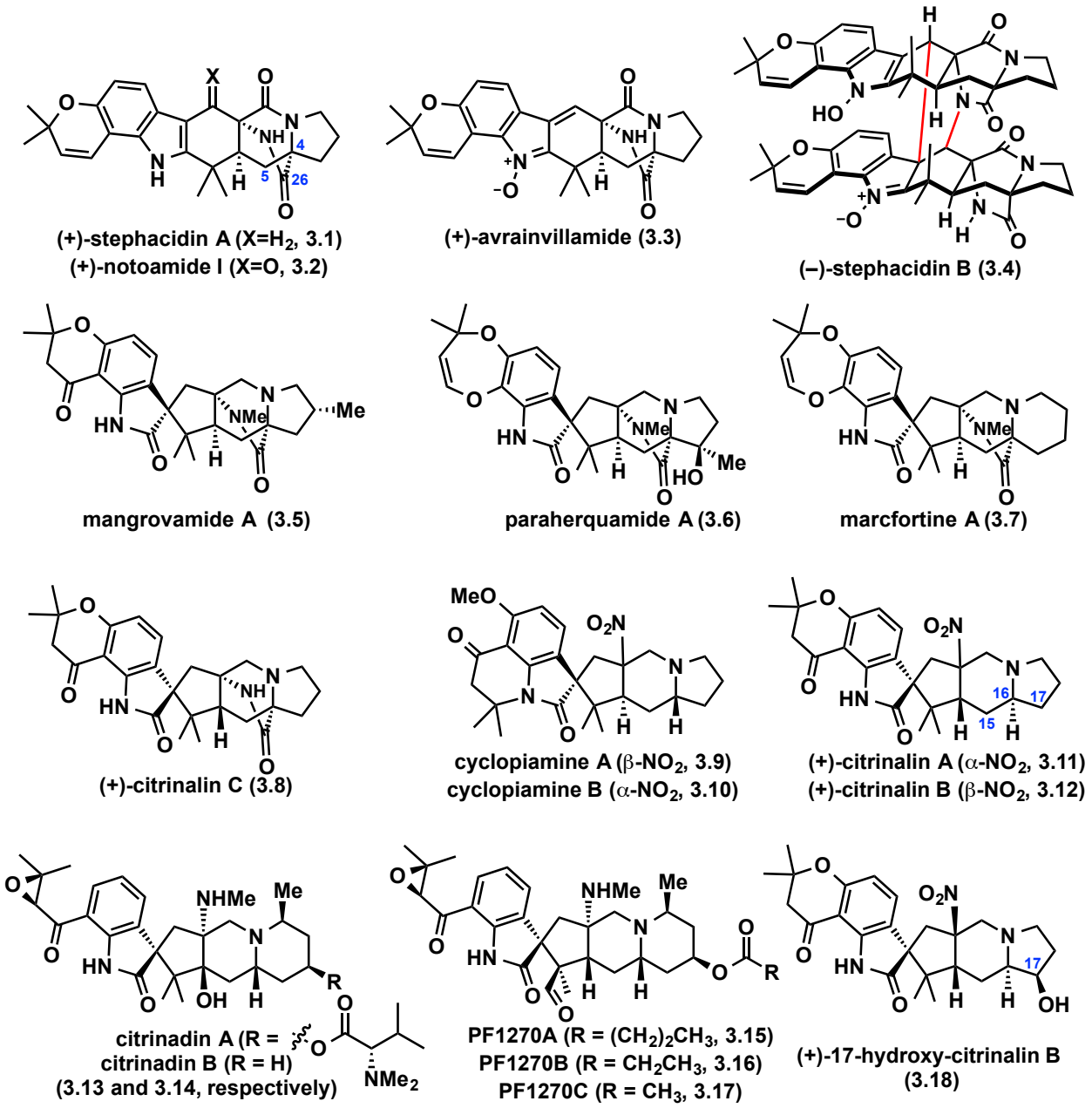

Figure 3.1: Selected examples of prenylated indole alkaloids.

3.1.2: Previous Synthetic Approaches to the Bicyclo[2.2.2]diazaoctane Ring System.

From our perspective, a unified synthetic approach that affords prenylated indole alkaloid congeners bearing the bicyclo[2.2.2]diazaoctane core as well as those lacking this structural moiety would provide the most *strategically efficient* approach to these natural products. However, to date, such an approach that encompasses both sub-types (of which **3.1** and **3.18** are representative) has not been reported. All the existing syntheses of this family of molecules have targeted either the subset that contains the [2.2.2] diazaoctane bicycle or those molecules that lack this structural feature.[7,8] As described in Chapter 1.4.1, all previous syntheses of natural products that contain the bicyclo[2.2.2]diazaoctane ring have focused on constructing the 2,5-diketopiperazine ring early in their synthetic routes (highlighted in red in Scheme 3.1), and rely on forming a C–C bond to construct the bridged bicyclic system.

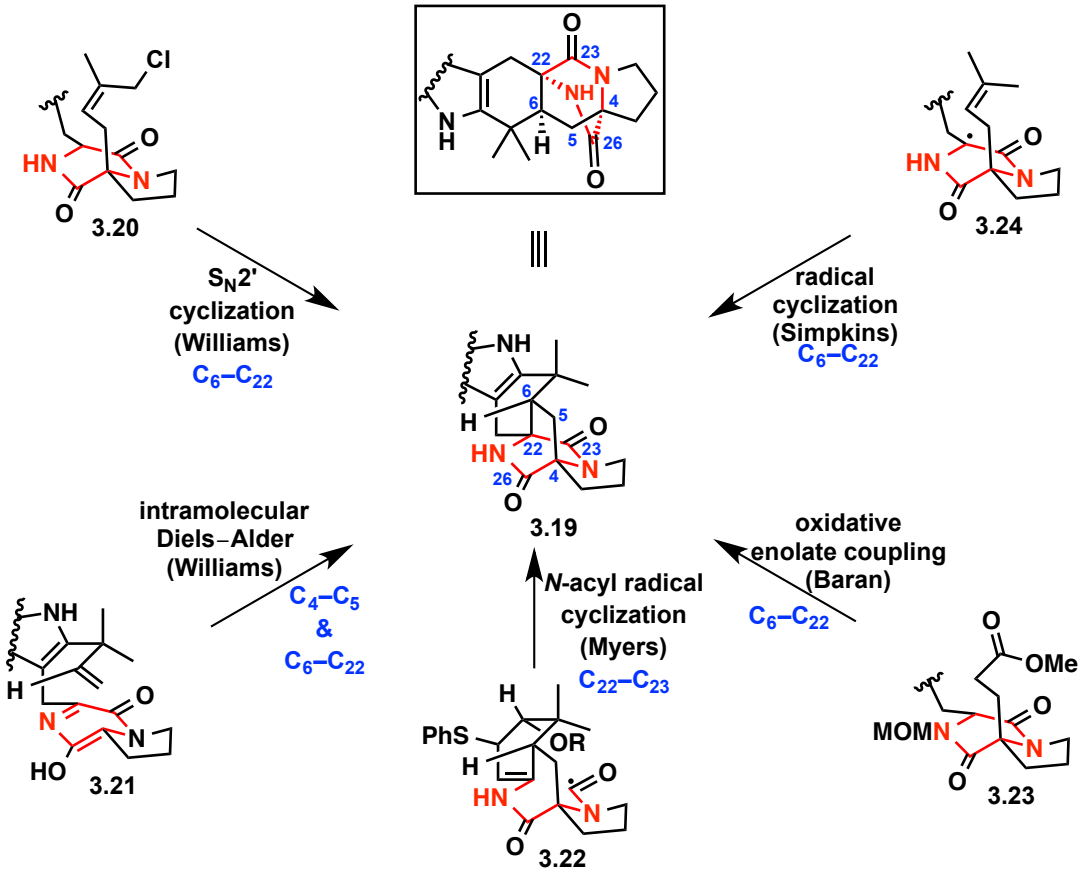

Scheme 3.1: Established approaches to the bicyclo[2.2.2]diazaoctane ring system of avarainvillamide and the stephacidins.

As shown in Scheme 3.1, the C4 tetrasubstituted center at the bicyclo[2.2.2] bridgehead (see compound **3.19** – in Scheme 3.1) is constructed at an early stage or through C4–C5 bond formation, which would necessitate its late-stage cleavage (in a complexity minimizing manipulation) in order to form compounds such as **3.18** from **3.1** (Figure 3.1). In this latter scenario, selective amide hydrolysis of the bicyclo[2.2.2]diazaoctane in **3.19** (Scheme 3.2) would produce **3.25**, which upon decarboxylation (cleavage of C4–C26), and a *diastereoselective* protonation at the ring junction C4 (the diastereoselectivity of which is not certain outside of an enzyme pocket) would then convert **3.19** to the sub-family that lacks the diazaoctane structural motif, **3.26**. While this sequence of events is the proposed biosynthesis for congeners that lack the bicyclo[2.2.2]diazaoctane ring (see Chapter 1.3), from a synthetic standpoint, this procedure would be both challenging and inefficient.[5c, 8c] Our approach to this collection of molecules, which constructs the bicyclo[2.2.2]diazaoctane ring late-stage from an advanced, all-fused precursor such as **3.26**, is complementary to this biosynthetic proposal as well as all previous syntheses.

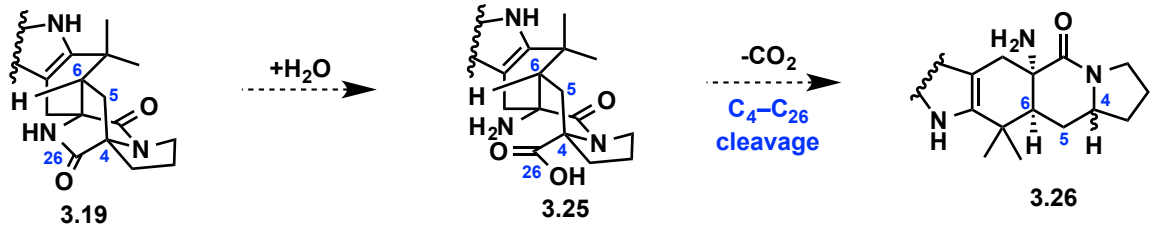

Scheme 3.2: Biomimetic degradation of the bicyclo[2.2.2]diazaoctane ring.

3.1.3: Retrosynthetic Design–Unifying Approach to Prenylated Indole Alkaloids.

In this Chapter, we present our studies toward identifying a common intermediate that can be advanced to natural products representative of both prenylated indole alkaloid structural motifs. These studies have led to the identification of **3.27** (Scheme 3.3) as such a common intermediate, which enables the first total synthesis of (–)-17-hydroxy-citrinalin B (**3.18**) as well as a synthesis of (+)-stephacidin A (**3.1**) and (+)-notoamide I (**3.2**).

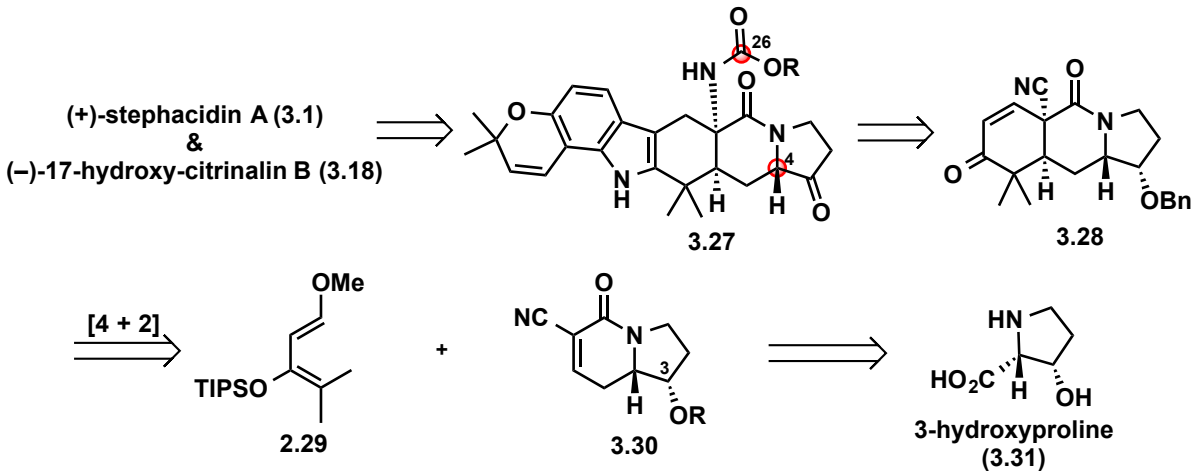

Scheme 3.3: Retrosynthesis–Unified approach to prenylated indole alkaloids.

Our synthetic strategy to these two natural products, which rests on 'network analysis'[9] considerations, diverges only at a late stage. Network analysis relies on strategic disconnections of C–C bonds in a polycylic-bridging framework to simpler fused structures, which are often easier to construct. Thus, strategic bond disconnection of the maximally bridged ring in, for example, **3.1** (i.e., the 2,5-diketopiperazine ring at C4-C26) leads back to carbamate **3.27**, where a bond can be formed at a late stage between C4 and the carbamate carbonyl group (C26) by a Dieckmann-type condensation.[10] Ultimately, tricycle **3.28** would arise from a Diels–Alder reaction between diene **3.29** and dienophile **3.30**, where the only difference from the dienophile we employed in the syntheses of the citrinalins and cyclopiamines (Chapter 2.3) is presence of the benzyloxy group at C3 of the pyrrolidine ring. We envisioned accessing benzyloxy dienophile **3.30** from 3-hydroxyproline (**3.31**), analogous to our previous synthetic approach. Moreover, the ketone functionality of the pyrrolidine ring in **3.32** (Scheme 3.4) would not only serve as a handle for forging the C4-C26 bond at a late stage but would also facilitate derivatization *en route* to other members in this family. For example, addition of methyl Grignard would allow access to the tertiary alcohol present in the paraherquamides (highlighted in red in **3.6**),[11] ring expansion chemistry (e.g. Tiffeneau-Demjanov rearrangement) would provide the piperdine ring of the marcfortine family (highlighted in red in **3.7**),[12] or enolate chemistry would enable the installation of alkyl groups such as those present in the mangrovamides (highlighted in red in **3.8**). Moreover, hexacycle **3.27** (Scheme 3.3) can in turn arise from tricycle **3.28** using an indole annulation reaction, which would provide opportunities to prepare other natural products such as paraherquamide A (**3.6**, Scheme 3.4) that differ in their indole substitution pattern (highlighted in blue). These directions are currently being investigated in the group by both post-docs and graduate students.

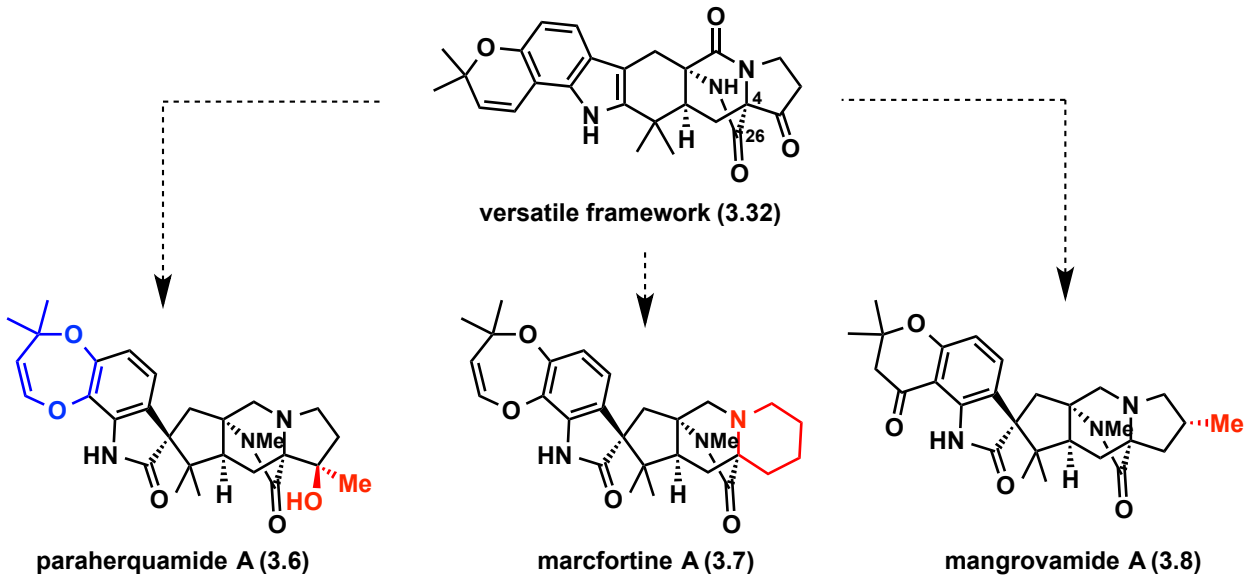

Scheme 3.4: Proposed use of versatile framework **3.32** toward other prenylated indole alkaloids.

In this way, the two sub-families of the prenylated indole alkaloids (e.g., **3.1** and **3.18**) can be connected by a synthesis sequence characterized by a progressive increase in structural complexity, which distinguishes this approach from prior syntheses of related prenylated indole alkaloids. More importantly, however, our retrosynthesis provides a unifying synthetic approach to this class of natural products, which would set the stage for the broad-ranging syntheses of congeners of the prenylated indole alkaloid family to facilitate in-depth studies on their biosynthesis and biological activity.

3.2 – Diels–Alder Reaction: Synthesis of 6-6-5 Tricycle.

3.2.1: Attempted C–H Functionalization Route to 3-Hydroxyproline.

Following the success of our previous synthetic route (see Chapter 2.3) we wondered if we could employ the same amino acid, proline, in the synthesis of 3-hydroxyproline by C–H functionalization, **3.34** (Scheme 3.5).

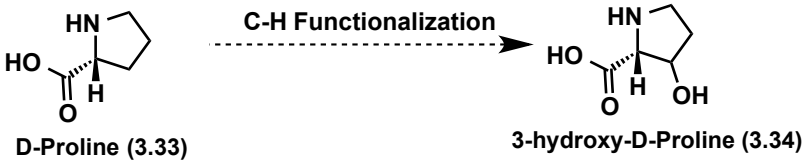

Scheme 3.5: C-H Functionalization of D-proline to 3-hydroxyproline.

Although enzymatic stereoselective hydroxylation of L-proline and L-pipecolic acids are known, these processes are unsuitable for large-scale chemical synthesis because the required enzymes must be expressed and isolated from *E. coli.* Moreover, they are unstable and require laborious product purifications.[13] As an alternative, we were drawn to results published by Corey and co-workers on the β-acetoxylation of amino acids.[14] Their approach utilizes a carboxamide to direct a Pd(II)-catalyzed oxidative conversion of the β-CH_2 group to β-CHOAc on various amino acids including *N*-phthaloyl-protected leucine, alanine, β-methylalanine, β-ethylalanine, and β-phenylalanine. It is worth noting that β-acetoxylation of proline derivatives has not been reported. We were eager to determine if this route could directly lead to the desired 3-oxoproline derivatives.

Our studies commenced with the synthesis of amide **3.37** (Scheme 3.6). Peptide coupling of Boc-D-proline (**3.35**) with 8-aminoquinoline (**3.36**) under conditions reported by Reddy and co-workers gave amide **3.37** in 83% yield.[15] When we subjected **3.37** to the conditions reported by Corey *et al.* (20 mol% $Pd(OAc)_2$, 10 equiv of Ac_2O, 1.2 equiv of $Mn(OAc)_2$, 5 equiv of *t*BuOOH as the oxidant in CH_3NO_2 at 80 °C) we recovered only starting material. Next, we utilized Oxone® as the oxidant, since Corey had also shown it to be a viable oxidant for this transformation. However, only diamide **3.38**, where the pyrrolidine nitrogen is acylated, was observed even with heating to 100 °C.

Although discouraging, we rationalized the absence of the β-acetoxylated proline derivative to be best explained by the highly strained *trans*-palladacycle fused 5-5 ring system that would have to be formed (see **3.39→3.40** in Scheme 3.6) assuming this reaction proceeds through intermediates analogous to those proposed by Corey and co-workers.[14]

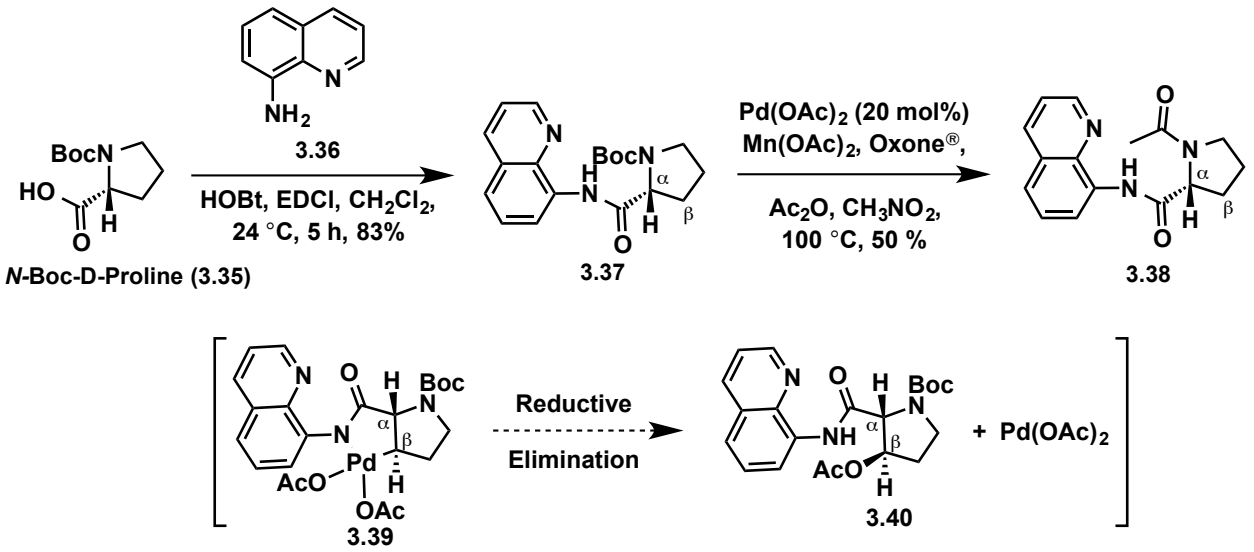

Scheme 3.6: Attempted β-acetoxylation of proline derivative **3.37**.

3.2.2: Asymmetric Baker's Yeast Reduction to 3-Hydroxyproline.

Next, we focused on previously reported asymmetric yeast reductions of racemic 3-ketoprolines (Scheme 3.7). We began with known 3-pyrrolidone **3.43**, which is readily obtained from a 1,4-addition of glycine ethyl ester (**3.41**) to ethyl acrylate followed by Boc protection of the amine to afford **3.42**. A Dieckmann condensation of **3.42** mediated by KO*t*Bu furnishes the desired 3-ketoproline **3.43**,[16] albeit in relatively low yield.

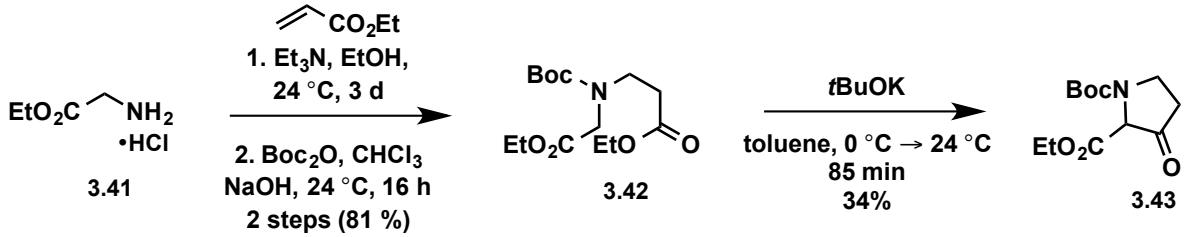

Scheme 3.7: Dieckmann condensation route to β-ketoester **3.43**.

The mixture of regioisomers obtained following the Dieckmann condensation was easily separated by partitioning between toluene and aqueous buffer, as reported by Rapoport and co-workers.[17] However, we ran into difficulty accessing large quantities of the desired ketoproline **3.43** through the low-yielding Dieckmann condensation route. For example, we could only obtain ~5.5 grams of **3.43** in a 28% overall yield on a single pass upon scale up. We were encouraged by a Rh(II) catalyzed N–H insertion route to access similar *β*-ketoesters reported by Sorensen and co-workers and decided to explore this alternative route.[18] Beginning with *N*-Boc-*β*-alanine (**3.44**, Scheme 3.8), a Masamune-Claisen condensation with potassium 3-ethoxy-3-oxopropanate (**3.45**) provided the linear *β*-keto ester **3.46**.

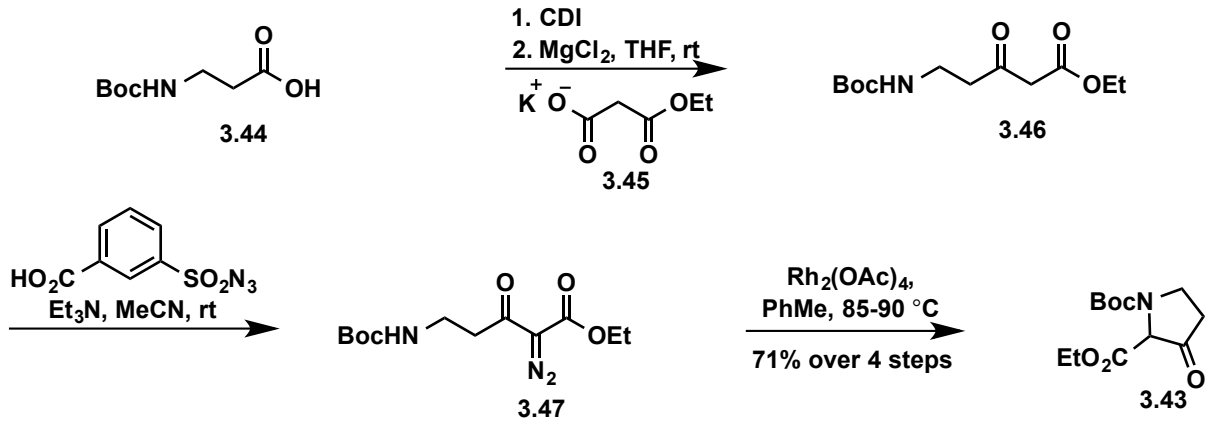

Scheme 3.8: N–H insertion route to β-ketoester **3.43**.

A diazo transfer using 3-carboxybenzenesulfonyl azide followed by a $Rh_2(OAc)_4$ catalyzed N–H insertion, gratifyingly gave the desired 3-keto-proline ester (**3.43**) in much improved yields and scalability. As an example, over 40 grams could be prepared in a single pass and requires only one silica gel purification step in 71% overall yield. Dynamic kinetic resolution of ketoproline **3.43** using an asymmetric Baker's yeast reduction afforded the 3-hydroxyproline derivative **3.48** in 90% e.e. and 90% isolated yield (Scheme 3.9).[16a, 19]

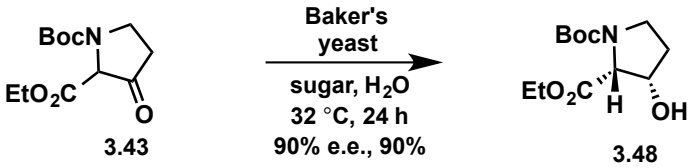

Scheme 3.9: Asymmetric Baker's yeast reduction of **3.43**.

3.2.3: Elaboration of 3-Hydroxyproline to Dienophile 3.59.

With ample quantities of **3.48** in hand, we began to explore hydroxyl protecting groups that would be stable to the conditions employed for the synthesis of dienophile **3.30** (Scheme 3.3). Silylation of alcohol **3.48** with TBSCl provided the corresponding silyl ether (**3.49**) in 94% isolated yield (Scheme 3.10).

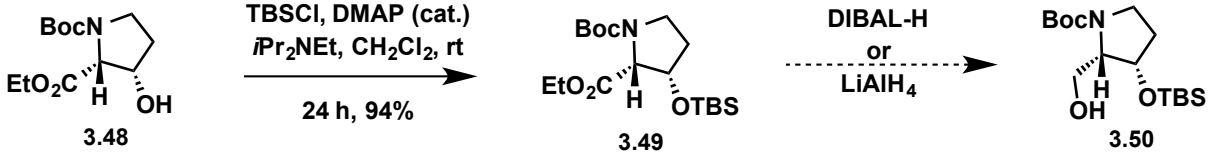

Scheme 3.10: Formation of silyl protected alcohol **3.49**.

However, reduction of the ethyl ester to either the alcohol or aldehyde proved to be troublesome. For instance, DIBAL-H consistently gave a mixture of the corresponding alcohol (**3.50**), aldehyde and starting material regardless of temperature or number of equivalents employed. When $LiAlH_4$ was employed, reduction of the ethyl ester to the alcohol was observed,

but this was accompanied by cleavage of the silyl protecting group to give the corresponding diol (not shown). To overcome this selectivity problem, we decided to switch the protecting group to the more robust benzyl ether (Scheme 3.11). Treating alcohol **3.48** with NaH in the presence of benzyl bromide and catalytic *n*-Bu_4NI provided the desired benzyl protected alcohol (**3.51**). Treatment of ethyl ester **3.51** with either DIBAL or $LiAlH_4$ provided the known alcohol in 89% and 90% isolated yields, respectively (not shown).[20] We decided to employ the $LiAlH_4$ reduction conditions upon scale up given the ease of workup and purification. With the known alcohol product in hand (not shown),[20] we began exploring conditions for the oxidation of the alcohol to the corresponding aldehyde (**3.52**). While the conditions described by Parikh and Doering[21] (DMSO, SO_3•pyridine, and Et_3N) led to epimerization at the α-stereocenter, Dess-Martin periodinane (DMP) oxidation, under buffered $NaHCO_3$ conditions, provided the desired aldehyde (**3.52**) in high yield with no observed epimerization.

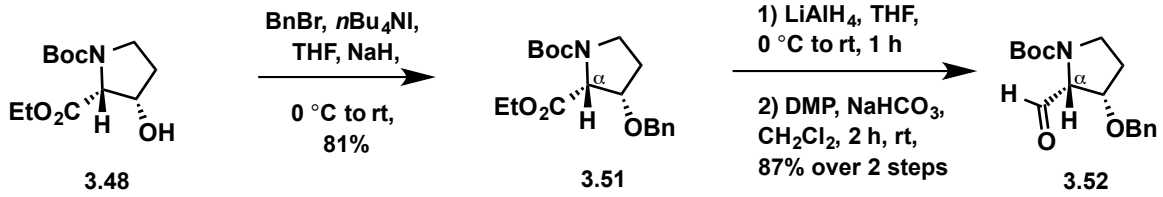

Scheme 3.11: Synthesis of aldehyde **3.52**.

Unfortunately, alkynylative homologation of the resulting aldehyde using the Ohira-Bestmann conditions (phosphonate **3.54**, K_2CO_3 in MeOH) led to epimerization of the α-stereocenter (Entry 1, Table 3.1).[16] Lowering the equivalents of base and the temperature at which the reaction is conducted only led to similar results (Entry 2, Table 3.1). It appears that the generation of the required methoxide ion for the deacylation of the 2-oxopropylphosphonate (**3.54**) competes with deprotonation of the α-stereocenter in **3.52** due to the enhanced acidity as a result of the presence of the β-oxygen substituent. Also, as previously observed by Zanato and co-workers with similar epimerizable aldehydes,[22] avoiding the use of protic solvents and conducting the reactions at lower temperatures suppresses the amount of epimerization observed. Given this precedent, we decided to investigate the generation of phosphonate anion under aprotic solvent conditions and at low temperatures prior to the introduction of aldehyde **3.52**. Using dimethyl (1-diazo-2-oxopropyl)phosphonate (**3.54**) in a suspension of NaOMe in THF at –78 °C prior to the introduction of the aldehyde **3.52** provided the desired alkyne (**3.53a**) in 60% yield with minimal epimerization (Entry 4, Table 3.1). Similarly, the use of the Seyferth-Gilbert reaction (dimethyl (diazomethyl)phosphonate (**3.55**), *t*BuOK, THF, –78 °C to rt, Entry 5 in Table 3.1) ultimately provided the desired aldehyde with no observed epimerization of the α-stereocenter. However, this procedure was not economical for scale-up as preparation of **3.55** requires a multi-step sequence. Therefore we decided to optimize the reaction using phosphonate **3.54** as it was significantly easier to access in large quantities. It was determined that decreasing the equivalents of both phosphonate **3.54** and NaOMe and conducting the reaction at –78 °C in THF delivered the desired alkyne (**3.53a**) in 76% yield with greater than 20:1 d.r. on multi-gram scale.

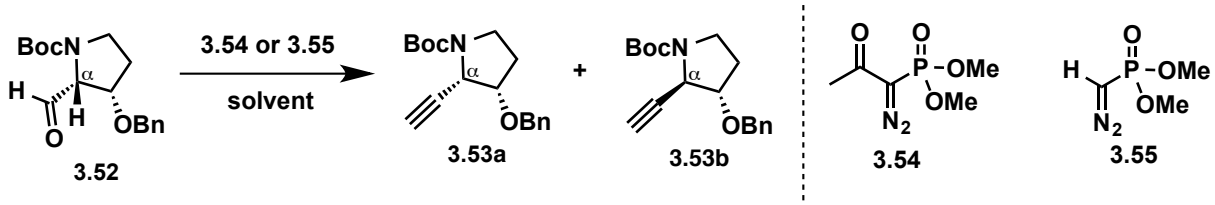

Entry	Phosphonate (equiv)	Base (equiv)	Solvent	Time/Temp (°C)	Yield (%)	Result	d.r. 3.53a:3.53b
1	**3.54** (1.3)	K_2CO_3 (excess)	MeOH	3 h / 0 °C to rt	71	**3.53a+b**	2:1
2	**3.54** (1.3)	K_2CO_3 (2.0)	MeOH	6 h / 0 °C	67	**3.53a+b**	nd
3	**3.54** (1.3)	K_2CO_3 (2.0)	MeOH	24 h / –18 °C	-	SM (**3.52**)	-
4	**3.54** (7.0)	NaOMe (6.0)	THF	5 h / –78 °C to rt	60	**3.53a+b**	>10:1
5	**3.55** (1.3)	*t*BuOK (1.4)	THF	14 h / –78 °C to rt	80	**3.53a**	-
6	**3.54** (1.5)	NaOMe (5.0)	THF	3 h / –78 °C to rt	76	**3.53a+b**	>20:1

Table 3.1: Synthesis and optimization of **3.53a**. (nd=not determined)

With the alkynylative homologation of aldehyde **3.52** using the Ohira-Bestmann reagent (**3.54**) established, we focused our efforts on the synthesis of dienophile **3.59** from alkyne **3.53a** (Scheme 3.12). Therefore, upon Boc-cleavage under acidic conditions, the resulting ammonium salt (not shown) was acylated with α-cyano acetylchloride to give alkyne **3.56**, analogous to our previously established sequence (see Chaper 2.3).[8c] A formal cycloisomerization of **3.56**, proceeding by anti-Markovnikov hydration of the terminal alkyne followed by Knoevanagel condensation of the incipient aldehyde (**3.58**), was effected using the Grotjahn complex (**3.57**)[23] to yield bicycle **3.59** in near quantitative yield.

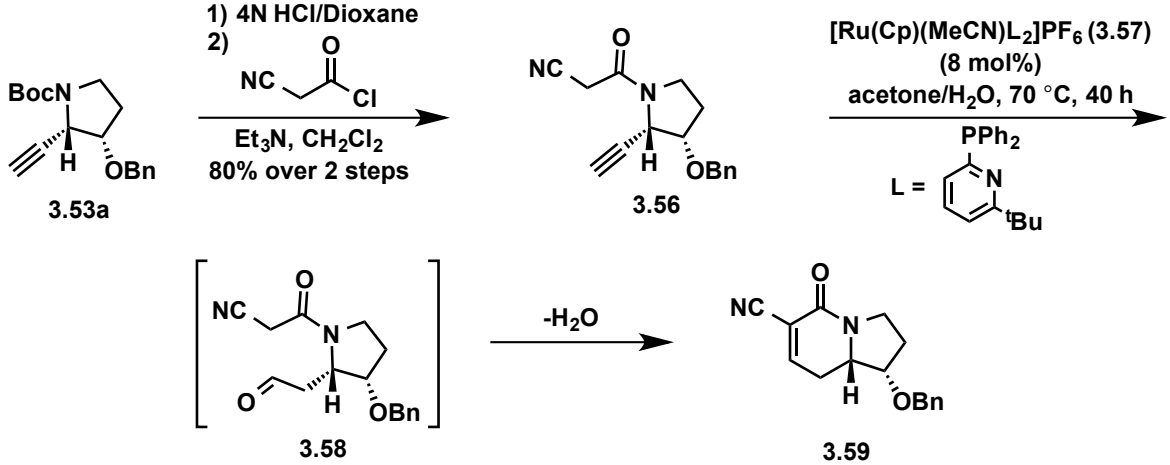

Scheme 3.12: Synthesis of benzyloxy dienophile **3.59**.

3.2.4: Diels–Alder reaction: Synthesis of Tricycle 3.28.

Diels–Alder cycloaddition of **3.59** with diene **3.29**, facilitated by $SnCl_4$ gives enone **3.28** upon basic workup. Even though we had previously accomplished the analogous synthesis of a tricycle lacking the benzyloxy group at C3 in Chapter 2.3 (see numbering in **3.59**), it was unclear what influence this added substituent would exert on the diastereoselectivity of the cycloaddition step and so we were gratified to obtain **3.28** as a single diastereomer in good yield.

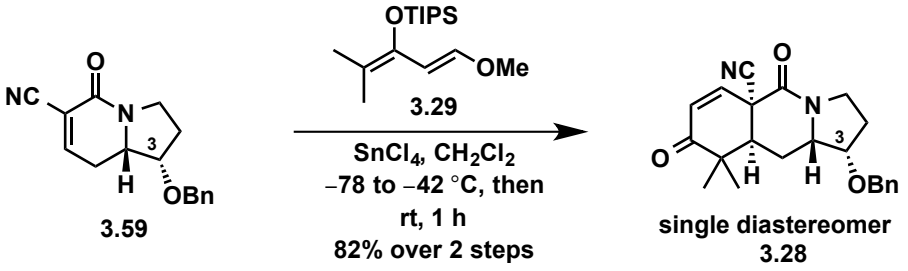

Scheme 3.13: Synthesis of tricycle **3.28** through a Diels–Alder reaction.

3.3 – Synthesis of Pentacyclic Indole Model Systems and Elaboration to the Bicyclo[2.2.2]diazaoctane.

3.3.1: Overview of the Model System and the Dieckmann Cyclization Step.

Having successfully accessed tricycle **3.28**, we decided to investigate a model system for the late-stage C4-C26 bond formation (stephacidin A numbering, Figure 3.1), which lacked substitution on the indole moiety (**3.61**, Scheme 3.14). This model system would be easily accessed from a Fischer indole synthesis using **3.60** and standard functional group manipulations. This model system would allow us to answer a few questions regarding the late-stage Dieckmann cyclization step: 1) What influence would the indole functional group have on the conformation of the system in the cyclization step? In other words, would the bridged bicyclic system be accessible with the indole functional group in place? If not, would C–C bond formation (i.e., C4-C26) have to be accomplished prior the installation of the indole functional group? 2) What conditions (i.e., acidic/basic, solvent and temperature) would be required for the *in situ* formation of the requisite isocyanate, **3.62**? 3) Will the free indole *N-H* act as a nucleophile and engage the isocyanate, via a *5-exo-dig* cyclization (blue arrows), forming [3.2.1] bicycle **3.63**? And if so, would this process be reversible? In the event that the indole does engage the isocyanate could protecting groups on the indole nitrogen favour the formation of bicyclo[2.2.2]diazaoctane **3.64**, via a *6-exo-dig* cyclization (red arrows)? Toward this end, we decided to target keto-alcohol **3.60** as the substrate for Fischer indole synthesis *en route* to addressing these questions. This model system would also provide a synthesis of premalbrancheamide (not shown), which has been shown to be a precursor to the malbrancheamide family of prenylated indole alkaloids.[24]

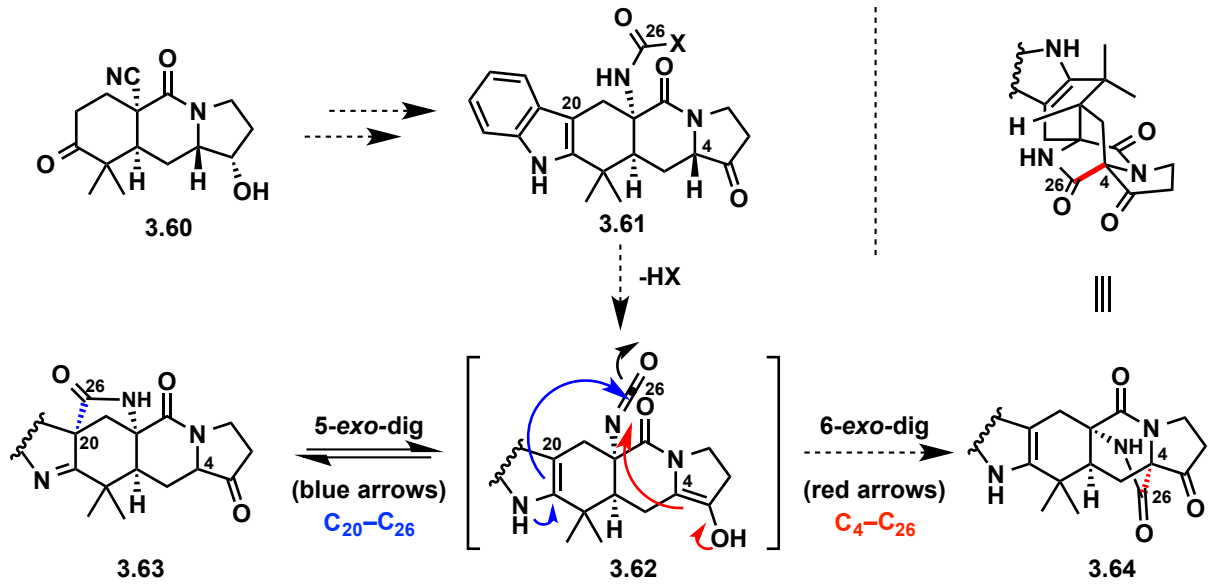

Scheme 3.14: Proposed application of the indole model system.

3.3.2: Synthesis of Nitrile-Indole Model System 3.69.

With tricycle **3.28** in hand we first investigated conditions for the direct one-pot hydrogenation of the enone and hydrogenolysis of the benzyl-ether to access the desired keto-alcohol **3.60** (Table 3.2). The use of heterogeneous conditions: Pd/C, Rh/Al_2O_3 or Pearlman's catalyst ($Pd(OH)_2$) over H_2 provided only the hydrogenation product **3.65** with no observable deprotection of the alcohol group, even at higher pressures (Entries 1-5, Table 3.2). However, the use of $PdCl_2$ did effect both the desired hydrogenation and hydrogenolysis processes but with concurrent reduction of the nitrile to the corresponding amine product **3.67**, as observed by LCMS (Entry 5, Table 3.2). The chemoselectivity issue could not be controlled as the rates of reduction (**3.28→3.66**) and hydrogenolysis (**3.28→3.67**) were competitive based on LCMS analysis of the reaction mixture. Even after surveying a variety of heterogeneous conditions we could not achieve the desired product due to chemoselectivity issues, therefore, we decided to pursue a step-wise sequence to access the desired keto-alcohol **3.60**.

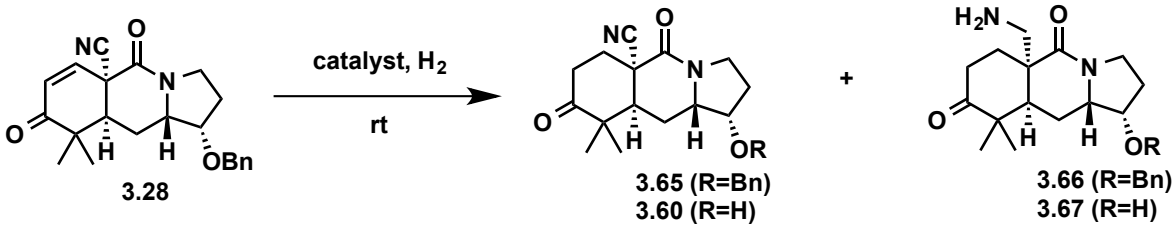

Entry	Catalyst	Solvent	Pressure	Result
1	Pd/C	EtOAc	1 atm	**3.65**
2	Pd/C	EtOH	1 atm	**3.65**
3	Rh/Al_2O_3	Et_2O	1 atm	**3.65+3.28**
4	$Pd(OH)_2$	EtOH	1 atm	**3.65**
5	Pd/C	EtOH	35 atm	**3.65**
6	$PdCl_2$	EtOH	1 atm	**3.66+3.67**

Table 3.2: Hydrogenation/hydrogenolysis conditions on tricycle **3.28**.

Next we investigated conditions to cleave the benzyl group of **3.65**, which was accessed by hydrogenation conditions (Entry 1, Table 3.2) in quantitative yield. The use of *in situ* generated TMSI, from TMSCl and NaI, or BCl_3•Me_2S only lead to decomposition of starting material. Gratifyingly, the use of BBr_3 at –42 °C after 30 minutes provided the desired keto-alcohol (**3.60**, Scheme 3.15) in moderate yield (60%). After optimization, it was determined that higher yields of **3.60** are obtained by decreasing the equivalents of BBr_3, conducting the reaction at lower temperature (–78 °C) and shortening the reaction time to 15 min. These conditions provided **3.60** in 74% yield over the two steps, with some amounts of isolated starting material as well (**3.65**, Table 3.2). The structure of **3.60** is unambiguously supported by single X-ray crystallographic analysis (see CYLview in Scheme 3.15).

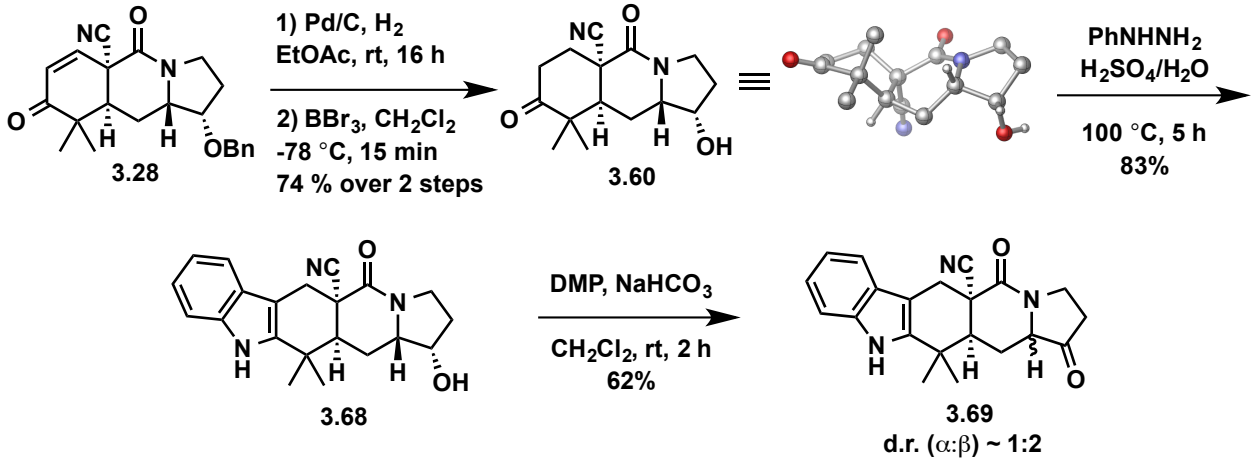

Scheme 3.15: Synthesis of pentacyclic indole **3.69**.

Fischer indole synthesis on keto-alcohol **3.60** with phenylhydrazine in aqueous sulfuric acid at 100 °C affords the pentacyclic indole **3.68** in 83% yield. Treating alcohol **3.68** with Dess-Martin periodinane (DMP) delivers ketone **3.69** as a single diastereomer, which epimerizes upon purification with silica gel chromatography to give an inseparable mixture of diastereomers in a ratio of 1:2 (*α:β* epimers). From these observations, we reasoned that if the hydration of the nitrile could be effected (**3.69→3.70**, Scheme 3.16), a Hofmann rearrangement performed in the absence of any external nucleophiles should generate isocyanate **3.71** in situ, which could be intercepted by the enol tautomer through a 6-*exo-dig* cyclization to provide the bicyclo[2.2.2]diazaoctane ring (**3.72**) in a single pot transformation. As previously described, this model system would find application in the syntheses of the premalbrancheamide (e.g., **3.73**) family of prenylated indole alkaloid natural products as well.

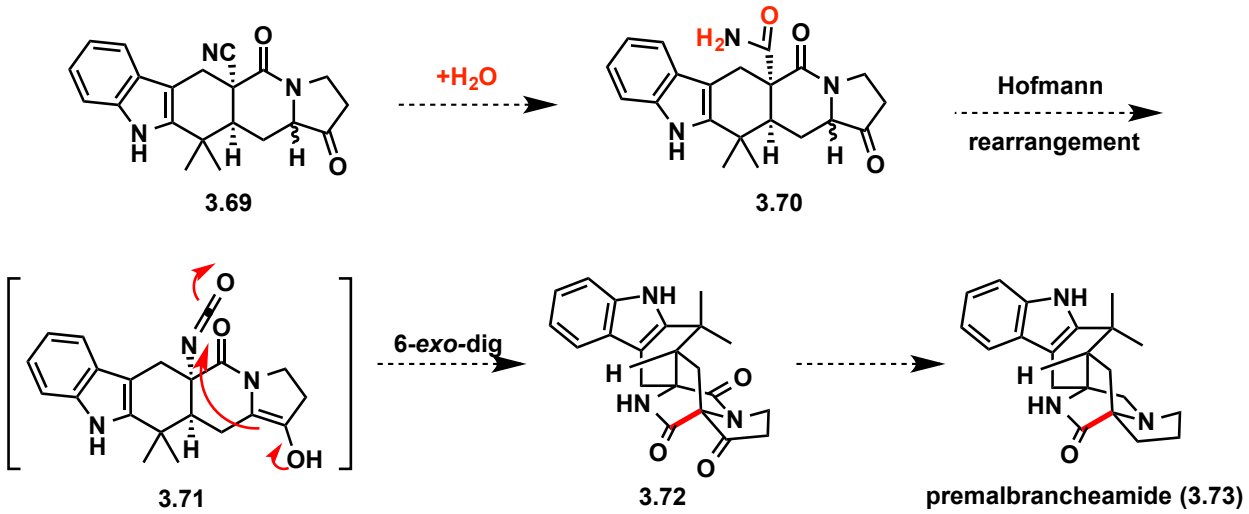

Scheme 3.16: Proposed one-pot transformation to the bicyclo [2.2.2] ring system.

Encouraged by this proposed sequence of events, we looked into conditions to effect the hydration of the nitrile group to the corresponding amide (**3.75**, Scheme 3.17). However, the use of Ghaffar-Parkins' platinum catalyst (**3.74**),[25] which has worked in similar systems in the past (see Chapter 2.3),[8c] failed to provide any desired hydrated product (**3.75**) but led to a complex product distribution by crude ^{1}H NMR and LCMS analysis. An alternative procedure reported by Sukbok Chang using Wilkinson's catalyst ($RhCl(PPh_3)_3$) and acetaldoxime as the water equivalent in refluxing toluene led only to decomposition of starting material.[26] We reasoned that due to the ease of enolization of the ketone, this enol may be coordinating the Rh/Pt metal catalysts as a ligand, shutting down the reactivity mode of the catalyst and/or leading to decomposition pathways. Support for this hypothesis comes from the fact that **3.60** and **3.68**, which lack the pyrrolidine ketone group, are both effectively hydrated in great yields using the Ghaffar-Parkins' catalytic system (Scheme 3.17). Given this outcome, we decided to utilize **3.77** in the forward route to test the one-pot Hofmann/isocyanate capture for forging the bicyclic framework (see Scheme 3.16).

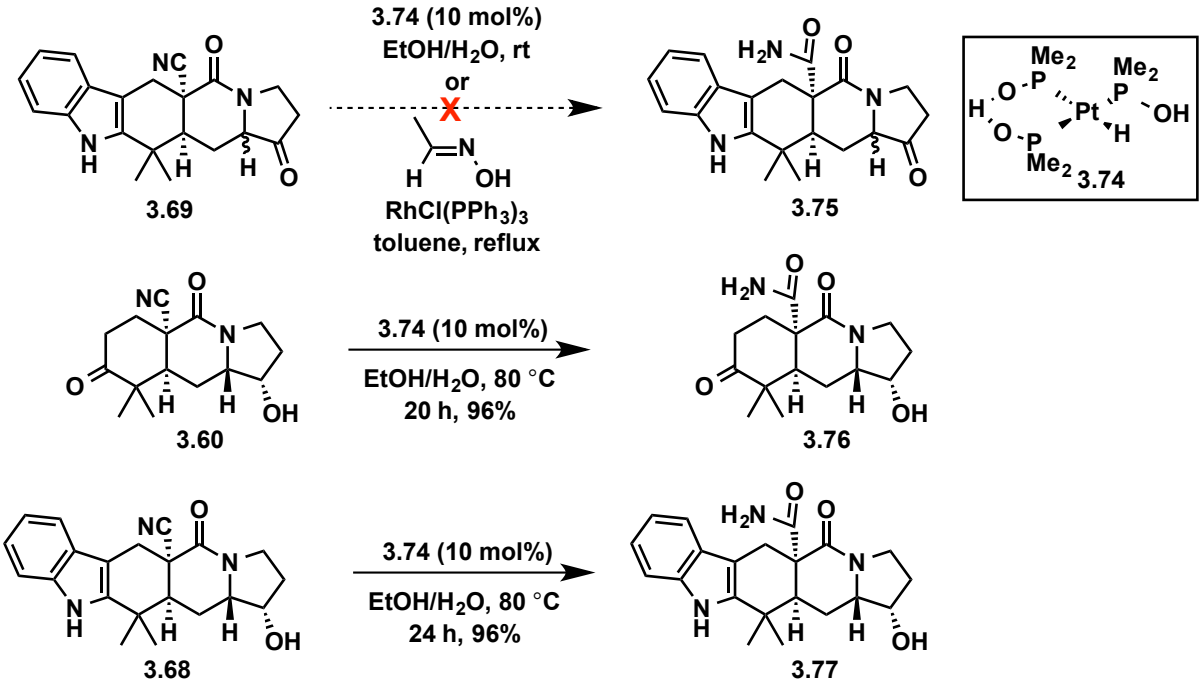

Scheme 3.17: Hydration of the nitrile functional group.

3.3.3: Elaboration of Primary Carboxamide-Indole Model System 3.77.

Having access to amide **3.77** following the hydration of the nitrile group using the Ghaffar-Parkins' catalytic system, we next investigated conditions for the oxidation of the alcohol functional group to the corresponding ketone group (**3.77→3.78**, Table 3.3). Dess-Martin periodinane (DMP), which worked successfully on alcohol **3.68** (Scheme 3.15), resulted in decomposition (Entry 1, Table 3.3). Turning to the Swern conditions (oxalyl chloride, DMSO, Et_3N, CH_2Cl_2)[27] provided only decomposition after 1.5 hours, however, the formation of product was detected by LCMS (Entry 2, Table 3.3). After decreasing the reaction time from 1.5 h to 30 minutes, small amounts of the desired product were obtained along with the majority of the mass balance accounted for by recovered starting material (Entry 3, Table 3.3). However, due to the inability to purify ketone **3.78** (even after preparative TLC) we were not convinced that the results of the forward chemistry would be conclusive and therefore, decided to look into alternative conditions for this oxidation sequence. Utilizing the Ley oxidation conditions (TPAP, NMO, 4Å MS, CH_2Cl_2),[28] caused decomposition of the starting material (Entry 4, Table 3.3). The Corey-Suggs reagent[29] (pyridinium chlorochromate, PCC) and the Parikh and Doering[21] conditions (DMSO, SO_3•pyridine, and Et_3N) only returned starting material (Entries 5 and 6, Table 3.3). Lastly, the classical Oppenauer oxidation conditions also failed to deliver the desired ketone **3.78** but instead returned starting material (Entry 7, Table 3.3). Recently, Zr(*t*OBu)$_4$ has been shown to be a superior catalyst for these transformations because it is monomeric in solution and the ligand exchange is very rapid.[30] Employing these modified Oppenauer conditions, however, also returned starting material (Entry 8, Table 3.3).

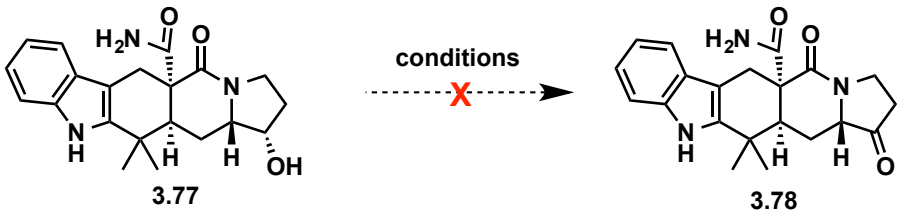

Entry	Conditions	Result
1	DMP, $NaHCO_3$, CH_2Cl_2, rt	Decomposition
2	$(COCl)_2$, DMSO, Et_3N, CH_2Cl_2, -78 °C to rt, *1.5 h*	Decomposition
3	$(COCl)_2$, DMSO, Et_3N, CH_2Cl_2, -78 °C to rt, *0.5 h*	~22% yield, messy
4	TPAP (10 mol%), NMO, 4Å MS, CH_2Cl_2, rt	Decomposition
5	PCC, NaOAc, CH_2Cl_2, rt	Starting Material
6	SO_3•pyr, Et_3N, DMSO/CH_2Cl_2, rt	Starting Material
7	Al(*i*OPr)$_3$, acetone/toluene, 90 °C	Starting Material
8	Zr(*t*OBu)$_4$, acetone/toluene, 90 °C	Starting Material

Table 3.3: Oxidation conditions on alcohol **3.77**.

We suspected that our lack of success in mediating this transformation was due to the more nucleophilic character of the primary amide with respect to the hydroxyl group, which would be interacting with the oxidants/catalysts in the cases above. Therefore, we decided to effect the Hofmann rearrangement on substrate **3.77** prior to the oxidation of the alcohol group to the corresponding ketone.

With alcohol-carboxamide **3.77** in hand, we investigated conditions to effect the Hofmann rearrangement (Table 3.4). Treating **3.77** with phenyliodoso trifluoromethyl acetate (PIFA) in the presence of methanol, in hopes of accessing the methyl carbamate (**3.79**), resulted in decomposition of the starting material (Entry 1, Table 3.4).[31] Interestingly, treating carboxamide **3.77** with $Pb(OAc)_4$ in a mixture of DMF/MeOH at room temperature, we observed the formation of [3.2.1] bicycle **3.80** as the sole product of the reaction in great yields (Entry 2, Table 3.4). The structure of **3.80** was confirmed by both 1D and 2D NMR analysis. In particular, a HMBC correlation between the ring fused methine at C6 and the carbonyl group of the bridging amide at C26 led to its assignment. We believe this [3.2.1] bicyclic system arises from an initial oxidation of the primary carboxamide to generate the *N*-acyl nitrene (**3.81**), which then interacts with the indole C2-C3 double bond forming aziridine **3.82**. The indole nitrogen can then open the aziridine via the C2 position, driven by release of ring strain (as shown by the red arrows), which, after a proton transfer, delivers **3.80**. Unfortunately, this unique ring system does not map onto any natural products scaffolds that have been reported thus far. We next investigated if we could override the selectivity of **3.79** vs **3.80** by increasing the temperature at which the reaction is conducted. As shown in Table 3.4, conducting the reaction at 70 °C again provided **3.80** as the major product of the reaction (Entry 3). Even after heating to 100 °C, **3.80** remained the major product of the reaction (Entry 4, Table 3.4).

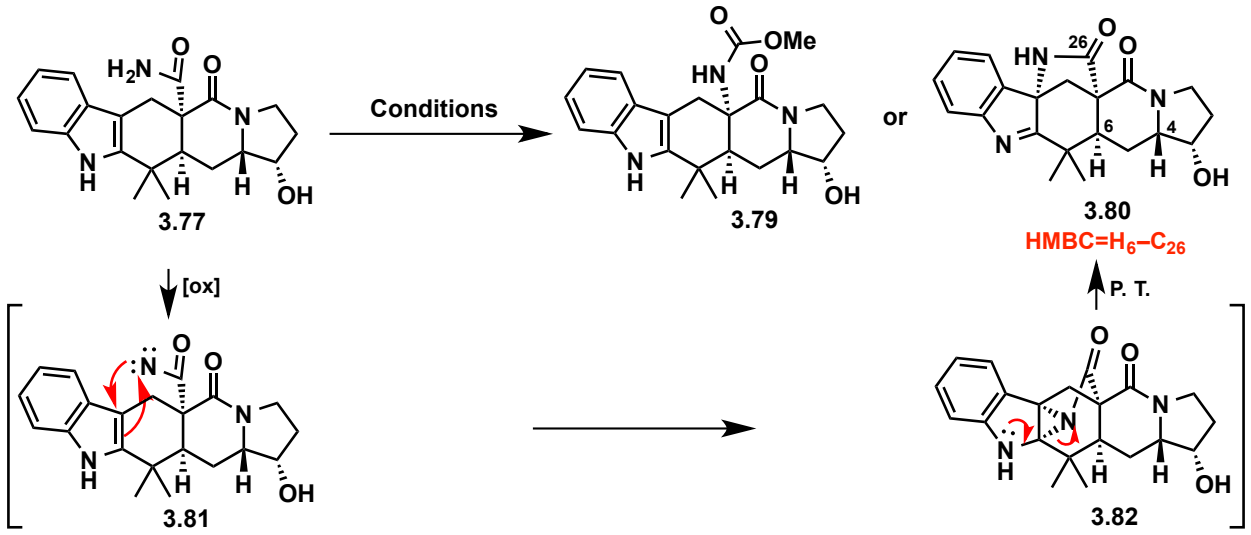

Entry	Conditions	Result (3.80:3.79), Yield
1	PIFA, MeOH, rt	Decomposition
2	$Pb(OAc)_4$, DMF/MeOH, rt, 2 h	1:0, 89%
3	$Pb(OAc)_4$, DMF/MeOH, 70 °C, 16 h	>5:1, nd
4	$Pb(OAc)_4$, DMF/MeOH, 100 °C, 16 h	3:1, nd

Table 3.4: Hofmann conditions on carboxamide **3.77**. (nd=not determined)

On the basis of these results, we suspected that the Hofmann rearrangement would have to be accomplished prior the installation of the indole moiety in order to avoid the formation of the [3.2.1] bicycle (**3.80**). Therefore, we directed our attention to carboxamide **3.76** (Scheme 3.17), which is predisposed for the Hofmann rearrangement and also contains the necessary ketone functional handle to implement the Fischer indole synthesis at a later stage.

3.3.4: Synthesis of Methyl Carbamate-Indole Model System 3.84.

Following our studies on the Hofmann rearrangement, we determined early on that $Pb(OAc)_4$ in the presence of MeOH at room temperature mediates this transformation to provide the desired methyl carbamate (**3.83**, Scheme 3.18) with varying amounts of recovered starting material. After some optimization, we established that elevated temperatures (70 °C) were required to attain full conversion of starting material. However, the yields of the reaction dropped dramatically upon scale up and required over 6 equivalents of the $Pb(OAc)_4$ to get complete consumption of starting material. Nevertheless, the methyl carbamate (**3.83**) was taken forward through the Fischer indole synthesis to provide indole **3.79** in 74% yield. Subsequent oxidation with Dess-Martin periodinane (DMP) gratifyingly provided **3.84**, which is predisposed for the late-stage

Dieckmann cyclization to afford the bicyclo[2.2.2]diazaoctane core. Unfortunately, trying a variety of bases (NaH, KHMDS, or KO*t*Bu) and acid (TFA), we could never detect any amount of the desired bicycle[2.2.2] product (**3.72**) by LCMS or ^{1}H NMR. We reasoned that the methyl carbamate might not be electrophilic enough for the cyclization step and the nucleofuge, in this case methoxide, may in fact act as a nucleophile (cleaving either C4-C26 or C3-C4) leading to decomposition. Therefore, we looked into installing different carbamates, which would be more electrophilic and contain better leaving groups such as phenols, *para*-nitro-phenols or polyfluoroalcohols. Furthermore, we envisioned the resulting nucleofuge from these carbamates would not be nucleophilic enough to lead to decomposition pathways.

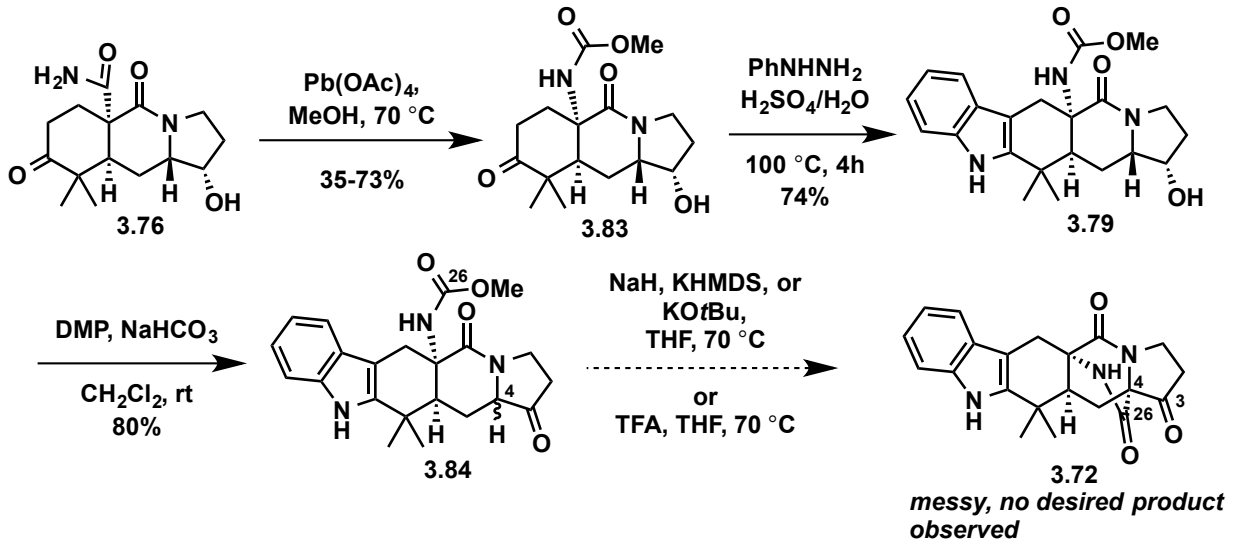

Scheme 3.18: Attempted Dieckmann condensation on methyl carbamate **3.84**.

3.3.5: Synthesis of Phenyl Carbamate-Indole Model System 3.91 and its Application to the Bicyclo[2.2.2]diazaoctane ring.

On the basis of the work of the Clive group,[32] we were encouraged that the use of a phenyl carbamate would be ideal to effect the desired Dieckmann condensation reaction. As depicted in Scheme 3.19, the Clive group was able to form 2,5-diketopiperizines in the presence of base (NaH) by the same Dieckmann cyclization we proposed for our system.

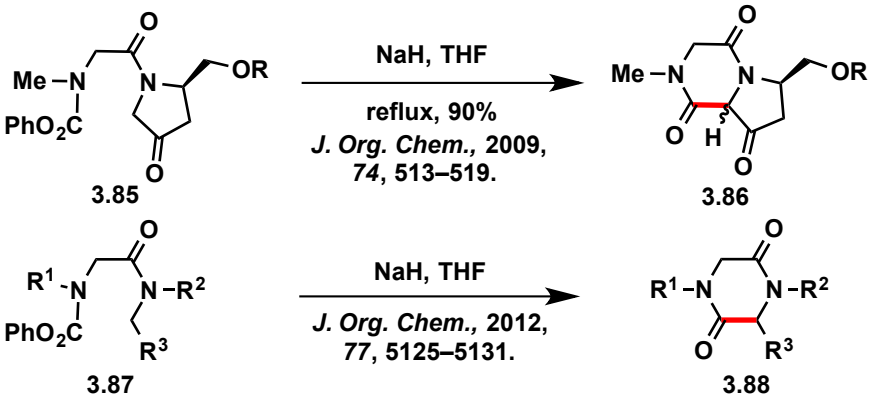

Scheme 3.19: Clive and co-worker's Dieckmann cyclization route to 2,5-diketopiperazines.

However, there are some notable differences between our system and those reported by the Clive group. First, all of the examples reported by Clive contain a tertiary carbamate (**3.85** and **3.87**, Scheme 3.19), meaning there is no N-H carbamate as is present in our system. This could be an issue in our system as deprotonation would render the carbamate carbonyl less electrophilic from an electrostatic and resonance standpoint. Second, the Clive group does not report the formation of any tetra-substituted carbons by this cyclization route (see **3.86** and **3.88**). In our case we envisioned forming a tetra-substituted carbon that is also bridging, which inherently is more sterically congested, strained and entropically less favourable. Nevertheless, we decided to pursue the synthesis of the phenyl carbamate to test out the Clive conditions for the Dieckmann cyclization.

Although we could access the corresponding amine product from **3.79** (Scheme 3.18), following cleavage of the methoxycarbonyl group of **3.79** with dimethylsulfide in methylsulfonic acid (91% yield, not shown), we decided to investigate alternative Hofmann rearrangement conditions (Table 3.5) seeing how $Pb(OAc)_4$ gave poor and irreproducible yields upon scale up. Furthermore, alternative conditions might furnish the desired amine **3.89** directly without having to go through the intermediacy of the methyl carbamate (**3.83**, see Table 3.5).

With access to **3.76**, we began our investigations for the preparation of either **3.83** or **3.89** in improved yields and scalability. Attempts to utilize $Pb(OAc)_4$ in the presence of water to afford the primary amine only led to decomposition of starting material (Entry 1, Table 3.5). Carrying out milder modifications of classical Hofmann rearrangement conditions (NBS and base at high temperatures) also led to decomposition (Entries 2-3, Table 3.5).[33] We next turned our attention to the catalytic formation of hypervalent aryl-iodane species to effect the Hofmann rearrangement, however, we observed either returned starting material or decomposition (Entries 4-5, Table 3.5).[34] Gratifyingly, other hypervalent aryl-iodanes such as PIDA or PIFA successfully provided the desired primary amine (**3.89**) but in low yields (Entries 6-7, Table 3.5).

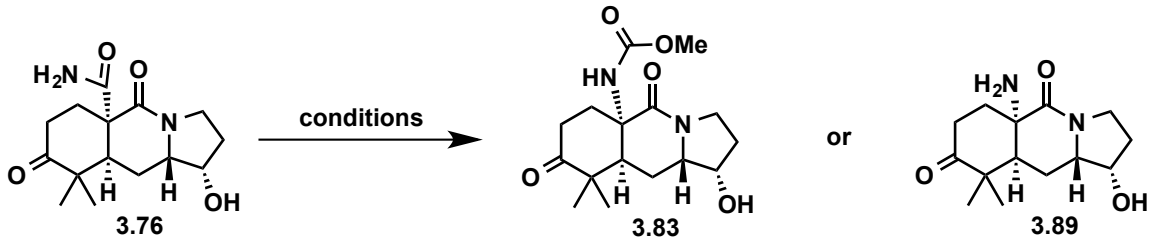

Entry	Conditions	Result
1	$Pb(OAc)_4$, H_2O, rt	Decomposition
2	NBS, NaOMe, MeOH, reflux	Decomposition
3	NBS, DBU, MeOH, reflux	Decomposition
4	PhI, *m*-CPBA, HBF_4, $MeCN/H_2O$	SM (**3.76**)
5	PhI, Oxone®, 40 °C, MeOH, HFIP, H_2O	Decomposition
6	PIDA, $MeCN/H_2O$, rt	**3.89** (<14%)
7	PIFA, $MeCN/H_2O$, rt	**3.89** (20%)
8	PhINTs, CH_2Cl_2, rt then aq. H_2SO_4	**3.89** (>80%)

Table 3.5: Optimized Hofmann rearrangement on carboxamide **3.76**.

After surveying the literature for other hypervalent aryl-iodanes that have been used for the Hofmann rearrangement, we came across (tosylimio)-phenyl-λ^3-iodane[35] (PhINTs), which in many cases has been shown to be a milder reagent than other hypervalent iodine reagents for these transformations. Treating carboxamide **3.76** with 1.2 equivalents of (tosylimio)-phenyl-λ^3-iodane (PhINTs) in CH_2Cl_2 at room temperature, we observed complete formation of the isocyanate after 2 hours by TLC and LCMS. In the same pot, the addition of aqueous sulfuric acid causes the hydrolysis of the isocyanate to the corresponding amine (**3.89**) in great yields (Entry 8, Table 3.5). Of note, the isocyanate is isolable following the Hofmann rearrangement by filtering the reaction mixture through a plug of silica gel. Moreover, the Fischer indole synthesis can be conducted in the same pot, following the Hofmann rearrangement, by the addition of phenyl hydrazine and heating to 100 °C overnight (Scheme 3.20).

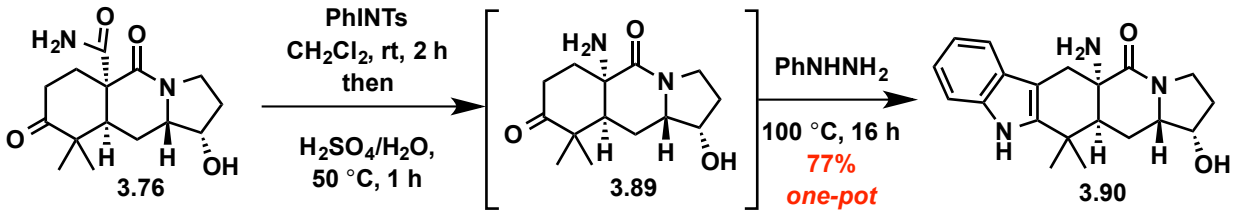

Scheme 3.20: One-pot Hofmann rearrangement and Fischer indole synthesis.

Having access to amino-indole **3.90** in reproducible yields through a scalable one-pot transformation from **3.76**, we turned to the installation of the phenyl carbamate and to testing the Dieckmann cyclization step (Table 3.6). Toward this end, chemoselective carbamoylation of the primary amine in **3.90** was achieved in high yield in the presence of the secondary hydroxyl with phenyl chloroformate to afford a phenyl carbamate (not shown). At this point, oxidation of the secondary hydroxyl group with Dess-Martin periodinane (DMP) was achieved to give the requisite ketone (**3.91**) as a mixture of diastereomers after purification, which is in position for the late-stage C4-C26 bond formation (red highlighted bond in **3.72**).

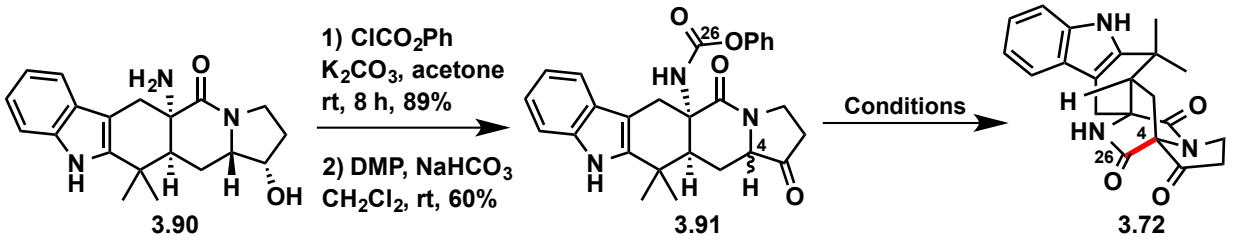

Entry	Base (equiv)	Solvent	Temperature	Time	Result
1	NaH (4.0)	THF	70 °C	15 min	Decomp.
2	KO*t*Bu (4.0)	THF	70 °C	15 min	Decomp.
3	NaH (1.1)	THF	50 °C	15 min	Trace **3.72**
4	KO*t*Bu (1.1)	THF	50 °C	15 min	Trace **3.72**
5	K_2CO_3 (5.0)	THF	50 °C	2 h	**3.72** (10%)
6	K_2CO_3 (5.0)	Acetone	50 °C	2 h	**3.72** (45%)
7	K_2CO_3 (2.0)	Acetone	50 °C	2 h	**3.72** (60%)
8 *	K_2CO_3 (2.0)	Acetone	50 °C	2 h	**3.72** (73%)

Table 3.6: Synthesis of bicyclo[2.2.2]diazaoctane ring (*pure starting material **3.91**).

Having successfully attained our desired phenyl carbamate (**3.91**), we began our investigation of the key Dieckmann cyclization to afford the bicyclo[2.2.2]diazaoctane core present in many members of the prenylated indole alkaloids. Applying the Clive conditions[32a] to **3.91** with either NaH or KO*t*Bu (4.0 equivalents) as base only resulted in decomposition of starting material (Entries 1-2, Table 3.6). We reasoned the large excess of base might be the cause for the decomposition since we had several acidic protons in **3.91** (α to the ketone, secondary amide N-H, and indole N-H groups). After decreasing the equivalents of base (NaH or KO*t*Bu) to 1.1 and the temperature to 50 °C we were enthused to observe the formation of **3.72** in trace amounts (Entries 3-4, Table 3.6). From our observation that ketone **3.91** epimerizes upon purification on silica gel, we reasoned that the proton at C4 is quite acidic and therefore decided to move to a milder base for this transformation. When potassium carbonate was utilized as the base in THF, we could isolate **3.72** in 10% yield (Entry 5, Table 3.6). Switching the solvent from THF to acetone provided **3.72** in much improved yield (Entry 6, Table 3.6). Next, decreasing the equivalents of potassium carbonate lead to an improvement in yield (Entry 7, Table 3.6).

Lastly, after optimizing purification of **3.91**, since we believed that trace DMP was leading to decomposition upon heating, application of these conditions provided a 73% yield of **3.72**.

We believe this transformation occurs *via* an isocyanate capture by the generated potassium enolate since treating the phenyl carbamate alcohol (not shown), obtained after carbamoylation of the primary amine of **3.91**, under the reaction conditions affords the isocyanate. Also, carbamates are commonly used as precursors for generating isocyanates *in situ* by industry.[36] Our synthesis of the bicyclo[2.2.2]diazaoctane ring system by a complexity building isocyanate capture step sets the stage for a unifying approach to the synthesis of these molecules, which is in sharp contrast to previous approaches toward this class of molecules (see Chapter 3.1.2).

Having successfully demonstrated the synthesis of the bicyclo[2.2.2]diazaoctane ring on our model system, we looked forward to applying this transformation to the synthesis of stephacidin A (**3.1**, Figure 3.1). However, before pursuing this endeavour, we realized that our model system, in particular **3.72**, could find application to the malbrancheamide family of prenylated indole alkaloids (Scheme 3.21).[24b, 37] This family of prenylated indole alkaloids is known to have calmodulin (CaM)-dependent phosphodiesterase (PDE1) inhibitory activity which has important implications in cancer, neurodegenerative and vascular diseases due to its effect on intercellular cAMP and cGMP concentrations.[38] In the forward sense, a one-pot Wolff-Kishner reduction[39] of the pyrrolidine ketone in **3.72** was performed to give known compound **3.92**.[24a] Following the precedence of Williams and co-workers, treating **3.92** with an excess of DIBAL-H completes the synthesis of premalbrancheamide **3.73**.[24a] Metal catalysed C–H functionalization methods for the installation of both chlorides and bromides at the C5 and C6 positions of the indole moiety in **3.72**, **3.92**, and **3.73** are currently being investigated in our group to access other malbrancheamide natural products and unnatural derivatives for structural activity relationship studies. We are also collaborating with David Sherman's group at the University of Michigan to investigate enzymatic C–H functionalization methods to accomplish the same task.

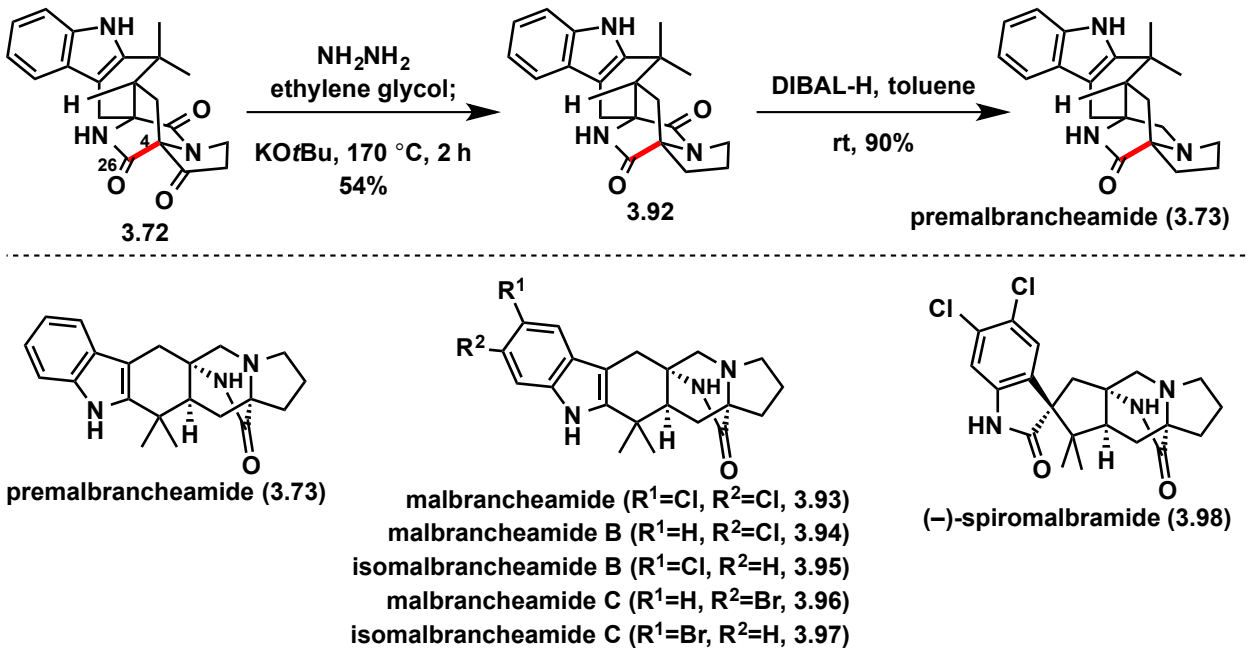

Scheme 3.21: Malbrancheamide family of natural products and synthesis of premalbrancheamide.

3.4 – Total Syntheses of (–)-17-hydroxy-citrinalin B, (+)-stephacidin A and (+)-notoamide I.

3.4.1: Synthesis of Divergent Intermediate 3.110.

Having successfully forged the bicyclo[2.2.2]diazaoctane ring at a late stage on our model system, we next focused on applying this same transformation on the fully functionalized indole fragment present in the stephacidin and citrinalin series of natural products (see Figure 3.1). These classes of natural products contain additional substitution at the indole C6 and C7 positions, a chromene in the case of the stephacidins and a chromanone in the citrinalin series. We reasoned that a common intermediate *en route* to both natural products should contain the lowest level oxidation state, in order to reduce the number of redox manipulations,[40] and therefore chose to target the chromene unit. Toward this end, we decided to take advantage of our previous success in the cyclopiamine and citrinalin series (see Chapter 2) and utilize the same reductive cyclization step to install the requisite indole moiety.[8c]

Starting from Diels–Alder adduct **3.28**, a Johnson iodination[41] provided **3.99** (Scheme 3.22), followed by hydration of the nitrile group using the Ghaffar-Parkins complex (**3.74**)[25] and subsequent Hofmann rearrangement of the resulting carboxamide (**3.100**) using phenyliodoso trifluoromethyl acetate (PIFA) in the presence of methanol provided methyl carbamate **3.101**.[33a] Following the precedent of Myers and Herzon,[7d] Suzuki cross-coupling of iodide **3.101** with pincacol boronic ester **3.102** followed by reductive cyclization, yielded indole annulated hexacycle **3.104**.

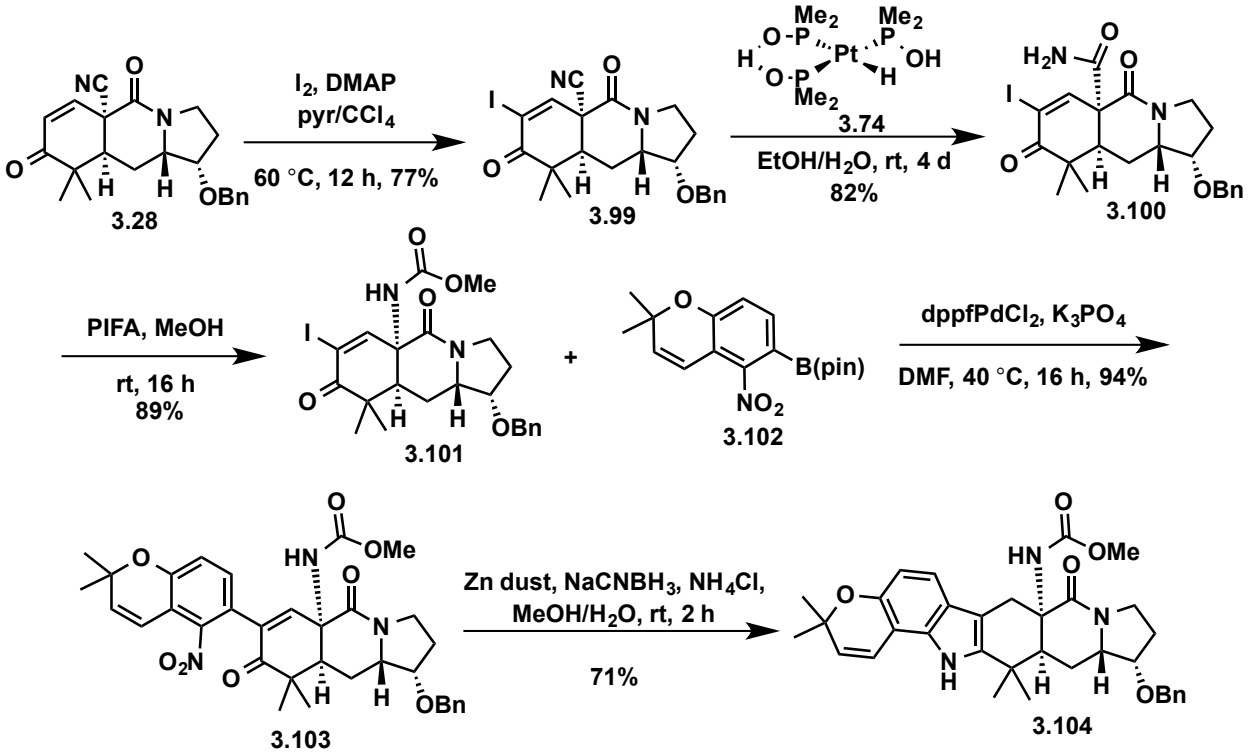

Scheme 3.22: Synthesis of indole annulated hexacycle **3.104**.

At this stage, we investigated cleaving both the methoxycarbonyl group as well as the benzyl protecting group of compound **3.104**. Treatment of **3.104** with dimethyl sulfide in the presence of methane sulfonic acid unveiled the amine and hydroxyl groups to provide **3.105**, but in low yields (Scheme 3.23).

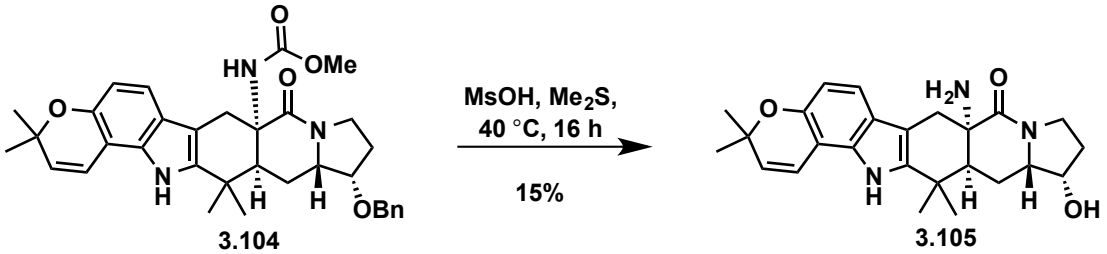

Scheme 3.23: Synthesis of amino-alcohol **3.105**.

In order to identify which of the two deprotection steps was the problematic one, we decided to investigate orthogonal deprotection conditions (Scheme 3.24). Treating **3.104** with sodium ethylthiolate unveiled the amine group to provide **3.106** in great yield, however, subjecting this material to Lewis acidic conditions (BBr_3) to cleave the benzyl protecting group afforded alcohol **3.105** in low yields. In order to rule out the amine

group as the cause of decomposition under the Lewis acidic conditions, **3.104** was treated directly with BBr_3 to obtain alcohol **3.107**, but again we observed significant decomposition under the reaction conditions.

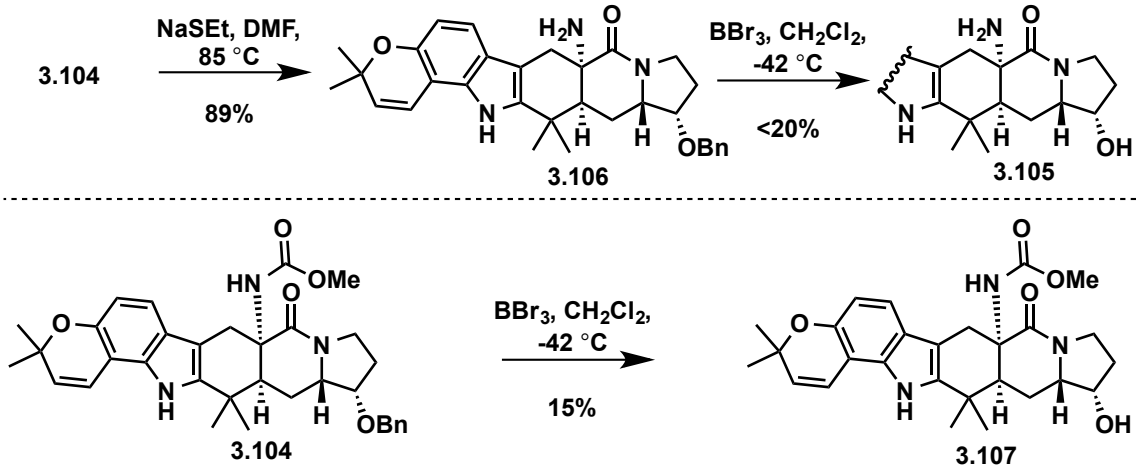

Scheme 3.24: Orthogonal deprotection sequences to access **3.105**.

With small amounts of amino alcohol **3.105** in hand (see Scheme 3.23), we began investigating the chemoselective carbamoylation of the primary amine in **3.105**, which could be achieved in high yield in the presence of the secondary hydroxyl with phenyl chloroformate to afford phenyl carbamate **3.108** (Scheme 3.25). However, oxidation of the secondary hydroxyl group with Dess-Martin periodinane (DMP) following our previously established protocol was unsuccessful (see Table 3.6). We reasoned that the chromene unit in **3.108** was the problematic functional group for both the benzyl deprotection and subsequent oxidation steps and therefore, we chose to mask the alkene as a ketone through a Wacker oxidation.

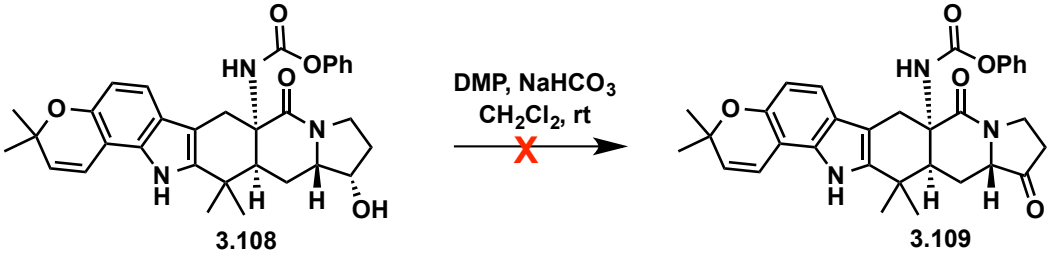

Scheme 3.25: Oxidation attempt on phenyl carbamate **3.108**.

Returning to methyl carbamate **3.104**, Wacker oxidation[42] of the chromene moiety and treatment of the resulting chromanone with dimethyl sulfide in the presence of methane sulfonic acid unveiled the amine and hydroxyl groups to provide **3.110** in excellent yield (Scheme 3.26), which would serve as the common intermediate to access both 17-hydroxy-citrinalin B as well as stephacidin A. Of note, while the synthesis of 17-hydroxy-citrinalin B would take advantage of the chromanone unit, a synthesis of

stephacidin A from **3.110** would require a reconstitution of the chromene moiety. However, in our hands, the chromanone moiety proved to be more robust (as compared to the chromene) in many of the subsequent steps and so **3.110** served as a more effective intermediate.

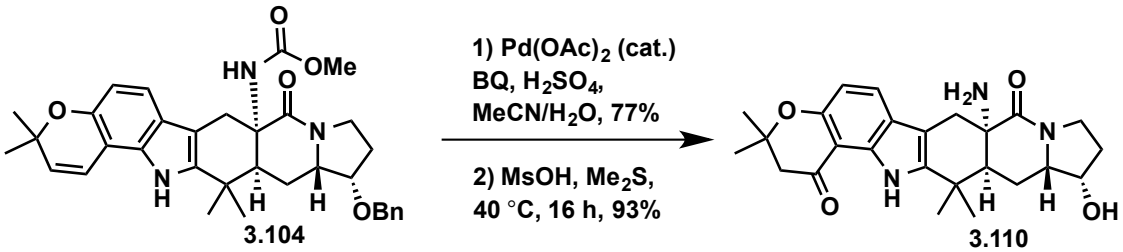

Scheme 3.26: Synthesis of divergent intermediate **3.110**.

3.4.2: Synthesis of (–)-17-Hydroxy-citrinalin B (3.18) From 3.110.

To complete the synthesis of 17-hydroxy-citrinalin B (**3.18**, Scheme 3.27), **3.110** was subjected to oxidative rearrangement using oxone, as previously described in the synthesis of citrinalin B[8c] (see Chapter 2.4.5), to provide **3.111**. This remarkable chemoselective oxidation cascade accomplished the conversion of the indole to the spirooxindole (corresponding to the desired diastereomer for **3.18**) as well as the oxidation of the amino group to the nitro group – all in the presence of the free secondary hydroxyl group.[43]

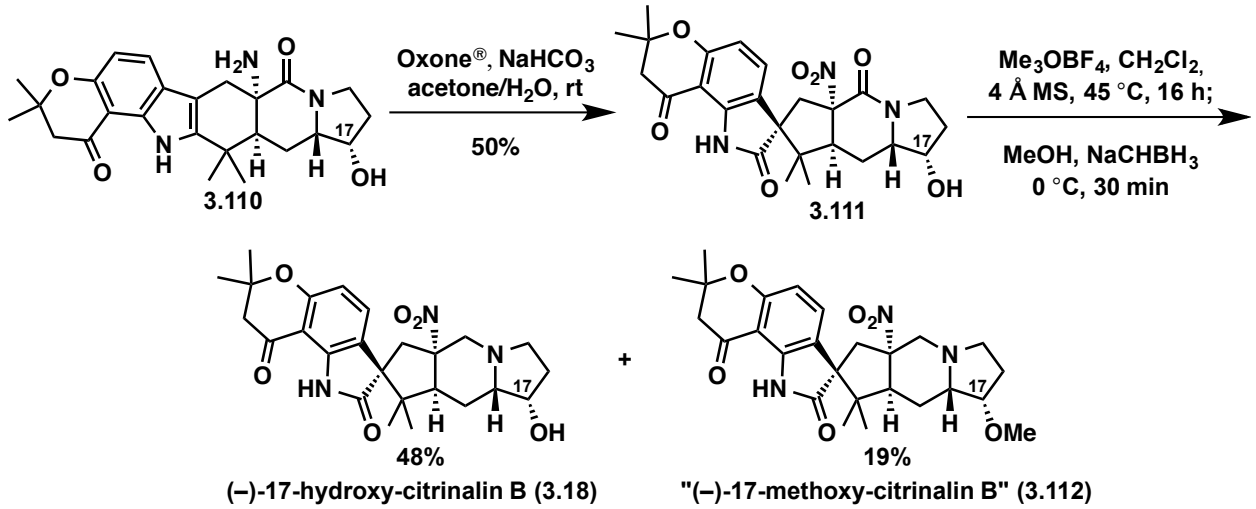

Scheme 3.27: Synthesis of (–)-17-hydroxy-citrinalin B (**3.18**).

With **3.111** in hand, chemoselective reductive removal of the tertiary amide carbonyl group (in the presence of several other functional groups that are susceptible to reduction) was accomplished following an adaptation of a procedure first reported by Borch.[44] Thus, subjection of **3.111** to Me_3OBF_4 followed by $NaCNBH_3$ proceeded in respectable yield to give (–)-17-hydroxy-citrinalin B (**3.18**) with the isolation of methyl

ether **3.112** in 19% yield as well (Note: This reaction was not optimized). Of note, in our hands, it was the TFA salt of **3.18** that provided analytical data identical in all respects to that of the natural isolate, which had been reported as the neutral compound.[8c,45]

Although our synthetic sequence for the preparation of (–)-17-hydroxy-citrinalin B mirrors closely our previous synthesis of citrinalin B (**3.12**, Figure 3.1) (see Chapter 2.4.6),[8c] it required a much more stringent level of chemoselectivity in the endgame. The success of this route is a testament to the robustness of our synthetic plan, which proceeded without event (especially in the endgame) even in the presence of a free hydroxyl group at C17 from intermediate **3.110** onwards.

3.4.3: Synthesis of (+)-stephacidin A (3.1) and (+)-notoamide I (3.2) from 3.110.

In an initial demonstration of the utility of **3.110** as an intermediate for the synthesis of prenylated indole alkaloid congeners possessing the bicyclo[2.2.2]diazaoctane structural motif, we have completed a synthesis of (+)-stephacidin A (**3.1**) and (+)-notoamide I (**3.2**) as outlined in Schemes 3.28 and 3.29. Thus, chemoselective carbamoylation of the primary amine of **3.110** (Scheme 3.28) was achieved in high yield in the presence of the secondary hydroxyl to afford phenyl carbamate **3.113**. Employing the optimized conditions from our model system (see Table 3.6), oxidation of the hydroxy group with DMP and treatment of the resulting ketone with K_2CO_3 forges the bicyclo[2.2.2]diazaoctane framework (**3.115**) of stephacidin A, presumably through a Dieckmann condensation via isocyanate/enolate intermediate **3.114**.[36]

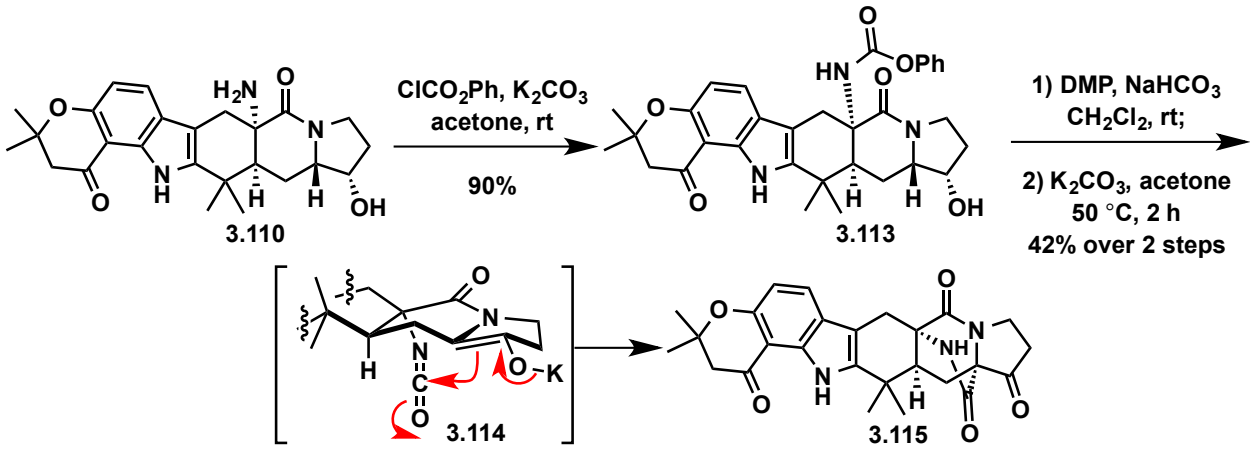

Scheme 3.28: Synthesis of versatile polycycle **3.115**.

These exceedingly simple conditions effectively accomplish the task of synthetically connecting the two major sub-families of the prenylated indole alkaloids. From our perspective, polycycle **3.115** represents a versatile framework that may be advanced to myriad prenylated indole alkaloids including mangrovamide A (**3.5**) and paraherquamide A (**3.6**) (see Figure 3.1).

To complete the synthesis of (+)-stephacidin A (**3.1**), removal of the ketone group in the pyrrolidine ring of **3.115** using a Wolff-Kishner protocol gave **3.116**. Reduction of the chromanone carbonyl group of **3.116** and elimination of the resulting hydroxyl gave (+)-stephacidin A (**3.1**) in 40% yield over the two steps (Scheme 3.29).[46] Analytical data for synthetic stephacidin A prepared by us matched perfectly previously reported spectra.[7a, 7e, 47] Furthermore, our X-ray analysis of a single crystal of **3.1** provided unambiguous support for the structure of the natural isolate (see CYLview in Scheme 3.29). Stephacidin A is a versatile starting point for the preparation of other prenylated indole alkaloids. For example, **3.1** was easily converted to (+)-notoamide I (**3.2**) upon treatment with MnO_2 in EtOAc (32% yield). Our synthesis of **3.1** also constitutes formal syntheses of (–)-notoamide B, (+)-avrainvillamide and (–)-stephacidin B.[7b, 7e]

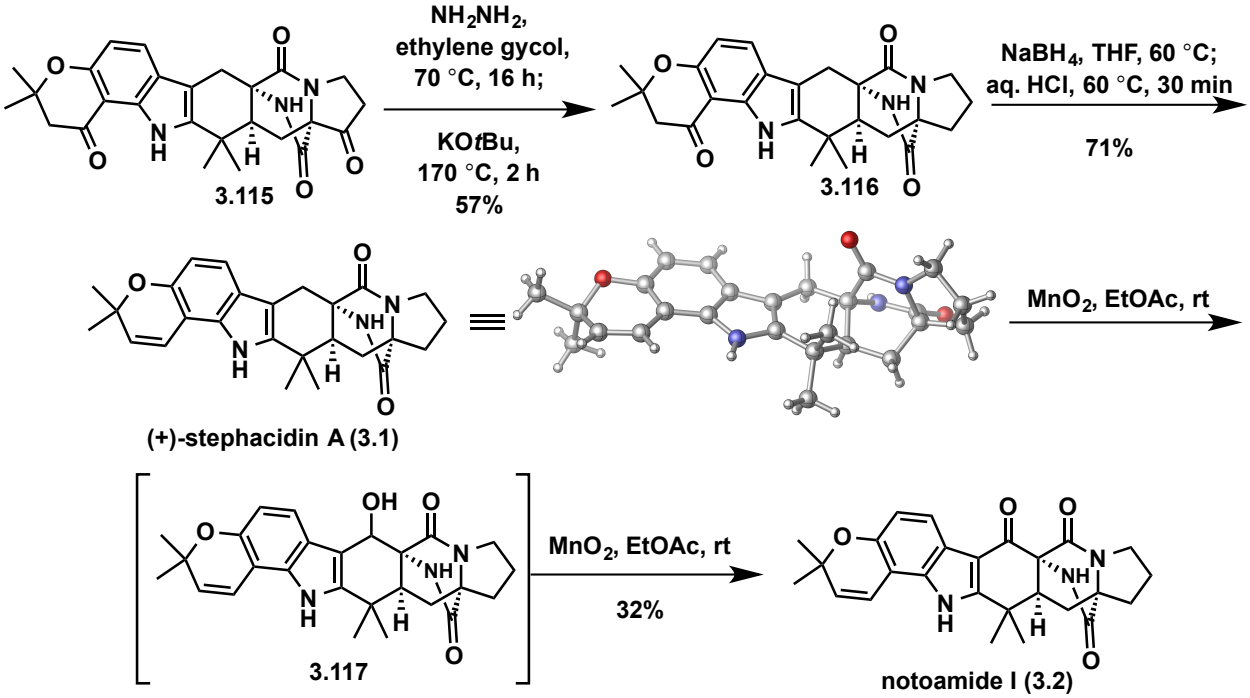

Scheme 3.29: Completed syntheses of stephacidin A (**3.1**) and notoamide I (**3.2**).

3.5 – Conclusion

In conclusion, we have achieved the first unified approach to the two sub-families of the prenylated indole alkaloids (i.e., that either lack or possess the bicyclo[2.2.2]diazaoctane structural motif). Our strategy has been exemplified with the first preparation of the natural product (–)-17-hydroxy-citrinalin B and of (+)-stephacidin A. Key to the success of the approach was the identification of a late-stage common intermediate (**3.110**), which could be advanced to either subclass of the prenylated indole alkaloids using a remarkably diastereoselective spirooxindole formation attended by a chemoselective oxidation of an amino group to a nitro group. Our synthesis of stephacidin A also featured a complexity building isocyanate capture to forge a [2.2.2]bicycle. Our studies now set the stage for the broad-ranging syntheses of congeners of the prenylated

indole alkaloid family to facilitate in-depth studies on their biosynthesis and biological activity.

3.6 – Experimental Contributors

All the work presented in this chapter was completed solely by Eduardo V. Mercado-Marin.

3.7 – Experimental Method and Procedure

3.7.1. General Experimental for the synthesis of compounds 3.1, 3.2, 3.18, 3.37-3.116.

Unless otherwise noted, all reactions were carried out under an atmosphere of nitrogen, and all reagents were purchased from commercial suppliers and used without further purification. All reactions were carried out in flame-dried glassware under a positive pressure of nitrogen in dry solvents using standard Schlenk techniques. Tetrahydrofuran (THF), diethyl ether (Et_2O), benzene, toluene (PhMe), methanol (MeOH) and triethylamine (Et_3N) were dried over alumina under an argon atmosphere in a GlassContour solvent system. Dichloromethane (CH_2Cl_2) and diisopropylethylamine (DIPEA) were distilled over calcium hydride under a nitrogen atmosphere. All other solvents and reagents were used as received unless otherwise noted. Reaction temperatures above room temperature (RT or rt), 23 °C, were controlled by an IKA® temperature modulator. Reaction progress was monitored by thin layer chromatography using SiliCycle silica gel 60 F254 precoated plates (0.25 mm) which were visualized using UV light (254 nm) and ninhydrin or $KMnO_4$ stain. Sorbtech silica gel (particle size 40-63 μm) was used for flash chromatography. Melting points were recorded on a Mel-Temp II by Laboratory Devices Inc., USA. Optical rotation was recorded on a Perkin Elmer Polarimeter 241 at the D line (1.0 dm path length), *c* = mg/mL. ^1H and ^{13}C NMR were recorded on Bruker AVB-400 and AV-600 MHz spectrometer with ^{13}C operating frequency of 100 and 150 MHz, respectively. Chemical shifts (δ) are reported in ppm relative to the residual solvent signal ($CDCl_3$ δ = 7.26 for ^1H NMR and δ = 77.16 for ^{13}C NMR; CD_3OD δ = 3.35 for ^1H NMR and δ = 49.3 for ^{13}C NMR; $(CD_3)_2SO$ δ = 2.50 for ^1H NMR and δ = 39.52 for ^{13}C NMR). Data for ^1H NMR are reported as follows: chemical shift (multiplicity, coupling constant, number of hydrogens). Multiplicity is abbreviated as follows: s (singlet), d (doublet), t (triplet), q (quartet), m (multiplet), br (broad). IR spectra were recorded on either a Nicolet MAGNA-IR 850 spectrometer or a Bruker Alpha Platinum ATR spectrometer and are reported in frequency of absorption (cm^{-1}). High-resolution mass spectral data were obtained from the University of California, Berkeley Mass Spectral Facility, on a VG Prospec Micromass spectrometer for EI.

3.7.2. Experimental Procedures for Compounds 3.1, 3.2, 3.18, 3.37-3.116.

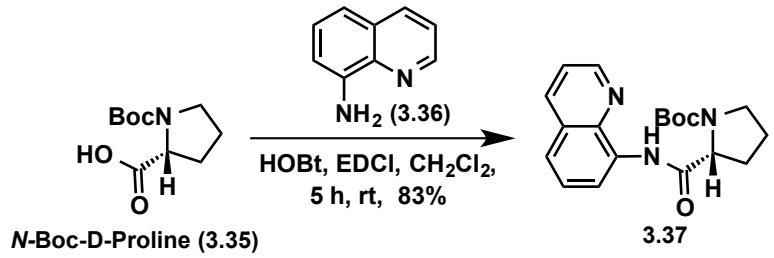

N-Boc-D-Proline (3.35) **3.37**

This procedure was adapted from a known procedure.[15] To a solution of *N*-Boc-D-proline **3.35** (200 mg, 0.929 mmol, 1.00 equiv) in dichloromethane (1.0 mL, 1.0M), was added 1-hydroxybenzotriazole (120 mg, 2.94 mmol, 3.16 equiv). The mixture was stirred for 15 minutes before it was cooled to 0 °C. 1-Ethyl-3-(3-dimethylaminopropyl)carbodiimide (230 mg, 6.59 mmol, 7.10 equiv) was added and the solution was stirred for an additional 20 minutes. A solution of 8-aminoquinoline (**3.36**) (260 mg, 8.11 mmol, 8.73 equiv) in dichloromethane (1.0 mL, 8.1M) was added to the solution, which was stirred for 5 h at rt. The reaction was quenched with water (10 mL) and the resulting mixture extracted with dichloromethane (3 x 10 mL). The combined organic layers were dried over Na_2SO_4, filtered and concentrated *in vacuo*. The crude oil was purified by silica gel chromatography (3:2 hexanes:ethyl acetate) to yield **3.37** (263 mg, 0.771 mmol, 83%) as a colorless solid. **^{1}H NMR** (600 MHz, $CDCl_3$, mixture of amide conformers 1.4:1) δ = 10.62–10.55 (br s, 0.4H), 10.37–10.28 (br s, 0.6H), 8.79–8.70 (m, 2H), 8.10–8.01 (m, 1H), 7.51–7.32 (m, 3H), 4.62–4.52 (m, 0.4H), 4.45–4.35 (m, 0.6H), 3.74–3.50 (m, 1.6H), 3.48–3.38 (m, 0.4H), 2.46–2.31 (m, 0.4H), 2.31–2.16 (m, 1.2H), 2.16–2.02 (m, 0.4H), 2.02–1.80 (m, 2H), 1.49 (s, 3.6H), 1.20 (s, 5.4H) ppm; **^{13}C NMR** (150 MHz, $CDCl_3$) δ = 171.2, 170.8, 155.1, 154.3, 148.2, 148.0, 138.4, 135.9, 134.3, 133.9, 127.7, 127.0, 121.4, 116.1, 80.3, 80.0, 62.2, 61.4, 47.0, 46.8, 31.1, 29.3, 28.3, 28.0, 24.3, 23.7. The spectroscopic data were consistent with those previously reported.[15]

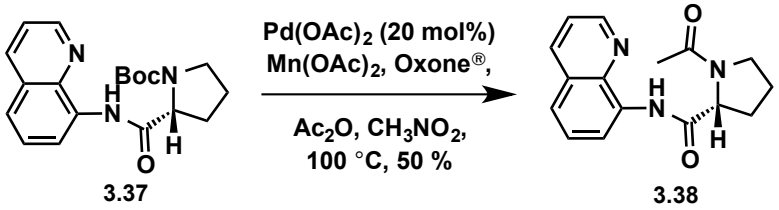

3.37 **3.38**

This procedure was adapted from a known procedure.[14] A mixture of amide **3.37** (34 mg, 0.100 mmol, 1.00 equiv), palladium(II)acetate (4.5 mg, 0.020 mmol, 0.20 equiv), manganese(II)acetate tetrahydrate (29 mg, 0.120 mmol, 1.20 equiv), Oxone® (76 mg, 0.500 mmol, 5.00 equiv), acetic anhydride (0.094 mL, 1.00 mmol, 10 equiv) and nitromethane (2 mL, 0.20M) was stirred at 100 °C for 27 h under an air atmosphere. The mixture was filtered through Celite™ and concentrated *in vacuo*. The crude brown oil was purified by silica gel chromatography (1:4 hexanes:ethyl acetate) to yield **3.38** (14 mg, 0.050 mmol, 50%) as a brown oil. **^{1}H NMR** (600 MHz, $CDCl_3$, mixture of amide conformers 3:1) δ = 10.54 (s, 0.75H), 10.39 (s,

0.25H), 8.89–8.80 (m, 1H), 8.77–8.69 (m, 1H), 8.21–8.10 (m, 1H), 7.59–7.41 (m, 3H), 4.87 (dd, J = 6.4, 3.3 Hz, 0.75H), 4.54 (dd, J = 7.8, 2.6 Hz, 0.25H), 3.95–3.86 (m, 0.25H), 3.81–3.73 (m, 1H), 3.64–3.54 (m, 0.75H), 2.47–2.39 (m, 1H), 2.24–2.03 (m, 6H) ppm; **^{13}C NMR** (150 MHz, $CDCl_3$) δ = 170.4, 170.1, 148.9, 148.4, 138.8, 136.3, 134.4, 128.0, 127.2, 127.1, 122.4, 121.8, 121.8, 121.5, 116.6, 63.4, 61.0, 48.2, 46.8, 32.3, 30.9, 29.7, 28.9, 25.0, 23.0, 22.5, 22.4 ppm; **IR** (NaCl, thin film) ν_{max}: 2926, 1685, 1647, 1531, 1425, 1324 cm^{-1}; **HRMS** (ESI) (*m/z*) $[M]^+$ calcd for $C_{16}H_{19}O_2N_3$, 284.1394; found, 284.1396.

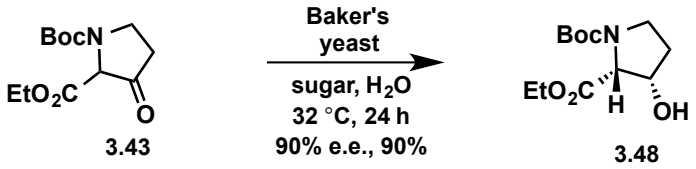

This procedure was adapted from a known procedure.[48] To a 2 L Erlenmeyer flask was added in succession 1-(*tert*-butyl) 2-ethyl 3-oxopyrrolidine-1,2-dicarboxylate[16,49] (**3.43**) (12.0 g, 46.7 mmol, 1.00 equiv), sugar (Trader Joe's Organic sugar™, 185 g, 1.03 mol, 22 equiv), and distilled water (940 mL, 0.05M). The mixture was placed in a water bath preheated to 32 °C and stirred until all the sugar had dissolved after which dry Baker's yeast (120 g, Red Star™) was added in one portion. The resulting mixture was stirred at 32 °C for 24 h then filtered using a Büchner funnel. The aqueous layer was extracted with ethyl acetate (5 x 700 mL) and the combined organic extracts were dried over Na_2SO_4, filtered, and concentrated *in vacuo*. The crude oil was purified by silica gel chromatography (150 mL SiO_2 with 2:3 ethyl acetate:hexanes) to yield **3.48** (9.65 grams, 37.2 mmol, 80%) as a clear, colorless oil. TLC (ethyl acetate:hexanes, 3:2 v/v): R_f=0.28; **^{1}H NMR** (600 MHz, $CDCl_3$, mixture of amide conformers 1:2) δ = 4.60–4.52 (m, 1H), 4.36 (d, J = 6.8 Hz, 0.33H), 4.29 (d, J = 6.8 Hz, 0.66H), 4.25 – 4.12 (m, 2H), 3.65 – 3.54 (m, 1H), 3.48 – 3.36 (m, 1H), 3.08 (br s, 1H), 2.11 – 2.02 (m, 1H), 2.02 – 1.93 (m, 1H), 1.42 (s, 3H), 1.38 (s, 6H), 1.29 – 1.22 (m, 3H); **^{13}C NMR** (150 MHz, $CDCl_3$, mixture of amide conformers 1:2) δ = 170.5, 170.3, 154.3, 153.8, 80.1, 80.0, 72.2, 71.3, 63.9, 63.4, 61.1, 61.0, 44.2, 43.7, 32.6, 32.1, 28.3, 28.2, 14.2, 14.1; $[\alpha]^{25}_D$ + 21.6 (c 1.21, CH_2Cl_2). The spectroscopic data were consistent with those previously reported. [16,48]

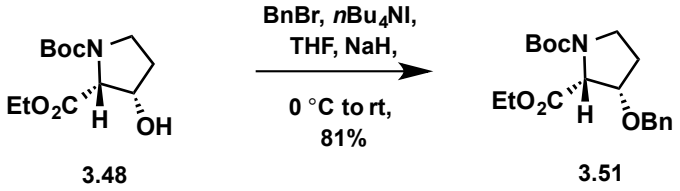

To a solution of 1-(*tert*-butyl) 2-ethyl (2*R*,3*S*)-3-hydroxypyrrolidine-1,2-dicarboxylate **(3.48)** (9.65 g, 37.2 mmol, 1.00 equiv), tetrabutylammonium iodide (3.71 g, 11.2 mmol, 0.30 equiv), and benzyl bromide (6.65 mL, 55.9 mmol, 1.5 equiv) in THF (250 mL, 0.15M) at 0 °C was added NaH (60% dispersion in mineral oil, 1.64 g, 40.9 mmol, 1.10 equiv) in three equal portions. The reaction mixture was slowly warmed to room temperature by allowing the ice bath to expire. After 4 h, additional benzyl bromide (4.0 mL, 16.2 mmol, 0.44 equiv) was added at room temperature and the resulting solution stirred for 15 h. The reaction was quenched by the addition of ice-cold water (100 mL) and the aqueous layer was extracted with ethyl acetate (4 x

150 mL). The combined organic layers were washed with brine (1 x 200 mL), dried over Na_2SO_4, filtered, and concentrated *in vacuo*. The crude oil was purified by silica gel chromatography (250 mL SiO_2 with 1:9 ethyl acetate:hexanes) to yield **3.51** (10.5 g, 30.1 mmol, 81%) as a clear, colorless oil. TLC (ethyl acetate:hexanes, 1:2 v/v): R_f=0.42; **^{1}H NMR** (600 MHz, $CDCl_3$, mixture of amide conformers 1:2) δ = 7.36 – 7.28 (m, 5H), 4.73 – 4.62 (m, 1H), 4.61 – 4.54 (m, 1.4H), 4.47 (d, *J* = 7.3 Hz, 0.6H), 4.35 – 4.13 (m, 3H), 3.73 – 3.60 (m, 1H), 3.41 – 3.31 (m, 1H), 2.22 – 2.11 (m, 1H), 2.10 – 2.02 (m, 1H), 1.46 (s, 3H), 1.43 (s, 6H), 1.28 – 1.19 (m, 3H); **^{13}C NMR** (150 MHz, $CDCl_3$, mixture of amide conformers 1:2) δ = 170.1, 170.0, 154.3, 153.8, 137.7, 137.6, 128.4, 128.3, 127.7, 127.6, 127.4, 80.1, 80.0, 78.8, 77.9, 72.1, 72.0, 62.0, 61.3, 60.9, 60.8, 43.9, 43.4, 29.8, 29.1, 28.4, 28.3, 28.2, 14.3, 14.1; **IR** (NaCl, thin film) ν_{max}: 3065, 2978, 1744, 1708, 1693, 1455, 1402 cm^{-1}; **HRMS** (ESI) calcd for $C_{19}H_{28}O_5N$ ([M]$^+$), 350.1962; found, 350.1968.

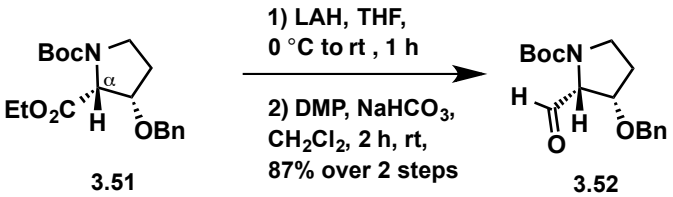

To a solution of 1-(*tert*-butyl) 2-ethyl (2*R*,3*S*)-3-(benzyloxy)pyrrolidine-1,2-dicarboxylate (**3.51**) (10.5 g, 30.1 mmol, 1.0 equiv) in THF (250 mL, 0.1M) cooled to 0 °C was added $LiAlH_4$ (2.85 g, 75.2 mmol, 2.5 equiv) in four equal portions. The resulting solution was stirred at 0 °C for 50 min then diluted with Et_2O (250 mL). The solution was cooled to 0 °C then 4.2 mL of distilled water was added dropwise, followed by 4.2 mL of 15% aqueous NaOH. After 5 min, 12.5 mL of distilled water was added and the solution was warmed to room temperature and stirred for 30 min. $MgSO_4$ (50 g) was then added and the solution was stirred at room temperature for 1.5 h, then filtered, and concentrated *in vacuo*. Analysis of the crude oil gave spectroscopic data consistent with those previously reported.[20] [**^{1}H NMR** (600 MHz, $CDCl_3$, mixture of amide conformers 1:2) δ = 7.38 – 7.28 (m, 5H), 4.68 – 4.56 (m, 1H), 4.54 – 4.45 (m, 1H), 4.35 – 4.22 (m, 1H), 4.19 – 4.10 (m, 0.7H), 4.02 – 3.71 (m, 3.3H), 3.49 – 3.32 (m, 2H), 2.73 (br s, 0.5H), 2.12 (br s, 0.5H), 2.05 – 1.88 (m, 2H), 1.46 (s, 9H); **^{13}C NMR** (150 MHz, $CDCl_3$, mixture of amide conformers 1:2) δ = 156.1, 154.3, 137.6, 137.3, 128.5, 128.4, 127.9, 127.8, 127.5, 80.0, 79.9, 79.5, 78.7, 71.9, 71.6, 63.2, 61.9, 61.8, 59.0, 44.4, 43.3, 29.2, 28.3.] The crude oil was dissolved in CH_2Cl_2 (170 mL, 0.18M) and $NaHCO_3$ (12.6 g, 150.3 mmol, 5.0 equiv) was added. The resulting solution was cooled to 0 °C and Dess-Martin periodinane (DMP) (14.0 g, 33.1 mmol, 1.1 equiv) was added in three equal portions. After 2.5 h, the resulting yellow solution was warmed to room temperature then poured into a separatory funnel containing 600 mL (1:1 v/v) saturated aqueous $NaHCO_3$ and saturated aqueous $Na_2S_2O_3$ and the layers separated. The aqueous layer was extracted with ethyl acetate (3 x 300 mL) and the combined organic extracts were dried over Na_2SO_4, filtered, and concentrated *in vacuo*. The crude oil was purified by silica gel chromatography (200 mL SiO_2 with 1:4 ethyl acetate:hexanes) to yield **3.52** (7.95 g, 26.1 mmol, 87% over 2 steps) as a clear, colorless oil. TLC (ethyl acetate:hexanes, 1:1 v/v): R_f=0.52; **^{1}H NMR** (600 MHz, $CDCl_3$, mixture of amide conformers 1:2) δ = 9.56 (d, *J* = 2.4 Hz, 0.33H), 9.50 (d, *J* = 3.6 Hz, 0.66H), 7.38 – 7.23 (m, 5H), 4.58 – 4.52 (m, 1H), 4.50 – 4.40 (m, 2H), 4.27 – 4.21 (m, 0.33H), 4.15 – 4.09 (m, 0.66H), 3.73 – 3.61 (m, 1.66H), 3.58 – 3.51 (m, 0.33H), 2.16 – 2.07 (m, 1H), 2.00 – 1.88 (m, 1H), 1.47 (s, 3H), 1.41 (s, 6H); **^{13}C NMR** (150 MHz, $CDCl_3$,

mixture of amide conformers 1:2) δ = 200.1, 154.7, 153.8, 137.2, 128.4, 127.9, 127.6, 127.5, 81.4, 80.8, 80.4, 80.2, 71.8, 71.6, 67.9, 67.6, 44.6, 44.5, 30.4, 29.8, 28.3, 28.2, 28.0; **IR** (NaCl, thin film) ν_{max}: 3032, 2977, 1737, 1704, 1455, 1397, 1367 cm^{-1}; **HRMS** (ESI) calcd for $C_{17}H_{23}O_4N_1Na$ ($[M+Na]^+$): 328.1519; found 328.1524.

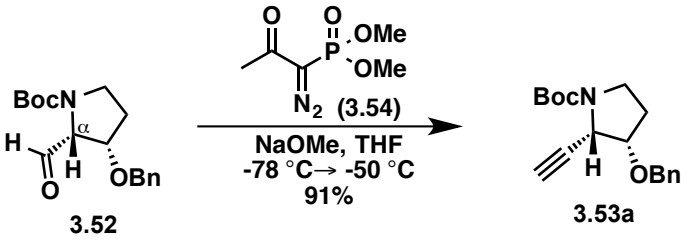

A solution of dimethyl (1-diazo-2-oxopropyl)phosphonate (**3.54**)[50] (15.04 g, 78.3 mmol, 1.5 equiv) in THF (200 mL, 0.39M) was added via cannula to a stirring suspension of NaOMe (13.5 g, 261 mmol, 5.0 equiv) in THF (200 mL, 1.30M) at –78 °C and stirred for 30 min. To this solution was added a cooled solution (–78 °C) of *tert*-butyl (2*R*,3*S*)-3-(benzyloxy)-2-formylpyrrolidine-1-carboxylate (**3.52**) (15.93 g, 52.2 mmol, 1.0 equiv) in THF (200 mL, 0.26M) via cannula along the side of the flask. The resulting solution was slowly warmed to –50 °C by allowing the dry ice/acetone bath to expire. Dry ice was added as needed to maintain a temperature of ≤ –50 °C. After TLC analysis indicated complete consumption of the starting material (approximately 2 h), saturated aqueous $NaHCO_3$ (400 mL) was added followed by Et_2O (500 mL). The solution was warmed to room temperature, the layers were separated, and the aqueous layer was extracted with Et_2O (3 x 500 mL). The combined organic extracts were dried over $MgSO_4$, filtered, and concentrated *in vacuo*. The crude yellow oil was purified by silica gel chromatography (300 mL SiO_2 with 1:9 ethyl acetate:hexanes) to yield **3.53a** (14.27 g, 47.4 mmol, 91%) as a white solid. **m.p.** 111-113 °C; TLC (ethyl acetate:hexanes, 1:1 v/v): R_f=0.75; **^{1}H NMR** (600 MHz, $CDCl_3$, mixture of amide conformers ~1:1) δ = 7.39 (d, *J* = 7.4 Hz, 2H), 7.35 (t, *J* = 7.4, 7.3 Hz, 2H), 7.30 (t, *J* = 7.3, 7.3 Hz, 1H), 4.76 – 4.69 (m, 1.5H), 4.60 (d, *J* = 6.2 Hz, 0.5H), 4.56 – 4.49 (m, 1H), 4.06 – 3.96 (m, 1H), 3.56 – 3.44 (m, 1H), 3.29 – 3.21 (m, 1H), 2.39 (s, 0.5H), 2.35 (s, 0.5H), 2.18 – 2.08 (m, 2H), 1.51 – 1.42 (m, 9H); **^{13}C NMR** (150 MHz, $CDCl_3$, mixture of amide conformers ~1:1) δ = 154.1, 137.6, 128.6, 128.1, 128.0, 80.3, 80.2, 79.9, 77.8, 77.4, 77.2, 77.02, 76.95, 73.3, 72.9, 72.2, 50.8, 50.2, 42.9, 42.3, 29.6, 28.8, 28.5; **IR** (NaCl, thin film) ν_{max}: 3288, 2978, 2892, 1694, 1497, 1477, 1455, 1393 cm^{-1}; **HRMS** (ESI) calcd for $C_{18}H_{23}O_3N_1Na$ ($[M+Na]^+$): 324.1570, found 324.1569.

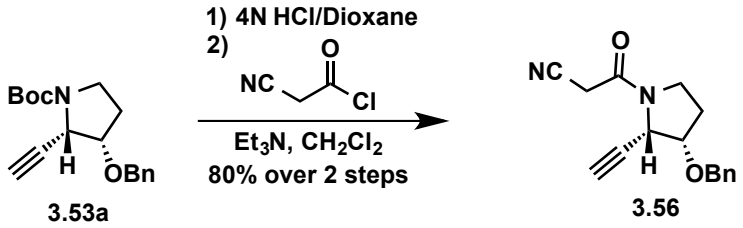

To a flask charged with *tert*-butyl (2*S*,3*S*)-3-(benzyloxy)-2-ethynylpyrrolidine-1-carboxylate (**3.53a**) (14.2 g, 47.2 mmol, 1.0 equiv) was added 4 N HCl/dioxane (60 mL, 236 mmol, 5.0 equiv) dropwise at 0 °C. The resulting solution was then warmed to room temperature and stirred for 30 min at which point the solvent was removed *in vacuo*. The excess HCl/dioxane was removed by azeotropic distillation with Et_2O (2 x 100 mL) and then hexanes (2 x 100 mL) to give a beige solid which was dried *in vacuo* overnight. The resulting crude mixture was suspended in CH_2Cl_2 (100 mL) and Et_3N (16.5 mL, 118 mmol, 2.5 equiv) was added dropwise at 0 °C, followed by the dropwise addition of cyanoacetylchloride (12.2 g, 118 mmol, 2.5 equiv) as a solution in CH_2Cl_2 (60 mL, 1.97 M). The resulting red solution was stirred at 0 °C for 2 h then warmed to room temperature and stirred for an additional 1 h. Saturated aqueous $NaHCO_3$ (200 mL) was added and the layers were separated. The aqueous layer was extracted with ethyl acetate (4 x 250 mL) and the combined organic extracts were dried over Na_2SO_4, filtered, and concentrated *in vacuo*. The crude red oil was purified by silica gel chromatography (400 mL SiO_2 with 2:3 to 3:2 ethyl acetate:hexanes) to yield **3.56** (9.52 g, 35.5 mmol, 75% over 2 steps) as an orange solid. **m.p.** 123-124 °C; TLC (ethyl acetate:hexanes, 4:1 v/v): R_f=0.47; **^{1}H NMR** (600 MHz, $CDCl_3$, mixture of amide conformers ~2:3) δ = 7.41 – 7.30 (m, 5H), 4.94 (dd, *J* = 6.4, 2.3 Hz, 0.4H), 4.74 (d, *J* = 11.6 Hz, 0.4H), 4.71 (d, *J* = 11.6 Hz, 0.6H), 4.64 – 4.58 (m, 1.2H), 4.55 (d, *J* = 11.6 Hz, 0.4H), 4.18 (dt, *J* = 9.1, 6.2 Hz, 0.6H), 4.06 (dt, *J* = 9.7, 6.3 Hz, 0.4H), 3.76 – 3.59 (m, 2H), 3.50 – 3.37 (m, 2H), 2.60 (d, *J* = 2.4 Hz, 0.6H), 2.44 (d, *J* = 2.2 Hz, 0.4H), 2.37 – 2.21 (m, 1H), 2.21 – 2.08 (m, 1H); **^{13}C NMR** (150 MHz, $CDCl_3$, mixture of amide conformers ~2:3) δ = 160.9, 160.4, 137.2, 137.1, 128.68, 128.65, 128.3, 128.2, 128.1, 128.0, 113.9, 113.5, 78.3, 77.9, 77.7, 76.6, 76.4, 74.3, 72.58, 72.5, 51.71, 50.67, 44.1, 43.7, 29.9, 28.4, 25.8, 25.4; **IR** (NaCl, thin film) ν_{max}: 3273, 3248, 2939, 2888, 2361, 1663, 1454, 1434, 1399 cm^{-1}; **HRMS** (ESI) calcd for $C_{16}H_{16}O_2N_2Na$ ($[M+Na]^+$): 291.1104, found 291.1103.

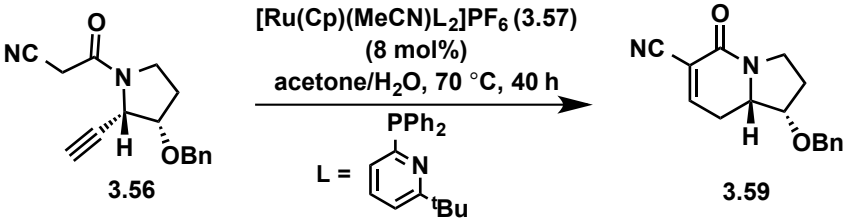

This procedure was adapted from a known procedure.[23] To a Schlenk flask charged with 3-((2*S*,3*S*)-3-(benzyloxy)-2-ethynylpyrrolidin-1-yl)-3-oxopropanenitrile (**3.56**) (832 mg, 3.10 mmol, 1.0 equiv) and a stir bar in a nitrogen atmosphere glove box was added acetonitrilebis[2-diphenylphosphino-6-*t*-butylpyridine]cyclopentadienylruthenium(II) hexafluorophosphate (**3.57**) (248 mg, 0.250 mmol, 0.08 equiv). A solution of acetone (6.3 mL) and HPLC grade water (0.280 mL) (deoxygenated by via three cycles of freeze/pump/thaw method) was added to the Schlenk flask in the glove box via syringe. The reaction vessel was then capped and removed from the

glove box and the resulting yellow solution was placed in a preheated oil bath and stirred at 70 °C for 24 h, at which time the reaction mixture was diluted with ethyl acetate (10 mL) and concentrated *in vacuo*. The resulting yellow oil was purified by silica gel chromatography (40 mL SiO_2 with 1:1 to 2:1 ethyl acetate:hexanes) to yield **3.59** (770 mg, 2.87 mmol, 93%) as a yellow solid. **m.p**. 94-96 °C; TLC (ethyl acetate:hexanes, 4:1 v/v): R_f=0.36; **^{1}H NMR** (600 MHz, $CDCl_3$) δ = 7.37 – 7.27 (m, 6H), 4.66 (d, *J* = 11.9 Hz, 1H), 4.46 (d, *J* = 11.9 Hz, 1H), 4.11 (t, *J* = 3.6 Hz, 1H), 3.86 (dt, *J* = 13.9, 4.5 Hz, 1H), 3.76 – 3.70 (m, 1H), 3.57 (td, *J* = 11.4, 7.3 Hz, 1H), 2.93 (ddd, *J* = 18.9, 14.0, 2.4 Hz, 1H), 2.47 (ddd, *J* = 18.9, 6.6, 5.0 Hz, 1H), 2.28 (dd, *J* = 13.9, 7.2 Hz, 1H), 1.87 (dtd, *J* = 13.8, 10.0, 3.7 Hz, 1H); **^{13}C NMR** (150 MHz, $CDCl_3$) δ = 157.3, 153.3, 137.6, 128.6 (2C), 128.0, 127.6 (2C), 114.8, 113.6, 78.0, 71.1, 59.6, 42.9, 28.1, 25.4; **IR** (NaCl, thin film) ν_{max}: 3032, 2952, 2233, 1665, 1608, 1453, 1346, 1302, 1210 cm^{-1}; **HRMS** (ESI) calcd for $C_{16}H_{17}O_2N_2$ ($[M+H]^+$): 269.1285, found 269.1282.

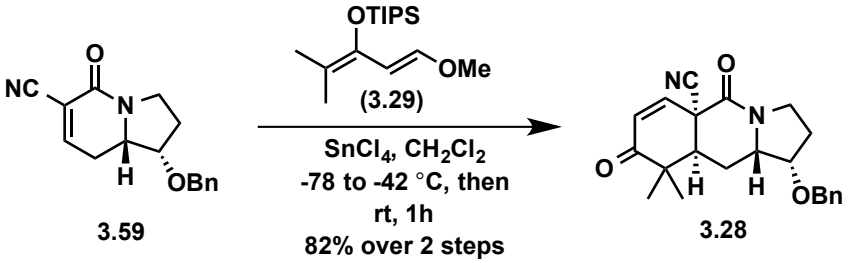

A solution of (1*S*,8a*S*)-1-(benzyloxy)-5-oxo-1,2,3,5,8,8a-hexahydroindolizine-6-carbonitrile (**3.59**) (2.82 g, 10.52 mmol, 1.0 equiv) and (*E*)-triisopropyl((1-methoxy-4-methylpenta-1,3-dien-3-yl)oxy)silane (**3.29**)[8c] (5.97 g, 21.0 mmol, 2.0 equiv) in CH_2Cl_2 (105 mL, 0.1M) was cooled to –78 °C and then $SnCl_4$ (1.0 M in CH_2Cl_2, 12.6 mL, 12.62 mmol, 1.2 equiv) was added dropwise. The resulting red solution was then warmed to –42 °C (MeCN/dry ice) and after 40 min, additional (*E*)-triisopropyl((1-methoxy-4-methylpenta-1,3-dien-3-yl)oxy)silane (**3.29**) (2.0 g, 7.03 mmol, 0.66 equiv) was added and the MeCN/dry ice bath removed. The solution was allowed to warm to room temperature and stirred for 30 min, then saturated aqueous $NaHCO_3$ (100 mL) was added and the mixture was stirred vigorously for 3 h. The resulting mixture was vacuum filtered through a fritted funnel and the layers separated. The aqueous layer was extracted with CH_2Cl_2 (3 x 100 mL), and the combined organic extracts were dried over Na_2SO_4, filtered, and concentrated *in vacuo*. The resulting oil was purified by silica gel chromatography (200 mL SiO_2 with 3:7 to 7:3 ethyl acetate:hexanes) to yield **3.28** (2.86 g, 7.85 mmol, 75%) as a yellow foam. TLC (ethyl acetate:hexanes, 2:1 v/v): R_f=0.30; **^{1}H NMR** (600 MHz, $CDCl_3$) δ = 7.38 – 7.27 (m, 5H), 6.81 (d, *J* = 10.1 Hz, 1H), 6.17 (d, *J* = 10.1 Hz, 1H), 4.66 (d, *J* = 12.2 Hz, 1H), 4.44 (d, *J* = 12.2 Hz, 1H), 3.98 (t, *J* = 3.7 Hz, 1H), 3.81 (ddd, *J* = 12.1, 9.8, 8.0 Hz, 1H), 3.58 – 3.52 (m, 1H), 3.48 (ddd, *J* = 12.1, 9.6, 2.2 Hz, 1H), 2.81 (dd, *J* = 7.5, 3.6 Hz, 1H), 2.53 (ddd, *J* = 14.9, 10.8, 7.5 Hz, 1H), 2.23 – 2.16 (m, 1H), 1.97 – 1.90 (m, 1H), 1.82 (dtd, *J* = 13.8, 9.8, 4.0 Hz, 1H), 1.39 (s, 3H), 1.15 (s, 3H); **^{13}C NMR** (150 MHz, $CDCl_3$) δ = 200.8, 161.8, 138.8, 137.7, 129.6, 128.6 (2C), 128.0, 127.5 (2C), 118.2, 78.2, 70.9, 59.6, 45.6, 45.3, 45.1, 44.3, 28.0, 24.8, 22.6, 22.4; **IR** (NaCl, thin film) ν_{max}: 2948, 2868, 2250, 1660, 1589, 1454, 1392, 1345 cm^{-1}; **HRMS** (ESI) calcd for $C_{22}H_{24}O_3N_2Na$ ($[M+Na]^+$): 387.1679, found 387.1676.

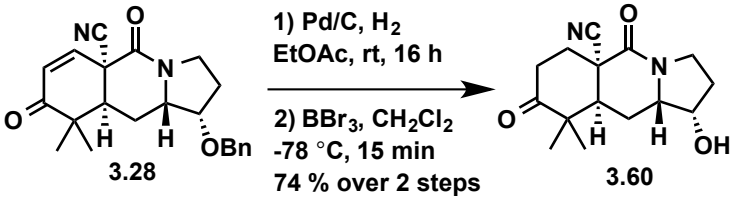

To a round-bottomed flask containing (1*S*,5a*R*,9a*S*,10a*S*)-1-(benzyloxy)-9,9-dimethyl-5,8-dioxo-1,2,3,8,9,9a,10,10a-octahydropyrrolo[1,2-*b*]isoquinoline-5a(5*H*)-carbonitrile (**3.28**) (930 mg, 2.55 mmol, 1.0 equiv) was added Pd/C (93 mg, 10 wt%) and ethyl acetate (2 mL) and the atmosphere purged with H_2 (three cycles of evacuation/backfill). Additional ethyl acetate (45 mL, 0.6M) was added and the resulting mixture was stirred at room temperature overnight. After 16 h, the reaction mixture was filtered through Celite and washed with ethyl acetate. The solvent was removed *in vacuo* and the resulting pale yellow oil was used without further purification. The crude oil was dissolved in CH_2Cl_2 (78 mL, 0.033M) and cooled to –78 °C. BBr_3 (1.10 mL, 11.7 mmol, 4.6 equiv) was then added dropwise along the side of the flask and stirred for 15 min at which point saturated aqueous $NaHCO_3$ (80 mL) was added and the mixture warmed to room temperature. The layers were separated and the aqueous layer was extracted with CH_2Cl_2 (4 x 80 mL). The combined organic extracts were dried over Na_2SO_4, filtered, and concentrated *in vacuo*. The resulting oil was purified by silica gel chromatography (40 mL SiO_2 with 2% to 5% methanol:dichloromethane) to yield **3.60** (524 mg, 1.89 mmol, 74% over 2 steps) as a white solid. **m.p.** 167-169 °C. TLC (methanol:dichloromethane, 1:9 v/v): R_f=0.60; **^{1}H NMR** (600 MHz, $CDCl_3$) δ = 4.24 – 4.14 (m, 1H), 3.93 (dt, *J* = 12.5, 9.0 Hz, 1H), 3.56 – 3.49 (m, 1H), 3.48 – 3.41 (m, 1H), 3.34 (ddd, *J* = 12.8, 7.7, 5.2 Hz, 1H), 2.73 – 2.63 (m, 2H), 2.60 – 2.36 (m, 4H), 2.00 (td, *J* = 8.5, 8.1, 3.3 Hz, 2H), 1.91 (dt, *J* = 14.7, 6.3 Hz, 1H), 1.37 (s, 3H), 1.12 (s, 3H); **^{13}C NMR** (150 MHz, $CDCl_3$) δ = 212.3, 164.2, 121.5, 72.3, 60.1, 48.0, 46.1, 43.9, 43.0, 34.3, 31.4, 29.8, 26.3, 22.8, 21.9; **IR** (NaCl, thin film) ν_{max}: 3413, 2927, 2360, 1712, 1647, 1456 cm^{-1}; **HRMS** (ESI) calcd for $C_{15}H_{20}O_3N_2Na$ ($[M+Na]^+$): 299.1366, found 299.1367.

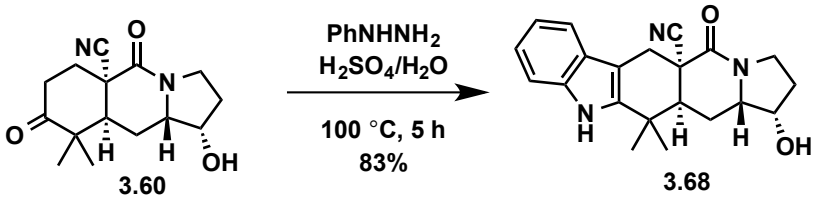

To a suspension of (1*S*,5a*R*,9a*S*,10a*S*)-1-hydroxy-9,9-dimethyl-5,8-dioxodecahydropyrrolo[1,2-*b*]isoquinoline-5a(5*H*)-carbonitrile (**3.60**) (524 mg, 1.90 mmol, 1.0 equiv) in aqueous H_2SO_4 (5% v/v, 32 mL, 0.06M) was added phenylhydrazine (0.75 mL, 7.60 mmol, 4.0 equiv) at room temperature and the resulting mixture was heated to 100 °C. After 14 h, the resulting reaction mixture was cooled to room temperature and then filtered through a Büchner funnel, layered with a medium porosity filter paper, and washed with water (30 mL) and then diethyl ether (2 x 30 mL). The beige solid was collected and dried *in vacuo* overnight to yield **3.68** (550 mg, 1.58 mmol, 83%) as a beige solid. **^{1}H NMR** (600 MHz, $(CD_3)_2SO$) δ = 11.02 (s, 1H), 7.44 (d, *J* = 7.8 Hz, 1H), 7.32 (d, *J* = 7.8 Hz, 1H), 7.07 (t, *J* = 7.5 Hz, 1H), 6.98 (t, *J* = 7.5 Hz, 1H), 5.16 (d, *J* = 4.8 Hz, 1H), 4.00 (q, *J* = 3.8 Hz, 1H), 3.72 (dt, *J* = 11.9, 8.9 Hz, 1H), 3.55 (d, *J* = 9.2 Hz, 1H), 3.24 – 3.16 (m, 2H), 3.05 (d, *J* = 15.8 Hz, 1H), 2.41 (dd, *J* = 13.0, 6.0 Hz, 1H), 2.26 (ddd, *J* =

14.3, 6.2, 2.2 Hz, 1H), 1.93 (dtd, *J* = 13.8, 9.6, 4.4 Hz, 1H), 1.78 (ddd, *J* = 12.7, 8.9, 2.6 Hz, 1H), 1.72 – 1.66 (m, 1H), 1.65 (s, 3H), 1.39 (s, 3H); **^{13}C NMR** (150 MHz, $(CD_3)_2SO$) δ = 165.3, 139.6, 136.2, 126.3, 122.4, 120.9, 118.5, 117.8, 110.9, 101.9, 72.1, 57.9, 45.1, 43.1, 42.8, 34.7, 30.5, 29.6, 27.3, 26.3, 20.4.; **HRMS** (ESI) calcd for $C_{21}H_{23}O_2N_3Na$ ($[M+Na]^+$): 372.1682, found 372.1682.

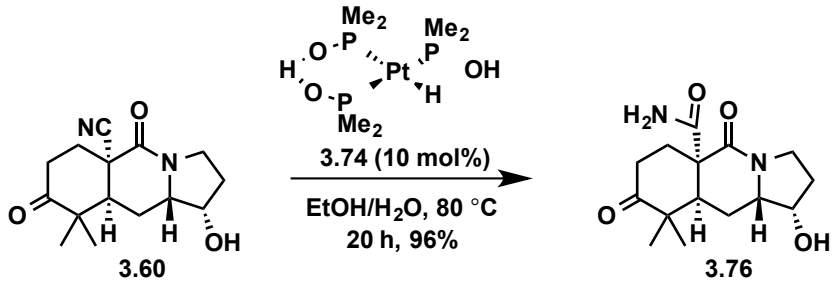

3.60 3.76

$(Me_2POH)_2Pt(H)(Me_2PO)$[25] (**3.74**) (68 mg, 0.16 mmol, 0.1 equiv) was added in one portion to a solution of (1*S*,5a*R*,9a*S*,10a*S*)-1-hydroxy-9,9-dimethyl-5,8-dioxodecahydropyrrolo[1,2-*b*]isoquinoline-5a(5*H*)-carbonitrile (**3.60**) (440 mg, 1.59 mmol, 1.0 equiv) in a mixture of EtOH/H_2O (4:1 v/v, 10.6 mL, 0.15M). The reaction mixture was heated to 80 °C for 16 hours and then cooled to room temperature. The resulting solution was then diluted with CH_2Cl_2 (10 mL) and passed through a short column containing silica gel (10 mL) layered with Na_2SO_4 (20 mL) and washed with 10% MeOH/CH_2Cl_2 (50 mL). The filtrate was concentrated *in vacuo* and purified by silica gel chromatography (20 mL SiO_2 with 5% to 10% methanol:dichloromethane) to yield **3.76** (451 mg, 1.53 mmol, 96%) as a white solid. **m.p.** 236-238 °C; TLC (methanol:dichloromethane, 1:9 v/v): R_f = 0.24; **^{1}H NMR** (600 MHz, $CDCl_3$) δ = 7.14 (s, 1H), 6.32 (s, 1H), 4.17 (s, 1H), 3.86 (dt, *J* = 11.5, 9.2 Hz, 1H), 3.52 (dd, *J* = 11.9, 5.7 Hz, 1H), 3.38 (ddd, *J* = 12.7, 8.7, 4.1 Hz, 1H), 3.06 – 3.00 (m, 1H), 2.62 (dt, *J* = 14.0, 6.4 Hz, 1H), 2.43 (t, *J* = 6.9 Hz, 2H), 2.23 (dt, *J* = 14.0, 6.9 Hz, 1H), 2.02 – 1.88 (m, 4H), 1.23 (s, 3H), 1.14 (s, 3H); **^{13}C NMR** (150 MHz, $CDCl_3$) δ = 214.6, 174.3, 171.2, 71.6, 61.2, 52.5, 46.9, 43.6, 41.4, 35.1, 31.4, 30.9, 25.2, 22.7, 21.4.

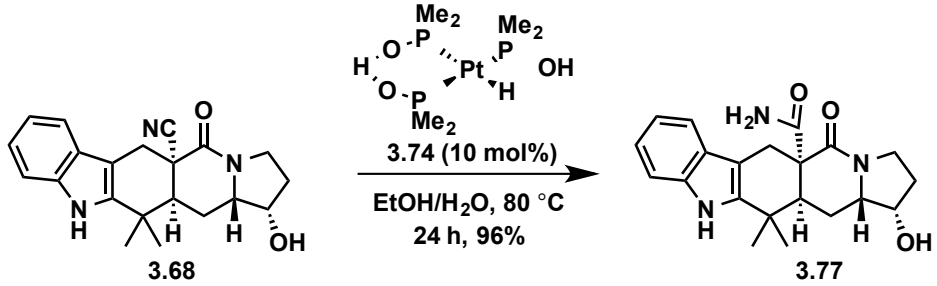

3.68 3.77

$(Me_2POH)_2Pt(H)(Me_2PO)$[25] (**3.74**) (43 mg, 0.10 mmol, 0.1 equiv) was added in one portion to a solution of (1*S*,5a*R*,12a*S*,13a*S*)-1-hydroxy-12,12-dimethyl-5-oxo-2,3,6,11,12,12a,13,13a-octahydro-1*H*-indolizino[7,6-*b*]carbazole-5a(5*H*)-carbonitrile (**3.68**) (350 mg, 1.0 mmol, 1.0

equiv) in a mixture of EtOH/H_2O (4:1 v/v, 10.0 mL, 0.10M). The reaction mixture was heated to 80 °C for 12 hours and then cooled to room temperature. The resulting solution was then diluted with CH_2Cl_2 (10 mL) and passed through a short column containing silica gel (10 mL) layered with Na_2SO_4 (20 mL) and washed with 20% MeOH/CH_2Cl_2 (50 mL). The filtrate was concentrated *in vacuo* and purified by silica gel chromatography (20 mL SiO_2 with 10% to 20% methanol:dichloromethane) to yield **3.77** (358 mg, 0.97 mmol, 97%) as a white foam. TLC (methanol:dichloromethane, 1:9 v/v): R_f= 0.20; **^{1}H NMR** (600 MHz, $(CD_3)_2SO$) δ = 10.68 (s, 1H), 7.37 (d, *J* = 7.7 Hz, 1H), 7.25 (d, *J* = 7.7 Hz, 1H), 7.00 (ddd, *J* = 8.1, 7.0, 1.2 Hz, 1H), 6.97 (s, 1H), 6.94 – 6.90 (m, 1H), 6.84 (s, 1H), 3.95 (dd, *J* = 4.8, 2.9 Hz, 1H), 3.67 (dt, *J* = 11.9, 8.6 Hz, 1H), 3.51 – 3.45 (m, 1H), 3.18 (d, *J* = 15.9 Hz, 1H), 3.09 (ddd, *J* = 11.9, 10.6, 3.2 Hz, 1H), 2.90 (d, *J* = 15.9 Hz, 1H), 2.66 (dd, *J* = 9.6, 5.9 Hz, 1H), 2.22 (dt, *J* = 14.0, 5.6 Hz, 1H), 1.99 – 1.91 (m, 1H), 1.79 – 1.63 (m, 2H), 1.48 – 1.39 (m, 1H), 1.34 (s, 3H), 1.33 (s, 3H).; **^{13}C NMR** (150 MHz, $(CD_3)_2SO$) δ = 174.6, 170.5, 140.0, 136.1, 126.6, 120.2, 117.9, 117.7, 110.6, 104.0, 71.6, 58.8, 53.2, 43.1, 42.1, 34.7, 31.2, 30.1, 26.7, 24.4, 20.8.; **IR** (neat) ν_{max}: 3276, 3187, 2951, 2883, 1665, 1613, 1460, 1297, 1196 cm^{-1}; **HRMS** (ESI) calcd for $C_{21}H_{25}O_3N_3Na$ ($[M+Na]^+$): 390.1788, found 390.1790.

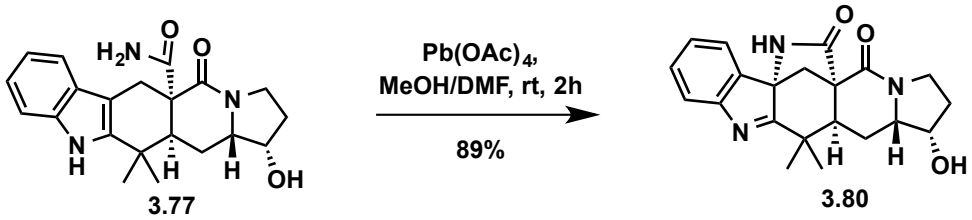

To a solution of (1*S*,5a*R*,12a*S*,13a*S*)-1-hydroxy-12,12-dimethyl-5-oxo-2,3,6,11,12,12a,13,13a-octahydro-1*H*-indolizino[7,6-*b*]carbazole-5a(5*H*)-carboxamide (**3.77**) (100 mg, 0.272 mmol, 1.0 equiv) in a mixture of DMF/MeOH (1:1 v/v, 9.1 mL, 0.03M) was added $Pb(OAc)_4$ (241 mg, 0.545 mmol, 2.0 equiv) at room temperature. The resulting brown-red mixture was stirred at room temperature for 2 h at which time sat. aq. $NaHCO_3$ (20 mL) was added. The biphasic mixture was then transferred to a 100 mL separatory funnel and the aqueous layer was extracted with ethyl acetate (5 x 40 mL). The combined organic layers were dried over Na_2SO_4, then filtered and concentrated *in vacuo*. The resulting residue was purified by silica gel chromatography (10 mL SiO_2 with 1% to 2% to 5% methanol:dichloromethane) to yield **3.80** (88 mg, 0.241 mmol, 89%) as a white foam. TLC (ethyl acetate:hexanes, 1:9 v/v): R_f= 0.27; **^{1}H NMR** (600 MHz, $(CD_3)_2SO$) δ = 8.26 (s, 1H), 7.55 (d, *J* = 7.3 Hz, 1H), 7.53 (d, *J* = 7.3 Hz, 1H), 7.42 (td, *J* = 7.4, 1.3 Hz, 1H), 7.27 (td, *J* = 7.4, 1.3 Hz, 1H), 5.08 (s, 1H), 4.01 (s, 1H), 3.65 (dt, *J* = 11.7, 8.4 Hz, 1H), 3.22 (d, *J* = 9.6 Hz, 1H), 3.05 (td, *J* = 11.2, 3.5 Hz, 1H), 2.39 (dd, *J* = 13.6, 5.2 Hz, 1H), 2.22 (dd, *J* = 13.9, 5.7 Hz, 1H), 2.11 (dd, *J* = 11.3, 1.7 Hz, 1H), 1.95 – 1.88 (m, 1H), 1.82 (td, *J* = 13.9, 9.5 Hz, 1H), 1.70 (ddd, *J* = 13.2, 9.1, 3.6 Hz, 1H), 1.37 (s, 3H), 1.32 (s, 3H); **^{13}C NMR** (150 MHz, $(CD_3)_2SO$) δ = 190.3, 177.0, 167.0, 154.7, 135.0, 129.7, 125.7, 123.2, 120.4, 71.8, 69.3, 58.1, 54.4, 41.7, 41.4, 38.5, 32.0, 30.7, 24.9, 21.5.; **HRMS** (ESI) calcd for $C_{21}H_{24}O_3N_3$ ($[M+H]^+$): 366.1812, found 366.1818.

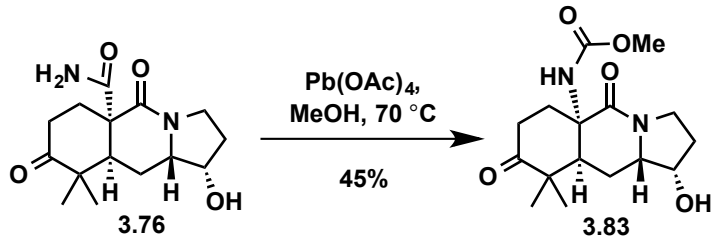

To a solution of (1*S*,5a*R*,9a*S*,10a*S*)-1-hydroxy-9,9-dimethyl-5,8-dioxodecahydropyrrolo[1,2-*b*]isoquinoline-5a(5*H*)-carboxamide (**3.76**) (224 mg, 0.761 mmol, 1.0 equiv) in anhydrous MeOH (7.6 mL, 0.10M) was added $Pb(OAc)_4$ (844 mg, 1.90 mmol, 2.5 equiv) in one portion at room temperature. The resulting mixture was heated to 70 °C for 3.5 h at which time the reaction mixture was cooled to room temperature. Additional $Pb(OAc)_4$ (844 mg, 1.90 mmol, 2.5 equiv) was added in one portion at room temperature and then the resulting mixture was heated to 70 °C for 2 h. The resulting reaction mixture was then cooled to room temperature and additional $Pb(OAc)_4$ (844 mg, 1.90 mmol, 2.5 equiv) was added in one portion at room temperature and then the resulting mixture heated to 70 °C for 1.5 h. The reaction mixture was then cooled to room temperature and poured into a 250 mL separatory funnel containing sat. aq. $NaHCO_3$ (60 mL). The aqueous layer was extracted with ethyl acetate (5 x 60 mL) and the combined organic layers were dried over Na_2SO_4, then filtered and concentrated *in vacuo*. The resulting residue was purified by silica gel chromatography (20 mL SiO_2 with 2% to 5% to 10% methanol:dichloromethane) to yield **3.83** (110 mg, 0.339 mmol, 45%) as a white foam and recovered **3.76** (17 mg, 0.0578 mmol, 7.6% recovery). TLC (methanol:dichloromethane, 1:9 v/v): R_f= 0.37; **^{1}H NMR** (600 MHz, $CDCl_3$) δ = 5.32 (s, 1H), 4.17 (s, 1H), 3.98 (q, *J* = 9.5 Hz, 1H), 3.67 (s, 3H), 3.43 – 3.35 (m, 1H), 3.27 (t, *J* = 11.3 Hz, 1H), 3.09 (t, *J* = 7.3 Hz, 1H), 2.75 – 2.65 (m, 1H), 2.41 – 2.25 (m, 3H), 2.09 – 2.00 (m, 1H), 1.99 – 1.91 (m, 1H), 1.80 (dt, *J* = 15.1, 7.6 Hz, 1H), 1.42 (s, 3H), 1.14 (s, 3H); **^{13}C NMR** (150 MHz, $CDCl_3$) δ = 214.7, 170.8, 157.1, 73.3, 59.6, 58.5, 52.4, 47.9, 45.3, 43.3, 33.5, 32.1, 31.0, 27.9, 23.3, 22.6.; **HRMS** (ESI) calcd for $C_{16}H_{25}O_5N_2$ ($[M+H]^+$): 325.1758, found 325.1761; calcd for $C_{16}H_{24}O_5N_2Na$ ($[M+Na]^+$): 347.1577, found 347.1578.

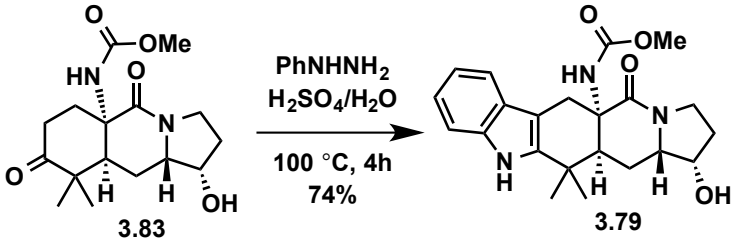

To a suspension of methyl ((1*S*,5a*S*,9a*S*,10a*S*)-1-hydroxy-9,9-dimethyl-5,8-dioxodecahydropyrrolo[1,2-*b*]isoquinolin-5a(5*H*)-yl)carbamate (**3.83**) (110 mg, 0.339 mmol, 1.0 equiv) in aqueous H_2SO_4 (5% v/v, 5.7 mL, 0.06M) was added phenylhydrazine (0.140 mL, 1.36 mmol, 4.0 equiv) at room temperature and the resulting mixture was heated to 100 °C. After 3.5 h, the resulting reaction mixture was cooled to room temperature and slowly poured into a 250 mL separatory funnel containing sat. aq. $NaHCO_3$ (60 mL) and stirred gently until bubbling ceased. The aqueous layer was then extracted with ethyl acetate (5 x 60 mL) and the combined

organic layers were dried over Na_2SO_4, then filtered and concentrated *in vacuo*. The resulting residue was purified by silica gel chromatography (20 mL SiO_2 with 2% to 5% to 10% methanol:dichloromethane) to yield **3.79** (100 mg, 0.252 mmol, 74%) as a yellow solid. TLC (methanol:dichloromethane, 1:9 v/v): R_f= 0.30; **^{1}H NMR** (600 MHz, $CDCl_3$) δ = 7.92 (s, 1H), 7.41 (d, *J* = 8.1 Hz, 1H), 7.35 (d, *J* = 8.1 Hz, 1H), 7.18 (t, *J* = 7.6 Hz, 1H), 7.11 (t, *J* = 7.6 Hz, 1H), 5.03 (s, 1H), 4.16 – 4.09 (m, 2H), 3.61 (s, 3H), 3.43 (d, *J* = 9.0 Hz, 1H), 3.31 – 3.24 (m, 1H), 3.17 (dd, *J* = 13.9, 5.5 Hz, 1H), 3.12 (d, *J* = 16.6 Hz, 1H), 2.95 (d, *J* = 16.6 Hz, 1H), 2.45 (dd, *J* = 14.6, 5.5 Hz, 1H), 2.16 – 2.08 (m, 1H), 2.01 – 1.94 (m, 1H), 1.87 – 1.80 (m, 2H), 1.47 (s, 3H), 1.41 (s, 3H); **^{13}C NMR** (150 MHz, $CDCl_3$) δ = 171.6, 156.6, 140.1, 136.4, 127.1, 121.8, 119.7, 117.8, 111.0, 101.9, 74.3, 59.2, 58.7, 52.3, 42.5, 40.9, 34.7, 32.0, 30.7, 28.7, 28.0, 22.2; **HRMS** (ESI) calcd for $C_{22}H_{28}O_4N_3$ ($[M+H]^+$): 398.2074, found 398.2077.

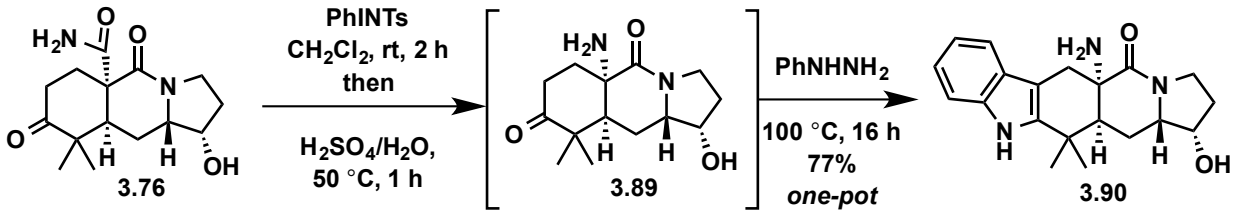

To a solution of (1*S*,5a*R*,9a*S*,10a*S*)-1-hydroxy-9,9-dimethyl-5,8-dioxodecahydropyrrolo[1,2-*b*]isoquinoline-5a(5*H*)-carboxamide (**3.76**) (500 mg, 1.70 mmol, 1.0 equiv) in anhydrous CH_2Cl_2 (34 mL, 0.05M) was added (tosylimio)-phenyl-λ^3-iodane[35] (PhINTs) (760 mg, 2.04 mmol, 1.2 equiv) in one portion at room temperature. The resulting solution was stirred at room temperature for 2 h, until TLC indicated complete consumption of starting material, and then aqueous H_2SO_4 (5% v/v, 34 mL) was added and the resulting solution was heated to 50 °C for 1 h. The biphasic reaction mixture was then cooled to room temperature and the organic layer was removed by pipette. To the remaining aqueous layer was added phenylhydrazine (0.67 mL, 6.80 mmol, 4.0 equiv) and the solution was then heated to 100 °C for 16 h. The solution was then cooled to 0 °C and solid K_2CO_3 was added portion-wise until bubbling had ceased followed by aqueous NaOH (5% w/v, 3 mL) to ensure a pH ≥ 12. The resulting reaction mixture was transferred to a 100 mL separatory funnel and the aqueous layer was extracted with ethyl acetate (5 x 40 mL). The combined organic layers were dried over Na_2SO_4, then filtered and concentrated *in vacuo*. The resulting residue was purified by silica gel chromatography (50 mL SiO_2 with 5% to 10% to 20% methanol:dichloromethane) to yield **3.90** (443 mg, 1.31 mmol, 77%) as an orange/brownish solid. TLC (methanol:dichloromethane, 1:9 v/v): R_f= 0.07; **^{1}H NMR** (600 MHz, $(CH_3)_2SO$) δ = 10.79 (s, 1H), 7.33 (d, *J* = 8.0 Hz, 1H), 7.29 (d, *J* = 8.0 Hz, 1H), 7.01 (t, *J* = 7.6 Hz, 1H), 6.92 (t, *J* = 7.6 Hz, 1H), 3.97 (d, *J* = 3.5 Hz, 1H), 3.67 (q, *J* = 9.7 Hz, 1H), 3.47 (d, *J* = 9.7 Hz, 1H), 3.16 (t, *J* = 11.1 Hz, 1H), 2.93 (d, *J* = 15.4 Hz, 1H), 2.49 (d, *J* = 15.4 Hz, 1H), 2.25 (ddd, *J* = 14.0, 6.6, 3.1 Hz, 1H), 1.96 – 1.85 (m, 2H), 1.80 – 1.74 (m, 1H), 1.63 – 1.57 (m, 1H), 1.55 (s, 3H), 1.35 (s, 3H); **^{13}C NMR** (150 MHz, $(CH_3)_2SO$) δ = 173.6, 140.0, 136.3, 127.3, 120.2, 118.0, 117.4, 110.6, 103.0, 71.9, 58.0, 56.4, 45.4, 42.6, 34.8, 30.9, 30.5, 30.0, 27.4, 21.8; **IR** (neat) ν_{max}: 3286, 2951, 2926, 2894, 1625, 1554, 1465, 1302, 1203, 1130 cm^{-1}; **HRMS** (ESI) calcd for $C_{20}H_{26}O_2N_3$ ($[M+H]^+$): 340.2020, found 340.2016.

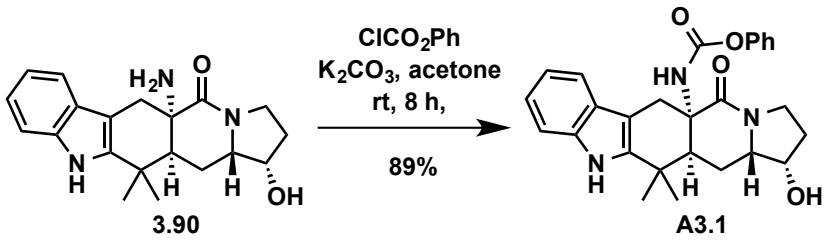

To a solution of (1*S*,5a*S*,12a*S*,13a*S*)-5a-amino-1-hydroxy-12,12-dimethyl-1,2,3,5a,6,11,12,12a,13,13a-decahydro-5*H*-indolizino[7,6-*b*]carbazol-5-one (**3.90**) (100 mg, 0.295 mmol, 1.0 equiv), and K_2CO_3 (81 mg, 0.59 mmol, 2.0 equiv) in anhydrous acetone (5.9 mL, 0.05M) was added phenyl chloroformate (45 μL, 0.354 mmol, 1.2 equiv) by syringe and stirred at room temperature. After 3.5 h, additional phenyl chloroformate (45 μL, 0.354 mmol, 1.2 equiv) was added by syringe and the mixture was stirred for an additional 3.5 h at which point water (6 mL) was added slowly. The resulting aqueous layer was extracted with ethyl acetate (4 x 8 mL) and the combined organic layers were dried over Na_2SO_4, then filtered and concentrated *in vacuo*. The resulting residue was purified by silica gel chromatography (10 mL SiO_2 with 2% to 5% to 10% methanol:dichloromethane) to yield **A3.1** (120 mg, 0.261 mmol, 89%) as an orange foam. TLC (methanol:dichloromethane, 1:9 v/v): R_f= 0.52; **^{1}H NMR** (600 MHz, $CDCl_3$) δ = 8.39 (s, 1H), 7.45 (d, *J* = 7.8 Hz, 1H), 7.38 (d, *J* = 8.0 Hz, 1H), 7.24 (t, *J* = 7.8 Hz, 2H), 7.19 (t, *J* = 7.6 Hz, 1H), 7.14 – 7.08 (m, 2H), 7.02 (d, *J* = 7.9 Hz, 2H), 5.43 (s, 1H), 4.09 – 4.00 (m, 2H), 3.40 (d, *J* = 10.0 Hz, 1H), 3.28 (td, *J* = 11.5, 3.5 Hz, 1H), 3.22 – 3.14 (m, 2H), 3.03 (d, *J* = 16.5 Hz, 1H), 2.45 – 2.39 (m, 1H), 2.05 – 1.97 (m, 1H), 1.89 (ddd, *J* = 13.7, 9.3, 3.5 Hz, 1H), 1.79 (td, *J* = 14.0, 9.5 Hz, 1H), 1.59 (s, 3H), 1.42 (s, 3H); **^{13}C NMR** (150 MHz, $CDCl_3$) δ = 171.1, 154.4, 150.9, 140.0, 136.4, 129.2, 127.1, 125.3, 121.92, 121.89, 119.8, 117.9, 111.1, 102.0, 74.3, 59.5, 58.6, 42.5, 40.8, 34.8, 31.9, 30.8, 28.7, 28.0, 22.2; **HRMS** (ESI) calcd for $C_{27}H_{30}O_4N_3$ ($[M+H]^+$): 460.2231, found 460.2238.

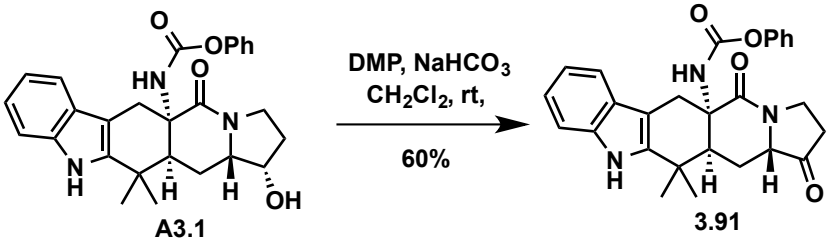

To a solution of phenyl ((1*S*,5a*S*,12a*S*,13a*S*)-1-hydroxy-12,12-dimethyl-5-oxo-2,3,6,11,12,12a,13,13a-octahydro-1*H*-indolizino[7,6-*b*]carbazol-5a(5*H*)-yl)carbamate (**A3.1**) (57.8 mg, 0.126 mmol, 1.0 equiv) in reagent grade CH_2Cl_2 (2.5 mL, 0.05M) was added Dess-Martin periodinane (DMP) (85.6 mg, 0.201 mmol, 1.6 equiv) in eight portions (8 x 10.7 mg) at 10 minute intervals at room temperature. After 20 minutes at room temperature sat. aq. $NaHCO_3$ (5.0 mL) was added and the biphasic mixture was stirred until the organic layer was no longer cloudy. The layers were separated and the aqueous layer was extracted with ethyl acetate (4 x 3 mL). The combined organic extracts were dried over Na_2SO_4, then filtered, and concentrated *in vacuo*. The resulting residue was purified by silica gel chromatography (10 mL SiO_2 with 20% to

40% to 60% ethyl acetate:hexanes) to yield **3.91** (35 mg, 0.0765 mmol, 60%) as an orange foam. TLC (methanol:dichloromethane, 1:19 v/v): R_f= 0.32; **^{1}H NMR** (600 MHz, $CDCl_3$) δ = 8.26 (s, 1H), 7.45 (d, *J* = 7.8 Hz, 1H), 7.38 (d, *J* = 8.1 Hz, 1H), 7.27 (d, *J* = 7.5 Hz, 2H), 7.20 (t, *J* = 7.7 Hz, 1H), 7.15 – 7.11 (m, 2H), 7.03 (d, *J* = 8.0 Hz, 2H), 5.43 (s, 1H), 4.64 (t, *J* = 10.7 Hz, 1H), 3.55 (d, *J* = 9.7 Hz, 1H), 3.31 (dt, *J* = 11.7, 8.6 Hz, 1H), 3.21 (d, *J* = 16.6 Hz, 1H), 3.04 (d, *J* = 16.6 Hz, 1H), 2.88 (dd, *J* = 13.9, 5.6 Hz, 1H), 2.57 – 2.39 (m, 3H), 1.90 (td, *J* = 14.2, 9.7 Hz, 1H), 1.57 (s, 3H), 1.42 (s, 3H); **^{13}C NMR** (150 MHz, $CDCl_3$) δ = 210.4, 171.2, 154.1, 150.8, 139.7, 136.4, 129.3, 127.0, 125.5, 122.2, 121.8, 120.0, 118.0, 111.1, 101.9, 60.0, 59.6, 41.0, 40.3, 35.8, 34.7, 30.4, 28.3, 28.2, 22.0; **HRMS** (ESI) calcd for $C_{27}H_{28}O_4N_3$ ($[M+H]^+$): 458.2074, found 458.2075.

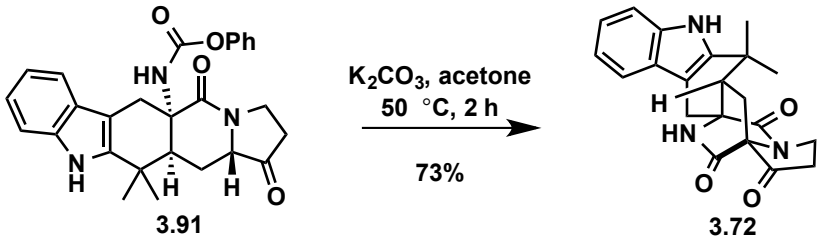

A solution of phenyl ((5a*S*,12a*S*,13a*S*)-12,12-dimethyl-1,5-dioxo-2,3,6,11,12,12a,13,13a-octahydro-1*H*-indolizino[7,6-*b*]carbazol-5a(5*H*)-yl)carbamate (**3.91**) (43.8 mg, 0.0958 mmol, 1.0 equiv), and K_2CO_3 (26.5 mg, 0.192 mmol, 2.0 equiv) in anhydrous acetone (3.8 mL, 0.025M) was heated to 50 °C for 2 h. After cooling the reaction mixture to room temperature sat. aq. NH_4Cl (4.0 mL) was added and the aqueous layer was extracted with ethyl acetate (4 x 4 mL). The combined organic extracts were dried over Na_2SO_4, and then filtered and concentrated *in vacuo*. The resulting residue was purified by silica gel chromatography (5 mL SiO_2 with 1% to 2% to 5% methanol:dichloromethane) to yield **3.72** (25.5 mg, 0.0702 mmol, 73%) as a white powder. TLC (methanol:dichloromethane, 1:19 v/v): R_f= 0.31; **^{1}H NMR** (600 MHz, $(CH_3)_2SO$) δ = 10.78 (s, 1H), 8.98 (s, 1H), 7.39 (d, *J* = 7.8 Hz, 1H), 7.28 (d, *J* = 8.0 Hz, 1H), 7.05 (t, *J* = 7.6 Hz, 1H), 6.97 (t, *J* = 7.3 Hz, 1H), 3.74 (td, *J* = 10.6, 4.1 Hz, 1H), 3.52 (q, *J* = 8.9 Hz, 1H), 3.47 (d, *J* = 15.4 Hz, 1H), 2.82 (q, *J* = 9.6 Hz, 1H), 2.78 – 2.71 (m, 2H), 2.56 (dd, *J* = 10.3, 4.8 Hz, 1H), 2.24 (dd, *J* = 13.4, 10.3 Hz, 1H), 2.17 (dd, *J* = 13.5, 4.8 Hz, 1H), 1.27 (s, 3H), 1.01 (s, 3H); **^{13}C NMR** (150 MHz, $(CH_3)_2SO$) δ = 205.6, 169.3, 169.0, 140.7, 136.4, 126.4, 120.7, 118.3, 117.5, 110.8, 103.0, 66.8, 60.5, 48.5, 38.2, 36.3, 34.6, 27.8, 27.1, 23.6, 21.9; **HRMS** (ESI) calcd for $C_{21}H_{22}O_3N_3$ ($[M+H]^+$): 364.1656, found 364.1656.

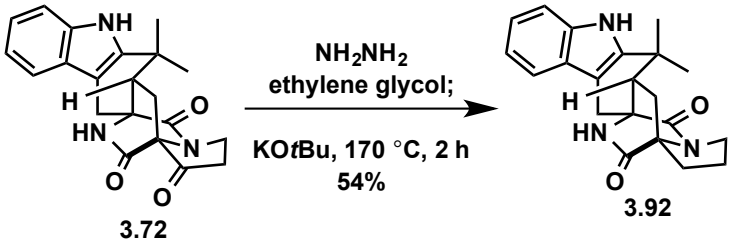

To a solution of (12a*S*,13a*S*)-12,12-dimethyl-2,3,11,12,12a,13-hexahydro-1*H*,5*H*,6*H*-5a,13a-(epiminomethano)indolizino[7,6-*b*]carbazole-1,5,14-trione (**3.72**) (39.0 mg, 0.107 mmol, 1.0 equiv) in deoxygenated (via three cycles of freeze/pump/thaw) ethylene glycol (4.3 mL, 0.025M) was added hydrazine (3.4 μL, 0.107 mmol, 1.0 equiv) via micro-syringe. The solution was then heated at 70 °C for 17 h, at which time the solution was cooled to room temperature and *t*BuOK (36.0 mg, 0.321 mmol, 3.0 equiv) was added in one portion at room temperature and the solution was then placed in a preheated heating block at 170 °C. After 2 h, the reaction was cooled to room temperature and saturated aqueous NH_4Cl (10 mL) was added and the aqueous layer was extracted with ethyl acetate (4 x 8 mL). The combined organic layers were dried over Na_2SO_4, filtered, and concentrated *in vacuo*. The resulting residue was purified by silica gel chromatography (3 mL SiO_2 with 1% to 3% to 5% methanol:dichloromethane) to yield **3.92** (20.0 mg, 0.0573 mmol, 54%) as a beige powder. **^{1}H NMR** (600 MHz, $CDCl_3$) δ = 10.74 (s, 1H), 8.70 (s, 1H), 7.37 (d, *J* = 7.7 Hz, 1H), 7.27 (d, *J* = 7.9 Hz, 1H), 7.04 (td, *J* = 7.7, 3.2 Hz, 1H), 6.97 (td, *J* = 7.5, 3.3 Hz, 1H), 3.44 (dd, *J* = 15.4, 3.4 Hz, 1H), 3.28 – 3.22 (m, 1H), 2.70 (dd, *J* = 15.5, 3.5 Hz, 1H), 2.57 – 2.52 (m, 1H), 2.46 (dd, *J* = 9.9, 4.7 Hz, 1H), 2.06 (td, *J* = 11.7, 10.0, 3.4 Hz, 1H), 2.02 – 1.94 (m, 2H), 1.89 – 1.79 (m, 2H), 1.28 (s, 3H), 1.00 (s, 3H); **^{13}C NMR** (150 MHz, $CDCl_3$) δ = 173.0, 168.5, 140.7, 136.4, 126.5, 120.6, 118.1, 117.5, 110.7, 103.3, 66.0, 59.7, 49.1, 43.5, 34.5, 30.1, 28.7, 27.9, 24.0, 23.8, 21.6. The spectroscopic data were consistent with those previously reported.[24a]

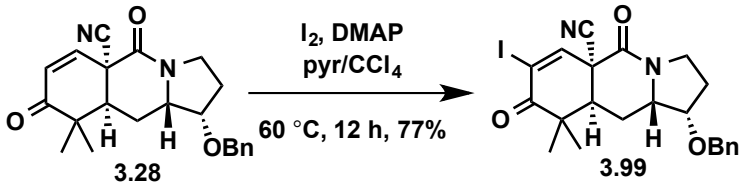

Iodine (2.10 g, 8.24 mmol, 1.5 equiv) and 4-dimethylaminopyridine (1.00g, 8.24 mmol, 1.5 equiv) were added sequentially to a solution of (1*S*,5a*R*,9a*S*,10a*S*)-1-(benzyloxy)-9,9-dimethyl-5,8-dioxo-1,2,3,8,9,9a,10,10a-octahydropyrrolo[1,2-*b*]isoquinoline-5a(5*H*)-carbonitrile (**3.28**) (2.00 g, 5.50 mmol, 1.0 equiv) in a mixture of pyridine/CCl_4 (1:1 v/v, 14.0 mL, 0.40M). The reaction flask was wrapped in aluminum foil and the resulting dark brown mixture was stirred at 60 °C in the dark for 15 h and then the reaction was cooled to room temperature. Additional iodine (2.10 g, 8.24 mmol, 1.5 equiv) and 4-dimethylaminopyridine (1.00g, 8.24 mmol, 1.5 equiv) were added sequentially to the solution, which was then stirred at 60 °C for 6 h, at which time the reaction mixture was cooled to room temperature. The reaction mixture was then poured into saturated aqueous $Na_2S_2O_3$ (80 mL) and the aqueous layer was extracted with a mixture of ethyl acetate/hexanes (1:1 v/v, 4 x 80 mL). The combined organic extracts were dried over Na_2SO_4, filtered, and concentrated *in vacuo*. The resulting dark oil was purified by silica

gel chromatography (50 mL SiO_2 with 1:4 to 3:2 ethyl acetate:hexanes) to yield **3.99** (2.08 g, 4.24 mmol, 77%) as a beige foam. TLC (ethyl acetate:hexanes, 4:1 v/v): R_f= 0.65; **^{1}H NMR** (600 MHz, $CDCl_3$) δ = 7.55 (s, 1H), 7.37 – 7.27 (m, 5H), 4.65 (d, *J* = 12.1 Hz, 1H), 4.43 (d, *J* = 12.2 Hz, 1H), 3.99 (t, *J* = 3.8 Hz, 1H), 3.84 – 3.77 (m, 1H), 3.53 – 3.45 (m, 2H), 2.85 (dd, *J* = 7.4, 3.7 Hz, 1H), 2.52 (ddd, *J* = 15.0, 10.7, 7.4 Hz, 1H), 2.20 (ddd, *J* = 14.1, 8.1, 2.3 Hz, 1H), 1.91 (dt, *J* = 15.0, 4.5 Hz, 1H), 1.88 – 1.80 (m, 1H), 1.44 (s, 3H), 1.19 (s, 3H); **^{13}C NMR** (150 MHz, $CDCl_3$) δ = 194.8, 160.6, 145.5, 137.6, 128.6 (2C), 128.0, 127.4 (2C), 117.1, 105.6, 78.2, 70.9, 59.5, 48.2, 45.8, 45.1, 44.4, 27.9, 25.2, 22.9, 22.5; **IR** (neat) ν_{max}: 3032, 2921, 1697, 1660, 1448, 1346, 1204 cm^{-1}; **HRMS** (ESI) calcd for $C_{22}H_{23}O_3N_2INa$ ([M+Na]$^+$): 513.0646, found 513.0670.

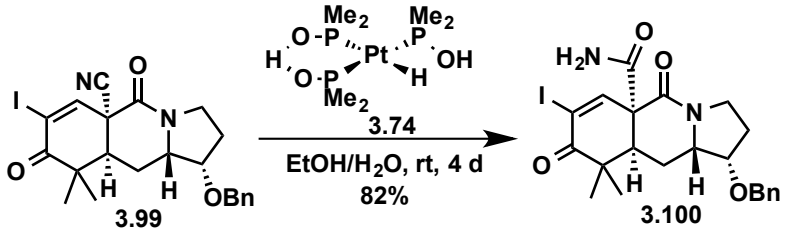

$(Me_2POH)_2Pt(H)(Me_2PO)$ (**3.74**)[25] (88 mg, 0.20 mmol, 0.2 equiv) was added in one portion to a solution of (1*S*,5a*S*,9a*S*,10a*S*)-1-(benzyloxy)-7-iodo-9,9-dimethyl-5,8-dioxo-1,2,3,8,9,9a,10,10a-octahydropyrrolo[1,2-*b*]isoquinoline-5a(5*H*)-carbonitrile (**3.99**) (500 mg, 1.02 mmol, 1.0 equiv) in a mixture of EtOH/H_2O (4:1 v/v, 5.1 mL, 0.2M). The reaction vessel was wrapped in aluminum foil and the resulting mixture stirred in the absence of light at room temperature. After 62 h, additional $(Me_2POH)_2Pt(H)(Me_2PO)$ (**3.74**) (44 mg, 0.10 mmol, 0.1 equiv) was added and the mixture stirred in the absence for light at room temperature for an additional 36 h. The resulting solution was then diluted with CH_2Cl_2 (10 mL) and passed through a short column containing silica gel (20 mL) layered with Na_2SO_4 (20 mL) and washed with 10% MeOH/CH_2Cl_2 (50 mL). The filtrate was concentrated *in vacuo* and purified by silica gel chromatography (20 mL SiO_2 with 2% to 5% methanol:dichloromethane) to yield **3.100** (423 mg, 0.832 mmol, 82%) as a yellow foam. TLC (methanol:dichloromethane, 1:19 v/v): R_f= 0.33; **^{1}H NMR** (600 MHz, $CDCl_3$) δ = 7.84 (s, 1H), 7.39 – 7.26 (m, 5H), 7.25 (s, 1H), 5.30 (s, 1H), 4.60 (d, *J* = 12.0 Hz, 1H), 4.45 (d, *J* = 12.0 Hz, 1H), 3.94 (t, *J* = 3.3 Hz, 1H), 3.86 (dt, *J* = 12.6, 9.1 Hz, 1H), 3.72 (ddd, *J* = 12.0, 5.4, 2.8 Hz, 1H), 3.45 (ddd, *J* = 12.6, 10.3, 2.2 Hz, 1H), 3.24 (dd, *J* = 5.4, 2.8 Hz, 1H), 2.35 (ddd, *J* = 14.9, 11.9, 5.4 Hz, 1H), 2.23 (ddd, *J* = 14.0, 8.6, 2.2 Hz, 1H), 2.07 – 2.01 (m, 1H), 1.91 – 1.83 (m, 1H), 1.34 (s, 3H), 1.16 (s, 3H); **^{13}C NMR** (150 MHz, $CDCl_3$) δ = 196.0, 168.0, 167.3, 152.6, 137.7, 128.6 (2C), 128.0, 127.5 (2C), 103.0, 77.7, 70.8, 60.9, 59.1, 45.2, 43.7, 39.4, 27.9, 23.3, 22.6, 20.7; **IR** (neat) ν_{max}: 3416, 3323, 2970, 2921, 1691, 1636, 1584, 1455, 1344, 1205 cm^{-1}; **HRMS** (ESI) calcd for $C_{22}H_{25}O_4N_2INa$ ([M+Na]$^+$): 531.0751, found 531.0739.

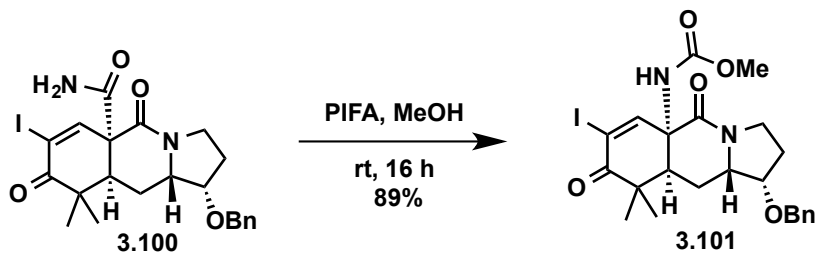

To a solution of (1*S*,5a*S*,9a*S*,10a*S*)-1-(benzyloxy)-7-iodo-9,9-dimethyl-5,8-dioxo-1,2,3,8,9,9a,10,10a-octahydropyrrolo[1,2-*b*]isoquinoline-5a(5*H*)-carboxamide (**3.100**) (700 mg, 1.38 mmol, 1.0 equiv) in methanol (14.0 mL, 0.1M) cooled to 0 °C was added [Bis(trifluoroacetoxy)iodo]benzene (PIFA) (650 mg, 1.51 mmol, 1.1 equiv) in one portion. The resulting mixture was stirred at room temperature for 16 h then poured into saturated aqueous $NaHCO_3$ (60 mL) and the aqueous layer extracted with ethyl acetate (4 x 60 mL). The combined organic extracts were dried over Na_2SO_4, filtered, and concentrated *in vacuo*. The resulting orange oil was purified by silica gel chromatography (40 mL SiO_2 with 2:3 to 4:1 ethyl acetate:hexanes) to yield **3.101** (658 mg, 1.22 mmol, 89%) as a pale yellow foam. TLC (ethyl acetate:hexanes, 4:1 v/v): R_f= 0.39; **^{1}H NMR** (600 MHz, $CDCl_3$) δ = 7.41 (s, 1H), 7.35 – 7.26 (m, 5H), 5.63 (bs, 1H), 4.61 (d, *J* = 12.0 Hz, 1H), 4.42 (d, *J* = 12.0 Hz, 1H), 3.95 (td, *J* = 3.8, 1.1 Hz, 1H), 3.78 – 3.71 (m, 1H), 3.64 (s, 3H), 3.45 – 3.38 (m, 2H), 3.11 (s, 1H), 2.39 (ddd, *J* = 14.7, 11.7, 7.7 Hz, 1H), 2.15 (ddt, *J* = 13.9, 7.5, 1.7 Hz, 1H), 1.90 (ddd, *J* = 14.8, 4.4, 2.0 Hz, 1H), 1.82 – 1.75 (m, 1H), 1.36 (s, 3H), 1.19 (s, 3H); **^{13}C NMR** (150 MHz, $CDCl_3$) δ = 197.0, 166.3, 155.8, 152.0, 137.7, 128.6 (2C), 128.0, 127.5 (2C), 104.0, 78.7, 71.1, 61.7, 59.5, 52.5, 45.5, 44.4, 44.2, 28.3, 27.4, 23.6, 22.4; **IR** (neat) ν_{max}: 3279, 3031, 2949, 1724, 1692, 1654, 1526, 1454, 1346, 1260 cm^{-1}; **HRMS** (ESI) calcd for $C_{23}H_{28}O_5N_2I$ ($[M+H]^+$): 539.1038, found 539.1049.

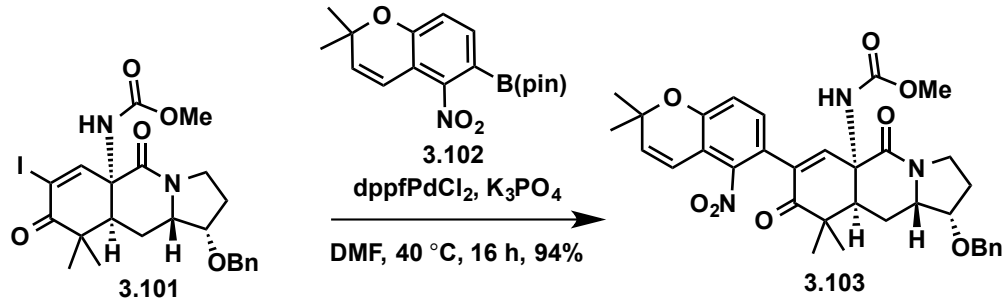

A round-bottomed flask was charged with methyl ((1*S*,5a*R*,9a*S*,10a*S*)-1-(benzyloxy)-7-iodo-9,9-dimethyl-5,8-dioxo-1,2,3,8,9,9a,10,10a-octahydropyrrolo[1,2-*b*]isoquinolin-5a(5*H*)-yl)carbamate (**3.101**) (670 mg, 1.24 mmol, 1.0 equiv), 2-(2,2-dimethyl-5-nitro-2*H*-chromen-6-yl)-4,4,5,5-tetramethyl-1,3,2-dioxaborolane (**3.102**)[7d] (620 mg, 1.87 mmol, 1.50 equiv), $dppfPdCl_2$ (101 mg, 0.124 mmol, 0.10 equiv) and K_3PO_4 (987 mg, 4.65 mmol, 3.75 equiv). *N,N*-dimethylformamide (12.4 mL, 0.1M) was added and the head space was deoxygenated with N_2 (three cycles of evacuation/backfill). The resulting brown mixture was stirred at 40 ºC. After 16 h, the reaction mixture was cooled to room temperature, poured into saturated aqueous NH_4Cl (100 mL) and the aqueous layer extracted with EtOAc (4 x 100 mL). The combined organic extracts were dried

with Na_2SO_4, filtered, and concentrated *in vacuo*. The resulting dark oil was purified by silica gel chromatography (40 mL SiO_2 with 2:3 to 4:1 ethyl acetate:hexanes) to yield **3.103** (715 mg, 1.16 mmol, 94%) as a dark brown foam. TLC (ethyl acetate:hexanes, 3:2 v/v): R_f= 0.23; **^{1}H NMR** (600 MHz, $CDCl_3$) δ = 7.37 – 7.27 (m, 5H), 6.95 (d, *J* = 8.3 Hz, 1H), 6.92 (d, *J* = 8.3 Hz, 1H), 6.62 (s, 1H), 6.40 (d, *J* = 10.3 Hz, 1H), 5.81 (d, *J* = 10.3 Hz, 1H), 5.29 (bs, 1H), 4.62 (d, *J* = 12.0 Hz, 1H), 4.44 (d, *J* = 12.0 Hz, 1H), 3.99 (t, *J* = 3.8 Hz, 1H), 3.79 (td, *J* = 11.3, 7.4 Hz, 1H), 3.69 (s, 3H), 3.53 – 3.47 (m, 2H), 3.02 (d, *J* = 7.8 Hz, 1H), 2.38 (ddd, *J* = 14.6, 11.6, 8.0 Hz, 1H), 2.18 (dd, *J* = 13.7, 7.2 Hz, 1H), 1.99 – 1.93 (m, 1H), 1.90 – 1.82 (m, 1H), 1.46 (s, 6H), 1.39 (s, 3H), 1.20 (s, 3H); **^{13}C NMR** (150 MHz, $CDCl_3$) δ = 200.9, 167.3, 156.4, 154.0, 146.8, 141.6, 137.9, 136.1, 134.2, 131.2, 128.5 (2C), 127.8, 127.5 (2C), 122.0, 119.5, 116.7, 114.6, 79.2, 76.8, 71.1, 59.5, 59.1, 52.3, 45.4, 45.0, 44.2, 28.5, 28.3, 28.0, 27.8, 23.5, 22.9; **IR** (neat) ν_{max}: 3289, 2977, 1722, 1654, 1527, 1456, 1353, 1278, 1205, 1119 cm^{-1}; **HRMS** (ESI) calcd for $C_{34}H_{37}O_8N_3Na$ ($[M+Na]^+$): 638.2473, found 638.2473.

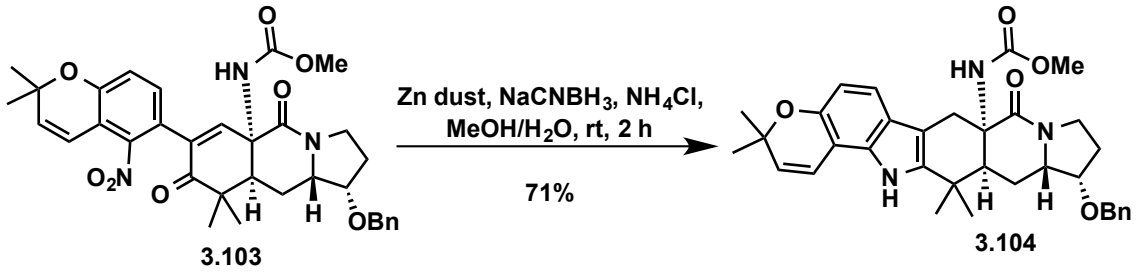

This procedure was adapted from a known procedure.[51] To a solution of methyl ((1*S*,5a*S*,9a*S*,10a*S*)-1-(benzyloxy)-7-(2,2-dimethyl-5-nitro-2*H*-chromen-6-yl)-9,9-dimethyl-5,8-dioxo-1,2,3,8,9,9a,10,10a-octahydropyrrolo[1,2-*b*]isoquinolin-5a(5*H*)-yl)carbamate (**3.103**) (110 mg, 0.179 mmol, 1.0 equiv) and saturated aqueous NH_4Cl (4.7 mL) in methanol (14.3 mL, 0.0125M) was added $NaCNBH_3$ (56 mg, 0.895 mmol, 5.0 equiv) followed by zinc dust[52] (89 mg, 1.43 mmol, 8.0 equiv). The resulting solution was then stirred at room temperature and zinc dust (267 mg, 4.29 mmol, 24 equiv) was added in three portions (3 x 89 mg) at 30 minute intervals. Two hours after the last addition, the reaction mixture was filtered using a Büchner funnel to remove the solids and to the resulting filtrate was added saturated aqueous $NaHCO_3$ (60 mL). The aqueous layer was extracted with ethyl acetate (3 x 60 mL) and the combined organic extracts were dried over Na_2SO_4, filtered, and concentrated *in vacuo*. The resulting beige powder was purified by silica gel chromatography (60 mL SiO_2 with 1% to 2% to 5% methanol:dichloromethane) to yield **3.104** (72 mg, 0.126 mmol, 71%) as an off white powder. TLC (methanol:dichloromethane, 1:19 v/v): R_f= 0.24; **^{1}H NMR** (600 MHz, $CDCl_3$) δ = 7.68 (s, 1H), 7.42 – 7.33 (m, 4H), 7.31 – 7.27 (m, 1H), 7.11 (d, *J* = 8.4 Hz, 1H), 6.65 (d, *J* = 8.4 Hz, 1H), 6.60 (d, *J* = 9.6 Hz, 1H), 5.68 (d, *J* = 9.6 Hz, 1H), 4.87 (s, 1H), 4.77 (d, *J* = 12.6 Hz, 1H), 4.41 (d, *J* = 12.6 Hz, 1H), 4.06 – 3.98 (m, 1H), 3.89 – 3.85 (m, 1H), 3.62 (s, 3H), 3.54 – 3.49 (m, 1H), 3.42 – 3.34 (m, 1H), 3.26 (dd, *J* = 13.3, 6.0 Hz, 1H), 3.03 (d, *J* = 16.5 Hz, 1H), 2.79 (d, *J* = 16.5 Hz, 1H), 2.37 – 2.30 (m, 1H), 2.21 – 2.14 (m, 1H), 1.90 – 1.80 (m, 1H), 1.76 – 1.68 (m, 1H), 1.47 (s, 3H), 1.46 (s, 6H), 1.33 (s, 3H); **^{13}C NMR** (150 MHz, $CDCl_3$) δ = 171.0, 156.2, 148.8, 138.8, 138.6, 132.8, 130.0, 128.5, 127.6, 122.0, 117.8, 117.3, 110.4, 105.3, 102.9, 80.0, 75.7, 70.5, 59.4, 57.8, 52.0, 43.3, 40.8, 34.8, 30.1, 28.7, 28.10, 27.56, 27.55, 27.4, 22.4; **IR** (neat) ν_{max}:

3434, 3307, 2972, 2923, 1715, 1638, 1502, 1455, 1356, 1253 cm^{-1}; **HRMS** (ESI) calcd for $C_{34}H_{39}O_5N_3Na$ ($[M+Na]^+$): 592.2782, found 592.2788.

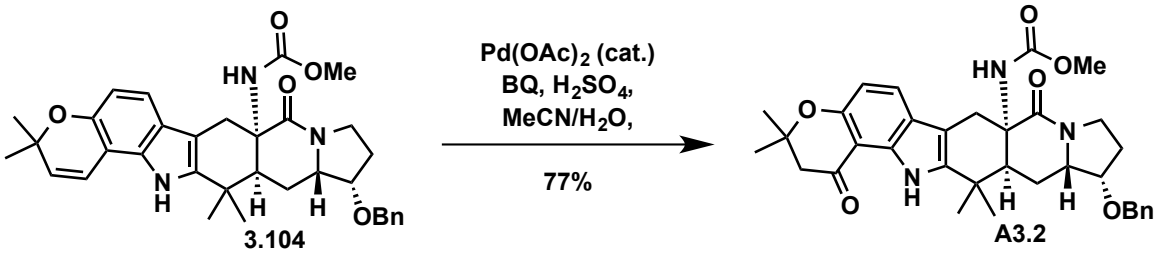

A 20 mL vial was charged with $Pd(OAc)_2$ (13.4 mg, 0.060 mmol, 0.40 equiv) and *p*-benzoquinone (BQ) (22.4 mg, 0.224 mmol, 1.50 equiv). The vial was fitted with a septum, purged with N_2 (three cycles of evacuation/backfill) and then MeCN (3.6 mL) and H_2O (1.06 mL) were added via syringe to give an orange solution. H_2SO_4 (11.4 µL, 95% wt in H_2O) was then added via syringe and the resulting pale yellow solution was stirred at room temperature for 5 min. In a separate vial, methyl ((7a*S*,12*S*,12a*S*,13a*S*)-12-(benzyloxy)-3,3,14,14-tetramethyl-8-oxo-3,7,10,11,12,12a,13,13a,14,15-decahydroindolizino[6,7-*h*]pyrano[3,2-*a*]carbazol-7a(8*H*)-yl)carbamate (**3.104**) (85 mg, 0.149 mmol, 1.0 equiv) was dissolved in MeCN (3.6 mL, 0.041M) under an N_2 atmosphere. To this was added, drop-wise, the catalyst solution described above and the resulting dark red mixture was stirred at room temperature. After 17 h, the resulting dark brown reaction mixture was poured into saturated aqueous $NaHCO_3$ (50 mL) and the aqueous layer extracted with EtOAc (3 x 50 mL). The combined organic extracts were dried over Na_2SO_4, filtered and concentrated *in vacuo*. The resulting red oil residue was purified by silica gel chromatography (30 mL SiO_2 with 1% to 2% to 3% methanol:dichloromethane) to yield **A3.2** (67 mg, 0.114 mmol, 77%) as a yellow foam. TLC (methanol:dichloromethane, 1:19 v/v): R_f= 0.33; **^{1}H NMR** (600 MHz, $CDCl_3$) δ = 9.74 (s, 1H), 7.46 (d, *J* = 8.4 Hz, 1H), 7.41 – 7.31 (m, 4H), 7.30 – 7.26 (m, 1H), 6.63 (d, *J* = 8.4 Hz, 1H), 4.89 (bs, 1H), 4.75 (d, *J* = 12.5 Hz, 1H), 4.39 (d, *J* = 12.5 Hz, 1H), 4.00 (dt, *J* = 12.1, 8.5 Hz, 1H), 3.85 (t, *J* = 3.9 Hz, 1H), 3.60 (s, 3H), 3.53 – 3.45 (m, 1H), 3.38 – 3.31 (m, 1H), 3.26 (dd, *J* = 13.1, 6.1 Hz, 1H), 3.02 (d, *J* = 16.6 Hz, 1H), 2.82 (d, *J* = 16.6 Hz, 1H), 2.73 (s, 2H), 2.36 – 2.29 (m, 1H), 2.19 – 2.10 (m, 1H), 1.88 – 1.78 (m, 1H), 1.73 – 1.63 (m, 1H), 1.49 – 1.44 (m, 9H), 1.34 (s, 3H); **^{13}C NMR** (150 MHz, $CDCl_3$) δ = 194.1, 170.8, 157.4, 156.1, 139.8, 138.5, 134.0, 128.4, 127.6, 127.5, 126.8, 121.6, 109.9, 105.3, 102.7, 79.9, 79.5, 70.4, 59.3, 57.7, 51.9, 48.8, 43.1, 40.6, 34.7, 29.90, 28.3, 27.9, 27.5, 26.7, 26.6, 22.3; **IR** (neat) ν_{max}: 3442, 3357, 2974, 2950 1732, 1709, 1653, 1618, 1580, 1457, 1369 cm^{-1}; **HRMS** (ESI) calcd for $C_{34}H_{40}O_6N_3$ ($[M+H]^+$): 586.2912, found 586.2918; calcd for $C_{34}H_{39}O_6N_3Na$ ($[M+Na]^+$): 608.2731, found 608.2726.

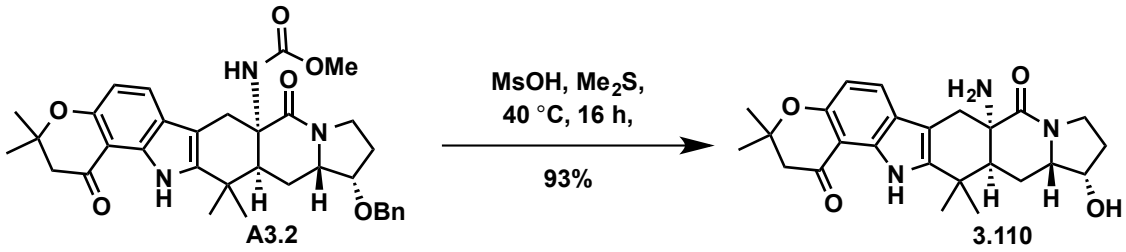

Dimethylsulfide (0.310 mL, 4.27 mmol, 20.0 equiv) was added to a solution of methyl ((7a*S*,12*S*,12a*S*,13a*S*)-12-(benzyloxy)-3,3,14,14-tetramethyl-1,8-dioxo-1,2,3,7,10,11,12,12a,13,13a,14,15-dodecahydroindolizino[6,7-*h*]pyrano[3,2-*a*]carbazol-7a(8*H*)-yl)carbamate (**A3.2**) (125 mg, 0.214 mmol, 1.0 equiv) in MsOH (4.3 mL, 0.05M) at room temperature. The reaction mixture was stirred at 40 ºC for 15 h and then cooled to room temperature. The resulting dark red reaction mixture was added dropwise to a stirring solution of saturated aqueous K_2CO_3 (50 mL) at 0 ºC. Stirring was continued until bubbling had ceased and then the aqueous solution was transferred to a separatory funnel and extracted with ethyl acetate (4 x 50 mL). The combined organic extracts were dried over Na_2SO_4, filtered, and concentrated *in vacuo*. The resulting yellow oil was purified by silica gel chromatography (20 mL SiO_2 with 2% to 20% methanol:dichloromethane) to yield **3.110** (87 mg, 0.199 mmol, 93%) as a yellow foam. TLC (methanol:dichloromethane, 1:9 v/v): R_f= 0.03; **^{1}H NMR** (600 MHz, $CDCl_3$) δ = 9.72 (s, 1H), 7.51 (d, *J* = 8.5 Hz, 1H), 6.63 (d, *J* = 8.5 Hz, 1H), 4.12 (t, *J* = 2.8 Hz, 1H), 3.97 (dt, *J* = 12.8, 8.7 Hz, 1H), 3.53 – 3.44 (m, 1H), 3.30 (dt, *J* = 13.1, 7.4 Hz, 1H), 3.03 (d, *J* = 15.8 Hz, 1H), 2.96 (bs, 2H), 2.75 (s, 2H), 2.70 (d, *J* = 15.8 Hz, 1H), 2.40 (ddd, *J* = 14.4, 6.4, 3.1 Hz, 1H), 2.18 (dd, *J* = 11.8, 6.2 Hz, 1H), 2.04 – 1.95 (m, 2H), 1.74 (ddd, *J* = 14.1, 11.8, 9.8 Hz, 1H), 1.61 (s, 3H), 1.49 (s, 6H), 1.41 (s, 3H); **^{13}C NMR** (150 MHz, $CDCl_3$) δ = 194.3, 174.0, 157.6, 139.1, 134.3, 127.3, 122.1, 109.8, 105.4, 104.5, 79.6, 73.5, 59.0, 57.2, 48.9, 45.6, 42.9, 35.1, 31.7, 31.0, 30.4, 28.0, 26.8, 26.7, 22.1; **IR** (neat) ν_{max}: 3440, 3395, 3364, 2976, 2934, 1620, 1584, 1463, 1370 cm^{-1}; **HRMS** (ESI) calcd for $C_{25}H_{31}O_4N_3$ ($[M+H]^+$): 438.2387, found 438.2384.

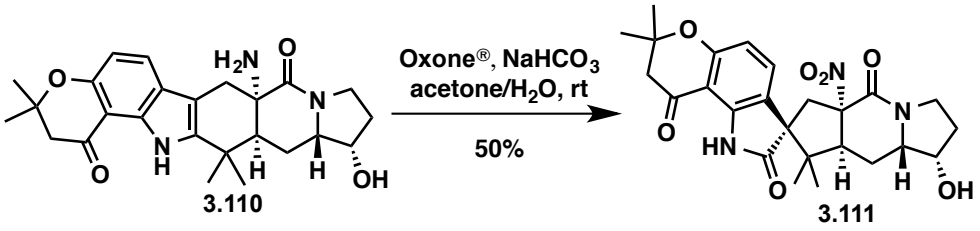

A saturated aqueous solution of $NaHCO_3$ (1.5 mL) was added to a solution of (7a*S*,12*S*,12a*S*,13a*S*)-7a-amino-12-hydroxy-3,3,14,14-tetramethyl-2,3,7,7a,10,11,12,12a,13,13a,14,15-dodecahydroindolizino[6,7-*h*]pyrano[3,2-*a*]carbazole-1,8-dione (**3.110**) (20.0 mg, 0.046 mmol, 1.0 equiv) in acetone (2.0 mL, 0.023M) at 0 ºC, resulting in precipitate formation. A solution of Oxone® (80 mg, 0.526 mmol, 11.4 equiv) in deionized water (1.00 mL, 0.53M) was added drop-wise and the mixture was warmed to room temperature by allowing the ice bath to expire. After 2 h, the resulting mixture was diluted with deionized water (3.0 mL) and extracted with ethyl acetate (4 x 5.0 mL). The combined organic extracts were dried with Na_2SO_4, filtered, and concentrated *in vacuo*. The resulting beige powder was purified by silica gel chromatography (10 mL SiO_2 with 1% to 2% to 3% to 5%

methanol:dichloromethane) to yield **3.111** (11.1 mg, 0.023 mmol, 50%) as a white powder. TLC (methanol:dichloromethane, 1:19 v/v): R_f= 0.29; **^{1}H NMR** (600 MHz, $(CD_3)_2SO$) δ = 10.21 (s, 1H), 7.46 (d, *J* = 8.4 Hz, 1H), 6.52 (d, *J* = 8.4 Hz, 1H), 5.07 (d, *J* = 4.1 Hz, 1H), 4.15 (q, *J* = 3.6 Hz, 1H), 3.74 (d, *J* = 11.9 Hz, 1H), 3.62 (d, *J* = 7.6 Hz, 1H), 3.59 – 3.51 (m, 1H), 3.41 – 3.35 (m, 1H), 3.18 (d, *J* = 16.1 Hz, 1H), 2.83 – 2.74 (m, 3H), 2.46 (dd, *J* = 13.2, 6.9 Hz, 1H), 1.98 – 1.88 (m, 2H), 1.84 (dd, *J* = 13.3, 7.9 Hz, 1H), 1.40 (s, 3H), 1.39 (s, 3H), 1.11 (s, 3H), 0.77 (s, 3H); **^{13}C NMR** (150 MHz, $(CD_3)_2SO$) δ = 192.6, 181.0, 162.6, 158.8, 142.7, 133.0, 118.7, 109.0, 104.9, 94.2, 79.2, 70.6, 61.1, 58.6, 49.8, 49.0, 48.0, 43.9, 40.1, 30.9, 26.3, 26.0, 22.7, 21.6, 19.0; **IR** (neat) ν_{max}: 3459, 3404, 2966, 2938, 1717, 1673, 1642, 1625, 1549, 1465, 1370, 1348, 1322, 1255 cm^{-1}; **HRMS** (ESI) calcd for $C_{25}H_{30}O_7N_3$ ($[M+H]^+$): 484.2078, found 484.2096.

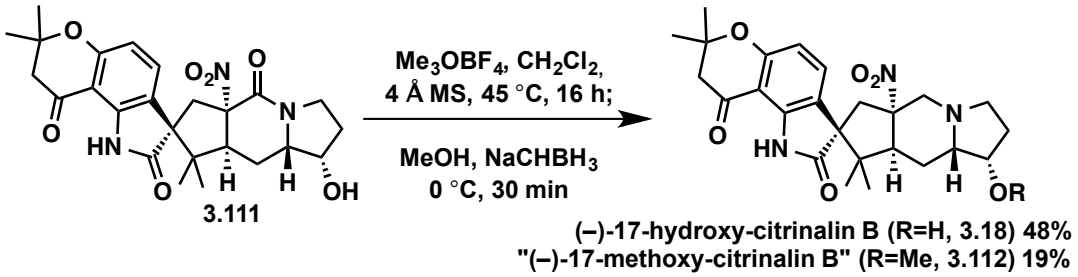

To a Schlenk tube charged with (1*S*,5a*S*,7*R*,8a*S*,9a*S*)-1-hydroxy-7',7',8,8-tetramethyl-5a-nitro-2,3,5a,6,7',8,8a,8',9,9a-decahydro-1*H*,2'*H*,5*H*-spiro[cyclopenta[*f*]indolizine-7,3'-pyrano[2,3-*g*]indole]-2',5,9'(1'*H*)-trione (**3.111**) (6.4 mg, 0.0132 mmol, 1.0 equiv) and a stir bar was added Me_3OBF_4 (23.5 mg, 0.159 mmol, 12.0 equiv) and activated 4 Å MS (64 mg) in a nitrogen atmosphere glove box. The reaction vessel was then removed from the glove box and CH_2Cl_2 (0.90 mL, 0.015M) was added by syringe under a nitrogen atmosphere and the mixture was stirred at 45 ºC for 16 h. After cooling to 0 ºC, anhydrous MeOH (0.90 mL) was added drop-wise followed by $NaCNBH_3$ (16.7 mg, 0.264 mmol, 20.0 equiv) in one portion. After 5 min, more $NaCNBH_3$ (16.7 mg, 0.264 mmol, 20.0 equiv) was added in one portion and the reaction mixture was stirred at 0 ºC for 30 min. The resulting reaction mixture was subsequently quenched by the addition of saturated aqueous $NaHCO_3$ (3.0 mL) and extracted with EtOAc (4 x 3.0 mL). The combined organic extracts were dried over Na_2SO_4, filtered, and concentrated *in vacuo*. The resulting yellow oil was purified by silica gel chromatography (5 mL SiO_2 with 1% to 2% to 3% to 5% methanol:toluene) to yield (–)-17-hydroxy-citrinalin B (**3.18**) (3.0 mg, 0.0064 mmol, 48%) as a yellow oil, methyl ether (**3.112**) (1.2 mg, 0.0025 mmol, 19%) as a yellow oil, and recovered **3.111** (0.7 mg, 0.0014 mmol, 11% recovery).

(–)-17-hydroxy-citrinalin B (**3.18**): TLC (methanol:toluene, 1:9 v/v): R_f= 0.31; **^{1}H NMR** (600 MHz, CD_3OD) δ = 7.47 (d, *J* = 8.4 Hz, 1H), 6.60 (d, *J* = 8.4 Hz, 1H), 4.18 (ddd, *J* = 7.3, 4.6, 2.3 Hz, 1H), 3.95 (d, *J* = 9.1 Hz, 1H), 3.85 (d, *J* = 13.1 Hz, 1H), 3.07 – 3.03 (m, 1H), 2.86 – 2.76 (m, 3H), 2.67 – 2.60 (m, 2H), 2.39 (td, *J* = 14.5, 14.1, 9.5 Hz, 1H), 2.28 (dt, *J* = 14.3, 7.3 Hz, 1H), 2.10 – 1.92 (m, 3H), 1.74 – 1.66 (m, 2H), 1.50 (s, 3H), 1.49 (s, 3H), 1.12 (s, 3H), 0.88 (s, 3H); **^{13}C NMR** (150 MHz, CD_3OD) δ = 195.19, 185.00, 161.25, 144.54, 134.17, 121.35, 111.10, 106.84, 96.06, 80.83, 72.98, 67.67, 66.54, 60.75, 53.64, 50.74, 49.3, 45.32, 44.00, 34.16, 27.05, 27.03, 24.43, 23.80, 21.46; **IR** (neat) ν_{max}: 3282, 2965, 2887, 1720, 1624, 1550, 1460, 1367 cm^{-1}; **HRMS** (ESI) calcd for $C_{25}H_{32}O_6N_3$ ($[M+H]^+$): 470.2286, found 470.2281.

methyl ether (**3.112**): $[\alpha]^{22}_D$ = -95.2 degrees (*c* = 1.46 , MeOH); TLC (methanol:toluene, 1:9 v/v): R_f= 0.41; **^{1}H NMR** (600 MHz, CD_3OD) δ = 7.46 (d, *J* = 8.4 Hz, 1H), 6.60 (d, *J* = 8.4 Hz, 1H), 3.92 (d, *J* = 9.2 Hz, 1H), 3.87 – 3.81 (m, 2H), 3.33 (s, 3H), 3.02 (td, *J* = 8.9, 1.8 Hz, 1H), 2.86 – 2.78 (m, 3H), 2.66 – 2.62 (m, 2H), 2.43 (ddd, *J* = 14.5, 12.7, 9.3 Hz, 1H), 2.19 – 2.13 (m, 1H), 2.10 – 2.01 (m, 2H), 1.80 (dtd, *J* = 13.7, 9.0, 2.5 Hz, 1H), 1.73 (dd, *J* = 14.5, 3.7 Hz, 1H), 1.50 (s, 3H), 1.48 (s, 3H), 1.12 (s, 3H), 0.87 (s, 3H); **^{13}C NMR** (150 MHz, CD_3OD) δ = 195.23, 184.96, 161.21, 144.50, 134.17, 121.29, 111.10, 106.80, 95.96, 82.41, 80.82, 67.34, 66.55, 60.71, 57.46, 53.91, 50.74, 49.3, 45.27, 44.02, 30.99, 27.05, 27.00, 24.36, 23.76, 21.32; **IR** (neat) ν_{max}: 3237, 2976, 2934, 1726, 1672, 1610, 1544, 1465, 1370 cm^{-1}; **HRMS** (ESI) calcd for $C_{26}H_{34}O_6N_3$ ($[M+H]^+$): 484.2442, found 484.2437.

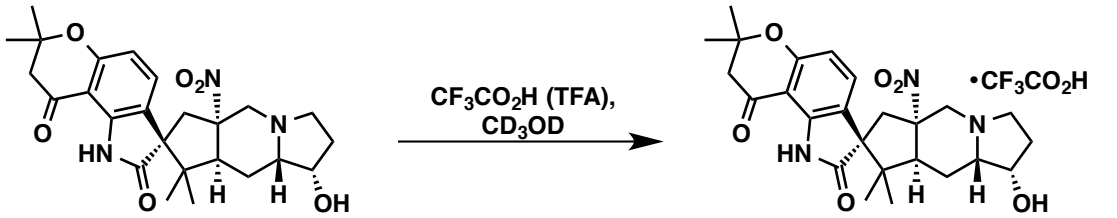

(–)-17-hydroxycitrinalin B (3.18) **(–)17-hydroxycitrinalin B•TFA (A3.3)**

To a solution of (–)-17-hydroxycitrinalin B (**3.18**) (1.7 mg, 0.0036 mmol, 1.0 equiv) in methanol-d_4 (1.0 mL) was added trifluoroacetic acid (TFA) (0.033 mL, 0.432 mmol, 120.0 equiv) at room temperature. The solvents were then removed *in vacuo*.

(–)-17-hydroxycitrinalin B•TFA (**A3.3**): $[\alpha]^{22}_D$ = -70.5 degrees (*c* = 1.8, MeOH) **^{1}H NMR** (600 MHz, CD_3OD) δ = 7.42 (d, *J* = 8.4 Hz, 1H), 6.60 (d, *J* = 8.4 Hz, 1H), 4.49 (dd, *J* = 5.8, 3.2 Hz, 1H), 4.41 (d, *J* = 14.5 Hz, 1H), 4.00 (d, *J* = 8.7 Hz, 1H), 3.80 – 3.71 (m, 2H), 3.25 (d, *J* = 13.3 Hz, 1H), 3.20 – 3.12 (m, 1H), 3.09 (d, *J* = 16.1 Hz, 1H), 2.77 (s, 2H), 2.75 – 2.67 (m, 1H), 2.66 – 2.58 (m, 1H), 2.55 – 2.45 (m, 1H), 2.12 (dd, *J* = 15.7, 3.6 Hz, 1H), 2.02 (dt, *J* = 14.0, 8.5 Hz, 1H), 1.46 (s, 3H), 1.45 (s, 3H), 1.17 (s, 3H), 0.88 (s, 3H); **^{13}C NMR** (150 MHz, CD_3OD) δ = 195.09, 184.21, 161.56, 144.58, 134.09, 120.23, 111.44, 107.03, 93.76, 80.97, 70.19, 69.46, 61.00, 60.69, 54.28, 51.11, 49.3, 46.09, 43.19, 32.52, 27.05, 26.99, 23.02 (2C), 20.02.

Reported Data for (+)-17-hydroxy-citrinalin B:[8c] $[\alpha]_D$ +76.9 degrees (*c* 1.6, MeOH)); **^{1}H NMR** (600 MHz, CD_3OD) δ = 7.38 (d, *J* = 8.4 Hz, 1H), 6.60 (d, *J* = 8.4 Hz, 1H), 4.47 (dd, *J* = 5.4, 3.2 Hz, 1H), 4.40 (d, *J* = 14.5 Hz, 1H), 3.99 (d, *J* = 8.7 Hz, 1H), 3.76 (m, 1H), 3.70 (d, *J* = 14.5 Hz, 1H), 3.20 (bd, *J* = 13.5 Hz, 1H), 3.12 (m, 1H), 3.08 (d, *J* = 16.1 Hz, 1H), 2.77 (d, *J* = 16.8 Hz, 1H), 2.75 (d, *J* = 16.8 Hz, 1H), 2.67 (d, *J* = 16.1 Hz, 1H), 2.60 (ddd, *J* = 15.6, 13.5, 8.7 Hz, 1H), 2.48 (m, 1H), 2.10 (dd, *J* = 15.6, 3.9 Hz, 1H), 2.00 (dt, *J* = 13.0, 8.7 Hz, 1H), 1.45 (s, 3H), 1.44 (s, 3H), 1.15 (s, 3H), 0.88 (s, 3H); **^{13}C NMR** (150 MHz, CD_3OD) δ = 195.02, 184.21, 161.58, 144.67, 133.98, 120.25, 111.38, 107.06, 93.74, 80.92, 70.19, 69.48, 61.00, 60.3 54.26, 51.09, 49.0, 45.99, 43.28, 32.55, 27.03, 26.99, 23.03 (2C), 20.05.[53]

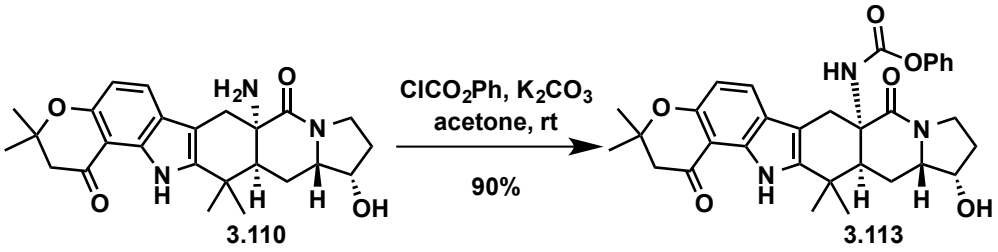

To a solution of (7a*S*,12*S*,12a*S*,13a*S*)-7a-amino-12-hydroxy-3,3,14,14-tetramethyl-2,3,7,7a,10,11,12,12a,13,13a,14,15-dodecahydroindolizino[6,7-*h*]pyrano[3,2-*a*]carbazole-1,8-dione (**3.110**) (20 mg, 0.0457 mmol, 1.0 equiv) and K_2CO_3 (63 mg, 0.457 mmol, 10.0 equiv) in anhydrous acetone (1.0 mL, 0.05M) was added phenyl chloroformate (0.060 mL, 0.457 mmol, 10.0 equiv) dropwise at room temperature. The resulting solution was stirred for 5 h then additional phenyl chloroformate (0.060 mL, 0.457 mmol, 10.0 equiv) was added dropwise, followed by more K_2CO_3 (63 mg, 0.457 mmol, 10.0 equiv). The resulting solution was stirred at room temperature for 16 h, at which time H_2O (2 mL) was added and the aqueous layer was extracted with ethyl acetate (4 x 2 mL). The combined organic extracts were dried over Na_2SO_4, filtered, and concentrated *in vacuo*. The resulting oil residue was purified by silica gel chromatography (5 mL SiO_2 with 1% to 2% to 5% methanol:dichloromethane) to yield **3.113** (23 mg, 0.0412 mmol, 90%) as a yellow oil. TLC (methanol:dichloromethane, 1:19 v/v): R_f= 0.23; **^{1}H NMR** (600 MHz, $CDCl_3$) δ = 9.79 (s, 1H), 7.53 (d, *J* = 8.5 Hz, 1H), 7.28 – 7.26 (m, 1H), 7.26 – 7.24 (m, 1H), 7.12 (t, *J* = 7.4 Hz, 1H), 7.04 (d, *J* = 8.0 Hz, 2H), 6.68 (d, *J* = 8.5 Hz, 1H), 5.38 (s, 1H), 4.06 (dt, *J* = 12.2, 8.3 Hz, 2H), 3.42 – 3.36 (m, 1H), 3.26 (td, *J* = 11.5, 3.6 Hz, 1H), 3.20 (dd, *J* = 13.7, 5.7 Hz, 1H), 3.12 (d, *J* = 16.7 Hz, 1H), 2.98 (d, *J* = 16.7 Hz, 1H), 2.78 (s, 2H), 2.76 – 2.69 (m, 1H), 2.43 (dd, *J* = 14.2, 5.7 Hz, 1H), 2.05 – 2.01 (m, 1H), 1.91 (ddd, *J* = 13.8, 9.3, 3.6 Hz, 1H), 1.78 (td, *J* = 14.0, 9.4 Hz, 1H), 1.60 (s, 3H), 1.51 (s, 6H), 1.44 (s, 3H); **^{13}C NMR** (150 MHz, $CDCl_3$) δ = 194.3, 171.1, 157.7, 154.4, 150.9, 139.8, 134.3, 129.3, 127.0, 125.4, 121.9, 121.5, 110.2, 105.5, 102.3, 79.7, 74.4, 59.5, 58.7, 48.9, 42.4, 40.8, 34.8, 32.0, 30.8, 28.5, 27.9, 26.8, 26.7, 22.3; **IR** (neat) ν_{max}: 3442, 3348, 2974, 1733, 1647, 1619, 1580, 1461, 1370, 1203 cm^{-1}; **HRMS** (ESI) calcd for $C_{32}H_{36}O_6N_3$ ($[M+H]^+$): 558.2599, found 558.2617.

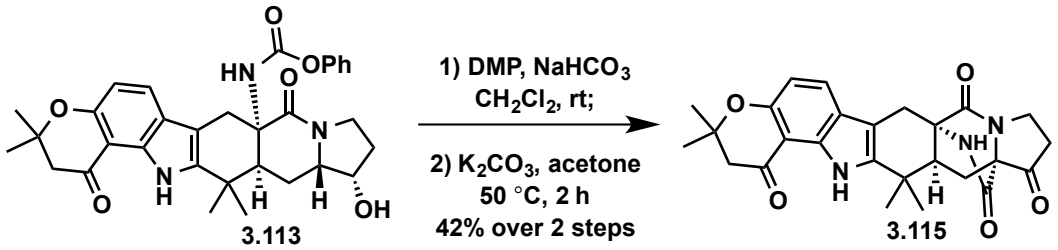

To a solution of phenyl ((7a*S*,12*S*,12a*S*,13a*S*)-12-hydroxy-3,3,14,14-tetramethyl-1,8-dioxo-1,2,3,7,10,11,12,12a,13,13a,14,15-dodecahydroindolizino[6,7-*h*]pyrano[3,2-*a*]carbazol-7a(8*H*)-yl)carbamate (**3.113**) (20.0 mg, 0.0359 mmol, 1.0 equiv) and $NaHCO_3$ (15.0 mg, 0.180 mmol, 5.0 equiv) in CH_2Cl_2 (0.720 mL, 0.05M) was added Dess-Martin periodinane (DMP) (23.0 mg, 0.0538 mmol, 1.5 equiv) in three portions (3 x 7.6 mg) at 5 minute intervals. The resulting solution was stirred at room temperature for 30 min then additional DMP (15.2 mg, 0.0359 mmol,

1.0 equiv) was added in two portions (2 x 7.6 mg) at 5 minute intervals. After 20 minutes at room temperature saturated aqueous $NaHCO_3$ (2.0 mL) was added and the mixture was stirred until the organic layer was no longer cloudy. The layers were separated and the aqueous layer was extracted with CH_2Cl_2 (4 x 2 mL) and the combined organic extracts were dried over Na_2SO_4, filtered, and concentrated *in vacuo*. The reaction mixture was subsequently diluted with CH_2Cl_2 and passed through a short column containing silica gel (2 mL) with 2:3 to 4:1 ethyl acetate:hexanes. The fractions containing the product were collected and concentrated *in vacuo*. [TLC (ethyl acetate:hexanes, 4:1 v/v): R_f=0.26]. The residue was dissolved in anhydrous acetone (1.4 mL, 0.025M) and K_2CO_3 (9.9 mg, 0.0718 mmol, 2.0 equiv) was added at room temperature and then the reaction was heated to 50 °C. After 2 h, the solution was cooled to 0 °C and saturated aqueous NH_4Cl (1 mL) was added and the aqueous layer was extracted with ethyl acetate (4 x 2 mL). The combined organic extracts were dried over Na_2SO_4, filtered and concentrated *in vacuo*. The resulting residue was purified by silica gel chromatography (4 mL SiO_2 with 1% to 3% to 5% methanol:dichloromethane) to yield **3.115** (6.9 mg, 0.0150 mmol, 42% over 2-steps) as a yellow oil. TLC (methanol:dichloromethane, 1:19 v/v): R_f= 0.31; **^{1}H NMR** (600 MHz, $CDCl_3$) δ = 9.67 (s, 1H), 7.61 (d, *J* = 8.5 Hz, 1H), 6.91 (s, 1H), 6.65 (d, *J* = 8.5 Hz, 1H), 3.95 (td, *J* = 11.1, 4.5 Hz, 1H), 3.81 (d, *J* = 15.4 Hz, 1H), 3.69 (dt, *J* = 11.9, 8.2 Hz, 1H), 2.93 (ddd, *J* = 18.2, 10.4, 7.4 Hz, 1H), 2.82 – 2.77 (m, 1H), 2.75 (s, 2H), 2.71 (d, *J* = 15.4 Hz, 1H), 2.66 (dd, *J* = 10.3, 4.7 Hz, 1H), 2.51 (dd, *J* = 13.6, 10.4 Hz, 1H), 2.01 (dd, *J* = 13.6, 4.7 Hz, 1H), 1.50 (s, 6H), 1.33 (s, 3H), 1.11 (s, 3H); **^{13}C NMR** (150 MHz, $CDCl_3$) δ = 204.3, 194.3, 169.6, 169.5, 157.9, 139.0, 134.5, 127.8, 121.2, 110.0, 105.3, 104.5, 79.7, 67.0, 61.5, 48.9, 48.8, 38.6, 36.5, 34.9, 28.5, 27.8, 26.8, 26.7, 24.6, 22.6; **IR** (neat) ν_{max}: 3441, 3234, 2972, 2929, 1768, 1695, 1583, 1461, 1373 cm^{-1}; **HRMS** (ESI) calcd for $C_{26}H_{28}O_5N_3$ ($[M+H]^+$): 462.2023, found 462.2022.

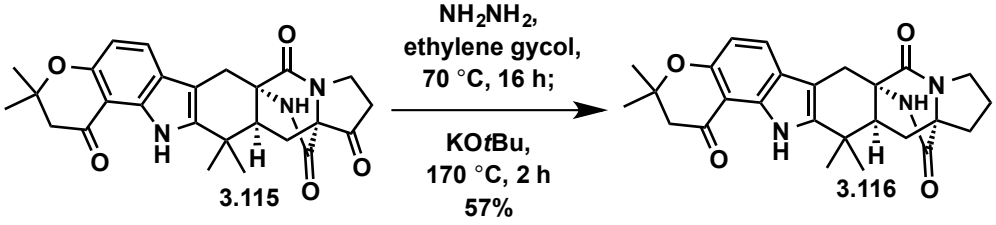

Stock solution A: Hydrazine (5.0 μL, 0.15 mmol) in deoxygenated (via three cycles of freeze/pump/thaw) ethylene glycol (5.0 mL). To a 4 mL vial equipped with a stir bar and (7a*S*,12a*R*,13a*S*)-3,3,14,14-tetramethyl-2,3,10,11,13,13a,14,15-octahydro-8*H*,12*H*-7a,12a-(epiminomethano)indolizino[6,7-*h*]pyrano[3,2-*a*]carbazole-1,8,12,16(7*H*)-tetraone (**3.115**) (6.2 mg, 0.013 mol, 1.0 equiv) was added 0.50 mL of stock solution A (0.015 mmol, 1.1 equiv) under a N_2 atmosphere. The solution was then heated at 70 °C for 17 h, at which time the solution was cooled to room temperature and *t*BuOK (7.5 mg, 0.067 mmol, 5.0 equiv) was added in one portion at room temperature and the solution was then placed in a preheated heating block at 170 °C. After 2 h, the reaction was cooled to room temperature and saturated aqueous NH_4Cl (2.0 mL) was added and the aqueous layer was extracted with ethyl acetate (4 x 2 mL). The combined organic layers were dried over Na_2SO_4, filtered, and concentrated *in vacuo*. The resulting residue was purified by silica gel chromatography (2 mL SiO_2 with 1% to 3% to 5% methanol:dichloromethane) to yield **3.116** (3.3 mg, 0.0074 mmol, 57%) as a beige powder. TLC (methanol:dichloromethane, 1:19 v/v): R_f= 0.33; **^{1}H NMR** (600 MHz, $CDCl_3$) δ = 9.66 (s, 1H),

7.61 (d, *J* = 8.6 Hz, 1H), 6.66 (d, *J* = 8.6 Hz, 1H), 5.95 (s, 1H), 3.82 (d, *J* = 15.0 Hz, 1H), 3.55 (dt, *J* = 12.5, 6.5 Hz, 1H), 3.41 (dt, *J* = 11.4, 7.1 Hz, 1H), 2.81 (dt, *J* = 13.3, 6.7 Hz, 1H), 2.75 (s, 2H), 2.61 (d, *J* = 15.0 Hz, 1H), 2.60 – 2.56 (m, 1H), 2.25 (dd, *J* = 13.5, 10.3 Hz, 1H), 2.06 – 1.97 (m, 3H), 1.89 (dt, *J* = 14.5, 7.5 Hz, 1H), 1.50 (s, 6H), 1.34 (s, 3H), 1.13 (s, 3H); **^{13}C NMR** (150 MHz, $CDCl_3$) δ = 194.3, 173.7, 168.6, 157.8, 139.5, 134.5, 127.7, 121.4, 109.9, 105.3, 104.8, 79.6, 66.7, 60.6, 49.6, 48.9, 44.3, 34.9, 31.1, 29.5, 28.6, 26.9, 26.6, 25.1, 24.7, 22.3; **IR** (neat) ν_{max}: 3441, 2964, 2930, 1686, 1656, 1618, 1582, 1457, 1370 cm^{-1}; **HRMS** (ESI) calcd for $C_{26}H_{29}O_4N_3Na$ ([M+Na]$^+$): 470.2050, found 470.2045.

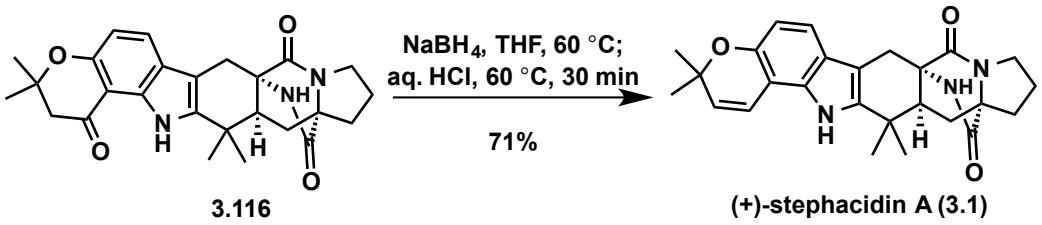

To a solution of (7a*S*,12a*S*,13a*S*)-3,3,14,14-tetramethyl-2,3,11,12,13,13a,14,15-octahydro-8*H*,10*H*-7a,12a-(epiminomethano)indolizino[6,7-*h*]pyrano[3,2-*a*]carbazole-1,8,16(7*H*)-trione (**3.116**) (3.2 mg, 0.0072 mmol, 1.0 equiv) in THF (0.20 mL, 0.035M) was added $NaBH_4$ (2.7 mg, 0.072 mmol, 10.0 equiv) in one portion at room temperature. The resulting solution was heated at 60 °C for 16 h, at which time the solution was cooled to room temperature and aqueous HCl (0.25 mL, 0.6M) was added dropwise. After bubbling had ceased, the solution was heated to 60 °C for 30 min and then cooled to room temperature. Saturated aqueous $NaHCO_3$ (1.5 mL) was added slowly and the aqueous layer was extracted with ethyl acetate (4 x 1.5 mL). The combined organic extracts were dried over Na_2SO_4, filtered, and concentrated *in vacuo*. The resulting residue was purified by silica gel chromatography (2 mL SiO_2 with 1% to 3% to 5% methanol:dichloromethane) to yield **(+)-stephacidin A** (**3.1**) (2.2 mg, 0.0051 mmol, 71%) as a white powder. **m.p.** >340 °C (decomp); $[\alpha]^{22}_D$ = + 79.1 degrees (*c* = 0.63, 1:1 CH_2Cl_2/MeOH); TLC (methanol:dichloromethane, 1:19 v/v): R_f = 0.35; **^{1}H NMR** (600 MHz, $(CD_3)_2SO$) δ = 10.45 (s, 1H), 8.68 (s, 1H), 7.09 (d, *J* = 8.3 Hz, 1H), 6.93 (d, *J* = 9.8 Hz, 1H), 6.47 (d, *J* = 8.3 Hz, 1H), 5.72 (d, *J* = 9.8 Hz, 1H), 3.38 – 3.35 (m, 1H), 3.32 – 3.29 (m, 1H), 3.27 – 3.21 (m, 1H), 2.63 (d, *J* = 15.5 Hz, 1H), 2.55 – 2.52 (m, 1H), 2.42 (dd, *J* = 10.1, 4.7 Hz, 1H), 2.10 – 2.02 (m, 1H), 2.02 – 1.94 (m, 2H), 1.88 – 1.79 (m, 2H), 1.37 (s, 3H), 1.36 (s, 3H), 1.28 (s, 3H), 1.00 (s, 3H); **^{13}C NMR** (150 MHz, $(CD_3)_2SO$) δ = 173.0, 168.4, 147.5, 139.6, 132.8, 128.9, 121.5, 118.2, 117.5, 108.6, 104.8, 103.8, 75.0, 66.0, 59.6, 49.2, 43.5, 34.6, 30.1, 28.7, 28.0, 27.1, 27.0, 24.0, 23.8, 21.5; **IR** (neat) ν_{max}: 3325, 2924, 1675, 1638, 1459 cm^{-1}; **HRMS** (ESI) calcd for $C_{26}H_{29}O_3N_3Na$ ([M+Na]$^+$): 454.2101, found 454.2097. The spectroscopic data were consistent with those previously reported.[7a, 7e]

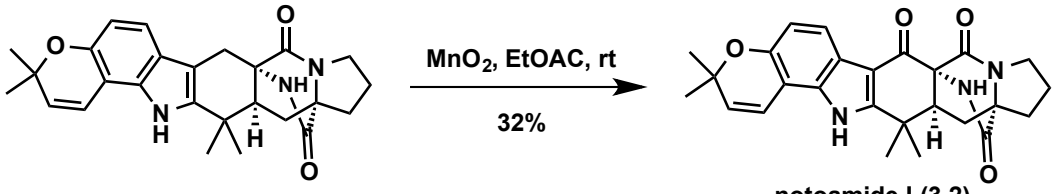

(+)-stephacidin A (3.1) notoamide I (3.2)

To a solution of (+)-stephacidin A (**3.1**) (3.6 mg, 0.0083 mmol, 1.00 equiv) in reagent grade ethyl acetate (3.6 mL, 0.0023M) was added MnO_2 (84 mg, 1.00 mmol, 120.0 equiv) in four portions (4 x 21 mg) at 2 h intervals. 30 minutes after the last addition, the reaction was filtered through Celite®, washed with ethyl acetate and the solvent removed *in vacuo*. The resulting residue was purified by silica gel chromatography (2 mL SiO_2 with 1% to 2% to 3% methanol:dichloromethane) to yield **(+)-notoamide I** (**3.2**) (1.2 mg, 0.0027 mmol, 32%) as a white powder. $[\alpha]^{22}_D$ = + 74.2 degrees (*c* = 0.22, 1:1 $CHCl_3$/MeOH); TLC (methanol:dichloromethane, 1:19 v/v): R_f= 0.30; **^{1}H NMR** (600 MHz, $(CD_3)_2SO$) δ = 11.65 (s, 1H), 8.73 (s, 1H), 7.76 (d, *J* = 8.4 Hz, 1H), 7.00 (d, *J* = 9.9 Hz, 1H), 6.70 (d, *J* = 8.4 Hz, 1H), 5.85 (d, *J* = 9.9 Hz, 1H), 3.38 – 3.34 (m, 1H), 3.32 – 3.29 (m, 1H), 2.82 (dd, *J* = 9.9, 5.6 Hz, 1H), 2.55 – 2.52 (m, 1H), 2.14 – 2.00 (m, 3H), 1.89 – 1.82 (m, 2H), 1.42 (s, 3H), 1.40 (s, 3H), 1.39 (s, 3H), 1.23 (s, 3H); **IR** (neat) ν_{max}: 3268, 2972, 2930, 1717, 1662, 1590, 1456, 1378 cm^{-1}; **HRMS** (ESI) calcd for $C_{26}H_{28}O_4N_3$ ($[M+H]^+$): 446.2074, found 446.2078. The spectroscopic data were consistent with those previously reported.[54]

3.8 – X-Ray Crystallography Data

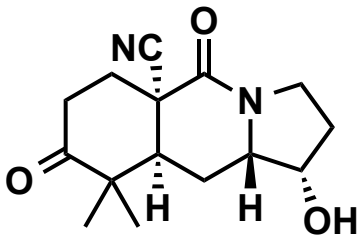

3.60

A colorless blade 0.100 x 0.040 x 0.020 mm in size was mounted on a Cryoloop with Paratone oil. Data were collected in a nitrogen gas stream at 100(2) K using phi and omega scans. Crystal-to-detector distance was 60 mm and exposure time was 10 seconds per frame using a scan width of 1.0°. Data collection was 99.9% complete to 67.000° in θ. A total of 10468 reflections were collected covering the indices, -9<=*h*<=9, -8<=*k*<=7, -15<=*l*<=15. 2538 reflections were found to be symmetry independent, with an R_{int} of 0.0262. Indexing and unit cell refinement indicated a primitive, monoclinic lattice. The space group was found to be P 21 (No. 4). The data were integrated using the Bruker SAINT software program and scaled using the SADABS software program. Solution by direct methods (SIR-2011) produced a complete heavy-atom phasing model consistent with the proposed structure. All non-hydrogen atoms were refined anisotropically by full-matrix least-squares (SHELXL-2012). All hydrogen atoms were placed using a riding model. Their positions were constrained relative to their parent atom using the appropriate HFIX command in SHELXL-2012. Absolute stereochemistry was unambiguously determined to be *R* at C1 and *S* at C6, C8, and C9, respectively. CCDC # 1400755 (**3.60**) contains the supplementary crystallographic data for this paper. These data can be obtained free of charge from The Cambridge Crystallographic Data Centre via www.ccdc.cam.ac.uk/data_request/cif.

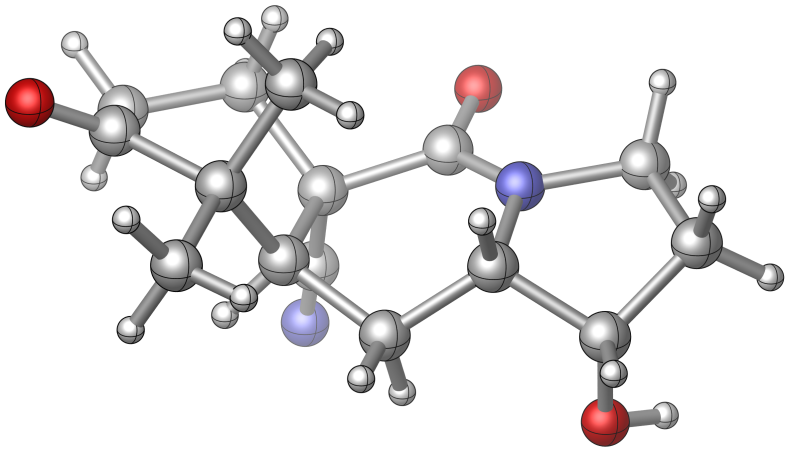

CYLview representation of **3.60**

Table 1. Crystal data and structure refinement for **3.60**.

X-ray ID	sarpong38	
Sample/notebook ID	EM03-093B	
Empirical formula	C15 H20 N2 O3	
Formula weight	276.33	
Temperature	100(2) K	
Wavelength	1.54178 Å	
Crystal system	Monoclinic	
Space group	P 21	
Unit cell dimensions	a = 7.9384(5) Å	α= 90°.
	b = 7.0246(5) Å	β= 98.464(4)°.
	c = 12.9394(8) Å	γ = 90°.
Volume	713.69(8) $Å^3$	
Z	2	
Density (calculated)	1.286 Mg/m^3	
Absorption coefficient	0.734 mm^{-1}	
F(000)	296	
Crystal size	0.100 x 0.040 x 0.020 mm^3	
Crystal color/habit	colorless blade	
Theta range for data collection	3.453 to 68.368°.	
Index ranges	-9<=h<=9, -8<=k<=7, -15<=l<=15	
Reflections collected	10468	
Independent reflections	2538 [R(int) = 0.0262]	
Completeness to theta = 67.000°	99.9 %	
Absorption correction	Semi-empirical from equivalents	
Max. and min. transmission	0.929 and 0.864	
Refinement method	Full-matrix least-squares on F^2	
Data / restraints / parameters	2538 / 1 / 184	
Goodness-of-fit on F^2	1.067	
Final R indices [I>2sigma(I)]	R1 = 0.0390, wR2 = 0.1064	
R indices (all data)	R1 = 0.0403, wR2 = 0.1078	
Absolute structure parameter	0.09(8)	
Extinction coefficient	n/a	
Largest diff. peak and hole	0.648 and -0.174 e.$Å^{-3}$	

Table 2. Atomic coordinates (x 10^4) and equivalent isotropic displacement parameters ($Å^2$x 10^3) for **3.60**. U(eq) is defined as one third of the trace of the orthogonalized U^{ij} tensor.

	x	y	z	U(eq)
C(1)	3422(3)	9265(4)	7290(2)	21(1)
C(2)	4152(3)	10654(4)	6533(2)	25(1)
C(3)	2904(3)	10899(5)	5523(2)	30(1)
C(4)	1232(3)	11738(4)	5726(2)	27(1)
C(5)	650(3)	11278(4)	6786(2)	24(1)
C(6)	1430(3)	9323(4)	7160(2)	21(1)
C(7)	845(3)	8469(4)	8138(2)	24(1)
C(8)	1608(3)	9456(4)	9136(2)	25(1)
C(9)	1460(3)	8392(5)	10146(2)	29(1)
C(10)	2824(4)	9376(5)	10920(2)	32(1)
C(11)	4310(4)	9715(4)	10300(2)	28(1)
C(12)	4368(3)	9595(4)	8408(2)	22(1)
C(13)	3927(3)	7318(4)	7019(2)	26(1)
C(14)	1176(4)	13004(4)	7498(2)	30(1)
C(15)	-1302(3)	11140(5)	6608(2)	31(1)
N(1)	3476(3)	9679(3)	9202(2)	23(1)
N(2)	4323(3)	5815(4)	6786(2)	40(1)
O(1)	400(3)	12762(4)	5101(2)	42(1)
O(2)	1768(3)	6432(3)	10013(2)	33(1)
O(3)	5946(2)	9707(3)	8531(1)	30(1)

Table 3. Bond lengths [Å] and angles [°] for **3.60**.

C(1)-C(13)	1.481(4)	C(8)-C(9)	1.525(4)
C(1)-C(12)	1.546(3)	C(8)-H(8)	1.0000
C(1)-C(2)	1.554(4)	C(9)-O(2)	1.413(4)
C(1)-C(6)	1.566(3)	C(9)-C(10)	1.528(4)
C(2)-C(3)	1.529(4)	C(9)-H(9)	1.0000
C(2)-H(2A)	0.9900	C(10)-C(11)	1.539(4)
C(2)-H(2B)	0.9900	C(10)-H(10A)	0.9900
C(3)-C(4)	1.510(4)	C(10)-H(10B)	0.9900
C(3)-H(3A)	0.9900	C(11)-N(1)	1.476(3)
C(3)-H(3B)	0.9900	C(11)-H(11A)	0.9900
C(4)-O(1)	1.204(4)	C(11)-H(11B)	0.9900
C(4)-C(5)	1.544(4)	C(12)-O(3)	1.242(3)
C(5)-C(15)	1.536(3)	C(12)-N(1)	1.333(3)
C(5)-C(14)	1.542(4)	C(13)-N(2)	1.155(4)
C(5)-C(6)	1.554(4)	C(14)-H(14A)	0.9800
C(6)-C(7)	1.532(3)	C(14)-H(14B)	0.9800
C(6)-H(6)	1.0000	C(14)-H(14C)	0.9800
C(7)-C(8)	1.512(4)	C(15)-H(15A)	0.9800
C(7)-H(7A)	0.9900	C(15)-H(15B)	0.9800
C(7)-H(7B)	0.9900	C(15)-H(15C)	0.9800
C(8)-N(1)	1.480(3)	O(2)-H(2)	0.8400

C(13)-C(1)-C(12)	104.4(2)	C(1)-C(6)-H(6)	105.4
C(13)-C(1)-C(2)	106.9(2)	C(8)-C(7)-C(6)	113.2(2)
C(12)-C(1)-C(2)	108.7(2)	C(8)-C(7)-H(7A)	108.9
C(13)-C(1)-C(6)	107.7(2)	C(6)-C(7)-H(7A)	108.9
C(12)-C(1)-C(6)	116.1(2)	C(8)-C(7)-H(7B)	108.9
C(2)-C(1)-C(6)	112.4(2)	C(6)-C(7)-H(7B)	108.9
C(3)-C(2)-C(1)	110.8(2)	H(7A)-C(7)-H(7B)	107.8
C(3)-C(2)-H(2A)	109.5	N(1)-C(8)-C(7)	111.7(2)
C(1)-C(2)-H(2A)	109.5	N(1)-C(8)-C(9)	101.9(2)
C(3)-C(2)-H(2B)	109.5	C(7)-C(8)-C(9)	115.8(2)
C(1)-C(2)-H(2B)	109.5	N(1)-C(8)-H(8)	109.0
H(2A)-C(2)-H(2B)	108.1	C(7)-C(8)-H(8)	109.0
C(4)-C(3)-C(2)	111.7(2)	C(9)-C(8)-H(8)	109.0
C(4)-C(3)-H(3A)	109.3	O(2)-C(9)-C(8)	109.7(2)
C(2)-C(3)-H(3A)	109.3	O(2)-C(9)-C(10)	113.7(2)
C(4)-C(3)-H(3B)	109.3	C(8)-C(9)-C(10)	101.7(2)
C(2)-C(3)-H(3B)	109.3	O(2)-C(9)-H(9)	110.5
H(3A)-C(3)-H(3B)	107.9	C(8)-C(9)-H(9)	110.5
O(1)-C(4)-C(3)	121.7(2)	C(10)-C(9)-H(9)	110.5
O(1)-C(4)-C(5)	121.0(3)	C(9)-C(10)-C(11)	104.6(2)
C(3)-C(4)-C(5)	117.3(2)	C(9)-C(10)-H(10A)	110.8
C(15)-C(5)-C(14)	108.5(2)	C(11)-C(10)-H(10A)	110.8
C(15)-C(5)-C(4)	107.9(2)	C(9)-C(10)-H(10B)	110.8
C(14)-C(5)-C(4)	106.0(2)	C(11)-C(10)-H(10B)	110.8
C(15)-C(5)-C(6)	109.7(2)	H(10A)-C(10)-H(10B)	108.9
C(14)-C(5)-C(6)	116.6(2)	N(1)-C(11)-C(10)	103.3(2)
C(4)-C(5)-C(6)	107.7(2)	N(1)-C(11)-H(11A)	111.1
C(7)-C(6)-C(5)	116.6(2)	C(10)-C(11)-H(11A)	111.1
C(7)-C(6)-C(1)	109.0(2)	N(1)-C(11)-H(11B)	111.1
C(5)-C(6)-C(1)	113.9(2)	C(10)-C(11)-H(11B)	111.1
C(7)-C(6)-H(6)	105.4	H(11A)-C(11)-H(11B)	109.1
C(5)-C(6)-H(6)	105.4	O(3)-C(12)-N(1)	122.6(2)

O(3)-C(12)-C(1)	118.1(2)
N(1)-C(12)-C(1)	119.2(2)
N(2)-C(13)-C(1)	178.5(3)
C(5)-C(14)-H(14A)	109.5
C(5)-C(14)-H(14B)	109.5
H(14A)-C(14)-H(14B)	109.5
C(5)-C(14)-H(14C)	109.5
H(14A)-C(14)-H(14C)	109.5
H(14B)-C(14)-H(14C)	109.5
C(5)-C(15)-H(15A)	109.5
C(5)-C(15)-H(15B)	109.5
H(15A)-C(15)-H(15B)	109.5
C(5)-C(15)-H(15C)	109.5
H(15A)-C(15)-H(15C)	109.5
H(15B)-C(15)-H(15C)	109.5
C(12)-N(1)-C(11)	121.9(2)
C(12)-N(1)-C(8)	126.3(2)
C(11)-N(1)-C(8)	111.15(19)
C(9)-O(2)-H(2)	109.5

Symmetry transformations used to generate equivalent atoms:

Table 4. Anisotropic displacement parameters ($Å^2 x\ 10^3$) for **3.60**. The anisotropic displacement factor exponent takes the form: $-2\pi^2[\ h^2\ a^{*2}U^{11} + ...\ + 2\ h\ k\ a^*\ b^*\ U^{12}\ ]$

	U^{11}	U^{22}	U^{33}	U^{23}	U^{13}	U^{12}
C(1)	19(1)	22(1)	23(1)	-2(1)	3(1)	-1(1)
C(2)	21(1)	29(2)	27(1)	0(1)	5(1)	-4(1)
C(3)	26(1)	41(2)	25(1)	3(1)	6(1)	-2(1)
C(4)	24(1)	35(2)	22(1)	2(1)	2(1)	-3(1)
C(5)	20(1)	29(2)	21(1)	3(1)	4(1)	2(1)
C(6)	18(1)	23(1)	22(1)	-1(1)	3(1)	-4(1)
C(7)	19(1)	24(1)	28(1)	4(1)	4(1)	-1(1)
C(8)	25(1)	24(1)	28(1)	5(1)	8(1)	3(1)
C(9)	27(1)	32(2)	28(1)	9(1)	10(1)	5(1)
C(10)	42(2)	30(2)	25(1)	2(1)	10(1)	3(1)
C(11)	37(1)	26(2)	21(1)	-2(1)	4(1)	-8(1)
C(12)	22(1)	18(1)	24(1)	-1(1)	3(1)	-2(1)
C(13)	22(1)	28(2)	29(1)	-2(1)	5(1)	-1(1)
C(14)	39(2)	22(2)	30(1)	4(1)	9(1)	4(1)
C(15)	22(1)	42(2)	30(1)	7(1)	5(1)	5(1)
N(1)	26(1)	21(1)	23(1)	2(1)	4(1)	-3(1)
N(2)	37(1)	31(2)	52(2)	-9(1)	9(1)	0(1)
O(1)	34(1)	64(2)	30(1)	17(1)	5(1)	9(1)
O(2)	30(1)	26(1)	40(1)	12(1)	-6(1)	-3(1)
O(3)	21(1)	42(1)	25(1)	-2(1)	1(1)	-7(1)

Table 5. Hydrogen coordinates ($x\ 10^4$) and isotropic displacement parameters ($Å^2 x\ 10^{\ 3}$) for **3.60**.

	x	y	z	U(eq)
H(2A)	4373	11907	6877	30
H(2B)	5247	10153	6368	30
H(3A)	3418	11742	5042	36
H(3B)	2693	9645	5179	36
H(6)	1032	8411	6583	25
H(7A)	-412	8551	8067	28
H(7B)	1162	7106	8185	28
H(8)	1077	10742	9164	30
H(9)	307	8590	10353	35
H(10A)	3185	8555	11534	38
H(10B)	2396	10597	11162	38
H(11A)	4860	10961	10479	33
H(11B)	5175	8696	10436	33
H(14A)	848	14182	7114	45
H(14B)	2412	12989	7713	45
H(14C)	602	12938	8117	45
H(15A)	-1710	10955	7279	47
H(15B)	-1656	10060	6147	47
H(15C)	-1785	12317	6282	47
H(2)	2546	6065	10482	49

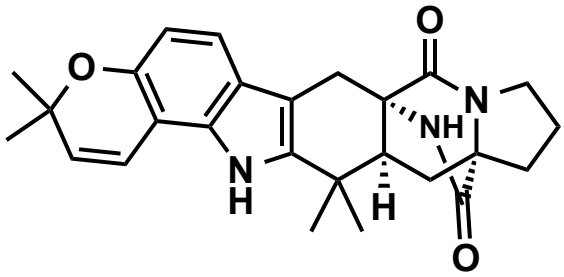

(+)-stephacidin A (3.1)

A colorless plate 0.060 x 0.040 x 0.020 mm in size was mounted on a Cryoloop with Paratone oil. Data were collected in a nitrogen gas stream at 100(2) K using phi and omega scans. Crystal-to-detector distance was 60 mm and exposure time was 10 seconds per frame using a scan width of 1.0°. Data collection was 97.8% complete to 67.000° in θ. A total of 39292 reflections were collected covering the indices, -10<=*h*<=10, -10<=*k*<=8, -42<=*l*<=42. 5366 reflections were found to be symmetry independent, with an R_{int} of 0.0438. Indexing and unit cell refinement indicated a primitive, orthorhombic lattice. The space group was found to be P 21 21 21 (No. 19). The data were integrated using the Bruker SAINT software program and scaled using the SADABS software program. Solution by iterative methods (SHELXT) produced a complete heavy-atom phasing model consistent with the proposed structure. All non-hydrogen atoms were refined anisotropically by full-matrix least-squares (SHELXL-2014). All hydrogen atoms were placed using a riding model. Their positions were constrained relative to their parent atom using the appropriate HFIX command in SHELXL-2014. CCDC # 1400756 (**3.1**) contains the supplementary crystallographic data for this paper. These data can be obtained free of charge from The Cambridge Crystallographic Data Centre via www.ccdc.cam.ac.uk/data_request/cif.

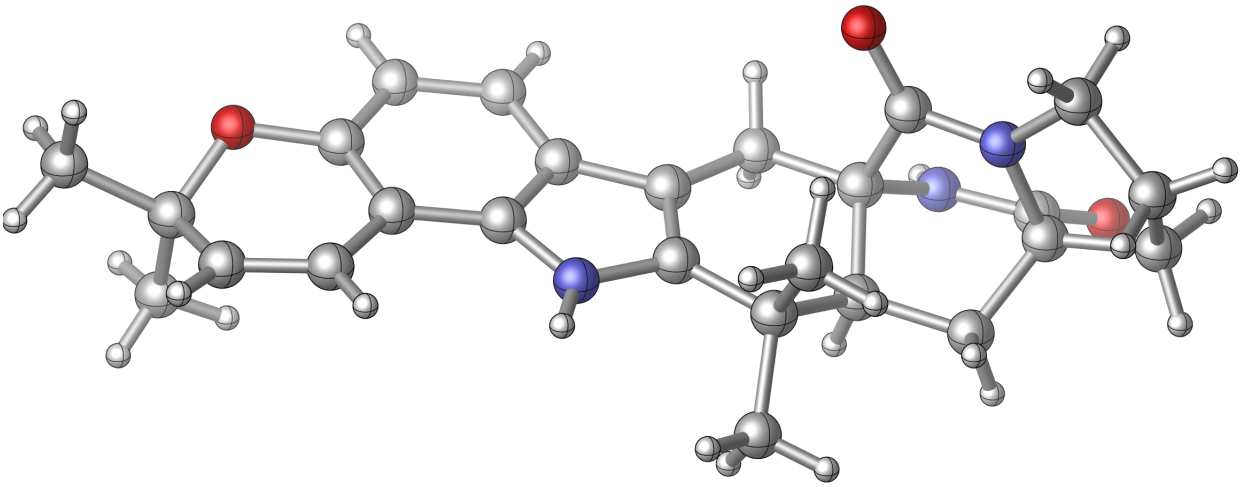

CYLview representation of (+)-stephacidin A (**3.1**)

Table 1. Crystal data and structure refinement for **3.1**.

X-ray ID	sarpong107	
Sample/notebook ID	EM07-137C	
Empirical formula	C26 H29 N3 O3	
Formula weight	431.52	
Temperature	100(2) K	
Wavelength	1.54178 Å	
Crystal system	Orthorhombic	
Space group	P 21 21 21	
Unit cell dimensions	a = 8.7961(4) Å	α= 90°.
	b = 9.7026(5) Å	β= 90°.
	c = 35.0914(18) Å	γ = 90°.
Volume	2994.9(3) $Å^3$	
Z	4	
Density (calculated)	0.957 Mg/m^3	
Absorption coefficient	0.506 mm^{-1}	
F(000)	920	
Crystal size	0.060 x 0.040 x 0.020 mm^3	
Theta range for data collection	2.518 to 68.506°.	
Index ranges	-10<=h<=10, -10<=k<=8, -42<=l<=42	
Reflections collected	39292	
Independent reflections	5366 [R(int) = 0.0438]	
Completeness to theta = 67.000°	97.8 %	
Absorption correction	Semi-empirical from equivalents	
Max. and min. transmission	0.929 and 0.777	
Refinement method	Full-matrix least-squares on F^2	
Data / restraints / parameters	5366 / 0 / 293	
Goodness-of-fit on F^2	1.055	
Final R indices [I>2sigma(I)]	R1 = 0.0628, wR2 = 0.1563	
R indices (all data)	R1 = 0.0660, wR2 = 0.1589	
Absolute structure parameter	-1.08(14)	
Extinction coefficient	n/a	
Largest diff. peak and hole	0.388 and -0.265 $e.Å^{-3}$	

Table 2. Atomic coordinates (x 10^4) and equivalent isotropic displacement parameters ($Å^2$x 10^3) for **3.1**. U(eq) is defined as one third of the trace of the orthogonalized U^{ij} tensor.

	x	y	z	U(eq)
C(1)	5760(5)	2190(5)	3456(1)	32(1)
C(2)	7122(5)	1545(5)	3268(1)	32(1)
C(3)	7302(4)	2022(5)	2870(1)	29(1)
C(4)	8333(4)	1546(4)	2581(1)	26(1)
C(5)	9424(4)	478(5)	2570(1)	29(1)
C(6)	10229(4)	243(5)	2235(1)	33(1)
C(7)	9971(5)	1075(5)	1914(1)	33(1)
C(8)	11049(6)	1892(5)	1329(1)	42(1)
C(9)	9579(6)	2719(6)	1266(1)	50(1)
C(10)	8620(6)	2868(6)	1563(1)	48(1)
C(11)	8870(5)	2119(5)	1908(1)	35(1)
C(12)	8070(4)	2348(5)	2251(1)	31(1)
C(13)	6487(4)	3075(5)	2711(1)	28(1)
C(14)	5288(5)	3920(4)	2893(1)	30(1)
C(15)	5500(5)	3696(5)	3335(1)	33(1)
C(16)	4178(5)	4330(5)	3572(1)	39(1)
C(17)	3510(5)	3176(5)	3824(1)	39(1)
C(18)	2001(6)	3495(6)	4021(2)	52(1)
C(19)	826(6)	2947(7)	3742(2)	54(1)
C(20)	1515(5)	1648(6)	3588(2)	48(1)
C(21)	4271(5)	1387(5)	3393(1)	31(1)
C(22)	4808(5)	2694(6)	4089(1)	41(1)
C(23)	12315(7)	2795(6)	1469(2)	55(1)
C(24)	11487(7)	1178(6)	956(2)	54(1)
C(25)	5505(5)	5463(5)	2811(1)	38(1)
C(26)	3708(5)	3500(5)	2737(1)	34(1)
N(1)	6948(4)	3272(4)	2337(1)	29(1)
N(2)	3155(4)	1987(4)	3581(1)	34(1)
N(3)	5959(4)	2220(4)	3876(1)	38(1)
O(1)	10765(4)	780(3)	1584(1)	39(1)
O(2)	4164(4)	338(3)	3194(1)	38(1)
O(3)	4792(4)	2780(4)	4434(1)	54(1)

Table 3. Bond lengths [Å] and angles [°] for **3.1**.

C(1)-N(3)	1.483(5)	C(16)-C(17)	1.541(7)
C(1)-C(2)	1.504(6)	C(16)-H(16A)	0.9900
C(1)-C(15)	1.539(7)	C(16)-H(16B)	0.9900
C(1)-C(21)	1.540(6)	C(17)-N(2)	1.468(6)
C(2)-C(3)	1.482(6)	C(17)-C(18)	1.529(6)
C(2)-H(2A)	0.9900	C(17)-C(22)	1.545(7)
C(2)-H(2B)	0.9900	C(18)-C(19)	1.519(8)
C(3)-C(13)	1.367(6)	C(18)-H(18A)	0.9900
C(3)-C(4)	1.435(6)	C(18)-H(18B)	0.9900
C(4)-C(5)	1.413(6)	C(19)-C(20)	1.499(8)
C(4)-C(12)	1.416(6)	C(19)-H(19A)	0.9900
C(5)-C(6)	1.391(6)	C(19)-H(19B)	0.9900
C(5)-H(5)	0.9500	C(20)-N(2)	1.480(6)
C(6)-C(7)	1.404(6)	C(20)-H(20A)	0.9900
C(6)-H(6)	0.9500	C(20)-H(20B)	0.9900
C(7)-O(1)	1.382(5)	C(21)-O(2)	1.237(5)
C(7)-C(11)	1.402(6)	C(21)-N(2)	1.318(6)
C(8)-O(1)	1.423(6)	C(22)-O(3)	1.214(5)
C(8)-C(23)	1.500(8)	C(22)-N(3)	1.341(6)
C(8)-C(24)	1.532(7)	C(23)-H(23A)	0.9800
C(8)-C(9)	1.538(7)	C(23)-H(23B)	0.9800
C(9)-C(10)	1.349(6)	C(23)-H(23C)	0.9800
C(9)-H(9)	0.9500	C(24)-H(24A)	0.9800
C(10)-C(11)	1.428(7)	C(24)-H(24B)	0.9800
C(10)-H(10)	0.9500	C(24)-H(24C)	0.9800
C(11)-C(12)	1.411(6)	C(25)-H(25A)	0.9800
C(12)-N(1)	1.367(5)	C(25)-H(25B)	0.9800
C(13)-N(1)	1.386(5)	C(25)-H(25C)	0.9800
C(13)-C(14)	1.481(6)	C(26)-H(26A)	0.9800
C(14)-C(25)	1.536(7)	C(26)-H(26B)	0.9800
C(14)-C(26)	1.548(6)	C(26)-H(26C)	0.9800
C(14)-C(15)	1.578(6)	N(1)-H(1)	0.8800
C(15)-C(16)	1.557(6)	N(3)-H(3)	0.8800
C(15)-H(15)	1.0000		

N(3)-C(1)-C(2)	110.4(3)	C(6)-C(5)-H(5)	120.3
N(3)-C(1)-C(15)	105.9(4)	C(4)-C(5)-H(5)	120.3
C(2)-C(1)-C(15)	113.1(4)	C(5)-C(6)-C(7)	120.0(4)
N(3)-C(1)-C(21)	104.7(3)	C(5)-C(6)-H(6)	120.0
C(2)-C(1)-C(21)	113.8(4)	C(7)-C(6)-H(6)	120.0
C(15)-C(1)-C(21)	108.3(3)	O(1)-C(7)-C(11)	119.1(4)
C(3)-C(2)-C(1)	111.7(4)	O(1)-C(7)-C(6)	118.1(4)
C(3)-C(2)-H(2A)	109.3	C(11)-C(7)-C(6)	122.7(4)
C(1)-C(2)-H(2A)	109.3	O(1)-C(8)-C(23)	111.6(4)
C(3)-C(2)-H(2B)	109.3	O(1)-C(8)-C(24)	103.8(4)
C(1)-C(2)-H(2B)	109.3	C(23)-C(8)-C(24)	110.9(4)
H(2A)-C(2)-H(2B)	107.9	O(1)-C(8)-C(9)	109.8(4)
C(13)-C(3)-C(4)	106.5(4)	C(23)-C(8)-C(9)	111.5(5)
C(13)-C(3)-C(2)	124.2(4)	C(24)-C(8)-C(9)	108.9(4)
C(4)-C(3)-C(2)	129.3(4)	C(10)-C(9)-C(8)	118.1(4)
C(5)-C(4)-C(12)	119.3(4)	C(10)-C(9)-H(9)	121.0
C(5)-C(4)-C(3)	133.3(4)	C(8)-C(9)-H(9)	121.0
C(12)-C(4)-C(3)	107.3(4)	C(9)-C(10)-C(11)	120.2(5)
C(6)-C(5)-C(4)	119.4(4)	C(9)-C(10)-H(10)	119.9

C(11)-C(10)-H(10)	119.9
C(7)-C(11)-C(12)	116.4(4)
C(7)-C(11)-C(10)	119.2(4)
C(12)-C(11)-C(10)	124.4(4)
N(1)-C(12)-C(11)	130.7(4)
N(1)-C(12)-C(4)	107.2(4)
C(11)-C(12)-C(4)	122.1(4)
C(3)-C(13)-N(1)	109.6(4)
C(3)-C(13)-C(14)	127.7(4)
N(1)-C(13)-C(14)	122.7(4)
C(13)-C(14)-C(25)	111.8(4)
C(13)-C(14)-C(26)	110.0(3)
C(25)-C(14)-C(26)	107.6(4)
C(13)-C(14)-C(15)	105.3(4)
C(25)-C(14)-C(15)	107.6(4)
C(26)-C(14)-C(15)	114.7(3)
C(1)-C(15)-C(16)	109.7(4)
C(1)-C(15)-C(14)	114.8(3)
C(16)-C(15)-C(14)	112.6(4)
C(1)-C(15)-H(15)	106.4
C(16)-C(15)-H(15)	106.4
C(14)-C(15)-H(15)	106.4
C(17)-C(16)-C(15)	107.7(4)
C(17)-C(16)-H(16A)	110.2
C(15)-C(16)-H(16A)	110.2
C(17)-C(16)-H(16B)	110.2
C(15)-C(16)-H(16B)	110.2
H(16A)-C(16)-H(16B)	108.5
N(2)-C(17)-C(18)	103.7(4)
N(2)-C(17)-C(16)	108.6(4)
C(18)-C(17)-C(16)	116.3(4)
N(2)-C(17)-C(22)	105.6(4)
C(18)-C(17)-C(22)	115.5(4)
C(16)-C(17)-C(22)	106.4(4)
C(19)-C(18)-C(17)	103.2(4)
C(19)-C(18)-H(18A)	111.1
C(17)-C(18)-H(18A)	111.1
C(19)-C(18)-H(18B)	111.1
C(17)-C(18)-H(18B)	111.1
H(18A)-C(18)-H(18B)	109.1
C(20)-C(19)-C(18)	104.6(4)
C(20)-C(19)-H(19A)	110.8
C(18)-C(19)-H(19A)	110.8
C(20)-C(19)-H(19B)	110.8
C(18)-C(19)-H(19B)	110.8
H(19A)-C(19)-H(19B)	108.9
N(2)-C(20)-C(19)	102.3(4)
N(2)-C(20)-H(20A)	111.3
C(19)-C(20)-H(20A)	111.3
N(2)-C(20)-H(20B)	111.3
C(19)-C(20)-H(20B)	111.3
H(20A)-C(20)-H(20B)	109.2
O(2)-C(21)-N(2)	126.1(4)
O(2)-C(21)-C(1)	124.2(4)
N(2)-C(21)-C(1)	109.7(4)
O(3)-C(22)-N(3)	126.1(5)
O(3)-C(22)-C(17)	124.8(4)
N(3)-C(22)-C(17)	109.1(4)
C(8)-C(23)-H(23A)	109.5
C(8)-C(23)-H(23B)	109.5
H(23A)-C(23)-H(23B)	109.5
C(8)-C(23)-H(23C)	109.5
H(23A)-C(23)-H(23C)	109.5
H(23B)-C(23)-H(23C)	109.5
C(8)-C(24)-H(24A)	109.5
C(8)-C(24)-H(24B)	109.5
H(24A)-C(24)-H(24B)	109.5
C(8)-C(24)-H(24C)	109.5
H(24A)-C(24)-H(24C)	109.5
H(24B)-C(24)-H(24C)	109.5
C(14)-C(25)-H(25A)	109.5
C(14)-C(25)-H(25B)	109.5
H(25A)-C(25)-H(25B)	109.5
C(14)-C(25)-H(25C)	109.5
H(25A)-C(25)-H(25C)	109.5
H(25B)-C(25)-H(25C)	109.5
C(14)-C(26)-H(26A)	109.5
C(14)-C(26)-H(26B)	109.5
H(26A)-C(26)-H(26B)	109.5
C(14)-C(26)-H(26C)	109.5
H(26A)-C(26)-H(26C)	109.5
H(26B)-C(26)-H(26C)	109.5
C(12)-N(1)-C(13)	109.3(3)
C(12)-N(1)-H(1)	125.3
C(13)-N(1)-H(1)	125.3
C(21)-N(2)-C(17)	118.7(4)
C(21)-N(2)-C(20)	129.5(4)
C(17)-N(2)-C(20)	111.9(4)
C(22)-N(3)-C(1)	118.1(4)
C(22)-N(3)-H(3)	121.0
C(1)-N(3)-H(3)	121.0
C(7)-O(1)-C(8)	117.3(3)

Symmetry transformations used to generate equivalent atoms:

Table 4. Anisotropic displacement parameters ($Å^2 x\ 10^3$)for **3.1**. The anisotropic displacement factor exponent takes the form: $-2\pi^2[\ h^2a^{*2}U^{11} + ... + 2\ h\ k\ a^*\ b^*\ U^{12}\ ]$

	U^{11}	U^{22}	U^{33}	U^{23}	U^{13}	U^{12}
C(1)	26(2)	34(2)	35(2)	1(2)	2(2)	-4(2)
C(2)	28(2)	36(3)	31(2)	4(2)	-1(2)	4(2)
C(3)	19(2)	35(2)	34(2)	-4(2)	-2(2)	-1(2)
C(4)	29(2)	17(2)	31(2)	1(2)	-1(2)	-3(2)
C(5)	16(2)	37(3)	34(2)	2(2)	-1(2)	3(2)
C(6)	22(2)	35(3)	43(2)	-2(2)	5(2)	5(2)
C(7)	23(2)	32(3)	44(2)	0(2)	4(2)	0(2)
C(8)	45(3)	37(3)	43(3)	-3(2)	10(2)	5(2)
C(9)	64(3)	59(4)	29(2)	12(2)	9(2)	21(3)
C(10)	41(3)	57(3)	44(3)	3(2)	13(2)	9(3)
C(11)	28(2)	36(3)	40(2)	-1(2)	3(2)	-9(2)
C(12)	24(2)	34(3)	36(2)	-4(2)	-3(2)	-4(2)
C(13)	23(2)	27(2)	36(2)	-1(2)	6(2)	-3(2)
C(14)	30(2)	21(2)	40(2)	0(2)	4(2)	-3(2)
C(15)	29(2)	32(3)	38(2)	-8(2)	-3(2)	-2(2)
C(16)	37(2)	39(3)	42(2)	-9(2)	7(2)	3(2)
C(17)	37(2)	40(3)	38(2)	-5(2)	6(2)	1(2)
C(18)	38(3)	59(4)	59(3)	1(3)	18(2)	1(2)
C(19)	32(2)	70(4)	60(3)	-8(3)	13(2)	13(3)
C(20)	27(2)	59(4)	58(3)	-1(3)	3(2)	3(2)
C(21)	31(2)	37(3)	25(2)	9(2)	3(2)	-2(2)
C(22)	37(2)	49(3)	37(2)	-11(2)	6(2)	-2(2)
C(23)	69(4)	49(3)	47(3)	-4(2)	6(3)	-9(3)
C(24)	57(3)	58(4)	47(3)	-2(3)	18(3)	6(3)
C(25)	29(2)	40(3)	44(2)	-1(2)	-1(2)	10(2)
C(26)	28(2)	39(3)	35(2)	-1(2)	6(2)	1(2)
N(1)	25(2)	33(2)	29(2)	2(1)	-1(1)	5(2)
N(2)	26(2)	39(2)	37(2)	2(2)	2(2)	-2(2)
N(3)	27(2)	50(3)	38(2)	-5(2)	-4(2)	1(2)
O(1)	36(2)	39(2)	41(2)	-2(1)	14(1)	2(1)
O(2)	42(2)	35(2)	36(2)	-7(1)	3(1)	-3(2)
O(3)	58(2)	79(3)	26(2)	-6(2)	6(2)	7(2)

Table 5. Hydrogen coordinates (x 10^4) and isotropic displacement parameters ($Å^2$x 10^3) for **3.1**.

	x	y	z	U(eq)
H(2A)	8047	1782	3415	38
H(2B)	7010	530	3271	38
H(5)	9606	-74	2788	35
H(6)	10955	-481	2223	40
H(9)	9354	3114	1025	60
H(10)	7775	3474	1543	57
H(15)	6439	4213	3408	40
H(16A)	4563	5091	3734	47
H(16B)	3385	4702	3401	47
H(18A)	1928	3019	4269	63
H(18B)	1875	4499	4061	63
H(19A)	-147	2751	3873	65
H(19B)	639	3618	3535	65
H(20A)	1308	854	3757	58
H(20B)	1130	1440	3329	58
H(23A)	12067	3141	1724	83
H(23B)	12446	3574	1294	83
H(23C)	13259	2260	1480	83
H(24A)	12372	585	999	81
H(24B)	11736	1874	764	81
H(24C)	10632	617	866	81
H(25A)	6542	5736	2880	56
H(25B)	4776	5997	2962	56
H(25C)	5337	5640	2540	56
H(26A)	3682	3645	2461	51
H(26B)	2922	4064	2859	51
H(26C)	3522	2525	2793	51
H(1)	6578	3895	2180	35
H(3)	6809	1934	3982	46

3.9 – References and Notes

1. Hudlicky, T.; Reed, J. W. *The Way of Synthesis*, Wiley-VCH, Weinheim, Germany, **2007**; pp 1–47.

2. (a) Jones, S. B.; Simmons, B.; Mastracchio, A.; MacMillan, D. W. C. *Nature* **2011,** *475*, 183–188; (b) Gravel, E.; Poupon, E. *Eur. J. Org. Chem.* **2008,** *2008*, 27–42.

3. Anagnostaki, E. E.; Zografos, A. L. *Chem. Soc. Rev.* **2012,** *41*, 5613–5625.

4. For an in-depth review on the isolation, biosynthesis and bioactivity of prenylated indole alkaloids containing the bridged bicyclo[2.2.2]diazaoctane ring system see: Finefield, J. M.; Frisvad, J. C.; Sherman, D. H.; Williams, R. M. *J. Nat. Prod.* **2012,** *75*, 812–833; For the isolation of mangrovamides see: Yang, B.; Dong, J.; Lin, X.; Zhou, X.; Zhang, Y.; Liu, Y. *Tetrahedron* **2014,** *70* , 3859–3863.

5. Citrinalins see: (a) Pimenta, E. F.; Vita-Marques, A. M.; Tinimis, A.; Seleghim, M. H. R.; Sette, L. D.; Veloso, K.; Ferreira, A. G.; Williams, D. E.; Patrick, B. O.; Dalisay, D. S.; Andersen, R. J.; Berlinck, R. G. S. *J. Nat. Prod.* **2010,** *73*, 1821–1832; Citrinadins see: (b) Tsuda, M.; Kasai, Y.; Komatsu, K.; Sone, T.; Tanaka, M.; Mikami, Y.; Kobayashi, J. I. *Org. Lett.* **2004,** *6*, 3087–3089; (c) Mugishima, T.; Tsuda, M.; Kasai, Y.; Ishiyama, H.; Fukushi, E.; Kawabata, J.; Watanabe, M.; Akao, K.; Kobayashi, J. I. *J. Org. Chem.* **2005,** *70*, 9430–9435; Cyclopiamines see: (d) Bond, R. F.; Boeyens, J. C. A.; Holzapfel, C. W.; Steyn, P. S. *J. Chem. Soc., Perkin Trans. 1,* **1979**, 1751; (e) Steyn, P. S.; Vleggaar, R.; Rabie, C. J. *Phytochemistry* **1981,** *20*, 538–539.

6. Kushida, N.; Watanabe, N.; Okuda, T.; Yokoyama, F.; Gyobu, Y.; Yaguchi, T. *J. Antibiot.* **2007,** *60*, 667–673.

7. For selected total syntheses of natural products containing the bicyclo[2.2.2]diazaoctane core see: (a) Baran, P. S.; Guerrero, C. A.; Ambhaikar, N. B.; Hafensteiner, B. D. *Angew. Chem. Int. Ed.* **2005,** *44*, 606–609; (b) Baran, P. S.; Guerrero, C. A.; Hafensteiner, B. D.; Ambhaikar, N. B. *Angew. Chem. Int. Ed.* **2005,** *44*, 3892–3895; (c) Baran, P. S.; Hafensteiner, B. D.; Ambhaikar, N. B.; Guerrero, C. A.; Gallagher, J. D. *J. Am. Chem. Soc.* **2006,** *128*, 8678–8693; (d) Herzon, S. B.; Myers, A. G. *J. Am. Chem. Soc.* **2005,** *127*, 5342-5344; (e) Greshock, T. J.; Grubbs, A. W.; Tsukamoto, S.; Williams, R. M. *Angew. Chem. Int. Ed.* **2007,** *46*, 2262–2265; (f) Artman III, G. D.; Grubbs, A. W.; Williams, R. M. *J. Am. Chem. Soc.* **2007,** *129*, 6336–6342; (g) Trost, B. M.; Cramer, N.; Bernsmann, H. *J. Am. Chem. Soc.* **2007,** *129*, 3086–3087; (h) Frebault, F.; Simpkins, N. S.; Fenwick, A. *J. Am. Chem. Soc.* **2009,** *131*, 4214–4215; (i) Laws, S. W.; Scheerer, J. R. *J. Org. Chem.* **2013,** *78*, 2422–2429; (j) Simpkins, N. S.; Pavlakos, I.; Weller, M. D.; Male, L. *Org. Biomol. Chem.* **2013,** *11*, 4957–4970; For reviews see: (k) Miller, K. A.; Williams, R. M. *Chem. Soc. Rev.* **2009,** *38*, 3160–3174; (l) Nising, C. F. *Chem. Soc. Rev.* **2010,** *39*, 591–599.

8. For selected total syntheses of natural products that lack the bicyclo[2.2.2]diazaoctane core see: (a) Bian, Z.; Marvin, C. C.; Martin, S. F. *J. Am. Chem. Soc.* **2013,** *135*, 10886–10889; (b) Kong, K.; Enquist, J. A., Jr.; McCallum, M. E.; Smith, G. M.; Matsumaru, T.; Menhaji-Klotz, E.; Wood, J. L. *J. Am. Chem. Soc.* **2013,** *135*, 10890–10893; (c) Mercado-Marin, E. V.; Garcia-Reynaga, P.; Romminger, S.; Pimenta, E. F.; Romney, D. K.;

Lodewyk, M. W.; Williams, D. E.; Andersen, R. J.; Miller, S. J.; Tantillo, D. J.; Berlinck, R. G. S.; Sarpong, R. *Nature* **2014,** *509*, 318–324.

9. (a) Corey, E. J.; Howe, W. J.; Orf, H. W.; Pensak, D. A.; Petersson, G. *J. Am. Chem. Soc.* **1975,** *97*, 6116–6124; (b) Heathcock, C. H. *Angew. Chem. Int. Ed.* **1992,** *31*, 665–681.

10. For a Dieckmann cyclization route to form 2,5-diketopiperazines see: (a) Aboussafy, C. L.; Clive, D. L. *J. Org. Chem.* **2012,** *77* (11), 5125–5131; For a review on the synthesis of 2,5-diketopiperazines see: (b) Borthwick, A. D. *Chem. Rev.* **2012,** *112*, 3641–3716.

11. (a) Lee, B. H.; Clothier, M. F. *J. Org. Chem.* **1997,** *62*, 1795–1798; (b) Lee, B. H.; Clothier, M. F.; Pickering, D. A. *J. Org. Chem.* **1997,** *62*, 7836–7840.

12. (a) Krow, G. R. *Tetrahedron* **1987,** *43*, 3–38; (b) Maruoka, K.; Concepcion, A. B.; Yamamoto, H. *J. Org. Chem.* **1994,** *59*, 4725–4726; (c) Macías, F. A.; Carrera, C.; Chinchilla, N.; Fronczek, F. R.; Galindo, J. C. G. *Tetrahedron* **2010,** *66*, 4125–4132; (d) McKinney, M. A.; Patel, P. P. *J. Org. Chem.* **1973,** *38*, 4059–4064; (e) Kürti, L.; Czakó, B.; Corey, E. J. *Org. Lett.* **2008,** *10*, 5247–5250.

13. Klein, C.; Hüttel, W. *Adv. Synth. Catal.* **2011,** *353*, 1375–1383.

14. Reddy, B. V. S.; Reddy, L. R.; Corey, E. J. *Org. Lett.* **2006,** *8*, 3391–3394.

15. Subba Reddy, B. V.; Bhavani, K.; Raju, A.; Yadav, J. S. *Tetrahedron: Asymmetry* **2011,** *22*, 881–886.

16. (a) Cooper, J.; Gallagher, P. T.; Knight, D. W. *J. Chem. Soc., Perkin Trans. 1,* **1993**, 1313–1317; (b) Cooper, J.; Gallagher, P. T.; Knight, D. W. *J. Chem. Soc., Chem. Commun.* **1988**, 509–510.

17. Blake, J.; Willson, C. D.; Rapoport, H. *J. Am. Chem. Soc.* **1964,** *86*, 5293–5299.

18. Moreau, R. J.; Sorensen, E. J. *Tetrahedron* **2007,** *63*, 6446–6453.

19. Williams, R. M.; Cao, J.; Tsujishima, H. *Angew. Chem. Int. Ed.* **2000,** *39*, 2540–2544.

20. Chakraborty, T. K.; Srinivasu, P.; Rao, R. V.; Kumar, S. K.; Kunwar, A. C. *J. Org. Chem.* **2004,** *69*, 7399–7402.

21. Parikh, J. R.; Doering, W. v. E. *J. Am. Chem. Soc.* **1967,** *89*, 5505–5507.

22. Zanato, C.; Pignataro, L.; Ambrosi, A.; Hao, Z.; Trigili, C.; Díaz, J. F.; Barasoain, I.; Gennari, C. *Eur. J. Org. Chem.* **2011**, 2643–2661.

23. Grotjahn, D. B.; Lev, D. A. *J. Am. Chem. Soc.* **2004,** *126*, 12232–12233.

24. (a) Ding, Y.; Greshock, T. J.; Miller, K. A.; Sherman, D. H.; Williams, R. M. *Org Lett* **2008,** *10*, 4863–4866; (b) Watts, K. R.; Loveridge, S. T.; Tenney, K.; Media, J.; Valeriote, F. A.; Crews, P. *J. Org. Chem.* **2011,** *76*, 6201–6208.

25. Ghaffar, T.; Parkins, A. W. *Tetrahedron Lett.* **1995,** *36*, 8657–8660.

26. Lee, J.; Kim, M.; Chang, S.; Lee, H.-Y. *Org. Lett.* **2009,** *11*, 5598–5601.

27. Omura, K.; Swern, D. *Tetrahedron* **1978,** *34*, 1651–1660.

28. Ley, S. V.; Norman, J.; Griffith, W. P.; Marsden, S. P. *Synthesis* **1994**, 639–666.

29. Corey, E. J.; Suggs, J. W. *Tetrahedron Lett.* **1975,** *16*, 2647–2650.

30. Krohn, K.; Knauer, B.; Küpke, J.; Seebach, D.; Beck, A. K.; Hayakawa, M. *Synthesis* **1996**, 1341–1344.

31. Moriarty, R. M.; Chany, C. J.; Vaid, R. K.; Prakash, O.; Tuladhar, S. M. *J. Org. Chem.* **1993,** *58*, 2478–2482.

32. (a) Aboussafy, C. L.; Clive, D. L. J. *J. Org. Chem.* **2012,** *77*, 5125–5131; (b) Peng, J.; Clive, D. L. J. *J. Org. Chem.* **2008,** *74* (2), 513–519.

33. (a) Huang, X.; Keillor, J. W. *Tetrahedron Lett.* **1997,** *38*, 313–316; (b) Huang, X.; Seid, M.; Keillor, J. W. *J. Org. Chem.* **1997,** *62*, 7495–7496.

34. (a) Yoshimura, A.; Middleton, K. R.; Luedtke, M. W.; Zhu, C.; Zhdankin, V. V. *J. Org. Chem.* **2012,** *77*, 11399–11404; (b) Miyamoto, K.; Sakai, Y.; Goda, S.; Ochiai, M. *Chem. Commun.* **2012,** *48*, 982–984.

35. Yoshimura, A.; Luedtke, M. W.; Zhdankin, V. V. *J. Org. Chem.* **2012,** *77*, 2087–2091.

36. (a) Wicks, D. A.; Wicks Jr, Z. W. *Prog. Org. Coat.* **1999,** *36*, 148–172; (b) Wicks, D. A.; Wicks Jr, Z. W. *Prog. Org. Coat.* **2001,** *41*, 1-83.

37. (a) Figueroa, M.; Gonzalez Mdel, C.; Mata, R. *Nat. Prod. Res.* **2008,** *22*, 709–714; (b) Martínez-Luis, S.; Rodríguez, R.; Acevedo, L.; González, M. C.; Lira-Rocha, A.; Mata, R. *Tetrahedron* **2006,** *62*, 1817–1822.

38. Miller, K. A.; Figueroa, M.; Valente, M. W.; Greshock, T. J.; Mata, R.; Williams, R. M. *Bioorg. Med. Chem. Lett.* **2008,** *18*, 6479–6481.

39. Cherney, E. C.; Lopchuk, J. M.; Green, J. C.; Baran, P. S. *J. Am. Chem. Soc.* **2014,** *136*, 12592–12595.

40. Burns, N. Z.; Baran, P. S.; Hoffmann, R. W. *Angew. Chem. Int. Ed.* **2009,** *48*, 2854–2867.

41. Johnson, C. R.; Adams, J. P.; Braun, M. P.; Senanayake, C. B. W.; Wovkulich, P. M.; Uskoković, M. R. *Tetrahedron Lett.* **1992,** *33*, 917–918.

42. Miller, D. G.; Wayner, D. D. M. *J. Org. Chem.* **1990,** *55*, 2924–2927.

43. Zhang, X.; Foote, C. S. *J. Am. Chem. Soc.* **1993,** *115*, 8867–8868.

44. Borch, R. F. *Tetrahedron Lett.* **1968,** *9*, 61–65.

45. Note: See 3.7 – Experimental Method and Procedure for more details.

46. Gruner, K. K.; Knolker, H.-J. *Org. Biomol. Chem.* **2008,** *6*, 3902–3904.

47. Greshock, T. J.; Williams, R. M. *Org. Lett.* **2007,** *9*, 4255–4258.

48. Williams, R. M.; Cao, J.; Tsujishima, H.; Cox, R. J. *J. Am. Chem. Soc.* **2003,** *125*, 12172–12178.

49. Note: The methyl ester varient of **3.43** was previously reported by Sorenson and co-workers by an intramolecular N-H insertion of a diazo-compound, Ref. 17 (R. Moreau, E. J. Sorensen, Tetrahedron, **2007**, *63*, 6446); this method was employed on large scale to access **3.43** by substituting methyl potassium malonate for ethyl potassium malonate in accordance with Sorenson's procedure.

50. Ohira, S. *Synth. Commun.* **1989,** *19*, 561–564.

51. Turner, T. C.; Shibayama, K.; Boger, D. L. *Org. Lett.* **2013,** *15*, 1100–1103.

52. Note: Zinc dust was freshly activated by sequential washing with 0.1 M aq. HCl (3 x 10 mL) and water (10 mL). The solid was collected by filtration and washed with ethanol (2 x 10 mL) and diethyl ether (2 x 10 mL), then dried under high vacuum to give a soft blue-gray solid, which was ground to a powder.

53. Note: The spectroscopic data for the TFA salt (**A3.3**) were consistent with those previously reported for the neutral form of the natural product 17-hydroxy-citrinalin B (**2.18**); see spectra in Appendix 2. Also see Ref: 8c.

54. Tsukamoto, S.; Kato, H.; Samizo, M.; Nojiri, Y.; Onuki, H.; Hirota, H.; Ohta, T. *J. Nat. Prod.* **2008,** *71*, 2064–2067.

Appendix 2:

Spectra Relevant to Chapter 3

EM01-071B_cdcl3/13
AV-600 ZBO proton starting parameters 11/16/08 RN

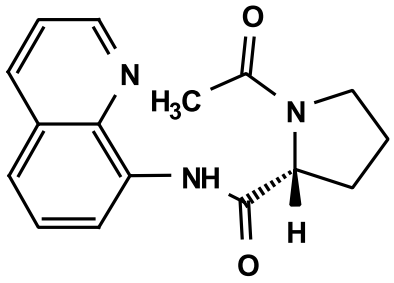

Figure A2.1: ^{1}H NMR of **3.38.**

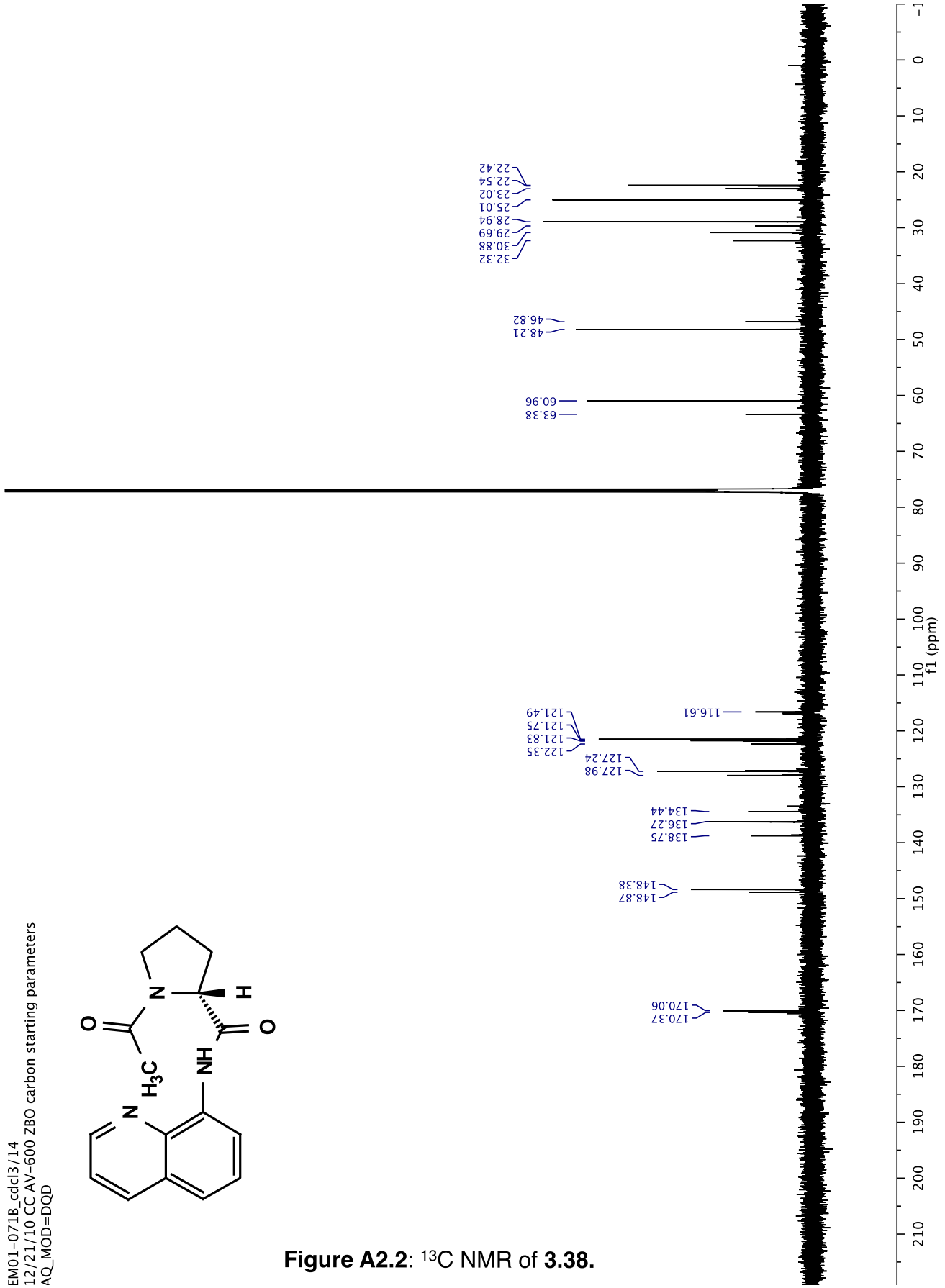

Figure A2.2: ^{13}C NMR of **3.38.**

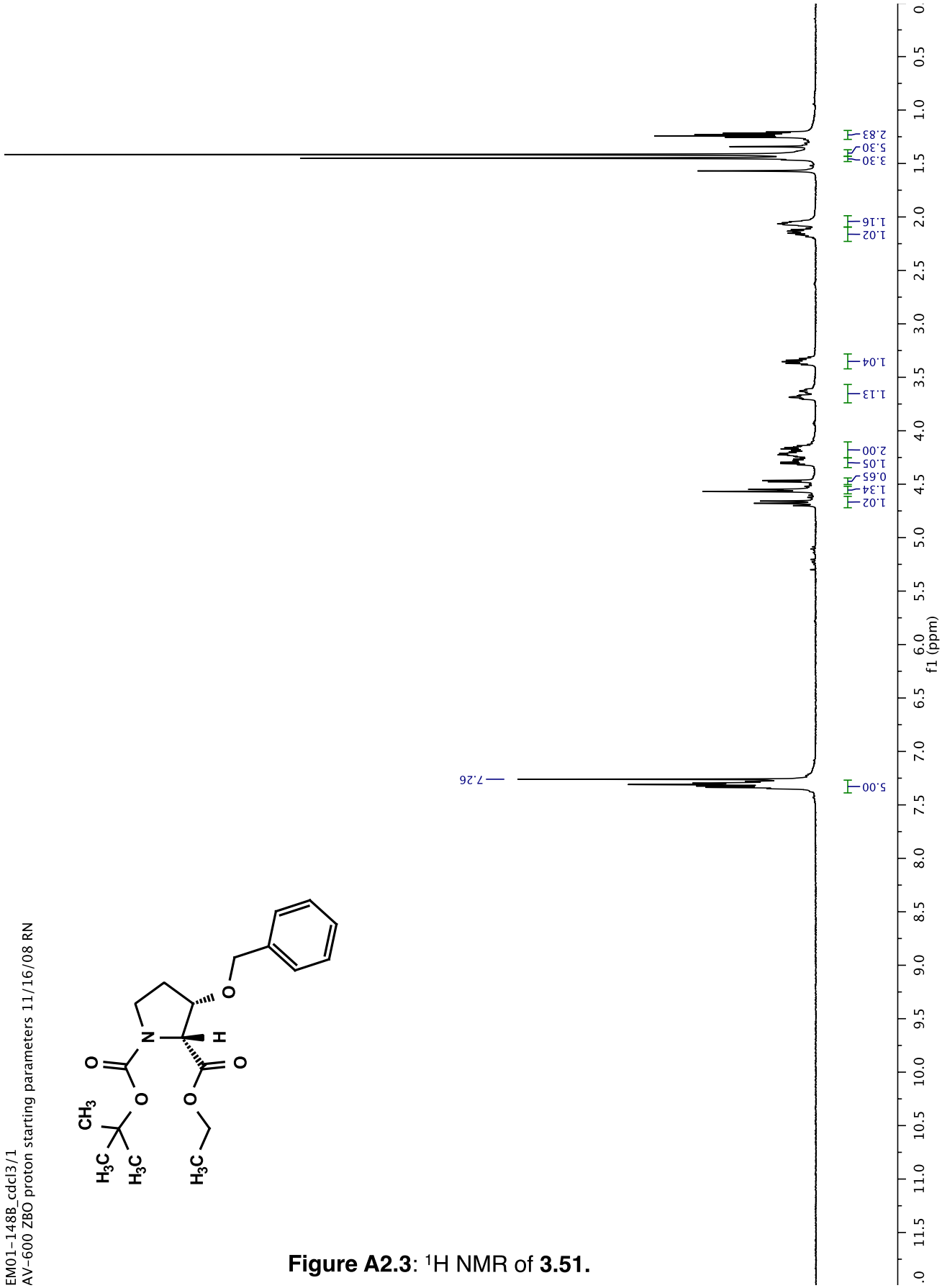

Figure A2.3: ^{1}H NMR of **3.51.**

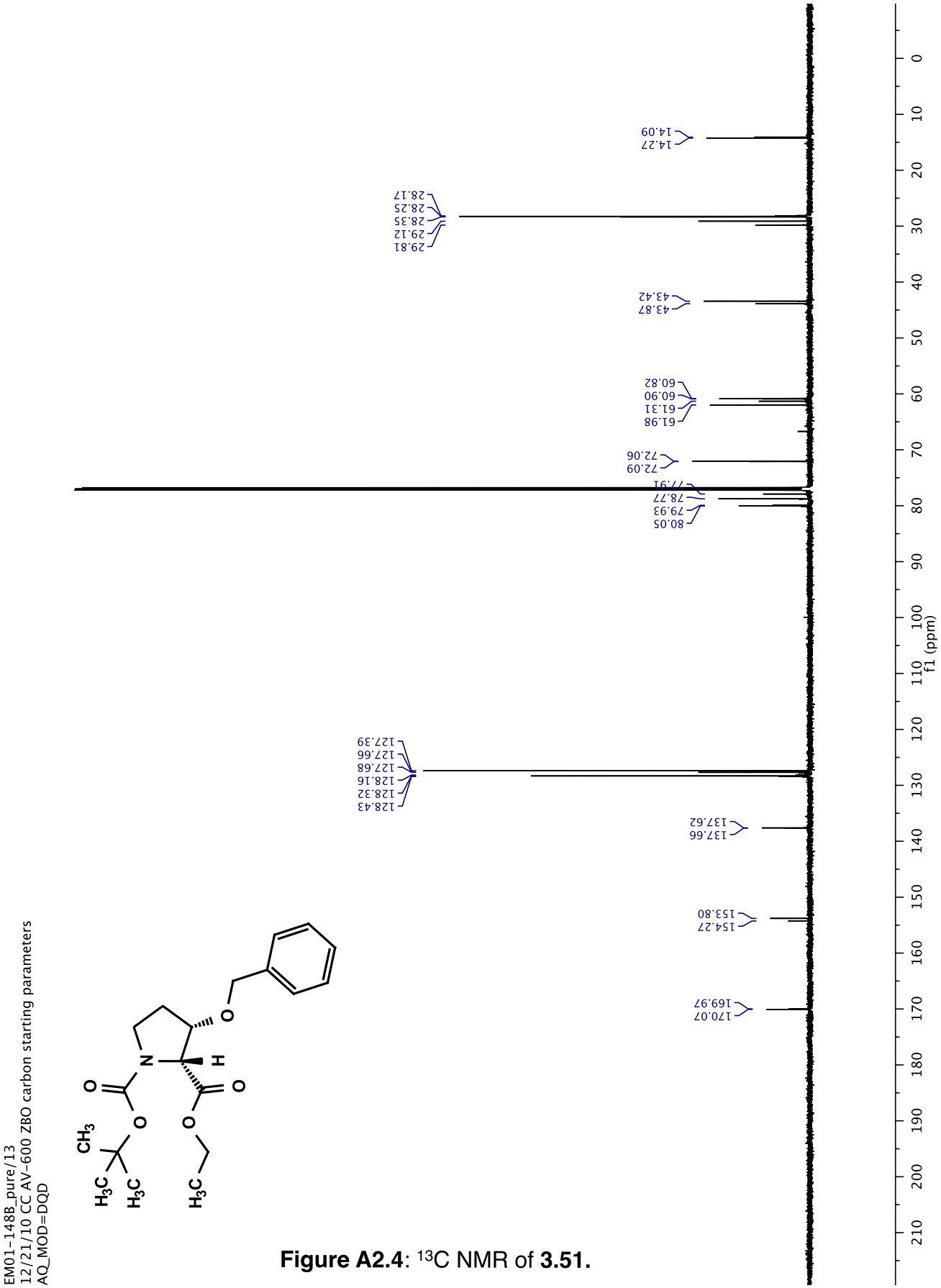

Figure A2.4: ^{13}C NMR of **3.51.**

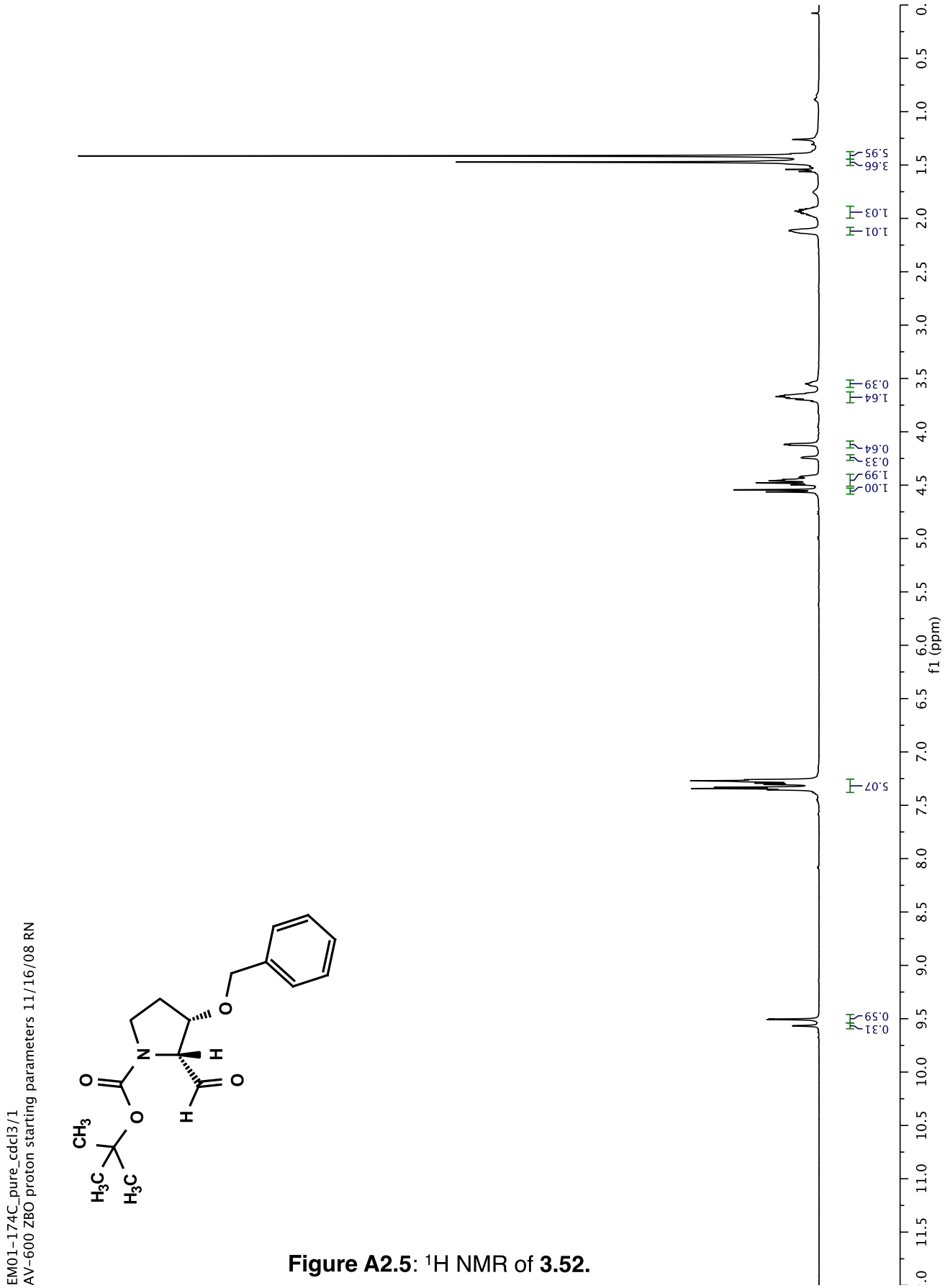

Figure A2.5: ^{1}H NMR of **3.52.**

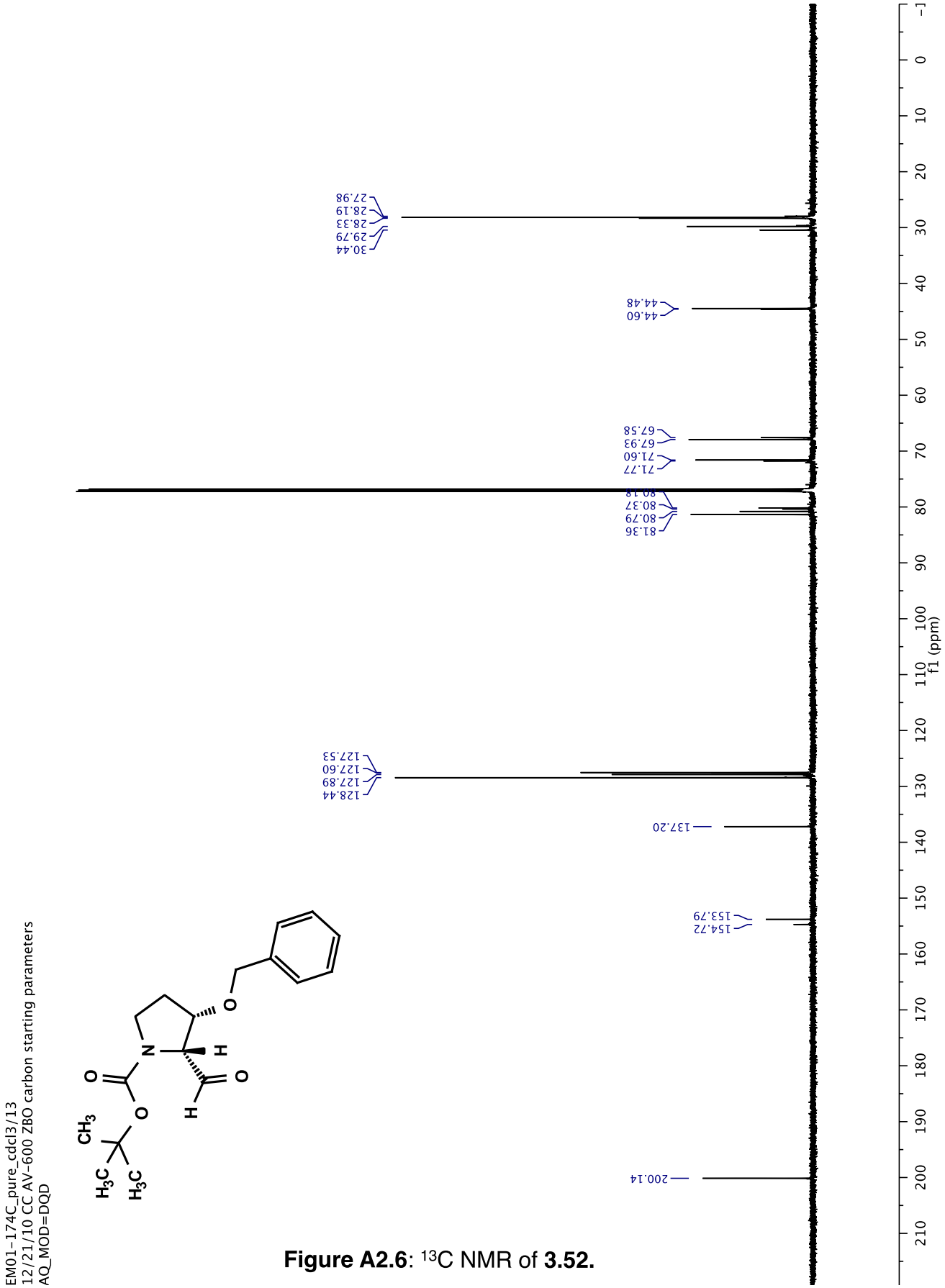

Figure A2.6: ^{13}C NMR of **3.52.**

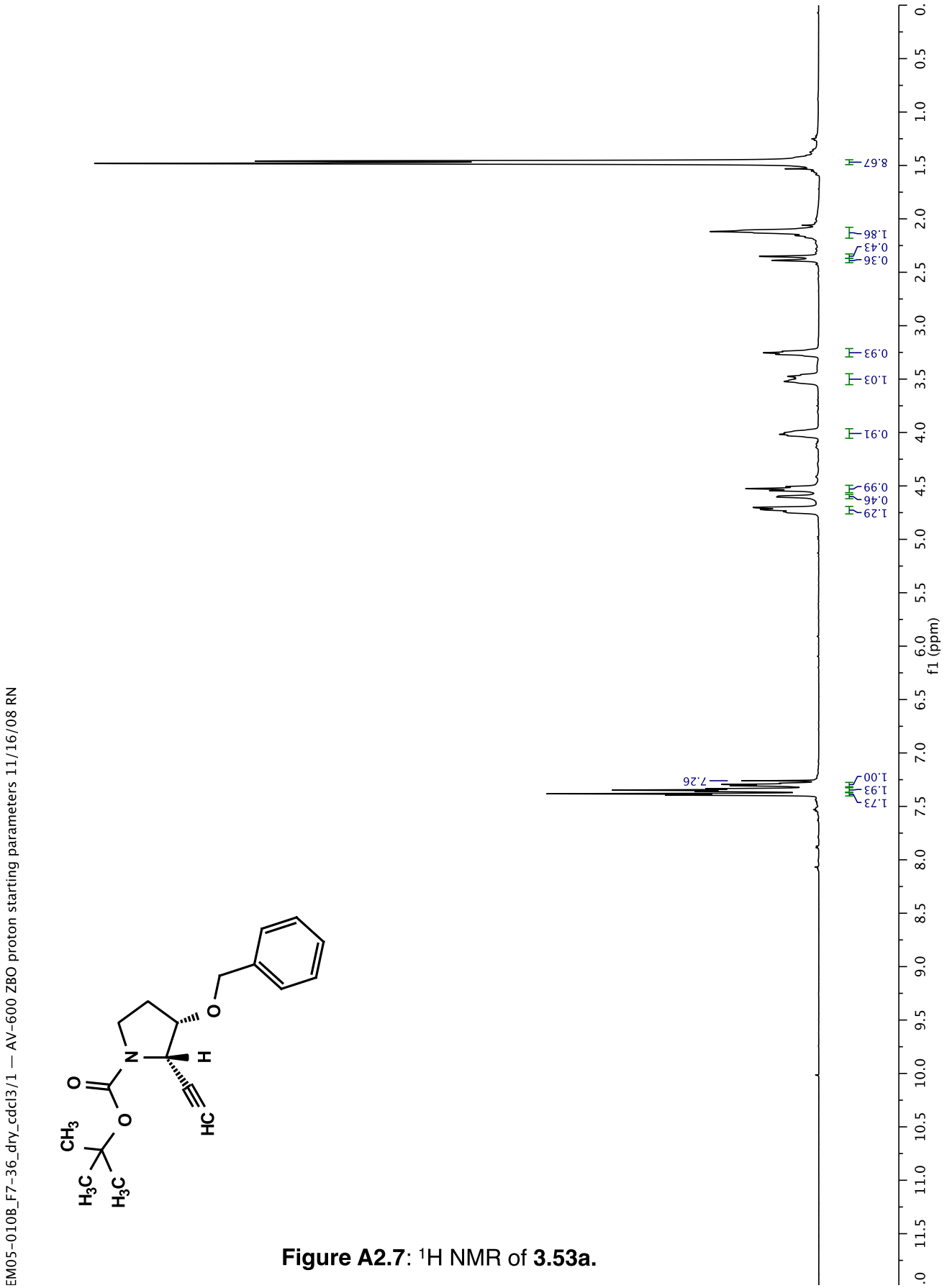

Figure A2.7: ^{1}H NMR of **3.53a.**

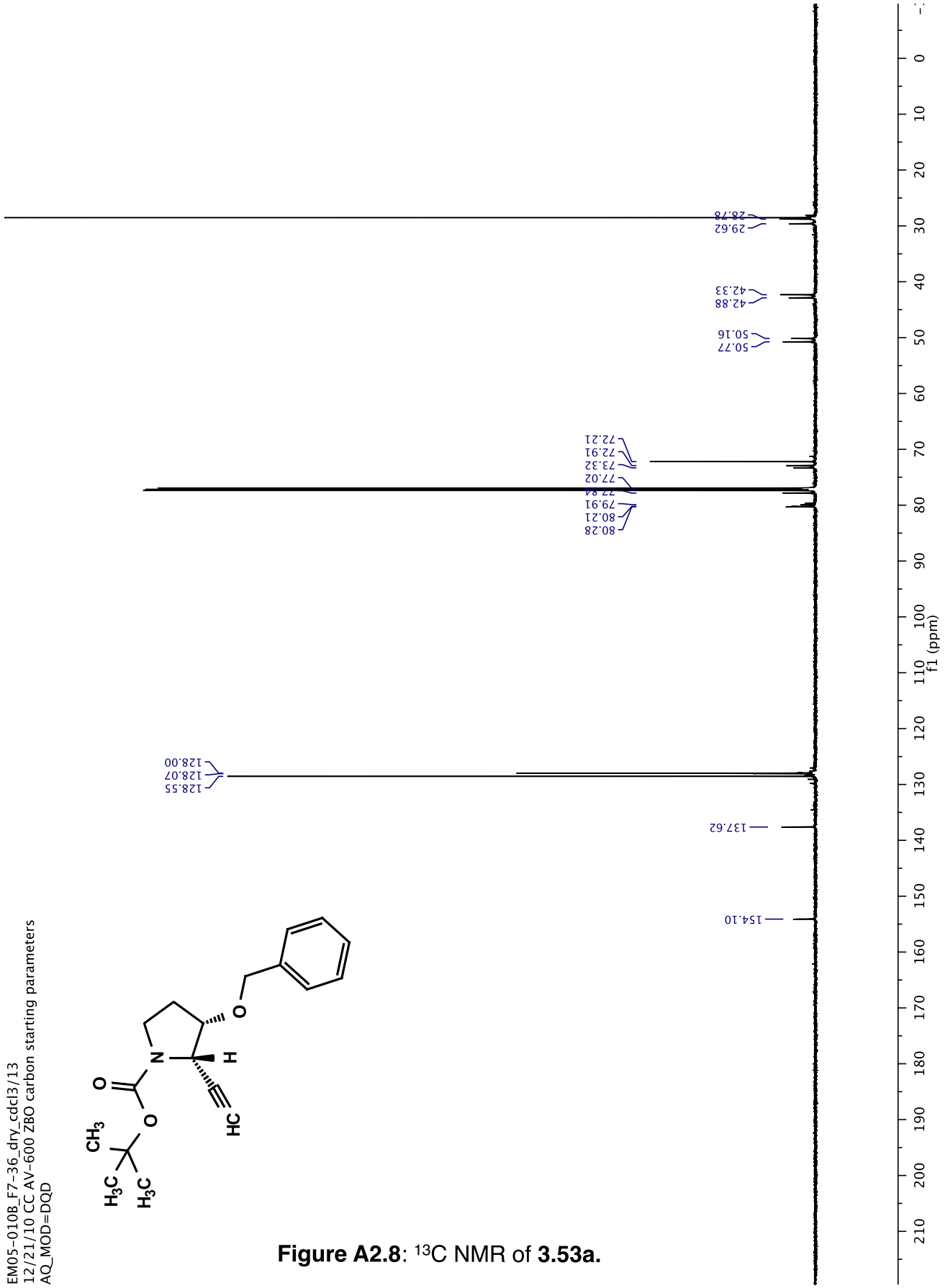

Figure A2.8: ^{13}C NMR of **3.53a.**

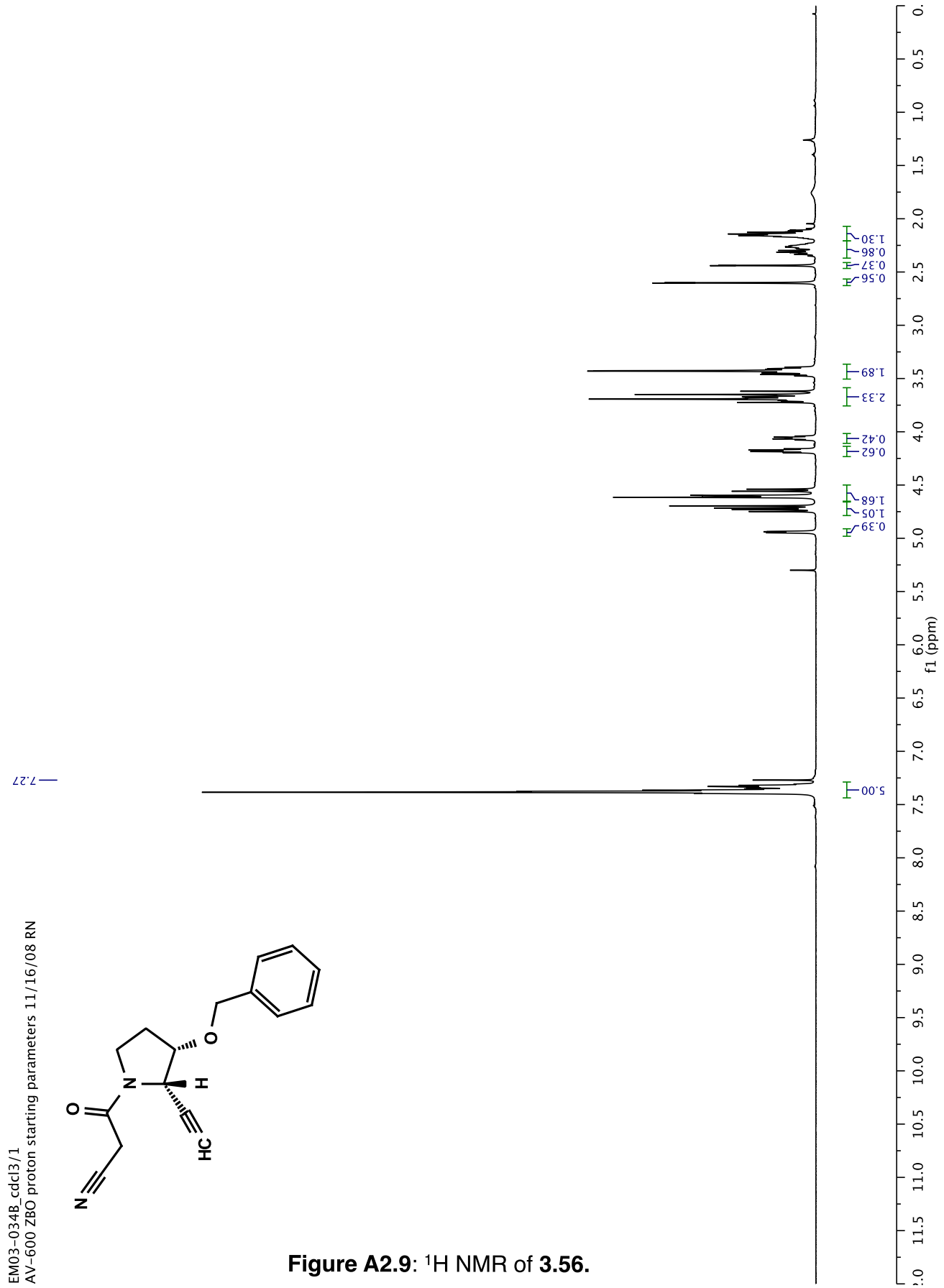

Figure A2.9: ^{1}H NMR of **3.56.**

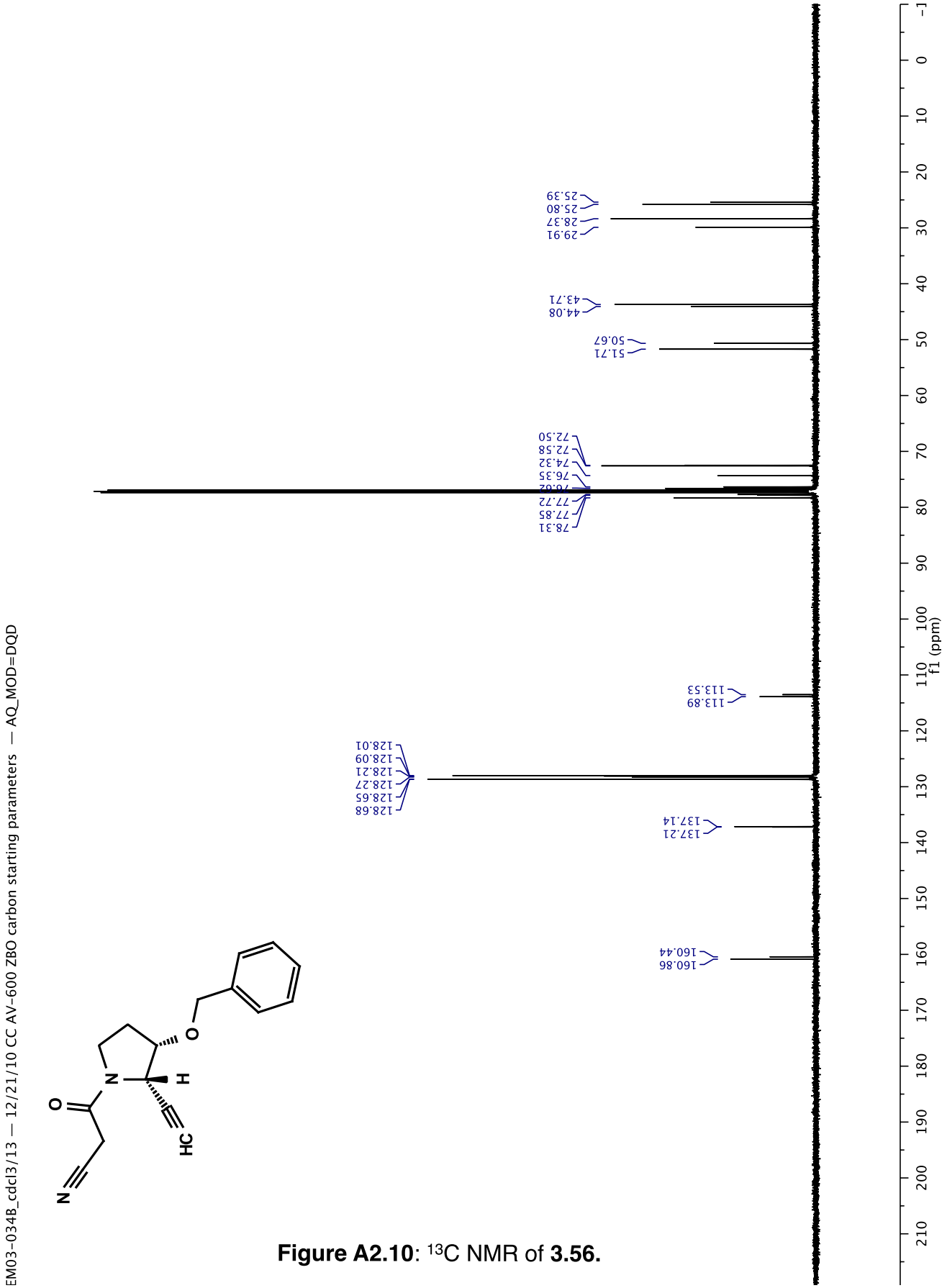

Figure A2.10: ^{13}C NMR of **3.56.**

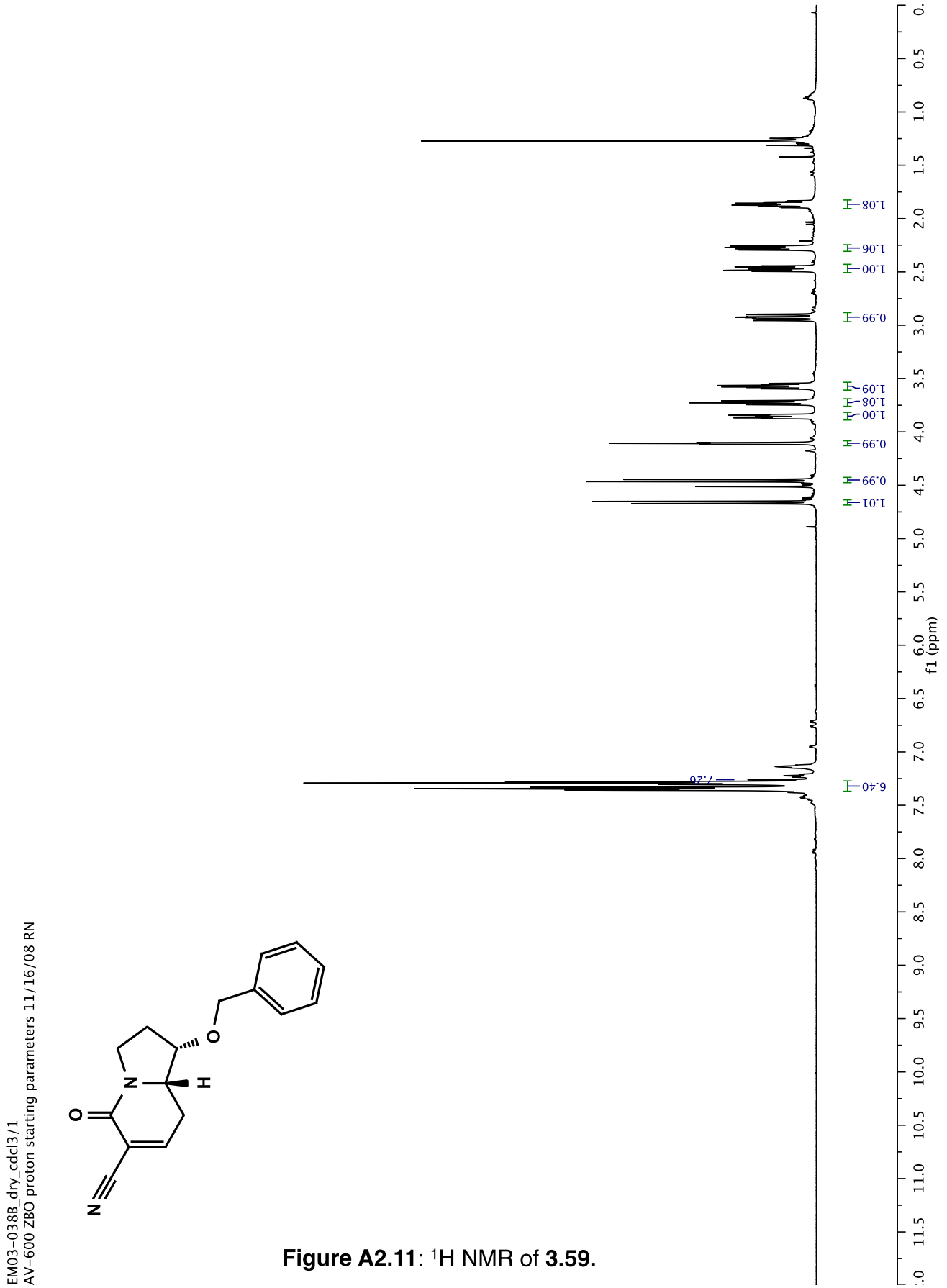

Figure A2.11: ^{1}H NMR of **3.59.**

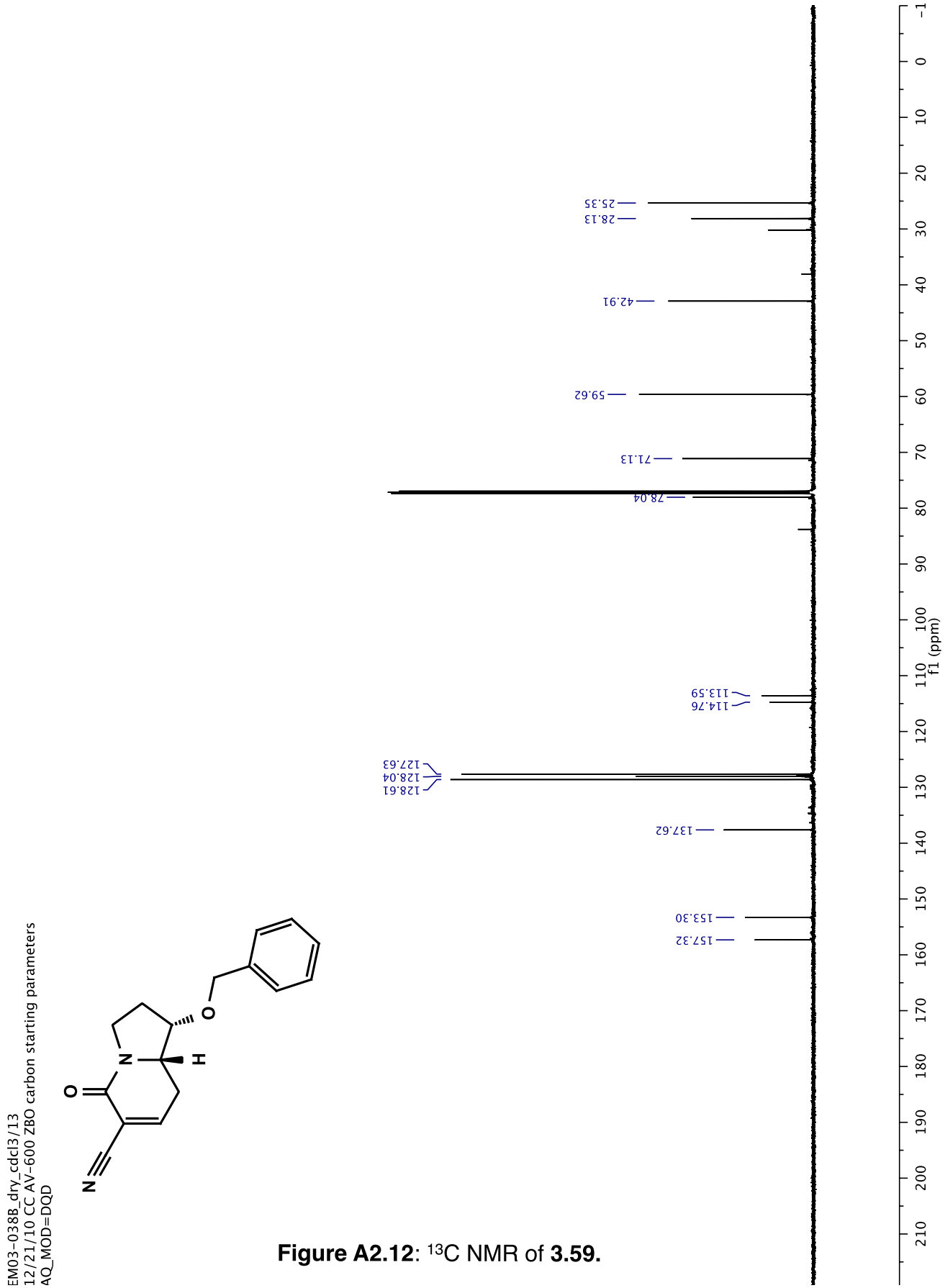

Figure A2.12: ^{13}C NMR of **3.59.**

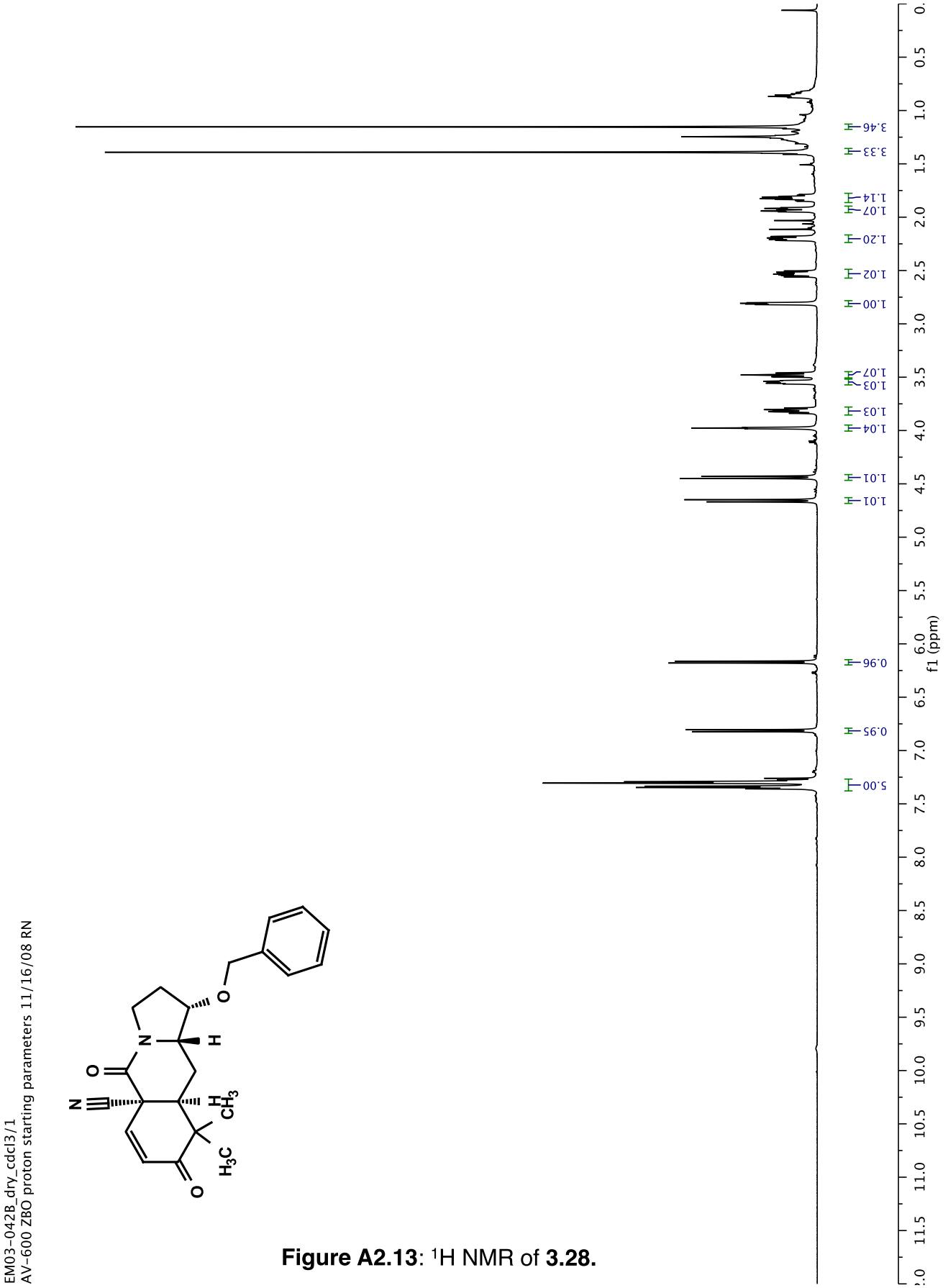

Figure A2.13: ^{1}H NMR of **3.28.**

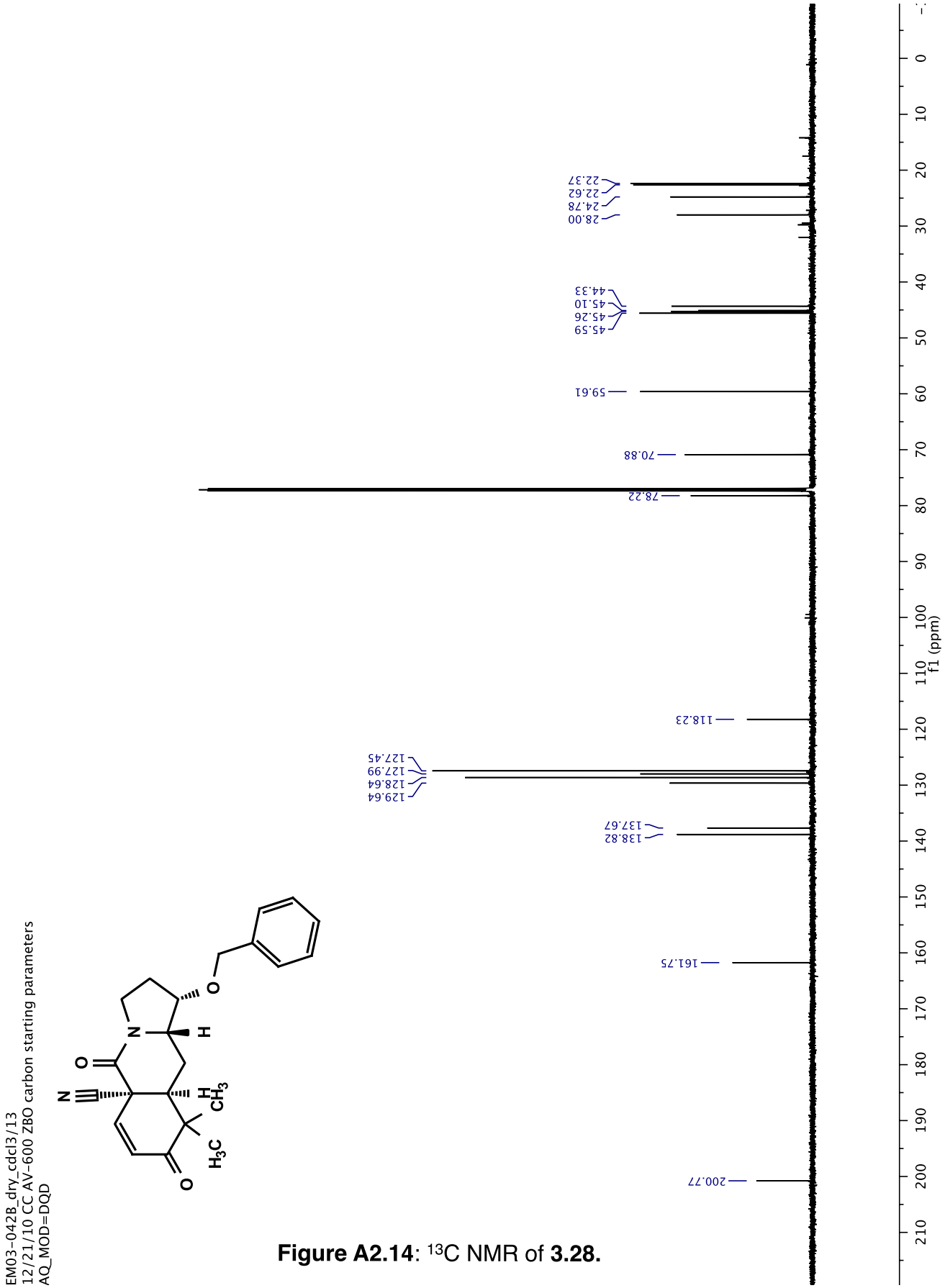

Figure A2.14: ^{13}C NMR of **3.28.**

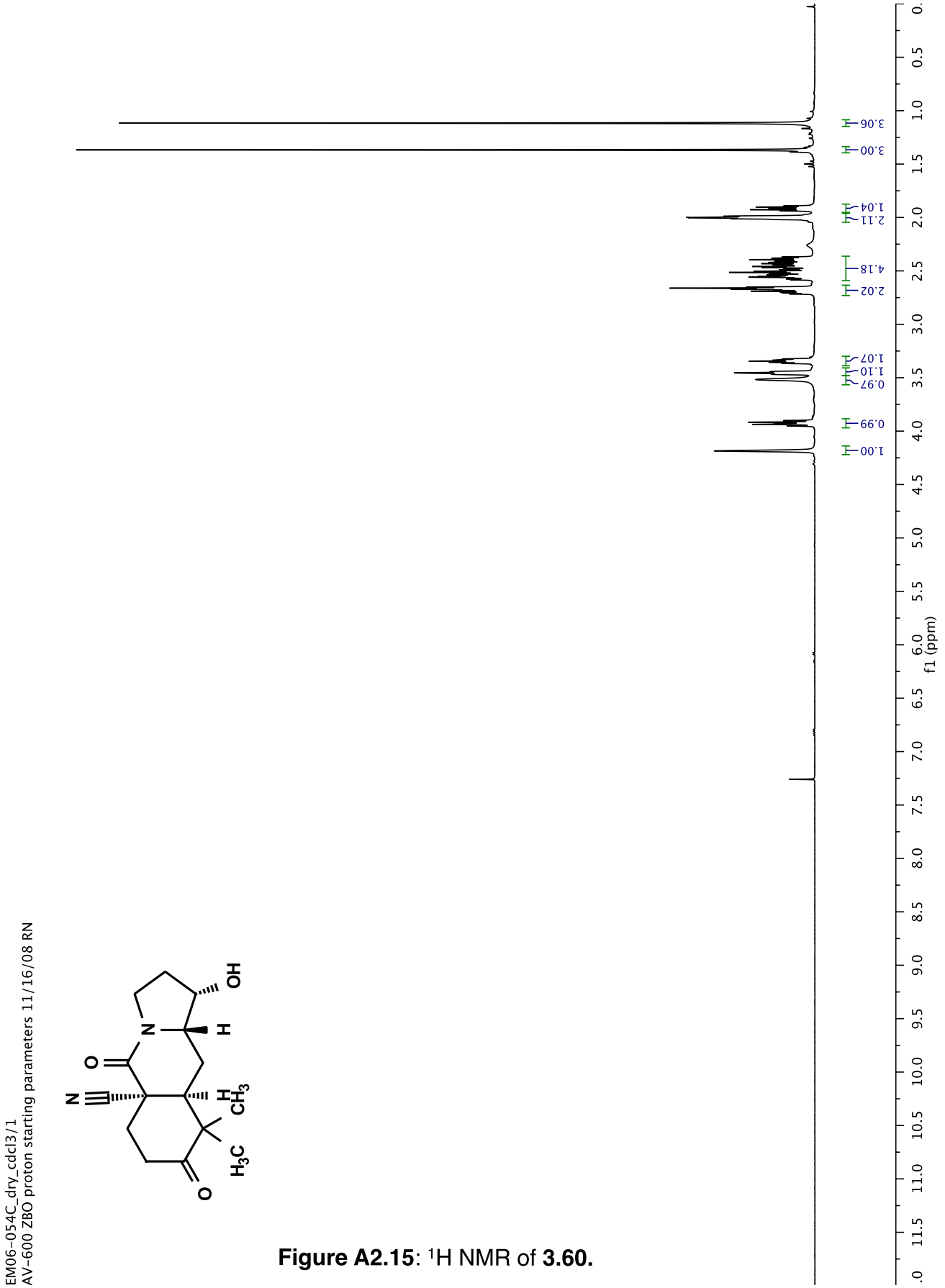

Figure A2.15: ^{1}H NMR of **3.60.**

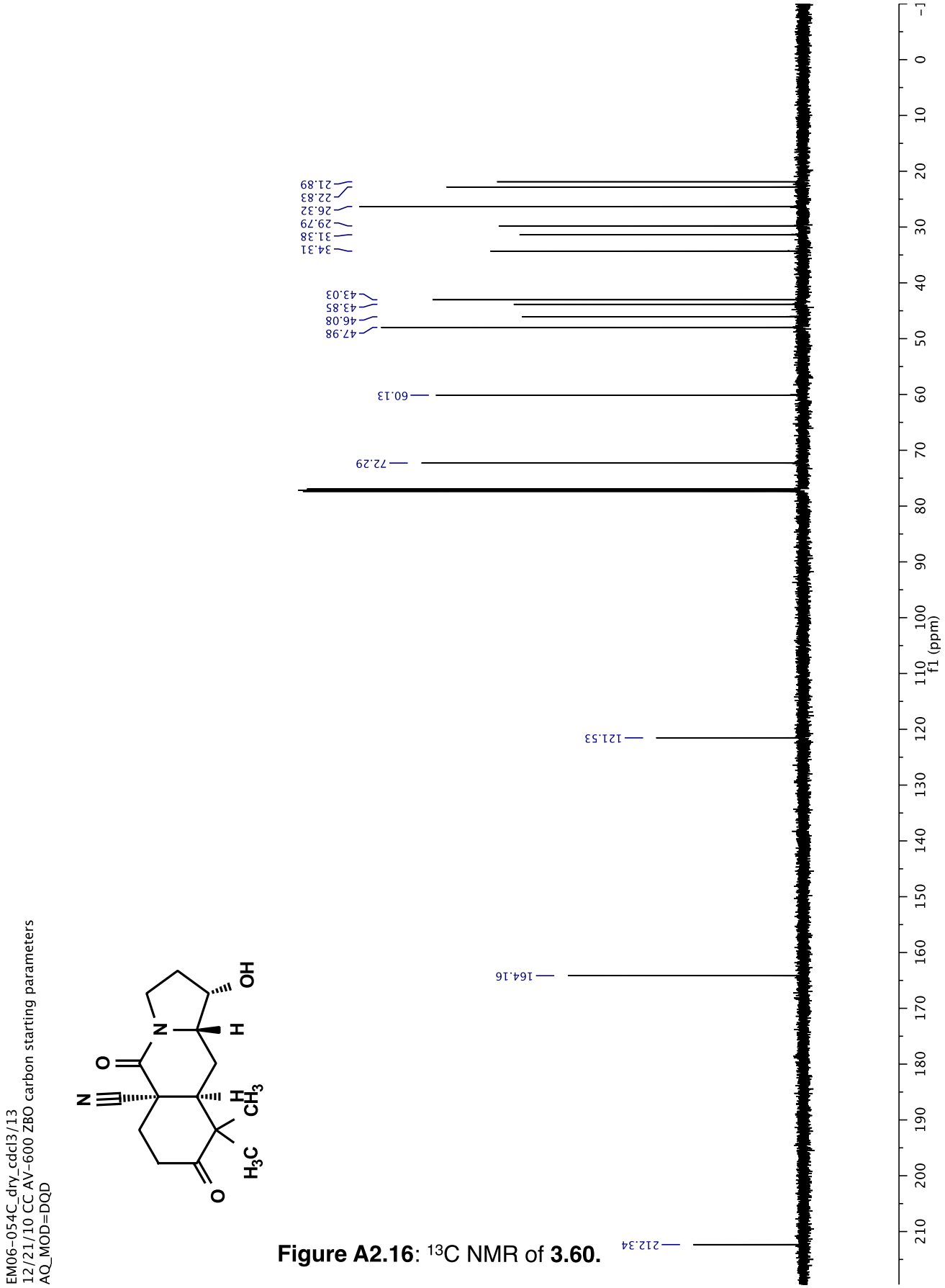

Figure A2.16: ^{13}C NMR of **3.60.**

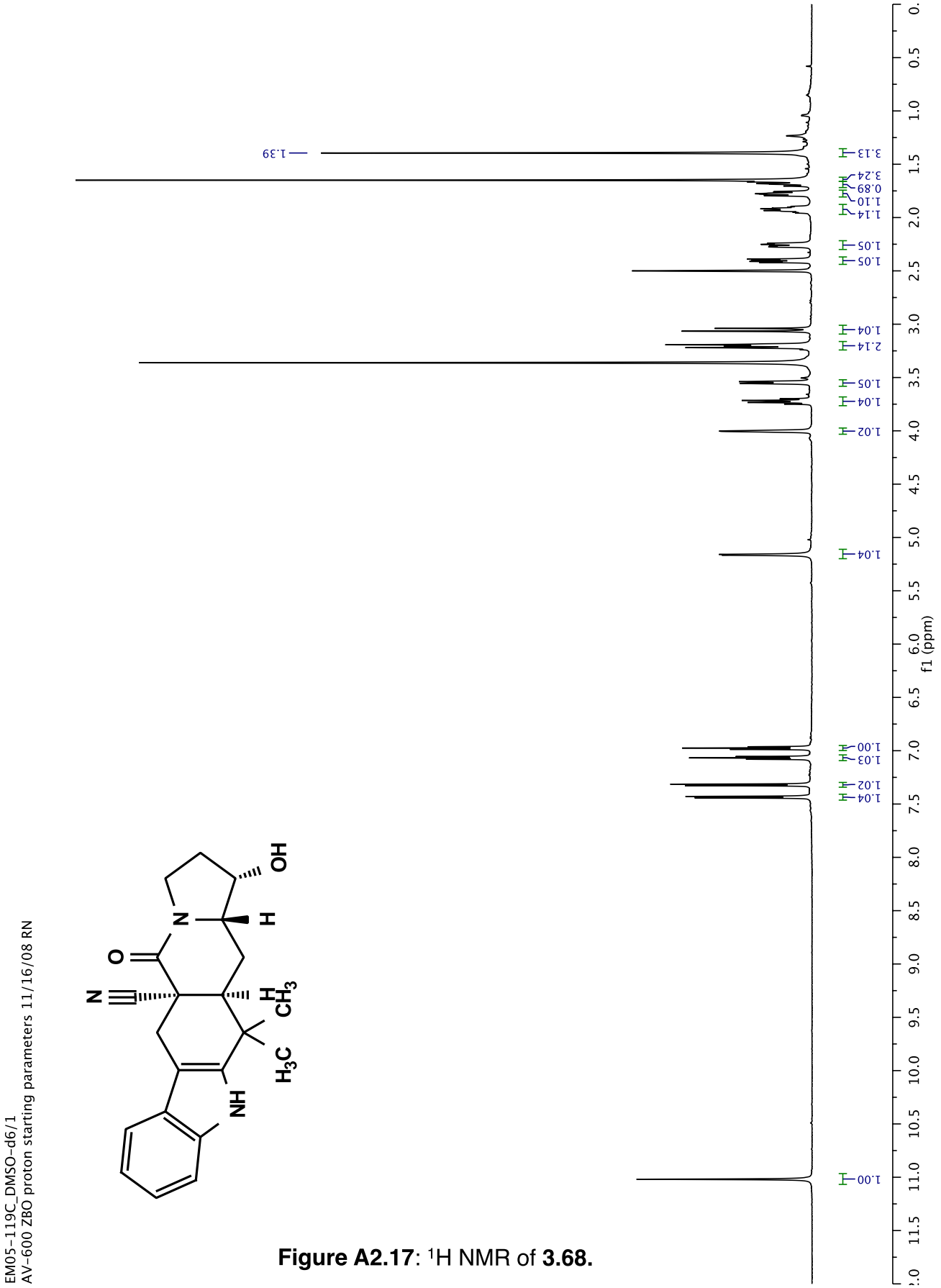

Figure A2.17: ^{1}H NMR of **3.68.**

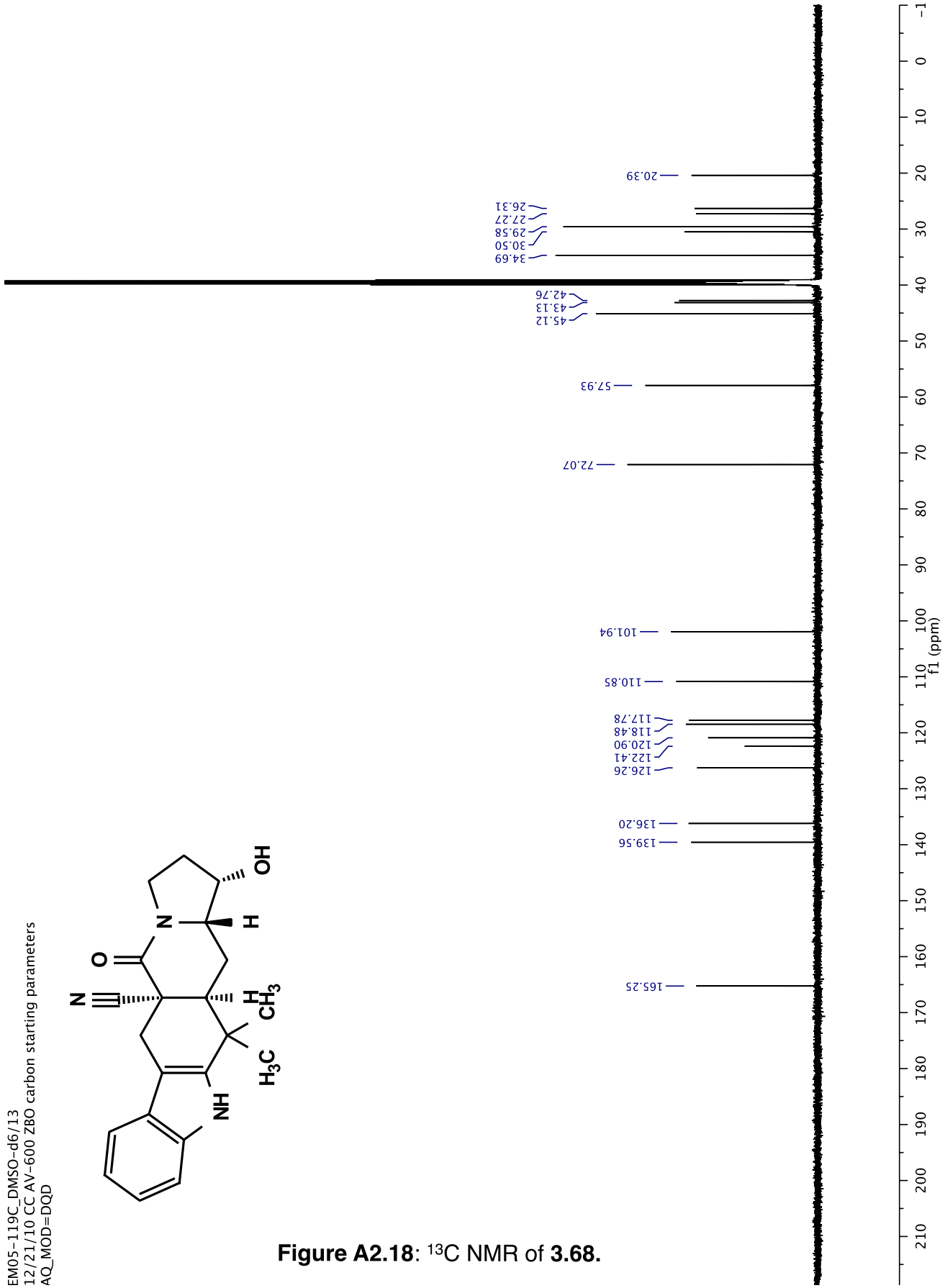

Figure A2.18: ^{13}C NMR of **3.68.**

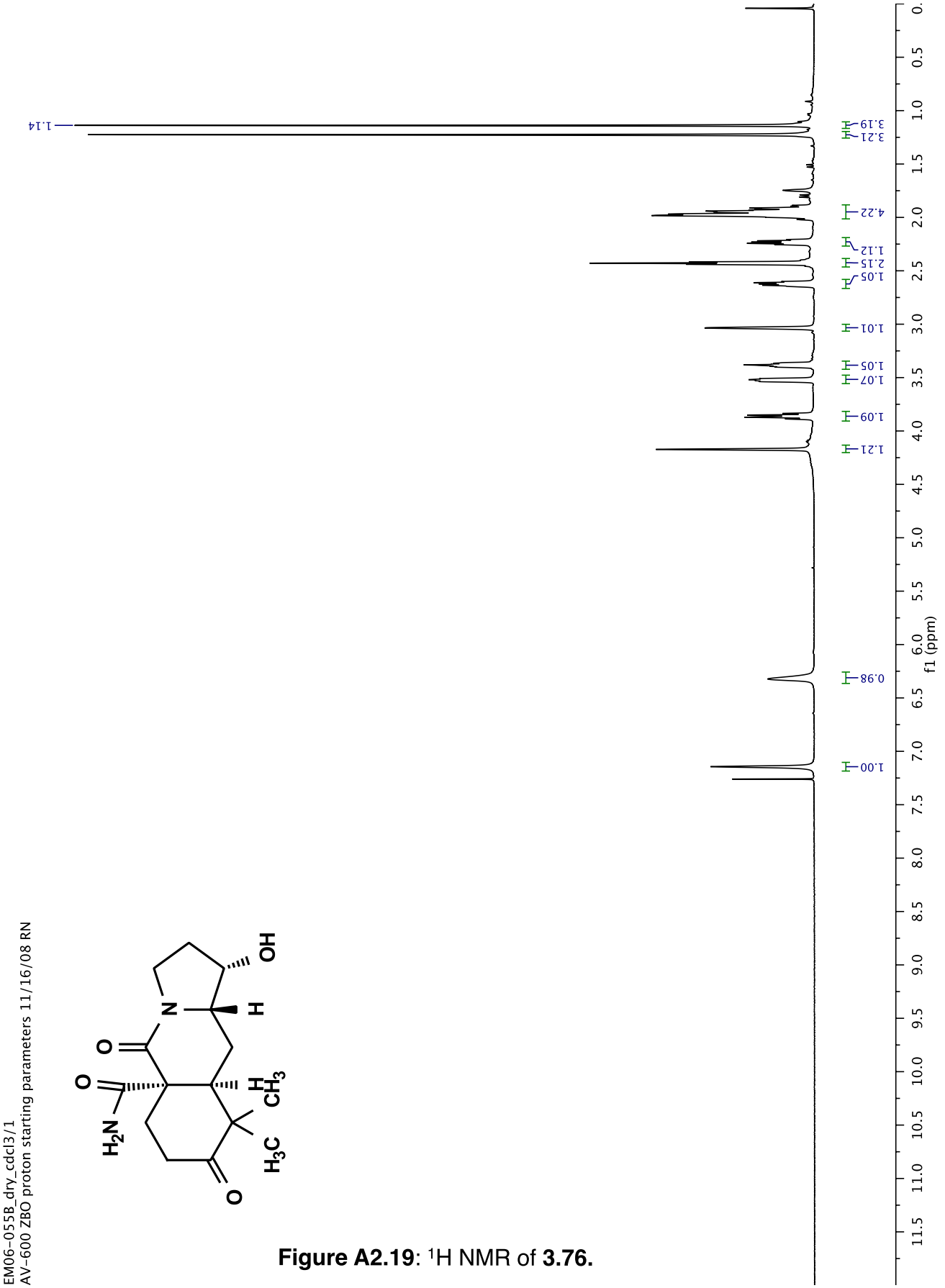

Figure A2.19: ^{1}H NMR of **3.76.**

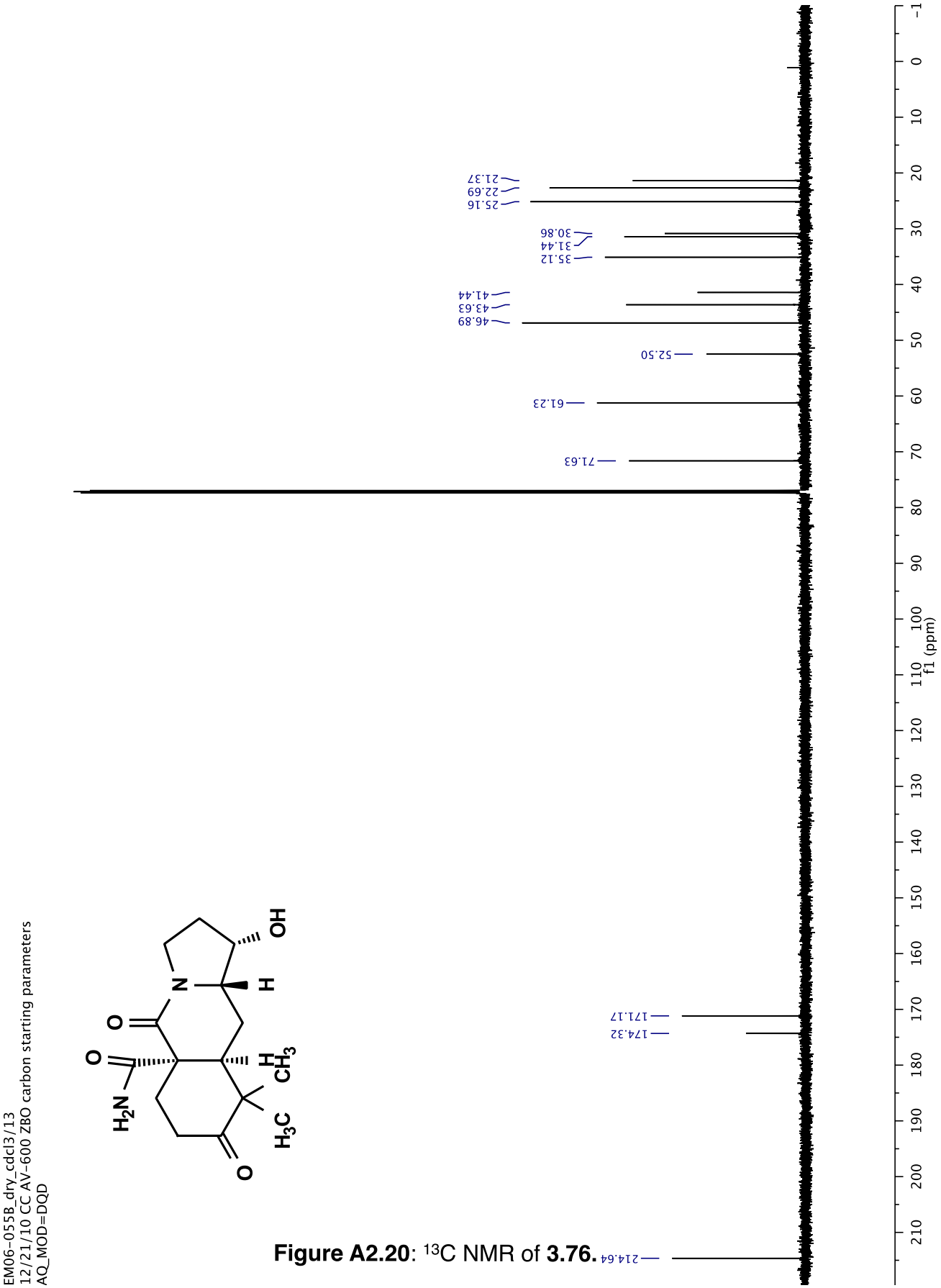

Figure A2.20: ^{13}C NMR of **3.76.**

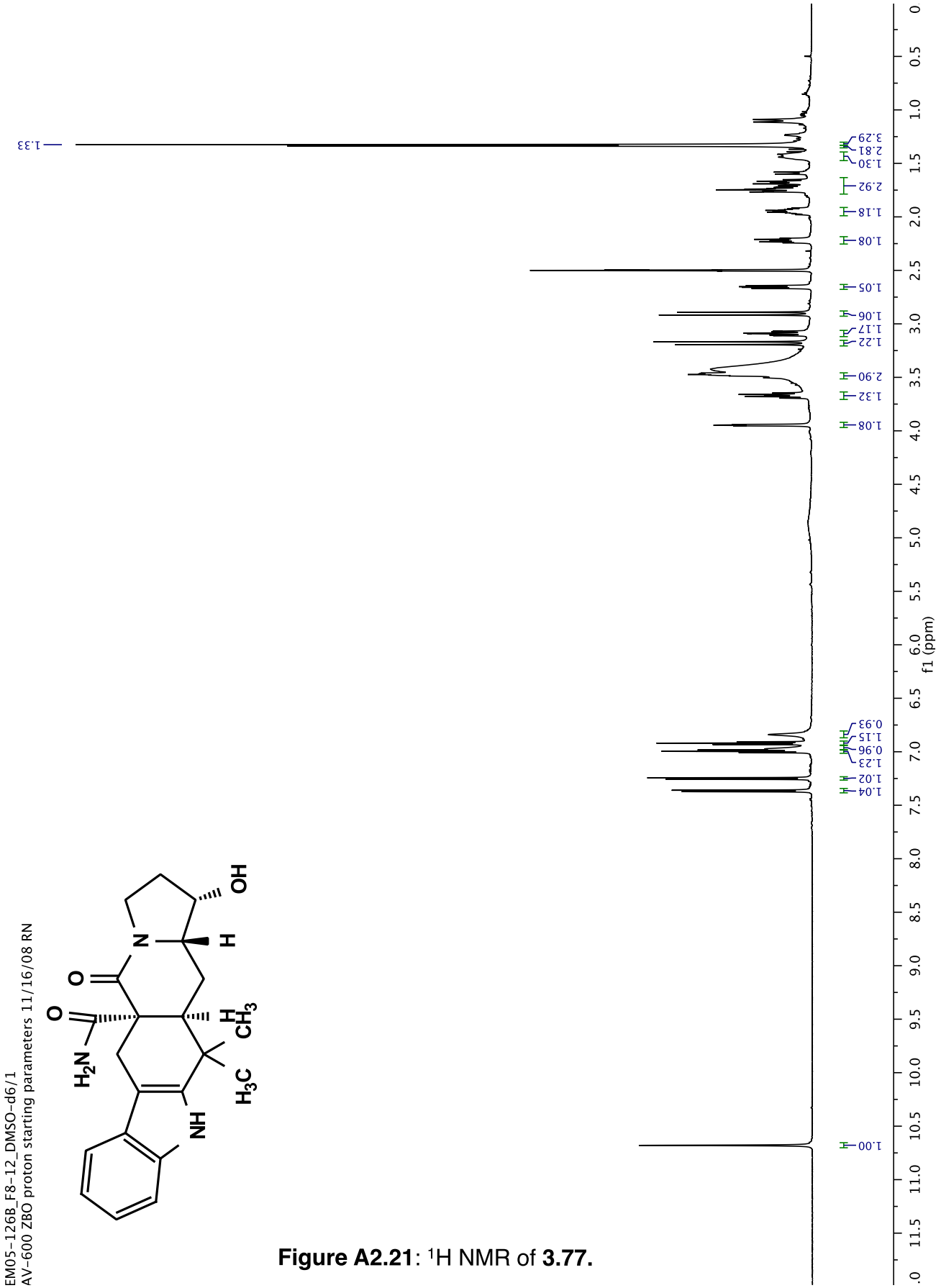

Figure A2.21: ^{1}H NMR of **3.77.**

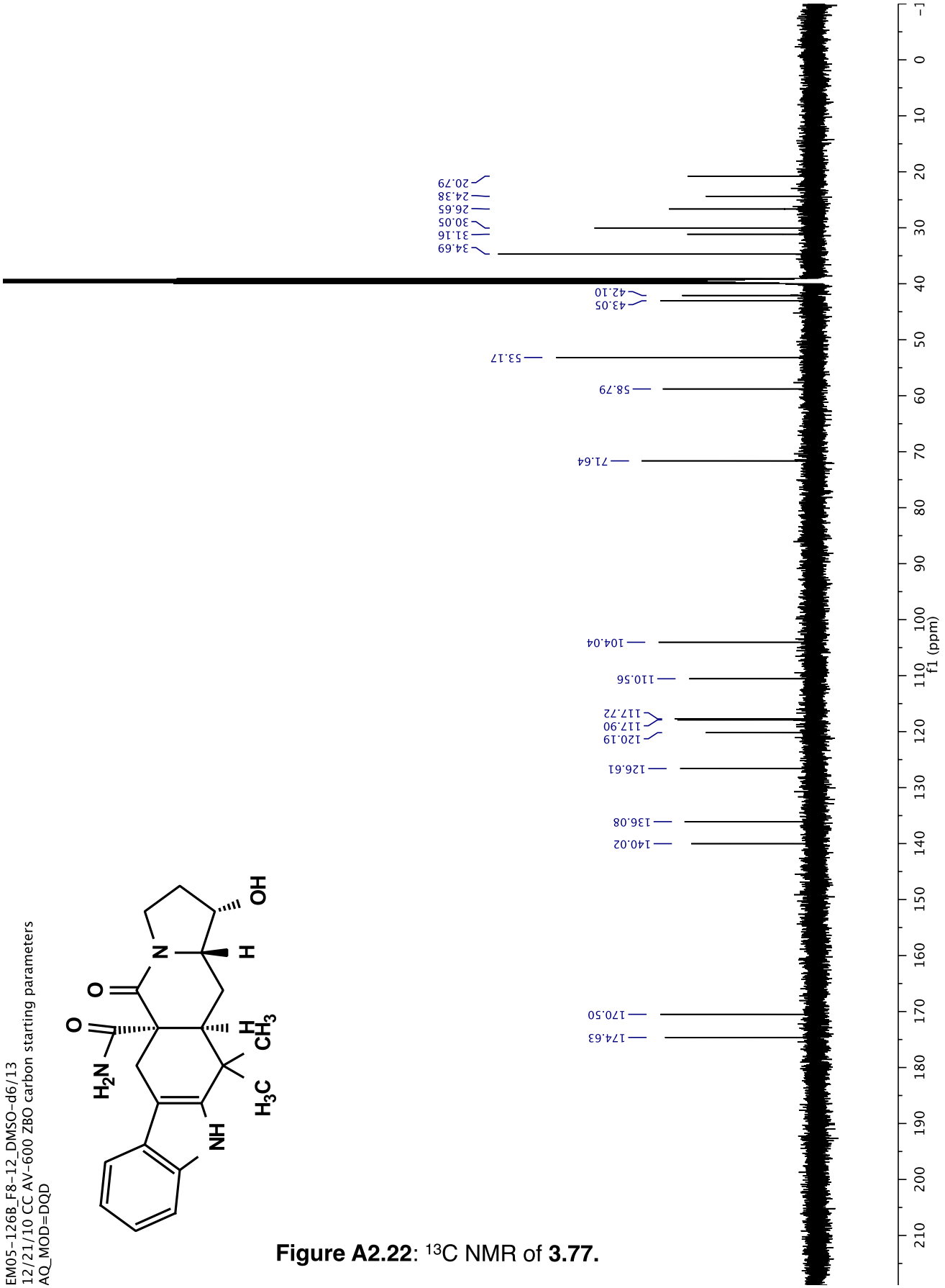

Figure A2.22: ^{13}C NMR of **3.77.**

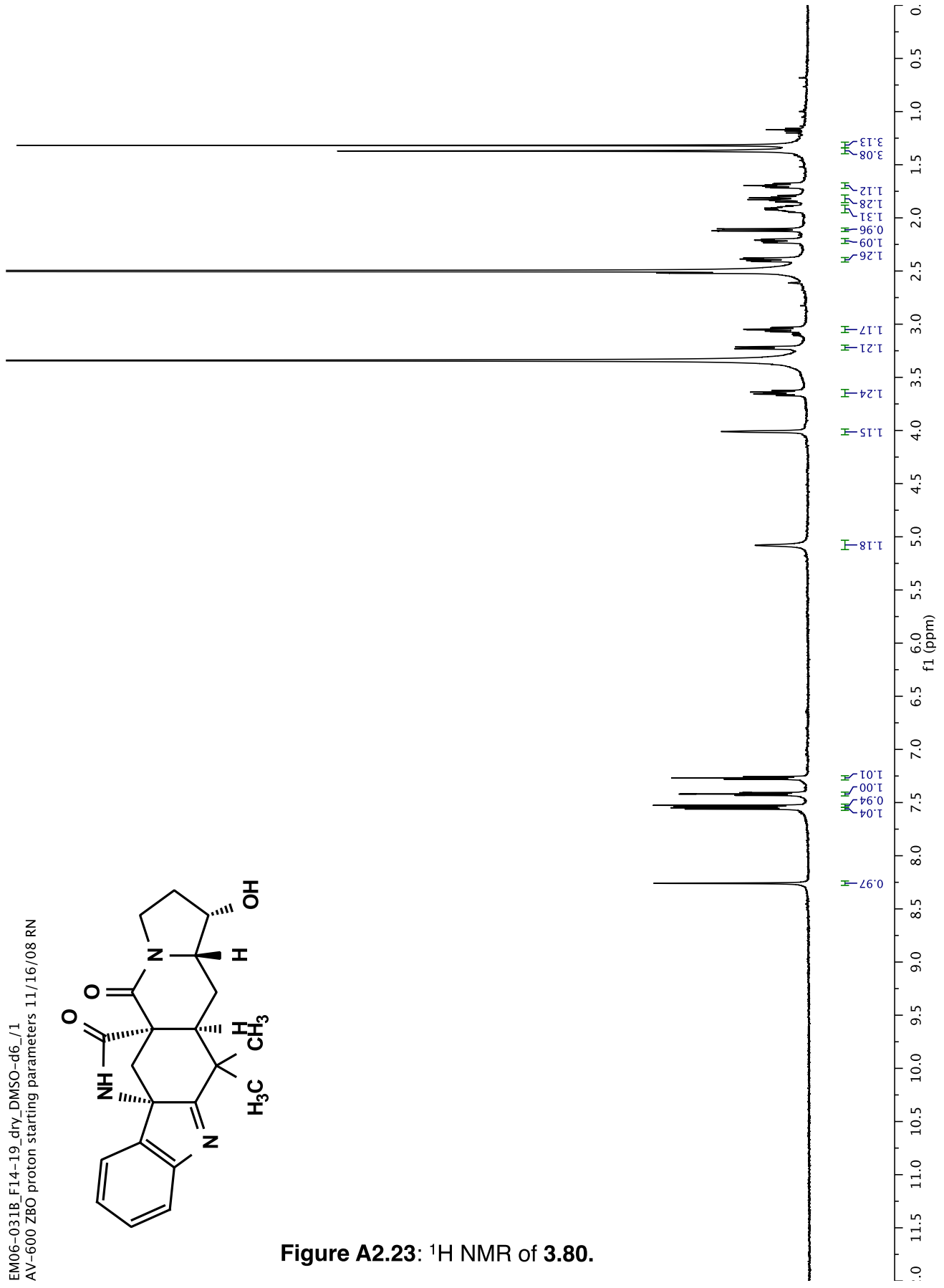

Figure A2.23: ^{1}H NMR of **3.80.**

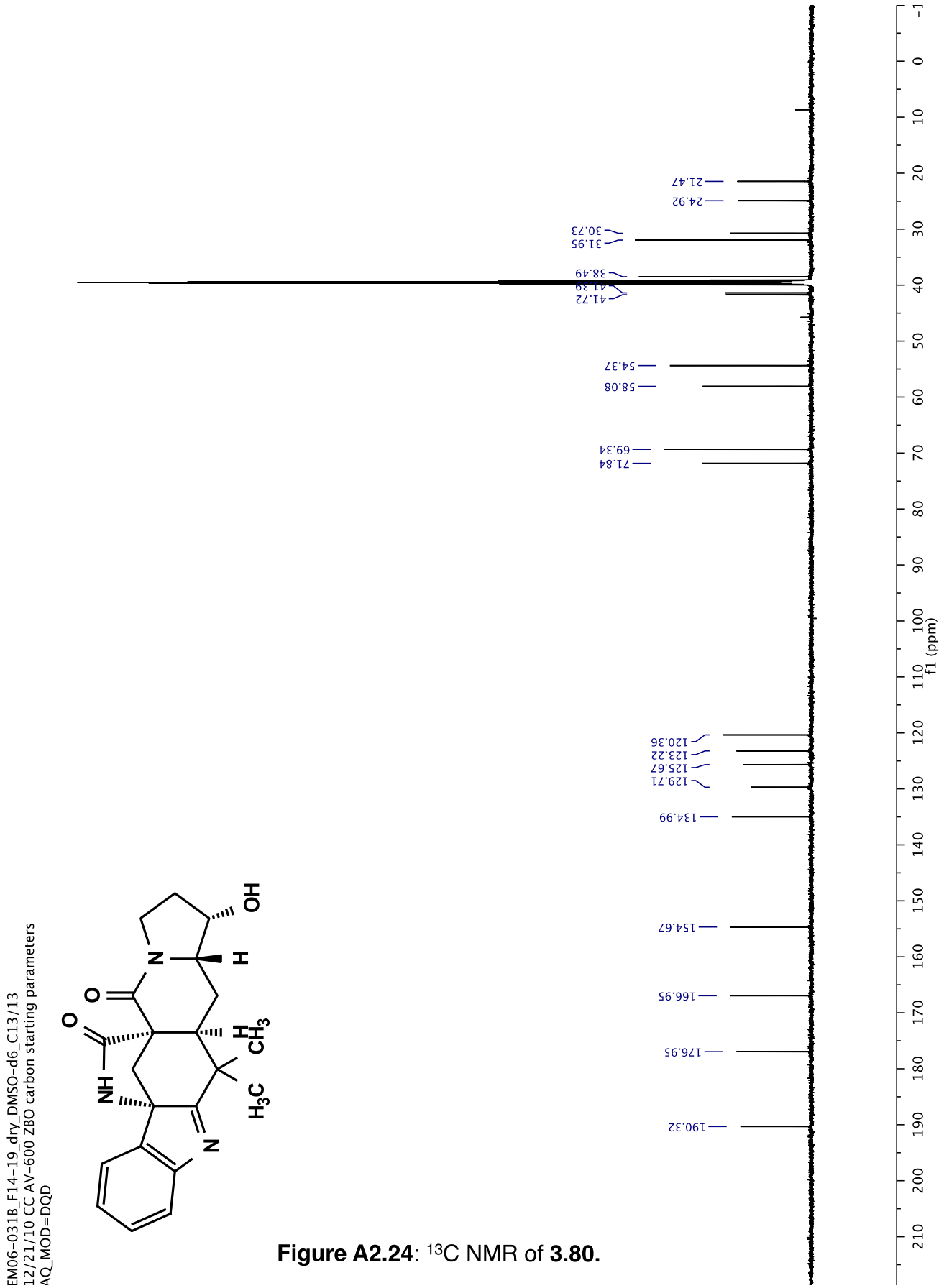

Figure A2.24: ^{13}C NMR of **3.80.**

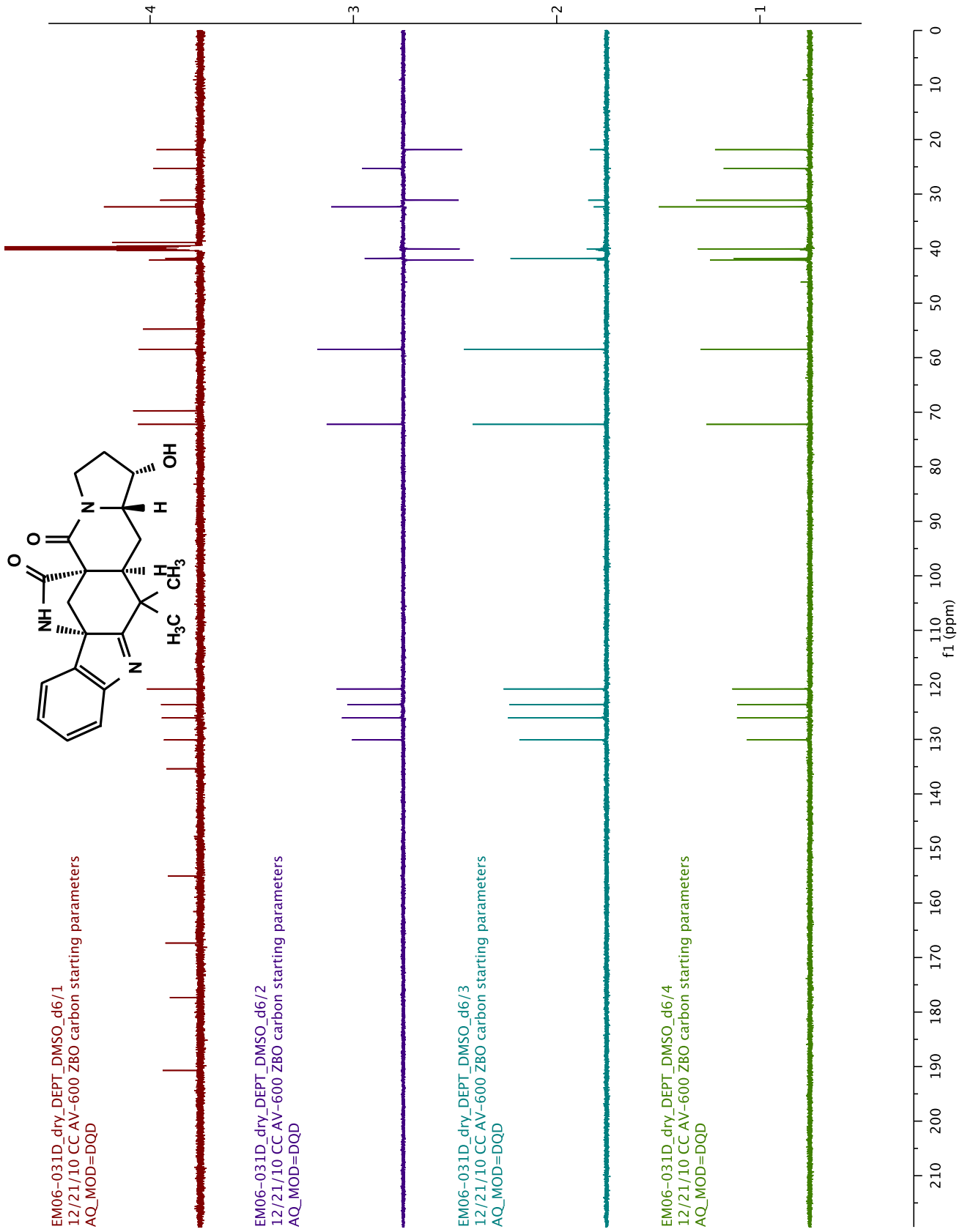

Figure A2.25: DEPT spectra of **3.80.**

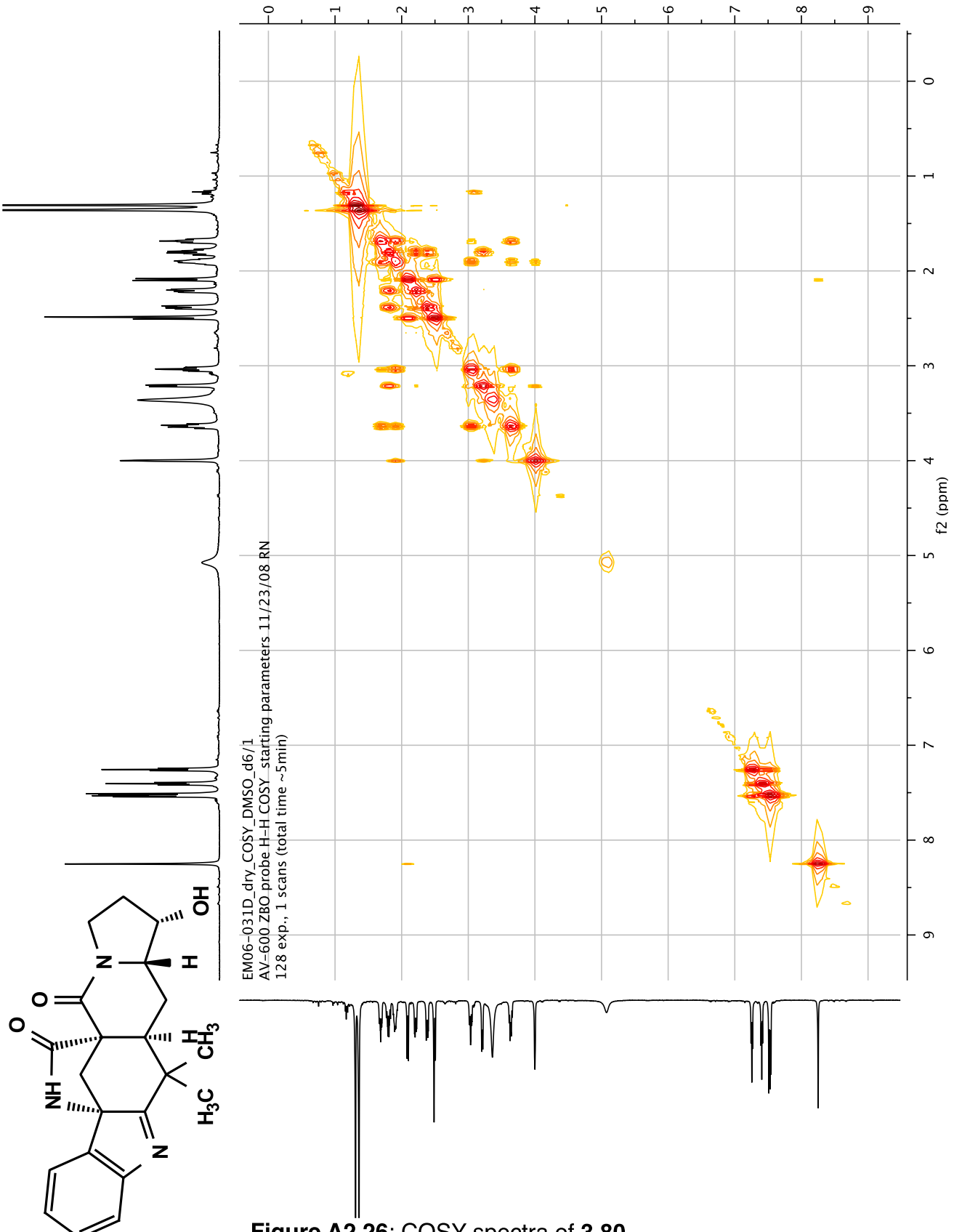

Figure A2.26: COSY spectra of **3.80.**

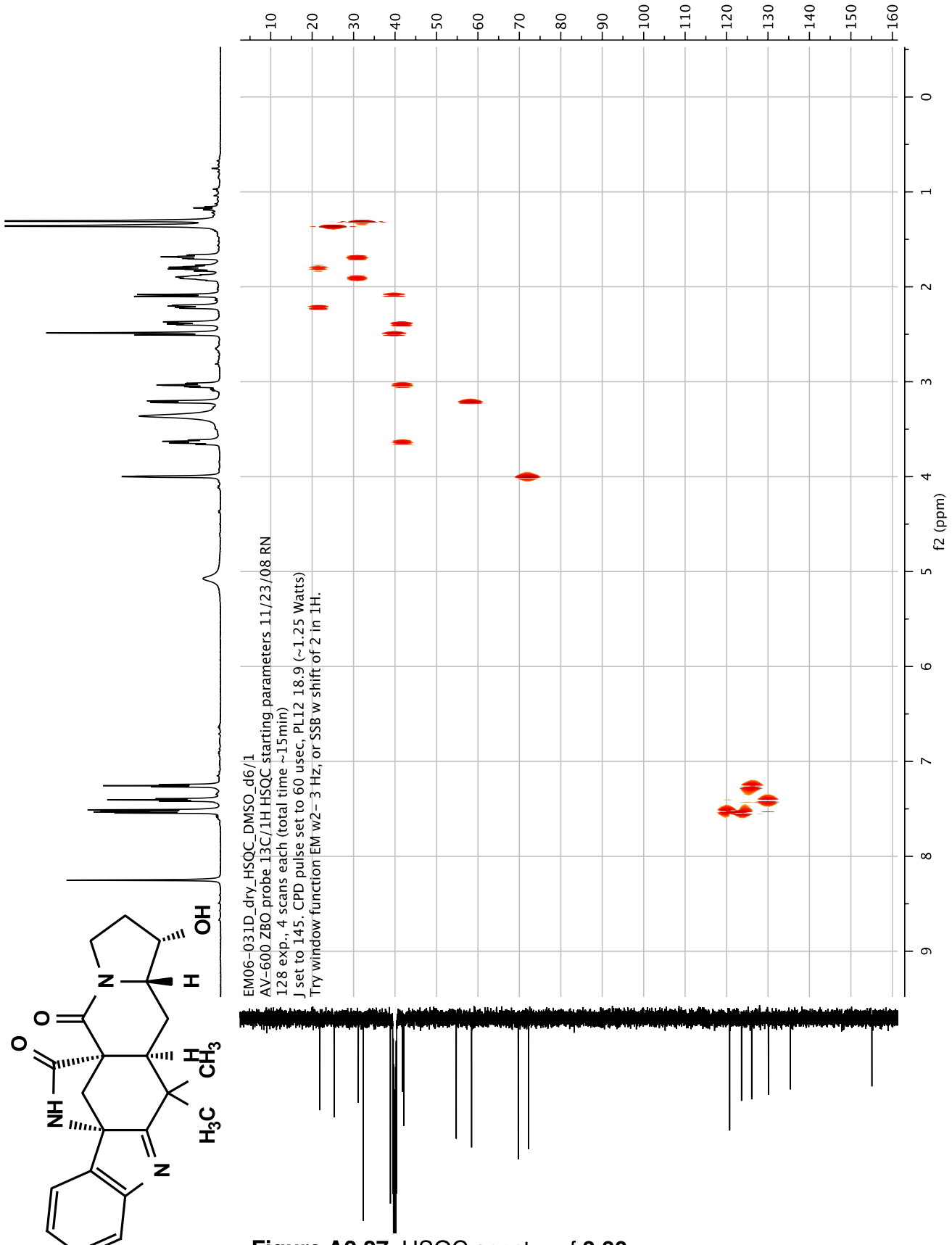

Figure A2.27: HSQC spectra of **3.80.**

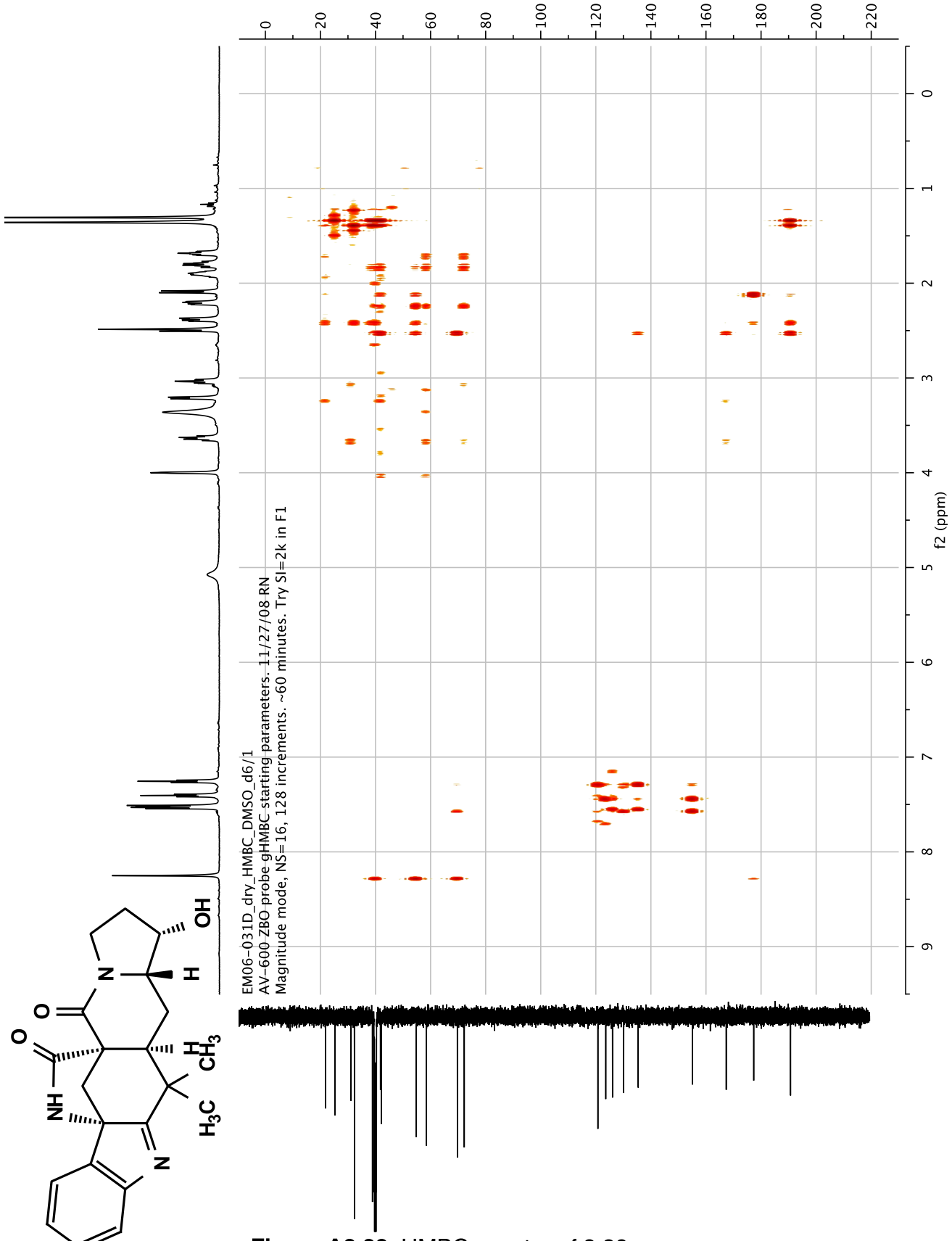

Figure A2.28: HMBC spectra of **3.80.**

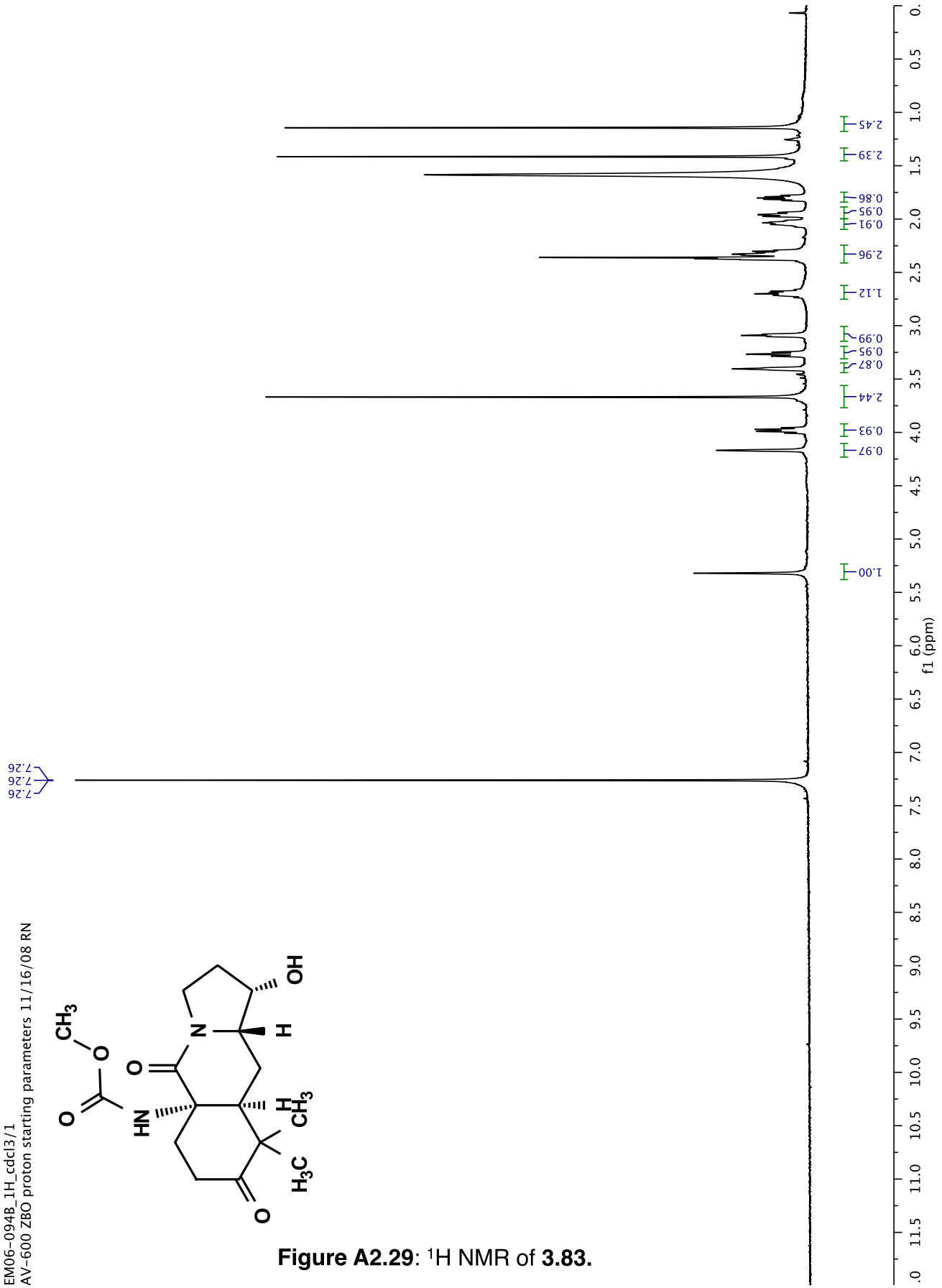

Figure A2.29: ^{1}H NMR of **3.83.**

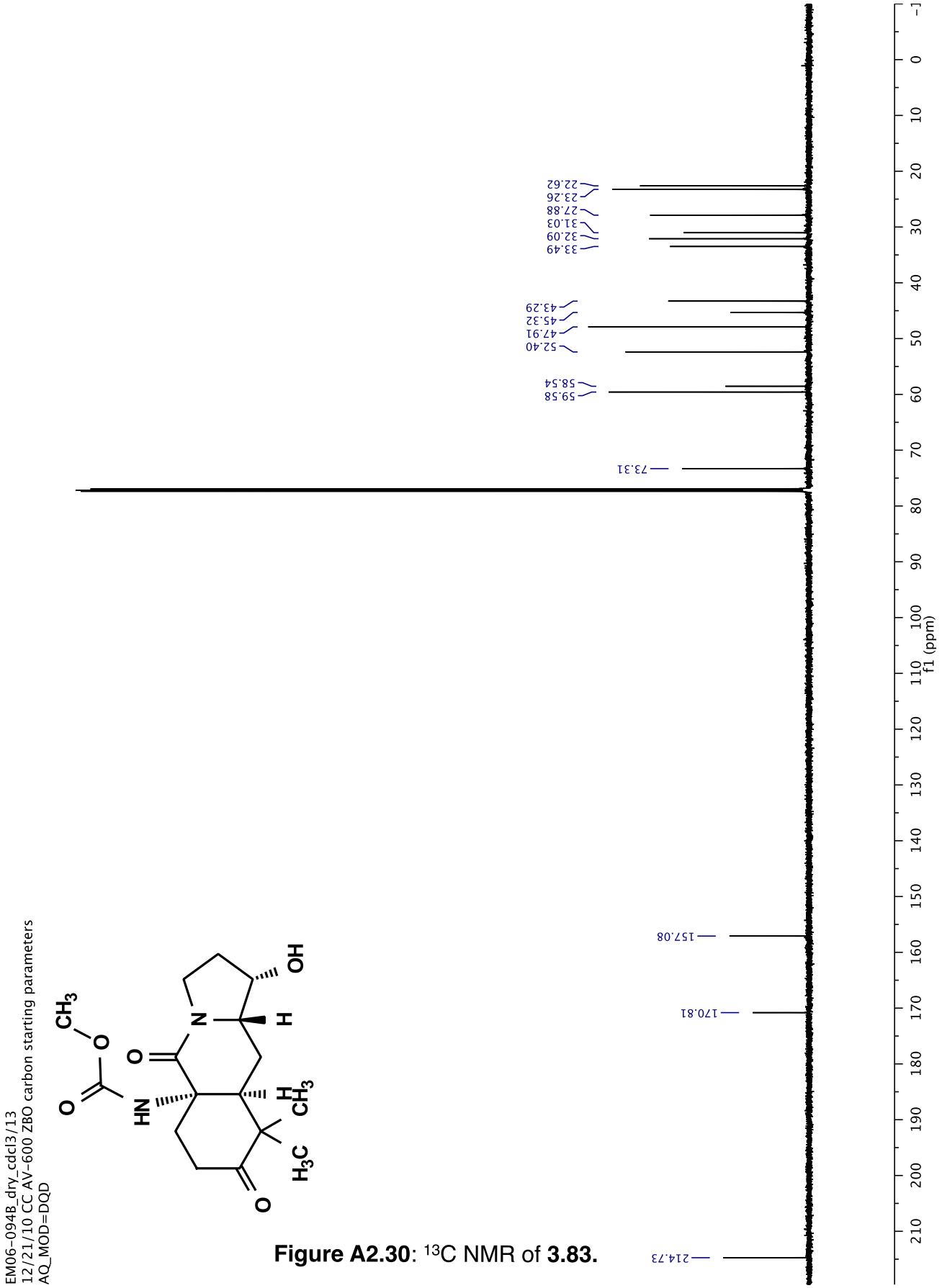

Figure A2.30: ^{13}C NMR of **3.83.**

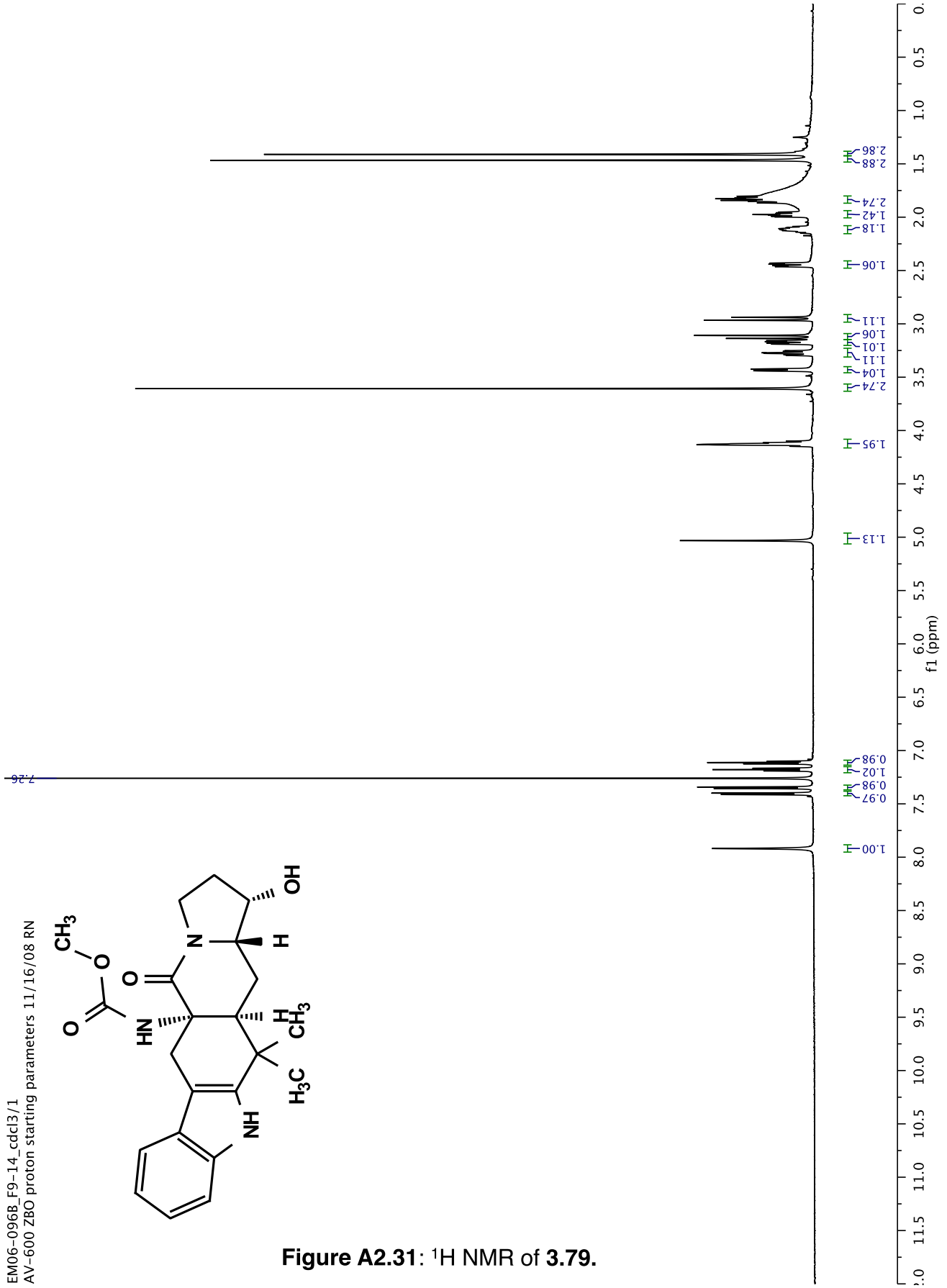

Figure A2.31: ^{1}H NMR of **3.79.**

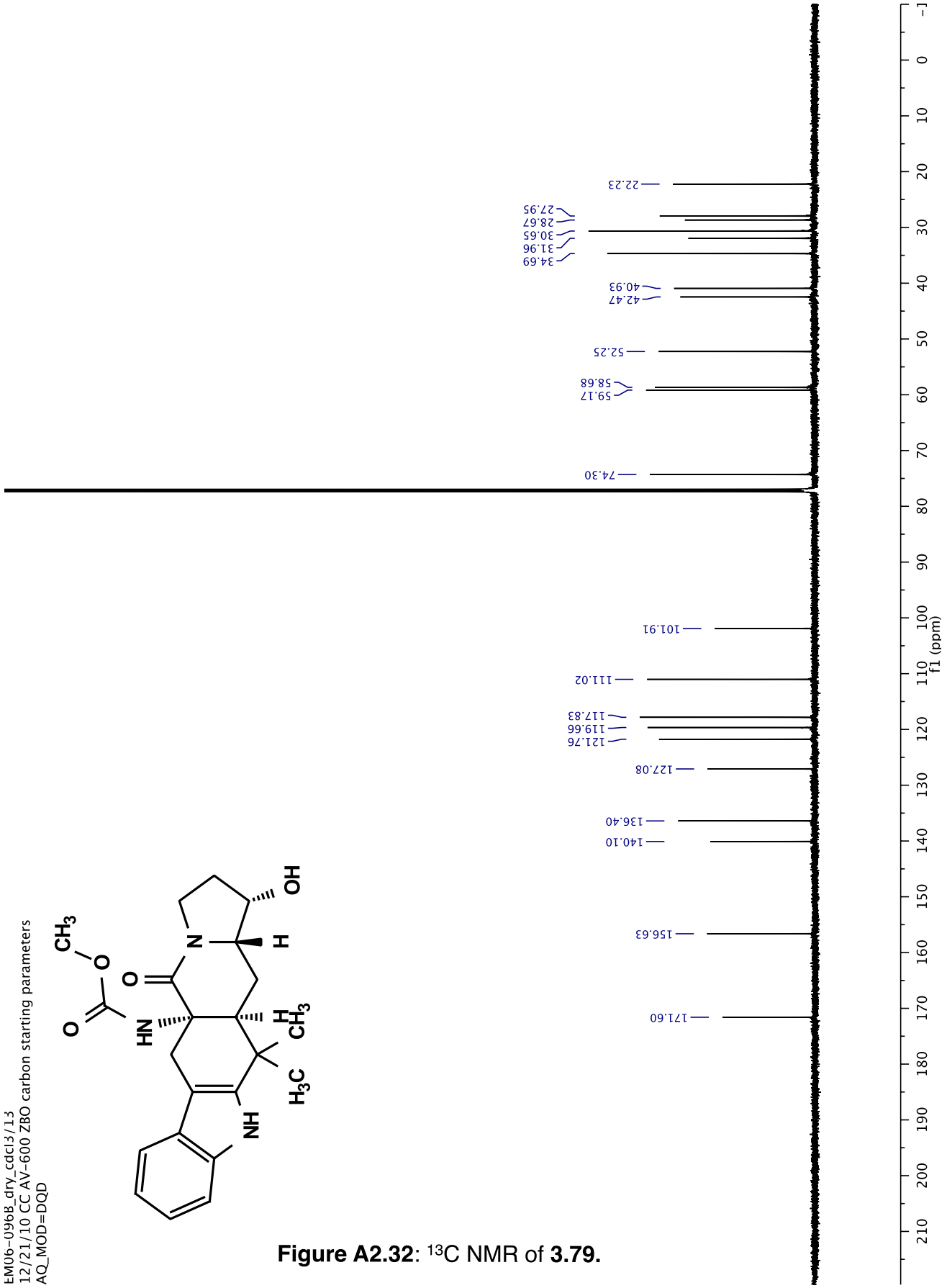

Figure A2.32: ^{13}C NMR of **3.79.**

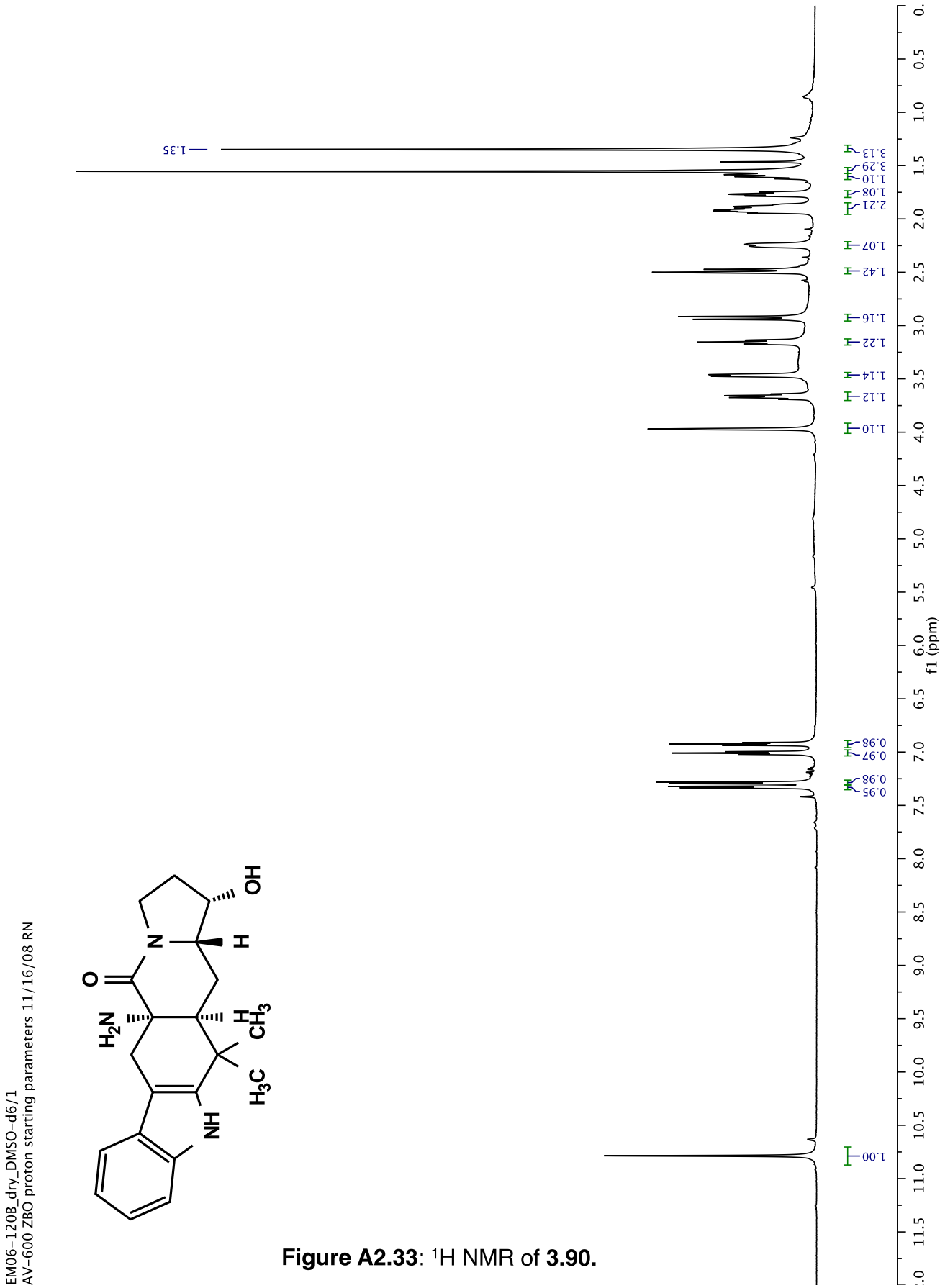

Figure A2.33: ^{1}H NMR of **3.90.**

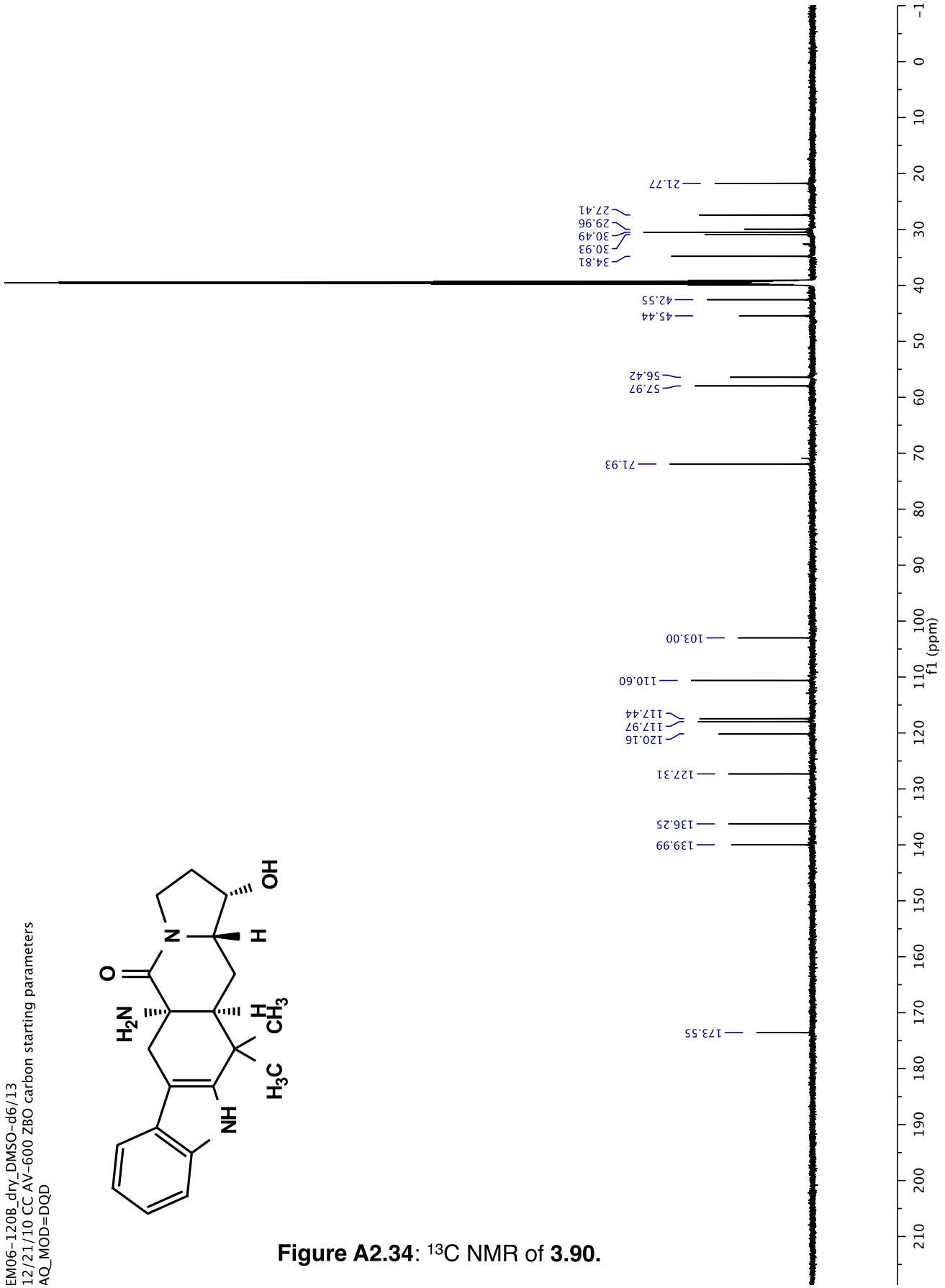

Figure A2.34: ^{13}C NMR of **3.90.**

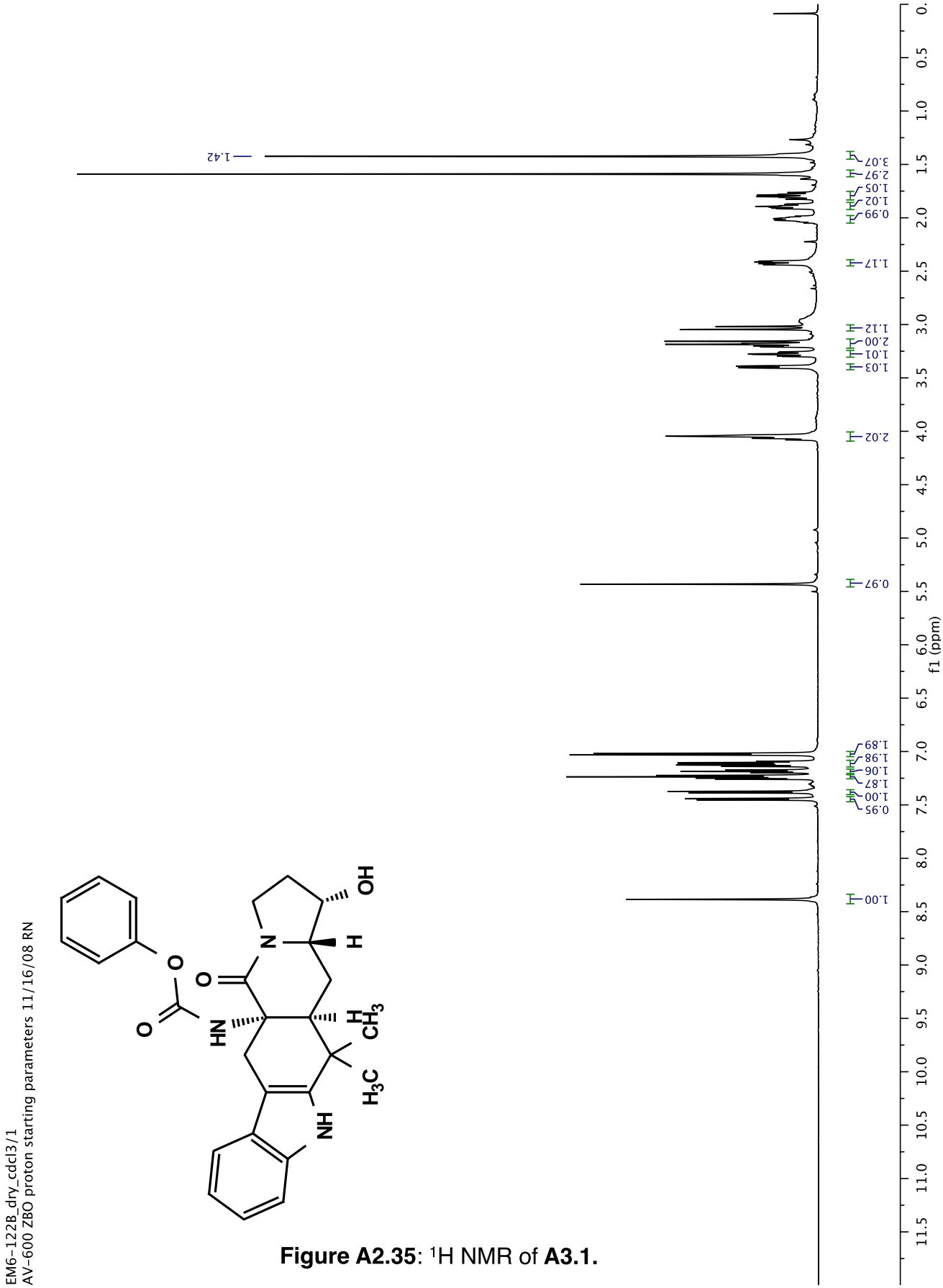

Figure A2.35: ^{1}H NMR of **A3.1.**

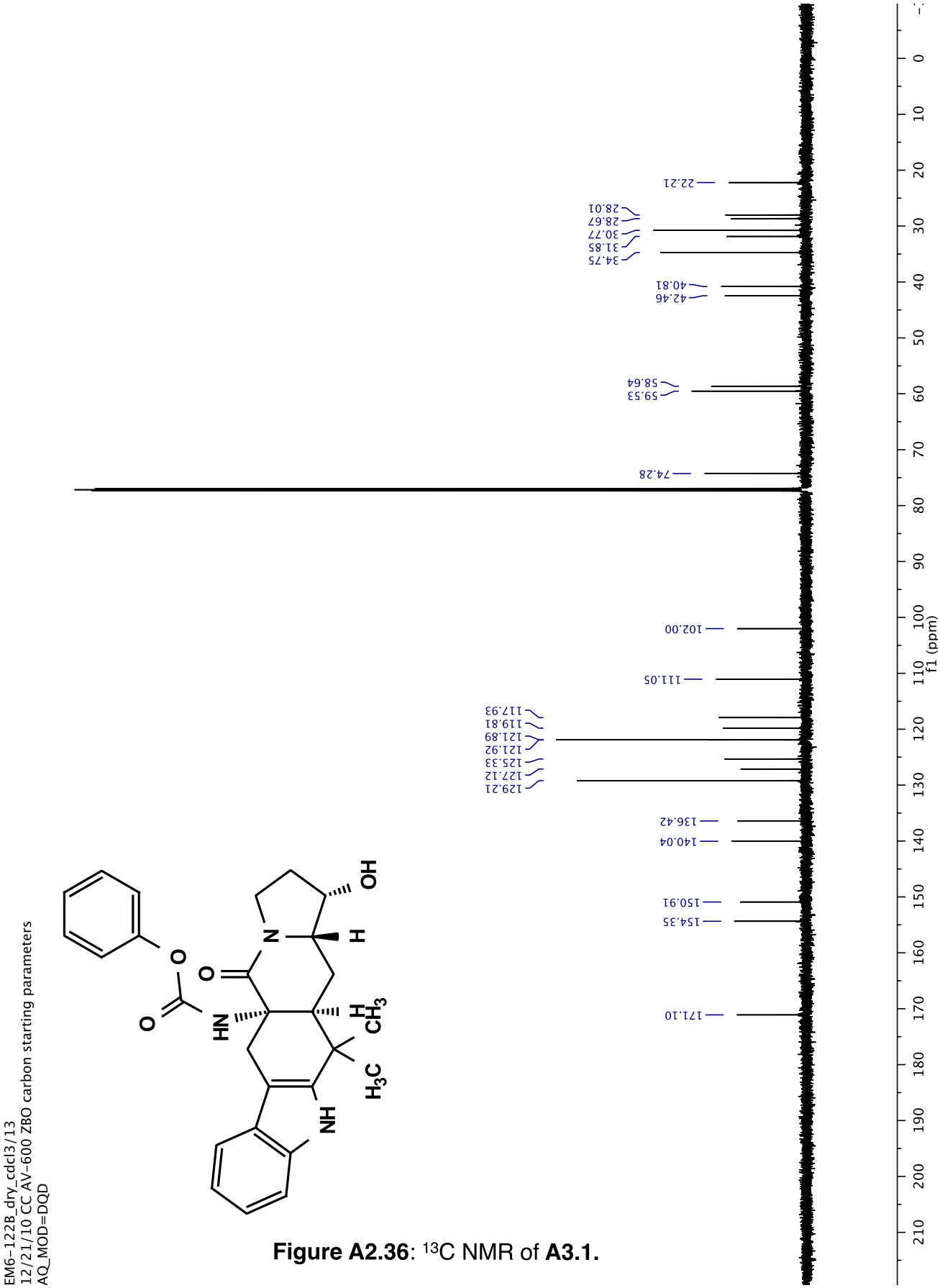

Figure A2.36: ^{13}C NMR of **A3.1.**

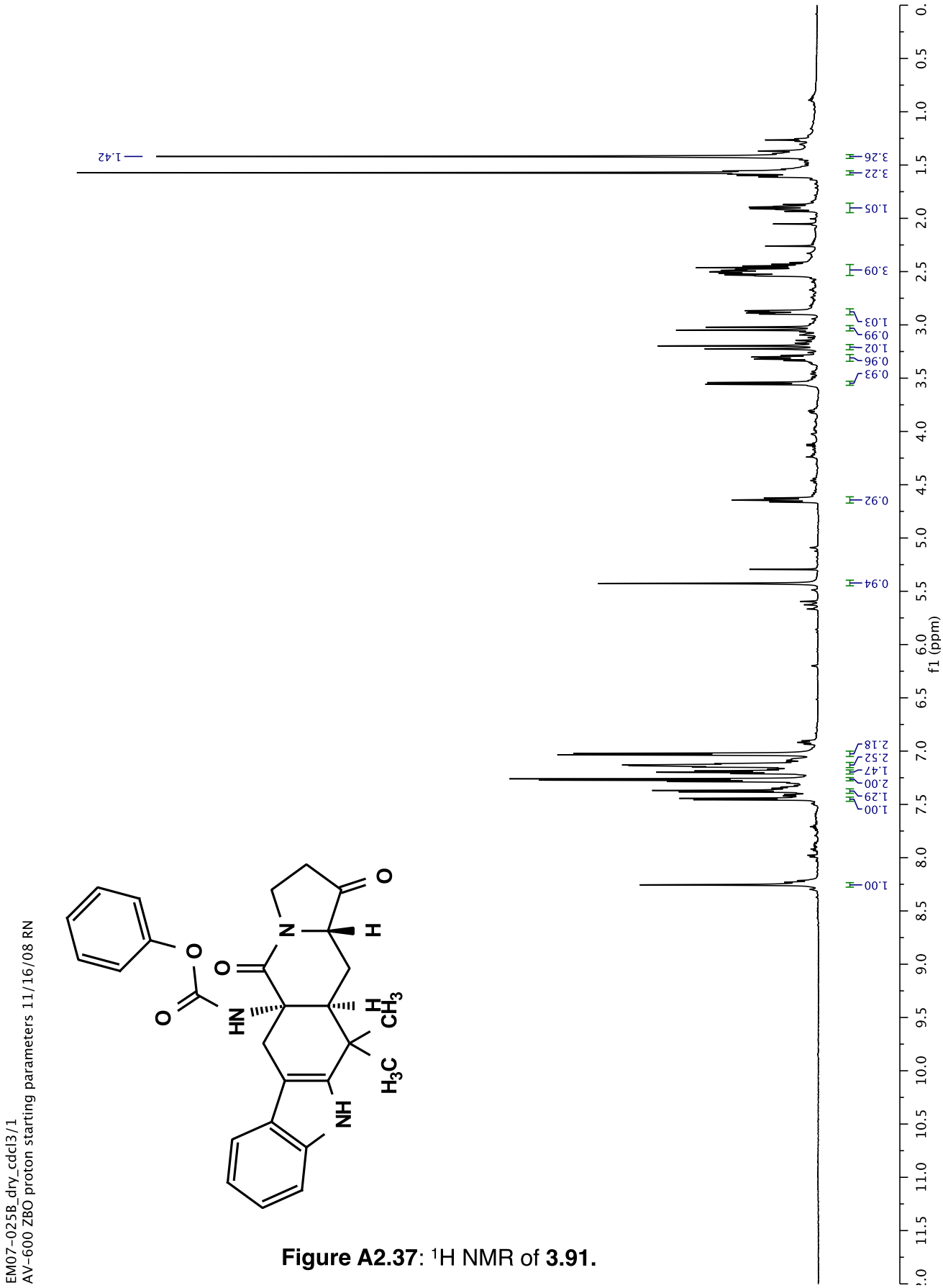

Figure A2.37: ^{1}H NMR of **3.91.**

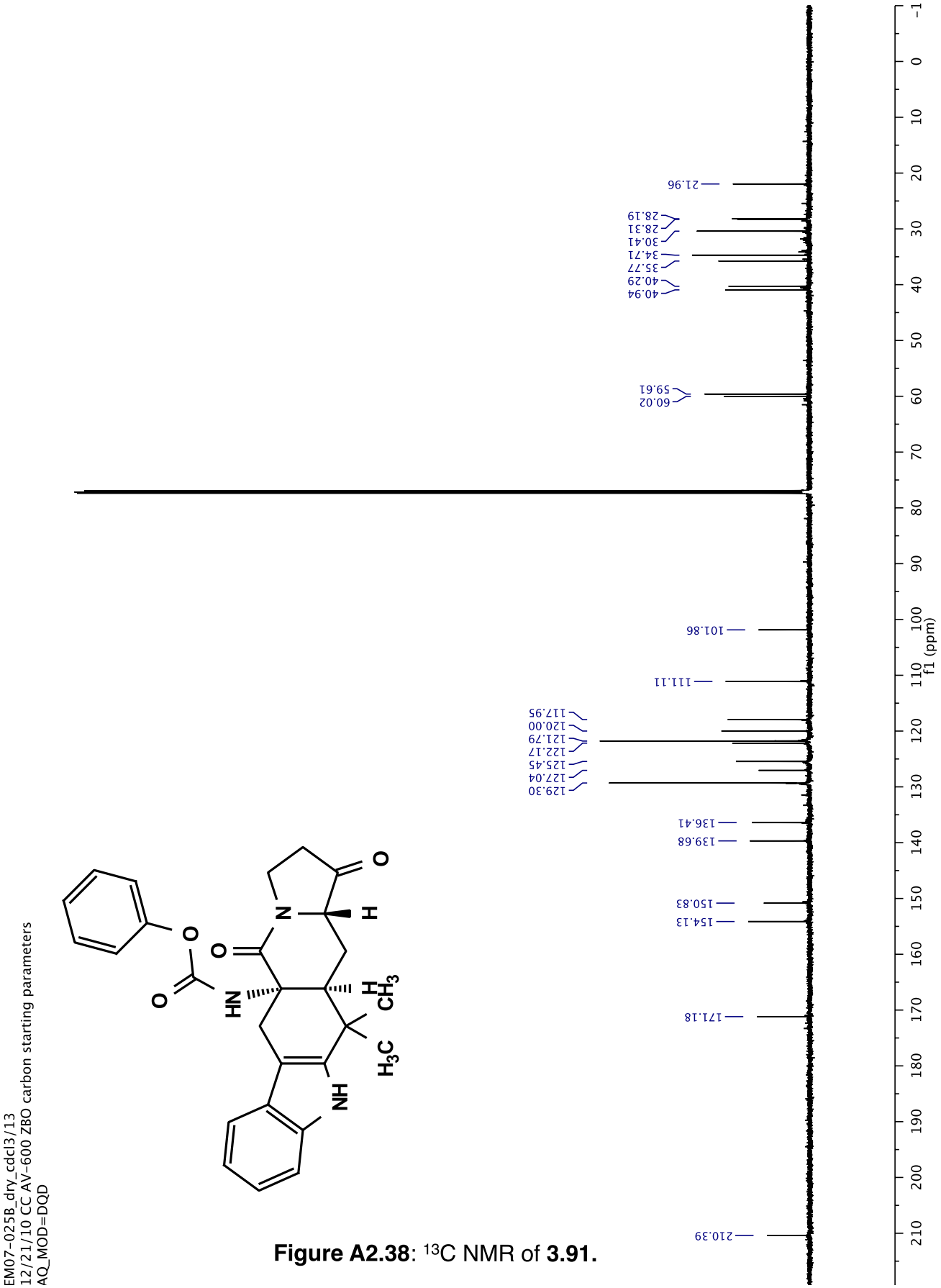

Figure A2.38: ^{13}C NMR of **3.91.**

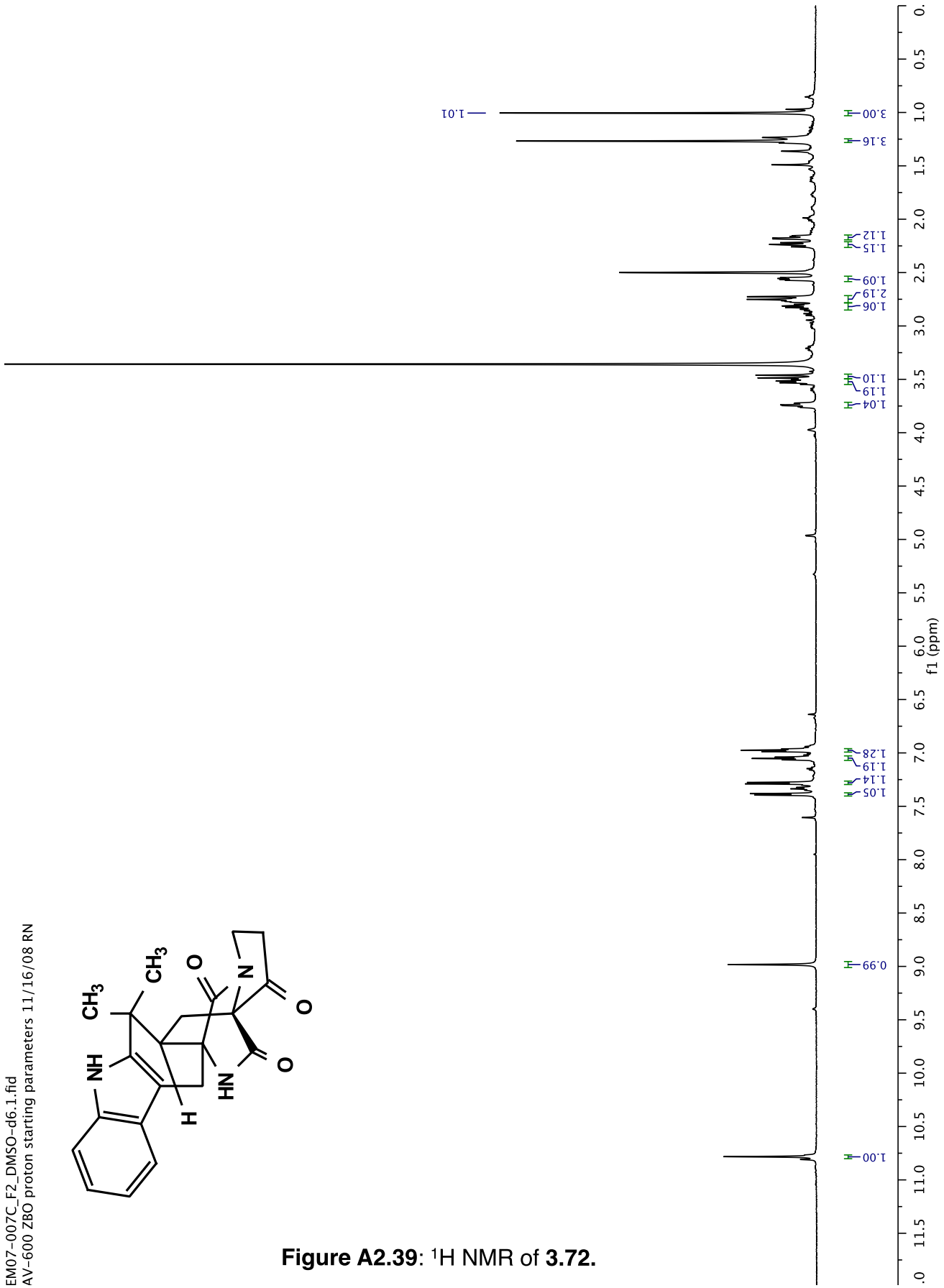

Figure A2.39: ^{1}H NMR of **3.72.**

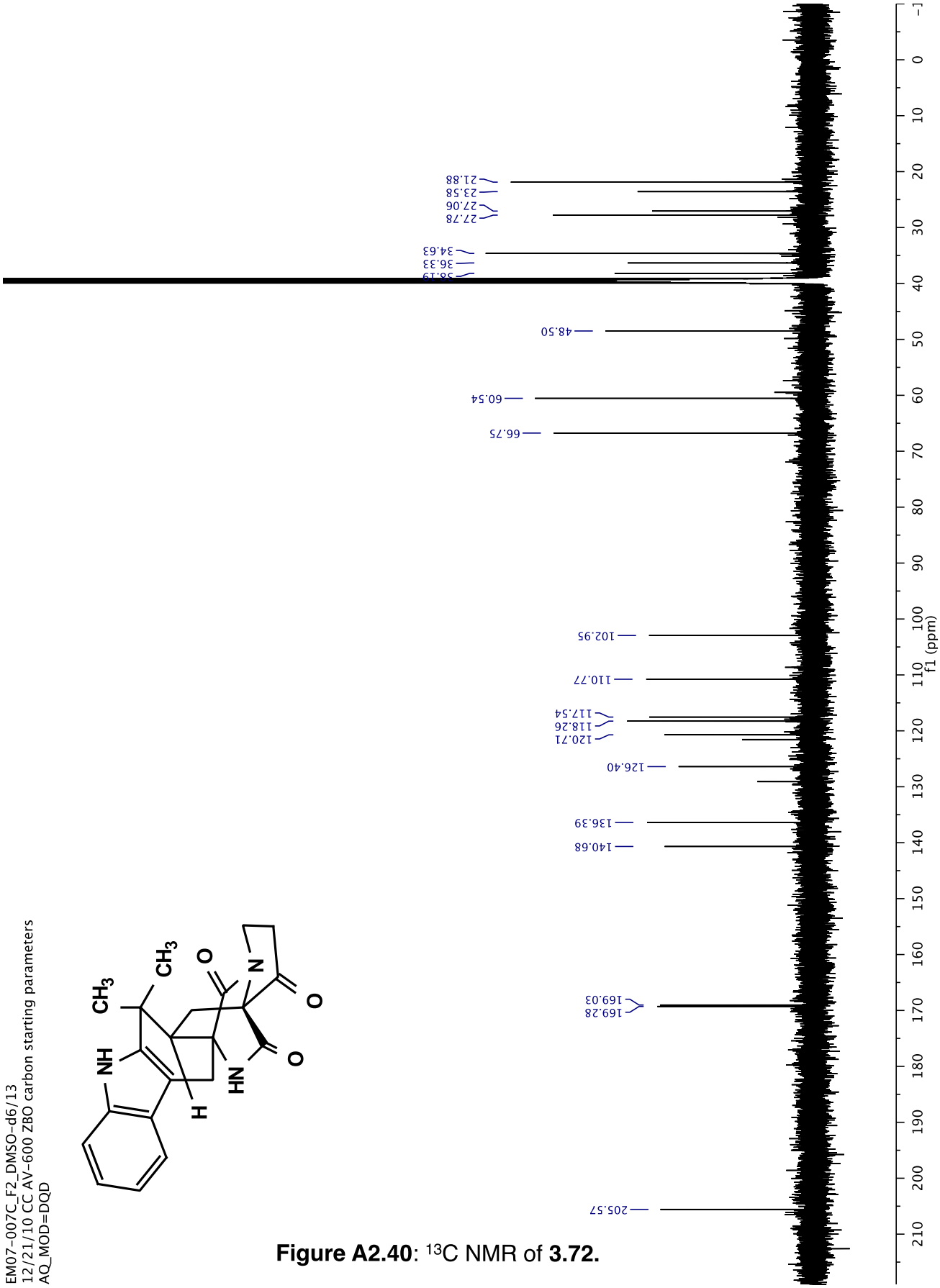

Figure A2.40: ^{13}C NMR of **3.72.**

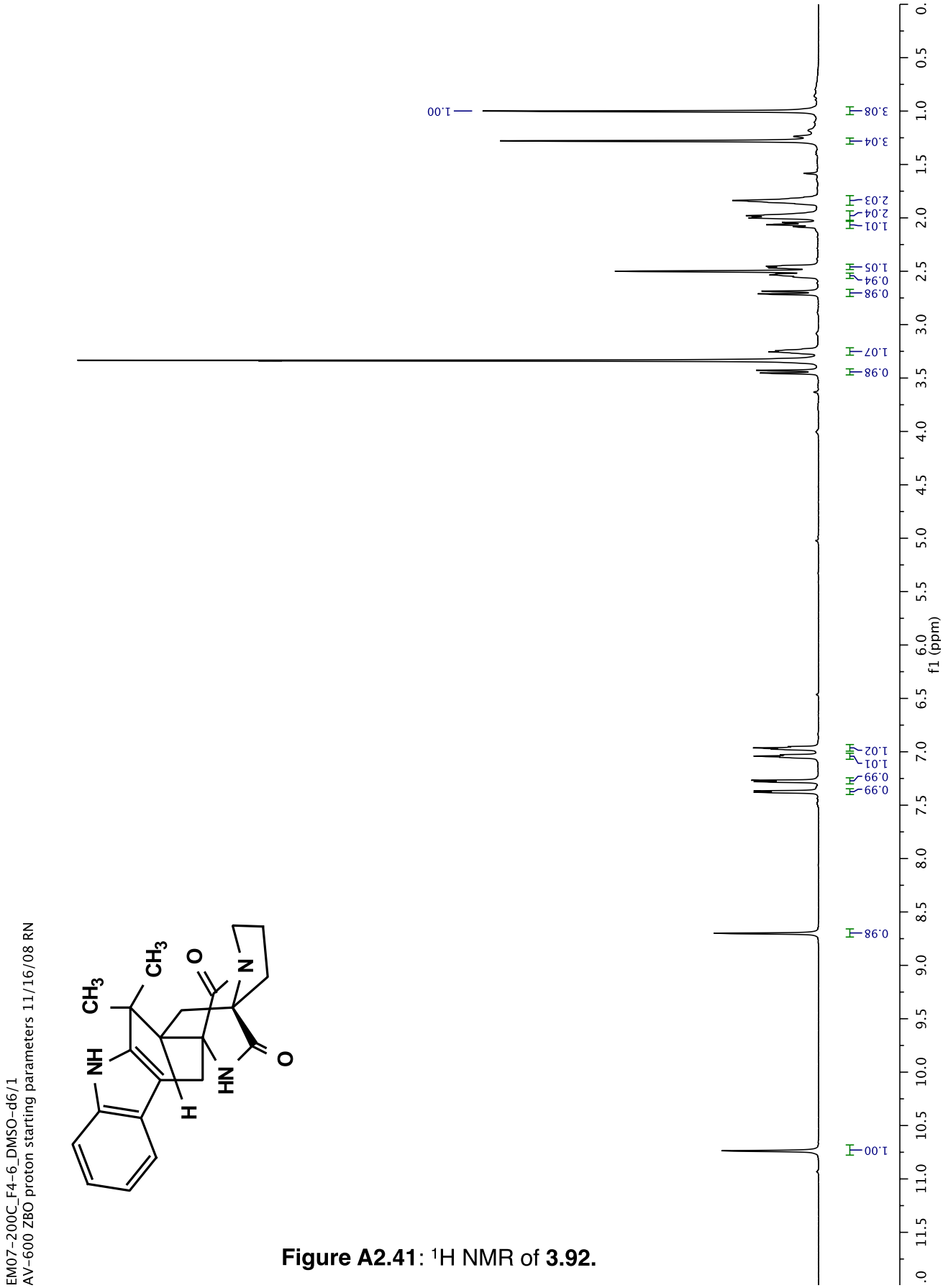

Figure A2.41: ^{1}H NMR of **3.92.**

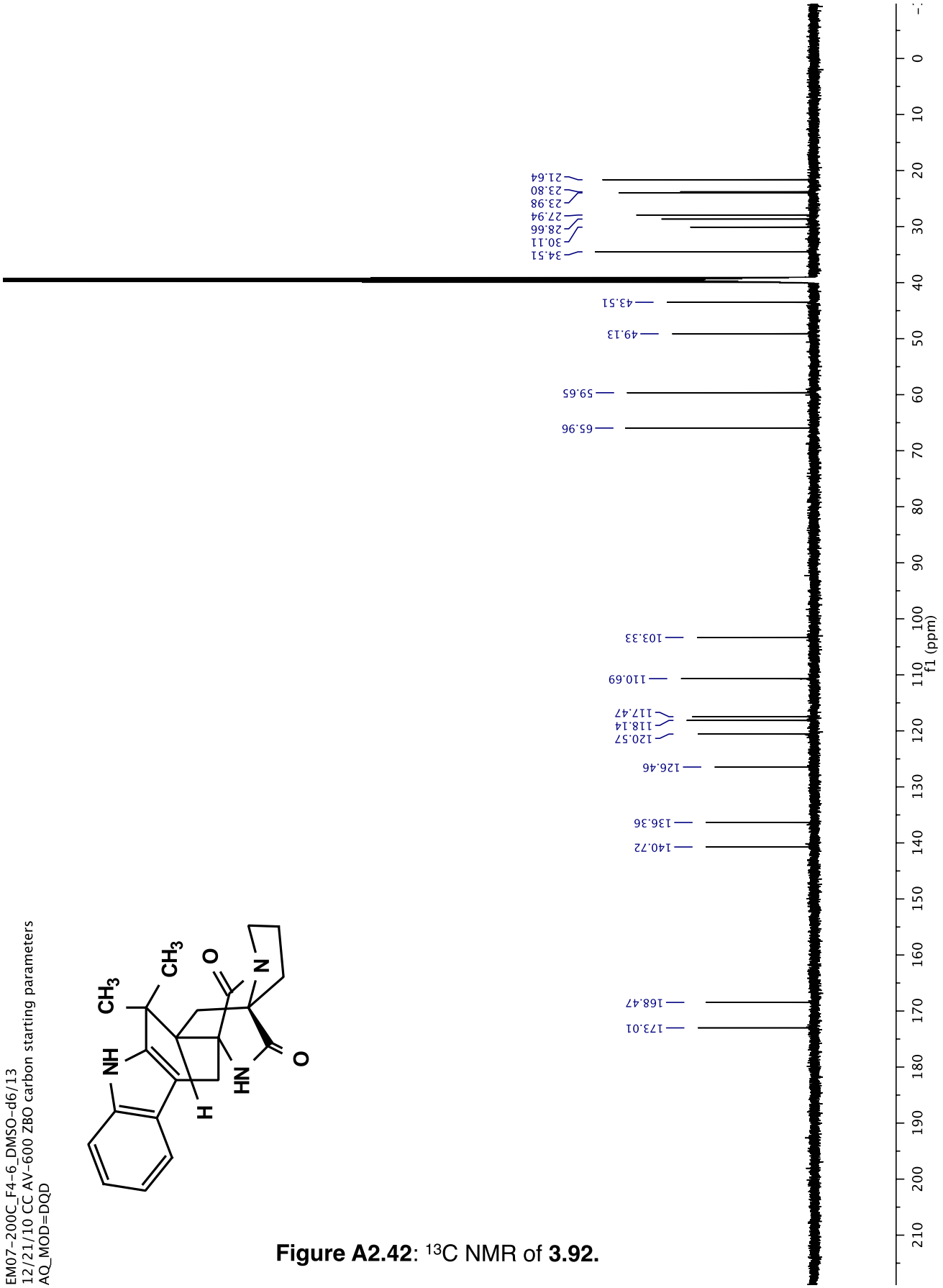

Figure A2.42: ^{13}C NMR of **3.92.**

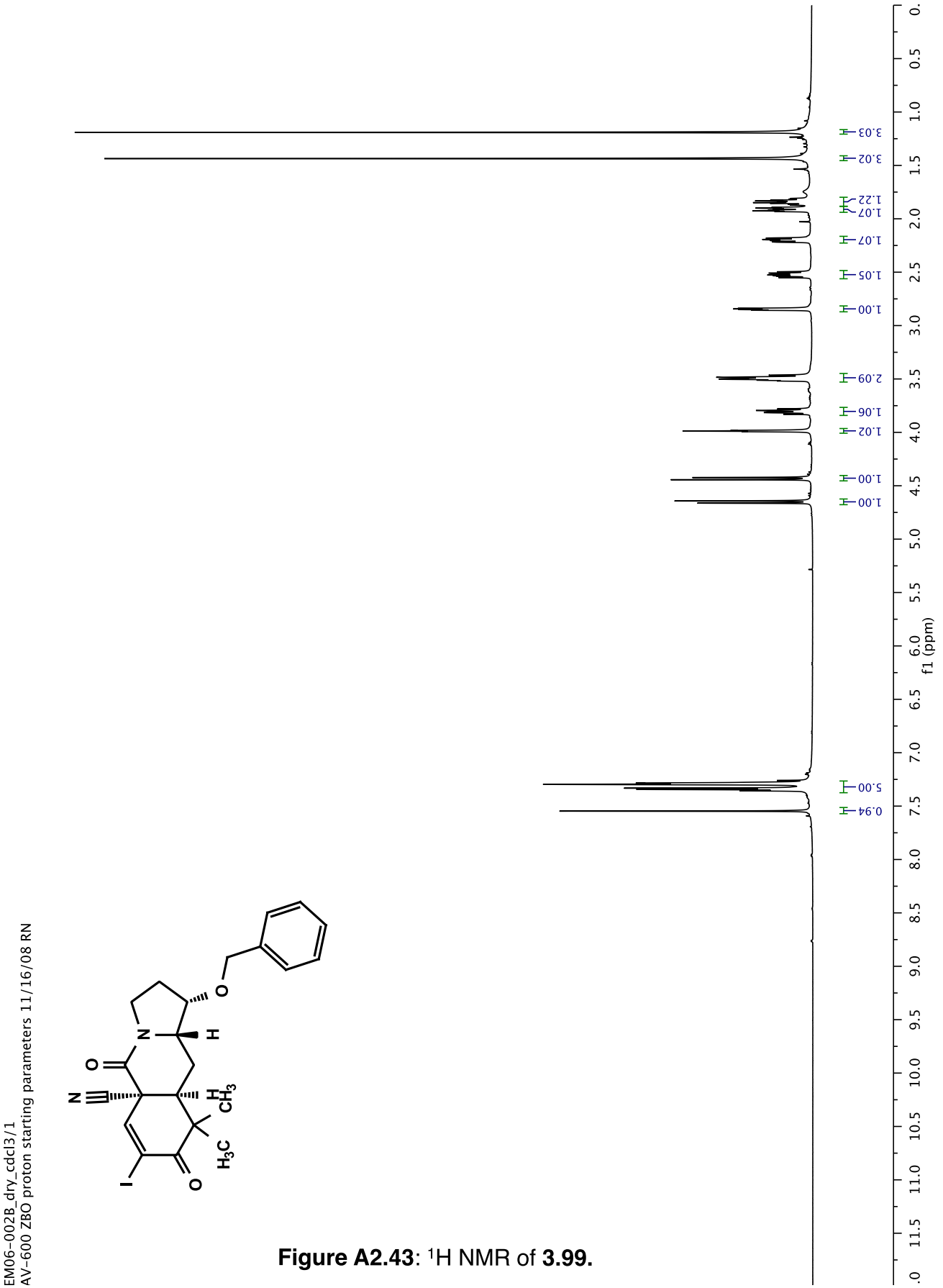

Figure A2.43: ^{1}H NMR of **3.99.**

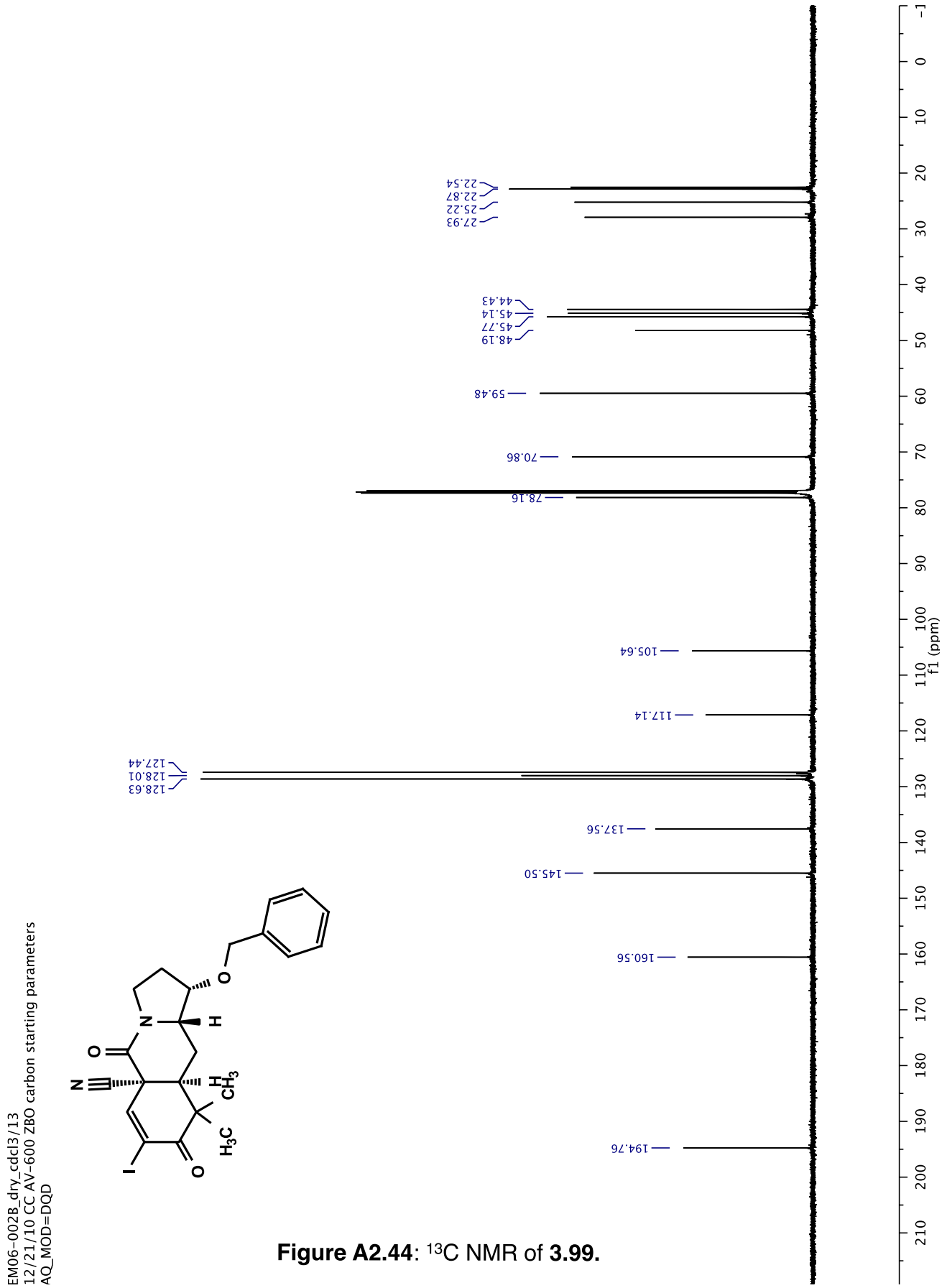

Figure A2.44: ^{13}C NMR of **3.99.**

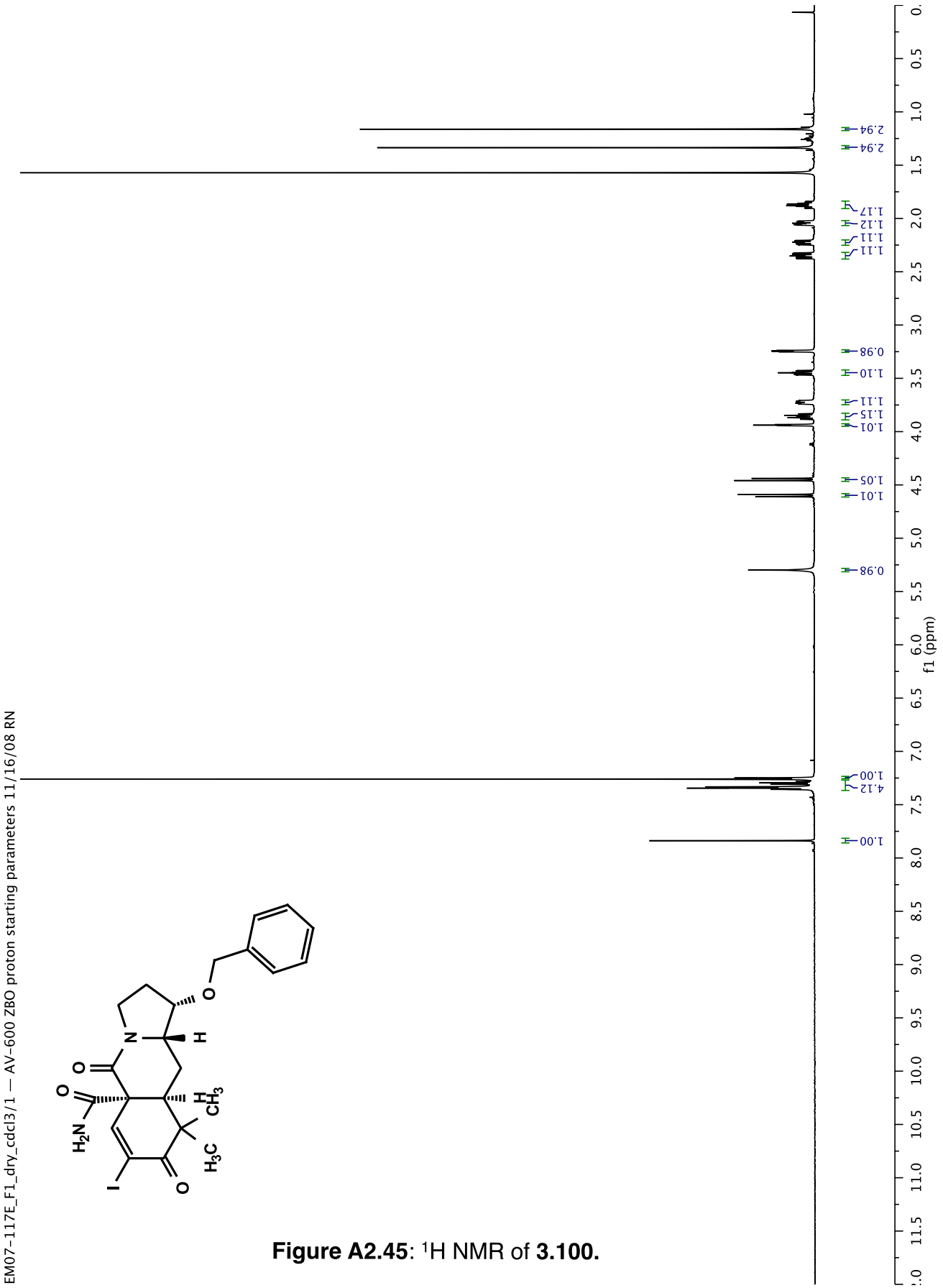

Figure A2.45: ^{1}H NMR of **3.100.**

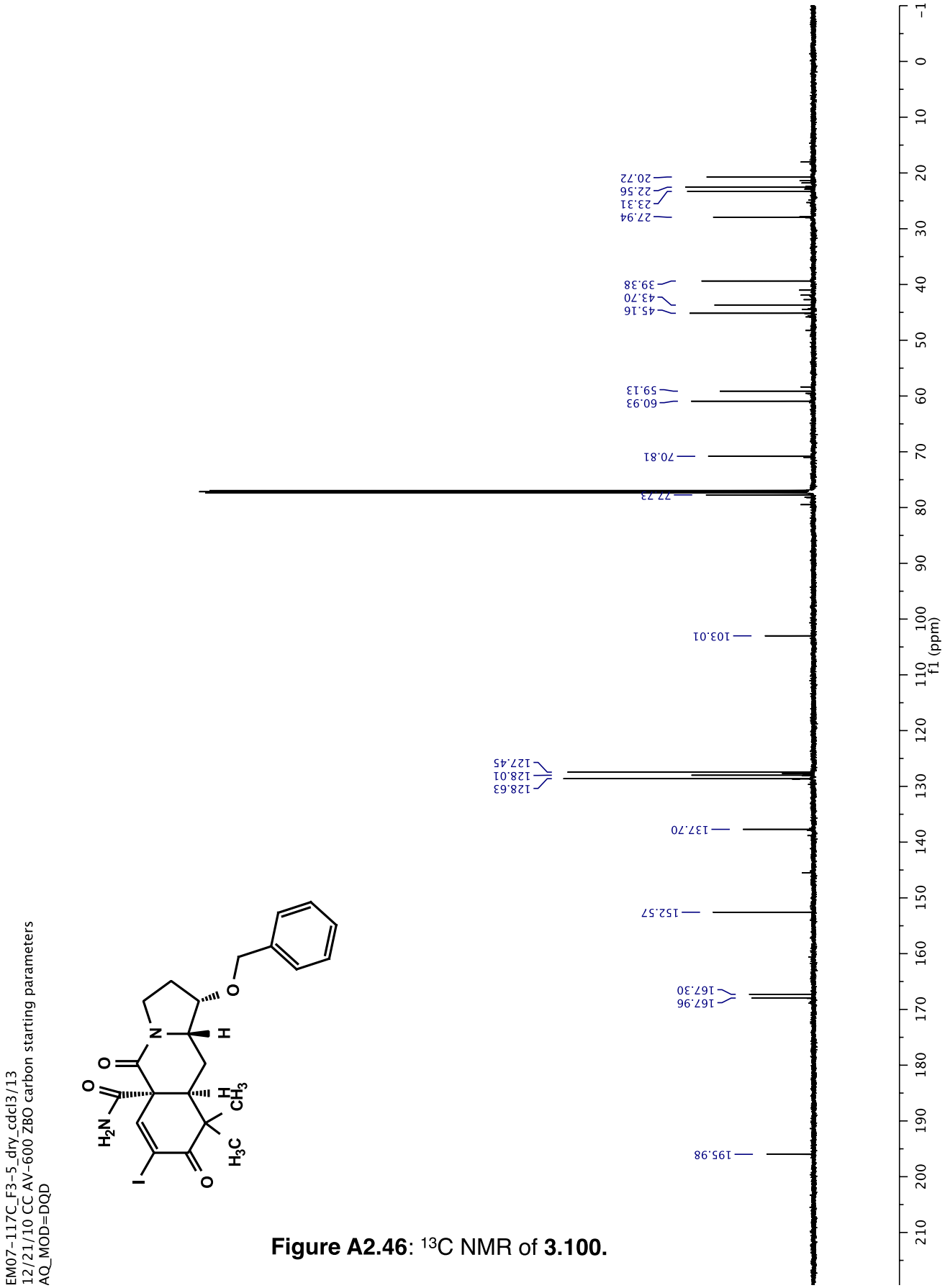

Figure A2.46: ^{13}C NMR of **3.100.**

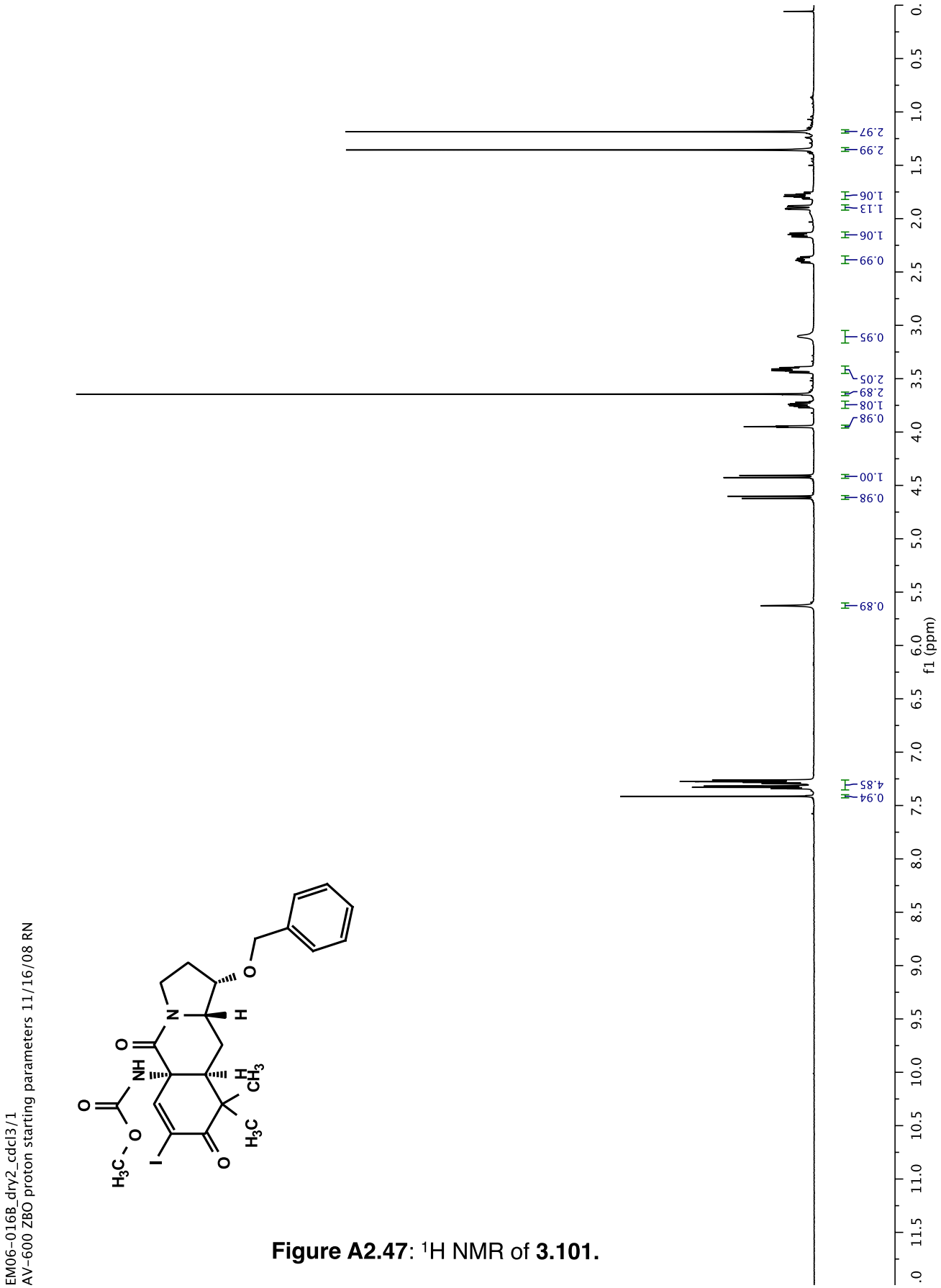

Figure A2.47: ^{1}H NMR of **3.101.**

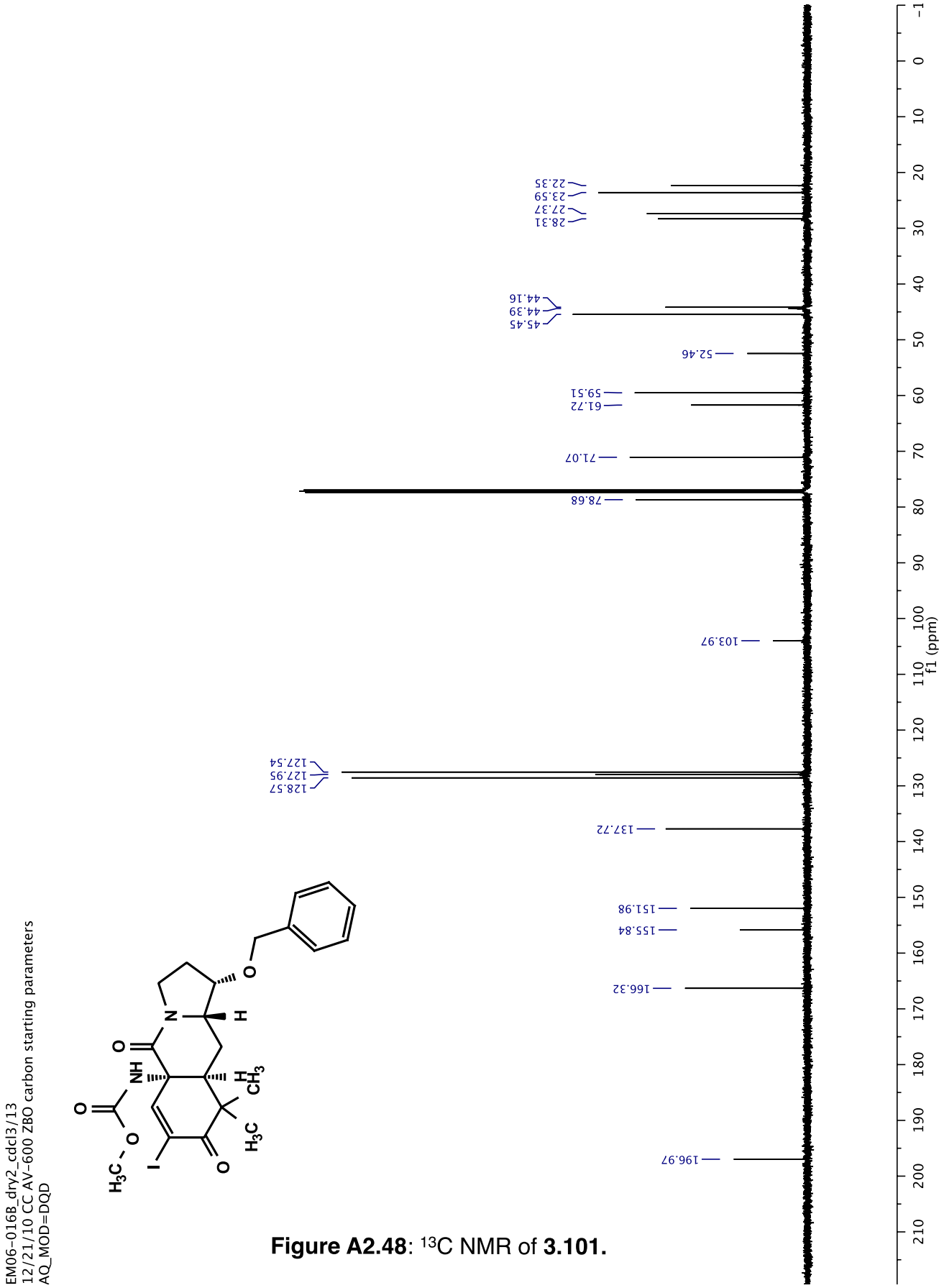

Figure A2.48: ^{13}C NMR of **3.101.**

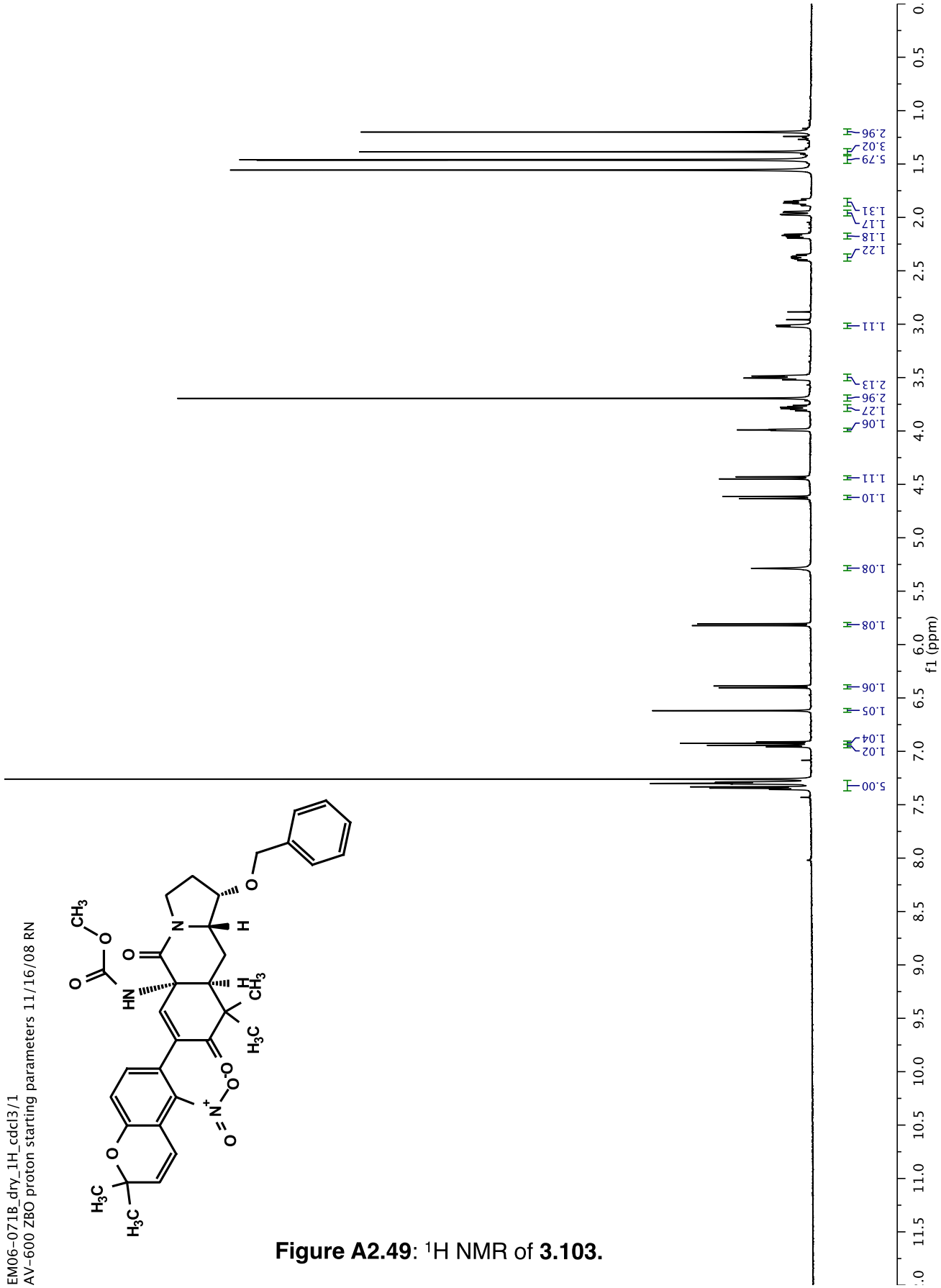

Figure A2.49: ^{1}H NMR of **3.103.**

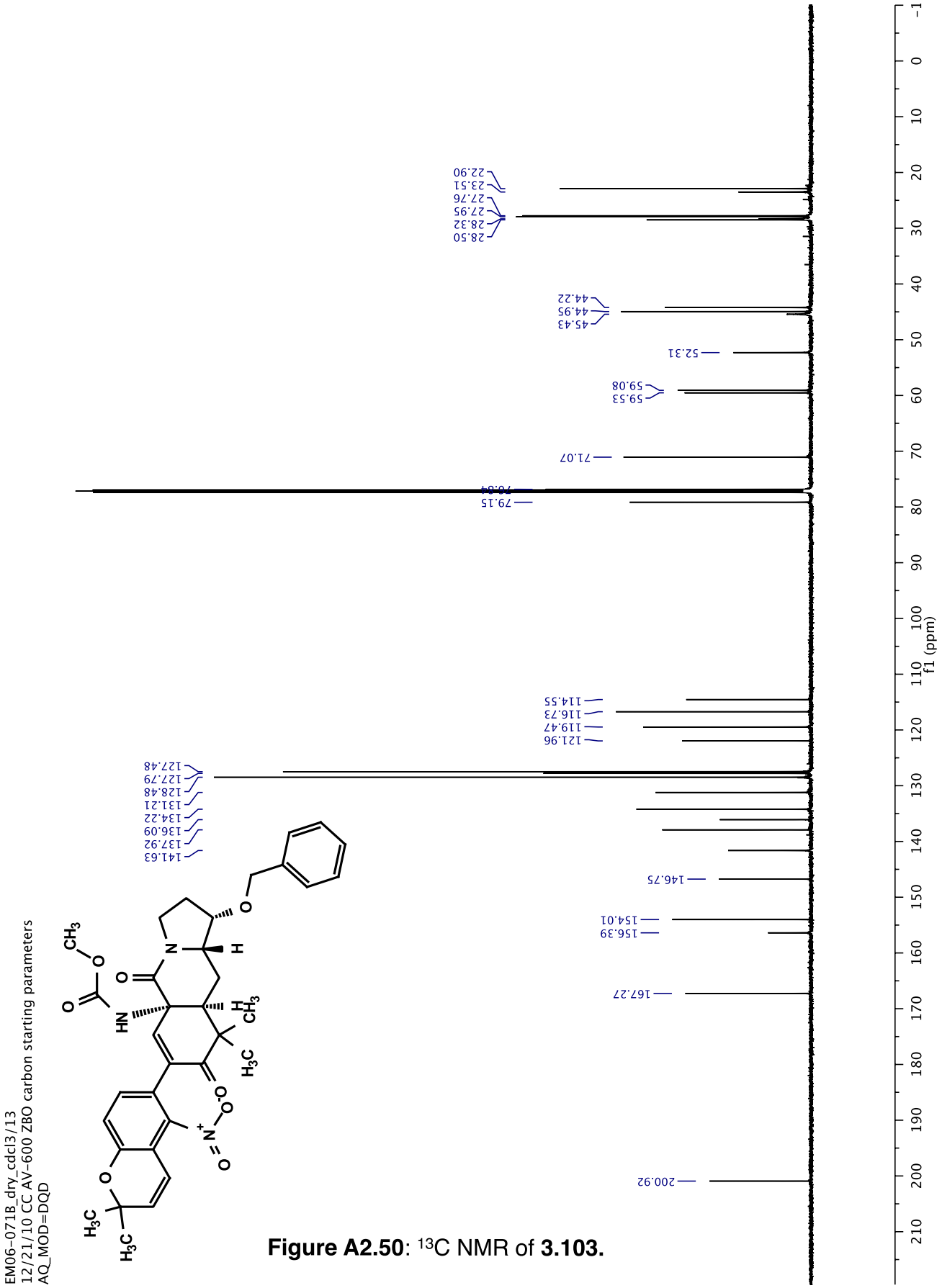

Figure A2.50: ^{13}C NMR of **3.103.**

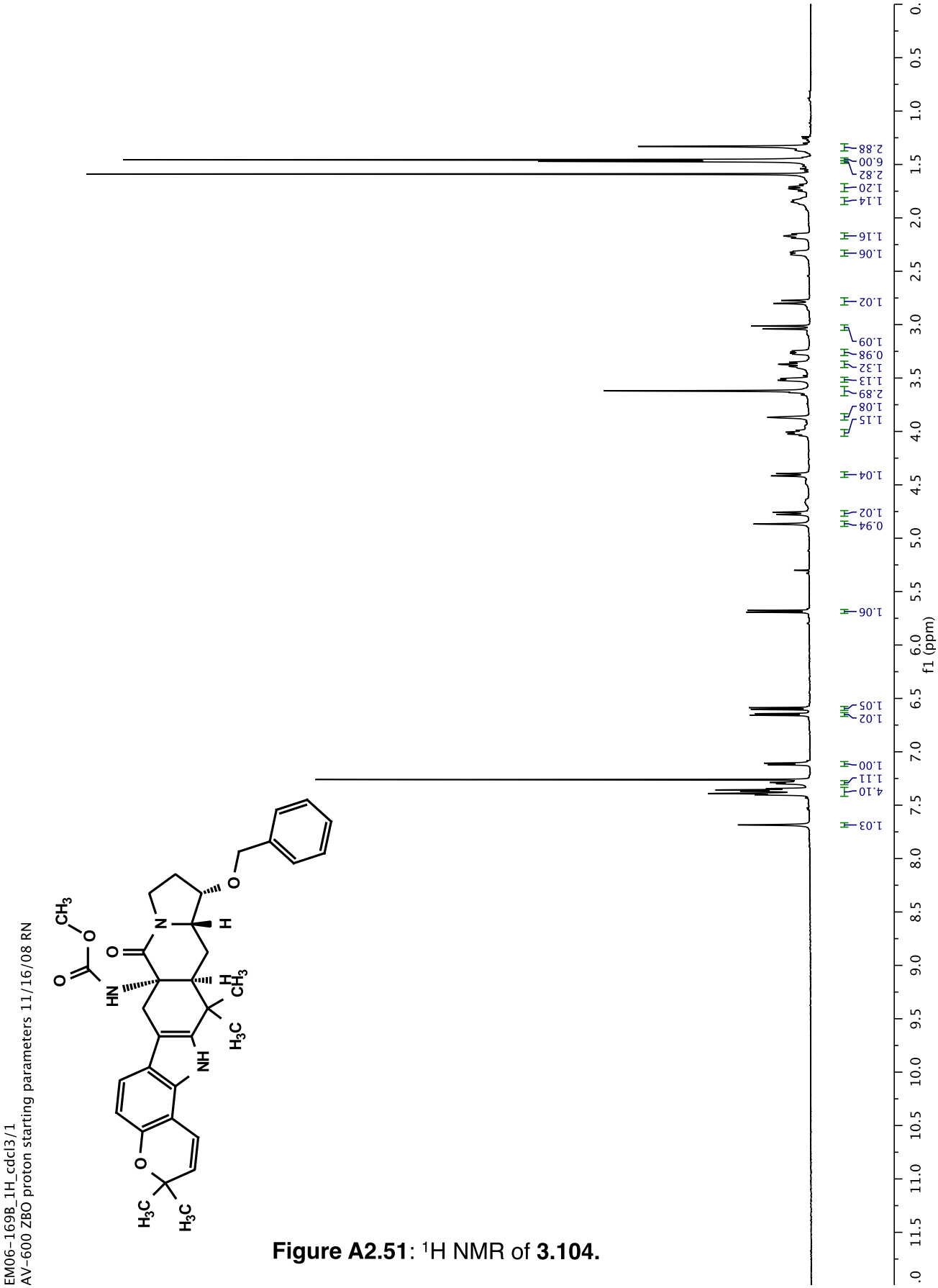

Figure A2.51: ^{1}H NMR of **3.104.**

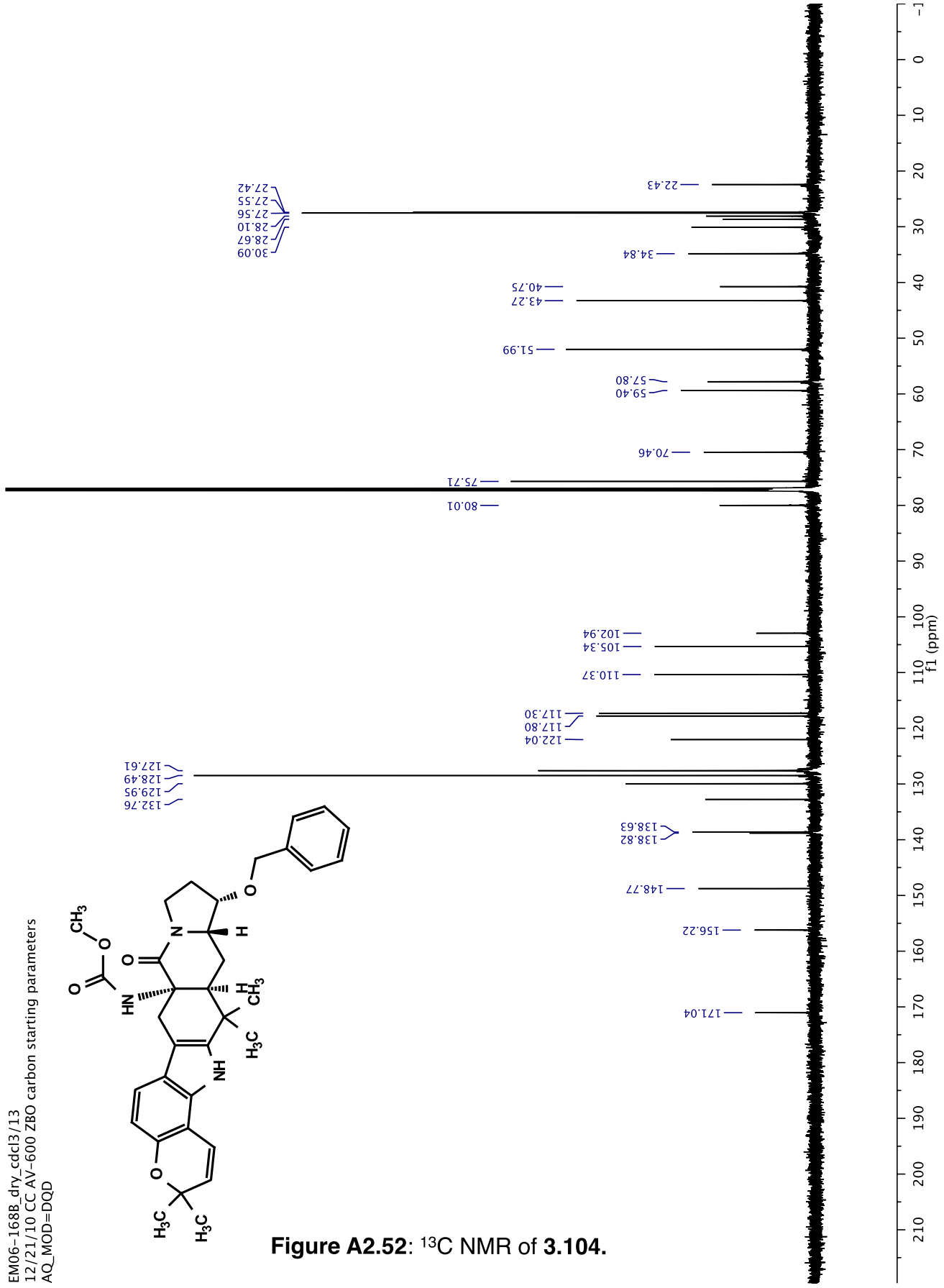

Figure A2.52: ^{13}C NMR of **3.104.**

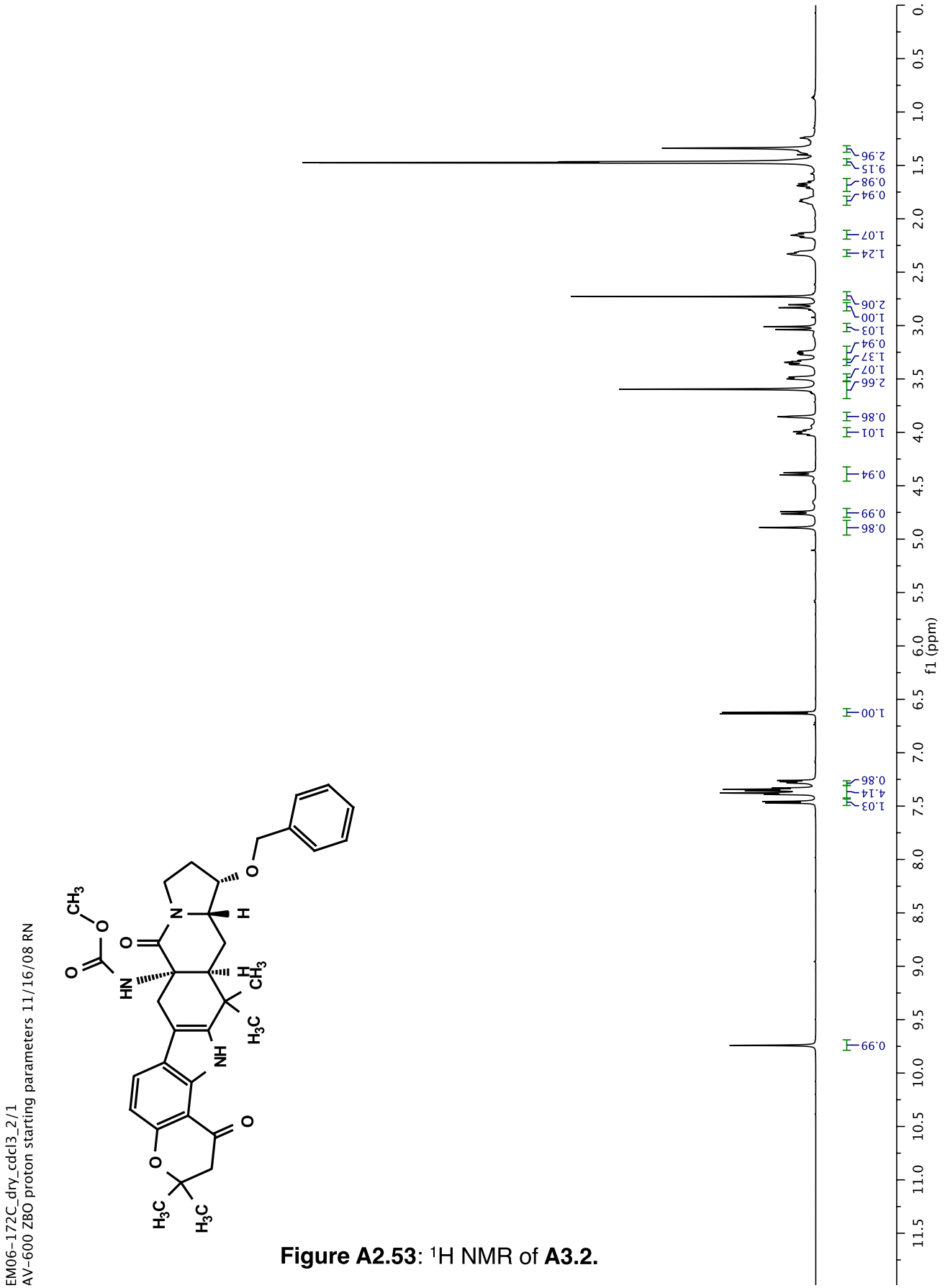

Figure A2.53: ^{1}H NMR of **A3.2.**

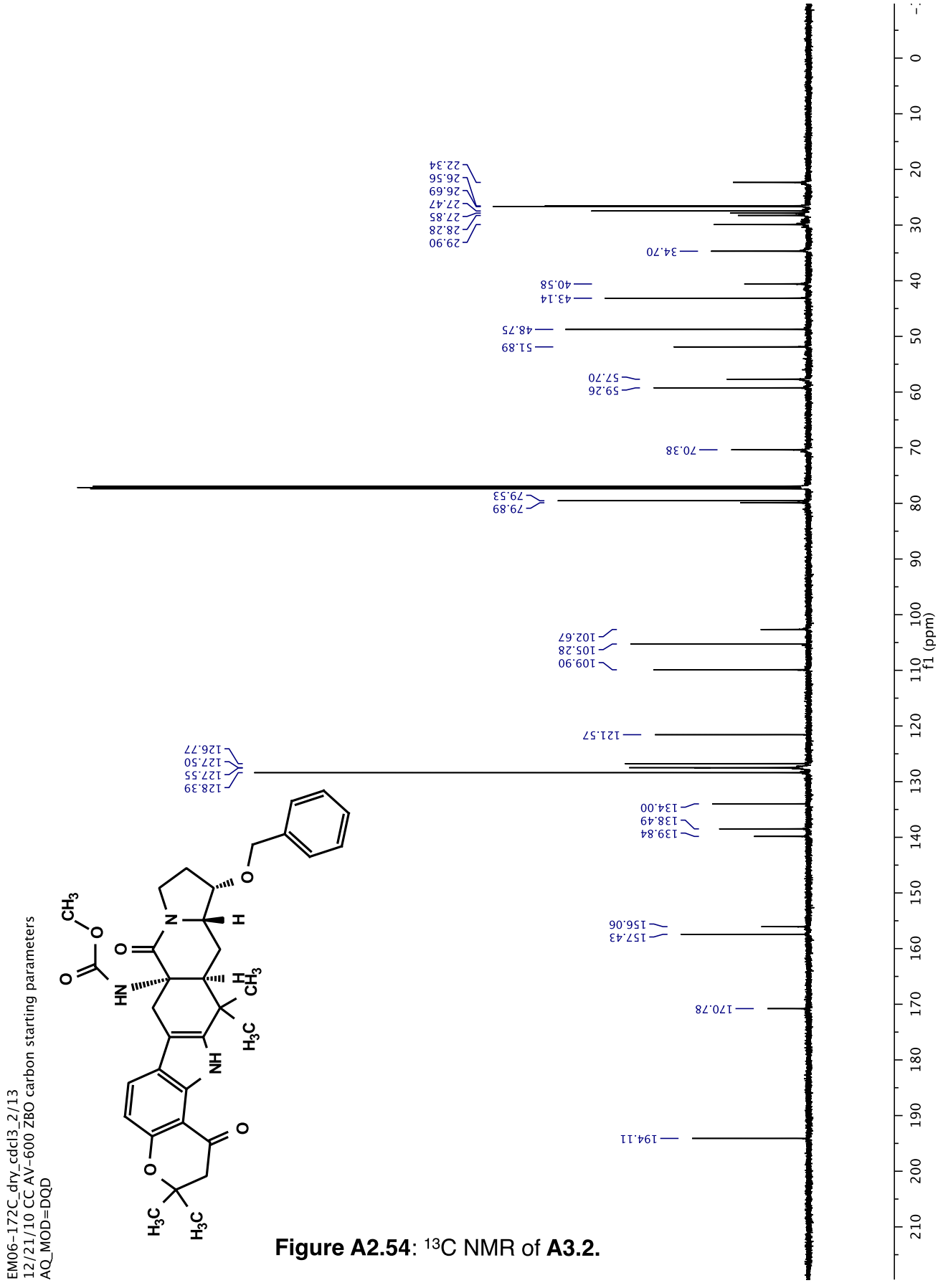

Figure A2.54: ^{13}C NMR of **A3.2.**

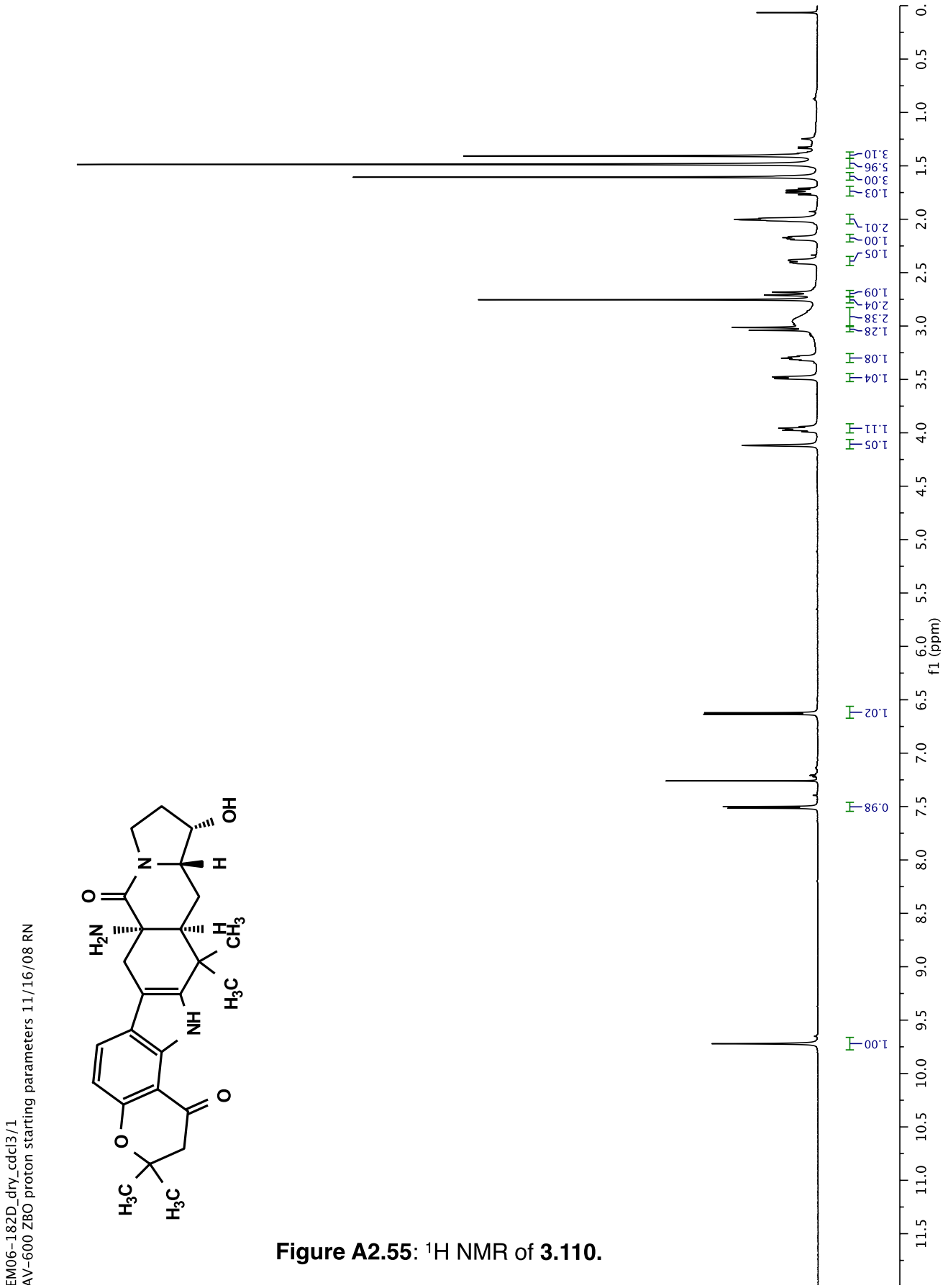

Figure A2.55: ^{1}H NMR of **3.110.**

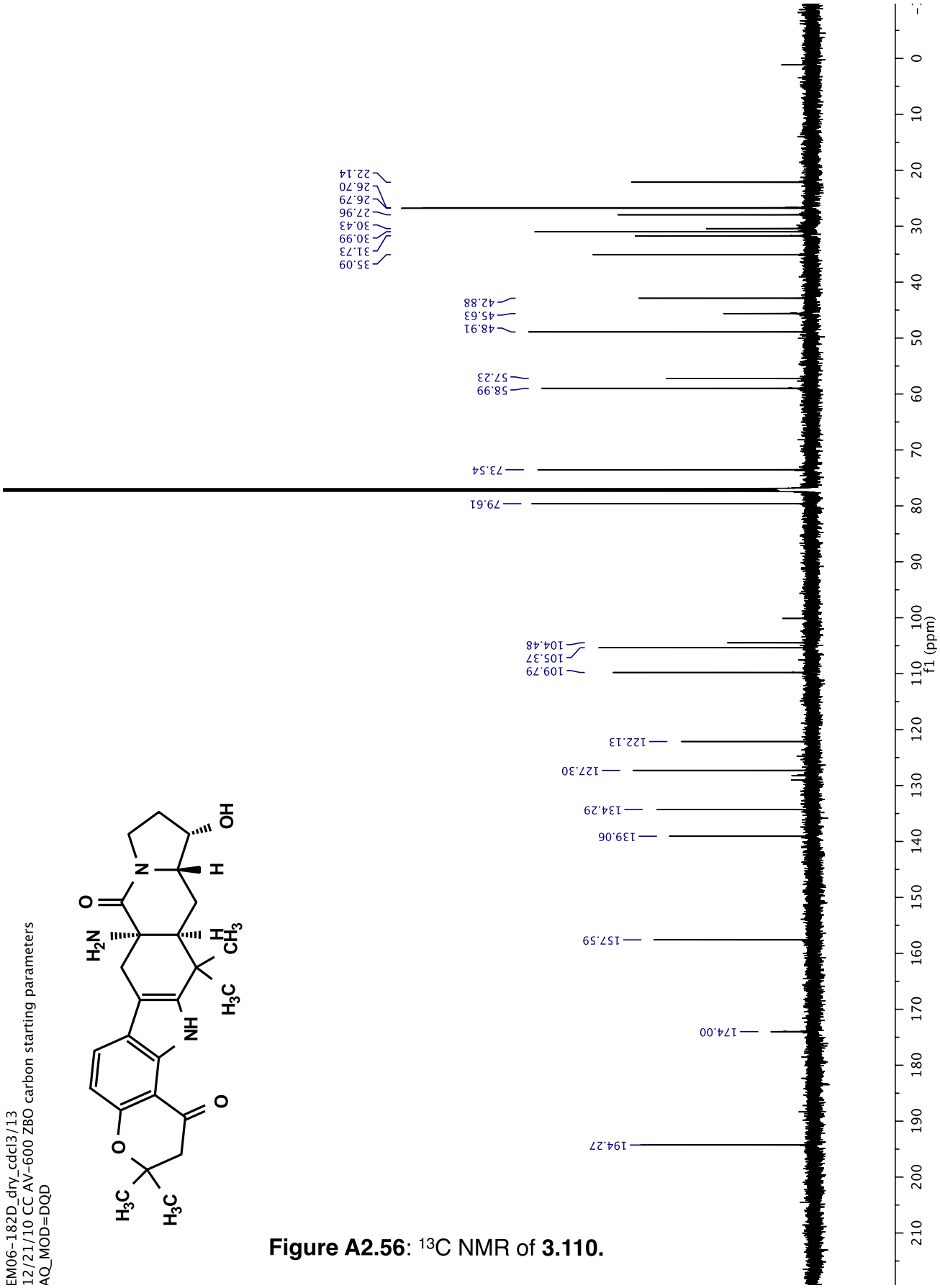

Figure A2.56: ^{13}C NMR of **3.110.**

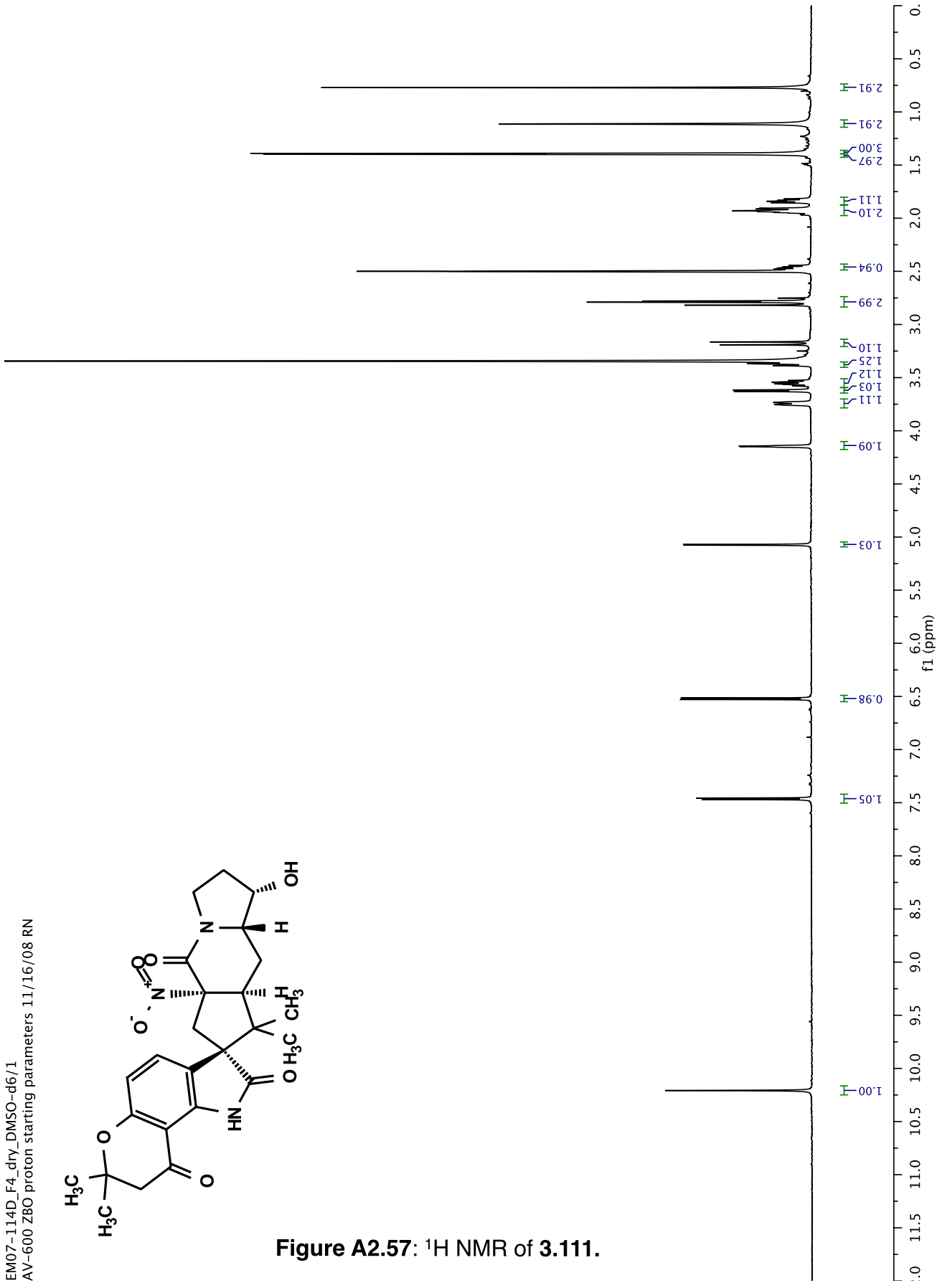

Figure A2.57: ^{1}H NMR of **3.111.**

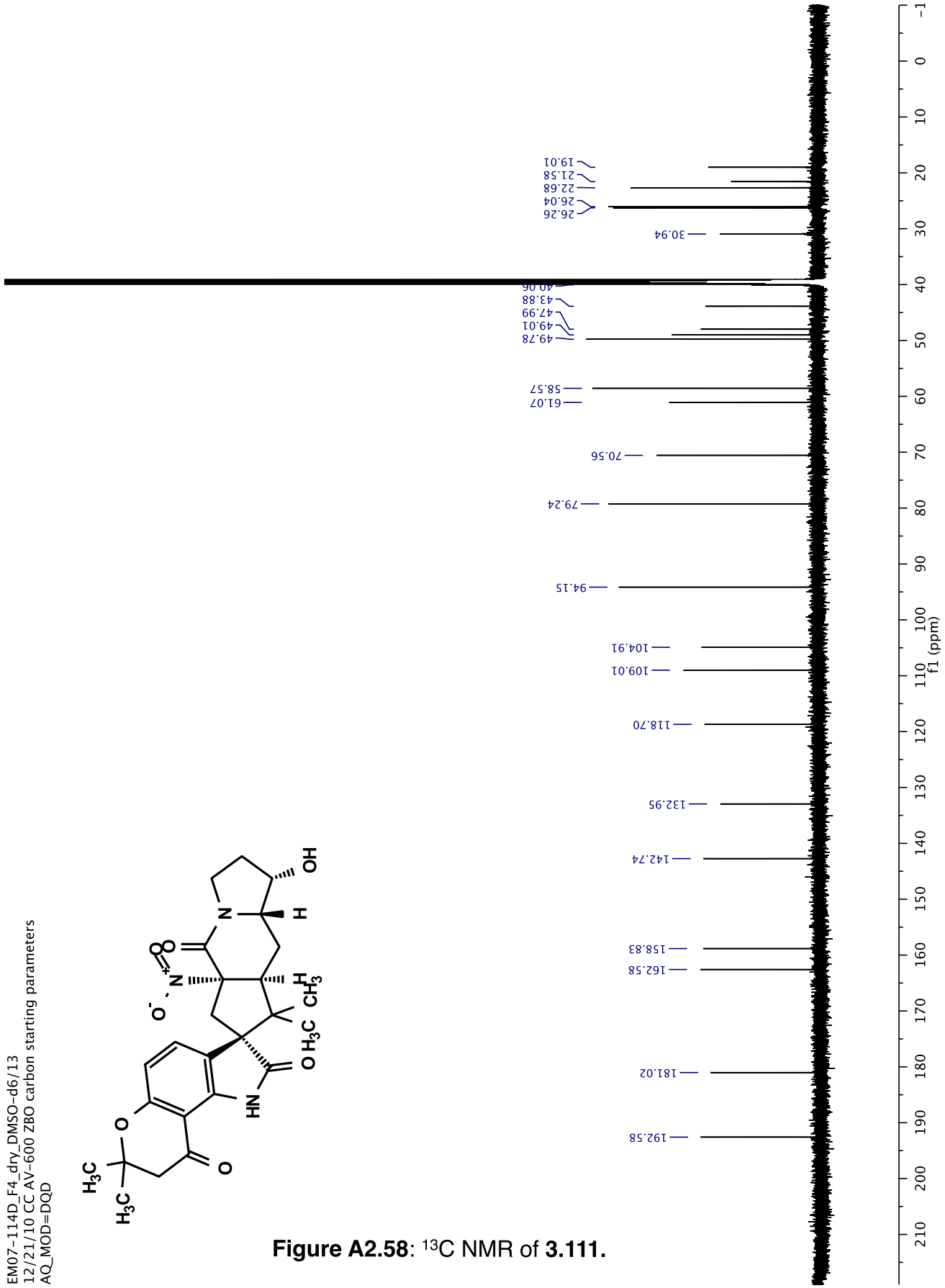

Figure A2.58: ^{13}C NMR of **3.111.**

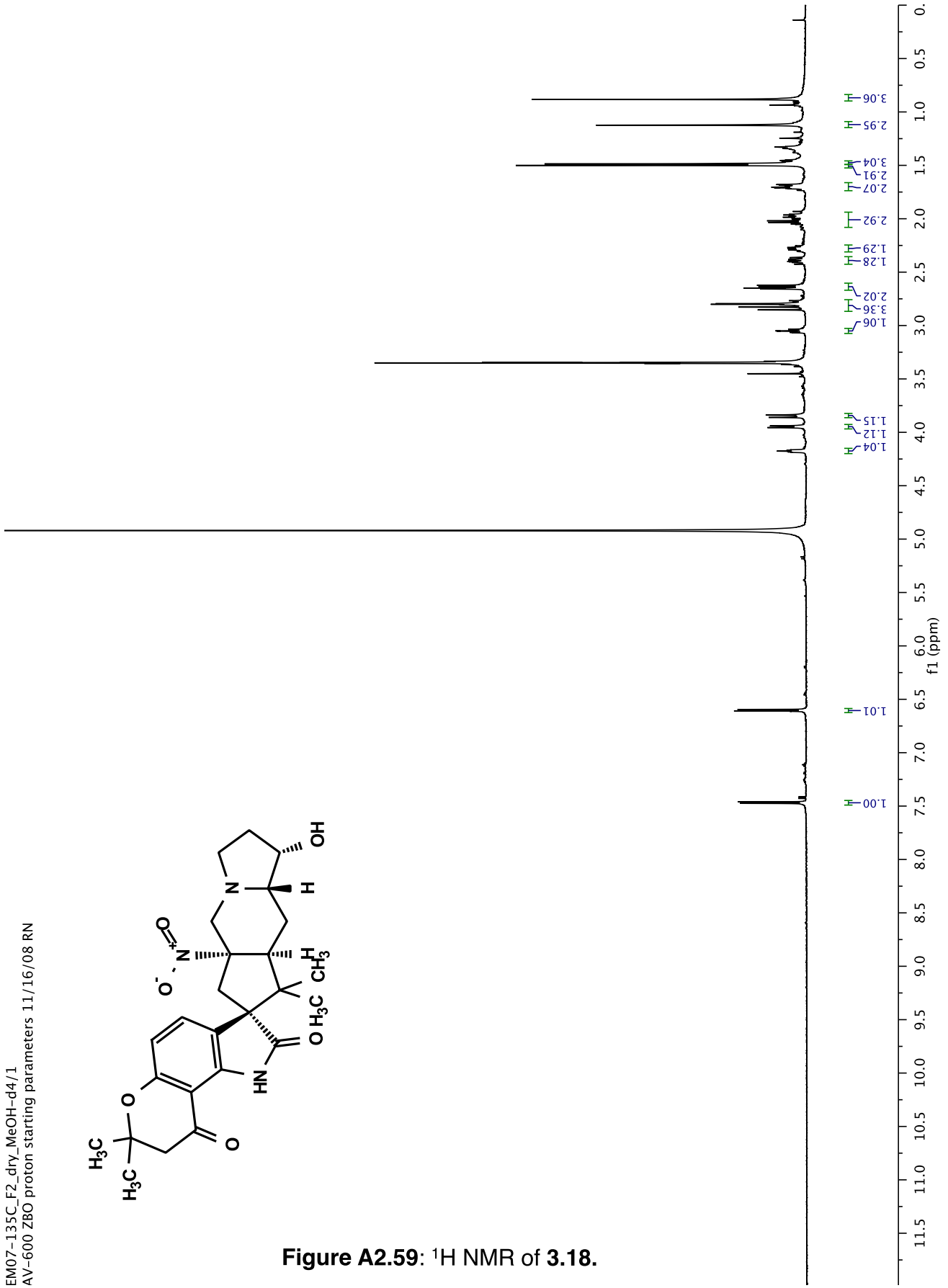

Figure A2.59: ^{1}H NMR of **3.18.**

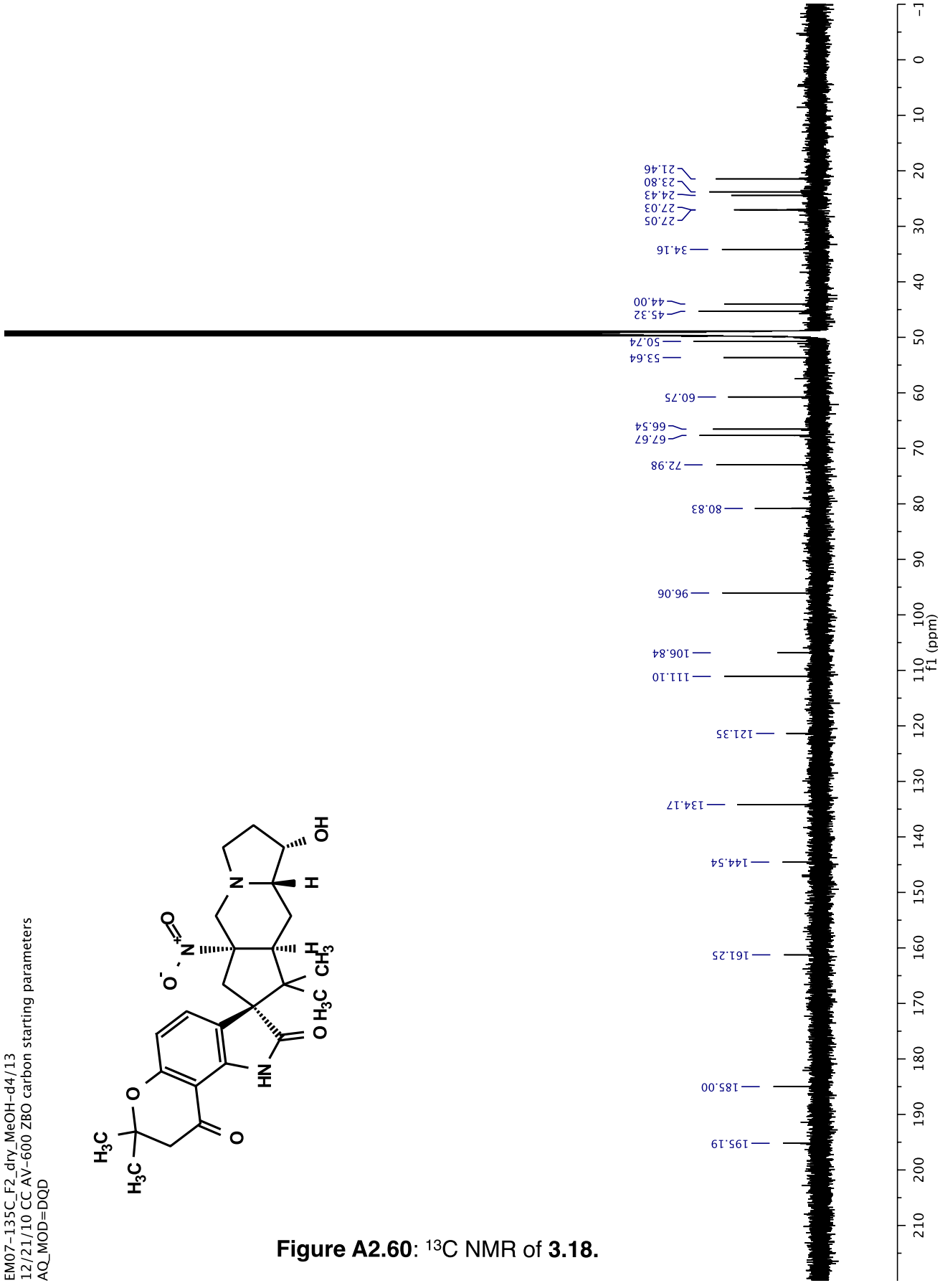

Figure A2.60: ^{13}C NMR of **3.18.**

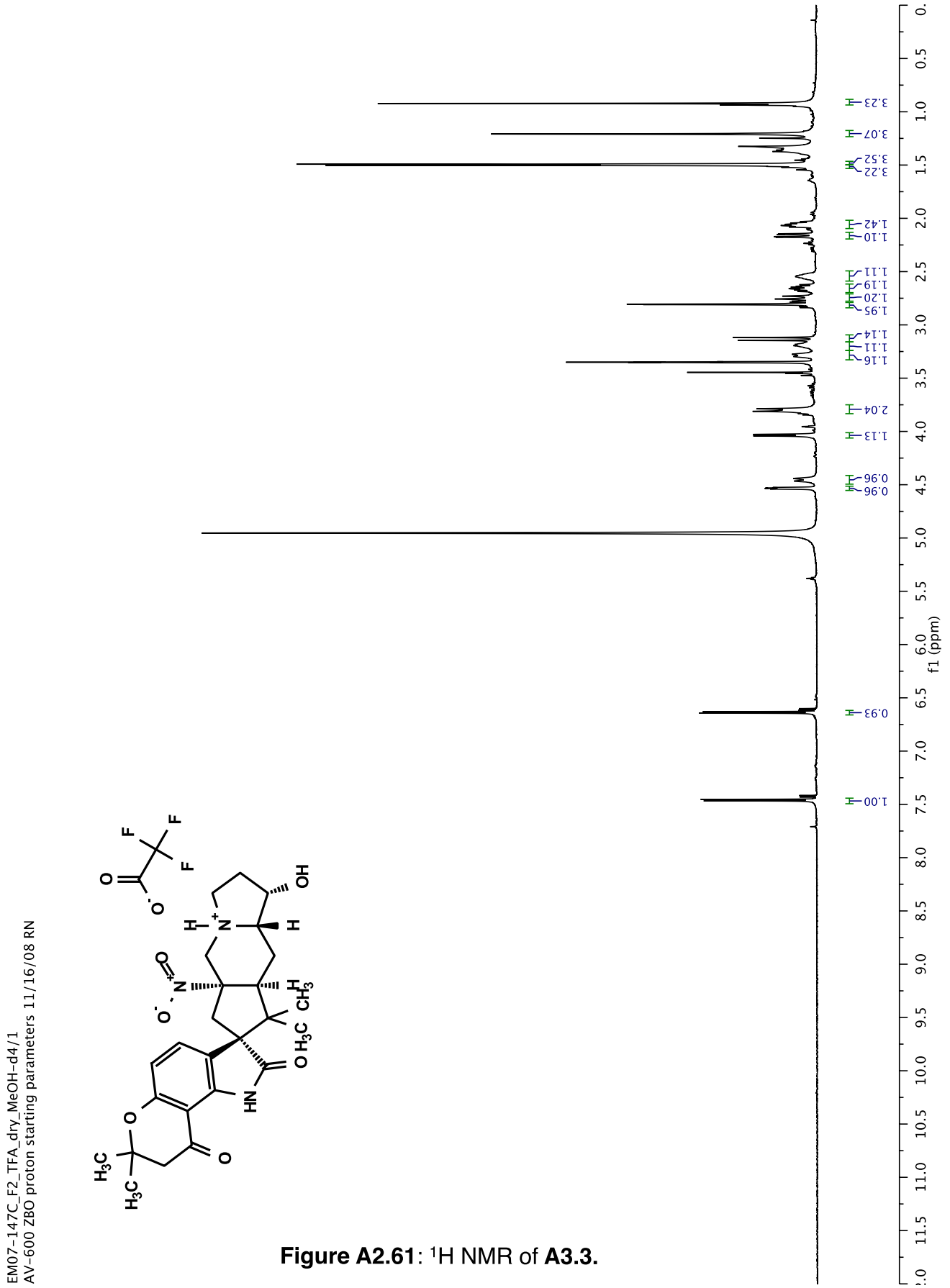

Figure A2.61: ^{1}H NMR of **A3.3.**

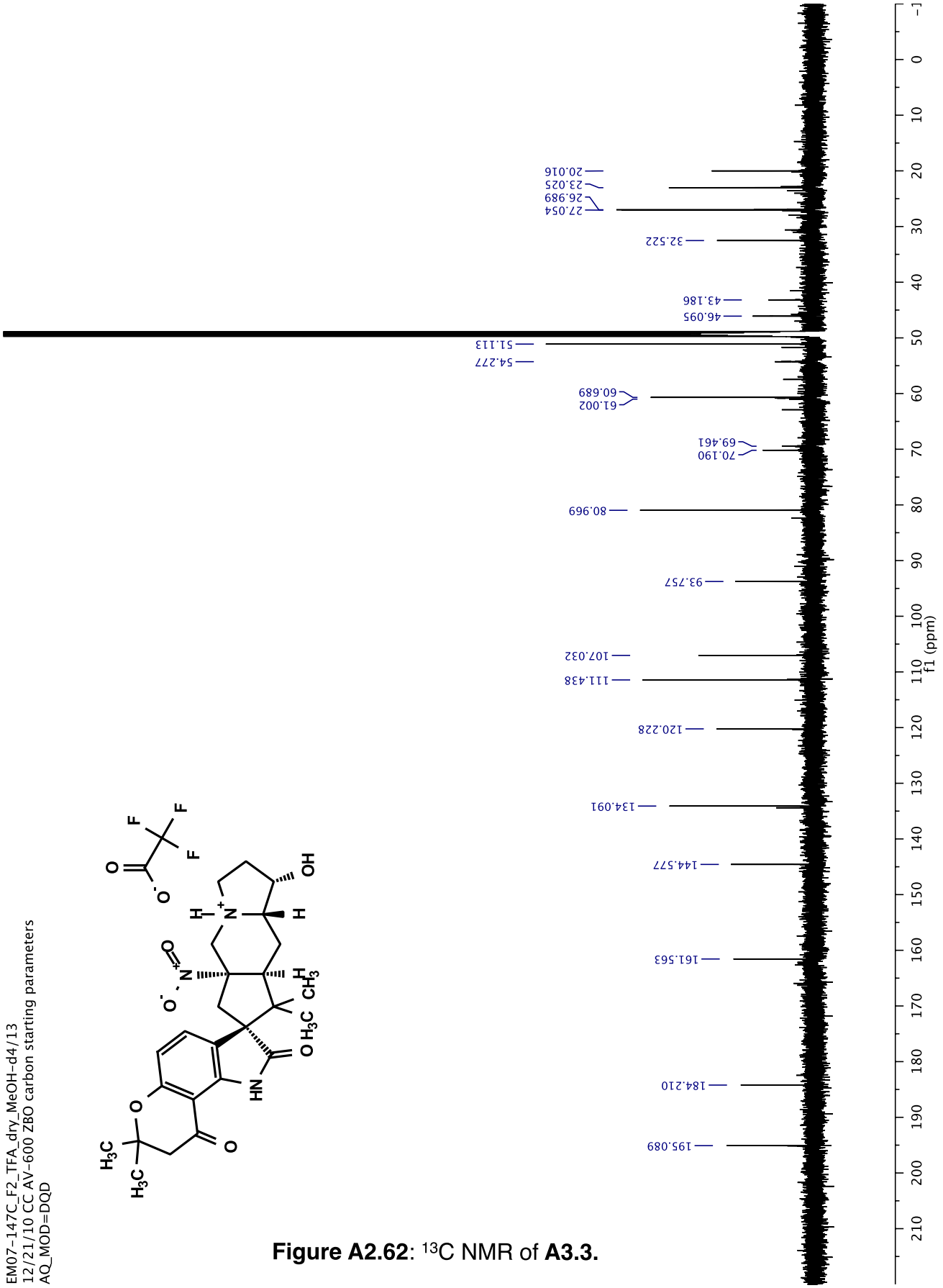

Figure A2.62: ^{13}C NMR of **A3.3.**

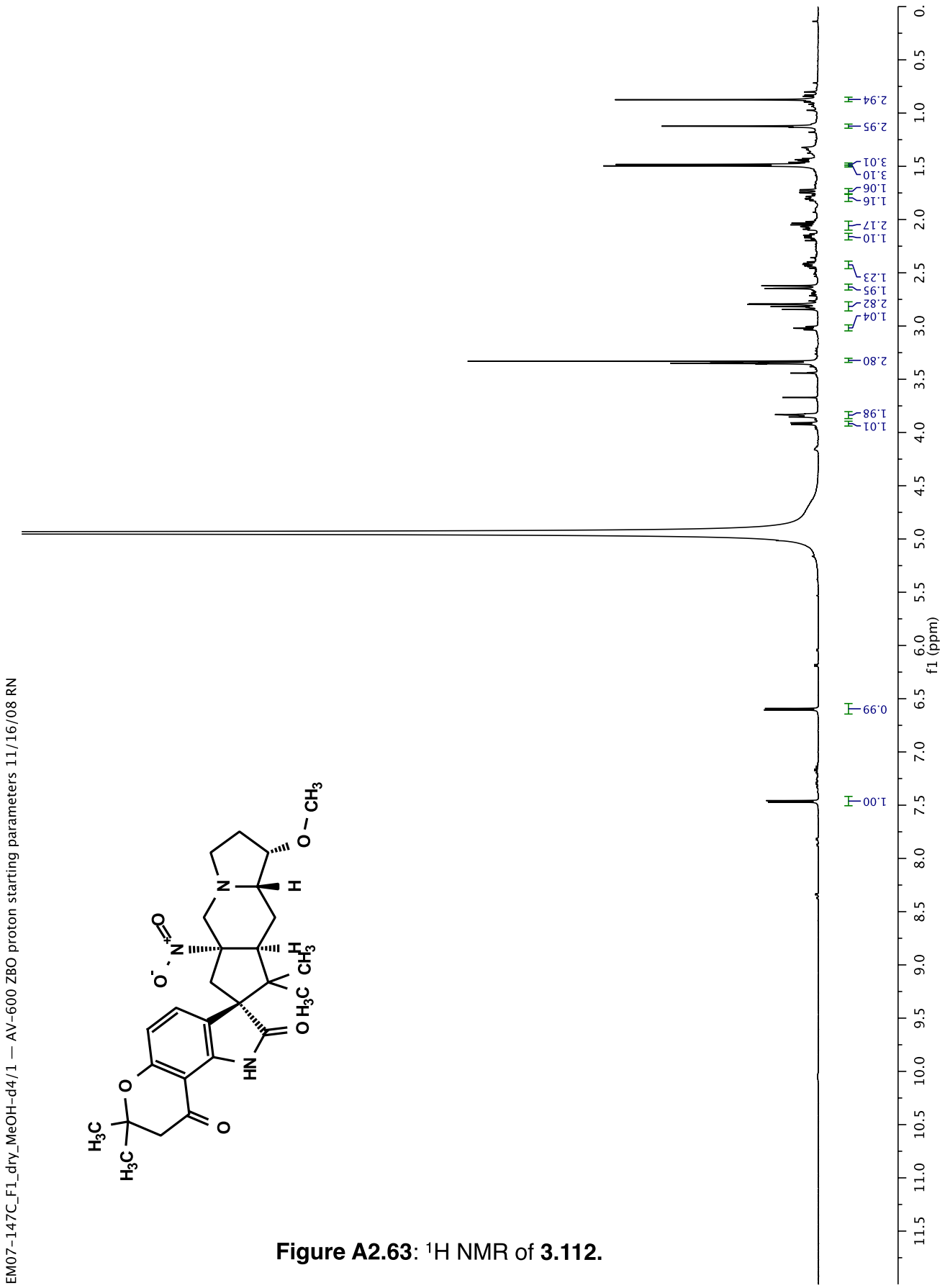

Figure A2.63: ^{1}H NMR of **3.112.**

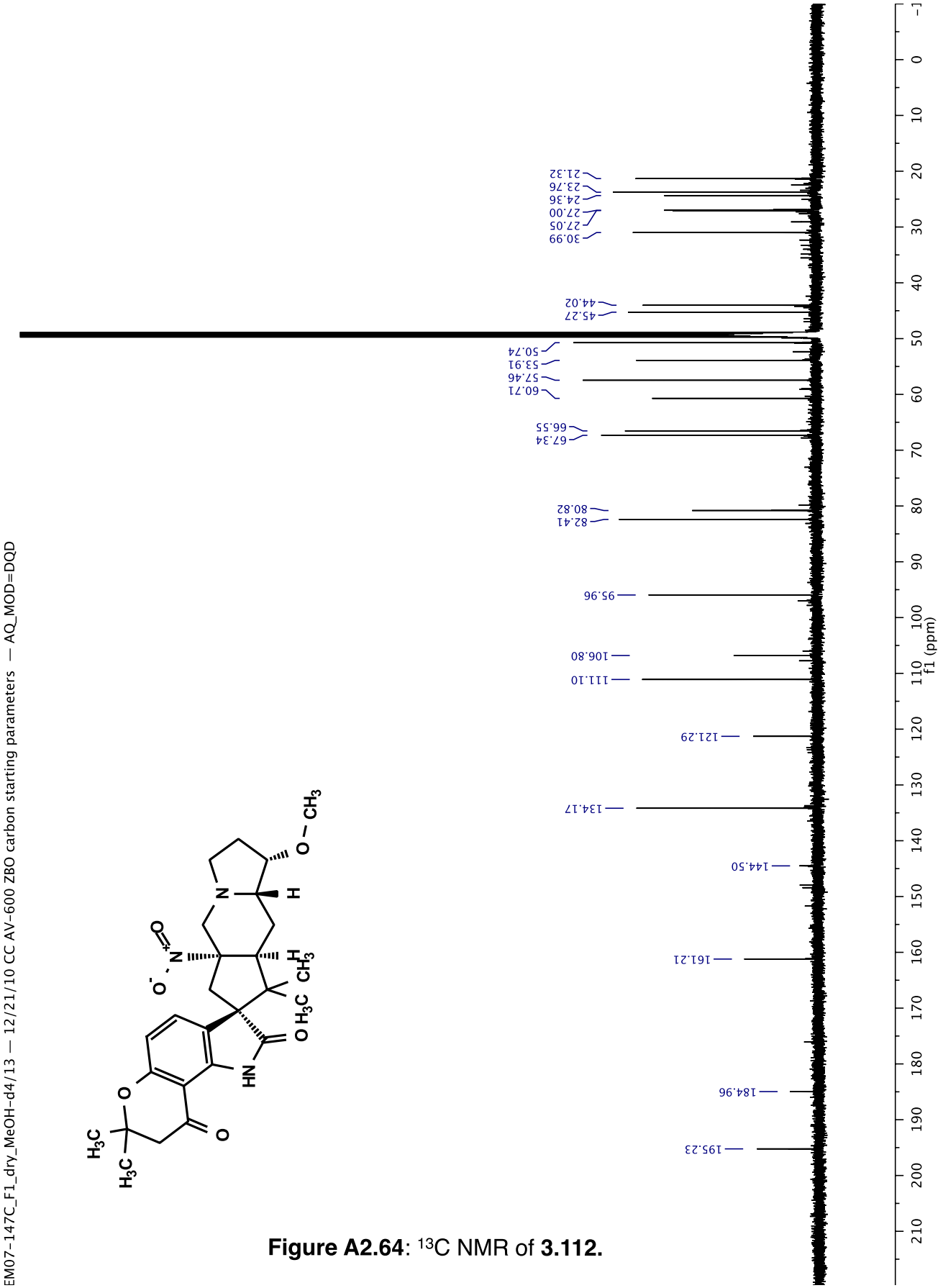

Figure A2.64: ^{13}C NMR of **3.112.**

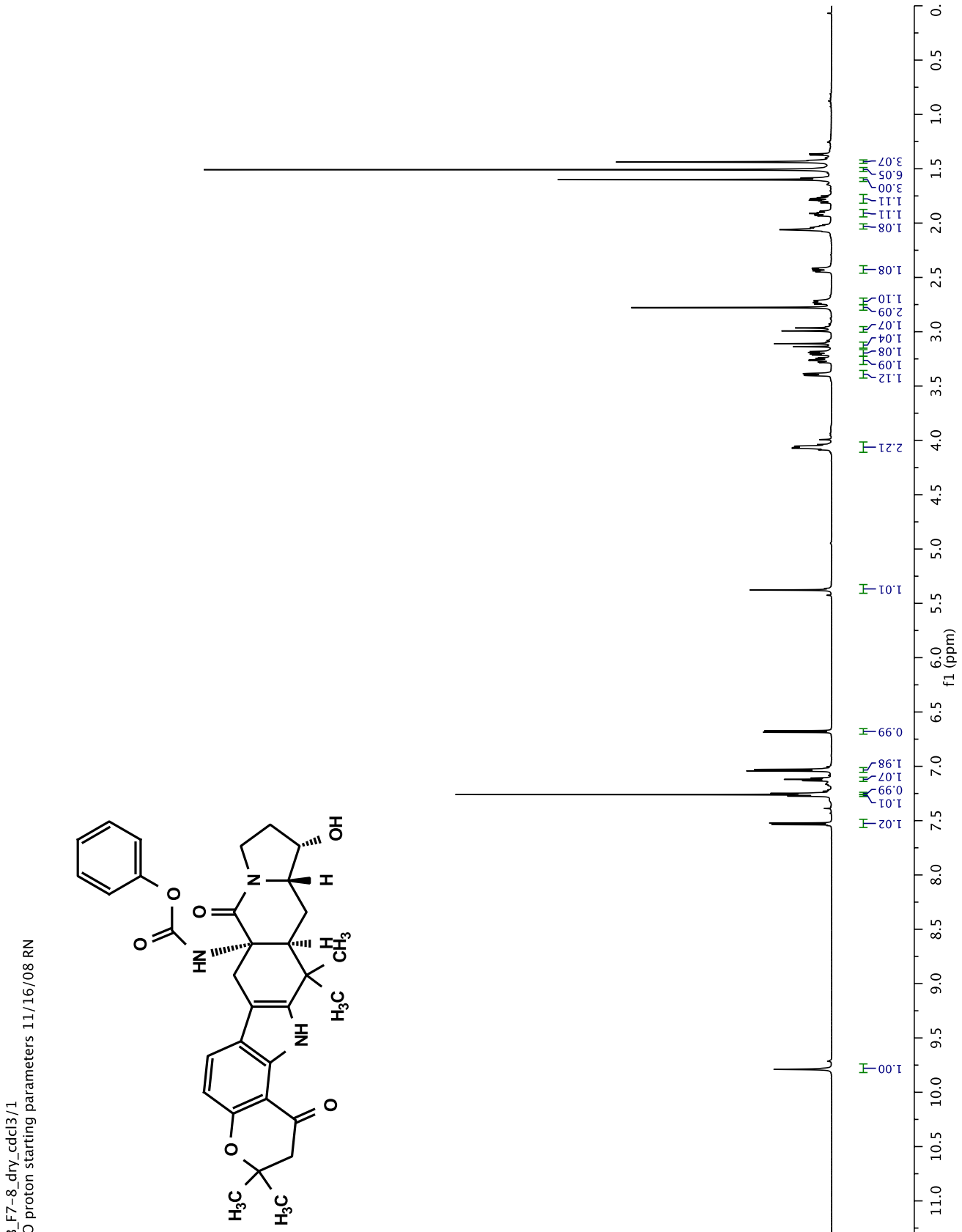

Figure A2.65: ^{1}H NMR of **3.113.**

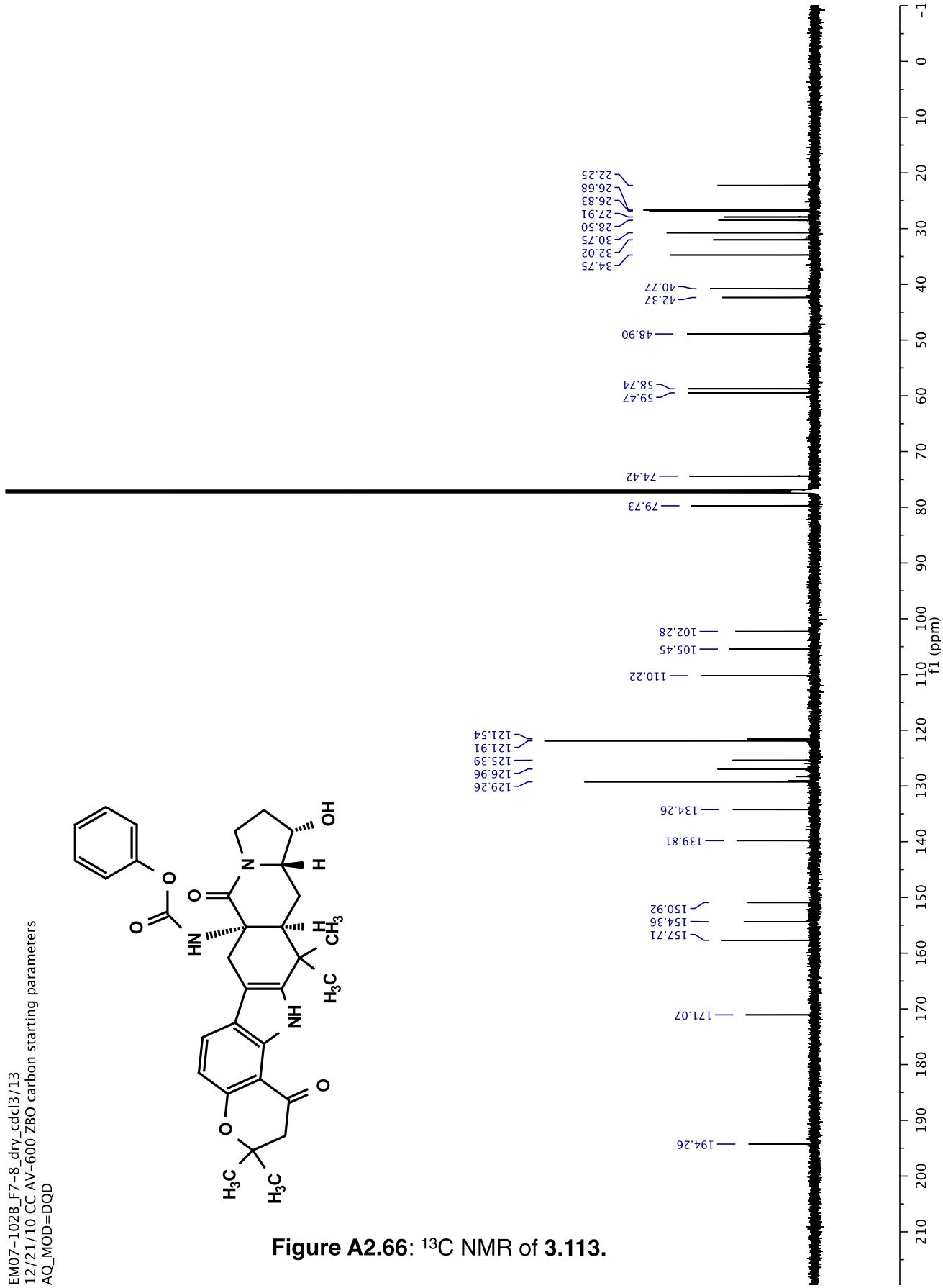

Figure A2.66: ^{13}C NMR of **3.113.**

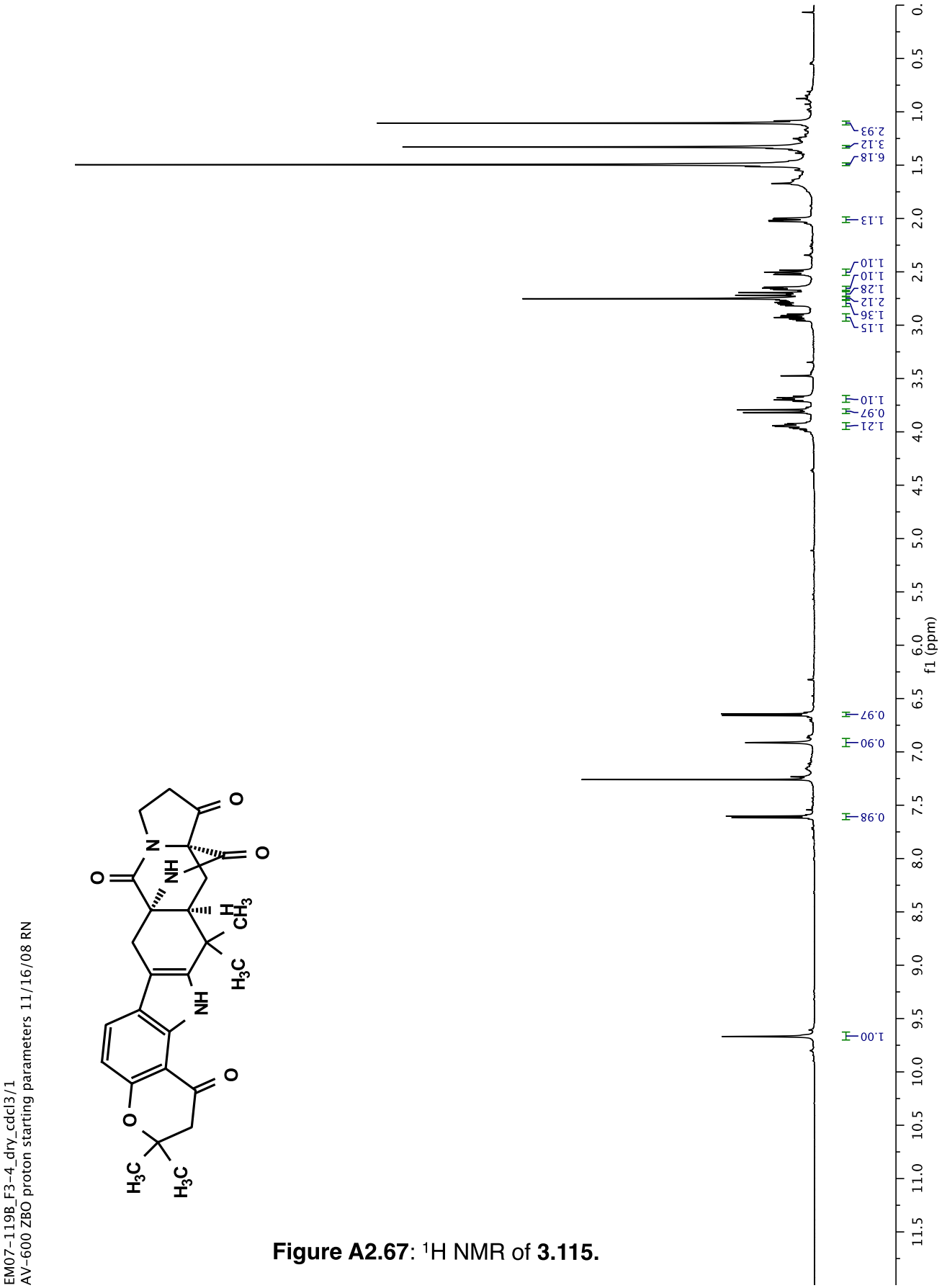

Figure A2.67: ^{1}H NMR of **3.115.**

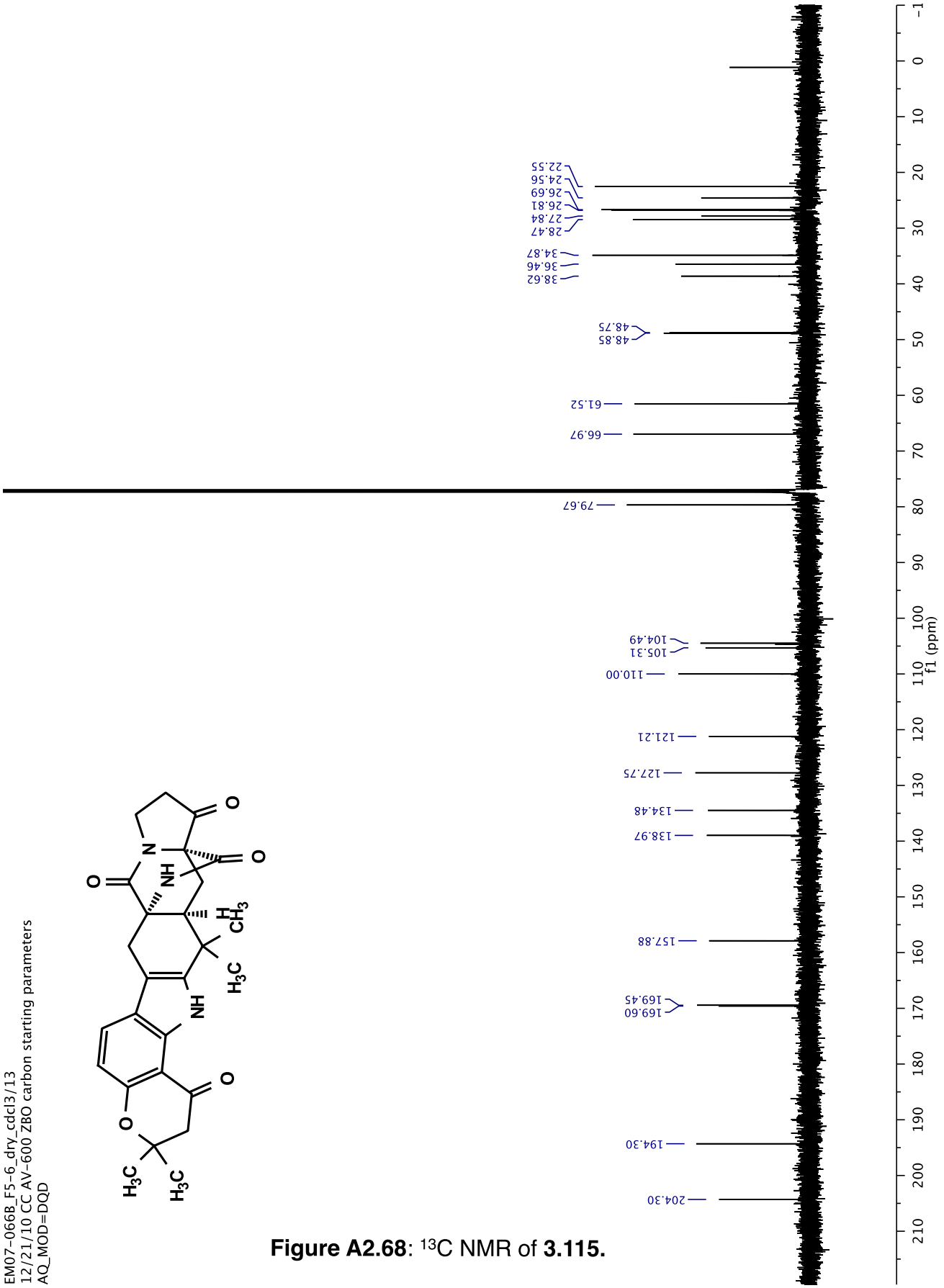

Figure A2.68: ^{13}C NMR of **3.115.**

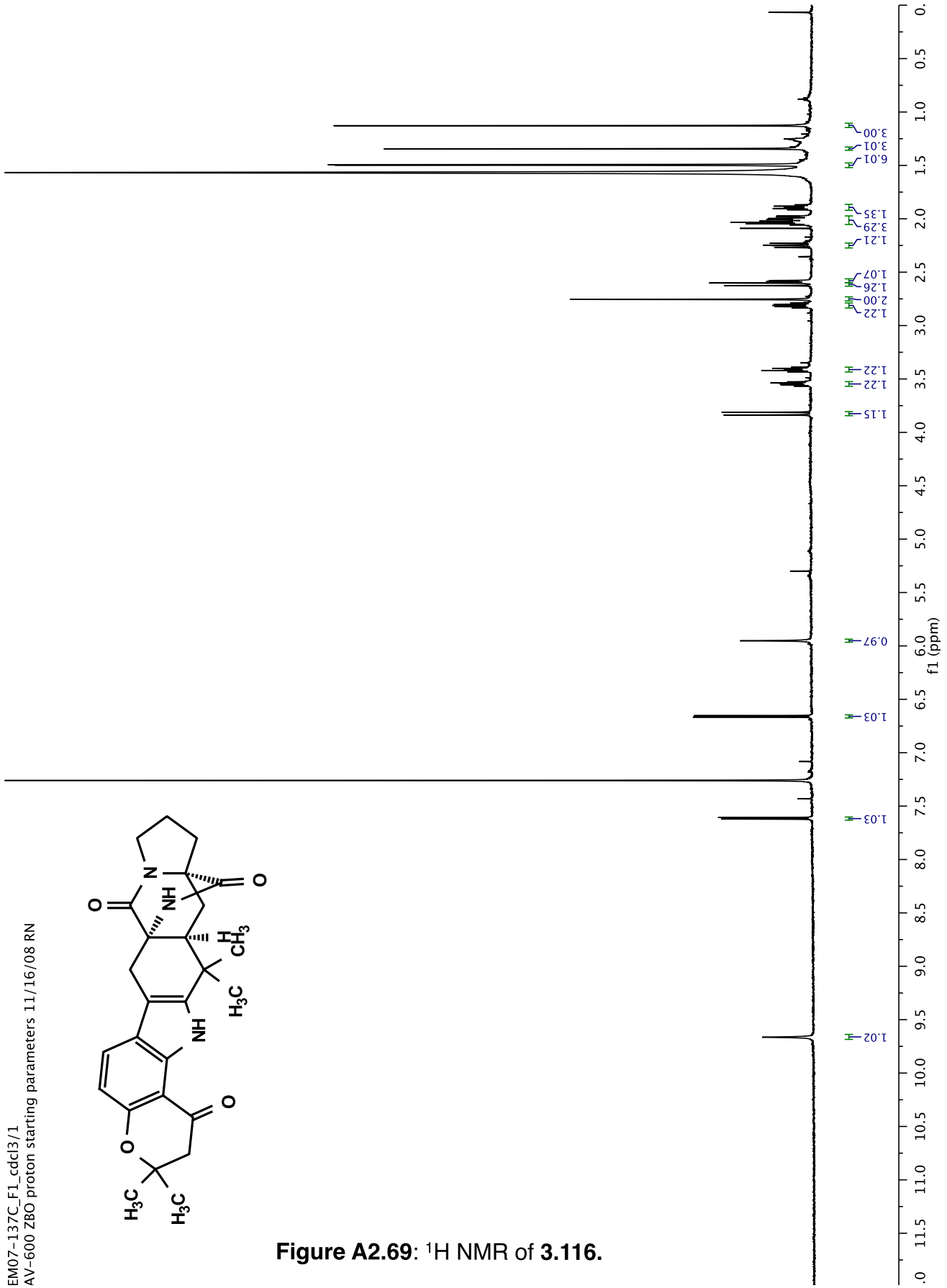

Figure A2.69: ^{1}H NMR of **3.116.**

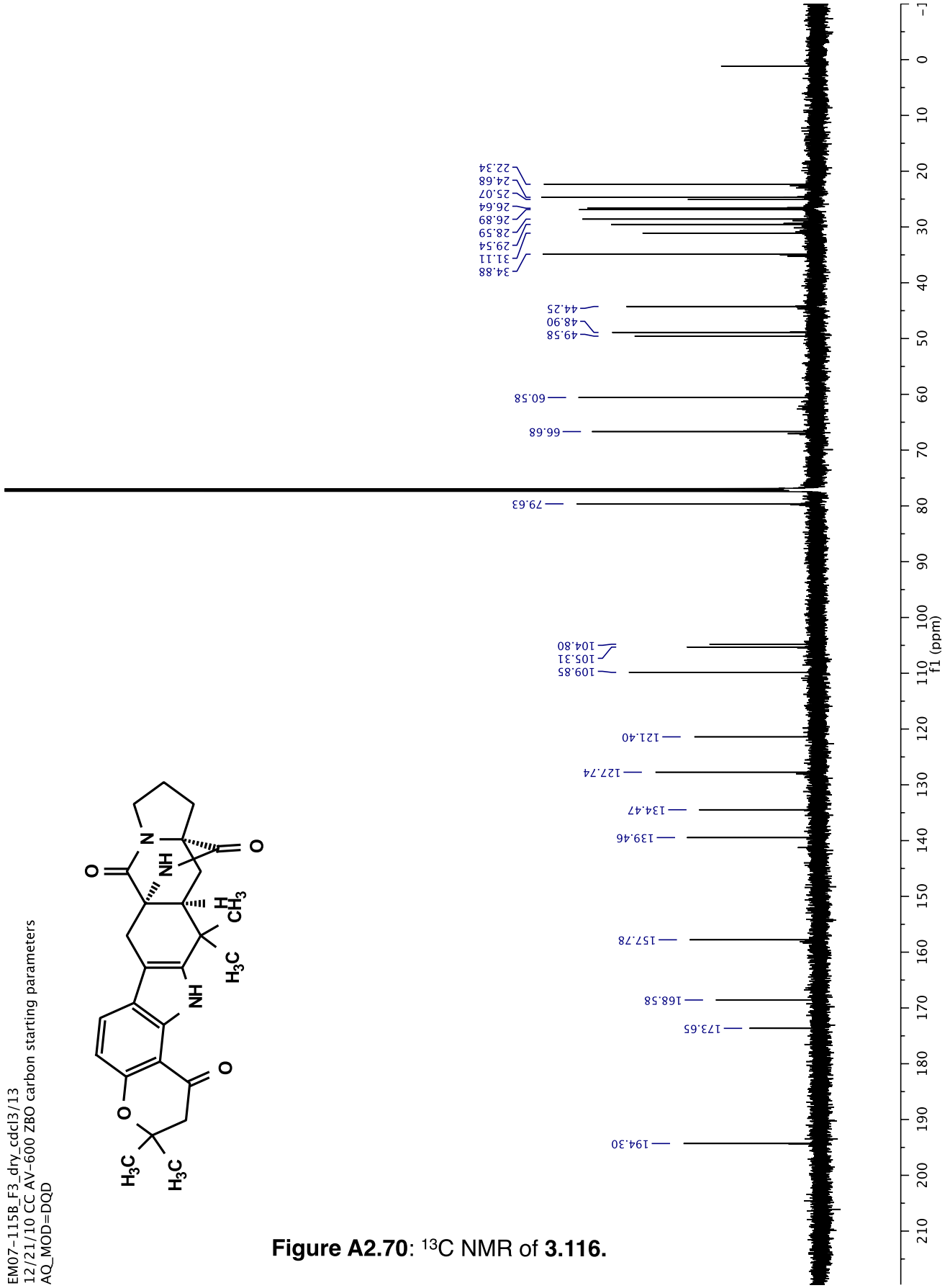

Figure A2.70: ^{13}C NMR of **3.116.**

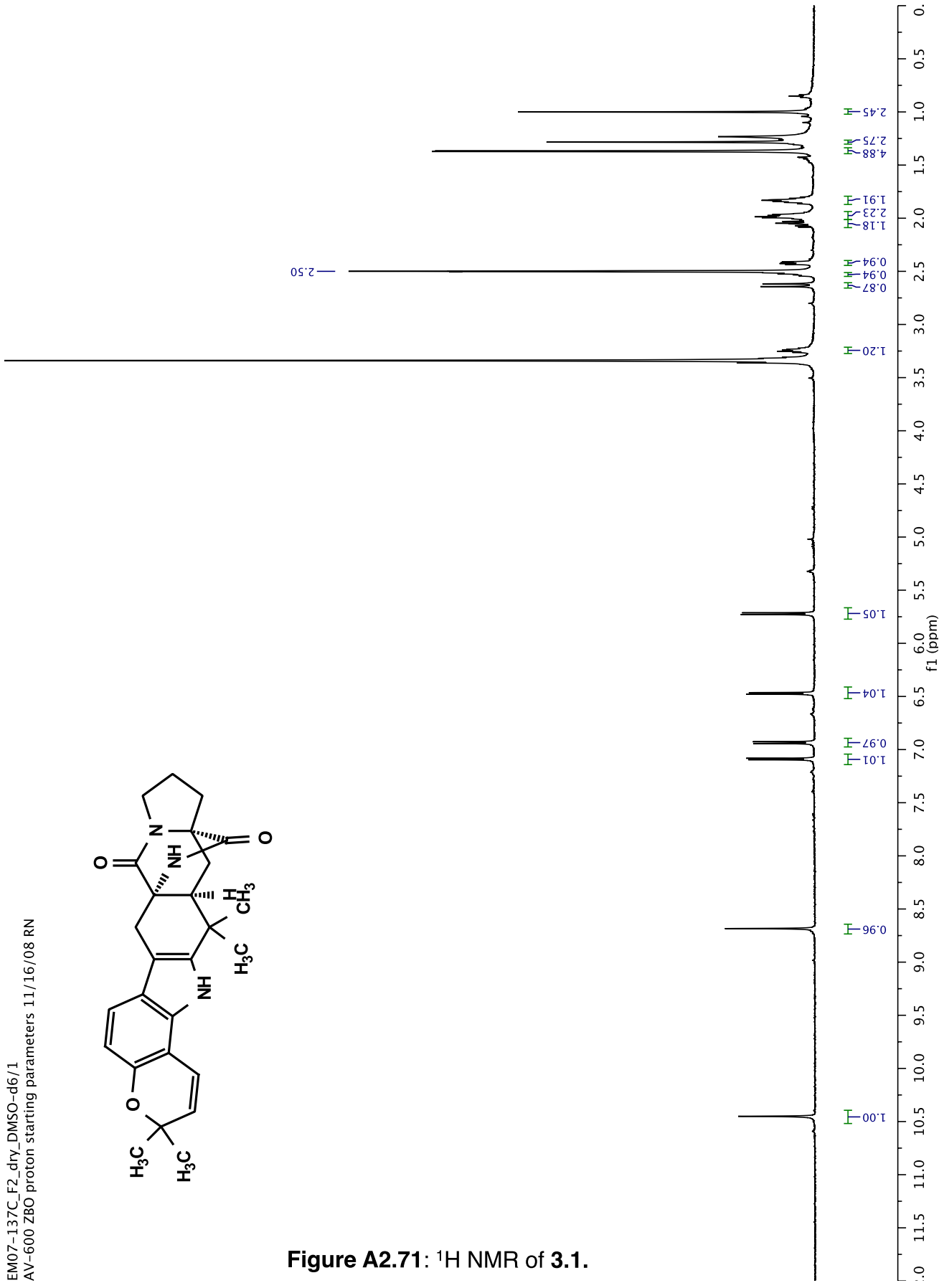

Figure A2.71: ^{1}H NMR of **3.1.**

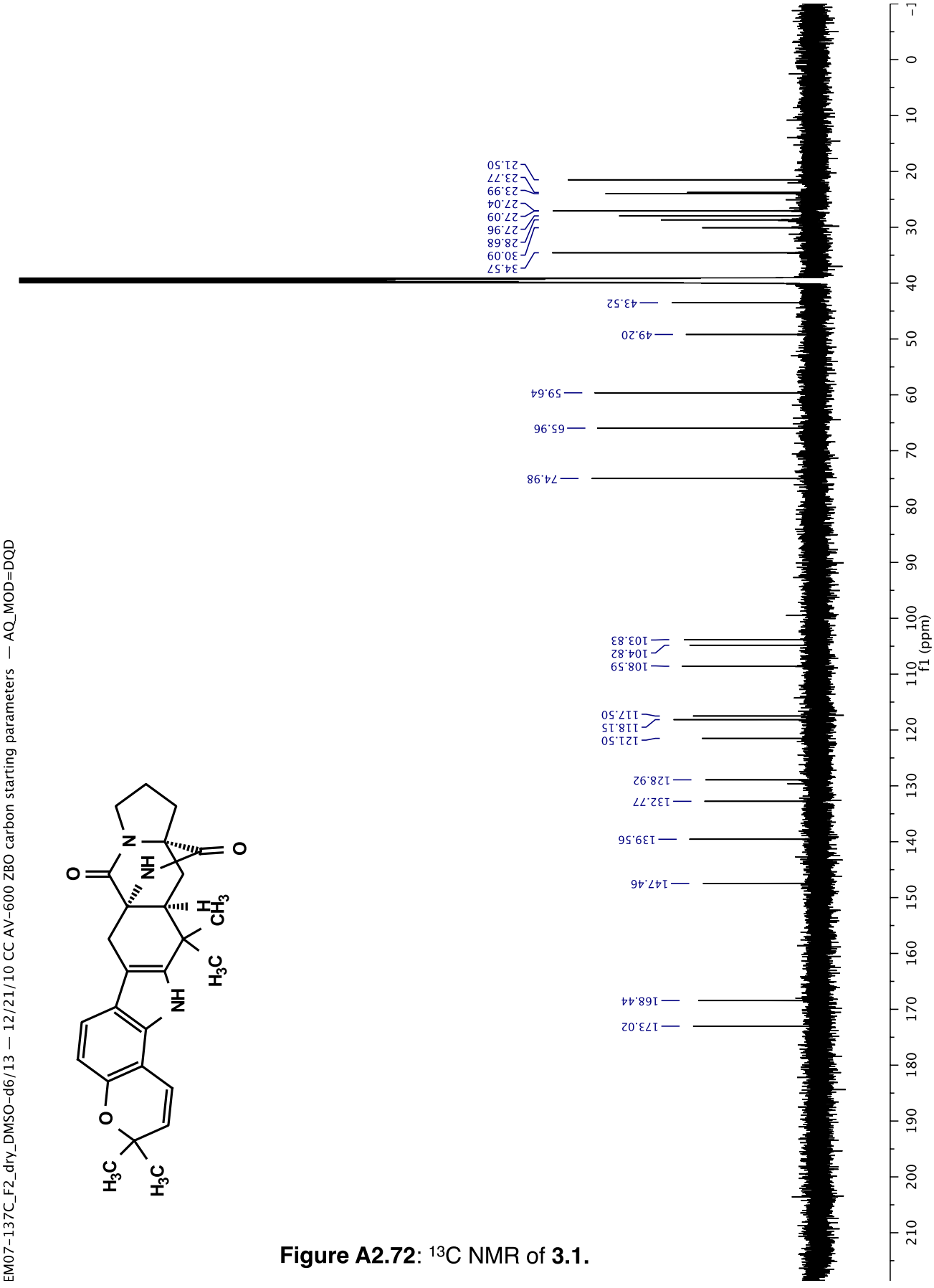

Figure A2.72: ^{13}C NMR of **3.1.**

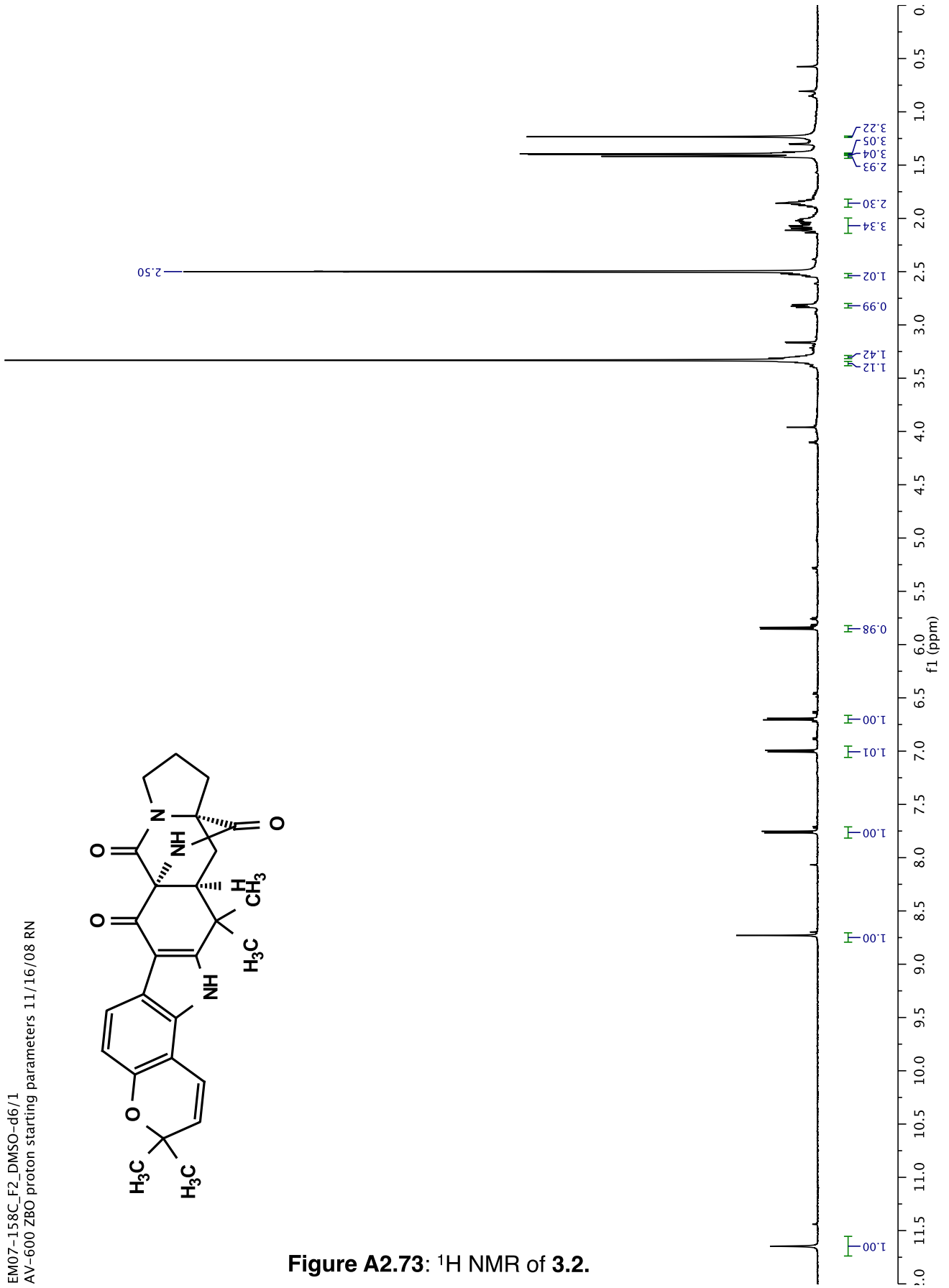

Figure A2.73: ^{1}H NMR of **3.2.**